

Faculty of Science, Masaryk University

National Centre for Biomolecular Research

Research Group Molecular Complexes of Chromatin

Mendel Centre for Plant Genomics and Proteomics

Central European Institute of Technology

**Epigenetic regulation of plant telomeres
and telomerases**

Habilitation thesis

Mgr. Miloslava Fojtová, CSc.

Brno, 2015

Acknowledgement

I would like to express great gratitude to my colleagues from the research group of Molecular Complexes of Chromatin for friendly and congenial working conditions and frequent fruitful discussions contributing to the successful work on my scientific topic. Many thanks to my students for their enthusiasm and youthful dynamism that have helped me to overcome failures and problems.

Prof. Jiří Fajkus, head of the group and the centre, is the best boss I can ever imagine. I acknowledge his tolerance and trust in my competence to develop my own research, and his endless optimism and support!

Contents:

1	Abstract.....	4
2	Telomeres.....	5
3	Telomerase.....	9
4	Epigenetic regulation.....	14
5	Epigenetic pattern of plant telomeres.....	15
6	Telomere maintenance in plants with hypomethylated genomes.....	20
7	References.....	24
8	Conclusion.....	30
9	Supplements.....	31

1 Abstract

My habilitation thesis „Epigenetics of plant telomeres and telomerases“ is presented as a summary of data on plant telomeres, telomerase, epigenetic mechanisms and involvement of epigenetic regulations in telomere homeostasis and developmental control of telomerase activity. The structure and function of telomeres and regulation of telomerase are characterised with respect to particularities described in plants. These topics have been intensively dealt with using mammalian models due to the tight correlation between telomere stability and telomerase activity, and serious pathological conditions. Epigenetics of plant telomeres and telomerases has had to wait until relatively recently to see any attention. Anyway, only plants exhibit specific features in developmental telomere stability and telomerase regulation, and have a broader range of epigenetic mechanisms available. Using plant models for the investigation of the epigenetic nature of telomeric chromatin and the involvement of epigenetic mechanisms in regulation of telomeres and telomerases, interesting results are thus expected to be obtained.

Relevant publications on which the applicant participated are marked as references in the text and presented as Supplements. Apart from the presentation of published data, topics of recent research of the applicant are outlined. In the list of publications the role of the applicant in the design of experiments, collection of experimental data, and writing and editing of manuscript is specified.

2 Telomeres

Ends of linear eukaryotic chromosomes are delimited by specialized structures, telomeres. Telomeres are crucial for the maintenance of genome stability and integrity. First, they distinguish natural chromosome ends from double-stranded DNA breaks and protect them from accidental fusions and undesirable activities of repair complexes. Second, telomeres prevent coding DNA settled inside of chromosomes from loss due to the incomplete replication of the distal most end of the lagging DNA strand. Due to the incapability of DNA polymerases to complete synthesis of the 3' DNA ends, telomeres are progressively shortened during successive replication cycles, and after the shortening to the minimum length, processes of cell senescence are started. Chromosome ends which are not effectively protected are fused together and DNA damage checkpoint responses are activated, contributing to the serious genome instability.

Telomeric DNA usually consists of short repetitive sequences of conservative structure; TTAGGG in animals (Cheng et al., 1989), TTTAGGG in most of plants (Richards and Ausubel, 1988). Only plants represent species with a colourful pattern of telomeric motives. Except canonical telomeric sequence TTTAGGG (so-called telomeric repeat of the *Arabidopsis* type), the human type of telomeric repeats was shown to delimit chromosome ends in representatives of the order of monocotyledonous plants Asparagales (Sykorova et al., 2003). Among Asparagales, species with the *Arabidopsis* type of telomeres are also present, and the structure of telomeric repeat of plants of the genus *Allium* remained scientific mystery for more than twenty years. Using sophisticated bioinformatic approaches, the telomeric sequence CTCGGTTATGGG was detected in *Allium* species (manuscript submitted). The same approach was successfully applied in analyses of the species of the genus *Cestrum* from the Solanaceae family in which the telomeric sequence TTTTTTAGGG was identified (Peska et al., 2015). Attempts to characterize the structure of telomeric repeats in these plants using classical approaches failed for a long time and only filtering abundant repeat sequences sensitive/insensitive to treatment by the BAL31 exonuclease enabled these breakthrough discoveries. *Cestrum* telomeric repeat is relatively similar to canonical plant sequence encompassing three extra Ts, while the

first part of the *Allium* telomere is less common even with Cs in the G-rich telomeric strand. Anyway, this situation is atypical, but it is not unique because recently TTTCAGG and TTCAGG telomeric motives were identified in carnivorous plants *Genlisea hispidula* and *Genlisea subglabra* (Tran et al., 2015). This structure of telomeric repeat may be of high interest due to the possible occurrence of methylated cytosine residues in both telomeric strands which may be important for epigenetic telomere regulation, as discussed below (see pp. 17, 21).

On the other hand, the common plant telomeric repeat TTTAGGG was identified at the ends of the chromosomes of dinoflagellates (Fojtova et al., 2010), the organization of the chromosomes of which is quite exceptional. Genomes of dinoflagellates are the largest in the Eukarya domain, the chromosomes lack histones and exist in a liquid crystalline state. Accordingly, the length of telomeres, 25 – 80 kb, is the largest among unicellular organisms analysed so far.

The length of telomeres is a variable parameter. In human cells, telomeres are 5 – 15 kb long, while in mice, telomeres range between 30 – 150 kb. Similarly in plants, telomeres in some algae species are about 0.5 kb, the length of telomeres in *Arabidopsis thaliana* is 2 – 9 kb depending on ecotype, and very long and heterogeneous telomeres were identified in *Nicotiana tabacum* (tobacco), 20 – 160 kb. Attempts to correlate the length of telomeres in respective species with any other parameter (e.g., longevity, number of chromosomes) have not been successful. Interesting data was obtained in analyses of inbred mouse populations and *A. thaliana* plants of different ecotypes. In the first study, the length of telomeres was determined in strains of mice derived from the wild population 20 years ago and strains inbred and outbred in a significantly longer time, more than 60 years (Hemann and Greider, 2000). Using two independent methodical approaches, it was shown that more recently inbred mouse strains had significantly shorter and more homogenous telomeres. Although it was suggested that the telomere length might be part of a complex mechanism determining organismal lifespan, no such correlation was observed in these mouse strains; mouse strains with shorter telomeres even had the longest lifespan. Authors concluded that, in contrast to observations using human cultured cells, there is no correlation between telomere length and longevity, and suggested that in wild mouse populations, selection for short telomere phenotypes existed. This selection was weakened in non-selective breeding conditions.

In *A. thaliana*, unique subtelomere sequences are present at most of the chromosome arms, making it possible to assess the lengths of individual telomeres. It was shown that the lengths of individual telomeres were co-ordinately regulated, because a single telomere band specific to the respective chromosome arm was detected even in DNA samples isolated from the whole plant body. The optimal size of telomere repeats at each chromosome arm seems to be thus established and maintained for each respective ecotype (Shakirov and Shippen, 2004).

Telomeric sequences are folded into regularly spaced nucleosomes in most organisms, except some lower organisms with short telomeres (Fajkus et al., 1995; Makarov et al., 1993). A specific feature of telomeric nucleosomes is their shorter periodicity compared to the bulk chromatin. For experiments described in this thesis, epigenetic modifications of telomeric histones are important; these are described below (see pp. 15 and following). Recently, participation of non-histone chromatin proteins on telomere homeostasis was demonstrated; loss of the high mobility group protein MHGB1 resulted in the short telomere phenotype in *A. thaliana* (Schrumpfova et al., 2011) and in mouse cells (Polanska et al., 2012).

Besides histones, other proteins associated with telomeres are crucial for their proper structure and function. In mammalian models, two distinct complexes of telomeric proteins were described; shelterin (de Lange, 2005) and CST complex (Surovtseva et al., 2009). Components of the CST complex are involved in telomere maintenance *via* the protection of single stranded G-rich telomere overhangs, and in the facilitation of telomere replication. CST complex was originally described in budding yeast (Gao et al., 2007) and is conserved in all eukaryotic organisms including plants (reviewed in (Price et al., 2010)). The shelterin complex has been characterised in detail in mammalian cells (de Lange, 2005). It comprises six components: TRF1 and TRF2 bind directly double-stranded part of telomeric DNA and mediate binding of two other shelterin proteins, RAP1 and TIN2. TIN2 *via* protein TPP1 interacts with POT1 which binds single-stranded telomere overhang. Shelterin proteins are involved in the formation of high-ordered telomere structures (D-loop, t-loop) which are crucial for the stability and protection of chromosome ends. The presence of shelterin components has not been convincingly documented in plants, although many candidate proteins have been proposed based on the presence of specific structural motives (reviewed in (Peska et al., 2011)). More detailed analyses

were done for representatives of the plant-specific single myb histone family, TRB proteins. In *A. thaliana*, co-localization of TRB1 with telomeres (Dvorackova et al., 2010), interaction with telomeric DNA *in vitro* (Schrumpfova et al., 2004) and *in vivo* (Schrumpfova et al., 2014) were demonstrated.

Because the characterisation of the set of proteins binding with or associated to plant telomeres is not a methodically trivial problem, at present two approaches are optimized for this purpose. PICh (Proteomics of Isolated Chromatin) utilizes a specific DNA probe for the isolation of telomeric DNA of high quality and purity and subsequent identification of bound proteins. Using this method set of telomeric proteins in human cancer cells with active telomerase and in cells maintaining the telomeres by alternative mechanisms was characterized (Dejardin and Kingston, 2009). Next, we will try to fish telomeric chromatin using specific TALE (Transcription Activator Like Effector) or CRISPR/dCas (Clustered Regularly Interspaced Short palindromic Repeats fused with deactivated Cas nuclease) telomeric probes; these are relatively novel approaches developed for the targeted genome editing (reviewed in (Gaj et al., 2013)).

In *A. thaliana*, telomere stability is significantly influenced by the activity of enzymes involved in repair and recombination processes. Our analysis of the moss *Physcomitrella patens*, a lower plant with the highly efficient system of homologous recombination - in contrast to common flowering plants preferring non-homologous end-joining for DNA repair - showed an absence of telomere phenotype and normal double-stranded break repair kinetics in *P. patens* cultures with loss of function of genes coding for proteins crucial for the repair of DNA double-stranded breaks (Fojtova et al., 2015). Thus, both conserved (structure of telomeric repeats and dynamics of telomerase activity) and distinct (telomere maintenance in the DNA repair mutants background) features in telomere biology of land and lower plants were presented.

In most eukaryotic organisms, telomeric repeats are located not only at chromosome termini forming genuine telomeres but also internally, in subtelomeric, centromeric and peri-centromeric regions, forming so called interstitial telomeric sequences (ITS). ITS contained a relatively high level of imprecise (degenerated) telomeric repeats and non-telomeric sequences. The functional importance of these structures remains enigmatic; their biological relevance is connected to their fragility

and genomic instability – DNA breakage, rearrangements and recombinations are common events in ITS. In mammals, ITSs are targets of common mutagens and carcinogens and are correlated with cancer breakpoints.

ITSs are relatively abundant in the *A. thaliana* genome encompassing 20-70% of total telomeric repeats (Gamez-Arjona et al., 2010; Uchida et al., 2002); the high discrepancy in data is related to the methodology used for analysis and data filtering. For the purpose of epigenetic analyses of telomeric chromatin, the presence of telomeric repeats outside of genuine telomeres represents a serious obstacle because it complicates the unambiguous interpretation of results, as discussed in more detail below (see pp. 17 and following).

3 Telomerase

Telomerase is a ribonucleoprotein complex which is able to add telomeric repeats at the G-rich telomere strand and in this way elongate telomeres and compensate for the replicative telomere shortening. Telomerase consists of a catalytic subunit, telomerase reverse transcriptase (TERT), and a telomerase RNA (TER) serving as a template for the telomere elongation by the TERT reverse transcriptase activity. The activity of telomerase is strictly regulated during plant and animal development. In plants, active telomerase was detected in organs and tissues containing highly dividing meristem cells as seedlings, root tips, blossoms and floral buds and in cell cultures (see e.g., (Fajkus et al., 1998; Fitzgerald et al., 1996)). In terminally differentiated tissues (stems, mature leaves), telomerase activity is abolished. Detailed analysis of telomerase activity during *A. thaliana* leaf development revealed high activity in young and middle-age leaves, while in mature leaf tissue telomerase activity was below the detection limit (**Ogrocka et al., 2012**). The pattern of telomerase activity in plants resembles that in humans, but a crucial difference is that active telomerase present throughout plant ontogenesis in meristems maintains stable telomere lengths in cells that these meristems produce by serial divisions and differentiations. Thus, in contrast to human ones, plant telomeres do not shorten during developmental progression (Fajkus et al., 1998). This phenomenon reflects the totipotent character of plant cells. Even in the absence of telomerase activity, as occurs in the case of *A. thaliana* telomerase knock-out mutants, alternative telomere

lengthening is activated, which partially compensates for the lack of telomerase function (Ruckova et al., 2008).

Using plant models, very interesting data regarding telomerase genes was obtained. In *A. thaliana*, two genes coding for the telomerase RNA, *TER1* and *TER2*, were identified (Cifuentes-Rojas et al., 2011), *TER2* even possessing a truncated variant (Cifuentes-Rojas et al., 2012). Although all TERs associate with the TERT catalytic subunit, only TER1 can serve as a template for telomere repeats synthesis while TER2 and its isoform participate in the modulation of telomerase activity. Next, in the allotetraploid *N. tabacum* plant three sequence variants of the *TERT* gene were described (Sykorova et al., 2012); two of them derived from *N. sylvestris* (*TERT_Cs*, *TERT_D*) and one variant with the high level of homology with the *TERT_Ct* sequence present in the donor of the paternal genome *N. tomentosiformis*. Original abbreviations are Cs for Coding putative functional *TERT* variant of the S-genome origin, Ct for Coding putative functional *TERT* variant of the T-genome origin, and D for putative pseuDogene *TERT* variant. All *TERT* gene variants are transcriptionally active, although *TERT_D* shows a lower level of sequence similarity with *TERT_C* variants, and due to insertions and deletions within exons and truncation at the 5' end it was originally supposed to be a pseudogene. In the analysis enabling specific amplification of *TERT* gene variants, *TERT_C* variant(s) transcripts were dominant in tobacco and *N. sylvestris* tissues indicating differential regulation of *TERT_C* and *TERT_D* transcription. In tobacco, *TERT_Ct* and *TERT_Cs* transcript levels were comparable and correlated to the telomerase activity in the respective tissues. A specific *TERT* transcription pattern was observed in samples of tobacco pollen (two stages of juvenile pollen, mature pollen and *in vitro* cultivated pollen tubes) where *TERT_Cs* transcript was significantly enriched. *TERT_Ct* transcript was at a level comparable to tobacco seedlings and corresponded to the telomerase activity. The reason for such a high level of *TERT_Cs* transcript in tobacco pollen and the potential function of the protein remain unclear (Jureckova et al., submitted).

The molecular mechanism of telomerase regulation at both cellular and organism levels is far from being elucidated. In a tobacco cell culture, cycle dependence of telomerase regulation was demonstrated with a peak of telomerase activity in the early S phase (Tamura et al., 1999). In the same work, induction of

telomerase activity by the plant hormone auxin was presented, although this was not confirmed in analyses of tobacco seedlings germinated in the auxin presence (**Jureckova et al., submitted**) indicating that telomerase activity is under more complex and more robust control in tobacco differentiated tissues compared to cell culture. The link between telomerase activity and cell cycle was also documented in the highly synchronized culture of green algae *Desmodesmus quadricauda*. Exceptionally highly active telomerase was present in all stages of the cell cycle with the peak in the dark period of culturing corresponding to the completion of cell division (**Sevcikova et al., 2013**).

Telomerase activity was correlated to the transcription of the protein subunit of telomerase TERT (Fitzgerald et al., 1996; **Ogrocka et al., 2012**), while the TER transcription was approximately the same in all plant tissues analyzed (Cifuentes-Rojas et al., 2011). Biosynthesis of TERT and TER subunits is not directly connected and their differential regulation raises questions of mechanisms of the active enzyme assembly including intracellular trafficking of telomerase components (reviewed in (Sykorova and Fajkus, 2009)). Regulation of telomerase activity at the posttranslational level *via* phosphorylation was reported in mammals (Liu et al., 2001) and in *Oryza sativa* (Oguchi et al., 2004). Moreover, the functional significance of alternatively spliced *TERT* transcript variants in the modulation of telomerase activity was demonstrated in a human system. In plants, number of alternatively spliced *TERT* variants was detected in *O. sativa* and species of the Asparagales order. In *A. thaliana*, *TERT* isoform retaining the intron 6 and with the stop codon inside the exon 8 revealed an ability to interact with the putative telomere binding protein POT1, determining possible functional relevance of this isoform (reviewed in (Sykorova and Fajkus, 2009)). Next, the telomerase activity is modulated by the dynamic structure of telomeres determining the accessibility of telomeres for telomerase enzyme, in the establishment of which telomere-binding and telomere-associated proteins play an important role. In animal models, the involvement of epigenetic mechanisms in the regulation of *TERT* gene transcription was convincingly documented; active *TERT* gene transcription in telomerase positive cells was correlated with euchromatic-specific epigenetic marks at histones in regulation regions, while heterochromatin specific modifications decorated *TERT* gene histones in telomerase negative cells (reviewed in (Zhu et al., 2010)). In the pilot study investigating involvement of epigenetic mechanisms in developmental regulation of telomerase activity in *A.*

thaliana, it was shown that the euchromatic character of the *TERT* gene in both telomerase positive and telomerase negative tissues was maintained (**Ogrocka et al., 2012**). These differences might reflect the totipotent character of plant cells and reversible and dynamic character of plant telomerase silencing.

Taking into consideration that even other factors including nucleosomal density in *TERT* regulatory regions, the binding of protein(s) activating or repressing telomerase protein subunit promoter, and the activity of telomere transcripts TERRA (see pp. 17) may influence telomerase transcription and subsequently activity, it is evident that the regulation of telomerase activity is a highly complex process, realized by the close interplay of multifarious pathways. The human telomerase interactome network encompassed tens of proteins (Cline et al., 2007); for plants this data has not been obtained yet.

The study of plant gene functions is commonly based on the analysis of *A. thaliana* T-DNA insertion lines, which are available from commercial databases. Collection of lines with T-DNA insertions in distinct *TERT* gene regions (N-terminal part with telomerase-specific motives, reverse transcriptase motif in the central part, C-terminal extension) and in the *TERT* upstream sequences was used for investigation of structure-function relationship of *TERT* domains. It was found that telomerase transcription and activity were abolished and telomeres were significantly shortened in all lines with T-DNA inserted inside the *TERT* gene regardless of position of the insertion. Telomerase function was maintained in lines with T-DNA inserted into the putative *TERT* promoter. Interestingly, putative regulatory elements were discovered in the 5' part of the *TERT* gene; in lines with T-DNA insertion in this region telomerase transcription was markedly upregulated even in telomerase negative tissue, with short telomere phenotype maintained (**Fojtova et al., 2011**). Complexity of the plant telomerase regulation pointed out in this work was further supported by analyses of *A. thaliana* plants transformed by functionally important parts of the *TERT* gene, full length *TERT* gene and *TERT* cDNA. Although *TERT* genomic constructs were efficiently transcribed and displayed correct mRNA splicing and protein translation, telomerase activity was not significantly affected in transformed wild type and *tert*^{-/-} plants, and in *tert*^{-/-} mutants the short telomere phenotype was maintained (**Zachova et al., 2013**). With reference to previous studies on human telomerase reconstruction (Bachand and Autexier, 1999; Banik et al., 2002), similar types of constructs were

used for transformation, but in spite of that we were not able to reconstitute functional telomerase in a plant system, evidencing that plant *TERT* expression differs from the human enzyme by more complex multi-level regulation, including probably cross-talk between regulatory elements located upstream and/or downstream of the *TERT* coding regions. In accordance with this hypothesis *TERT* gene constructs containing relevant regulatory regions have been designed and transformed to *A. thaliana tert*^{-/-} plants and preliminary analyses have produced very promising results.

Besides being active in the maintenance of chromosome ends, telomerase also exerts non-telomeric activities. In mammalian models, telomerase was documented to be active, e.g. in anti-apoptotic, cytoprotective and pro-proliferative processes and in protection of mitochondria from the oxidative stress. High-throughput analysis revealed that a protein subunit of human telomerase modulates expression of more than 300 genes involved mainly in cell cycle progression, differentiation and proliferation (reviewed in (Majerska et al., 2011)). Transcriptome analysis of *A. thaliana tert*^{-/-} plants revealed more than 1 000 genes with significantly changed transcription. The comparison of transcriptomes of different generations of mutant plants permitted to separate effects corresponding predominantly to the telomerase absence (the second generation of mutants) and to the severe genome damage (the seventh generation of mutants) (Amiard et al., 2014). In this study marked differences in the transcriptome of telomerase-deficient mice and plants were pointed out, demonstrating different ways of cellular response to the chronic telomere erosion.

In tobacco culture cells cultivated in the presence of cadmium ions, apoptotic fragmentation of DNA was observed (Fojtova and Kovarik, 2000). Increased activity of telomerase (Fojtova et al., 2002) together with the accumulation of phytochelatin, plant-specific metallothioneins (Fojta et al., 2006) were detected in the phase of genome recovery from the genotoxic stress. This promising research is being further developed now to better define the role and significance of telomerase in stress-response processes.

Similarly, telomerase was shown to be involved in the healing of *Luzula elegans* holocentric chromosomes fragmented due to the exposure of the plant to ionizing radiation (Jankowska et al., 2015).

4 Epigenetic regulation

Studies of epigenetic molecular mechanisms including DNA methylation, modifications of histones and processes of RNAi, undergo significant boom in last decades. It is due to the involvement of epigenetic regulations in plenty of pivotal processes such as gene expression, replication timing and differentiation which are part of cellular programming and re-programming and of the complex response to the developmental and environmental stimuli. These intensive efforts have resulted into applications to the clinical practice, namely in the form of epigenetically active drugs (for recent review see (Bojang and Ramos, 2014)).

In the epigenetic studies plant models are of high significance. Plants, as sessile organisms, have developed sophisticated and complex systems of epigenetic tools enabling them to cope with suboptimal living conditions and environmental changes. Some epigenetic mechanisms are even unique for plants. In animals, methylated cytosines are located preferentially or almost exclusively in CG doublets, although in recent studies a fraction of methylated cytosines in non-CG motives was detected in non-differentiated human cells (Lee et al., 2010; Lister et al., 2009). In plants, methylated cytosines are located in symmetrical sequence motives CG and CHG (H = C, A, T) and even in non-symmetrical sequences. Correspondingly, three DNA methyltransferases were identified in plant cells. MET1 (functional analogue of mammalian DDM1 enzyme) is responsible primarily for methylation of CG cytosines and consecutively for the stability of the general epigenetic pattern including non-CG methylation and histone modifications (Mathieu et al., 2007). CMT3 is a plant-specific methyltransferase modifying cytosines in CHG triplets. This methyltransferase functions in close interplay with histone methyltransferases. *De novo* methyltransferase DRM2 (functional analogue of mammalian DNMT3a/b) mediates the transfer of the methyl group on cytosines in all sequence contexts. In this process, a signal indicating the position of cytosines – substrates for *de novo* methylation – has to be active. The involvement of RNA molecules in the driving of *de novo* DNA methylation, RNA-directed DNA methylation (RdDM), was described in plants (Jones et al., 1999), and plant specific RNA polymerases IV and V participating in this process were characterized (Herr et al., 2005; Wierzbicki et al., 2012). Inspired by

plant achievements in this field, the involvement of RdDM in the silencing of human promoters was also demonstrated (Kawasaki and Taira, 2004; Morris et al., 2004).

Compared to relatively straightforward and simple DNA methylation, the pattern of covalent modifications of histones is extremely complex, constituting so-called histone code. This code is not universal among species. A striking example of this is distribution of methyl residues at lysine 9 of histone H3 and lysine 20 of histone H4. In *A. thaliana*, mono-methylated H3K9 and H4K20 are associated with heterochromatic regions and tri-methylated with euchromatic regions while in mouse cells the pattern is completely the opposite – H3K9me and H4K20me in euchromatin, H3K9me₃ and H4K20me₃ in heterochromatin (reviewed in (Fransz et al., 2006)).

Results obtained in analyses using plant models significantly contributed even to the elucidation of the RNAi, a breakthrough discovery demonstrating the fundamental role of RNA molecules in many regulation processes. The mechanism of RNAi was described on *Caenorhabditis elegans* (Fire et al., 1998) but years ago co-suppression, posttranscriptional silencing of plant transgenes based on the sequence homology and of the same mechanistic background as RNAi, was presented (Napoli et al., 1990).

Epigenetic regulation is not realized only and simply *via* modulation of gene expression. The final impact of interplay of different epigenetic mechanisms including additive processes like the activity of chromatin remodelling complexes and deposition of variant histones is realized at the level of the chromatin structure. Changes in chromatin structure may result in modulation of the accessibility of the region to transcription factors, replication timing, activity of transposable elements and DNA repair resulting in changes in proteome and metabolome, and possibly to the establishment of a new cell phenotype.

5 Epigenetic pattern of plant telomeres

Telomeres, due to their repetitive character and main function as protective chromosomal structures, have been traditionally considered as heterochromatic

regions. This assumption has been supported by an amount of convincing data from mammalian studies. Heterochromatin-specific histone modifications at telomeres and subtelomeres were shown to be essential for proper structure and function of telomeres, and the loss of these marks correlated with disruption of telomere maintenance and genome instabilities in mouse cells (reviewed in (Blasco, 2007; Galati et al., 2013)). *A vice versa*, telomeric and subtelomeric chromatin in telomerase-deficient mice with eroded telomeres was depleted by heterochromatic H3K9me3 and H4K20me3 marks (Benetti et al., 2007), and genome-wide hypomethylation was observed as a consequence of critically short telomeres in telomerase-negative embryonic stem cells (Pucci et al., 2013), evidencing the mutual relationship between the mammalian telomeres stability and their epigenetic pattern. Interestingly, some studies of telomeric chromatin properties in mammalian models have brought rather controversial results. Firstly, in mouse embryonic stem cells, both heterochromatin-specific H3K9me3 and euchromatic mark H3K4me3 were detected, although the H3K9me3 exhibited a higher level. Moreover, in cells deficient in H3K4 methyltransferase function H3K9 methylation increased markedly, suggesting dynamics between these opposing types of histone modifications at mouse telomeres (Cao et al., 2009). Secondly, in mouse embryos and adult tissues with impaired function of important epigenetic modifiers, the length of telomeres was maintained (Roberts et al., 2011), in contrast to previous reports implicating involvement of epigenetic mechanisms in the regulation of mammalian telomeres stability.

Extraordinary dynamic of telomeric chromatin structure is related to stem cell differentiation. Telomeric chromatin in pluripotent stem cells exists in a relatively open formation, and during differentiation a switch to a more condensed state arises. Interestingly, reprogramming somatic cells to induced pluripotent cells is connected with inverse changes – the telomeric chromatin adopts a more open embryonic stem cell-like organization. These observations point out that the specific structure of telomeric chromatin plays a role in determining the unique character of embryonic stem cells (reviewed in (Wong, 2010)).

In contrast to a number of studies dealing with the epigenetic properties of mammalian telomeres, significantly less effort has been devoted to analogous analyses in plants, although plants as model organisms are no less interesting in this respect, quite the contrary in fact. A good example of this fact is that plant cells possess

enzymatic apparatus enabling methylation of cytosines located in all sequence contexts and, correspondingly, cytosines in the C-rich strand of the telomeric repeat CCCTAAA are natural targets for methylation. Data from the whole genome *A. thaliana* methylation study did confirm the presence of methylated cytosines in telomeric sequences (Cokus et al., 2008). Another discovery demonstrating the colourful pattern of plant telomere epigenetics concerns telomeric transcripts. Telomeric-repeat containing RNA (TERRA) was described in 2007 in mammalian cells (Azzalin et al., 2001). It was shown that TERRA comprises primarily the G-rich telomeric RNA strands (UUAGGG repeats), and transcription thus originates in subtelomeric regions. In plant models *A. thaliana* (Vrbsky et al., 2010) and *Nicotiana tabacum* (Majerová et al., 2014) not only TERRA but also complementary C-rich telomeric transcripts ARRET (nomenclature here is still chaotic, see below) were detected at comparable levels. Similarly, C-rich telomeric transcripts were revealed in fission yeast (Bah et al., 2012). Telomeric transcriptome in fission yeast is even more complex because besides the G-rich telomeric transcripts TERRA, and C-rich telomeric transcripts (here named ARIA), subtelomeric RNA complementary to the subtelomeric part of TERRA lacking the perfect telomeric repeats ARRET, and its complementary strand α ARRET, were described (Bah et al., 2012).

In the pilot study on epigenetic properties of *A. thaliana* telomeric chromatin, its dual character was reported, as both heterochromatin- and euchromatin-specific histone modifications were associated with telomeric histones and a fraction of telomeric cytosines was methylated. The methylation of cytosines in telomeric repeats was maintained by the RdDM pathway *via* siRNA molecules derived from telomeric transcripts (Vrbsky et al., 2010). However, analysis of telomeric histone modifications is routinely done by chromatin immunoprecipitation (ChIP) followed by the hybridization of the immunoprecipitated fraction of DNA against labelled telomeric probe. In such analyses, the hybridization signal is yielded not only by genuine telomeres, but also by internally located telomeric repeats, ITS (see pp. 8, 9) which are common components of plant and vertebrate genomes (Azzalin et al., 2001; Uchida et al., 2002). To our knowledge, interference of ITS has not routinely been taken into consideration in interpretation of epigenetic analyses of telomeric chromatin in mammalian studies. Fortunately, the structures of genuine telomeres and ITS are not identical; telomeres consist of arrays of perfect telomeric repeats while in ITS, telomeric repeats are irregular and interspersed by random DNA sequences. This fact

is commonly utilized in analyses of telomere lengths by the terminal restriction fragments method when genomic DNA (including ITS) is digested by the frequently cutting restriction enzyme while tracks of telomeres remain intact. Experimental conditions used in epigenetic analyses of *A. thaliana* telomeres should strongly favour detection of signals from genuine telomeres (Vrbsky et al., 2010). Nevertheless, in an alternative study, when telomeric and non-telomeric (ITS-containing) fractions of the *A. thaliana* genome were analysed separately, euchromatin-specific modifications of telomeric histones and non-methylated telomeric cytosines, and heterochromatic character (including cytosine methylation) of subtelomeric chromatin and telomeric repeats located internally were reported (Vaquero-Sedas et al., 2011). This pattern was confirmed by evaluation of *A. thaliana* ChIP-seq data (Vaquero-Sedas et al., 2012).

These sets of rather contradictory results have initiated scientific discussions on the proper interpretation of epigenetic analyses of plant telomeric chromatin (Majerova et al., 2011a; Vaquero-Sedas and Vega-Palas, 2011). Although in the Vrbsky et al. study on *A. thaliana* (Vrbsky et al., 2010) (i) the pattern of telomeric cytosines methylation corresponded to previous observations (Cokus et al., 2008), (ii) detailed analysis directly proved the presence of methylated cytosines at least in the specific part of the proximal telomere region, and (iii) conditions of histone modifications analyses were optimized to provide a signal just/primarily from the genuine telomeres, possible contribution of ITS cannot be excluded. To avoid these difficulties, plants with contrasting distributions of genuine telomeres and ITS were studied (Majerová et al., 2014): *N. tabacum*, a species with long telomeres and non-detectable fraction of ITSs (Majerova et al., 2011a), and an endemic Australian cruciferous plant *Ballantinia antipoda* with huge blocks of ITS in pericentromeric regions of all chromosomes and relatively short telomeres (Mandakova et al., 2010). It was shown that cytosines in telomeres and ITS are methylated with some gradient towards distal parts of *Nicotiana* telomeres and significantly different levels of methylation of respective ITS. Regarding histone modifications, telomeres were associated with both heterochromatin- and euchromatin-specific marks, with a prevalence of heterochromatic H3K9me₂, while ITSs were exclusively heterochromatic. Interestingly, in accordance with the previous observation (Vaquero-Sedas et al., 2012), H3K27me₃, a mark of the chromatin of developmentally silenced genes, was loaded at telomeric histones. The significance of this modification – and generally significance of all histone marks – for a proper structure and function of

plant telomeres is yet to be determined, and this topic is a subject of our recent research.

The H3.3 histone variant is commonly associated with transcriptionally active euchromatic regions where it replaces for canonical H3.1 histone. However, H3.3 accumulation was found also at telomeres and pericentric heterochromatin in mouse embryonic stem cells and mouse embryonic fibroblasts, respectively (reviewed in (Szenker et al., 2011)). Surprisingly, in contrast to the proposed role of H3.3 in marking active chromatin, its presence at telomeres in mammalian embryonic stem cells is required for the transcriptional repression of telomeric repeats (Goldberg et al., 2010). ChIP-seq data from dividing and non-dividing *A. thaliana* tissues is in agreement with the general enrichment of transcriptionally active chromatin in H3.3 (Stroud et al., 2012; Wollmann et al., 2012). However, evaluation of telomeric sequences was included in neither of these reports. Vaquero-Sedas and Vega-Palas sorted ChIP-seq data corresponding to perfect telomeric repeats (presumed genuine telomeres) and imperfect telomeric repeats (presumed ITS) and compared the distribution of H3.1 and H3.3 histone variants in telomeres, ITS and centromeric repeats (Vaquero-Sedas and Vega-Palas, 2013). They found the enrichment of H3.3 at telomeres and H3.1 at centromeres and ITS. Interestingly, the association of telomeres with the H3.3 variant (which compromises purely heterochromatic nature of the telomeric chromatin) makes the reports on the presence of H3K27me3 histone mark at plant telomeres (**Majerová et al., 2014**; Vaquero-Sedas et al., 2012) rather surprising, because the occurrence of H3.3 and H3K27me3 epigenetic marks was shown as mutually exclusive in the genome-wide study (Stroud et al., 2012).

All these findings demonstrate specific properties of plant telomeric chromatin, to a certain extent probably similar to that of mammalian embryonic stem cells. The “intermediate” character of plant telomeric chromatin may constitute a reason why the so-called telomere position effect, i.e. silencing of genes adjacent to telomeres, could not be demonstrated in plants (reviewed in (**Fojtova and Fajkus, 2014**)). Due to the lack of wholly consistent results in *A. thaliana*, well-designed studies using other model plants are required to draw convincing general conclusions and a detailed map of epigenetic landscape of plant telomeres.

6 Telomere maintenance in plants with hypomethylated genomes

As mentioned above (see pp. 16), in mammalian cells the interrelation between epigenetic state of telomeres and their stability was reported. On the other hand, just a few analogous plant studies are available so far. Telomere maintenance was analysed in *A. thaliana* plants hypomethylated either chemically or genetically (Ogrocka et al., 2014). *A. thaliana* seedlings were germinated in the presence of two different hypomethylation drugs. One of them, zebularine (1-(β -D-ribofuranosyl)-2(1H)-pyrimidin-one) is a cytidine analogue, which is able to be incorporated into DNA and form a covalent adduct with DNA methyltransferases. This compound acts similarly to commonly used cytidine analogues 5-azacytidine (5-azaC) and 5-aza-deoxycytidine (5-aza-dC, decitabine) which are used in clinics for cancer therapy (reviewed in (Yoo and Jones, 2006)). Nevertheless, there are several important differences between actions of 5-azaC and 5-aza-dC on one hand and zebularine on the other. Big advantages of zebularine include its significantly lower toxicity and higher stability in aqueous solutions (Cheng et al., 1989); opposite properties markedly complicate the admission of 5-azaC and 5-aza-dC (Beisler, 1978; Ghoshal and Bai, 2007). Moreover, the incorporation of zebularine into DNA increased the DNA binding of methyltransferases while no such effect was observed for 5-aza-dC (Champion et al., 2010). A lot of effort was exerted to elucidate the detailed mechanism of the drug – DNA – methyltransferase interaction. Although formation of the irreversible covalent complex for both 5-aza-dC- and zebularine-containing DNA with DNA methyltransferase was reported (Hurd et al., 1999; Taylor et al., 1993), according to the more recent data formation of a reversible although highly stable complex between the zebularine-containing DNA and the DNA methyltransferase appears more probable (Champion et al., 2010). The very recent report compromised previously obtained data on the mechanisms of the zebularine hypomethylation activity showing extremely low level of the zebularine incorporation into DNA and demonstrating DNA damage induced at least partially by zebularine-DNA methyltransferase nucleoprotein complex (Liu et al., 2015).

The other hypomethylation drug used in the analysis of epigenetic regulation of plant telomeres was DHPA ((*S*)-9-(2,3dihydroxypropyl) adenine), a competitive inhibitor of S-adenosyl-L-homocystein hydrolase (Holy, 1975). This enzyme catalyses hydrolytic

degradation of S-adenosyl-L-homocysteine, a by-product of transmethylation reactions and a potent inhibitor of all DNA and histone methyltransferases. The hypomethylation effect of DHPA is thus more general concerning the spectrum of methylation reactions affected, compared with the zebularine which influences DNA methylation only.

As an alternative approach for obtaining *A. thaliana* plants with the hypomethylated genome, mutant plants with the T-DNA insertion in genes coding for the proteins essential for the maintenance of stable DNA methylation were analysed. These plants exhibited loss of function of either (i) the MET1 methyltransferase (Mathieu et al., 2007) (see pp. 14), or (ii) DDM1, a chromatin remodelling factor which is involved in the maintenance of methylated cytosines in all sequence contexts (Vongs et al., 1993). In both types of mutant plants, a significant drop of methylated cytosines in centromeric repetitive sequence as well as in telomere repeats was observed. Similar results were obtained for the plants hypomethylated chemically (Ogrocka et al., 2014). While in mammalian cells, the genome hypomethylation led to telomere elongation (Gonzalo et al., 2006), telomeres in hypomethylated plants were significantly shortened and the short telomere phenotype was stably transmitted to the subsequent generation of plants which were not more exposed to the epigenetic stress. The hypomethylation is thus essential for the induction of telomere length changes, but the maintenance of the modulated telomere phenotype is not dependent on the genome methylation status. Loss of methylation of cytosines in telomeric repeats was also observed in plants lacking RNA-dependent RNA polymerase 2 (Vrbsky et al., 2010), an essential component of the RdDM pathway. It would be interesting to analyse telomere length in these mutants to elucidate whether the loss of methylation of non-symmetrically located telomeric cytosines (or more precisely, loss of methylation of cytosines in non-symmetrical sequence contexts generally) represents a necessary and sufficient condition for the induction of the telomere instabilities. This appears probable, because telomeres in *A. thaliana* mutants with loss of functions of non-CpG DNA methyltransferases were also significantly shorter (Vaquero-Sedas and Vega-Palas, 2014). Interestingly, changes of telomere length in *met1* and *ddm1* mutants and in drug-treated plants were not correlated to the changes of the activity and transcription of telomerase (Ogrocka et al., 2014). In agreement with these observations, no significant contribution of DNA methylation to the developmental silencing of telomerase transcription and activity in the terminally

differentiated *A. thaliana* tissues was observed (**Ogrocka et al., 2012**). The process of telomere maintenance is rather complex and many factors involved in it may be under epigenetic control. These factors may influence, for example, the formation of a functional telomerase complex or the accessibility of telomeres for telomerase, important parameters that are not possible to notice in *in vitro* analysis of the telomerase activity.

The next study on epigenetic modulation of plant telomere maintenance was performed using tobacco culture cells cultivated in the presence of hypomethylation drugs zebularine or DHPA (**Majerova et al., 2011b**). The treatment caused the genome-wide cytosine hypomethylation including significant decrease of the level of methylated cytosines located in telomeric repeats. This observation is very important in the point mentioned above i.e., that tobacco – in contrast to other common model plants including other representatives of the Solanaceae family (He et al., 2013) – does not contain a significant fraction of ITS in its genome (**Majerova et al., 2011a**). Results of this study thus, with a high probability, reflect changes in the methylation level of genuine telomeres. Surprisingly, in contrast to analyses of *A. thaliana* hypomethylated plants, the length of telomeres in hypomethylated tobacco cells was unaffected, although markedly increased telomerase activity was detected in the quantitative assay (**Majerova et al., 2011b**).

The distinct involvement of epigenetic mechanisms in the telomere and telomerase regulation in *A. thaliana* and *N. tabacum* may be more comprehensible considering the differences in the genome and epigenome composition between these two model plants. Compared to *N. tabacum*, *A. thaliana* has a significantly smaller genome with a low content of repetitive sequences and, correspondingly, a low number of heterochromatic regions. In agreement with this, the overall level of DNA methylation in *A. thaliana* is significantly lower and methylated cytosines are located preferentially in CpG doublets. Even the general methylation landscape differs between these plants. In *A. thaliana*, a mosaic methylation pattern, similar to the one in invertebrates, was observed, with methylated cytosines residing mainly in transposons, repetitive elements and gene body regions. By contrast, in plants with huge genomes (e.g., tobacco, maize), although detailed methylation analyses have not been done yet, non-methylated (or body-gene methylated) genes are separated by long

tracts of methylated transposons and other types of repetitive sequences (reviewed in (Suzuki and Bird, 2008)).

As in mammalian cells, plant telomeres are under epigenetic control, at least in the model plants analysed. The principles of this regulation are not uniform and not trivial, since the loss of heterochromatin-specific epigenetic modifications, including DNA methylation, led to the telomere elongation and increased recombination capacity in most mammalian studies (Gonzalo et al., 2006; Vera et al., 2008), while, on the other hand, telomere shortening due to the telomerase transcription down-regulation was observed in 5-aza-dC-treated chronic myeloid leukemia cell lines (Grandjennette et al., 2014). The different effects of the hypomethylation stress on the telomere stability and telomerase activity observed in *A. thaliana* and tobacco may indicate different involvements of epigenetic mechanisms in the regulation of crucial cellular processes in these species (Vaughn et al., 2007), and their contribution to the colourful pattern of the plant epigenetic and telomere stories (reviewed in **(Dvorackova et al., 2015)**). Definitely, analyses of other plants with genomes/epigenomes similar to those of either *A. thaliana* or *N. tabacum* will bring new data essential for verbalization of generally valid and species-specific aspects of epigenetic regulation of plant telomeres.

7 References:

- Amiard, S., Da Ines, O., Gallego, M.E., and White, C.I. (2014). Responses to telomere erosion in plants. *PLoS One* 9.
- Azzalin, C.M., Nergadze, S.G., and Giulotto, E. (2001). Human intrachromosomal telomeric like repeats: sequence organization and mechanisms of origin. *Chromosoma* 110, 75-82.
- Bah, A., Wischnewski, H., Shchepachev, V., and Azzalin, C.M. (2012). The telomeric transcriptome of *Schizosaccharomyces pombe*. *Nucleic Acids Res* 40, 2995-3005.
- Bachand, F., and Autexier, C. (1999). Functional reconstitution of human telomerase expressed in *Saccharomyces cerevisiae*. *J Biol Chem* 274, 38027-38031.
- Banik, S.S.R., Guo, C.H., Smith, A.C., Margolis, S.S., Richardson, D.A., Tirado, C.A., and Counter, C.M. (2002). C-terminal regions of the human telomerase catalytic subunit essential for in vivo enzyme activity. *Mol Cell Biol* 22, 6234-6246.
- Beisler, J.A. (1978). Isolation, characterization, and properties of a labile hydrolysis product of anti-tumor nucleoside, 5-azacytidine. *J Med Chem* 21, 204-208.
- Benetti, R., Garcia-Cao, M., and Blasco, M.A. (2007). Telomere length regulates the epigenetic status of mammalian telomeres and subtelomeres. *Nat Genet* 39, 243-250.
- Blasco, M.A. (2007). The epigenetic regulation of mammalian telomeres. *Nat Rev Genet* 8, 299-309.
- Bojang, P., and Ramos, K.S. (2014). The promise and failures of epigenetic therapies for cancer treatment. *Cancer Treat Rev* 40, 153-169.
- Cao, F., Li, X., Hiew, S., Brady, H., Liu, Y., and Dou, Y. (2009). Dicer independent small RNAs associate with telomeric heterochromatin. *RNA* 15, 1274-1281.
- Cifuentes-Rojas, C., Kannan, K., Tseng, L., and Shippen, D.E. (2011). Two RNA subunits and POT1a are components of Arabidopsis telomerase. *Proc Natl Acad Sci USA* 108, 73-78.
- Cifuentes-Rojas, C., Nelson, A.D.L., Boltz, K.A., Kannan, K., She, X.T., and Shippen, D.E. (2012). An alternative telomerase RNA in Arabidopsis modulates enzyme activity in response to DNA damage. *Gene Dev* 26, 2512-2523.
- Cline, M.S., Smoot, M., Cerami, E., Kuchinsky, A., Landys, N., Workman, C., Christmas, R., Avila-Campilo, I., Creech, M., Gross, B., *et al.* (2007). Integration of biological networks and gene expression data using Cytoscape. *Nat Protoc* 2, 2366-2382.
- Cokus, S.J., Feng, S., Zhang, X., Chen, Z., Merriman, B., Haudenschild, C.D., Pradhan, S., Nelson, S.F., Pellegrini, M., and Jacobsen, S.E. (2008). Shotgun bisulphite sequencing of the Arabidopsis genome reveals DNA methylation patterning. *Nature* 452, 215-219.
- de Lange, T. (2005). Shelterin: the protein complex that shapes and safeguards human telomeres. *Gene Dev* 19, 2100-2110.
- Dejardin, J., and Kingston, R.E. (2009). Purification of proteins associated with specific genomic loci. *Cell* 136, 175-186.
- Dvorackova, M., Fojtova, M., and Fajkus, J. (2015). Chromatin dynamics of plant telomeres and ribosomal genes. *Plant J* 83, 18-37.
- Dvorackova, M., Rossignol, P., Shaw, P.J., Koroleva, O.A., Doonan, J.H., and Fajkus, J. (2010). AtTRB1, a telomeric DNA-binding protein from Arabidopsis, is concentrated in the nucleolus and shows highly dynamic association with chromatin. *Plant J* 61, 637-649.
- Fajkus, J., Fulneckova, J., Hulanova, M., Berkova, K., Riha, K., and Matyasek, R. (1998). Plant cells express telomerase activity upon transfer to callus culture, without extensively changing telomere lengths. *Mol Gen Genet* 260, 470-474.

- Fajkus, J., Kovarik, A., Kralovics, R., and Bezdek, M. (1995). Organization of telomeric and subtelomeric chromatin in the higher plant *Nicotiana tabacum*. *Mol Gen Genet* 247, 633-638.
- Fire, A., Xu, S.Q., Montgomery, M.K., Kostas, S.A., Driver, S.E., and Mello, C.C. (1998). Potent and specific genetic interference by double-stranded RNA in *Caenorhabditis elegans*. *Nature* 391, 806-811.
- Fitzgerald, M.S., McKnight, T.D., and Shippen, D.E. (1996). Characterization and developmental patterns of telomerase expression in plants. *Proc Natl Acad Sci U S A* 93, 14422-14427.
- Fojta, M., Fojtova, M., Havran, L., Pivonkova, H., Dorcak, V., and Sestakova, I. (2006). Electrochemical monitoring of phytochelatin accumulation in *Nicotiana tabacum* cells exposed to sub-cytotoxic and cytotoxic levels of cadmium. *Anal Chim Acta* 558, 171-178.
- Fojtova, M., and Fajkus, J. (2014). Epigenetic regulation of telomere maintenance. *Cytogenet Genome Res* 143, 125-135.
- Fojtova, M., Fulneckova, J., Fajkus, J., and Kovarik, A. (2002). Recovery of tobacco cells from cadmium stress is accompanied by DNA repair and increased telomerase activity. *J Exp Bot* 53, 2151-2158.
- Fojtova, M., and Kovarik, A. (2000). Genotoxic effect of cadmium is associated with apoptotic changes in tobacco cells. *Plant Cell Environ* 23, 531-537.
- Fojtova, M., Peska, V., Dobsakova, Z., Mozgova, I., Fajkus, J., and Sykorova, E. (2011). Molecular analysis of T-DNA insertion mutants identified putative regulatory elements in the *AfTERT* gene. *J Exp Bot* 62, 5531-5545.
- Fojtova, M., Sykorova, E., Najdekrova, L., Polanska, P., Zachova, D., Vagnerova, R., Angelis, K.J., and Fajkus, J. (2015). Telomere dynamics in the lower plant *Physcomitrella patens*. *Plant Mol Biol* 87, 591-601.
- Fojtova, M., Wong, J.T.Y., Dvorackova, M., Yan, K.T.H., Sykorova, E., and Fajkus, J. (2010). Telomere maintenance in liquid crystalline chromosomes of dinoflagellates. *Chromosoma* 119, 485-493.
- Fransz, P., ten Hoopen, R., and Tessadori, F. (2006). Composition and formation of heterochromatin in *Arabidopsis thaliana*. *Chromosome Res* 14, 71-82.
- Gaj, T., Gersbach, C.A., and Barbas, C.F. (2013). ZFN, TALEN, and CRISPR/Cas-based methods for genome engineering. *Trends Biotechnol* 31, 397-405.
- Galati, A., Micheli, E., and Cacchione, S. (2013). Chromatin structure in telomere dynamics. *Front Oncol* 3, 46.
- Gamez-Arjona, F.M., Lopez-Lopez, C., Vaquero-Sedas, M.I., and Vega-Palas, M.A. (2010). On the organization of the nucleosomes associated with telomeric sequences. *Biochim Biophys Acta* 1803, 1058-1061.
- Gao, H., Cervantes, R.B., Mandell, E.K., Otero, J.H., and Lundblad, V. (2007). RPA-like proteins mediate yeast telomere function. *Nat Struct Mol Biol* 14, 208-214.
- Ghoshal, K., and Bai, S.M. (2007). DNA methyltransferases as targets for cancer therapy. *Drugs Today* 43, 395-422.
- Goldberg, A.D., Banaszynski, L.A., Noh, K.M., Lewis, P.W., Elsaesser, S.J., Stadler, S., Dewell, S., Law, M., Guo, X.Y., Li, X., *et al.* (2010). Distinct factors control histone variant H3.3 localization at specific genomic regions. *Cell* 140, 678-691.
- Gonzalo, S., Jaco, I., Fraga, M.F., Chen, T.P., Li, E., Esteller, M., and Blasco, M.A. (2006). DNA methyltransferases control telomere length and telomere recombination in mammalian cells. *Nat Cell Biol* 8, 416-U466.
- Grandjenette, C., Schnekenburger, M., Karius, T., Ghelfi, J., Gaigneaux, A., Henry, E.,

- Dicato, M., and Diederich, M. (2014). 5-aza-2'-deoxycytidine-mediated c-myc Down-regulation Triggers Telomere-dependent Senescence by Regulating Human Telomerase Reverse Transcriptase in Chronic Myeloid Leukemia. *Neoplasia* 16, 511-528.
- He, L., Liu, J., Torres, G.A., Zhang, H.Q., Jiang, J.M., and Xie, C.H. (2013). Interstitial telomeric repeats are enriched in the centromeres of chromosomes in *Solanum* species. *Chromosome Res* 21, 5-13.
- Hemann, M.T., and Greider, C.W. (2000). Wild-derived inbred mouse strains have short telomeres. *Nucleic Acids Res* 28, 4474-4478.
- Herr, A.J., Jensen, M.B., Dalmay, T., and Baulcombe, D.C. (2005). RNA polymerase IV directs silencing of endogenous DNA. *Science* 308, 118-120.
- Holy, A. (1975). Nucleic acid components and their analogs .172. Aliphatic analogs of nucleosides, nucleotides, and oligonucleotides. *Collect Czech Chem C* 40, 187-214.
- Hurd, P.J., Whitmarsh, A.J., Baldwin, G.S., Kelly, S.M., Waltho, J.P., Price, N.C., Connolly, B.A., and Hornby, D.P. (1999). Mechanism-based inhibition of C5-cytosine DNA methyltransferases by 2-H pyrimidinone. *J Mol Biol* 286, 389-401.
- Champion, C., Guianvarc'h, D., Senamaud-Beaufort, C., Jurkowska, R.Z., Jeltsch, A., Ponger, L., Arimondo, P.B., and Guiesse-Peugeot, A.L. (2010). Mechanistic insights on the inhibition of C5 DNA methyltransferases by zebularine. *Plos One* 5.
- Cheng, J.F., Smith, C.L., and Cantor, C.R. (1989). Isolation and characterization of a human telomere. *Nucleic Acids Res* 17, 6109-6127.
- Jankowska, M., Fuchs, J., Klocke, E., Fojtova, M., Polanska, P., Fajkus, J., Schubert, V., and Houben, A. (2015). Holokinetic centromeres and efficient telomere healing enable rapid karyotype evolution. *Chromosoma*. doi: 10.1007/s00412-015-0524-y.
- Jones, L., Hamilton, A.J., Voinnet, O., Thomas, C.L., Maule, A.J., and Baulcombe, D.C. (1999). RNA-DNA interactions and DNA methylation in post-transcriptional gene silencing. *Plant Cell* 11, 2291-2301.
- Kawasaki, H., and Taira, K. (2004). Induction of DNA methylation and gene silencing by short interfering RNAs in human cells. *Nature* 431, 211-217.
- Lee, J., Jang, S.J., Benoit, N., Hogue, M.O., Califano, J.A., Trink, B., Sidransky, D., Mao, L., and Moon, C. (2010). Presence of 5-methylcytosine in CpNpG trinucleotides in the human genome. *Genomics* 96, 67-72.
- Lister, R., Pelizzola, M., Dowen, R.H., Hawkins, R.D., Hon, G., Tonti-Filippini, J., Nery, J.R., Lee, L., Ye, Z., Ngo, Q.M., *et al.* (2009). Human DNA methylomes at base resolution show widespread epigenomic differences. *Nature* 462, 315-322.
- Liu, C.H., Finke, A., Diaz, M., Rozhon, W., Poppenberger, B., Baubec, T., and Pecinka, A. (2015). Repair of DNA damage induced by the cytidine analog zebularine requires ATR and ATM in *Arabidopsis*. *Plant Cell* 27, 1788-1800.
- Liu, K.B., Hodes, R.J., and Weng, N.P. (2001). Cutting edge: Telomerase activation in human T lymphocytes does not require increase in telomerase reverse transcriptase (hTERT) protein but is associated with hTERT phosphorylation and nuclear translocation. *J Immunol* 166, 4826-4830.
- Majerova, E., Fojtova, M., Mandakova, T., and Fajkus, J. (2011a). Methylation of plant telomeric DNA: what do the results say? (Vaquero-Sedas, M.I. and Vega-Palas, M.A.: DNA methylation at tobacco telomeric sequences). *Plant Mol Biol* 77, 533-536.
- Majerova, E., Fojtova, M., Mozgova, I., Bittova, M., and Fajkus, J. (2011b). Hypomethylating drugs efficiently decrease cytosine methylation in telomeric DNA and activate telomerase without affecting telomere lengths in tobacco cells. *Plant Mol Biol* 77, 371-380.
- Majerová, E., Mandáková, T., Vu, G.T.H., Fajkus, J., Lysak, M.A., and Fojtová, M. (2014).

- Chromatin features of plant telomeric sequences at terminal vs. internal positions. *Front Plant Sci* 5, 593.
- Majerska, J., Sykorova, E., and Fajkus, J. (2011). Non-telomeric activities of telomerase. *Mol Biosyst* 7, 1013-1023.
- Makarov, V.L., Lejnine, S., Bedoyan, J., and Langmore, J.P. (1993). Nucleosomal organization of telomere-specific chromatin in rat. *Cell* 73, 775-787.
- Mandakova, T., Joly, S., Krzywinski, M., Mummenhoff, K., and Lysak, M.A. (2010). Fast diploidization in close mesopolyploid relatives of *Arabidopsis*. *Plant Cell* 22, 2277-2290.
- Mathieu, O., Reinders, J., Caikovski, M., Smathajitt, C., and Paszkowski, J. (2007). Transgenerational stability of the *Arabidopsis* epigenome is coordinated by CG methylation. *Cell* 130, 851-862.
- Morris, K.V., Chan, S.W., Jacobsen, S.E., and Looney, D.J. (2004). Small interfering RNA induced transcriptional gene silencing in human cells. *Science* 305, 1289-1292.
- Napoli, C., Lemieux, C., and Jorgensen, R. (1990). Introduction of a chimeric chalcone synthase gene into *Petunia* results in reversible co-suppression of homologous genes in trans. *Plant Cell* 2, 279-289.
- Ogrocka, A., Polanska, P., Majerova, E., Janeba, Z., Fajkus, J., and Fojtova, M. (2014). Compromised telomere maintenance in hypomethylated *Arabidopsis thaliana* plants. *Nucleic Acids Res* 42, 2919-2931.
- Ogrocka, A., Sykorova, E., Fajkus, J., and Fojtova, M. (2012). Developmental silencing of the *AtTERT* gene is associated with increased H3K27me3 loading and maintenance of its euchromatic environment. *J Exp Bot* 63, 4233-4241.
- Oguchi, K., Tamura, K., and Takahashi, H. (2004). Characterization of *Oryza sativa* telomerase reverse transcriptase and possible role of its phosphorylation in the control of telomerase activity. *Gene* 342, 57-66.
- Peska, V., Fajkus, P., Fojtova, M., Dvorackova, M., Hapala, J., Dvoracek, V., Polanska, P., Leitch, A.R., Sykorova, E., and Fajkus, J. (2015). Characterisation of an unusual telomere motif (TTTTTTAGGG)(n) in the plant *Cestrum elegans* (Solanaceae), a species with a large genome. *Plant J* 82, 644-654.
- Peska, V., Schrupfova, P.P., and Fajkus, J. (2011). Using the telobox to search for plant telomere binding proteins. *Curr Protein Pept Sc* 12, 75-83.
- Polanska, E., Dobsakova, Z., Dvorackova, M., Fajkus, J., and Stros, M. (2012). HMGB1 gene knockout in mouse embryonic fibroblasts results in reduced telomerase activity and telomere dysfunction. *Chromosoma* 121, 419-431.
- Price, C.M., Boltz, K.A., Chaiken, M.F., Stewart, J.A., Beilstein, M.A., and Shippen, D.E. (2010). Evolution of CST function in telomere maintenance. *Cell Cycle* 9, 3157-3165.
- Pucci, F., Gardano, L., and Harrington, L. (2013). Short telomeres in ESCs lead to unstable differentiation. *Cell Stem Cell* 12, 479-486.
- Richards, E.J., and Ausubel, F.M. (1988). Isolation of a higher eukaryotic telomere from *Arabidopsis thaliana*. *Cell* 53, 127-136.
- Roberts, A.R., Blewitt, M.E., Youngson, N.A., Whitelaw, E., and Chong, S. (2011). Reduced dosage of the modifiers of epigenetic reprogramming *Dnmt1*, *Dnmt3L*, *SmcHD1* and *Foxo3a* has no detectable effect on mouse telomere length in vivo. *Chromosoma* 120, 377-385.
- Ruckova, E., Friml, J., Schrupfova, P.P., and Fajkus, J. (2008). Role of alternative telomere lengthening unmasked in telomerase knock-out mutant plants. *Plant Mol Biol* 66, 637-646.
- Sevcikova, T., Bisova, K., Fojtova, M., Lukesova, A., Hrckova, K., and Sykorova, E. (2013).

- Completion of cell division is associated with maximum telomerase activity in naturally synchronized cultures of the green alga *Desmodesmus quadricauda*. *Febs Lett* *587*, 743-748.
- Shakirov, E.V., and Shippen, D.E. (2004). Length regulation and dynamics of individual telomere tracts in wild-type *Arabidopsis*. *Plant Cell* *16*, 1959-1967.
- Schrumpfova, P., Kuchar, M., Mikova, G., Skrisovska, L., Kubicarova, T., and Fajkus, J. (2004). Characterization of two *Arabidopsis thaliana* myb-like proteins showing affinity to telomeric DNA sequence. *Genome* *47*, 316-324.
- Schrumpfova, P.P., Fojtova, M., Mokros, P., Grasser, K.D., and Fajkus, J. (2011). Role of HMGB proteins in chromatin dynamics and telomere maintenance in *Arabidopsis thaliana*. *Curr Protein Pept Sc* *12*, 105-111.
- Schrumpfova, P.P., Vychodilova, I., Dvorackova, M., Majerska, J., Dokladal, L., Schorova, S., and Fajkus, J. (2014). Telomere repeat binding proteins are functional components of *Arabidopsis* telomeres and interact with telomerase. *Plant J* *77*, 770-781.
- Stroud, H., Otero, S., Desvoves, B., Ramirez-Parra, E., Jacobsen, S.E., and Gutierrez, C. (2012). Genome-wide analysis of histone H3.1 and H3.3 variants in *Arabidopsis thaliana*. *P Natl Acad Sci USA* *109*, 5370-5375.
- Surovtseva, Y.V., Churikov, D., Boltz, K.A., Song, X.Y., Lamb, J.C., Warrington, R., Leehy, K., Heacock, M., Price, C.M., and Shippen, D.E. (2009). Conserved telomere maintenance Component 1 interacts with STN1 and maintains chromosome ends in higher eukaryotes. *Mol Cell* *36*, 207-218.
- Suzuki, M.M., and Bird, A. (2008). DNA methylation landscapes: provocative insights from epigenomics. *Nat Rev Genet* *9*, 465-476.
- Sykorova, E., and Fajkus, J. (2009). Structure-function relationships in telomerase genes. *Biol Cell* *101*, 375-392.
- Sykorova, E., Fulneckova, J., Mokros, P., Fajkus, J., Fojtova, M., and Peska, V. (2012). Three TERT genes in *Nicotiana tabacum*. *Chromosome Res* *20*, 381-394.
- Sykorova, E., Lim, K.Y., Kunicka, Z., Chase, M.W., Bennett, M.D., Fajkus, J., and Leitch, A.R. (2003). Telomere variability in the monocotyledonous plant order Asparagales. *P Roy Soc B-Biol Sci* *270*, 1893-1904.
- Szenker, E., Ray-Gallet, D., and Almouzni, G. (2011). The double face of the histone variant H3.3. *Cell Res* *21*, 421-434.
- Tamura, K., Liu, H.T., and Takahashi, H. (1999). Auxin induction of cell cycle regulated activity of tobacco telomerase. *J Biol Chem* *274*, 20997-21002.
- Taylor, C., Ford, K., Connolly, B.A., and Hornby, D.P. (1993). Determination of the order of substrate addition to MspI DNA methyltransferase using a novel mechanism-based inhibitor. *Biochem J* *291*, 493-504.
- Tran, T.D., Cao, H.X., Jovtchev, G., Neumann, P., Novák, P., Fojtová, M., Vu, G.T., Macas, J., Fajkus, J., Schubert, I., *et al.* (2015). Centromere and telomere sequence alterations reflect the rapid genome evolution within the carnivorous plant genus *Genlisea*. *Plant J*. doi: 10.1111/tpj.13058.
- Uchida, W., Matsunaga, S., Sugiyama, R., and Kawano, S. (2002). Interstitial telomere-like repeats in the *Arabidopsis thaliana* genome. *Genes Genet Syst* *77*, 63-67.
- Vaquero-Sedas, M.I., Gamez-Arjona, F.M., and Vega-Palas, M.A. (2011). *Arabidopsis thaliana* telomeres exhibit euchromatic features. *Nucleic Acids Res* *39*, 2007-2017.
- Vaquero-Sedas, M.I., Luo, C., and Vega-Palas, M.A. (2012). Analysis of the epigenetic status of telomeres by using ChIP-seq data. *Nucleic Acids Res* *40*, e163.
- Vaquero-Sedas, M.I., and Vega-Palas, M.A. (2011). DNA methylation at tobacco telomeric sequences. *Plant Mol Biol* *77*, 529-531; author reply 533-526.
- Vaquero-Sedas, M.I., and Vega-Palas, M.A. (2013). Differential association of *Arabidopsis*

- telomeres and centromeres with histone H3 variants. *Sci Rep* 3, 1202.
- Vaquero-Sedas, M.I., and Vega-Palas, M.A. (2014). Determination of *Arabidopsis thaliana* telomere length by PCR. *Sci Rep-Uk* 4.
- Vaughn, M.W., Tanurdzic, M., Lippman, Z., Jiang, H., Carrasquillo, R., Rabinowicz, P.D., Dedhia, N., McCombie, W.R., Agier, N., Bulski, A., *et al.* (2007). Epigenetic natural variation in *Arabidopsis thaliana*. *Plos Biol* 5, 1617-1629.
- Vera, E., Canela, A., Fraga, M.F., Esteller, M., and Blasco, M.A. (2008). Epigenetic regulation of telomeres in human cancer. *Oncogene* 27, 6817-6833.
- Vongs, A., Kakutani, T., Martienssen, R.A., and Richards, E.J. (1993). *Arabidopsis thaliana* DNA methylation mutants. *Science* 260, 1926-1928.
- Vrbsky, J., Akimcheva, S., Watson, J.M., Turner, T.L., Daxinger, L., Vyskot, B., Aufsatz, W., and Riha, K. (2010). siRNA-mediated methylation of *Arabidopsis* telomeres. *PLoS Genet* 6, e1000986.
- Wierzbicki, A.T., Cocklin, R., Mayampurath, A., Lister, R., Rowley, M.J., Gregory, B.D., Ecker, J.R., Tang, H., and Pikaard, C.S. (2012). Spatial and functional relationships among Pol V-associated loci, Pol IV-dependent siRNAs, and cytosine methylation in the *Arabidopsis* epigenome. *Genes Dev* 26, 1825-1836.
- Wollmann, H., Holec, S., Alden, K., Clarke, N.D., Jacques, P.E., and Berger, F. (2012). Dynamic deposition of histone variant H3.3 accompanies developmental remodeling of the *Arabidopsis* transcriptome. *Plos Genetics* 8.
- Wong, L.H. (2010). Epigenetic regulation of telomere chromatin integrity in pluripotent embryonic stem cells. *Epigenomics-Uk* 2, 639-655.
- Yoo, C.B., and Jones, P.A. (2006). Epigenetic therapy of cancer: past, present and future (vol 5, pg 37, 2006). *Nat Rev Drug Discov* 5.
- Zachova, D., Fojtova, M., Dvorackova, M., Mozgova, I., Lermontova, I., Peska, V., Schubert, I., Fajkus, J., and Sykorova, E. (2013). Structure-function relationships during transgenic telomerase expression in *Arabidopsis*. *Physiol Plantarum* 149, 114-126.
- Zhu, J.Y., Zhao, Y.J., and Wang, S.W. (2010). Chromatin and epigenetic regulation of the telomerase reverse transcriptase gene. *Protein Cell* 1, 22-32.

8 Conclusion

This habilitation thesis is presented as a review on plant telomeres and telomerases and the involvement of epigenetic mechanisms in their regulation. Experimental data referred in the thesis was obtained in the research group Molecular Complexes of Chromatin at Masaryk University, Brno, and data before 2009 in the research group Molecular Epigenetics at Institute of Biophysics, Academy of Sciences of the Czech Republic, Brno.

The presented data demonstrated plants as important and interesting models for epigenetics and telomere and telomerase research. Due to specific mechanisms and pathways activated in plant cells, significant contributions to these fields have been achieved. Until now we were able to demonstrate that plant telomeres are under epigenetic control, and that significant differences in epigenetic regulation of telomere homeostasis and the involvement of epigenetic mechanisms to regulation of telomerase activity do exist between different model plants. Significant effort was devoted to analyse epigenetic properties of terminally and internally located telomeric repeats in respective model plants. To continue this promising research, analysis of telomeres and telomerase in *A. thaliana* mutant plants with loss of function of enzymes responsible for histone methylation / demethylation is in progress and a study of a complex response of *A. thaliana* and *N. tabacum* plants and calli to the cadmium genotoxic stress was initiated. As the next topic, novel methods are optimized to characterize set of proteins associated with plant telomeres as a background for further functional studies.

9 Supplements

Relevant publications of the applicant arranged in chronological order.

All publications referred in Supplements have been included in the thesis (references in bold in the text).

List of publications:

Fojtova, M., and Kovarik, A. (2000). Genotoxic effect of cadmium is associated with apoptotic changes in tobacco cells. *Plant Cell Environ* 23, 531-537.

MF performed all experiments, evaluated data and participated in the ms editing

Fojtova, M., Fulneckova, J., Fajkus, J., and Kovarik, A. (2002). Recovery of tobacco cells from cadmium stress is accompanied by DNA repair and increased telomerase activity. *J Exp Bot* 53, 2151-2158.

MF performed experiments except analysis of telomerase activity, evaluated data and participated in the ms editing

Fojta, M., Fojtova, M., Havran, L., Pivonkova, H., Dorcak, V., and Sestakova, I. (2006). Electrochemical monitoring of phytochelatin accumulation in *Nicotiana tabacum* cells exposed to sub-cytotoxic and cytotoxic levels of cadmium. *Anal Chim Acta* 558, 171-178.

MF was involved in the experimental part (cultivation of cells and preparation of protein extracts for electrochemical analysis) and participated in the ms editing

Fojtova, M., Wong, J.T.Y., Dvorackova, M., Yan, K.T.H., Sykorova, E., and Fajkus, J. (2010). Telomere maintenance in liquid crystalline chromosomes of dinoflagellates. *Chromosoma* 119, 485-493.

MF was significantly involved in the experimental part (more than 50% of experiments) and evaluation of data, and participated in the ms writing and editing

Fojtova, M., Peska, V., Dobsakova, Z., Mozgova, I., Fajkus, J., and Sykorova, E. (2011). Molecular analysis of T-DNA insertion mutants identified putative regulatory elements in the *AtTERT* gene. *J Exp Bot* 62, 5531-5545.

MF was significantly involved in the experimental part (~ 50% of experiments) and evaluation of data, and participated in the ms writing and editing

Majerova, E., Fojtova, M., Mozgova, I., Bittova, M., and Fajkus, J. (2011b). Hypomethylating drugs efficiently decrease cytosine methylation in telomeric DNA and activate telomerase without affecting telomere lengths in tobacco cells. *Plant Mol Biol* 77, 371-380.

MF participated in the design of experiments, evaluation of data and the ms writing and editing

Majerova, E., Fojtova, M., Mandakova, T., and Fajkus, J. (2011a). Methylation of plant telomeric DNA: what do the results say? (Vaquero-Sedas, M.I. and Vega-Palas, M.A.: DNA methylation at tobacco telomeric sequences). *Plant Mol Biol* 77, 533-536.

MF participated in the ms writing and editing

Schrumpfova, P.P., Fojtova, M., Mokros, P., Grasser, K.D., and Fajkus, J. (2011). Role of HMGB proteins in chromatin dynamics and telomere maintenance in *Arabidopsis thaliana*. *Curr Protein Pept Sc* 12, 105-111.

MF was involved in the experimental part (~ 20% of experiments), data evaluation and ms writing and editing

Ogrocka, A., Sykorova, E., Fajkus, J., and Fojtova, M. (2012). Developmental silencing of the *AtTERT* gene is associated with increased H3K27me3 loading and maintenance of its euchromatic environment. *J Exp Bot* 63, 4233-4241.

MF designed the research, was involved in data evaluation, wrote the ms

Sykorova, E., Fulneckova, J., Mokros, P., Fajkus, J., Fojtova, M., and Peska, V. (2012). Three TERT genes in *Nicotiana tabacum*. *Chromosome Res* 20, 381-394.

MF was involved in the experimental part (~ 10% of experiments) and ms editing

Zachova, D., Fojtova, M., Dvorackova, M., Mozgova, I., Lermontova, I., Peska, V., Schubert, I., Fajkus, J., and Sykorova, E. (2013). Structure-function relationships during transgenic telomerase expression in *Arabidopsis*. *Physiol Plantarum* 149, 114-126.

MF participated in the design of experiments, experimental part (~ 20% of experiments), evaluation of data and ms writing end editing

Sevcikova, T., Bisova, K., Fojtova, M., Lukesova, A., Hrcikova, K., and Sykorova, E. (2013). Completion of cell division is associated with maximum telomerase activity in naturally synchronized cultures of the green alga *Desmodesmus quadricauda*. *Febs Lett* 587, 743-748.

MF participated in the design of experiments, experimental part (~ 10% of experiments), evaluation of data and ms writing end editing

Majerová, E., Mandáková, T., Vu, G.T.H., Fajkus, J., Lysak, M.A., and Fojtová, M. (2014). Chromatin features of plant telomeric sequences at terminal vs. internal positions. *Front Plant Sci* 5, 593.

MF designed the research, was involved in data evaluation, wrote the ms

Ogrocka, A., Polanska, P., Majerova, E., Janeba, Z., Fajkus, J., and Fojtova, M. (2014). Compromised telomere maintenance in hypomethylated *Arabidopsis thaliana* plants. *Nucleic Acids Res* 42, 2919-2931.

MF designed the research, was involved in data evaluation, wrote the ms

Fojtova, M., and Fajkus, J. (2014). Epigenetic regulation of telomere maintenance. *Cytogenet Genome Res* 143, 125-135. **Review**

MF participated in ms writing (~ 50%)

Dvorackova, M., Fojtova, M., and Fajkus, J. (2015). Chromatin dynamics of plant telomeres and ribosomal genes. *Plant J* 83, 18-37. **Review**

MF participated in ms writing (~ 50%)

Fojtova, M., Sykorova, E., Najdekrova, L., Polanska, P., Zachova, D., Vagnerova, R., Angelis, K.J., and Fajkus, J. (2015). Telomere dynamics in the lower plant *Physcomitrella patens*. *Plant Mol Biol* 87, 591-601.

MF participated in the design of experiments, experimental part (~ 20% of experiments), evaluation of data and ms writing and editing

Jankowska, M., Fuchs, J., Klocke, E., Fojtova, M., Polanska, P., Fajkus, J., Schubert, V., and Houben, A. (2015). Holokinetic centromeres and efficient telomere healing enable rapid karyotype evolution. *Chromosoma*. doi: 10.1007/s00412-015-0524-y.

MF was involved in the experimental part (~ 10% of experiments) and ms editing

Peska, V., Fajkus, P., Fojtova, M., Dvorackova, M., Hapala, J., Dvoracek, V., Polanska, P., Leitch, A.R., Sykorova, E., and Fajkus, J. (2015). Characterisation of an unusual telomere motif (TTTTTTAGGG)(n) in the plant *Cestrum elegans* (Solanaceae), a species with a large genome. *Plant J* 82, 644-654.

MF was involved in the experimental part (~ 5% of experiments) and ms editing

Tran, T.D., Cao, H.X., Jovtchev, G., Neumann, P., Novák, P., Fojtová, M., Vu, G.T., Macas, J., Fajkus, J., Schubert, I., *et al.* (2015). Centromere and telomere sequence alterations reflect the rapid genome evolution within the carnivorous plant genus *Genlisea*. *Plant J*. doi: 10.1111/tpj.13058.

MF was involved in the experimental part (~ 10% of experiments) and ms writing and editing

Jureckova, J., Sykorova, E., Honys, D., Fajkus, J., Fojtova, M. Tissue-specific expression of telomerase reverse transcriptase gene variants in *Nicotiana tabacum*. submitted.

MF designed the research, was involved in data evaluation, wrote the ms

Genotoxic effect of cadmium is associated with apoptotic changes in tobacco cells

MILOSLAVA FOJTOVÁ & ALEŠ KOVAŘÍK

Institute of Biophysics, Academy of Sciences of the Czech Republic, Královopolská 135, 612 65 Brno, Czech Republic

SUMMARY

This work explores the influence of cadmium on a suspension cell culture of *Nicotiana tabacum* (TBY-2) by examining cell morphology, viability and DNA integrity. Changes in these parameters were strikingly dependent on concentration of cadmium in the culture medium: a concentration of 50–100 mmol m⁻³ CdSO₄ induced apoptotic changes including DNA fragmentation into oligonucleosomal units, while 1 mol m⁻³ Cd²⁺ showed strong cytotoxicity, but no fragmentation of DNA. Low cadmium concentrations (below 10 mmol m⁻³) affected neither cell viability nor DNA integrity. A detailed kinetic study showed a significant delay in the onset of apoptosis after the application of high concentrations of cadmium. From days 0–3 after the application of 50 mmol m⁻³ CdSO₄, the morphology of the cells, their viability and growth were indistinguishable between control and treated cells, and ‘domain’ DNA fragmentation into 50–200 kb fragments was observed at the DNA level. After this (days 4–7), there was a characteristic and rapid decrease in cell viability, distinct changes in cell morphology and oligonucleosomal fragmentation. The results suggest that chronic exposure of plant cells to cadmium can trigger programmed cell death.

Key-words: apoptosis; cadmium; plant cell; oligonucleosomal DNA fragmentation.

INTRODUCTION

Cadmium is a toxic metal with a long biological half-life, and represents a serious environmental pollutant for both animals and plants. As with other heavy metals, cadmium is known to interact with proteins, influencing protein–protein and protein–DNA interactions (Freedman *et al.* 1988). Although cadmium has been shown to be a genotoxic metal, the molecular mechanism of cadmium toxicity to plants is not well understood. In plants, cadmium is known to inhibit seed germination and root growth (Chakravarty & Srivastava 1992; Liu, Jiang & Li 1992), induce chromosomal aberrations and micronucleus formation (Zhang & Xiao 1998) and cause faster wilting and a grey-green leaf colour (Czuba & Kraszewski 1994).

Apoptosis is a physiological process that causes cells to die in response to developmental and environmental

changes. In animals, cadmium-induced apoptosis has been described in isolated bovine liver nuclei (Lohmann & Beyersmann 1993), in mouse liver (Habeebu, Liu & Klaassen 1998) and in human T cells (El Azzouzi *et al.* 1994). To our knowledge, there are no reports about cadmium-induced apoptosis in plant cells. Plants are known to activate apoptotic pathways:

- (a) in specific developmental situations necessary for growth and survival (Barlow 1982; Woodson *et al.* 1992; Pennell & Lamb 1997),
- (b) as a hypersensitive response to the influence of pathogen spread (Keen 1990; Greenberg 1996), and
- (c) as a response to changes in environmental conditions (Greenberg *et al.* 1994; Reyrson & Heath 1996; Koukalová *et al.* 1997; Danon & Gallois 1998).

Apoptotic hallmarks are similar in animals and plants (for review see Havel & Durzan 1996). In both cases, apoptosis is characterized by cell shrinkage, membrane blebbing, re-organization of the cell nucleus and chromatin fragmentation. At the DNA level, fragmentation occurs in two consecutive steps. The early stage of the apoptotic process is characterized by fragmentation of the DNA into 50–200 kb fragments resulting from cleavage of the matrix-attached domains (Oberhammer *et al.* 1993; Walker & Sikorska 1994; Walker, Padney & Sikorska 1995). In most cases, this ‘domain’ fragmentation is followed by cleavage of DNA into nucleosomal linker regions yielding a typical DNA ladder on conventional agarose gels (Wyllie 1980). It has not been elucidated so far whether one or more enzymatic activities participate in these processes (Sun & Cohen 1994; Walker *et al.* 1995).

In this report we describe a study of cadmium-induced changes in cell viability, morphology and DNA integrity in tobacco suspension culture.

MATERIALS AND METHODS

Chemicals

CdSO₄ and fluorescein diacetate (FDA) were obtained from Sigma (USA).

Cell culture

The tobacco bright yellow (TBY-2) cells (Nagata, Nemoto & Hasezawa 1992) were propagated in standard liquid

Correspondence: Miloslava Fojtová. Fax: +420 5 41211293; e-mail: fojtova@ibp.cz

Murashige & Skoog (MS) media supplemented with sucrose (3%, w/v), thiamine (1 g m^{-3}), KH_2PO_4 (200 g m^{-3}), myoinositol (100 g m^{-3}) and 2,4-dichlorophenoxyacetic acid (0.2 g m^{-3}) in 100 cm^3 Erlenmeyer flasks under constant shaking (130 rev min^{-1}) at 27°C . Cell suspensions at a density of about 3 million cells per cm^3 were then passaged at 1:10 dilution into MS media with or without CdSO_4 . Cells were collected at the time intervals indicated.

DNA isolation

Total DNA (< 50 kb) was isolated by a modified cetyltrimethylammonium bromide method (CTAB) (Saghai-Marooof *et al.* 1984). Lyophilized TBV-2 cells were homogenized in liquid nitrogen. After chloroform–octanol extraction, DNA was precipitated with isopropanol, dissolved and treated with RNase A ($40 \mu\text{g cm}^{-3}$) for 30 min at 37°C and treated with proteinase K ($0.1 \mu\text{g cm}^{-3}$) for 2 h at 55°C . After phenol–chloroform extraction, DNA was precipitated with ethanol and dissolved in TE buffer (10 mol m^{-3} Tris–HCl, 1 mol m^{-3} EDTA, pH 8.0). DNA concentration and purity were determined by measuring absorbance at 260 and 280 nm, respectively.

High-molecular-weight (HMW) DNA for pulsed-field gel electrophoresis (PFGE) were prepared from TBV-2 cells. About 3 million cells (1 mL of cell culture suspension) were gently centrifuged (1500 g for 2 min), and the pellet was resuspended in MS medium and cooled on ice. The cells were resuspended in homogenization buffer (10 mol m^{-3} 2-[N-morpholino]ethanesulphonic acid (MES), pH 5.6, 10 mol m^{-3} NaCl, 5 mol m^{-3} EDTA). To homogenize the cells, about 10 glass beads (2 mm in diameter) were added to the cell suspension and this was mixed well by vortexing ($5 \times 30 \text{ s}$) at 4°C . The efficiency of homogenization was monitored using a phase-contrast microscope. The nuclei were centrifuged (5500 g , 4°C , for 10 min, GS-15R Beckman centrifuge), mixed with an equal volume of molten 1.5% (w/v) low gelling temperature agarose in 400 mol m^{-3} mannitol, 20 mol m^{-3} MES, pH 5.6, and transferred to a mould. After solidification at 4°C , agarose blocks were transferred into a lysis buffer (500 mol m^{-3} EDTA, pH 9.2, N-lauroylsarcosine (1%, w/v), 0.1 mg cm^{-3} proteinase K, and incubated at 55°C for 48 h.

Conventional and pulsed-field gel electrophoresis

Genomic DNA (< 50 kb) was size-fractionated on 2% agarose gels; gels were stained with ethidium bromide and photographed.

High molecular weight (HMW) DNA was size-fractionated on 1% agarose gel with the Gene Navigator System (Pharmacia Biotech, Uppsala, Sweden) using 45 mol m^{-3} Tris-borate, 1 mol m^{-3} EDTA, pH 8.0, as a running buffer. The running conditions were as follows: 200 V, pulse ramping time from $T_1 = 5 \text{ s}$ to $T_2 = 50 \text{ s}$, 10°C , 24 h. After electrophoresis, the gel was stained with ethidium bromide ($1.0 \mu\text{g cm}^{-3}$) and photographed.

Southern blot hybridization

DNA was blotted onto a nylon membrane (Hybond XL, Amersham, UK) and hybridized against the HRS60 probe. The cloned 360 bp dimer of the HRS60 tandem repeated sequence (Koukalová *et al.* 1989) was labelled by ^{32}P -dCTP using a random priming method (DNA Labelling Kit, MBI Fermentas, Vilnius, Lithuania). Hybridization was performed according to standard protocol (Sambrook, Fritsch & Maniatis 1988).

Cell morphology, estimation of cell viability

Cell morphology was monitored with a phase-contrast light microscope (Carl Zeiss, Jena, Germany). Total cell counts were determined manually and expressed as an average from five independent counts.

Viable cell count was determined by the fluorescein diacetate (FDA) method combined with fluorescence intensity measurements on a PhosphorImager (Storm, Molecular Dynamics, Sunnyvale, USA) (Kovařík & Fojtová 1999). Briefly, cell suspensions at appropriate dilutions were mixed with equal volumes of FDA reagent, prepared by diluting stock solution (3 mg FDA/cm^3 of acetone) with MS medium at 1:200. After 5 min incubation at 25°C , 20 mm^3 drops were transferred onto a nylon membrane (Hybond N, Amersham, UK) and air-dried. Fluorescence signals were scanned with a blue-fluorescence laser channel (excitation wavelength 450 nm) at a high resolution (100 pixels) using a PhosphorImager. Signals were evaluated with the ImageQuant program using an ellipse integration method, and viable cell counts were calculated from the calibration curve (a linear plot of fluorescence units and the number of viable cells).

RESULTS

Cadmium induces nucleosomal chromatin fragmentation

TBV-2 cells were grown in the presence of 10, 50, 75, 100 or 1000 mmol m^{-3} CdSO_4 for 1 week. The cells were then collected and extracted total DNA analysed by electrophoresis on 2% agarose gel (Fig. 1). Exposure of cells to cadmium lead to concentration-dependent changes in DNA integrity. At 50 mmol m^{-3} cadmium (lane 3), the fragmentation was most pronounced, forming a ladder of evenly distributed bands. The $180 \pm 5 \text{ bp}$ periodicity corresponded to the tobacco nucleosomal repeat (Fig. 4). Intact, non-degraded DNA was observed in lanes with DNA extracted from cells cultivated in the presence of the lowest (10 mmol m^{-3} , Fig. 1, lane 2) and paradoxically the highest (1000 mmol m^{-3} , Fig. 1, lane 6) concentrations of CdSO_4 .

Kinetics of DNA fragmentation and cell viability

Cell viability was measured for control and cadmium-treated (50 mmol m^{-3} CdSO_4) cells during 7 d of cultiva-

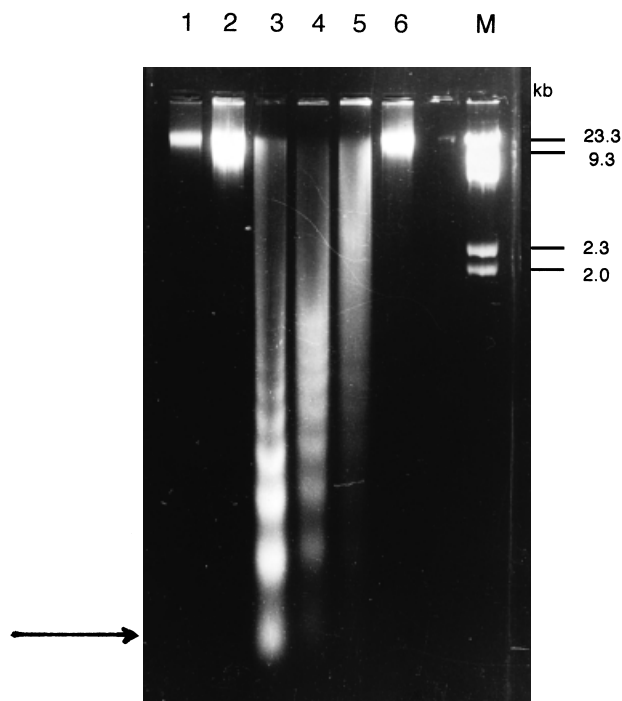


Figure 1. DNA fragmentation in TBY-2 cells after cadmium treatment. DNA was isolated from control and cadmium-treated cells after 7 d of cultivation and analysed by agarose gel electrophoresis. Lane 1, control DNA; lanes 2–6, DNA from cadmium treated cells; lane 2, 10 mmol m⁻³ CdSO₄; lane 3, 50 mmol m⁻³ CdSO₄; lane 4, 75 mmol m⁻³ CdSO₄; lane 5, 100 mmol m⁻³ CdSO₄; lane 6, 1000 mmol m⁻³ CdSO₄; lane M, DNA markers (lambda phage DNA/*Hind*III). The arrow indicates the position of a 180 bp fragment.

tion. Viability was assayed in aliquots by FDA staining at 24 h intervals. The fluorescence was counted using a PhosphorImager (Fig. 2). For days 0–3, cadmium treated-cells followed the same growth curve as control cells, suggesting the absence of a direct cytotoxic effect of cadmium at this concentration. However, on day 4, cell viability dramatically decreased. Finally, on day 5, only 7% of cells were viable, and essentially no viable cells were detected at day 7. Data obtained from viable and total cell counts are summarized in Table 1.

The morphology of cells cultivated for three days in 50 mmol m⁻³ CdSO₄ did not significantly differ from that of control cells (Fig. 3a). Longer incubation in cadmium, however, resulted in an increased proportion of cells with aberrant morphology (Fig. 3b). The most common phenotype was cells with condensed protoplasts and irregular profiles, both being hallmarks of apoptosis (Havel & Durzan 1996).

We were interested in a possible relationship between cell viability and chromatin fragmentation. DNA integrity was assayed in parallel with the cell viability test at 24 h intervals (Fig. 4). It is evident that nucleosomal chromatin

fragmentation started at day 5 of cadmium treatment (lane 5), i.e. at the time when a considerable proportion of the cell population were already FDA-negative and presumably dead.

Similar effects were observed for treatment of TBY-2 cells with 100 mmol m⁻³ CdSO₄; the cell viability began to decrease at day 3, followed by DNA fragmentation at day 4. When 1 mol m⁻³ CdSO₄ was applied, only about 10% of cells were viable after 24 h (Table 1).

Cadmium rapidly induces DNA breaks in matrix-attached domains

Conventional electrophoresis did not show any DNA degradation for the first 5 d following cadmium treatment. Consequently, we wished to study the integrity of high-molecular-weight DNA by pulsed-field gel electrophoresis. HMW DNA was isolated from control and 50 mmol m⁻³ CdSO₄-treated cells at different intervals of cell culture following cadmium treatment. Figure 5a shows the ethidium bromide-stained gel; Southern hybridization with the HRS60 probe hybridizing to the sub-telomeric heterochromatin (Koukalová *et al.* 1989) is shown in Fig. 5b. The electrophoretic profile of DNA isolated from cells treated with cadmium for 24 h (lane 1) was indistinguishable from that of control DNA (lane 0). Both DNAs showed only negligible PFGE mobility, suggesting the presence of intact DNA (the majority of the signal was in the 'compression zone', corresponding to DNA > 2 Mb). However, starting from day 3, a significant fraction of molecules of 50–200 kb in size was seen (Fig. 5a,b, lanes 3–5).

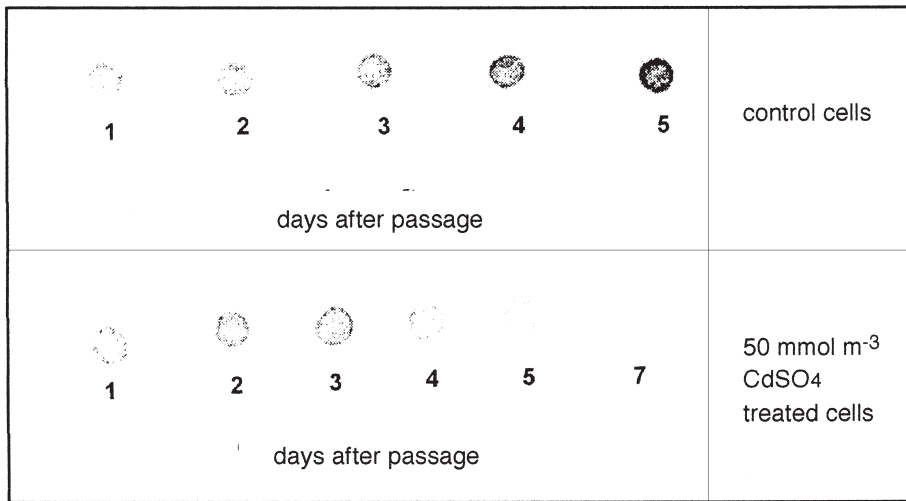
The distribution of radioactivity along each track was graphically expressed to emphasize the changes in DNA integrity (Fig. 6). The compression zone (the left peak) contains HMW DNA (> 2 Mb). From day 3, the amount of radioactivity in the compression zone decreased and the peak of radioactivity was shifted to the region of 50–200 kb, indicating fragmentation of sub-telomeric HRS60 heterochromatin.

Table 1. Viable cell counts in control and cadmium-treated TBY-2 cell culture

Cadmium concentration (mmol/m ³)	Day						
	0	1	2	3	4	5	7
–	0.4	0.8	1.1	1.9	3.2	4.8	5.2
10	0.4	0.8	1.1	1.8	3.3	5.0	5.3
50	0.4	0.6	1.1	1.5	0.5	0.1	0
100	0.4	0.6	1.0	0.4	0.2	0	0
1000	0.4	0.3	0	0	0	0	0

On each day of incubation, viable cell count was determined by FDA staining combined with measurement of intensity of fluorescence on the PhosphorImager. Cell counts are presented in millions per cm³. Day 0, cell counts at the beginning of the experiment.

(a)



(b)

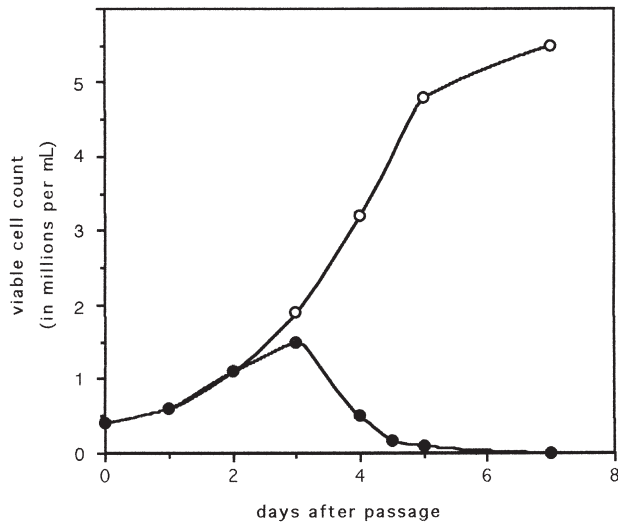


Figure 2. Cell viability of TBY-2 cells grown in the presence of 50 mmol m⁻³ CdSO₄. (a) PhosphorImager scans of control and cadmium-treated cells stained by fluorescein diacetate. Aliquots of the cell culture were diluted and stained with FDA at 24 h intervals. Cells were spotted onto nylon membrane, air dried and a fluorescence image was obtained. (b) Time dependence of viable cell count. (○) control; (●) 50 mmol m⁻³ CdSO₄. The data were obtained by integration of fluorescence signals (a). Cell numbers were calculated from a calibration curve.

DISCUSSION

In their natural environment, plants are exposed to cadmium, a frequent soil pollutant. Furthermore, cadmium is a major industrial pollutant influencing many plant and animal communities. Therefore, a deeper understanding of the mechanism of cadmium toxicity is important.

Here we report cadmium-induced apoptotic changes in a tobacco cell culture. Cells grown for 1 week in the presence of 50–100 mmol m⁻³ CdSO₄ exhibited oligonucleosomal DNA fragmentation associated with cell death. The lowest cadmium concentration used (10 mmol m⁻³) had no effect on cell viability or DNA integrity, while 1000 mmol m⁻³ CdSO₄ killed cells rapidly without chromatin fragmentation. Thus it seems that the cytotoxic effect of cadmium involves at least two mechanisms of cell death depending on the concentration used. Rapid death of cells at the highest cadmium concentration without apparent DNA degradation suggested necrosis as a cause of cell death. By

contrast, 50–100 mmol m⁻³ cadmium triggered an apoptotic pathway, demonstrating a true genotoxic effect of this metal on plant cells.

The occurrence of DNA fragmentation in the presence of cadmium has been well documented in human cells (El Azzouzi *et al.* 1994; Habeebu *et al.* 1998). However, differences between plant and animal cells in response to cadmium can be distinguished:

- in tobacco cells, apoptosis-inducing concentrations were about 10-fold higher than in animal cells,
- cell necrosis in tobacco cell culture was observed at a cadmium concentration that was 20-fold higher than in lymphocyte culture, and
- in lymphocyte culture, oligonucleosomal fragmentation preceded a decrease in cell viability, while in TBY-2 cells DNA ladders appeared when about 90% of cells were already dead (defined by FDA fluorescence).

Another difference between tobacco and animal cells

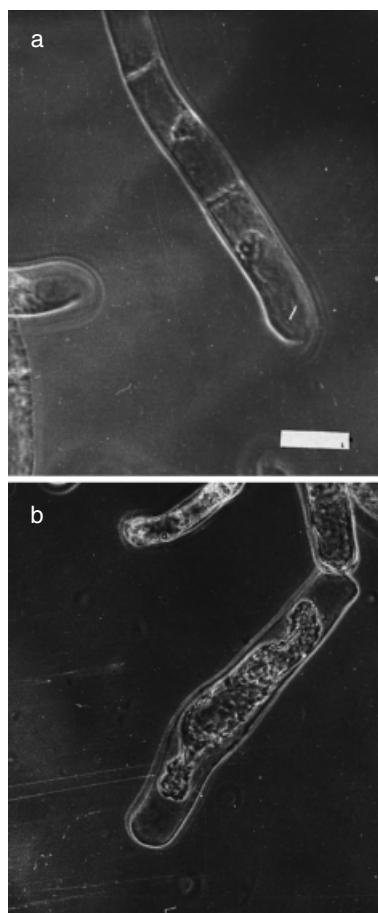


Figure 3. Morphology of TBY-2 cells. Morphology changes were monitored using phase-contrast light microscopy. (a) Control cells; (b) cells maintained in the presence of $50 \text{ mmol m}^{-3} \text{ CdSO}_4$ for 5 d. Note the irregular profiles of cadmium-treated cells with condensed protoplasts. Bar = $50 \mu\text{m}$.

concerns the kinetics of apoptosis. El Azzouzi *et al.* (1994) reported death of lymphocyte cell lines almost immediately after addition of cadmium. On the other hand, TBY-2 cells completed almost two rounds of the cell cycle (Table 1) before rapid cell death at day 4. The fact that tobacco cell cultures tolerated higher concentrations of cadmium compared to animal cells suggests that plant cells possess an efficient mechanism to cope with limited exposure to relatively high concentrations of cadmium. Possibly activation of protective metallothioneins could account for the observed short-term resistance. In carrot cell culture, selection of metal-resistant cells was observed (Ojima & Ohira 1983). However, this was not the case with TBY-2 since longer exposures to cadmium lead inevitably to cell death and DNA fragmentation. Application of $50 \text{ mmol m}^{-3} \text{ CdSO}_4$ to seeds completely prevented germination, suggesting the apoptotic changes might also occur in plant tissue (not shown). Adaptation processes, however, cannot be excluded under the lowest concentration of cadmium (10 mmol m^{-3}).

What might be the mechanism of the apoptotic process

triggered by cadmium in cell culture? The oligonucleosomal ladders were correlated with about 20% and 0% cell viability at days 5 and 7 of cadmium treatment (50 mmol m^{-3}), casting doubts that the primary effect of cadmium is nucleosomal cleavage. It is likely that the oligonucleosomal fragmentation in TBY-2 cells is merely a consequence of cell death rather than its direct cause. The decrease of viable cell counts occurred relatively late after cadmium administration. Early intervals of cadmium treatment (up to day 3) did not have any apparent effect on cell morphology and growth. The dynamics of cell death suggest that, with moderate doses of cadmium, genetic and epigenetic changes accumulate to reach a threshold beyond which the apoptotic pathway is triggered. At the molecular level, we were able to detect double-strand breaks at early intervals following cadmium treatment, while the cell culture behaved 'normally' with respect to growth, viability and cell morphology. The shift from $> 2 \text{ Mb}$ to $50\text{--}200 \text{ kb}$ DNA fragments from day 3–5 of incubation with cadmium indicated that double-strand breaks became more frequent after prolonged exposure to cadmium. Most fragments occurred in the $50\text{--}200 \text{ kb}$ region, suggesting cleavage of phosphodiester bonds at matrix attachment regions and fractionation of chromatin into chromatin domains. Thus, nucleosomal fragmentation and cell death is clearly preceded by fragmentation of chromatin into chromatin domains (loops). It has been reported that the matrix

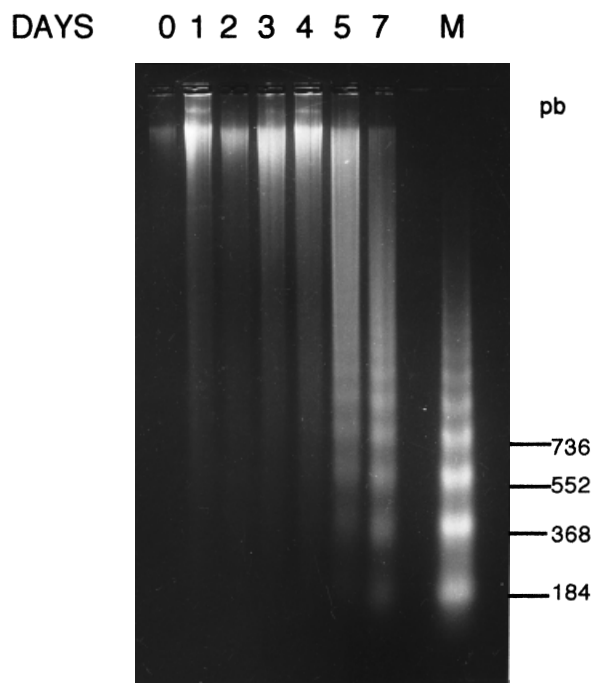


Figure 4. Time dependence of oligonucleosomal DNA fragmentation. TBY-2 cells were grown in the presence of $50 \text{ mmol m}^{-3} \text{ CdSO}_4$ for up to 7 d. Cells were harvested at the indicated time intervals and extracted DNA was analysed by conventional agarose gel electrophoresis. The duration of cadmium treatment is indicated above each lane; lane M, tobacco chromatin digested with micrococcal nuclease.

attachment sites are in a close contact with topoisomerase II enzyme (Gromova, Thomsen & Razin 1995; Laemmli *et al.* 1995) whose inhibition, e.g. by denaturation of enzyme molecules, results in selective cleavage of DNA into domains (Sander & Hsieh 1983; Liu 1989). Moreover, the activity of topoisomerase II was shown to be sensitive to thiol-reactive compounds (Frydman *et al.* 1997). Since divalent cadmium ion possesses high affinity towards sulphhydryl groups, we speculate that cadmium may inhibit topoisomerase II or some enzyme modulating topoisomerase II activity, leading to DNA breakage. The extent of DNA damage may be critical for triggering of the apoptotic pathway.

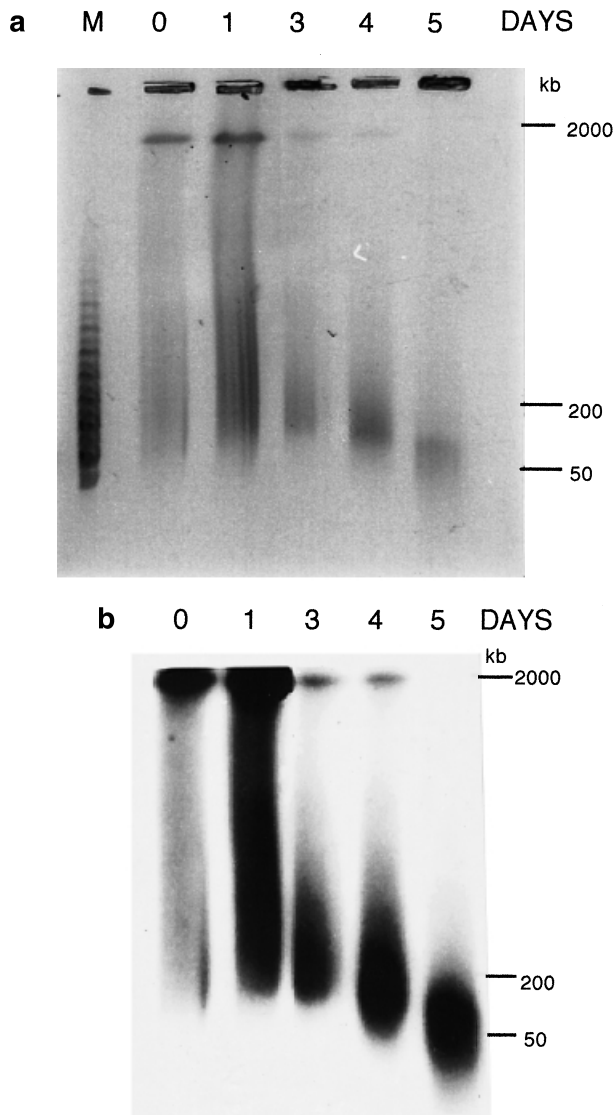


Figure 5. Pulsed-field gel electrophoresis of high-molecular-weight DNA isolated from control and cadmium-treated cells. TBV-2 cells were grown in the presence of $50 \text{ mmol m}^{-3} \text{ CdSO}_4$ for the time intervals indicated. DNA was run on an agarose gel under conditions enabling separation of fragments of 50–2000 kb in size, and stained with ethidium bromide (a). To detect fragmentation in a defined sequence, DNA was blotted onto a nylon membrane and hybridized against the HRS60 probe (b). Lane M, DNA marker (λ phage DNA concatemers).

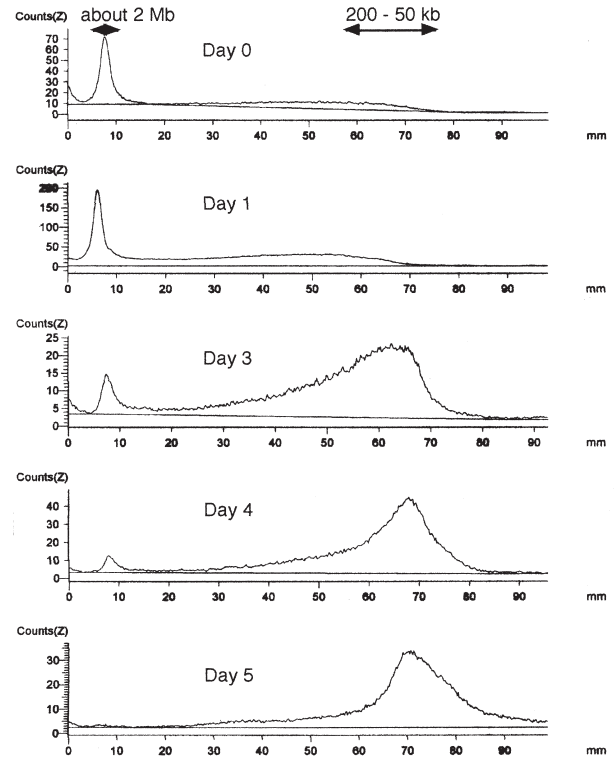


Figure 6. Densitometric scanning of radioactive signals along the electrophoretic tracks. Radioactivity in tracks (Fig. 5b) was scanned using a PhosphorImager and processed with the ImageQuant program. Molecular weights of fragments are indicated by arrows. *x* axis, distance from the start (mm); *y* axis, radioactivity counts

merase II activity, leading to DNA breakage. The extent of DNA damage may be critical for triggering of the apoptotic pathway.

In conclusion, we show that the genotoxic properties of cadmium in plant cells are manifested by directed chromatin fragmentation. The 'domain' and oligonucleosomal DNA fragmentation are clearly separated by relatively long time intervals, making the TBV-2 cells a convenient model for molecular studies of individual apoptotic steps.

ACKNOWLEDGMENTS

We thank Dr B. Koukalová, Dr M. Bezděk (Institute of Biophysics, Brno) and Dr A. R. Leitch (School of Biological Sciences, Queen Mary and Westfield College, University of London) for critical reading of the manuscript. The excellent technical assistance of Mrs L. Jedličková and Mrs E. Koudelková is highly appreciated. Financial support for this work was provided by the Grant Agency of the Czech Republic (grant no. 521/98/0045).

REFERENCES

Barlow P.W. (1982) *Plant Growth Regulator Group Monograph No. 8*, pp. 27–45. Plant Growth Regulator Group, Wantage, UK.

- Chakravarty B. & Srivastava S. (1992) Toxicity of some heavy metals in vivo and in vitro in *Helianthus annuus*. *Mutation Research* **283**, 287–294.
- Czuba M. & Kraszewski A. (1994) Long-term cadmium exposure accelerates oxidant injury: significance of bound/free water states during long-term metal stress. *Ecotoxicology and Environmental Safety* **29**, 330–348.
- Danon A. & Gallois P. (1998) UV-C radiation induces apoptotic-like changes in *Arabidopsis thaliana*. *FEBS Letters* **437**, 131–136.
- El Azzouzi B., Tsangaris G.T., Pellegrini O., Manuel Y., Benveniste J. & Thomas Y. (1994) Cadmium induces apoptosis in a human T cell line. *Toxicology* **88**, 127–139.
- Freedman L.P., Luisi B.F., Korszun Z.R., Basavappa R., Sigler P.B. & Yamanoto K.R. (1988) The function and structure of the metal coordination sites within the glucocorticoid receptor DNA binding domain. *Nature* **334**, 543–546.
- Frydman B., Marton J.S., Sun K., Neder K.K., Liu H.M., Wang Y., Mao H.Y., Wu H.Y., Sanders M.M. & Liu L.F. (1997) Induction of DNA topoisomerase II-mediated DNA cleavage by beta-lapachone and related naphthoquinones. *Cancer Research* **57**, 620–627.
- Greenberg J.T. (1996) Programmed cell death: a way of life for plants. *Proceedings of the National Academy of Sciences of the USA* **93**, 12094–12097.
- Greenberg J.T., Guo A., Klessig D.F. & Ausubel F.M. (1994) *Cell* **77**, 551–563.
- Gromova I.I., Thomsen B. & Razin S.V. (1995) Different topoisomerase II antitumour drugs direct similar specific long-range fragmentation of amplified *c-myc* gene locus in living cells and in high salt-extracted nuclei. *Proceedings of the National Academy of Sciences of the USA* **92**, 102–106.
- Habeebu S.M.S., Liu J. & Klaassen C.D. (1998) Cadmium-induced apoptosis in mouse liver. *Toxicology and Applied Pharmacology* **149**, 203–209.
- Havel L. & Durzan D.J. (1996) Apoptosis in plants. *Botanical Acta* **109**, 268–277.
- Keen N.T. (1990) Gene for gene complementarity in plant-pathogen interactions. *Annual Review of Genetics* **24**, 447–463.
- Koukalová B., Kovařík A., Fajkus J. & Široký J. (1997) Chromatin fragmentation associated with apoptotic changes in tobacco cells exposed to cold stress. *FEBS Letters* **414**, 289–292.
- Koukalová B., Reich J., Matyášek R., Kuhrová V., Bezděk, M. (1989) A *Bam*HI family of highly repetitive DNA sequences of *Nicotiana tabacum*. *Theoretical and Applied Genetics* **78**, 77–80.
- Kovařík A. & Fojtová M. (1999) Estimation of viable cell count after fluorescein diacetate staining using PhosphorImager. *Biotechniques* **27**, 685–688.
- Laemmli U.K., Kas E., Poljak L. & Adachi Y. (1995) Physical mapping of the human *hprt* chromosomal region (Xq26). *Mutation Research* **326**, 39–49.
- Liu D.H., Jiang W.S. & Li M.X. (1992) Effects of cadmium on root growth and cell division of *Allium cepa*. *Acta Scientiae Circumstantiae* **12**, 339–406.
- Liu L.F. (1989) DNA topoisomerase poisons as antitumour drugs. *Annual Review of Biochemistry* **58**, 351–375.
- Lohmann R.D. & Beyersmann D. (1993) Cadmium and zinc mediated changes of the Ca²⁺-dependent endonuclease in apoptosis. *Biochemical and Biophysical Research Communications* **190**, 1097–1103.
- Nagata T., Nemoto Y. & Hasezawa S. (1992) Tobacco BY-2 cell line as the 'HeLa' cell in the cell biology of higher plants. *International Review of Cytology* **132**, 1–30.
- Oberhammer F., Wilson J.W., Dive C., Morris I.D., Hickman J.A., Wakeling A.E., Walker P.R. & Sikorska M. (1993) Apoptotic death in epithelial cells: cleavage of DNA to 300 and/or 50 kb fragments prior to or in the absence of internucleosomal fragmentation. *EMBO Journal* **12**, 3679–3684.
- Ojima K. & Ohira K. (1983) Characterisation of aluminium and manganese tolerant cell lines selected from carrot cell cultures. *Plant Cell Physiology* **24**, 789–797.
- Pennell R.I. & Lamb C. (1997) Programmed cell death in plants. *Plant Cell* **9**, 1157–1168.
- Reyerson D.E. & Heath M.C. (1996) Cleavage of nuclear DNA into oligonucleosomal fragments during cell death induced by fungal infection or by abiotic treatments. *Plant Cell* **8**, 393–402.
- Saghai-Marooif M.A., Soliman K.M., Jorgensen R.A. & Allard R.W. (1984) Ribosomal DNA spacer/length polymorphism in barley, Mendelian inheritance, chromosomal location and population dynamics. *Proceedings of the National Academy of Sciences of the USA* **81**, 8014–8018.
- Sambrook J., Fritsch E.F. & Maniatis T. (1988) *Molecular Cloning: A Laboratory Manual*. Cold Spring Harbor Laboratory Press, Cold Spring Harbor, New York.
- Sander M. & Hsieh T. (1983) Double strand DNA cleavage by type II DNA topoisomerase from *Drosophila melanogaster*. *Journal of Biological Chemistry* **258**, 8421–8428.
- Sun X.M. & Cohen G.M. (1994) Mg²⁺-dependent cleavage of DNA into kilobase pair fragments is responsible for the initial degradation of DNA in apoptosis. *Journal of Biological Chemistry* **269**, 14857–14860.
- Walker P.R. & Sikorska M. (1994) Endonuclease activities, chromatin structure, and DNA degradation in apoptosis – review. *Biochemistry and Cell Biology* **72**, 615–623.
- Walker P.R., Padney S. & Sikorska M. (1995) Degradation of chromatin in apoptosis. *Cell Death and Differentiation* **2**, 97–104.
- Woodson W.R., Park K.Y., Drory A., Larsen P.B. & Wang H. (1992) Expression of ethylene biosynthetic pathway transcripts in senescing carnation flowers. *Plant Physiology* **99**, 526–532.
- Wyllie A.H. (1980) Glucocorticoid-induced thymocyte apoptosis is associated with endogenous endonuclease activation. *Nature* **284**, 555–556.
- Zhang Y. & Xiao H. (1998) Antagonistic effect of calcium, zinc and selenium against cadmium induced chromosomal aberrations and micronuclei in root cells of *Hordeum vulgare*. *Mutation Research* **420**, 1–6.

Received 17 September 1999; received in revised form 13 January 2000; accepted for publication 13 January 2000

Recovery of tobacco cells from cadmium stress is accompanied by DNA repair and increased telomerase activity

Miloslava Fojtová¹, Jana Fulnečková², Jiří Fajkus^{1,2} and Aleš Kovařík^{1,3}

¹ Institute of Biophysics, Academy of Sciences of the Czech Republic, Královopolská 135, Brno, CZ-612 65, Czech Republic

² Department of Functional Genomics and Proteomics, Masaryk University Brno, CZ-612 65, Czech Republic

Received 14 December 2001; Accepted 3 July 2002

Abstract

It has been shown previously that apoptosis of tobacco cells induced by cadmium ions shows a relatively long lag period between exposure and cell death. This lag phase lasts for 3 d in TBY-2 cell cultures and is characterized by the maintenance of full cell viability despite extensive fragmentation of DNA into pieces of chromatin loop size. Experiments reported here demonstrate that cell death can be prevented if 50 μ M CdSO₄ is removed from the growth medium during the lag phase, suggesting that an irreversible apoptotic trigger is delivered within 24 h, between the third and fourth days of cadmium treatment. The post-cadmium recovery phase was characterized by DNA repair at the level of 50–200 kb and increased telomerase activity. Analysis of high-molecular-weight DNA by pulsed-field-gel electrophoresis revealed that the majority of DNA strand breaks was repaired within 48 h after cadmium withdrawal. Telomerase activity increased 2.5-fold in the recovery phase, but elevated levels were also found in cell extracts from apoptotic cells suggesting that telomerase might be associated with DNA repair, but it is not capable of inhibiting ongoing apoptosis. Limited exposure of TBY-2 cells to cadmium elicits non-random DNA damage of relatively high magnitude that can be repaired. It is proposed that plants might have developed a highly efficient DNA repair system to cope with transient genotoxic stress.

Key words: Apoptosis, cadmium, DNA domain fragmentation, telomerase, tobacco BY-2 cells.

Introduction

Cadmium is a known carcinogen and represents a serious environmental problem for both humans and animals (Freedman *et al.*, 1988). Although cadmium is a genotoxic metal, the molecular basis of cadmium genotoxicity is not well defined. In mammalian cells, cadmium enhances the mutagenicity of UV light, suggesting its interference with DNA repair processes and the activity of detoxifying enzymes (reviewed in Beyersmann and Hechtenberg, 1997; Hartwig, 1994). In plants, cadmium induces a number of genome-related changes including chromosomal aberrations (Zhang and Xiao, 1998), decrease of mitotic index in root cells (Zhang and Yang, 1994), and abnormalities in nucleolar structure (Jiang *et al.*, 1994; Zhang and Yang, 1994). At the biochemical level, the accumulation of oxidized proteins and lipid peroxides was observed in pea upon cadmium stress (Sandalo *et al.*, 2001).

Apoptosis in plants occurs in response to pathogens (Keen, 1990) and to changes in environmental conditions. Typical DNA fragmentation and changes in the morphology of nuclei were observed during temperature stress (Koukalová *et al.*, 1997; McCabe and Leaver, 2000), after UV-irradiation (Danon and Gallois, 1998) and after exposure to chemicals and toxins (Wang *et al.*, 1996). Apoptosis of tobacco cells, manifested by chromatin condensation and DNA fragmentation after exposure to chemicals (salicylic acid, okadaic acid, hydrogen peroxide, camptothecin), can be reversible during the early stages following the removal of the inducing agent (O'Brien *et al.*, 1998). DNA lesions induced by ongoing apoptosis may represent an abundant substrate for healing by telomerase,

³ To whom correspondence should be addressed. Fax: +420 5 41211293. E-mail: kovarik@ibp.cz

Abbreviations: dNTP, deoxynucleotide triphosphate; DTT, 1,4-dithio-DL-threitol; FDA, fluorescein diacetate; Mb, megabase; MES, 2[*N*-morpholino]ethanesulphonic acid; MS medium, Murashige and Skoog medium; PFGE, pulsed-field-gel electrophoresis; Topoll, topoisomerase II; TRAP, telomere repeat amplification protocol.

and a number of reports from the animal kingdom are consistent with this theory (Leteurtre *et al.*, 1997; Hande *et al.*, 1998). To date, the up-regulation of telomerase in response to DNA damaging agents has not been reported in plants.

In a previous paper on cadmium sulphate-triggered apoptosis in tobacco BY-2 cells (Fojtová and Kovařík, 2000), the most striking observation was the relatively late onset of cell death upon exposure to 50 μM CdSO_4 . During the first 3 d of cadmium treatment, cell proliferation and morphology were similar to non-treated cells. On the third day, DNA cleavage into units 50–200 kb in length, termed as domain fragmentation, was observed and prolonged exposure (4–7 d) led to a rapid decrease of cell viability and further degradation of DNA to oligonucleosomal units. Thus, in TBY-2 cells, the domain and oligonucleosomal DNA fragmentation are separated by at least 24 h and this experimental system can be used to study the kinetics of domain DNA fragmentation in plant apoptosis.

Here the focus is on the reversibility of cadmium-induced DNA fragmentation during the first 3 d of cadmium treatment and on DNA repair processes taking place after the removal of Cd^{2+} ions. A relationship between recovery of genome integrity and telomerase activity is demonstrated.

Materials and methods

Chemicals

CdSO_4 and fluorescein diacetate were obtained from Sigma (USA), [^{14}C]thymidine (specific activity 4 MBq ml^{-1}) from UVVVR (Czech Republic).

Cell culture and cadmium treatment

The tobacco bright yellow (TBY-2) cells (Kato *et al.*, 1972) were grown in standard liquid Murashige and Skoog (MS) medium supplemented with sucrose (3%, w/v), thiamine (1 mg l^{-1}), KH_2PO_4 (200 mg l^{-1}), myoinositol (100 mg l^{-1}) and 2,4-dichlorophenoxyacetic acid (0.2 mg l^{-1}) in 100 ml Erlenmeyer flasks at 27 °C with shaking at 120 rev min^{-1} . The cells were regularly subcultured twice a week.

For cadmium stress studies, the cells at a density of about 3 millions cells ml^{-1} were subcultured at dilution of 1:10 into MS medium with CdSO_4 (final concentration 50 μM). After 3 d and 4 d of cultivation, respectively, cells were extensively washed with MS medium and further cultivated without cadmium sulphate for 1–4 d, defined as the post-cadmium phase.

In double strand break induction/rejoining experiments, the DNA was metabolically pre-labelled with [^{14}C] thymidine as follows: about 3×10^6 of TBY-2 cells were cultivated in 10 ml of MS medium containing 0.4 MBq of [^{14}C]thymidine for 3 d. The incorporated [^{14}C]thymidine was measured in a β -scintillation counter Wallac 1410 (LKB, Pharmacia) after DNA precipitation with trichloroacetic acid. Typically, incorporated radioactivity reached a plateau (0.2–1.0 dpm per cell) after 24 h when about 50% of the total had been incorporated.

Analysis of high-molecular-weight DNA

Cells from about 3 ml of TBY-2 cell suspension culture were lyophilized at -20 °C, then homogenized in liquid nitrogen and immediately resuspended in a buffer containing 10 mM 2[*N*-morpholino]ethanesulphonic acid (MES), pH 5.6, 10 mM NaCl, and 5 mM EDTA. The suspension was mixed with an equal volume of molten 2% (w/v) low melting temperature agarose in 0.4 M mannitol, 20 mM MES, pH 5.6 and transferred to a mould. Agarose blocks were incubated in a lysis buffer (0.5 M EDTA, pH 8.0, 1% (w/v) *N*-lauroylsarcosine, 0.1 mg ml^{-1} proteinase K) at 55 °C for 2×24 h and stored in 0.5 M EDTA. The DNA was analysed within 1 week to avoid diffusion of low molecular weight fragments.

Electrophoresis was performed on the Gene Navigator System (Pharmacia Biotech, Sweden) using 1% agarose gel in 45 mM Tris-borate, 1 mM EDTA, pH 8.0. The running conditions (pulse ramping time from 5 s to 50 s, voltage 200 V, temperature 10 °C, time 24 h) enabled separation of fragments between 50–1000 kb in size. After electrophoresis, gels were stained by ethidium bromide and photographed. Gels containing [^{14}C]thymidine-labelled DNA were blotted onto a nylon membrane, exposed to a screen and scanned using a PhosphorImager STORM 860 (Molecular Dynamics, USA).

Southern blot hybridization

DNA separated on pulsed-field-gel electrophoresis (PFGE) was blotted onto nylon membranes (Hybond XL, Amersham Pharmacia Biotech, UK) and hybridized with the 360 bp dimer of the subtelomeric tandem repeated sequence HRS60 (Koukalová *et al.*, 1989) labelled with ^{32}P -dCTP by random priming (DNA Labelling Kit, MBI Fermentas, Lithuania) according to a standard protocol (Sambrook *et al.*, 1988). The radioactive signals were visualized using a PhosphorImager and analysed by ImageQuant software (Molecular Dynamics, USA).

Estimation of total and viable cell count, studies of nuclei morphology

Total cell counts were determined manually in Burkler chamber using phase-contrast light microscope (Carl Zeiss, Jena, Germany). Counts of viable TBY-2 cells were determined by fluorescein diacetate staining followed by evaluation of fluorescence of living cells using the blue-fluorescence mode of a PhosphorImager STORM (Kovařík and Fojtová, 1999). Briefly, diluted cell suspensions were mixed with equal volumes of FDA reagent, prepared by diluting stock solution (3 mg FDA ml^{-1} of acetone) with MS medium at 1:200. After 5 min incubation, 20 μl drops were transferred onto a nylon membrane (Hybond XL) and dried. Fluorescence signals were scanned with a blue fluorescence laser channel (excitation wavelength 450 nm) at a high resolution (100 pixels) using a PhosphorImager. Signals were evaluated with an ImageQuant program using an ellipse integration method, viable cell counts were calculated from the calibration curve (a linear plot of fluorescence units and the number of viable cells determined manually by fluorescence microscopy).

The morphology of nuclei was studied by fluorescence microscopy using cells fixed in a Carnoy's fixative (methanol:acetic acid, 3:1), transferred onto microscope slides, stained with Hoechst 33258 (1 μg ml^{-1}) for 10 min, and destained in distilled water. Blue fluorescence was visualized using an epifluorescence microscope Olympus AX 70 with image capture and processing; image analysis was performed by the ISIS program (Metasystems, Germany).

Preparation of cell extract for telomerase assay

Cell extracts from TBY-2 cells was prepared as described previously (Fitzgerald *et al.*, 1996). Approximately 0.25 g of lyophilized cells were ground in liquid nitrogen, suspended in 1 ml of buffer W (50 mM Tris-acetate pH 7.5, 5 mM MgCl_2 , 100 mM potassium

glutamate, 20 mM EGTA, 1 mM DTT, 0.1 mM PMSF, 0.6 mM vanadyl ribonucleoside complex (NEB), 1.5% (w/v) polyvinylpyrrolidone, 10% glycerol) and centrifuged at 16 000 *g* for 15 min at 4 °C. The supernatant was supplemented with PEG 8000 (Sigma) to a final concentration of 10%, stirred for 30 min at 4 °C, and centrifuged at 20 000 *g* for 5 min at 4 °C. The pellet was resuspended in 250 µl of buffer W for 30 min on ice and centrifuged at 20 000 *g* for 2 min at 4 °C. The supernatant was stored at -70 °C until use. The concentration of total protein in cell extracts was determined according to Bradford (Bradford, 1976).

Telomerase assay

Telomerase was assayed using a modified plant version of the telomere repeat amplification protocol (TRAP) (Fitzgerald *et al.*, 1996; Fajkus *et al.*, 1998). In the first step of the assay, telomerase adds a number of telomeric repeats (GGTTAG) onto the 3' end of a substrate oligonucleotide. In the second step, the extended products are amplified by PCR using the substrate and reverse primers, generating a ladder of products with seven base increments. Assay buffer contained 50 mM Tris-acetate, pH 8.3, 50 mM potassium glutamate, 0.1% Triton-X-100, 1 mM spermidine, 1 mM DTT, 50 µM of each dNTP, 5 mM MgCl₂, 10 mM EGTA, and 100 µg ml⁻¹ BSA. The primer 47F (5'-CGCGGTAGTGATGTGGTTGTGTT-3') was denatured for 5 min at 95 °C and cooled on ice prior to addition to reactions. The reaction mixture, composed of telomerase assay buffer (45.5 µl), 10 pmol of primer 47F and cell extract, was incubated at 26 °C for 45 min in a thermocycler. Controls for false-positive results were run in parallel using heat-treated extracts (94 °C, 10 min). Elongation was terminated by heating the reaction mixture at 94 °C for 10 min and 10 pmol of TP primer (5'-CCGAATCAACCCTAAACCCTAAACCCTAAACCC-3') and 2 units of DyNAzyme II DNA polymerase (Finnzymes, Finland) were added immediately to each reaction at 80 °C. The extension products were amplified by 35 cycles of PCR (94 °C for 30 s, 55 °C for 30 s, and 72 °C for 45 s), followed by a terminal extension step (72 °C for 5 min). The products were separated on a 12.5% polyacrylamide gel which was stained with SYBR Green I (Molecular Probes) and scanned on a PhosphorImager STORM in a blue fluorescence mode and the resulting product ladder bands (see above) were quantified using ImageQuant software in each sample. The activity of each sample was then expressed as the percentage telomerase activity with respect to the activity found at the corresponding protein concentration in control cells (cultured in the absence of cadmium).

Results

Early cadmium removal may prevent apoptosis

Previous reports indicated that the death of TBY-2 cells occurs only after 4 d of exposure to 50 µM cadmium sulphate (Fojtová and Kovařík, 2000). Here the aim was to find out whether the removal of cadmium after different intervals of treatment would prevent apoptosis. In order to determine the point of reversibility, defined as the maximum time interval beyond which cell damage reaches a critical threshold inevitably leading to death, cells were treated with 50 µM CdSO₄ for 3 d or 4 d, respectively, then washed and subcultured for up to 4 d in cadmium-free medium. Viable (Fig. 1) and total cell counts were determined and expressed as a ratio (Table 1). TBY-2 cells growing in the presence of the cadmium sulphate for up to 3 d displayed full viability (Table 1). Immediately

after transfer to cadmium-free medium, the growth slowed slightly, but then recovered to the control rate (Fig. 1). On the other hand, cells exposed to cadmium for 4 d showed only ~30% viability and viability fell to zero after transfer to cadmium-free medium. This indicated that the changes during the first 3 d of cadmium treatment were fully reversible, while more extended exposure led inevitably to cell death even after the removal of the stress factor. Similar results were obtained in three independent experiments.

Repair of double strand DNA breaks after cadmium removal

The preapoptotic phase of cadmium treatment was accompanied by DNA fragmentation into chromatin loops 50–200 kb in length (Fojtová and Kovařík, 2000). Next it was determined whether this initial DNA damage was repaired during the recovery phase described above. Pulsed-field-gel electrophoresis was used to analyse high-molecular-weight DNA from cells treated with 50 µM CdSO₄ for 3 d and from a post-cadmium culture (Fig. 2A). On day 3 of the cadmium treatment (lane 2), and 24 h after cadmium removal (lane 3), DNA migrated at the gel front as a smear of unresolved fragments 50–200 kb in length indicating the severe breakdown of genomic DNA. Starting from day 2 following cadmium removal, the signals were shifted to higher molecular weight fractions (Fig. 2A, lanes 4, 5) and on the 4th day of the post-cadmium period, most DNA migrated in the compression

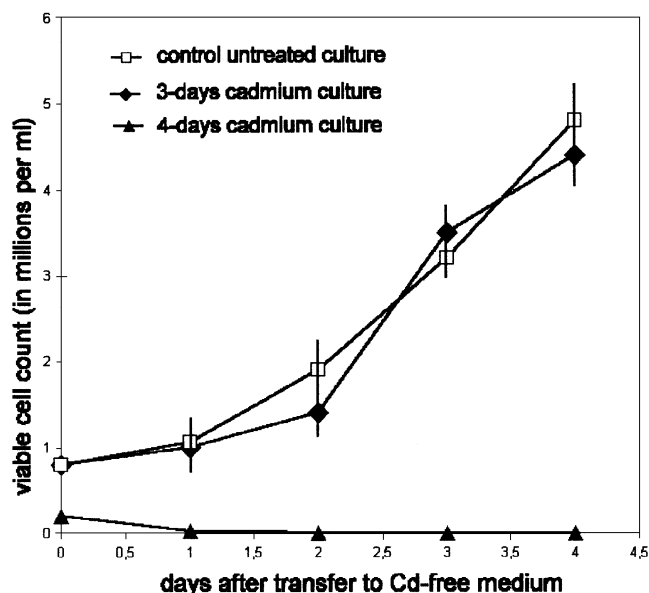


Fig. 1. Growth of TBY-2 cells in post-cadmium phase. The cells were grown with 50 µM CdSO₄ for 3 d or 4 d, respectively, and transferred into cadmium-free medium for a further 4 d. A viable cell count was determined for each time point interval by a fluorescence method described in Materials and Methods. The results represent the mean of three independent experiments.

Table 1. Viability of *TBY-2* cells recovered from cadmium stress

Cells were exposed to 50 μM CdSO_4 for 3 d and 4 d, respectively, then transferred to cadmium-free medium and cultivated for 4 d. Viability is expressed as a ratio between viable and total cell counts.

Cadmium exposure	Recovery phase (days following cadmium removal)				
	0	1	2	3	4
0 d	0.88	0.88	0.92	0.93	0.96
3 d	0.88	0.8	0.84	0.93	0.88
4 d	0.28	0.02	0	0	0

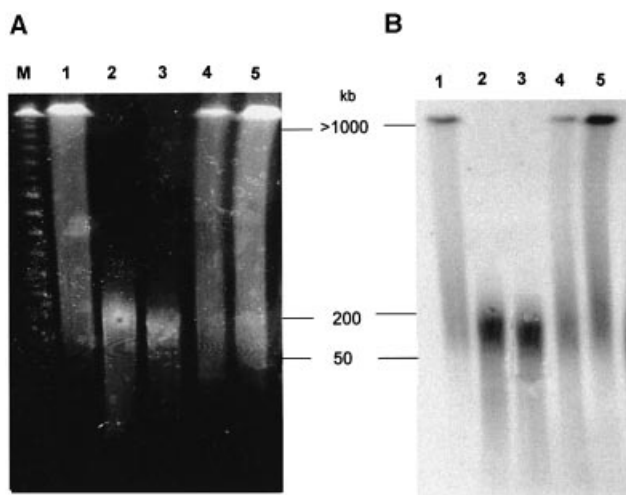


Fig. 2. Analysis of high-molecular weight DNA by PFGE. Cells were grown for 3 d in the presence of 50 μM CdSO_4 and transferred into cadmium-free medium for another 4 d. High-molecular-weight DNA was prepared and analysed by PFGE. (A) Stained with ethidium bromide; (B) hybridized with the subtelomeric probe HRS60. Lane 1, control DNA; lane 2, 3 d with cadmium sulphate; lanes 3, 4, 5, 1, 2 or 4 d, respectively, after removal of cadmium sulphate; lane M, DNA marker (λ phage DNA concatemers).

zone (about 1 Mb in length) (lane 5). Subsequent Southern hybridization with the subtelomeric probe HRS60 (Fig. 2B) or with telomeric probe (not shown) revealed similar patterns.

The extensive domain fragmentation of DNA and the virtual absence of dead cells in preapoptotic and post-cadmium phases suggest that restoration of DNA integrity during the post-cadmium period was caused by a repair process, rather than by selection of a rare subpopulation of cells with non-fragmented DNA. In order to demonstrate that double strand breaks are rejoined, cellular DNA was prelabelled with [^{14}C]thymidine during cadmium treatment, then the cells were washed and incubated in cadmium-free medium for 1, 2 or 3 d. An increase of incorporated label was not observed during the post-cadmium period showing the effective removal of free [^{14}C]thymidine (not shown). DNA from cadmium-treated

and non-treated cells was separated by PFGE and transferred to a nylon membrane which was exposed to a PhosphorImager screen for 60 d. DNA from non-treated cells migrated to the high-molecular-weight region (Fig. 3, lane 5). As expected, after 3 d with 50 μM CdSO_4 most DNA was in the 50–200 kb region at the gel front (lane 1). The removal of cadmium resulted in a shift of the radioactive DNA towards a higher molecular weight after 2 d, when a band in the compression zone (>1 Mb) became visible (lane 3) and its intensity increased after 3 d (lane 4). Thus, recovery of *TBY-2* cells from cadmium-induced genotoxic stress is accompanied by the repair of double strand DNA breaks.

Recovery of genome integrity is accompanied by an increase in telomerase activity

Broken chromosomes become highly unstable and fuse with other broken chromosome ends which leads to overall genomic instability. This may be prevented by ‘healing’ which involves the addition of telomere sequences at the breakpoints by telomerase (reviewed in Gill and Friebe, 1998). To resolve whether telomerase participates in the recovery from the genotoxic stress imposed by cadmium, telomerase activity was monitored in the course of cadmium sulphate treatment and the post-cadmium phase; serial dilutions of nuclear extracts from each phase of the experiment were used for TRAP assays. The final values of relative telomerase activity (see Materials and methods) were then calculated as an average of 5–7 values obtained at individual extract concentrations for each time-point. A remarkable increase in telomerase activity was detected during the phase of recovery from cadmium sulphate treatment (Fig. 4C, D, E), reaching a maximum (234% of the activity in control cells) on the second day of the recovery phase (Fig. 4D; and day 5 of the experiment II in Fig. 5), and falling slightly below the normal level on the fourth day of the recovery phase (see Fig. 4F and day 7 of the experiment II). A small increase in telomerase activity could be observed in cells treated with cadmium for 3 d (Fig. 4B) or 4 d (beyond the ‘point of reversibility’)—see Fig. 5, days 3 and 4 of experiment I. The addition of 50 μM CdSO_4 to the TRAP reaction mixtures did not affect the assay, suggesting that the

presence of cadmium itself does not directly influence telomerase activity either positively or negatively (not shown). These observations suggest that telomerase participates in the genotoxic-stress-response and, together

with DNA polymerases, is involved in the re-establishment of genome integrity.

Discussion

A previous report indicated that apoptosis induced by cadmium ions in TBY-2 cell cultures can be dissected into a relatively long initial phase lasting for 3 d, followed by cell death associated with oligonucleosomal fragmentation of DNA (Fojtová and Kovařík, 2000). It is shown here that death is prevented if cadmium is removed from the medium during the initial phase. Since on day 4, viable cells could not be recovered even after removal of 50 μM cadmium, the critical phase of this type of apoptosis is limited to about 24 h between days 3 and 4 of cadmium treatment, when a cell death signal is irreversibly triggered and DNA degradation is manifested.

The progressive breakdown of high-molecular-weight DNA has been regularly observed during the initial phase. In these experiments, it was not possible to detect significant amounts of intact DNA of >1 Mb after 3 d of cadmium treatment suggesting that most cells possessed severely damaged DNA. During the first 24 h of the post-cadmium phase, the DNA was still significantly fragmented, but after 48 h it showed a dramatic shift towards higher molecular weight and after 4 d most DNA was of >1 Mb in length. This suggests that DNA repair mechanisms were activated in the post-cadmium phase. To demonstrate directly that ligation of breaks had indeed occurred *in vivo*, pulsed-field-gel-electrophoresis was used to show that, in the post-cadmium phase, the average size of the ^{14}C -

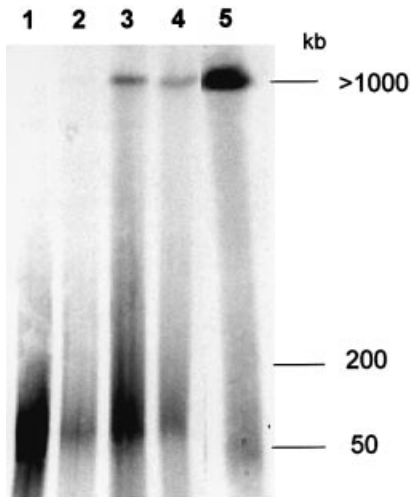


Fig. 3. End-joining of strand breaks in [^{14}C]thymidine-labelled DNA. TBY-2 cells were grown in the presence of [^{14}C]thymidine with or without 50 μM CdSO_4 for 3 d. After the removal of cadmium ions and radioactive thymidine, the cells were cultivated in MS medium for another 1, 2 or 3 d. High-molecular-weight DNA was prepared at the indicated times. After separation by PFGE, DNA was blotted onto a nylon membrane which was scanned using a PhosphorImager STORM. Lane 1, DNA from cells exposed to cadmium for 3 d; lanes 2, 3, 4, DNA extracted from cells after 1, 2 or 3 d following the removal of cadmium, respectively; lane 5, control DNA.

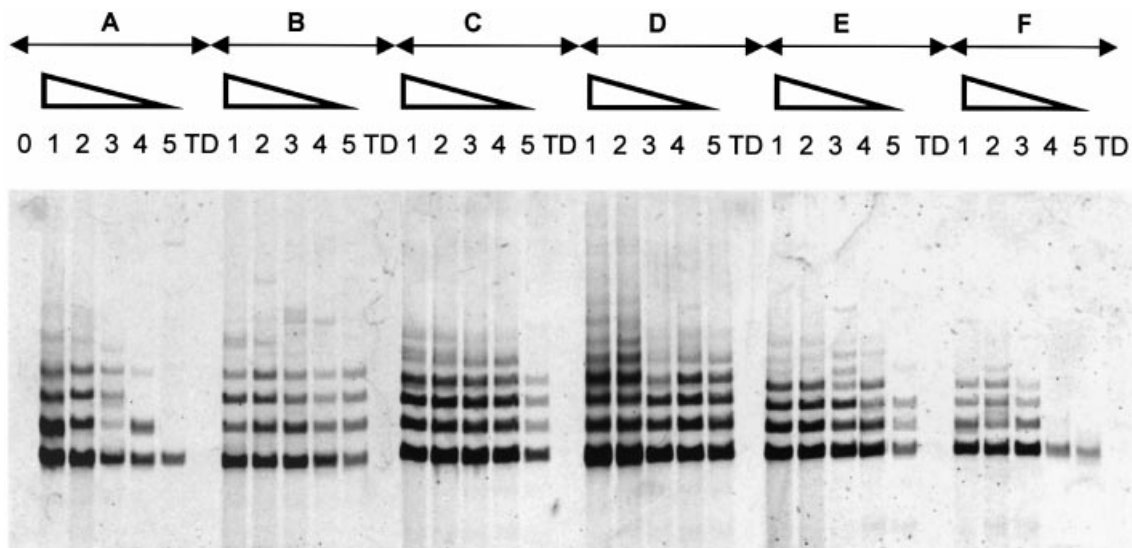


Fig. 4. Changes in telomerase activities in response to cadmium-induced genotoxic stress. Protein extracts from cadmium sulphate-treated and control cells were analysed for telomerase activity by the TRAP assay using dilutions containing 1000, 500, 250, 100 ng or 10 ng of total protein (lanes 1–5 in each panel, respectively). Lane 0, no cell extract; lanes TD, as lane 1 but using thermally-denatured telomerase. (A) Telomerase activity in control cells; (B) cells exposed to cadmium sulphate for 3 d; (C, D, E, F) cells after 1, 2, 3 or 4 d following the removal of cadmium, respectively.

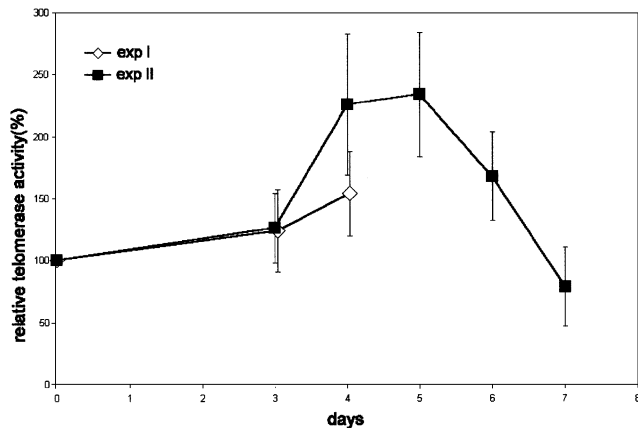


Fig. 5. Dynamics of telomerase activity in cell extracts during cadmium and post-cadmium period. TBY-2 cells were treated with 50 μM CdSO_4 . Telomerase activity was determined in protein extracts at indicated time intervals. Relative telomerase activity was expressed as percentage of activity with respect to control non-treated cells. Exp I, 4 d treatment with cadmium without recovery phase. At day 4 apoptotic phenotype was already manifested leading irreversibly to cell death (Fig. 1). Exp II, 3 d treatment with cadmium, followed by 4 d recovery in Cd-free medium.

thymidine-labelled DNA molecules increased markedly compared to the initial apoptotic phase. Gorbunova and Levy (1997) recently reported end-joining of transfected plasmid DNA in tobacco cells. Thus, end-joining of double strand breaks may significantly contribute to the recovery of plant cells from the temporal genotoxic stress. The DNA cleavage patterns accompanying cadmium stress clearly differed from those observed after gamma irradiation of cells (Hall *et al.*, 1992). While in the latter study the sizes of the DNA fragments were randomly distributed, these results are most consistent with targeted fragmentation into chromatin loops of 50–200 kb. This conclusion is supported by the similarity between the size of ‘pre-apoptotic’ DNA fragments and that of fragments obtained after treatment of maize protoplasts with VM-26, an inhibitor of topoisomerase II (TopoII) (Espinosa and Carballo, 1993). TopoII sites frequently (but not always) co-localize with matrix attachment regions (Gromova *et al.*, 1995). Hence, TopoII and/or other nuclease sensitive sites in chromatin could be primary targets of the cadmium genotoxicity.

Telomerase could be considered as a key enzyme in maintaining chromosomal integrity (reviewed in Blackburn, 2000). In this study’s experiments, the maximum increase of activity of telomerase was found in the 48 h interval of a post-cadmium phase. Interestingly, over this interval the intensive repair of double strand breaks was observed. Correlative evidence for a link between the end-joining of double strand breaks and telomerase was thus obtained. Presumably, the recovery of cells from cadmium stress requires multiple enzyme activities involved in the re-establishment of genome integrity. It

will be interesting to examine whether the activation of telomerase would also occur in other systems that involve increased DNA repair, for example, after UV irradiation. The weakly elevated levels of telomerase activity were found in extracts from cells in the apoptotic phase (day 4 in cadmium). Since about 70% of cells are already dead at this stage, this activity may originate from the remaining viable cells that might contain high enzyme activity. Nevertheless, activated telomerase cannot inhibit the apoptosis already initiated between days 3 and 4 of cadmium treatment (Fig. 1). Although tobacco contains exceptionally long telomeres (Fajkus *et al.*, 1995), the double strand breaks occurring in telomeric or subtelomeric regions (not shown and Fig. 2B) might result in short telomeres or chromosomes without telomeres. Possibly, active telomerase helps even very short telomeres to be functionally capped.

Perhaps the most interesting aspect of cadmium stress is the relationship between cell viability and the extent of the DNA damage. The initiation stage and the early post-cadmium phase are characterized by extensive DNA cleavage into chromatin loops. In most animal systems, once this type of fragmentation is initiated, cell death and, in some cases, oligonucleosomal fragmentation inevitably occur (Huang *et al.*, 1995). However, TBY-2 cells remained fully viable and oligonucleosomal fragmentation did not appear in the post-cadmium phase (not shown). The morphology of cell nuclei at day 3 of cadmium treatment did not show significant condensation of chromatin; in fact, the nuclear volume was slightly larger than controls (Fig. 6), which could indicate the arrest of cells in the G2 phase or a certain degree of aneuploidy. How can the observed severe DNA fragmentation be explained in the context of full cell viability? A trivial explanation is that the DNA became fragmented in the course of its preparation. But this possibility is considered unlikely. Domain fragmentation of DNA from lymphocytes was only seen under conditions of low EDTA concentration (Szabo and Bacso, 1996), whereas here all buffers contained 0.5 M EDTA. Moreover, DNA from control cells prepared in parallel did not show the fragmentation and elevation of telomerase activity correlated with end-joining of double strand breaks. The interpretation that fragmentation of high-molecular-weight DNA into 50–200 kb pieces represents a repairable DNA damage in transient cadmium stress is favoured. Saturation of DNA repair enzymes with prolonged genotoxic stress could lead to the activation of apoptotic signals sensing the ‘irreparable’ DNA damage. This assumption is strengthened because the addition of 100 μM cadmium shortened the initial preapoptotic period of cadmium tolerance to about 48 h (Fojtová and Kovařík, 2000). As in other studies that use DNA-damaging drugs to induce apoptosis, it is difficult to separate breaks introduced by treatment from those that represent the initial breaks of apoptosis. Possibly, the cleavage of DNA to

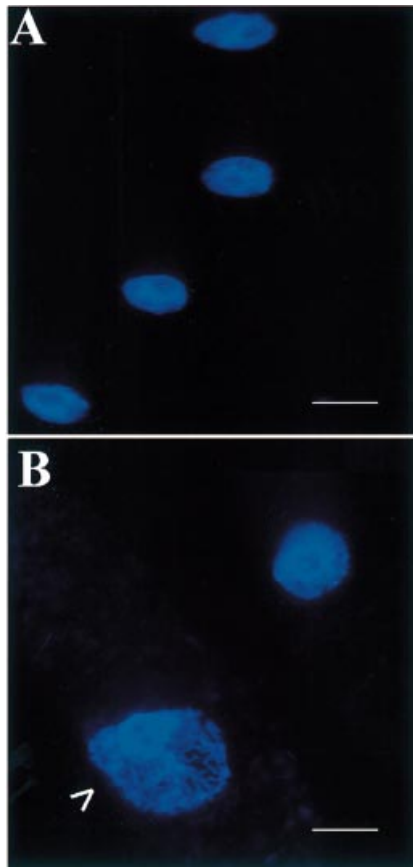


Fig. 6. Morphology of nuclei of cadmium-treated cells. TBY-2 cells grown with 50 μM CdSO_4 for 3 d were fixed, stained with Hoechst 33258 and visualized by epifluorescence microscopy. About 200 nuclei from each sample were examined. Approximately 10% of cadmium-treated cells contained enlarged nuclei (indicated by arrow). (A) control; (B) cells exposed to 50 μM CdSO_4 for 3 d. Bar=50 μm .

50–200 kb fragments could represent a regular phase of the apoptotic pathway (Oberhammer *et al.*, 1993). In this context the reversibility of the early stages of apoptosis induced with various stresses has been described in plant cells (O'Brien *et al.*, 1998).

An open question remains as to how genome integrity is restored to allow cells to resume the cell cycle after the removal of cadmium. a central role is proposed for matrix-attachment regions in this process. The assembly of an extensively fragmented genome on the nuclear matrix may contribute to the correct repair via DNA recombination and repair machinery, an idea supported because (i) the size of fragments in the 'reversible phase' corresponds to the size of chromatin loops, (ii) chromosome breaks and recombination events preferentially occur at nuclear matrix attachment sites where DNA is bound to topoisomerase II (Blasquez *et al.*, 1989) and (iii) the DNA fragmentation induced by TopoII inhibitor was reversible in maize protoplasts (Espinass and Carballo, 1993). Most likely, the contacts between the ends of chromatin loops

and the nuclear matrix proteins probably survive the reversible stage of cadmium-induced genome fragmentation and thus DNA–protein bonds would provide a way of conserving the nuclear position and function of individual loop domains. The maintenance of the loop organization of nuclear chromatin may thus be functionally more important than the simple integrity of the sugar–phosphate backbone of genomic DNA. Hence, the reconstruction of the genome could hardly be possible without the maintenance or re-establishment of chromatin loop attachments to the nuclear matrix.

Acknowledgements

We thank Dr B Koukalová (Institute of Biophysics, Brno, Czech Republic) and Dr R Hancock (Laval University Cancer Research Center, Quebec, Canada) for helpful comments and critical reading of the manuscript and Dr A Levy (Weizman Institute of Sciences, Rehovot, Israel) for a useful discussion. The excellent technical assistance of Mrs L Jedličková and Miss D Fridrichová is highly appreciated. The work was supported by the Grant Agency of the Czech Republic (grants no. 521/01/P042, Z 5004920 and 204/02/0027) and the Ministry of Education of the Czech Republic (MSM143100008).

References

- Beyersmann D, Hechtenberg S.** 1997. Cadmium, gene regulation, and cellular signalling in mammalian cells. *Toxicology and Applied Pharmacology* **144**, 247–261.
- Blackburn EH.** 2000. Telomere states and cell fates. *Nature* **408**, 53–56.
- Blasquez VC, Sperry AO, Cockerill PN, Garrard WT.** 1989. Protein:DNA interactions at chromosomal loop attachment sites. *Genome* **31**, 503–509.
- Bradford MM.** 1976. A rapid and sensitive method for the quantitation of microgram quantities of protein utilizing the principle of protein–dye binding. *Analytical Biochemistry* **72**, 248–254.
- Danon A, Gallois P.** 1998. UV-C radiation induces apoptotic-like changes in *Arabidopsis thaliana*. *FEBS Letters* **437**, 131–136.
- Espinass ML, Carballo M.** 1993. Pulsed-field-gel-electrophoresis analysis of higher-order chromatin structures of *Zea mays*. Highly methylated DNA in the 50 kb chromatin structure. *Plant Molecular Biology* **21**, 847–857.
- Fajkus J, Kovařík A, Kralovics R, Bezděk M.** 1995. Organization of telomeric and subtelomeric chromatin in the higher plant *Nicotiana tabacum*. *Molecular and General Genetics* **247**, 633–638.
- Fajkus J, Fulnečková J, Hulánova M, Berková K, Říha K, Matyášek R.** 1998. Plant cells express telomerase activity upon transfer to callus culture, without extensively changing telomere lengths. *Molecular and General Genetics* **260**, 470–474.
- Fitzgerald MS, McKnight TD, Shippen DE.** 1996. Characterization and developmental patterns of telomerase expression in plants. *Proceedings of the National Academy of Sciences, USA* **93**, 14422–14427.
- Fojtová M, Kovařík A.** 2000. Genotoxic effect of cadmium is associated with apoptotic changes in tobacco cells. *Plant, Cell and Environment* **23**, 531–537.
- Freedman LP, Luisi BF, Korszun ZR, Basavappa R, Sigler PB, Yamamoto KR.** 1988. The function and structure of the metal

- coordination sites within the glucocorticoid receptor DNA binding domain. *Nature* **334**, 543–546.
- Gill BS, Friebe B.** 1998. Plant cytogenetics at the dawn of the 21st century. *Current Opinion in Plant Biology* **1**, 109–115.
- Gorbunova V, Levy AA.** 1997. Non-homologous DNA end joining in plant cells is associated with deletions and filler DNA insertions. *Nucleic Acids Research* **25**, 4650–4657.
- Gromova I, Thomsen B, Razin SV.** 1995. Different topoisomerase II antitumor drugs direct similar specific long-range fragmentation of an amplified c-MYC gene locus in living cells and in high-salt-extracted nuclei. *Proceedings of the National Academy of Sciences, USA* **92**, 102–106.
- Hall RD, Rouwendal GJ, Krens FA.** 1992. Asymmetric somatic cell hybridization in plants. II. Electrophoretic analysis of radiation-induced DNA damage and repair following the exposure of sugarbeet (*Beta vulgaris* L.) protoplasts to UV and gamma rays. *Molecular and General Genetics* **234**, 315–324.
- Hande MP, Lansdorp PM, Natarajan AT.** 1998. Induction of telomerase activity by *in vivo* X-irradiation of mouse splenocytes and its possible role in chromosome healing. *Mutation Research* **404**, 205–214.
- Hartwig A.** 1994. Role of DNA repair inhibition in lead- and cadmium-induced genotoxicity: a review. *Environmental and Health Perspectives* **102**, Supplement 3, 45–50.
- Huang P, Robertson LE, Wright S, Plunkett W.** 1995. High molecular weight DNA fragmentation: a critical event in nucleoside analogue-induced apoptosis in leukemia cells. *Clinical Cancer Research* **1**, 1005–1013.
- Jiang WS, Liu DH, Li MX.** 1994. Effect of Cd²⁺ on the nucleus in root tip cells of *Allium cepa*. *Journal of Environmental Sciences* **6**, 382–386.
- Kato K, Matsumoto T, Koiwai A, Mizusaki S, Nishida K, Noguchi M, Tamaki E.** 1972. In: Terui G, ed. *Fermentation technology today*. Osaka: Society of Fermentation Technology, 689–695.
- Keen NT.** 1990. Gene-for-gene complementarity in plant–pathogen interactions. *Annual Review of Genetics* **24**, 447–463.
- Koukalová B, Kovařík A, Fajkus J, Šíroky J.** 1997. Chromatin fragmentation associated with apoptotic changes in tobacco cells exposed to cold stress. *FEBS Letters* **414**, 289–292.
- Koukalová B, Reich J, Matyášek R, Kuhrová V, Bezděk M.** 1989. A *BamHI* family of highly repetitive DNA sequences of *Nicotiana tabacum*. *Theoretical and Applied Genetics* **78**, 77–80.
- Kovařík A, Fojtová M.** 1999. Estimation of viable cell count after fluorescein diacetate staining using PhosphorImager analysis. *Biotechniques* **27**, 685–688.
- Leteurtre F, Li X, Gluckman E, Carosella ED.** 1997. Telomerase activity during the cell cycle and in gamma-irradiated hematopoietic cells. *Leukemia* **11**, 1681–1689.
- McCabe PF, Leaver CJ.** 2000. Programmed cell death in cell cultures. *Plant Molecular Biology* **44**, 359–368.
- Oberhammer F, Wilson JW, Dive C, Morris ID, Hickman JA, Wakeling AE, Walker PR, Sikorska M.** 1993. Apoptotic death in epithelial cells: cleavage of DNA to 300 and/or 50 kb fragments prior to or in the absence of internucleosomal fragmentation. *EMBO Journal* **12**, 3679–3684.
- O'Brien IE, Baguley BC, Murray BG, Morris BA, Ferguson IB.** 1998. Early stages of the apoptotic pathway in plant cells are reversible. *The Plant Journal* **13**, 803–814.
- Sambrook J, Fritsch EF, Maniatis T.** 1988. *Molecular cloning: a laboratory manual*. New York: Cold Spring Harbor Laboratory Press.
- Sandalio LM, Dalurzo HC, Gomez M, Romero-Puertas MC, del Rio LA.** 2001. Cadmium-induced changes in the growth and oxidative metabolism of pea plants. *Journal of Experimental Botany* **52**, 2115–2126.
- Szabo Jr G, Bacso Z.** 1996. Chromatin isolated from viable human PBLs contains DNA fragmented to > 50 kb. *Cell Death and Differentiation* **3**, 237–241.
- Wang H, Li J, Bostock RM, Gilchrist DG.** 1996. Apoptosis: a functional paradigm for programmed plant cell death induced by a host-selective phytotoxin and invoked during development. *The Plant Cell* **8**, 357–391.
- Zhang Y, Xiao H.** 1998. Antagonistic effect of calcium, zinc and selenium against cadmium-induced chromosomal aberrations and micronuclei in root cells of *Hordeum vulgare*. *Mutation Research* **420**, 1–6.
- Zhang Y, Yang X.** 1994. The toxic effects of cadmium on cell division and chromosomal morphology of *Hordeum vulgare*. *Mutation Research* **312**, 121–126.

Electrochemical monitoring of phytochelatin accumulation in *Nicotiana tabacum* cells exposed to sub-cytotoxic and cytotoxic levels of cadmium

Miroslav Fojta^{a,*}, Miloslava Fojtová^b, Luděk Havran^a,
Hana Pivoňková^a, Vlastimil Dorčák^a, Ivana Šestáková^c

^a *Laboratory of Biophysical Chemistry and Molecular Oncology, Institute of Biophysics, Academy of Sciences of the Czech Republic, Kralovopolska 135, 612 65 Brno, Czech Republic*

^b *Laboratory of Molecular Epigenetics, Institute of Biophysics, Academy of Sciences of the Czech Republic, Kralovopolska 135, 612 65 Brno, Czech Republic*

^c *J. Heyrovsky Institute of Physical Chemistry, Academy of Sciences of the Czech Republic, Dolejskova 3, 182 23 Prague 8, Czech Republic*

Received 9 August 2005; received in revised form 26 October 2005; accepted 31 October 2005

Available online 2 December 2005

Abstract

Cadmium belongs to the most dangerous environmental pollutants among the toxic heavy metals seriously affecting vital functions in both animal and plant cells. It has been previously shown that cadmium ions at 50–100 μM concentrations caused tobacco BY-2 (TBY-2) cells to enter apoptosis within several days of exposure. Phytochelatins (PCs), the “plant metallothioneins”, are cysteine-rich peptides involved in detoxification of heavy metals in plants. The PCs are synthesized in response to the heavy metal exposure. In this paper, we utilized electrochemical analysis to monitor accumulation of PCs in the TBY-2 cells exposed to cadmium ions. Measurements of a characteristic PC signal at mercury electrode in the presence of cobalt ions made it possible to detect changes in the cellular PC levels during the time of cultivation, starting from 30 min after exposure. Upon TBY-2 cultivation in the presence of cytotoxic cadmium concentrations, the PC levels remarkably increased during the pre-apoptotic phase and reached a limiting value at cultivation times coinciding with apoptosis trigger. The PC level observed for a sub-cytotoxic cadmium concentration (10 μM) was about three-times lower than that observed for the 50 or 100 μM cadmium ions after 5 days of exposure. We show that using a simple electrochemical analysis, synthesis of PCs in plant cells can be easily followed in parallel with other tests of the cellular response to the toxic heavy metal stress.

© 2005 Elsevier B.V. All rights reserved.

Keywords: Cadmium; Phytochelatins; Electrochemical analysis; Brdicka reaction; Plant cell; Apoptosis

1. Introduction

Cadmium belongs to the most important industrial pollutants among the toxic heavy metals, representing serious problem for the ecosystem [1–4]. Cadmium at sub-cytotoxic concentrations interferes with DNA repair processes in mammalian cells, inhibits activity of detoxifying enzymes and enhances genotoxicity of mutagens (e.g. UV light). Upregulation of the intracellular signaling pathways leading to increased mitogenesis due to chronic exposure to cadmium ions is supposed to be involved in cadmium carcinogenic activity [5]. In plants,

cadmium was shown to be extremely toxic element inhibiting seed germination and root growth [6,7] and inducing chromosomal aberrations and micronuclei formation [8]. Cadmium ions at the 50–100 μM levels were shown to trigger apoptosis (programmed cell death) in the *Nicotiana tabacum* cell culture TBY-2 [9,10]. Cytotoxic effects of cadmium were concentration-dependent and followed a distinct time course. During the first 3 days of cultivation in medium containing 50 μM CdSO_4 , the cells grew apparently normally, albeit DNA domain fragmentation (a hallmark of early stages of apoptosis) was detected as early as 24 h after exposure [9]. Within this period, the process could be reverted upon transferring the cells into fresh cadmium-free medium [10]. For longer exposure times, typical apoptotic markers were observed, including characteristic changes in cell morphology, DNA fragmentation at the

* Corresponding author. Tel.: +420 5 41517197; fax: +420 5 41211293.
E-mail address: fojta@ibp.cz (M. Fojta).

oligonucleosomal level and considerable decrease of the cell viability.

Phytochelatins (PCs), the “plant metallothioneins”, are the most abundant heavy metal-binding peptides in plants. General formula of the PCs is $(\gamma\text{-Glu-Cys})_n\text{-Gly}$ (where Glu is glutamic acid, Cys cysteine, Gly glycine and n can vary between 2 and 11) [11,12]. Synthesis of the PCs (as well as glutathione, $\gamma\text{-Glu-Cys-Gly}$, the precursor of PCs in the biosynthetic pathway [13–15]) is remarkably induced in the presence of heavy metals (such as zinc, lead, silver and especially cadmium) and thence these peptides are considered to play a crucial role in defense of plant cells against toxic effects of the metals [12,16–20]. The PCs have been utilized also as biomarkers of heavy metal pollution [21].

PCs similarly as animal metallothioneins (MTs) possess a distinct electrochemical behavior. Voltammetric and constant current stripping chronopotentiometry (SCP) analysis in connection with carbon [22], hanging mercury drop (HMDE) [22–28] or solid amalgam electrodes [29] have been employed to study interactions of MTs or PCs with heavy metal ions (zinc, cadmium) and for determination of these species. Due to a high cysteine content these substances exhibit remarkable catalytic hydrogen evolution processes at the HMDE, either in presence (Brdicka reaction [23,25,26,30–33]) or absence (peak H [27,34–37]) of cobalt ions. Both peak H [27] and the Brdicka currents have been utilized in techniques of MT determination in animal tissues [23–26]. Although these processes are not sufficiently selective for the MTs (being yielded also by other SH-containing proteins), the analytical protocols have included a pretreatment step conferring selective removal of higher molecular mass proteins. Some of us recently studied voltammetric behavior of two PC species $(\gamma\text{-Glu-Cys})_2\text{-Gly}$ and $(\gamma\text{-Glu-Cys})_3\text{-Gly}$ (PC2 and PC3, respectively), as well as smaller peptides glutathione and its dipeptidic fragments, at HMDE in the presence of cobalt(II) ions [32]. These peptides underwent, depending on their nature and on conditions used, complex electrode processes including several cobalt prewaves, a signal due to reduction of stable PC–Co complexes, and one or two catalytic Brdicka responses. Results of that study [32] suggested that under certain conditions, the PCs can be distinguished from the other thiol peptides on the basis of their characteristic electrochemical behavior in the presence of cobalt ions.

In this paper, we proposed an electrochemical technique based on SCP measurements in the presence of $[\text{Co}(\text{NH}_3)_6]^{3+}$ complex for monitoring PC synthesis in TBY-2 cells cultured in the presence of sub-cytotoxic and cytotoxic levels of cadmium. Selectivity of a SCP signal, peak a, for the PC species in cell extracts was tested. We show that using a simple electrochemical protocol, changes in the PC levels in plant cell extracts can be easily followed in response to toxic heavy metal exposure.

2. Experimental

2.1. Chemicals

Phytochelatin $(\gamma\text{-Glu-Cys})_3\text{-Gly}$ (PC3) was synthesized and analyzed [38] in the Institute of Organic Chemistry and Bio-

chemistry, Academy of Sciences of the Czech Republic, Prague. Glutathione and CdSO_4 were purchased from Sigma (USA). Other chemicals were of analytical grade.

2.2. Cell culturing, cadmium treatment and preparation of extract

The tobacco bright yellow (TBY-2) cells [39] were grown in standard liquid Murashige and Skoog (MS) medium supplemented with sucrose (3%, w/v), myoinositol (100 mg l^{-1}) and 2,4-dichlorophenoxyacetic acid (0.2 mg ml^{-1}) in 100 ml Erlenmeyer flasks at 27°C with shaking at 120 rpm. The cells were subcultured twice a week. Cell culture at the density about 3 millions cells per ml was passaged with dilution 1:10 to the MS medium supplemented with CdSO_4 to the final concentrations 0, 10, 50 or $100 \mu\text{M}$. After a given time of cultivation, the cells were extensively washed with 0.14 M NaCl, 3 mM KCl, 4 mM Na_2PO_4 , pH 7.4 (PBS), manually homogenized using the homogenization pestle (Eppendorf) and the cell debris was removed by centrifugation (13,000 rpm, 30 min, Eppendorf Minispin centrifuge) (Fig. 1). Prior to the electrochemical measurements, dilution of the cell extracts was normalized to same average protein content through measurements of absorbance at 280 nm [40] (Hewlett-Packard 8452A spectrophotometer). Although this technique offers only fair accuracy when used for determining concentrations of individual proteins and suffers from interference of nucleic acids, components of the cell extracts are expected to yield an average signal which is sufficient for the sample normalization (the PCs themselves do not contribute to A_{280} due to absence of aromatic amino acid residues). All samples were pre-diluted by PBS to $A_{280} = 0.28$ (half of the lowest absorbance observed within the first set of samples).

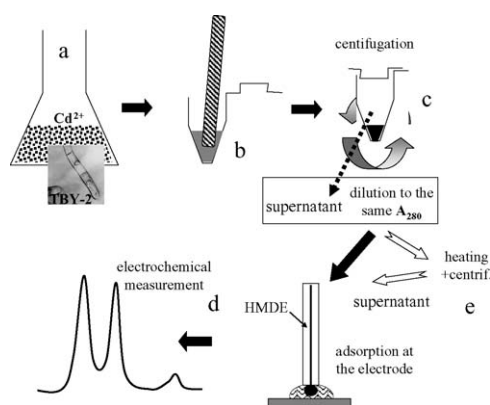


Fig. 1. Schematic representation of the experimental procedure. The TBY-2 cells were cultured in medium containing appropriate concentration of cadmium ions (a). After the given time, the cells were harvested, homogenized (b), and the extracts were clarified by spinning (c). The supernatants were diluted by PBS to reach the same total protein concentration (measured as absorbance at 280 nm; all samples were pre-diluted to $A_{280} = 0.28$). After further dilution (usually to $A_{280} = 0.0028$) by PBS, aliquots of the samples were analyzed electrochemically using the adsorptive transfer stripping procedure (d). Alternatively, the supernatants were thermally treated in boiling water bath (to precipitate selectively high molecular weight proteins) and spun prior to the final dilution (e).

2.3. Electrochemical measurements

The normalized samples were further diluted 100-times (if not stated otherwise) by PBS (in some cases, the supernatants were thermally treated in boiling water bath and spun to remove high molecular weight proteins prior to the final dilution). The diluted extracts were analyzed using the adsorptive transfer stripping (AdTS) procedure [27,30,36,37,41–44]. The HMDE was modified with the cell extracts via immersing the HMDE into 5 μ l aliquots of the samples (Fig. 1) for 60 s. Then the electrode was rinsed in PBS to wash off weakly adsorbed species, transferred into supporting electrolyte (0.1 M ammonium buffer, pH 9.5) containing 1 mM $[\text{Co}(\text{NH}_3)_6]\text{Cl}_3$, and the electrochemical responses were recorded.

All electrochemical measurements were performed in a three electrode setup (using HMDE as working, Ag/AgCl/3 M KCl as reference and platinum wire as counter electrode) with an Autolab analyzer (Eco Chemie, The Netherlands) connected to a VA-Stand 663 (Metrohm, Switzerland). In linear sweep voltammetry, the following settings were used: initial potential -0.1 V, final potential -1.75 V, scan rate 10 – 500 mV s^{-1} , potential step 5 mV. SCP was applied with the following parameters: initial potential -0.1 V, final potential -1.65 V, stripping current -5 μA (if not stated otherwise). All measurements were carried out on air at room temperature.

3. Results and discussion

3.1. Adsorptive transfer stripping electrochemical analysis of TBY-2 cell extracts

Medium exchange (adsorptive transfer stripping, AdTS) techniques have proven advantageous in electrochemical analysis of biomolecules strongly adsorbing at electrode surfaces (thus, creating a biomolecule-modified electrode). Having been originally developed for analysis of nucleic acids [41–44], the procedures based on adsorptive accumulation of the analyte at electrodes from small droplet of sample solutions followed by measurements of the electrochemical signals in blank supporting electrolytes were later successfully applied in studies of bioactive peptides and proteins [30,36,37,42], including metallothioneins [27]. Here, we utilized the AdTS procedure to analyze the extracts of the TBY-2 cells cultured in presence of cytotoxic levels of cadmium ions (Fig. 1).

3.1.1. Linear scan voltammetry

The linear scan voltammetry (LSV) was used as the first-choice technique. Voltammogram recorded with the bare HMDE (not modified with the cell extract) in the $[\text{Co}(\text{NH}_3)_6]\text{Cl}_3$ -containing supporting electrolyte displayed a peak at -1.17 V related to the cobalt reduction (peak Co, Fig. 2). At HMDE modified with extract from TBY-2 cultivated for 2 days in 100 μM CdSO_4 , the peak Co was strongly depressed; instead of it, two poorly developed waves were observed at potentials -1.03 and -1.19 V (Fig. 2). In addition, a large peak appeared at potential around -1.54 V (peak P, Fig. 2). When the HMDE was modified with extract from control TBY-2 cells (cultured in cadmium-free

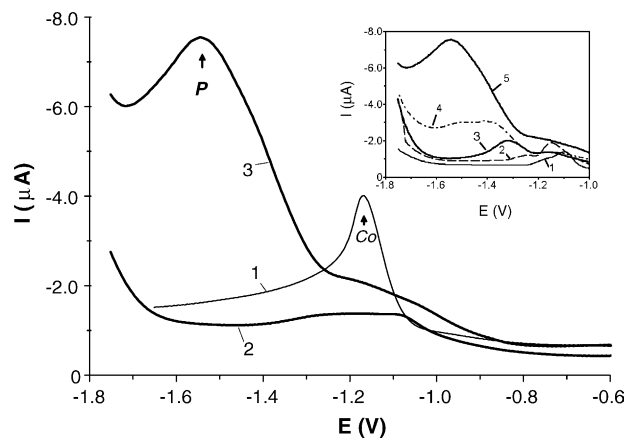


Fig. 2. Sections of AdTS linear sweep voltammograms obtained at the HMDE for supporting electrolyte containing 1 mM $[\text{Co}(\text{NH}_3)_6]\text{Cl}_3$ (with bare HMDE) (curve 1); extract of control TBY-2 cells cultured for 2 days in absence of cadmium (curve 2); extract of TBY-2 cultured for 2 days in 100 μM CdSO_4 (curve 3). The clarified cell extracts were diluted to $A_{280} = 0.0028$ (without any other treatment). The HMDE was immersed to 5 μl droplets of the samples for 60 s, followed by washing and transfer into supporting electrolyte to perform the measurement. The voltammograms were recorded with scan rate 500 mV s^{-1} . Inset, AdTS LS voltammograms of the extract of the cadmium-exposed TBY-2 measured at scan rates 10 (curve 1); 50 (curve 2); 100 (curve 3); 250 (curve 4); 500 mV s^{-1} (curve 5); other details as above.

medium under otherwise the same conditions), the signal due to cobalt reduction was influenced in the same way as in the case of the extract of cells cultivated in the presence of cadmium. On the contrary, no significant current signal in the potential region ≤ -1.30 V was detected with the control extract (Fig. 2).

To check the nature of the peak P, LSV responses of the cell extracts were measured as a function of scan rate (inset in Fig. 2). Intensity of the peak P yielded by the extract from cadmium-exposed cells strongly increased with increasing scan rate and its potential was remarkably shifted towards more negative values. Such behavior resembled that of peak IV previously observed with two synthetic phytochelatin, PC2 and PC3 [32] which was attributed to electrochemical reduction of a stable PC–Co complex formed at the electrode surface, in analogy to complexes $\text{RS}_2\text{–Co}$ formed at the HMDE by animal MTs [23]. The peak IV was characteristic for the PCs rather than for glutathione or its fragments producing a different pattern of signals [32]. Although an exact comparison (based on, e.g. the peak potential values) of the peak IV [32] and peak P (Fig. 2) is difficult due to different conditions used, we suggest that the peak P was yielded PCs synthesized in the TBY-2 cells upon their cultivation in the presence of cadmium ions.

3.1.2. Constant current stripping chronopotentiometry

The LSV measurements (Fig. 2), although revealing large differences between the cadmium-treated and control cell extracts, yielded ill-defined signals not suitable for quantitative evaluation. We therefore tested the SCP that has been successfully applied as a highly sensitive technique in analysis of peptides and proteins at both carbon [45,46] and mercury electrodes [27,30,35]. It proved particularly advantageous in measurements of catalytic signals at the HMDE such as peak H as well as the

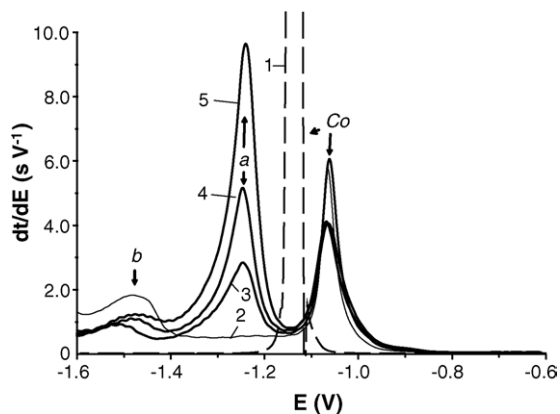


Fig. 3. Sections of AdTS constant current stripping chronopotentiograms obtained for supporting electrolyte containing 1 mM $[\text{Co}(\text{NH}_3)_6]\text{Cl}_3$ (curve 1); extract of control TBY-2 cells cultured for 2 days in absence of cadmium (curve 2); extract of TBY-2 cultured for 2 days in 10 (curve 3); 50 (curve 4); or 100 μM CdSO_4 (curve 5). Stripping current was $-5 \mu\text{A}$; other conditions as in Fig. 2.

Brdicka currents. For example, a peptide vasopressin containing two cysteine residues (forming an S–S bond in the vasopressin native state) yielded two well defined SCP signals in cobalt-containing solutions [30]. Here, we used SCP in the presence of $[\text{Co}(\text{NH}_3)_6]\text{Cl}_3$ for the AdTS measurements using HMDE modified with the TBY-2 cell extracts. Similarly as in the LSV, a remarkable signal related to the cobalt reduction (peak Co) was observed with the bare HMDE (when stripping current of $-5 \mu\text{A}$ was used, Fig. 3). Due to modification of the electrode with the control TBY-2 extract, the peak Co was considerably decreased and shifted to less negative potentials, and two additional signals appeared: one at -1.23 V (peak a which was very small) and -1.48 V (a better developed peak b, Fig. 3). Notably, with the extract from cells cultivated for 2 days in the presence 100 μM CdSO_4 , a large, sharp peak a was obtained (curve 5 in Fig. 3) whose intensity was increased by two orders of magnitude, compared to the same signal yielded by the control extract. On the other hand, intensities of the peak b and peak Co were decreased by 62 and 36%, respectively, compared to the cadmium-untreated control.

The most striking differences between the responses of control and the cadmium-treated cells were observed in the intensity of peak a. In contrast to the LSV peak P (Fig. 2), the SCP peak a (Fig. 3) was narrower, more symmetrical, possessing a flat baseline, and apparently well separated from signals related to other electrode processes. The SCP peak a was therefore chosen as the analytical signal in the following experiments. In SCP, a critical parameter influencing the measured signals is the magnitude of stripping current [47]. We therefore tested the effect of negative stripping current on the peak a yielded by the cadmium-treated TBY-2 extract (Fig. 4). In general, the peak a intensity decreased with increasing value of the negative stripping current ($-i$) and it was shifted to more negative potentials. For $-i = 7.5 \mu\text{A}$, only negligible peak a was obtained, and no signal was detected for $-i = 10 \mu\text{A}$. On the other hand, for $-i$ values $< 3 \mu\text{A}$ the measured peak a heights were affected by partial overlapping with peak b and peak Co (inset in Fig. 4). Intensities of the latter signals exhibited more steep dependences on the stripping cur-

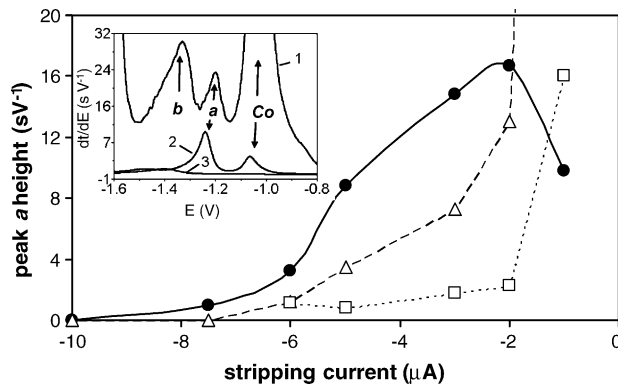


Fig. 4. Dependence of intensities of SCP signals on the stripping current: peak a (●); peak Co (Δ); peak b (□). Inset, sections of AdTS chronopotentiograms obtained at stripping current $-1.0 \mu\text{A}$ (curve 1), $-5.0 \mu\text{A}$ (curve 2) and $-7.5 \mu\text{A}$ (curve 3). Extract of the TBY-2 cells cultured in 100 μM CdSO_4 for 2 days was used for the measurements. For other details see Figs. 2 and 3.

rent (Fig. 4): for $-i = 1 \mu\text{A}$, both peak b and peak Co were more intense than peak a. Due to increasing the $-i$ value, the peak a became dominant (Figs. 3 and 4) and at $-i$ values higher than $5 \mu\text{A}$, the peak b and peak Co practically disappeared. The differences between the behavior of peak a and that of the other two peaks suggest different nature of electrode processes related to these signals. It is likely that the peak a corresponded to the LSV peak P (Fig. 2) (or peak IV [32]) related to the PC–Co complex reduction rather than to a catalytic Brdicka process. This assumption is supported by its specificity for the cadmium-treated cell extracts as well as for the synthetic PC3 (see below). For next measurements, we chose a stripping current value of $-5 \mu\text{A}$ which conferred a good separation of the peak a from the neighboring signals on one hand as well as a reasonable peak a intensity and a good reproducibility on the other.

3.2. Effects of cadmium concentration and of time of TBY-2 cultivation

The SCP responses were measured with extracts of TBY-2 cell cultivated in control (cadmium-free) medium and in the presence of 10, 50 and 100 μM CdSO_4 for 1, 2, 3 and 5 days. The time of the cells cultivation in the control medium influenced significantly intensities of neither peak a (Fig. 5A) nor the other SCP signals observed (not shown). On the other hand, in the presence of cadmium, the peak a height responded remarkably to both CdSO_4 concentration and time of cultivation. For example, sections of SCP curves (showing the peak a) obtained with extracts from cells cultured in different cadmium concentrations for 2 days are shown in Fig. 3. The peak a heights increased with the CdSO_4 concentrations between 10 and 100 μM almost linearly, showing values of 2.3, 4.4 and 6.6 s V^{-1} for 10, 50 and 100 μM , respectively (Figs. 3 and 5B). A similar but less steep dependence was obtained after 1 day of cultivation while after 5 days, the signal increased steeply between 0 and 50 μM cadmium and did not change significantly between 50 and 100 μM CdSO_4 (Fig. 5B).

Dependences of the peak a height on the time of cultivation for different CdSO_4 concentrations are shown in Fig. 5A. In the

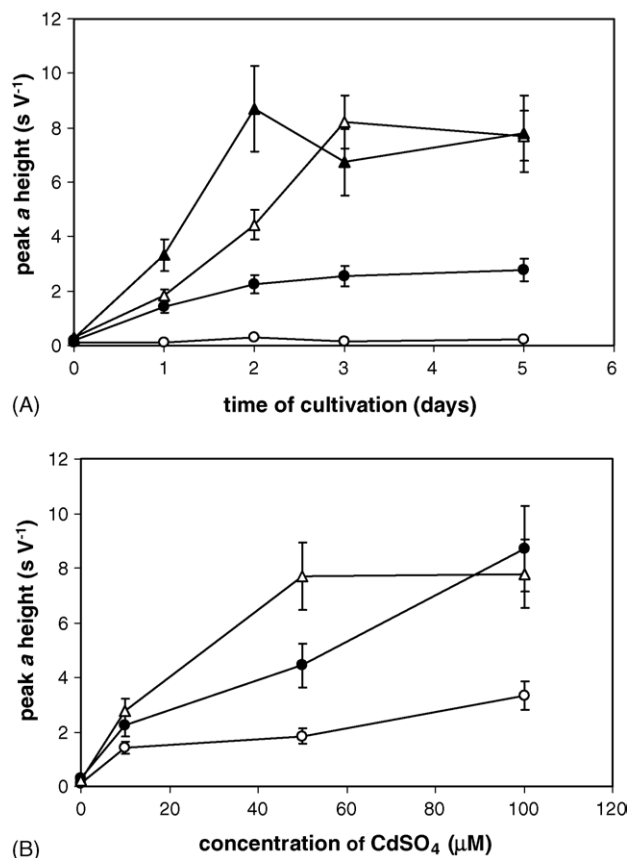


Fig. 5. (A) Dependence of the SCP peak a height on time of TBXY-2 cultivation in absence of cadmium (○); in 10 μM CdSO₄ (●); in 50 μM CdSO₄ (△); or in 100 μM CdSO₄ (▲). (B) Dependence of the SCP peak a height on concentration of CdSO₄ in cultivation medium measured with the TBXY-2 extracts after 1 (○), 2 (●) or 5 (△) days of cultivation. For other details see Figs. 2 and 3.

first day, similar increases in the signal intensity were observed for 10 and 50 μM CdSO₄ (the value obtained for 50 μM was by about 17% higher, compared to signal observed for cells exposed to 10 μM CdSO₄, Fig. 5A), while for 100 μM cadmium the peak a was about twice higher. For longer cultivation times, the 10 μM cadmium ions caused only moderate increase of the signal intensity (compared to the first day) which leveled off after 3 days. On the contrary, the peak a height measured for the extracts of cells cultivated in the presence 50 μM cadmium ions continued to increase steeply (about linearly) up to 3 days. The peak a intensity obtained for 5-day cultivation in 50 μM CdSO₄ was similar (within the relative standard error) as that measured after 3 days for the same cadmium concentration but about three-times higher than the value obtained after 5 days with cells exposed to 10 μM cadmium ions. For cultivation in 100 μM CdSO₄, the peak a intensity exhibited a steep increase only up to 2 days of cultivation. Interestingly, the limiting peak a heights observed after the cells exposure to 50 and 100 μM cadmium were similar (around 8.0 s V⁻¹).

We were further interested how exposure of the TBXY-cells to 10 or 50 μM cadmium ions for short time intervals (1–5 h) influences SCP responses of the cell extracts. Because lower concentrations of the cadmium-induced species were expected to be detected under these conditions, the extracts were ther-

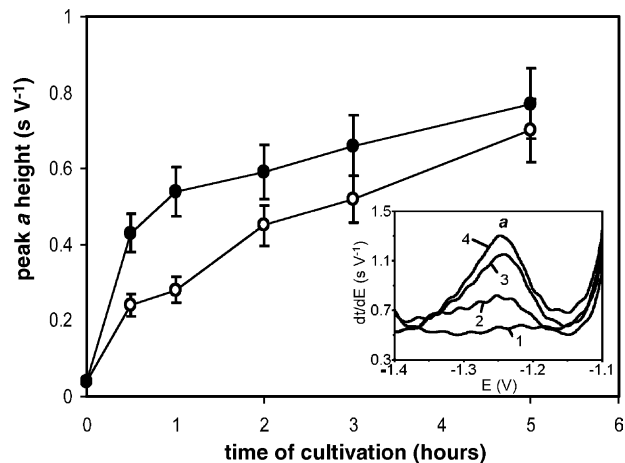


Fig. 6. Dependence of the SCP peak a height on time of TBXY-2 cultivation in 10 μM CdSO₄ (○); or in 50 μM CdSO₄ (●). Inset, sections of chronopotentiograms obtained with extracts of TBXY-2 cultured in absence of cadmium for 5 h (curve 1) or in 10 μM CdSO₄ for 1 h (curve 2), 2 h (curve 3) and 5 h (curve 4). After dilution to A₂₈₀ = 0.28, the extracts were heated in boiling water bath for 10 min followed by removal of precipitate by spinning and dilution of the samples 10-times by PBS. Other conditions as in Figs. 2 and 3.

mally treated (using the procedure usually applied in the metallothionein analysis [23,27,48]) prior to the AdTS procedure to decrease the content of high molecular mass proteins, thus, making the background/signal ratio more favorable. After the heat treatment and spinning-off the precipitate, the samples were 10-times diluted by PBS. A significant increase of the peak a height was observed already after 30 min of exposure of the cells to both 10 and 50 μM CdSO₄ (Fig. 6). For cells exposed to 50 μM cadmium ions, the initial increase of the signal was relatively steep but starting from 1 h, the peak a height increased slowly, following an about linear dependence. For TBXY-2 cultivation in 10 μM cadmium, the signal increased less steeply immediately after exposure (after 1 h reaching about half the value observed upon exposure to 50 μM cadmium) and then followed a similar course as observed for the 50 μM cadmium exposure (up to 1 day after exposure, see above). When the thermal treatment was omitted, reasonable changes in the peak a intensities were observed after 1 h of exposure to 10 or 50 μM CdSO₄ and the signal further changed in similar way as observed with the thermally treated samples (not shown).

3.3. Testing selectivity of the SCP signal and calibration

As shown above, the SCP peak a measured in the TBXY-2 extracts responded remarkably to the cell exposure to cadmium ions. Based on this behavior—and on analogy with a LSV peak P/peak IV [32] (see above)—we assumed that the peak a was due to PCs induced in the tobacco cells by the cadmium. To confirm this assumption, we measured the SCP responses of two synthetic peptides, glutathione and PC3, added to the control TBXY-2 extract. No significant changes on the SCP curve were observed upon addition of 1 μM glutathione while glutathione at concentrations 10 μM, 100 μM and 1 mM yielded (in the region corresponding to the peak a) only a broad, poorly developed signal at potentials around -1.25 V (Fig. 7A). On the contrary,

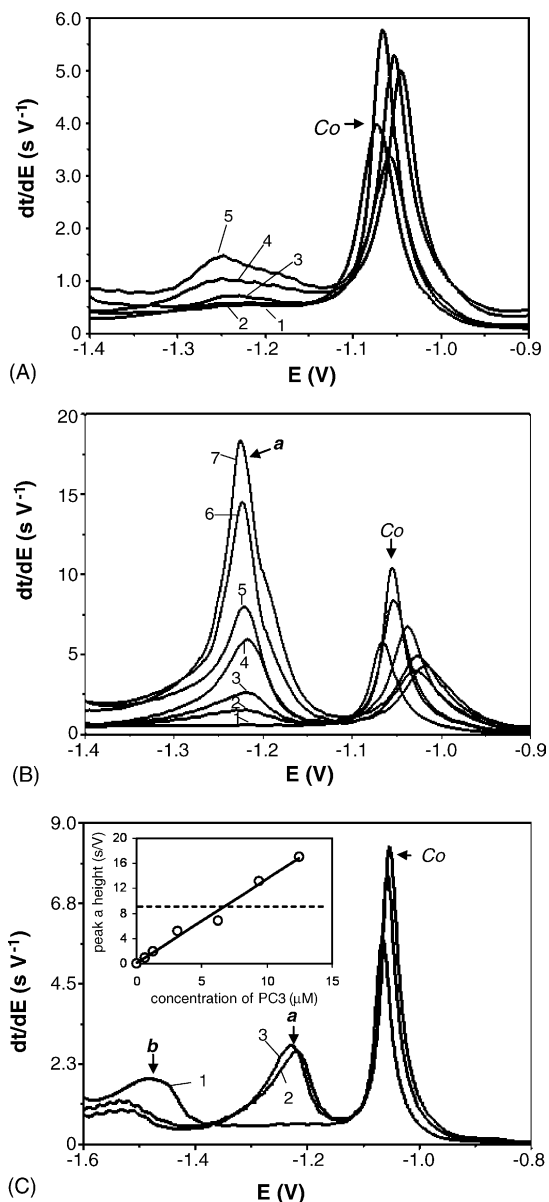


Fig. 7. (A) Sections of chronopotentiograms of the control TBY-2 extract (2-day cultivation, thermally untreated, diluted to $A_{280} = 0.0028$) (curve 1) and the same extract with additions of glutathione: 1 μM (curve 2), 10 μM (curve 3), 100 μM (curve 4), 1 mM (curve 5). (B) Sections of chronopotentiograms of the control TBY-2 extract (as in A) (curve 1) and the same extract with additions of PC3: 0.7 μM (curve 2), 1.25 μM (curve 3), 3.1 μM (curve 4), 6.3 μM (curve 5), 9.4 μM (curve 6), 12.5 μM (curve 7). (C) Sections of chronopotentiograms obtained for extract of control TBY-2 (as in A) (curve 1); the same control extract with addition of 1.25 μM PC (curve 2); extract of TBY-2 cultured in 10 μM CdSO_4 for 1 day (curve 3). Inset, dependence of the SCP peak a height on concentration of PC3 added to the control TBY-2 extract. The dashed line corresponds to maximum peak a heights obtained with cell cultured in 50–100 μM CdSO_4 . For other details see Figs. 2 and 3.

additions of PC3 at concentrations between 0.7 and 12.5 μM resulted in formation of a well defined peak a whose height linearly increased with the PC3 concentration (Fig. 7B and C). Interestingly, extracts from cadmium-treated cells and the control extracts with appropriate additions of synthetic PC3 yielded SCP curves of practically identical shape (in Fig. 7C shown for extract from TBY-2 after 1-day exposure to 10 μM cadmium

and for 1.25 μM PC3 added into 1-day control extract). It can be therefore concluded that the peak a was actually due to phytochelatins synthesized in the tobacco cells under the cadmium stress.

The maximum values of peak a intensity observed with the cadmium-treated cell extracts lay within the linear dependence of the peak a height on concentration of added PC3. The dependence could be therefore used as a calibration curve for estimation of cellular PC levels. The limiting signals obtained for cells exposed to 50 or 100 μM cadmium ions corresponded to about 6 μM PC3 in the solution used for the SCP measurement, while after exposure to 10 μM cadmium the maximum signal corresponded to 2 μM PC3. Considering the cell extracts dilution by two orders of magnitude (the pre-dilution to $A_{280} = 0.28$ was performed by a factor of about 2 for all samples), this corresponded to hundreds-of- μM cellular PC levels. The lowest detectable changes in the PC levels, observed after 60 min exposure of the cells to 10 μM cadmium ions (see above), corresponded to an increase of the PC3 concentration by 0.2 μM . It should be noted that a more precise determination of the PCs in the cells is difficult in this way because in the cells, a mixture of different PC species (differing in the number of $\gamma\text{-Glu-Cys}$ -motifs) occurs and there is no information available either about the SCP behavior of the longer PCs, or about the relative content of individual PCs in the TBY-2 extracts. The current techniques used for monitoring phytochelatin levels in plant material include high performance liquid chromatography, capillary electrophoresis and mass spectroscopy [17,49–51]. These techniques can inherently provide information about distribution of molecular weights of the PC species; on the other hand, they require expensive instrumentation and are more laborious and time consuming, compared to the technique presented here. In some cases estimation of the sum PC level using the electrochemical analysis may be sufficient, as documented by the remarkable correlation between the electrochemically estimated PC levels and other aspects of the cellular response to the presence of the toxic heavy metal (growth suppression, loss of viability, apoptosis, etc.; see below).

3.4. Changes of the PC levels and trigger of apoptosis

Our results suggest a massive PC synthesis in the TBY-2 cells exposed to cytotoxic levels of cadmium in the lag phase that precedes triggering of irreversible apoptotic processes [9,10]. During this lag phase the cells exhibited apparently full cell viability, albeit extensive domain fragmentation of DNA (into pieces of chromatin loop size) was observed. In this phase the cells can be recovered from the cadmium stress via passaging into a fresh cadmium-free medium [10]. The pre-apoptotic phase coincided with the phase of continuously increasing PC levels (detected through measurements of the SCP peak a). Treatment of the cells with cytotoxic cadmium concentrations resulted in reaching a limiting PC level which was similar for both 50 and 100 μM CdSO_4 but was observed after different exposure times (3 and 2 days, respectively; Figs. 5A and 8). Strikingly, attainment of the critical PC level was followed by the apoptosis onset in both cases [9]. On the other hand, 10 μM cadmium (which

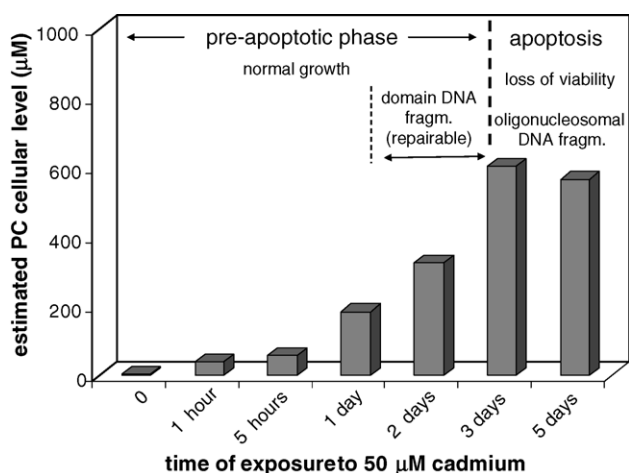


Fig. 8. Correlation between phytochelatin levels, TB Y-2 cell growth and apoptosis manifestation during 5 days of TB Y-2 cultivation in the presence of 50 μM CdSO_4 . The PC levels continuously increased in first 3 days of cultivation. During this period, the cells grew practically normally despite an extensive domain DNA fragmentation (observed mainly in the second day) [9]. This DNA damage was repairable upon passing the cells into fresh cadmium-free medium; the cells were recovered from the cadmium stress and survived [10]. In the third day, the PC content reached a limiting level which coincided with loss of the cells viability and appearance of apoptotic markers such as the oligonucleosomal DNA fragmentation in the next days [9]. When cultured in the presence of 100 μM cadmium ions, the critical PC level was reached in the second day after exposure (Fig. 5), again followed by the apoptosis onset [9].

did not exhibit cytotoxic effects under the same conditions [9]) caused induction of considerably lower PC levels within the time intervals tested. In the initial stage after exposure, the effects of 10 and 50 μM cadmium ions (up to 1 day) were apparently similar. Later, the content of PCs induced by the 10 μM CdSO_4 leveled off while the cells were surviving suggesting that the cadmium ions were successfully eliminated by the PC detoxifying system. When cultivated in the presence of 50 μM cadmium ions, the cells continued to produce the PCs until reaching the critical level in the third day and then started dying (Fig. 8). For 100 μM CdSO_4 both the limiting PC level and the markers of irreversible apoptosis were observed in shorter exposure times. Existence of the critical PC level suggests that trigger of the cadmium-induced apoptosis may be somehow related to depletion of capacity of the heavy metal detoxification pathway involving the PCs. Alternatively, the high cellular levels of PCs (and/or their cadmium complexes) may be cytotoxic by themselves in accordance with observations that overexpression of PC synthase leads to cadmium hypersensitivity rather than tolerance in *Arabidopsis thaliana* transgenic lines [49].

3.5. Conclusions

Electrochemical techniques, especially those utilizing catalytic signals at mercury electrodes, have been successfully applied in analysis of animal metallothioneins. On the other hand, similar applications in analysis of plant phytochelatin are still scarce; the existing literature on PC electrochemistry is focused on basic electrochemical studies of these peptides and/or of their metal complexes [22,28,29,32,38,46,52–54] rather than

to detection of PCs in plant cells or tissues. In this paper, we utilized characteristic chronopotentiometric signals yielded by the PCs in cobalt-containing solutions [32] to monitor PC synthesis in the TB Y-2 cells exposed to cytotoxic and sub-cytotoxic concentrations of cadmium. Using adsorptive transfer stripping procedure and a SCP peak a, it was possible to follow the PC levels in the cell extracts with an acceptable relative standard error (below 20% for parallel TB Y-2 culture samples; the reproducibility of the transfer stripping step itself corresponded to a relative standard deviation of about 8% when five successive measurements of the same sample were performed). The signal clearly increased with the time of the cells exposure to cadmium (10–100 μM) starting from 30 min up to initiation of the cell death. No sample pretreatment except normalization on the total protein content and suitable dilution was in principle necessary. Upon cultivation with cytotoxic cadmium concentrations, the cellular PC concentrations remarkably increased until reaching a limiting level (6×10^{-4} M, normalized to PC3). The phase of continuous PC synthesis coincided with a phase in which the cells exhibited apparently normal growth [9,10], and reaching the critical PC level correlated with loss of the cells viability and their entry into apoptosis. Our results demonstrate that a simple electrochemical technique can be applied to determine the cysteine-rich peptides phytochelatin in the cellular extracts and to monitor changes in the PC levels in response to the toxic heavy metal exposure.

Acknowledgements

This work was supported by a grant A4004402 from the Grant Agency of the Academy of Sciences of the Czech Republic, a grant COST OC D21-002 from the Ministry of Education, Youth and Sports of the Czech Republic, and a grant No. AVOZ50040507.

References

- [1] M. Valko, H. Morris, M.T.D. Cronin, *Curr. Med. Chem.* 12 (2005) 1161.
- [2] M. Satoh, H. Koyama, T. Kaji, H. Kito, C. Tohyama, *Tohoku J. Exp. Med.* 196 (2002) 23.
- [3] P. Das, S. Samantaray, G.R. Rout, *Environ. Pollut.* 98 (1997) 29.
- [4] L.P. Freedman, B.F. Luisi, Z.R. Korszun, R. Basavappa, P.B. Sigler, K.R. Yamamoto, *Nature* 334 (1988) 543.
- [5] D. Beyersmann, S. Hechtenberg, *Toxicol. Appl. Pharm.* 144 (1997) 247.
- [6] D.H. Liu, W.S. Jiang, M.X. Li, *Acta Scientiae Circumstantiae* 12 (1992) 339.
- [7] B. Chakravarty, S. Srivastava, *Mutat. Res.* 283 (1992) 287.
- [8] Y. Zhang, H. Xiao, *Mutat. Res.* 420 (1998) 1.
- [9] M. Fojtova, A. Kovarik, *Plant Cell Environ.* 23 (2000) 531.
- [10] M. Fojtova, J. Fulneckova, J. Fajkus, A. Kovarik, *J. Exp. Bot.* 53 (2002) 2151.
- [11] M.H. Zenk, *Gene* 179 (1996) 21.
- [12] W.E. Rauser, *Plant Physiol.* 109 (1995) 1141.
- [13] E. Grill, S. Löffler, E.L. Winnacker, M.H. Zenk, *Proc. Natl. Acad. Sci. U.S.A.* 86 (1989) 6838.
- [14] O.K. Vatamaniuk, S. Mari, A. Lang, S. Chalasani, L.O. Demkiv, P.A. Rea, *J. Biol. Chem.* 279 (2004) 22449.
- [15] M.J. Dominguez, F. Gutierrez, R. Leon, C. Vilchez, J.M. Vega, J. Vigar, *Plant Physiol. Biochem.* 41 (2003) 828.
- [16] M. Wojcik, J. Vangronsveld, A. Tukiendorf, *Environ. Exp. Bot.* 53 (2005) 151.

- [17] M. Wojcik, A. Tukiendorf, *Plant Growth Regul.* 44 (2004) 71.
- [18] W.E. Rauser, R. Schupp, H. Rennenberg, *Plant Physiol.* 97 (1991) 128.
- [19] W.E. Rauser, *Plant Sci.* 51 (1987) 171.
- [20] S. Clemens, C. Simm, *N. Phytol.* 159 (2003) 323.
- [21] W.G. Keltjens, M.L. van Beusichem, *J. Plant Nutr.* 21 (1998) 635.
- [22] I. Sestakova, P. Mader, *Cell. Mol. Biol.* 46 (2000) 257.
- [23] B. Raspor, M. Paic, M. Erk, *Talanta* 55 (2001) 109.
- [24] C. Mouneyrac, C. Amiard-Triquet, J.C. Amaird, P.S. Rainbow, *Comp. Biochem. Phys. C* 129 (2001) 193.
- [25] R.W. Olafson, P.E. Olsson, *Methods Enzymol.* 205 (1991) 205.
- [26] R.W. Olafson, *J. Biol. Chem.* 256 (1981) 1263.
- [27] R. Kizek, L. Trnkova, E. Palecek, *Anal. Chem.* 73 (2001) 4801.
- [28] H. Vodickova, V. Pacakova, I. Sestakova, P. Mader, *Chem. Listy* 95 (2001) 477.
- [29] B. Yosypchuk, I. Sestakova, L. Novotny, *Talanta* 59 (2003) 1253.
- [30] M. Tomschik, L. Havran, M. Fojta, E. Palecek, *Electroanalysis* 10 (1998) 403.
- [31] R. Brdicka, *Collect. Czech. Chem. C* 5 (1933) 112.
- [32] V. Dorcak, I. Sestakova, *Bioelectrochemistry* 68 (2005) 14.
- [33] M. Heyrovsky, *Electroanalysis* 16 (2004) 1067.
- [34] R. Kizek, J. Vacek, L. Trnkova, B. Klejdus, L. Havel, *Chem. Listy* 98 (2004) 166.
- [35] M. Tomschik, L. Havran, E. Palecek, M. Heyrovsky, *Electroanalysis* 12 (2000) 274.
- [36] L. Havran, S. Billova, E. Palecek, *Electroanalysis* 16 (2004) 1139.
- [37] M. Masarik, A. Stobiecka, R. Kizek, F. Jelen, Z. Pechan, W. Hoyer, T.M. Jovin, V. Subramaniam, E. Palecek, *Electroanalysis* 16 (2004) 1172.
- [38] B.H. Cruz, J.M. Diaz-Cruz, I. Sestakova, J. Velek, C. Arino, M. Esteban, *J. Electroanal. Chem.* 520 (2002) 111.
- [39] T. Nagata, Y. Nemoto, S. Hasezawa, *Int. Rev. Cytol.* 132 (1992) 1.
- [40] C.M. Schoscheck, *Methods Enzymol.* 182 (1990) 50.
- [41] E. Palecek, I. Postbieglova, *J. Electroanal. Chem.* 214 (1986) 359.
- [42] E. Palecek, F. Jelen, C. Teijeiro, V. Fucik, T.M. Jovin, *Anal. Chim. Acta* 273 (1993) 175.
- [43] E. Palecek, M. Fojta, F. Jelen, V. Vetterl, in: A.J. Bard, M. Stratsmann (Eds.), *The Encyclopedia of Electrochemistry*, vol 9: *Bioelectrochemistry*, Wiley/VCH, Weinheim, 2002, p. 365.
- [44] M. Fojta, *Collect. Czech. Chem. C* 69 (2004) 715.
- [45] X. Cai, G. Rivas, P.A.M. Farias, H. Shiraishi, J. Wang, M. Fojta, E. Palecek, *Anal. Chim. Acta* 332 (1996) 49.
- [46] I. Sestakova, M. Kopanica, L. Havran, E. Palecek, *Electroanalysis* 12 (2000) 100.
- [47] J. Wang, *Analytical Electrochemistry*, VCH Publishers Inc., New York, 1994.
- [48] M. Erk, D. Ivankovic, B. Raspor, J. Pavicic, *Talanta* 57 (2002) 1211.
- [49] S. Lee, J.S. Moon, T.S. Ko, D. Petros, P.B. Goldsbrough, S.S. Korban, *Plant Physiol.* 131 (2003) 656.
- [50] E.A. Maier, R.D. Matthews, J.A. McDowell, R.R. Walden, B.A. Ahner, *J. Environ. Qual.* 32 (2003) 1356.
- [51] S. Mounicou, V. Vacchina, J. Szpunar, M. Potin-Gautier, R. Lobinski, *Analyst* 126 (2001) 624.
- [52] G. Scarano, E. Morelli, *Electroanalysis* 10 (1998) 39.
- [53] I. Sestakova, H. Vodickova, P. Mader, *Electroanalysis* 10 (1998) 764.
- [54] B.H. Cruz, J.M. Diaz-Cruz, C. Arino, M. Esteban, *Environ. Sci. Technol.* 39 (2005) 778.

Telomere maintenance in liquid crystalline chromosomes of dinoflagellates

Miloslava Fojtová · Joseph T. Y. Wong ·
Martina Dvořáčková · Kosmo T. H. Yan ·
Eva Sýkorová · Jiří Fajkus

Received: 29 January 2010 / Revised: 11 March 2010 / Accepted: 11 March 2010 / Published online: 6 April 2010
© Springer-Verlag 2010

Abstract The organisation of dinoflagellate chromosomes is exceptional among eukaryotes. Their genomes are the largest in the Eukarya domain, chromosomes lack histones and may exist in liquid crystalline state. Therefore, the study of the structural and functional properties of dinoflagellate chromosomes is of high interest. In this work, we have analysed the telomeres and telomerase in two Dinoflagellata species, *Karenia papilionacea* and *Cryptocodinium cohnii*. Active telomerase, synthesising exclusively *Arabidopsis*-type telomere sequences, was detected in cell extracts. The terminal position of TTTAGGG repeats was determined by in situ hybridisation and BAL31 digestion methods and provides evidence for the linear characteristic of dinoflagellate chromosomes. The length of telomeric tracts, 25–80 kb, is the largest among unicellular eukaryotic organisms to date. Both the presence

of long arrays of perfect telomeric repeats at the ends of dinoflagellate chromosomes and the existence of active telomerase as the primary tool for their high-fidelity maintenance demonstrate the general importance of these structures throughout eukaryotes. We conclude that whilst chromosomes of dinoflagellates are unique in many aspects of their structure and composition, their telomere maintenance follows the most common scenario.

Introduction

The development of nucleosomes and chromosomes probably allowed for the evolution of larger genomes in the eukaryotes. However, the largest known eukaryotic genomes are harboured by nucleosomeless chromosomes of unicellular microorganisms from the phylum Dinoflagellata. As many dinoflagellates are autotrophic, the group is normally considered to be an algal group. Molecular phylogenetic analysis suggests that the dinoflagellates, the apicomplexans and the ciliates form the Alveolates (Fast et al. 2002). The haploid genomes of dinoflagellates can be as large as 400 pg (cf. 3 pg in humans; Spector et al. 1981). Most interestingly, the chromosomes of dinoflagellates are completely devoid of core histones, but contain a group of histone-like proteins related to the prokaryotic HU protein (Rizzo and Nooden 1972; Wong et al. 2003). The ratio of nuclear proteins to DNA content in dinoflagellate chromosomes (1:10) is much lower than in most eukaryotes (1:1; Bohrmann et al. 1993; Kellenberger and Arnold-Schulz-Gahmen 1992). As much as 70% of thymine bases in the total DNA of dinoflagellates are modified and replaced with the rare bases 5-hydroxymethyluracil (Rae 1973, 1976). Transmission electron microscopy, polarising light microscopy and analysis of circular dichroism suggest that the

Communicated by I. Schubert

M. Fojtová · M. Dvořáčková · E. Sýkorová · J. Fajkus (✉)
Department of Functional Genomics and Proteomics, Institute
of Experimental Biology, Faculty of Science, Masaryk University,
Kotlářská 2,
CZ-61137 Brno, Czech Republic
e-mail: fajkus@sci.muni.cz

M. Fojtová · M. Dvořáčková · E. Sýkorová · J. Fajkus
Institute of Biophysics,
Academy of Sciences of the Czech Republic, v.v.i.,
Královopolská 135,
CZ-61265 Brno, Czech Republic

J. T. Y. Wong · K. T. H. Yan
Department of Biology,
Hong Kong University of Science & Technology,
Clear Water Bay,
Kowloon, Hong Kong Special Administrative Region,
People's Republic of China

dinoflagellate chromosomes are in liquid crystalline states (Livolant 1978, 1984; Rill et al. 1989).

Telomeres are structurally and functionally important parts of linear eukaryotic chromosomes and distinguish the natural chromosome ends from unrepaired chromosomal breaks. The main functions of telomeres are the maintenance of genomic loci at chromosome termini during DNA replication and the prevention of chromosome end fusions. Incomplete lagging strand synthesis leads to chromosome shortening during each successive replication cycle. When a critical minimum length is reached, telomere protective function is abolished and chromosome ends become indistinguishable from DNA breaks. Cells with non-functional telomeres become senescent or undergo apoptosis. Alternatively, inappropriate repair events can occur, resulting in progressive genome instability (reviewed in Blackburn 2001). Sequence composition of telomere minisatellite repeats is highly conserved throughout eukaryotic organisms: TTAGGG in humans and other vertebrates (Moyzis et al. 1988), TTTAGGG in most plants (Richards and Ausubel 1988), TTGGGG in *Tetrahymena* (Blackburn and Gall 1978) and TTAGG in insects (Okazaki et al. 1993). In a more detailed view, the human-type telomeric motif has been found also in many invertebrates, as well as in *Trypanosoma brucei* and *Leishmania major* from the Trypanosomatida order, in slime moulds *Didymium iridis* and *Physarum polycephalum*, in fungi *Magnaporthe grisea*, *Neurospora crassa* and *Histoplasma capsulatum* (reviewed in Teixeira and Gilson 2005) and in species from the order of monocotyledonous plants Asparagales (Sykorova et al. 2006a, b). Telomeric sequence referred to as “insect” is in fact a common motif found in divergent species of the Arthropoda phylum. The occurrence of telomeric repeats of the common sequence pattern (dT/A_{1–4}dG_{1–8})_n across the protozoa, fungi, metazoa and higher plants demonstrates their universal function in chromosome protection and genome stability. The length of telomeric arrays is highly variable not only among species but also among different chromosome ends in the same cell. So far, no direct or universal relationship has been found between telomere length and other factors like genome size, chromosome size or chromosome arm size. Moreover, attempts to detect these canonical telomeres failed in some orders of insect (Sahara et al. 1999) and some genera of plant families Solanaceae and Alliaceae (Sykorova et al. 2003a, b; Sykorova et al. 2006a, b).

Telomeres are typically maintained by telomerase, an enzyme responsible for adding telomeric repeats to the chromosomes ends, using the mechanism of reverse transcription. Telomerase consists of at least two subunits, the catalytic subunit TERT (telomerase reverse transcriptase) and the TR subunit (telomerase RNA) which serves as a template for the telomere motif elongation. Both essential telomerase subunits were characterised in many model organisms (yeast, protozoa, human and plants). Besides telomerase, alternative

(telomerase-independent) mechanisms of telomere lengthening (ALT) have been described in various model organisms. These can function as the essential telomere maintenance system as seen in plants in the genera *Allium* or *Cestrum* (Sykorova et al. 2003a, b; Sykorova et al. 2006a, b) and in the dipteran genus *Chironomus* (Saiga and Edstrom 1985). Alternatively, these mechanisms can act as a backup system, functioning in case of the loss of telomerase activity, as demonstrated in yeast, human and plant telomerase mutants (Bryan et al. 1997; Lundblad and Blackburn 1993; Ruckova et al. 2008). The wide repertoire of organisms using ALT at least in the latter role suggests that ALT is probably the original, ancestral mechanism of telomere maintenance which preceded the advent of the apparently more aggressive (in terms of its fast and early expansion throughout all today's major eukaryotic kingdoms) telomerase system (Fajkus et al. 2005; Nosek et al. 2006).

The presence of telomeres at chromosome ends is supposed to be a general attribute of linear eukaryotic chromosomes. In this respect, the extremely large and specifically organised genomes of the dinoflagellates are of high interest. Dinoflagellate chromosomes stay condensed throughout the cell cycle and replicate via closed mitosis (Soyer-Gobillard et al. 1999). Microtubules are formed in tunnels (cytoplasmic channels) surrounded by the nuclear envelope. In mitotic cells, two daughter chromatids begin to split at one end and attach to the membrane of cytoplasmic channels at the other end (Bhaud et al. 2000; Leadbeater and Dodge 1967). It is still uncertain whether the dinoflagellate chromosomes attach directly or indirectly to the extranuclear microtubules through the nuclear envelope (Leadbeater and Dodge 1967). These observations suggest that ends of dinoflagellate chromosomes have novel properties and additional functions in chromosome segregation. Although in situ hybridisation has confirmed the presence of eukaryotic telomeric sequences on dinoflagellate chromosomes (Alverca et al. 2007), a detailed characterisation of canonical telomere structures has not yet been performed, and evidence of active telomerase is still lacking. In this paper, we demonstrate the presence of plant-type telomeric tracts at the ends of dinoflagellate chromosomes which are tens of kilobases long. Moreover, active telomerase synthesising these repeats was detected in dinoflagellate cell extracts.

Materials and methods

Cultivation of Dinoflagellata species *C. cohnii* and *K. papilionacea*

The *Cryptothecodinium cohnii* Biecheler strain 1649 was obtained from the Culture Collection of Algae at the

University of Texas at Austin maintained in MLH liquid medium (Tuttle and Loeblich 1975) and incubated at 28°C in the dark (Fig. 1a).

Karenia papilionacea was an isolated strain from seawater collected at the university pier of Hong Kong University of Science and Technology (Yeung et al. 2005; Yeung and Wong 2008) and maintained in f/2 medium (Guillard and Ryther 1962) at 18°C under a daily cycle of 12-h light and 12-h darkness (Fig. 1b).

Analysis of telomerase activity

Preparation of protein extracts *K. papilionacea* culture (100 ml) with a density of about 5×10^3 cells per millilitre was gently centrifuged (2,000 rpm, 10 min, 4°C). Cells were resuspended in 50 μ l nuclear preparation buffer [NPB; 1 mM Tris-HCl, pH 8.0, 1.5 mM MgCl₂, 10 mM KCl, 0.1 mM DTT, 0.5% NP-40 (BDH Chemicals, Poole, UK); 1×

protease inhibitors (phenylmethylsulphonyl fluoride, PMSF; 0.5 μ g/ml (Sigma, St. Louis, MO, USA); aprotinin 0.01 μ g/ml (USB, Cleveland, Ohio, USA); pepstatin 0.01 μ g/ml, (USB); leupeptin 0.01 μ g/ml (Sigma)]. *C. cohnii* culture (30 ml) with a density of about 3×10^5 cells per millilitre was centrifuged (2,000 rpm, 10 min, 4°C). The pellet was resuspended in 800 μ l NPB and cells were disintegrated using a disruptor (Constant Systems, Daventry, UK). For the telomere repeat amplification protocol (TRAP) assay, both extracts were diluted 1:20 with NPB. As a control, a protein extract from 7-day-old *Arabidopsis thaliana* seedlings was prepared according to the protocol described previously (Fitzgerald et al. 1996; Sykorova et al. 2003a, b).

In vitro telomerase activity assay Telomerase activity was determined by a two-step TRAP assay (Sykorova et al. 2003a, b). First, 1 μ l of 10 μ M substrate primer was mixed with 1 μ l of telomerase extract (10^4 cell equivalent). Primer

Fig. 1 Bright field and fluorescence photomicrographs of *C. cohnii* (a) and *K. papilionacea* (b). Fluorescence staining was carried out with DNA-binding dye DAPI according to protocol previously published (Yeung et al. 2005). The scale bar is 10 μ m

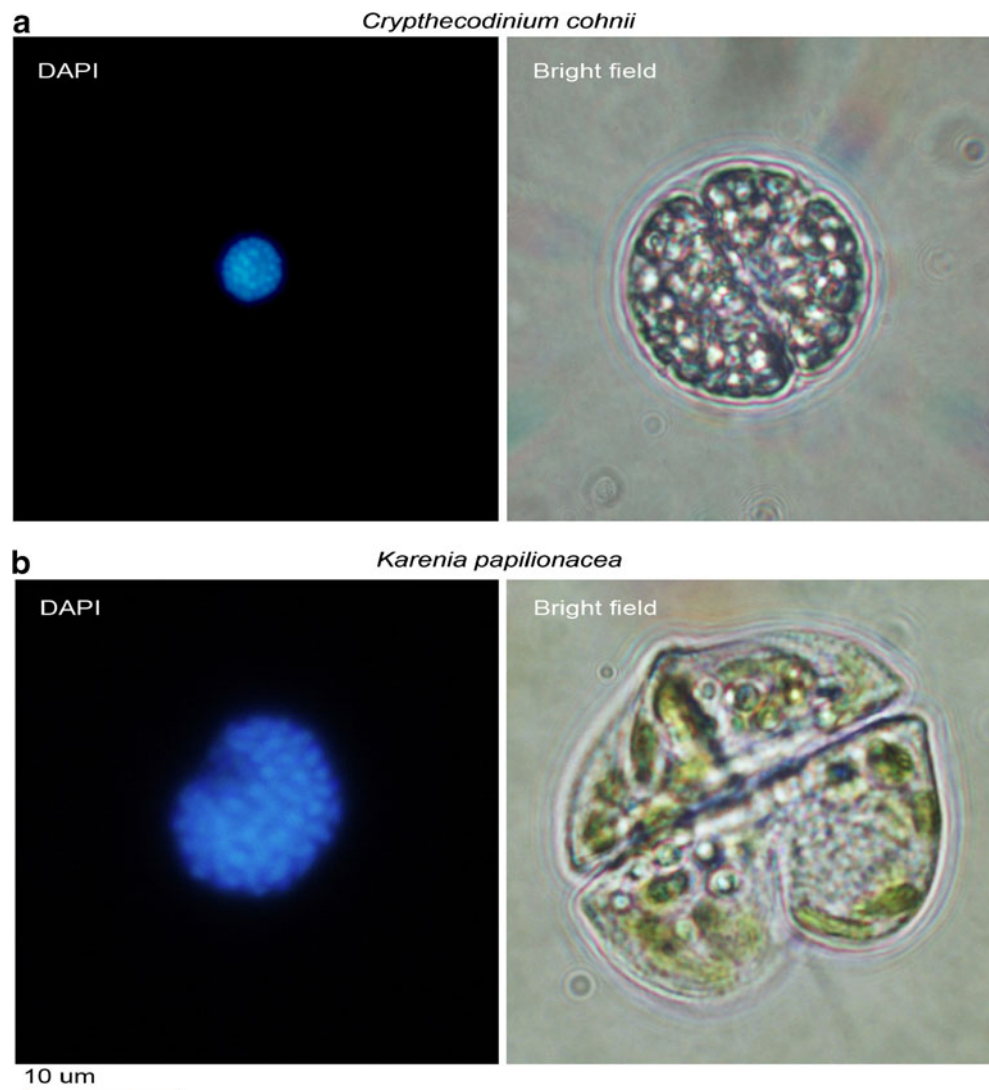


Table 1 Sequences of the primers used in the TRAP assay

Forward (substrate) primers	Reverse primers
TS21 5'GACAATCCGTC GAGCAGAGTT 3'	TelPr 5'CCGAATTCAACCCT (AAACCCT) ₂ AAACCC3' TTSBCN 5'(CAACCC) ₄ 3' HUTC 5'(AACCCCT) ₃ AAC 3'
GG21 5'CACTATCGACT ACGCGATCGG 3'	PLTC 5'(CCCTAAA) ₃ 3'

elongation proceeded in 25 µl of reaction buffer at 26°C (unless otherwise stated) for 45 min. After extension, telomerase was heat-inactivated for 10 min at 95°C and cooled to 80°C. One microlitre of 10 µM of the reverse primer and 2 U of Taq DNA Polymerase (NEB, Beverly, MA, USA) were added to start the PCR step of the TRAP (35 cycles of 95°C/30 s, 65°C/30 s, 72°C/30 s) followed by a final extension of 72°C/5 min. Electrophoresis was performed on products of the TRAP reaction on a 12.5% polyacrylamide gel in 0.5× TBE buffer; gel was stained with SybrGreen I dye (Roche Applied Science, Mannheim, Germany). Gel imaging was performed using the LAS-3000 system (Fuji Film, Tokyo, Japan). Primer sequences are given in Table 1.

Cloning of TRAP products Products of the TRAP reactions were cloned into the pCRII-TOPO vector and transformed into TOP10 chemically competent *Escherichia coli* cells according to the instructions in the TOPO TA cloning kit (Invitrogen, Carlsbad, CA, USA). Eight clones each from *K. papilionacea* and *C. cohnii* were sequenced using M13 forward and M13 reverse primers, respectively.

Telomere length analysis

Cells from 300 ml of the *K. papilionacea* culture (about 1.5×10^6 cells) were collected by centrifugation (2,000 rpm, 5 min, 4°C). The cell pellet was lysed by washing it four times with 1 ml of hypotonic buffer (NPB), and the final nuclear sediment was resuspended in 100 µl NPB. The nuclear suspension was added to an equal volume of 2% low-melting-point agarose in water equilibrated to 42°C and homogenised by pipetting up and down. The resulting mixture was pipetted into a disposable plug mould (Bio-Rad, Hercules, CA, USA). After solidifying, plugs were incubated in TES buffer (0.5 M EDTA, pH 8.0; 10 mM Tris-HCl, pH 8.0; 1.0% lauroylsarcosine) for 30 min at 37°C and then at 50°C in fresh TES buffer with proteinase K (Roche Diagnostics, final concentration 500 µg/ml) for 24 h. Deproteinised plugs were washed twice in TE (10 mM Tris-HCl, pH 8.0; 1 mM EDTA, pH 8.0) for 30 min, then

twice in TE with 1 mM PMSF for 30 min, and finally in 0.1×TE buffer (3×30 min).

BAL31 digestion was performed according to previously published protocol (Sykorova et al. 2006a, b). Briefly, the samples in agarose plugs were equilibrated in BAL31 nuclease buffer (NEB) for 30 min and digested with 3 U of BAL31 nuclease (NEB) for 15, 30, 45, 90 or 120 min in a Thermomixer (Eppendorf AG, Hamburg, Germany) at 30°C. Reactions were terminated by buffer exchange with 50 mM EGTA, pH 8.0, and BAL31 nuclease was irreversibly inactivated by incubation at 58°C for 15 min. The plugs were then washed three times in 0.1× TE buffer and subsequently equilibrated in the appropriate restriction enzyme buffer. Restriction enzyme digestion was performed as described previously (Fajkus et al. 1998). After digestion, the solution containing low-molecular-mass fractions of digested DNA was ethanol-precipitated and dissolved in TE for analysis by conventional agarose gel electrophoresis and Southern hybridisation. High-molecular-mass fractions, which were retained in the agarose plugs, were analysed by pulsed-field gel electrophoresis (PFGE) using the Gene Navigator system (GE Healthcare, Little Chalfont, UK) under the following conditions: 1% agarose gel (Serva, Heidelberg, Germany) in 0.5× TBE buffer, 190 V, pulses 2 s for 1 h, followed by 18 h of pulse time ramping from 2 to 20 s, and then 20 s for 1 h at 14°C. Both conventional and PFGE gels were alkali-blotted and hybridised with end-labelled telomeric oligonucleotide probe (CCCTAAA)₄. Hybridisation signals were visualised with a FLA-7000 phosphorimaging system (Fuji Film).

In situ analysis of telomeres

Sample preparation *K. papilionacea* nuclear suspension (1 ml) in NPB was spun down (2,000 rpm, 5 min, 4°C) and the pellet washed several times in 1 ml of freshly made cold fixative (3:1 EtOH/acetic acid). Nuclei were resuspended in a final volume of 200 µl, and 10 µl of this suspension was dropped on a microscopic slide, mixed with 10 µl of 60% acetic acid, and the slide was heated briefly in a flame three times to remove the cytoplasm. Chromosomes were squashed, followed by an additional fixation for 2 min in 3:1 EtOH/acetic acid.

Fluorescence in situ hybridisation Slides were washed in 2× standard saline citrate (SSC) for 5 min, treated with RNase A (100 µg/ml, Sigma) for 1 h at 37°C, washed in 2× SSC for 2× 5 min, in 0.01 M HCl for 1×2 min and treated with pepsin (10 µg/ml) for 10 min at 37°C, followed by three 5-min washes in 2× SSC. The sample was then post-fixed in 10% formaldehyde/1× PBS (phosphate buffered saline) for 10 min and washed in 2× SSC for 2×5 min. Twenty microlitres of hybridisation mix (10% dextran sulphate, 65% deionised formamide and 0.2 µl of telomeric peptide nucleic acid probe

(TTTAGGG)_n) was applied to each slide. The denaturation step was carried out in a microwave oven for 1 min at 500 W and hybridisation overnight at 37°C. Non-specific signals were removed in two washing steps, 2× SSC at 60°C for 3× 3 min and 2× SSC at 42°C for 3× 3 min, and slides viewed on a Zeiss Axio imager microscope (<http://www.zeiss.cz/>). All incubation steps were performed in a moist chamber. Acquired images were processed with Image J software (<http://rsbweb.nih.gov/ij/>).

Results

Active telomerase in the dinoflagellate cell extracts

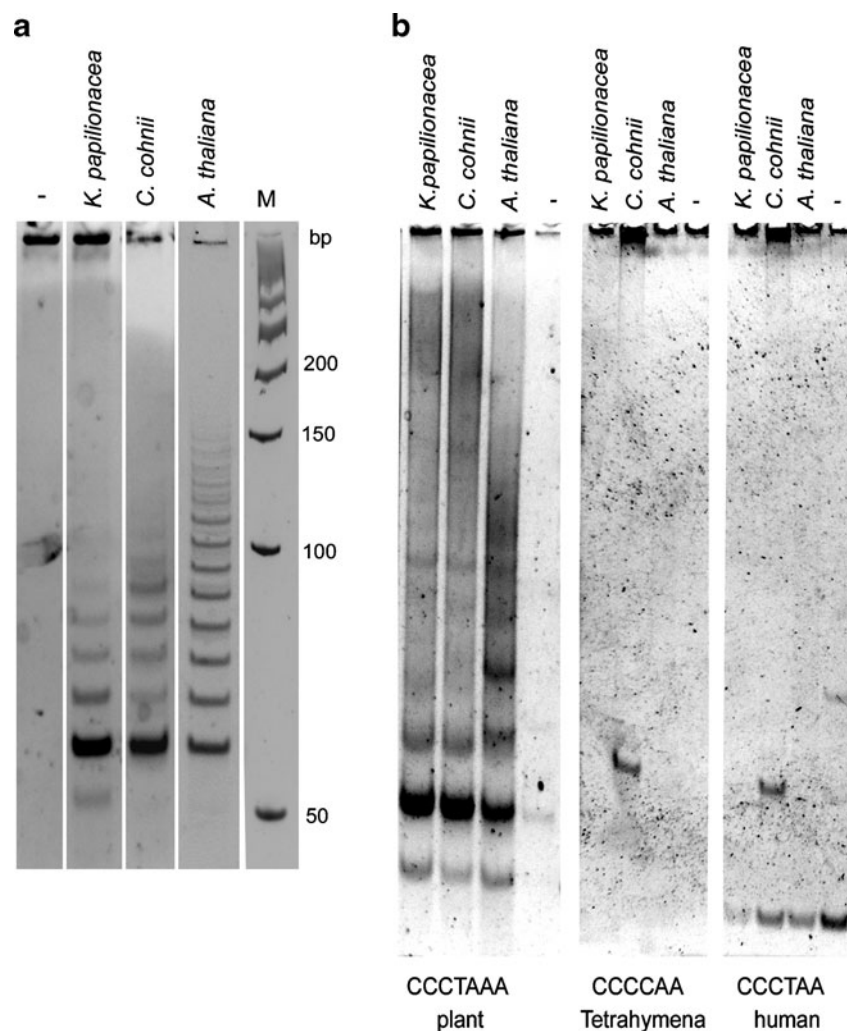
The ladders presented after PAGE separation of the TRAP products using plant-specific primers TS21 and TelPr (Table 1) corresponded to the ladder observed in the control reaction with the telomerase extract from *A. thaliana*

seedlings (Fig. 2a). Adjacent products in these ladders differ by 7 bp in length. A processive telomerase activity has been observed in both analysed Dinoflagellata species, but a higher processivity was observed in *Crypthecodinium*.

The presence of *Arabidopsis*-type telomere repeats in the Dinoflagellata species was confirmed using also the primer set GG21 and PLTC (Table 1) for the plant TRAP assay according to Fitzgerald et al. (1996) (Fig. 2b, left panel). When the reverse primer specific for the *Tetrahymena*-type telomeric sequence (TTSBCN) and human-type telomeric sequence (HUTC) was used for the amplification of telomerase products, no specific PCR product was obtained (Fig. 2b, middle and right panels, respectively). These results are consistent with the idea that the dinoflagellate chromosome ends are formed by TTTAGGG repeats.

Taking into consideration different cultivation temperatures of *Karenia* and *Crypthecodinium* cells (18°C and 28°C, respectively), the extension step of the TRAP assay was performed also at 18°C (instead of 26°C in the standard protocol). No differences in *Karenia* telomerase processivity

Fig. 2 In vitro telomerase activity assay. **a** Telomerase activity was determined in *K. papilionacea* and *C. cohnii* cell extracts according to the TRAP protocol using the primer set TS21 and TelPr (see Table 1). **b** In vitro telomerase activity assay with the alternative primer sets. The TRAP assay was performed with GG21 and PLTC primers (specific for amplification of the plant-type telomeric repeat), TS21 and TTSBCN primers (*Tetrahymena*-type telomeric repeats) and TS21 and HUTC primers (human-type telomeric repeats). The sequence motifs of the reverse primers and telomere types are depicted below the panels. The negative controls (– lanes) contain no protein extract. An extract from *A. thaliana* 7-day-old seedlings was used as a control. Lane M contains a 50-bp DNA ladder (GeneRuler, Fermentas)



were observed (not shown), suggesting in vitro enzyme tolerance to a higher temperature.

To unambiguously identify the sequence or sequences, which were produced by telomerases in *Cryptothecodinium* and *Karenia* species, the products of TRAP assays were cloned into the TOPO vector and sequenced from both ends. Clones of various insert sizes, ranging from one to nine added telomeric repeats, were obtained in *Cryptothecodinium* and *Karenia*, thus reflecting the ladder-like pattern of TRAP products. In *Karenia*, eight clones containing one to eight telomeric repeats were obtained, and eight clones containing two to nine repeats were obtained in *Cryptothecodinium*. Thus, 52 telomeric repeats (harbouring 364 nucleotides) were sequenced in total in both species. The results show that telomerases of both *Cryptothecodinium* and *Karenia* synthesise exclusively the *Arabidopsis*-type telomere repeat sequence (TTTAGGG)_n. The absence of any inaccuracy in a total of 364 analysed nucleotides points to the astonishing fidelity of telomerases in both species.

Length of dinoflagellate telomeric repeats ranges between 25 and 80 kb

The length of telomeres in the *Karenia* cells was assessed as terminal restriction fragments (TRFs). In this method, high-molecular-weight (HMW) DNA is digested by frequently cutting enzymes with recognition sites which are supposedly absent in the highly conserved G/C asymmetrical telomere repeats. Due to the absence of a relevant protocol for isolation of HMW DNA from *Cryptothecodinium* species, telomere lengths could only be determined for *Karenia* in this study. HMW DNA isolated from *Karenia* cells was digested by two restriction endonucleases commonly used in TRF analysis: *Hinf*I (G↓ANTC) and *Hae*III (GG↓CC). Restriction fragments ranging between 25 and 80 kb were detected by Southern blot hybridisation with an end-labelled plant telomeric probe (Fig. 3).

To confirm the localisation of the TTTAGGG repeats at chromosome ends, BAL31 exonuclease (degrading both 3' and 5' termini of duplex DNA, without generating internal scissions) was applied for increasing time intervals prior to *Hae*III digestion. With progressive BAL31 cleavage, the positive bands were associated with decreasing molecular weight positions and lower intensity of hybridisation signal (Fig. 4a, lanes 0 to 120). This result thus reflects the terminal, i.e. telomeric, position of the hybridising fragments.

The low-molecular-weight DNA eluted from the agarose plugs during enzyme digestions was collected by ethanol precipitation and analysed by conventional agarose electrophoresis and Southern hybridisation (Fig. 4b). Multiple weakly hybridising bands can be observed which are resistant to BAL31 cleavage, possibly representing short clusters of internal telomeric repeats.

Dinoflagellate telomeres in situ

Distribution of *Arabidopsis*-type telomeric sequence (TTTAGGG)_n on *K. papilionacea* chromosomes was analysed in detail by fluorescence in situ hybridisation (FISH) with a peptide nucleic acid (PNA) probe. The telomeric probe clearly labelled chromosome ends, although signal intensity was rather variable, suggesting a certain level of heterogeneity in telomere lengths among individual chromosomes (Fig. 5a, b). These FISH results are thus consistent with the TRF analysis reported above (Fig. 3) where telomere lengths showed a range of 25–80 kb.

Fluorescence signals were mostly present at chromosome ends, but a few interstitial telomeric blocks were also detected (arrowed in Fig. 5c). Majority of the nuclei contained compacted chromosomes, suggesting that the cells were at the G1 stage, as evaluated in accordance to previous observations (Bhaud et al. 2000). In cells with less condensed chromatin (these can be more easily evaluated), more than one telomeric signal was found at a single chromosomal end, as shown in Fig. 5c in detail.

Discussion

We demonstrate for the first time that telomeres of dinoflagellate chromosomes are maintained by telomerase. This further supports the hypothesis that a markedly different way and degree of folding of dinoflagellate

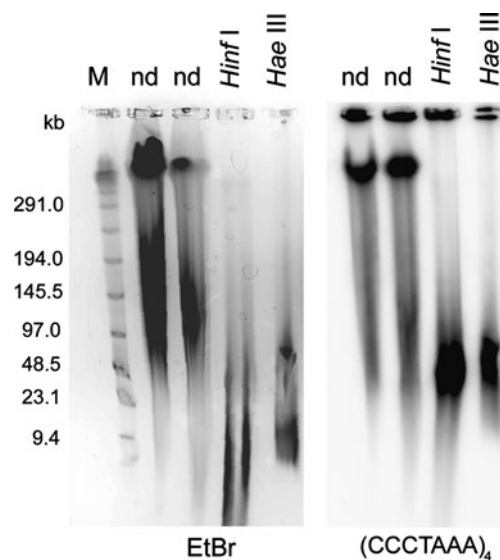


Fig. 3 Analysis of telomere length in *K. papilionacea* by the TRF method. High-molecular-weight DNA from *K. papilionacea* cells was digested by *Hinf*I and *Hae*III restriction endonucleases, respectively, separated using pulsed-field gel electrophoresis and hybridised with radioactively labelled oligonucleotide probe (CCCTAAA)₄. Hybridisation signals correspond to compact telomeric blocks. *nd* non-digested DNA, *M* DNA size marker (low-range PFG Marker, NEB)

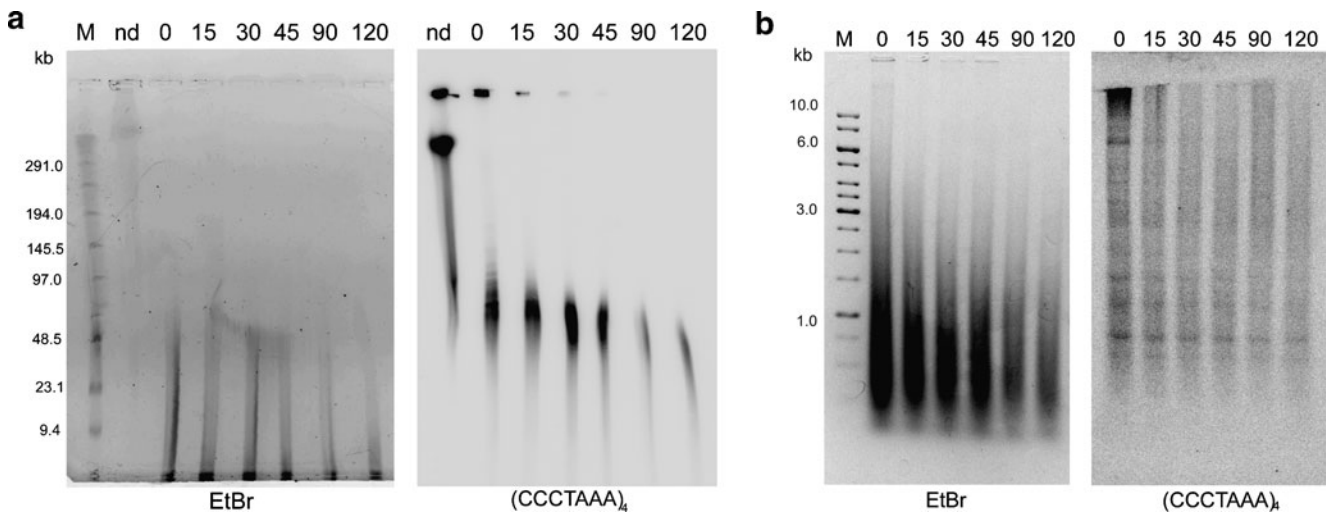


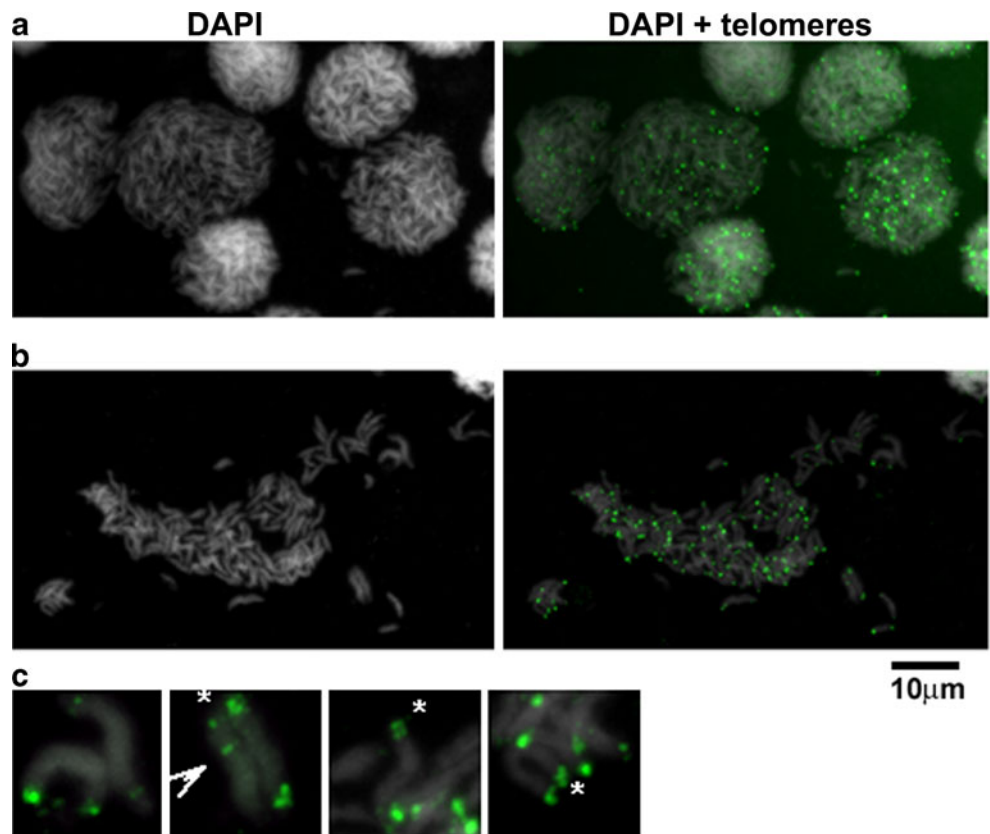
Fig. 4 Telomeric sequences of *K. papilionacea* are sensitive to BAL31 digestion. High-molecular-weight DNA from *K. papilionacea* cells was digested by BAL31 exonuclease followed by *Hae*III cleavage and separated using pulsed-field gel electrophoresis (a). The low-molecular-weight fraction was subjected to conventional 1% agarose gel electrophoresis (b). DNA transferred to a nylon membrane was analysed by Southern hybridisation with radioactively labelled oligonucleotide probe (CCCTAAA)₄. The numbers above lines (0, 15, 30, 45, 90, 120) indicate the length of BAL31 digestion in minutes. *nd*

non-digested DNA, *M* DNA size markers (low-range PFG Marker, NEB in a; GeneRuler 1 kb DNA ladder, Fermentas in b). Reduced hybridisation signal intensity with prolonged BAL31 treatment in (a) proves the terminal position of the restriction fragments. Weak hybridisation signals insensitive to BAL31 in (b) represent interstitial telomeric sequences in the *Karenia* genome. Apparent decrease of signal intensity reflects variation in sample loading (compare to the EtBr panel) rather than changes due to BAL31 treatment

chromatin does not contradict their eukaryotic character. Moreover, the presence of telomeres and telomerase points to the linear character of dinoflagellate chromosomes, in

accordance with previous evidence showing telomere-like signals in FISH experiments using the *Arabidopsis*-type telomeric probe (Alverca et al. 2007). In addition to

Fig. 5 Fluorescence in situ labelling of *Karenia* chromosomes to localise telomeric sequences (a, b). All nuclei are equally labelled with (TTTAGGG)_n telomeric PNA probe, green, which clearly labels chromosome ends. DNA is stained with DAPI (1 µg/µl), grey. c Detail of telomeric FISH showing occurrence of multiple telomeric signals at individual chromosome ends (asterisk) and interstitial telomeric blocks (arrowhead)



confirming the presence of *Arabidopsis*-type telomere sequences in dinoflagellates, we also present evidence of direct telomerase involvement in telomere maintenance and observe striking sequence fidelity of telomere synthesis in both *Karenia* and *Cryptothecodinium* telomerases. This precision of synthesis is particularly interesting since it does not seem to be common among the closest relatives of the phylum Dinoflagellata. For example, in the related phylum of Apicomplexa, the species *Theileria parva* (Nene et al. 2000) comprises mixed telomeric arrays consisting of TTTTAGGG and TTTAGGG units which constitute <10 kb blocks at its chromosome ends. In the genus *Plasmodium*, again from the phylum Apicomplexa, the sequence TT(T/C)AGGG constitutes telomeres of 1.2 kb in *Plasmodium falciparum* and 6.7 kb in *Plasmodium vivax* (see Scherf et al. 2001 for a review). In *Cryptosporidium parvum*, imperfect repeats of the general formula $T_{[2-12]}AG_{[2-6]}$ were found with the TTTAGG sequence unit occurring most frequently. The second sister phylum, Ciliophora, includes several classical model organisms used in telomere biology: *Tetrahymena* species with TTGGGG repeats, *Paramecium* species possessing TTGGG(T/G) units and *Stylonychia*, *Oxytricha* and *Euplotes* with TTTTGGGG telomeric repeats. Telomere lengths in this group are typically several kilobases in the micronucleus, but significantly shorter (only tens of base pairs) in the macronucleus (see Prescott 1994 for a review). The above diversity of telomeric DNA sequences among representatives of the phyla Ciliophora and Apicomplexa, as well as the frequent occurrence of degenerated telomere motifs within these phyla, is in sharp contrast with those features present in both species of the Dinoflagellata phylum analysed in this work. *Karenia* and *Cryptothecodinium* belong to two separate major orders of dinoflagellates, the GPP complex (Gymnodinales, Peridinales and Procentrales plus others) and the Gonyaulacales, respectively, together encompassing most of the living families of dinoflagellates (Benett and Wong 2006; Gast and Caron 1996; Haywood et al. 2004; Saunders et al. 1997). The two species also represent very different mode of lives: *K. papilionacea* is an athecate autotrophic species, whereas *C. cohnii* is a thecat heterotrophic dinoflagellate. The *Arabidopsis*-type telomere repeat seems to be a common feature even among evolutionarily distant dinoflagellate genera as it is present in *Prorocentrum micans* and *Amphidinium arterae* (Alverca et al. 2007) as well as in *K. papilionacea* and *C. cohnii* (this study).

In addition, the telomere lengths determined in *K. papilionacea* in this work (25–80 kb) are more than an order of magnitude longer than any others previously described in Alveolata. In fact, they possibly represent the longest telomeres ever observed in unicellular organisms. Dinoflagellates have the largest genomes among eukaryotic

organisms, with the haploid DNA content per nucleus (the DNA *C* value) ranging between 4 and 400 pg. The DNA *C* values vary over five orders of magnitude among eukaryotic organisms—from 0.005 pg in yeast up to 400 pg in dinoflagellates. The mean *C* value in mammals is 3.4 pg, ranging from 1.7 to 8.4 pg (i.e., ~5-fold). The *C* value in angiosperms is varying through a much wider range—from 0.06 to 127.4 pg (i.e., 2,000-fold; reviewed in Kejnovsky et al. 2009). Considering the aforementioned DNA *C* values in dinoflagellates, these species are on the top of this scale. Moreover, non-coding repetitive sequences may make up 60% of dinoflagellate genomes, and their distribution may be linked to the specific and atypical chromosome organisation found in these species (Moreau et al. 1998). In this respect, the unusual length of telomeric tracts may reflect these specificities of dinoflagellate genomes. However, more extensive studies are needed to judge whether telomeres that are markedly longer but homogeneous in sequence are typically present in most dinoflagellates, as well as whether these telomeres are in any way related to the unique way of chromatin structure in these enigmatic organisms. In this perspective, analysis of sequence composition and length of telomeric regions of symbiotic dinoflagellates, whose genomes consist of significantly fewer chromosomes than those of their free-living counterparts, may possess particularly interesting results.

Dinoflagellates are unique unicellular model organisms displaying both prokaryotic and eukaryotic features. Nevertheless, the presence of long telomeric arrays of conserved *Arabidopsis*-type telomeric repeats which are maintained by telomerase demonstrates the general importance of telomere maintenance for the stability and proper function of linear eukaryotic chromosomes even if these chromosome exist in a liquid crystalline state as in the case of free-living dinoflagellate species.

Acknowledgements This work has been supported by the Grant Agency of the Czech Republic (521/09/1912), Czech Ministry of Education (LC06004), institutional funding (MSM0021622415, AV0Z50040507, AV0Z50040702) and by CERG grants HKUST6421/06M from the Research Grant Council of Hong Kong and RPC06/07.SC10 (from the University Grant Council of Hong Kong) to J. T. Y. Wong. The technical assistance of Jana Kapustová and Marcela Šefčíková is highly appreciated. Elizabeth McCarthy (School of Biological and Chemical Sciences, Queen Mary, University of London) is acknowledged for language revision.

References

- Alverca E, Cuadrado A, Jouve N, Franca S, de la Espina SMD (2007) Telomeric DNA localization on dinoflagellate chromosomes: structural and evolutionary implications. *Cytogenet Genome Res* 116:224–231
- Benett MJ, Wong JTY (2006) Evolution and diversity of dinoflagellates: molecular perspectives. In: Sharma AK, Sharma A (eds)

- Plant genome: biodiversity and evolution. Science Publishers, Enfield, pp 89–116
- Bhaud Y, Guillebault D, Lennon J, Defacque H, Soyer-Gobillard MO, Moreau H (2000) Morphology and behaviour of dinoflagellate chromosomes during the cell cycle and mitosis. *J Cell Sci* 113(Pt 7):1231–1239
- Blackburn EH (2001) Switching and signaling at the telomere. *Cell* 106:661–673
- Blackburn EH, Gall JG (1978) A tandemly repeated sequence at the termini of the extrachromosomal ribosomal RNA genes in *Tetrahymena*. *J Mol Biol* 120:33–53
- Bohrmann B, Haider M, Kellenberger E (1993) Concentration evaluation of chromatin in unstained resin-embedded sections by means of low-dose ratio-contrast imaging in STEM. *Ultra-microscopy* 49:235–251
- Bryan TM, Englezou A, Dalla-Pozza L, Dunham MA, Reddel RR (1997) Evidence for an alternative mechanism for maintaining telomere length in human tumors and tumor-derived cell lines. *Nat Med* 3:1271–1274
- Fajkus J, Fulneckova J, Hulanova M, Berkova K, Riha K, Matyasek R (1998) Plant cells express telomerase activity upon transfer to callus culture, without extensively changing telomere lengths. *Mol Gen Genet* 260:470–474
- Fajkus J, Sykorova E, Leitch AR (2005) Telomeres in evolution and evolution of telomeres. *Chromosome Res* 13:469–479
- Fast NM, Xue L, Bingham S, Keeling PJ (2002) Re-examining alveolate evolution using multiple protein molecular phylogenies. *J Eukaryot Microbiol* 49:30–37
- Fitzgerald MS, McKnight TD, Shippen DE (1996) Characterization and developmental patterns of telomerase expression in plants. *Proc Natl Acad Sci USA* 93:14422–14427
- Gast RJ, Caron DA (1996) Molecular phylogeny of symbiotic dinoflagellates from planktonic foraminifera and radiolaria. *Mol Biol Evol* 13:1192–1197
- Guillard RRL, Ryther JH (1962) Studies of marine planktonic diatoms. *Cyclotella nana* Hustedt and *Detonula confervacea* Cleve. *Can J Microbiol* 8:229–239
- Haywood AJ, Steidinger KA, Truby EW, Bergquist PR, Bergquist PL, Adamson J, Mackenzie L (2004) Comparative morphology and molecular phylogenetic analysis of three new species of the genus *Karenia* (Dinophyceae) from New Zealand. *J Phycol* 40:165–179
- Kejnovsky E, Leitch IJ, Leitch AR (2009) Contrasting evolutionary dynamics between angiosperms and mammalian genomes. *Trends Ecol Evol* 24:572–582
- Kellenberger E, Arnold-Schulz-Gahmen B (1992) Chromatins of low-protein content: special features of their compaction and condensation. *FEMS Microbiol Lett* 79:361–370
- Leadbeater B, Dodge JD (1967) An electron microscope study of nuclear and cell division in a dinoflagellate. *Arch Mikrobiol* 57:239–254
- Livolant F (1978) Positive and negative birefringence in chromosomes. *Chromosoma* 68:45–58
- Livolant F (1984) Cholesteric organization of DNA in vivo and in vitro. *Eur J Cell Biol* 33:300–311
- Lundblad V, Blackburn EH (1993) An alternative pathway for yeast telomere maintenance rescues est1- senescence. *Cell* 73:347–360
- Moreau H, Geraud ML, Bhaud Y, Soyer-Gobillard MO (1998) Cloning, characterization and chromosomal localization of a repeated sequence in *Cryptocodinium cohnii*, a marine dinoflagellate. *Int Microbiol* 1:35–43
- Moyzis RK, Buckingham JM, Cram LS, Dani M, Deaven LL, Jones MD, Meyne J, Ratliff RL, Wu JR (1988) A highly conserved repetitive DNA sequence, (TTAGGG)_n, present at the telomeres of human chromosomes. *Proc Natl Acad Sci USA* 85:6622–6626
- Nene V, Bishop R, Morzaria S, Gardner MJ, Sugimoto C, ole-MoiYoi OK, Fraser CM, Irvin A (2000) *Theileria parva* genomics reveals an atypical apicomplexan genome. *Int J Parasitol* 30:465–474
- Nosek J, Kosa P, Tomaska L (2006) On the origin of telomeres: a glimpse at the pre-telomerase world. *BioEssays* 28:182–190
- Okazaki S, Tsuchida K, Maekawa H, Ishikawa H, Fujiwara H (1993) Identification of a pentanucleotide telomeric sequence, (TTAGG)_n, in the silkworm *Bombyx mori* and in other insects. *Mol Cell Biol* 13:1424–1432
- Prescott DM (1994) The DNA of ciliated protozoa. *Microbiol Rev* 58:233–267
- Rae PM (1973) 5-Hydroxymethyluracil in the DNA of a dinoflagellate. *Proc Natl Acad Sci USA* 70:1141–1145
- Rae PM (1976) Hydroxymethyluracil in eukaryote DNA: a natural feature of the pyrophyta (dinoflagellates). *Science* 194:1062–1064
- Richards EJ, Ausubel FM (1988) Isolation of a higher eukaryotic telomere from *Arabidopsis thaliana*. *Cell* 53:127–136
- Rill RL, Livolant F, Aldrich HC, Davidson MW (1989) Electron microscopy of liquid crystalline DNA: direct evidence for cholesteric-like organization of DNA in dinoflagellate chromosomes. *Chromosoma* 98:280–286
- Rizzo PJ, Nooden LD (1972) Chromosomal proteins in the dinoflagellate alga *Gyrodinium cohnii*. *Science* 176:796–797
- Ruckova E, Friml J, Prochazkova Schrupfova P, Fajkus J (2008) Role of alternative telomere lengthening unmasked in telomerase knock-out mutant plants. *Plant Mol Biol* 66:637–646
- Sahara K, Marec F, Traut W (1999) TTAGG telomeric repeats in chromosomes of some insects and other arthropods. *Chromosome Res* 7:449–460
- Saiga H, Edstrom JE (1985) Long tandem arrays of complex repeat units in Chironomus telomeres. *EMBO J* 4:799–804
- Saunders GW, Hill DRA, Sexton JP, Andersen RA (1997) Small-subunit ribosomal RNA sequences from selected dinoflagellates: testing classical evolutionary hypotheses with molecular systematic models. In: Bhattacharya D (ed) *Plant systematics and evolution*. Springer, New York, pp 237–259
- Scherf A, Figueiredo LM, Freitas-Junior LH (2001) Plasmodium telomeres: a pathogen's perspective. *Curr Opin Microbiol* 4:409–414
- Soyer-Gobillard MO, Gillet B, Geraud ML, Bhaud Y (1999) Dinoflagellate chromosome behaviour during stages of replication. *Int Microbiol* 2:93–102
- Spector DL, Vasconcelos AC, Triemer RE (1981) DNA duplication and chromosome structure in the dinoflagellates. *Protoplasma* 105:185–194
- Sykorova E, Lim KY, Chase MW, Knapp S, Leitch IJ, Leitch AR, Fajkus J (2003a) The absence of *Arabidopsis*-type telomeres in *Cestrum* and closely related genera *Vestia* and *Sessea* (Solanales): first evidence from eudicots. *Plant J* 34:283–291
- Sykorova E, Lim KY, Kunicka Z, Chase MW, Bennett MD, Fajkus J, Leitch AR (2003b) Telomere variability in the monocotyledonous plant order Asparagales. *Proc Biol Sci* 270:1893–1904
- Sykorova E, Fajkus J, Meznikova M, Lim KY, Nepelchova K, Blattner FR, Chase MW, Leitch AR (2006a) Minisatellite telomeres occur in the family Alliaceae but are lost in *Allium*. *Am J Bot* 93:814–823
- Sykorova E, Leitch AR, Fajkus J (2006b) Asparagales telomerases which synthesize the human type of telomeres. *Plant Mol Biol* 60:633–646
- Teixeira MT, Gilson E (2005) Telomere maintenance, function and evolution: the yeast paradigm. *Chromosome Res* 13:535–548
- Tuttle RC, Loeblich AR (1975) An optimal growth medium for the dinoflagellate *Cryptocodinium cohnii*. *Phycologia* 14:1–8
- Wong JT, New DC, Wong JC, Hung VK (2003) Histone-like proteins of the dinoflagellate *Cryptocodinium cohnii* have homologies to bacterial DNA-binding proteins. *Eukaryot Cell* 2:646–650
- Yeung PKK, Hung VKL, Chan FK, Cand JTY (2005) Characterization of a *Karenia*-like dinoflagellate from the South China Sea. *J Mar Biol Assoc UK* 85:779–781
- Yeung PKK, Wong JTY (2008) A *Karenia papilionacea* species complex in the Western Pacific. The 13th International Conference on Harmful Algae, Hong Kong

RESEARCH PAPER

Molecular analysis of T-DNA insertion mutants identified putative regulatory elements in the *AtTERT* gene

Miloslava Fojtová^{1,2}, Vratislav Peška^{1,2}, Zuzana Dobšáková^{1,*}, Iva Mozgová², Jiří Fajkus^{1,2} and Eva Sýkorová^{1,2,†}

¹ Institute of Biophysics, Academy of Sciences of the Czech Republic, v.v.i., Královopolská 135, CZ-61265 Brno, Czech Republic

² Department of Functional Genomics and Proteomics, Faculty of Science and CEITEC - Central European Institute of Technology, Masaryk University, Kotlářská 2, CZ-61137 Brno, Czech Republic

* Present address: Cytogenetics Laboratory Brno, Ltd, Veveří 39, CZ-60200 Brno, Czech Republic

† To whom correspondence should be addressed. E-mail: evin@ibp.cz

Received 13 April 2011; Revised 1 July 2011; Accepted 5 July 2011

Abstract

Analysis of plants bearing a T-DNA insertion is a potent tool of modern molecular biology, providing valuable information about the function and involvement of genes in metabolic pathways. A collection of 12 *Arabidopsis thaliana* lines with T-DNA insertions in the gene coding for the catalytic subunit of telomerase (*AtTERT*) and in adjacent regions was screened for telomerase activity [telomere repeat amplification protocol (TRAP) assay], telomere length (terminal restriction fragments), and *AtTERT* transcription (quantitative reverse transcription-PCR). Lines with the insertion located upstream of the start codon displayed unchanged telomere stability and telomerase activity, defining a putative minimal *AtTERT* promoter and the presence of a regulatory element linked to increased transcription in the line SALK_048471. Lines bearing a T-DNA insertion inside the protein-coding region showed telomere shortening and lack of telomerase activity. Transcription in most of these lines was unchanged upstream of the T-DNA insertion, while it was notably decreased downstream. The expression profile varied markedly in mutant lines harbouring insertions at the 5' end of *AtTERT* which showed increased transcription and abolished tissue specificity. Moreover, the line FLAG_385G01 (T-DNA insertion inside intron 1) revealed the presence of a highly abundant downstream transcript with normal splicing but without active telomerase. The role of regulatory elements found along the *AtTERT* gene is discussed in respect to natural telomerase expression and putative intron-mediated enhancement.

Key words: *Arabidopsis thaliana*, regulation element, T-DNA insertion, telomerase, transcription.

Introduction

Telomerase is a ribonucleoprotein complex able to add telomeric repeats to chromosome ends and thus to elongate telomeres. Telomerase consists of the catalytic subunit TERT (Telomerase Reverse Transcriptase), and the TR (Telomerase RNA) subunit which serves as a template for the telomere motif elongation. Both telomerase subunits have been characterized in many model organisms (yeast, protozoa, and humans). In plants, the *TERT* gene has been cloned in *Arabidopsis* (Fitzgerald *et al.*, 1999), *Oryza* (Heller-Uszynska *et al.*, 2002), and Asparagales species (Sykorova *et al.*, 2006), and more plant TERT genes were

identified *in silico* in sequenced genomes (reviewed in Podlevsky *et al.*, 2008; Sykorova and Fajkus, 2009). The plant *TERT* genes consist of 12 exons (Fitzgerald *et al.*, 1999; Oguchi *et al.*, 1999) (Fig. 1C), and all the basic functional domains reported previously for *TERT* genes from other model organisms (Nakamura *et al.*, 1997) have been identified in *Arabidopsis thaliana TERT (AtTERT)* (Fig. 1A, C). The original identification of the *AtTERT* gene was achieved using a T-DNA insertion line with the insertion inside the telomerase-specific T motif. T-DNA insertion in exon 9 of the *AtTERT* gene (SALK_061434,

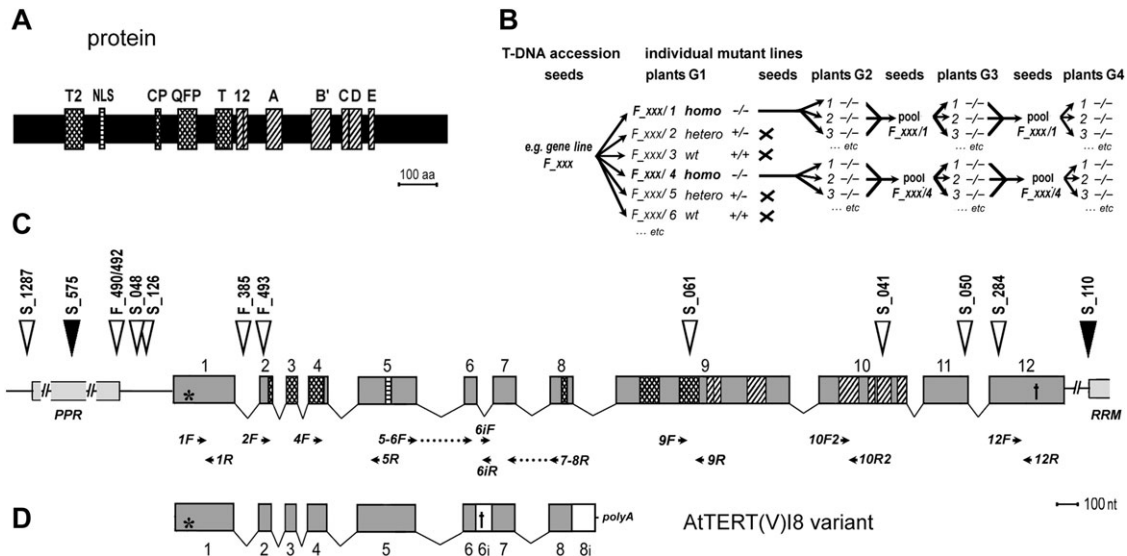


Fig. 1. Description of the *AtTERT* gene and of the experimental strategy. (A) Conserved motifs in the *AtTERT* protein are highlighted: reverse transcriptase motifs (1, 2, A, B', C, D, E); telomerase-specific motifs (T2, CP, QFP, T); NLS, nuclear localization-like signal. Details are given in Sykorova et al. (2006) and Sykorova and Fajkus (2009). (B) Scheme of the experimental strategy. T-DNA insertion lines obtained from the respective collections were propagated (generation 1; G1 plants represent T_3 progeny of the original accession) and genotyped in each generation. Two homozygous ($-/-$) individual gene lines and four homozygous individual upstream lines were propagated up to the fourth generation (G4); pool, seeds from all plants of the respective individual mutant line were pooled for subsequent cultivation. (C) Structure of the *AtTERT* gene and positions of T-DNA insertion lines. Exons (boxes, grey) and introns (lines) are depicted approximately true to scale according to their lengths. Positions of conserved regions are highlighted as in A. Triangles indicate the positions of T-DNA insertion; names of mutant lines are shortened as noted in the text. Lines marked by black triangles (S_575 and S_110) were excluded from the analysis. Positions of primers (Supplementary Table S1 at JXB online) used in analysis of *AtTERT* transcription are given below the gene map. (D) Splicing variant of the *AtTERT* gene. Open boxes indicate introns retained in the mRNA sequence. The asterisk in exon 1 (C, D) shows the position of the start codon according to Rossignol et al. (2007); the cross in intron 6 (and in exon 12) shows the position of the stop codon.

Fig. 1A, C) resulted in disruption of telomerase activity in telomerase-positive tissues and progressive telomere shortening during propagation of the mutant line, but without apparent phenotypic defects at least in early plant generations (Fitzgerald et al., 1999; Ruckova et al., 2008).

The detailed molecular mechanisms of telomerase regulation at both the cellular and organism levels are far from being elucidated. Analysis of tobacco suspension cell cultures showed low telomerase activity except in early S phase (Tamura et al., 1999), demonstrating cell cycle-dependent telomerase regulation. In both plant and animal models, a correlation between the level of TERT mRNA and telomerase activity was reported, pointing to regulation of TERT transcription as an important factor (Meyerson et al., 1997; Fitzgerald et al., 1999; Oguchi et al., 1999). Moreover, post-translational regulation of telomerase activity by phosphorylation was reported in mammals (Liu et al., 2001) and in rice (Oguchi et al., 2004). The dynamic structure of telomeres represents another level of regulation of telomerase activity (reviewed in Blackburn, 2000) in which telomere binding- and telomere-associated proteins play a crucial role.

Alternatively spliced *TERT* transcript variants and their specific function in the regulation of telomerase activity and telomere homeostasis have been described in both human

and plant systems. In humans, two basic TERT deletion variants have been identified: an α deletion (Colgin et al., 2000; Yi et al., 2000) and a β deletion (Kilian et al., 1997). These hTERT forms are enzymatically inactive; moreover, an overexpressed α deletion variant can act as a strong telomerase inhibitor. Apart from these splicing events, their combination ($\alpha+\beta$), insertions, and intron retentions were described (for a review, see Sykorova and Fajkus, 2009); expression of the respective variants was quantified and correlated with distinct cell types, developmental stage, or pathological processes (Ulaner et al., 1998, 2001; Kaneko et al., 2006). Reconstitutions of human telomerase reveal 'minimal' hTERT regions indispensable for the formation of an active enzyme complex which differ under *in vitro* and *in vivo* experimental conditions (Beattie et al., 2000).

In plants, a number of alternatively spliced *TERT* isoforms have been identified in *Oryza* (Heller-Uszynska et al., 2002; Oguchi et al., 2004) and Asparagales (Sykorova et al., 2006). Detailed analysis of the *A. thaliana* TERT V(I8) isoform (Fig. 1D; GenBank accession no. AM384991; Rossignol et al., 2007) revealed its ability to bind the telomere-binding protein AtPOT1a effectively, pointing to a biological significance of the splicing variant in the plant system.

The identification and description of plant gene functions are mainly based on analysis of T-DNA insertion lines.

Insertion into either an exon or an intron in the protein-coding region is equally effective in knocking out the target gene (86%), while insertions before the start codon or after the stop codon are slightly less effective (Wang, 2008). However, when a transcript is produced due to expression of a fusion transcript driven by a strong T-DNA promoter or is truncated due to transcription termination by the insertion, it can still be translated into a functional protein (Ren *et al.*, 2004; Dohmann *et al.*, 2005; Ohtomo *et al.*, 2005; Wilmoth *et al.*, 2005) or into a truncated protein lacking essential domains (Kim *et al.*, 2004; Henderson *et al.*, 2005; for a review, see Wang, 2008). To investigate structure–function relationships in *TERT* subdomains in plants, a collection of *A. thaliana* T-DNA insertion lines has been utilized (Fig. 1C; Supplementary Fig. S1A available at *JXB* online) in which the insertion was in distinct *AtTERT* regions encompassing the N-terminal part with telomerase-specific motifs, the central part (reverse transcriptase motifs), and the C-terminal extension (Fig. 1A), or in the upstream and downstream sequences. Telomerase activity was abolished and telomeres were shortened in all the mutant lines with a T-DNA insertion in the *AtTERT* gene regardless of the T-DNA position. On the other hand, telomerase function was maintained in the mutant lines with a T-DNA insertion within the *AtTERT* upstream region, and a correlation between increased transcription level and telomerase activity was observed. T-DNA insertions at the 5' end of the *AtTERT* gene or in the region upstream of the ATG start codon led to the activation of putative regulatory elements. Possible outcomes of these observations are discussed.

Materials and methods

Plant material and genotyping

Arabidopsis thaliana lines with a T-DNA insertion in the gene coding for telomerase reverse transcriptase *AtTERT* (At5g16850; Supplementary Fig. S1A at *JXB* online) were selected from the public T-DNA Express database established by the Salk Institute Genomic Analysis Laboratory accessible at the SIGnAL website <http://signal.salk.edu>. Seeds were obtained from the Nottingham Arabidopsis Stock Centre [SALK and SAIL lines, Columbia wild type (wt) (Sessions *et al.*, 2002; Alonso *et al.*, 2003) and Versailles INRA collection (FLAG lines, Wassilevskija-4 wt (Brunaud *et al.*, 2002)]; for the T-DNA positions, see Fig. 1C. Note that the lines FLAG_490F05 and FLAG_492C08 (F_490/492 in Fig. 1C) represent flanking sequence tags (FSTs) of the same accession (Brunaud *et al.*, 2002).

Seeds were placed onto half-strength Murashige and Skoog (MS; Duchefa) agar plates and grown under cycles of 8 h light, 21 °C and 16 h dark, 19 °C (except root elongation analysis; see Supplementary methods at *JXB* online). After 2 weeks, seedlings were potted and grown for 3 weeks under the same conditions until samples of plant material (leaves) for genotyping and genomic DNA were collected. Plants were then grown under 16 h/8 h light/dark cycles suitable for flowering, and seeds from each plant were collected. Individual plants (generation G1) from each T-DNA insertion line were genotyped (see Supplementary Table S1 at *JXB* online for primer sequences) to select individual segregated wt, heterozygous, and homozygous individual mutant lines. At least two mutant lines for each T-DNA accession (referred to here as individual mutant lines) were propagated up

to the fourth generation (G4) and each individual plant was genotyped (Fig. 1B). The seeds from homozygous plants in G2, G3, and G4 were pooled. Heterozygous and wt plants were revealed by genotyping of the line SALK_126201 which is referred to as homozygous for T-DNA insertion in the T-DNA Express database. The lines SALK_110053 and SAIL_575_F07 were excluded from the study because of mis-mapping of their position in the T-DNA Express database. Two control lines were used, the line SALK_061434 previously described in detail (Ruckova *et al.*, 2008) for the telomere repeat amplification protocol (TRAP) analysis, and the line SAIL_1287_C04 located 3174 bp upstream of the start codon (Fig. 1C) for the analysis of root growth.

DNA isolation and telomere length analysis

Genomic DNA for genotyping was isolated according to the 'modified IRR1 method' (Collard *et al.*, 2007) from leaves of 4- to 5-week-old plants. DNA for analysis of telomere length by the terminal restriction fragments (TRFs) method was isolated according to Dellaporta *et al.* (1983) from rosette leaves of 5- to 7-week-old plants. The quality of DNA was checked and the concentration estimated using electrophoresis on 0.8% (w/v) agarose gels stained with ethidium bromide. The Gene Ruler 1-kb DNA Ladder (Fermentas) was used as a standard and data were analysed by Multi Gauge software (FujiFilm).

Telomere length was assessed as the length of TRFs resulting from the digestion of genomic DNA by a frequently cutting restriction endonuclease whose recognition site is not located within the telomeric region. DNAs (500 ng) isolated from individual plants were cleaved overnight at 65 °C by *Tru*II (*Mse*I) (Fermentas) and separated in 0.8% (w/v) agarose gels at 1.5 V cm⁻¹ for 16 h. Agarose gels were alkali blotted onto Hybond XL membranes (GE Healthcare). Membranes were hybridized overnight at 55 °C with the radioactively labelled telomeric oligonucleotide (GGTTAG)₄ and washed twice at 55 °C for 30 min in 2× SSC (1× SSC=150 mM NaCl, 15 mM Na₃ citrate, pH 7.0), 0.1% SDS. Signals were visualized using a FLA7000 phosphorimager (FujiFilm). Evaluation of fragment lengths was done by using the Gene Ruler 1-kb DNA Ladder (Fermentas) as a standard; Multi Gauge software (FujiFilm) was used to analyse hybridization patterns. Mean telomere lengths were calculated by the Telometric tool (Grant *et al.*, 2001).

Analysis of telomerase activity (TRAP assay)

Protein extracts from undeveloped buds and 7-day-old seedlings were prepared as described (Fitzgerald *et al.*, 1996; Sykorova *et al.*, 2003) and tested for telomerase activity according to the protocol in Fajkus *et al.* (1998). Briefly, 1 µl of 10 µM CAMV or TS21 substrate primer (Supplementary Table S1 at *JXB* online) was mixed with 1 µl of telomerase extract (protein concentration 50 ng µl⁻¹). Primer elongation proceeded in 25 µl of the reaction buffer at 26 °C for 45 min. After extension, telomerase was heat inactivated for 10 min at 95 °C and the sample was cooled to 80 °C. A 1 µl aliquot of 10 µM TELPR reverse primer (Supplementary Table S1) and 2 U of DyNAzymeII DNA Polymerase (Finnzymes) were added to start the PCR step of the TRAP assay (35 cycles of 95 °C/30 s, 65 °C/30 s, 72 °C/30 s) followed by a final extension (72 °C/5 min). Products of the TRAP reactions were analysed by electrophoresis on a 12.5% polyacrylamide gel in 0.5× TBE buffer, the gel was stained with GelStar Nucleic Acid Gel Stain (LONZA), and signals were visualized using the LAS-3000 system (FujiFilm).

The quantitative variant of the TRAP analysis was performed as described in Herbert *et al.* (2006) using FastStart SYBR Green Master (Roche) and TS21 and TELPR primers. Samples were analysed in triplicate. A 1 µl aliquot of extract diluted to 50 ng µl⁻¹ protein concentration was added to the 20 µl reaction mix. Ct values were determined using the RotorGene3000 (Qiagen) machine

software, and relative telomerase activity was calculated by the Δ Ct method (Pfaffl, 2004).

RNA isolation and analysis of *AtTERT* transcription

Total RNA was isolated from undeveloped buds, 7-day-old seedlings, and mature leaves with the RNeasy Plant Mini Kit (Qiagen) followed by treatment by DNase I (TURBO DNA-free, Applied Biosystems/Ambion) according to the manufacturer's instructions. The quality and quantity of RNA were checked by electrophoresis on 1% (w/v) agarose gels and by absorbance measurement (NanoPhotometr IMPLÉN). cDNA was prepared by reverse transcription of 1 μ g of RNA using the M-MuLV (NEB) reverse transcriptase and Random Nonamers (Sigma). Quantification of the *AtTERT* transcript level relative to the ubiquitin reference gene was done using FastStart SYBR Green Master (Roche) by the Rotorgene3000 (Qiagen) machine. A 1 μ l aliquot of cDNA was added to the 20 μ l reaction mix; the final concentration of each forward and reverse primer (sequences are given in Supplementary Table S1) was 0.25 μ M. Reactions were done in triplicate; the PCR cycle consisted of 15 min of initial denaturation followed by 40 cycles of 20 s at 94 °C, 20 s at 56 °C, and 20 s at 72 °C. SYBR Green I fluorescence was monitored consecutively after the extension step. The amount of the respective transcript was determined for at least two individual mutant lines, and *AtTERT* transcription was calculated as the fold increase/decrease relative to the wt plant tissue ($\Delta\Delta$ Ct method; Pfaffl, 2004).

Analysis of alternatively spliced *AtTERT* transcripts was done by PCR using DyNAzyme II (Finnzymes) polymerase. The 20 μ l reaction mix consisted of 1 μ l of cDNA, 1 \times DyNAzyme II reaction buffer (Finnzymes), 0.25 μ M forward and reverse primers, 1 mM MgCl₂, 350 μ M of each dNTP, and 1 U of DyNAzyme II polymerase; PCR conditions were the same as for quantitative reverse transcription-PCR (qRT-PCR). Reaction products were analysed by electrophoresis on a 2% (w/v) agarose gel, stained by ethidium bromide, and visualized using the LAS3000 (FujiFilm).

Results

Characterization of T-DNA insertion lines

Publicly accessible *A. thaliana* lines with insertions mapped inside the *AtTERT* gene sequence (At5g16850) and adjacent regions were searched for and selected. The *AtTERT* gene is located on chromosome 5; upstream of its start codon is the At5g16860 gene coding for a putative pentatricopeptide repeat-containing protein (*PPR*), and downstream of the stop codon is the At5g16840 gene coding for a putative RNA recognition motif-containing protein (*RRM*) (Fig. 1C; Supplementary Fig. S1A at *JXB* online). The set of T-DNA insertion lines included accessions from three T-DNA libraries derived from Columbia (Col wt, SALK, and SAIL lines) and from Wassilevskija ecotypes (WS4 wt, FLAG lines). They covered the *AtTERT* gene region (six lines), the upstream region (five lines), and the downstream region (one line) (Fig. 1C). The lines FLAG_490F05 and FLAG_492C08 from the INRA collection were supplied as one accession because they represent FSTs of the same T-DNA insertion (Supplementary Fig. S1A, B; Brunaud *et al.*, 2002). Genotyping of the insertion lines (primer sequences are given in Supplementary Table S1 at *JXB* online) showed that the lines SALK_110053 and SAIL_575_F07 did not contain T-DNA insertions at the

mapped positions (the *RRM* gene and *PPR* gene, respectively) and they were excluded from this study.

The region upstream of the *AtTERT* start codon was covered by lines SALK_126201, SALK_048471, FLAG_490F05/FLAG_492C08, and SAIL_1287_C04 (designated here as S_126, S_048, F_490/492, and S_1287; 'upstream lines', Fig. 1C) and the gene region from the start to the stop codon was covered by lines FLAG_385G01, FLAG_493F06, SALK_061434, SALK_041265, SALK_050921, and SAIL_284_B07 (designated here as F_385, F_493, S_061, S_041, S_050, and S_284; 'gene lines', Fig. 1C). For subsequent analysis, at least two individual mutant lines derived from each gene line and four individual mutant lines from each upstream line classified as homozygous for T-DNA insertion from each T-DNA accession were propagated (Fig. 1B). These individual mutant lines were cultivated up to the fourth generation (G4) which was originally described as critical for telomere shortening but not for plant survival (Ruckova *et al.*, 2008).

Furthermore, experiments were conducted to determine if T-DNA insertions upstream of *AtTERT* and in the gene region may influence the development of roots, the typical telomerase-positive tissue (Fitzgerald *et al.*, 1996). Analysis of the root growth of all lines via calculation of root elongation dynamics (Supplementary Figs S2, S3 at *JXB* online) did not reveal any changes related to the position of T-DNA insertions in comparison with the segregated wts (Supplementary Figs S2, S3).

Plant lines with T-DNA insertions inside the *AtTERT* coding region show telomere shortening independently of the T-DNA position

The telomere length was estimated by measuring TRFs, which involves hybridization of digested genomic DNA on Southern blots with a telomeric repeat probe. The hybridization pattern represents the telomeres plus the region adjacent to the most telomere-proximal recognition site of the restriction enzyme used. The lengths of telomeric tracts differ in *A. thaliana* ecotypes (Gallego and White, 2001; Riha *et al.*, 2002; Shakirov and Shippen, 2004), giving a different starting point for telomere shortening. The TRF lengths reach 2–4 kb in the Columbia ecotype (wt of the SALK and SAIL mutant lines) and 3.5–8 kb in the Wassilevskija ecotype (wt of the FLAG mutant lines). The upstream lines S_126, S_048, and F_490/492 showed telomere lengths fully comparable with the corresponding wts (examples are shown in Fig. 2C). Telomeric tracts in all gene lines were remarkably shortened as compared with the wt (as shown for F_385/22 in Fig. 2A, B) using three criteria for evaluation of TRFs: absolute maximum and minimum per generation, and weighted mean TRF length for each individual plant (Fig. 2B, C). Weighted mean TRF length was calculated as the mean TRF adjusted by the decreased signal of the telomere probe in the shorter TRF in relation to the unchanged portion of the non-telomeric part of the TRF (Grant *et al.*, 2001). Similar shortening of telomeres was reported previously for the original *AtTERT* mutant

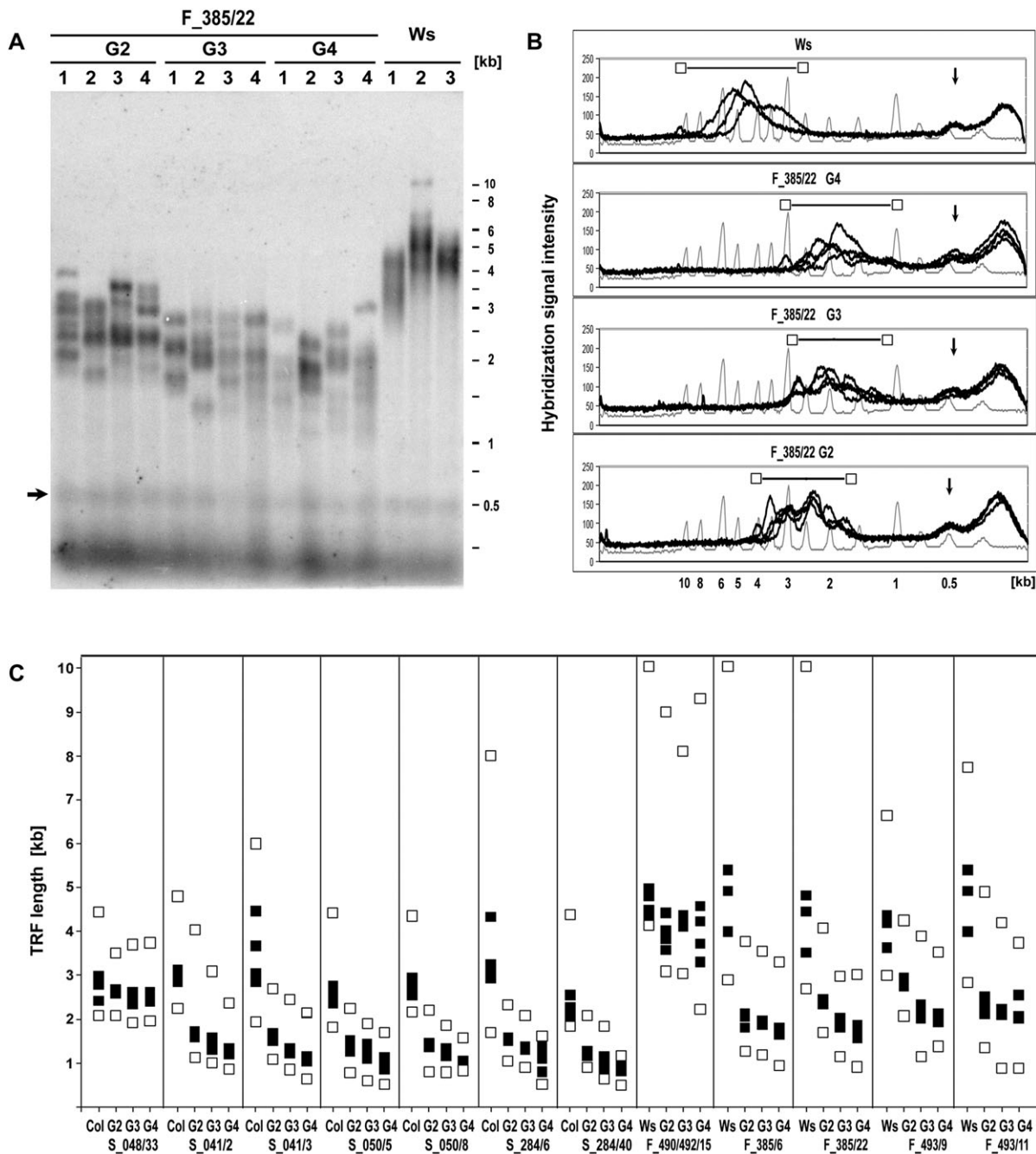


Fig. 2. Analysis of the telomere length in T-DNA insertion lines. (A) Example of the telomere length analysis. The lengths of the terminal restriction fragments (TRFs) were determined in four individual plants (numbers above the panel) of each generation (G2, G3, and G4) of the individual mutant line F_385/22 and compared with Wassilevskija-4 wt (Ws, three plants). Note a significant shift of hybridization signals to lower molecular weights in the mutant samples. The arrow delimits the position of the internal telomere-like sequence near the centromere (~500 bp) which serves as a control (A, B). Marker lengths are shown in kb (1-kb DNA Gene Ruler Ladder, Fermentas). (B) An example of TRF evaluation is shown using lane intensity charts in which the x-axis of the graphs shows a reference value (marker in kb) and the y-axis value corresponds to the pixel intensity at each point along the lane. Open squares show the absolute maximum and minimum per generation in mutant and control plants (as in C). (C) Graphical representation of the TRF results shown in A. Evaluation of TRF lengths from one and two individual mutant lines of upstream and gene lines, respectively, in comparison with the wild types is shown. The TRF lengths were calculated using the Multi Gauge program (FujiFilm) from the hybridization pattern of four individual mutant plants of each generation (G2, G3, and G4) and wt plants (Col, four plants; Ws, three plants). The absolute minimum and maximum (open squares) are shown per generation; the weighted mean telomere length from each line (filled squares) was calculated using the Telometric tool (Grant *et al.*, 2001).

line S_061 (shortening by 250–500 bp per generation; Fitzgerald *et al.*, 1999; Ruckova *et al.*, 2008).

The splicing variant *AtTERT* V(18) (Fig. 1D) with suggested telomeric function as an interaction partner of AtPOT1a (Rossignol *et al.*, 2007) could possibly be transcribed and translated in the gene lines S_041, S_050, and S_284 that have the T-DNA insertion at the 3' end of the *TERT* gene and downstream of the *AtTERT* V(18) region (see Fig. 1C). However, no difference was observed in telomere length dynamics between gene lines with the T-DNA insertion located at the 5' and the 3' regions of the *AtTERT* gene (Fig. 2C). These results suggest that (i) shortening of telomeres in gene lines was not influenced by the position of the T-DNA insertion and (ii) telomere maintenance was not affected in upstream lines.

Telomerase activity is disrupted in lines with a T-DNA insertion inside the *AtTERT* coding region, while insertion upstream of the ATG start codon shows no effect

To investigate whether the distance of the T-DNA insertion from the *AtTERT* start codon in upstream lines influences telomerase activity, TRAP assays were performed in homozygous, heterozygous, and segregated wt plants of S_126 (insertion at position –271 bp relative to the ATG start codon), S_048 (–360 bp), F_490/492 (–441 bp), and S_1287 (–3 174 bp, not shown) using the CAMV and TELPR primer set (Fig. 3; Supplementary Table S1 at *JXB* online). Telomerase extracts prepared from buds of the first generation (G1, Fig. 1B) of all upstream lines showed telomerase activity comparable with that in the corresponding wt tissues (Fig. 3, left panels). This result and the position of the T-DNA insertion in S_126 suggest that the region of 271 bp upstream of the ATG start codon is sufficient to act as a putative ‘minimal promoter’ (E Šýkorová *et al.*, unpublished results). Telomerase activities in gene lines harbouring insertions inside the protein-coding region (F_385, F_493,

S_061, S_050, S_041, and S_284) were examined using protein extracts prepared from G1 buds of homozygous, heterozygous, and segregated wt individual plants. Extracts from heterozygous plants showed telomerase activity similar to that of wt plants, but no activity was observed in homozygous mutant plants (Fig. 3, right panels).

The TRAP assay with the TS21 substrate primer (Supplementary Table S1) confirmed the loss of telomerase activity in gene lines, and active telomerase was detected in seedlings and buds of all upstream lines analysed up to the fourth generation (Supplementary Fig. S5). The primer TS21 was chosen as an alternative substrate primer also suitable for the modified quantitative TRAP assay (see below) instead of the CAMV primer which showed the presence of high molecular weight TRAP products (details in Supplementary methods and Supplementary Figs S4, S5 at *JXB* online).

Quantitative TRAP assays using TS21+TELPR primers showed increased telomerase activity in buds and seedlings of the S_048 upstream line, while activity in S_126 and F_490/492 lines was comparable with that of the wts (Fig. 4). These results point to the presence of a putative regulatory element in the upstream region whose function was changed in the S_048 line by T-DNA insertion.

Reduced telomerase activity is thus tightly correlated with the shortening of telomeric repeats in mutant lines. In upstream lines with the telomere length comparable with that of the wts, high telomerase activity was observed in telomerase-positive tissues but, on the other hand, no telomerase activity was detected in gene lines in accordance with their progressively shortened telomeres.

AtTERT transcription is comparable with that of the wt in telomerase-positive upstream lines but decreases downstream of the T-DNA insertion in 3' gene lines

The *AtTERT* gene was identified via its T-DNA insertion mutant (S_061, insertion in exon 9) in which the loss of

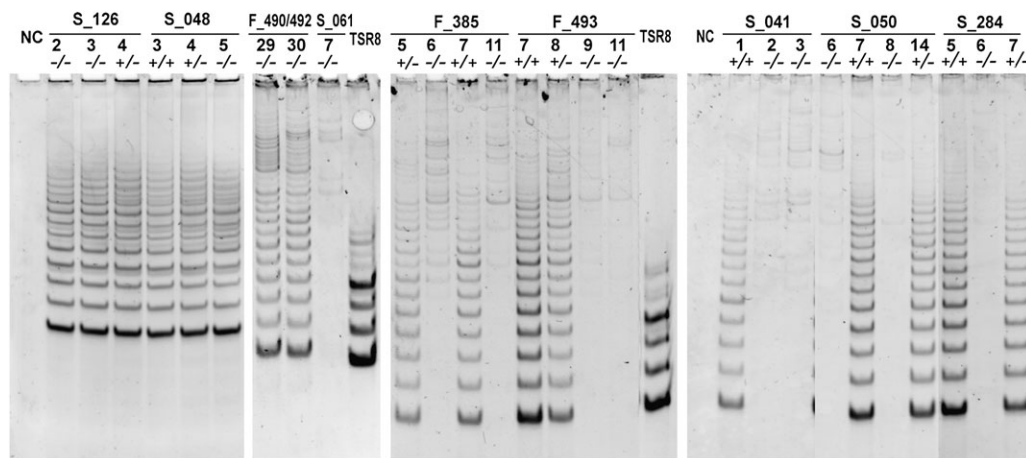


Fig. 3. Analysis of telomerase activity in buds collected from plants of the first generation of T-DNA insertion lines. High telomerase activity was detected in all upstream line samples homozygous (–/– lines) or heterozygous (+/–) for T-DNA insertions and in segregated wt plants (+/+) using the CAMV×TELPR primer set. In individuals of gene lines heterozygous for T-DNA insertion and in segregated wt plants, active telomerase was revealed; no telomerase activity was detected in individuals of gene lines homozygous for T-DNA insertion (except for bands of high molecular weight; see Supplementary methods, Supplementary Figs S4, S5 at *JXB* online). NC, negative control (no protein extract in TRAP reaction); TSR8, control template from the TRAPeze® XL Telomerase Detection Kit (Millipore); S_061/7, control line homozygous for T-DNA insertion in exon 9 of the *AtTERT* gene (Ruckova *et al.*, 2008).

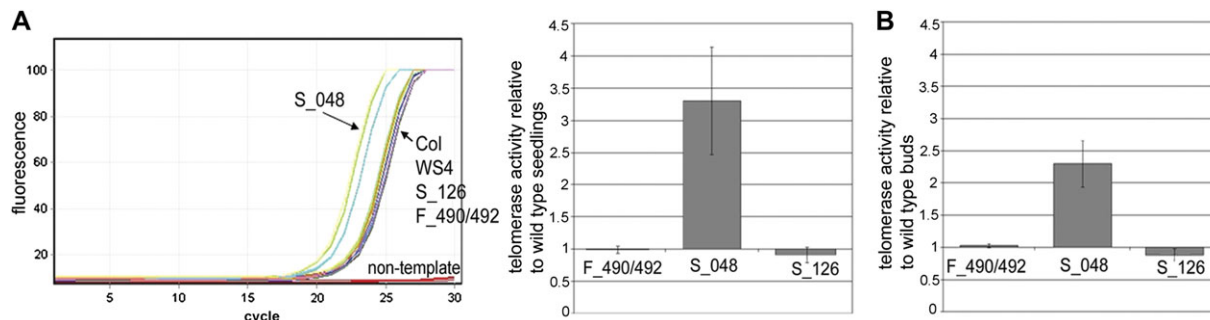


Fig. 4. Quantitative telomerase activity assay using the TS21 and TELPR primer set in G4 seedlings (A) and G4 buds (B) of the upstream lines. Two individual mutant lines of the F_490/492 accession, four individual mutant lines of S_126 and S_048, and wts (Col, Columbia; WS4, Wassilevskija) were analysed. Representative raw data for cycling (A, left panel) grouped curves for individual mutant lines S_048 and curves for wts and other upstream lines as marked by arrows. A slight but reproducible increase of telomerase activity relative to Columbia wt was observed in S_048 tissues. (This figure is available in colour at *JXB* online.)

telomerase activity and shortening of telomeres was observed (Fitzgerald *et al.*, 1999; Ruckova *et al.*, 2008). However, the presence/absence of *AtTERT* transcripts from regions upstream/downstream of the T-DNA insertion site has not been demonstrated yet. Previous studies of *A. thaliana* telomerase revealed the presence of the alternatively spliced isoform *AtTERT* V(18) (Fig. 1D; Rossignol *et al.*, 2007) with suggested telomeric function as a putative AtPOT1a binding partner. The presence of *TERT* transcripts including the variant *AtTERT* V(18) from regions located upstream and downstream of T-DNA insertions (Figs 5–7) was investigated using RT-PCR and qRT-PCR in telomerase-positive tissues (seedlings and buds) and telomerase-negative tissues (mature leaves; see below).

In telomerase-positive tissues, upstream lines generally showed levels of transcripts originating from exons 1 and 10 comparable with or slightly higher than those in the wts (Figs 5, 6; Table 1). The transcription of the *PPR* gene (At5g16860) located upstream of *AtTERT* (Fig. 1C, Supplementary Fig. S1A) was also examined, and no RT-PCR product in buds, seedlings, or leaves was observed in either upstream lines or in Columbia wt plants (not shown).

All gene lines showed a level of the exon 1 transcript (upstream of the T-DNA insertion for all lines) similar to that in the wt (except for F_385 and F_493; see below), while transcription from exon 12 (downstream of T-DNA insertions for all lines) was significantly decreased (except for F_385; see below) (Figs 5, 6; Table 1). The level of transcription from exon 10 was markedly decreased in F_493 (Fig. 6) and similar to that in the wt in S_041/2, S_050, and S_284 (Fig. 5), thus corresponding to the relative position of the T-DNA insertion. In some cases, differences were observed in the transcript level among individual mutant line representatives; for example, line S_048/23 showed a more pronounced increase in expression of exons 1 and 10 (by more than one order of magnitude; Table 1) in comparison with other individual mutant lines of the same accession (S_048/2, 8, 33; Table 1), and a similar difference was observed between individual mutant lines of S_041 (see Supplementary methods for analysis of the individual mutant line S_041/3; Supplementary Table S2 at

JXB online). Previous results revealed that transcription was not reduced upstream of T-DNA insertion sites and there is a possibility that the alternatively spliced isoform of *AtTERT* could be present and even functional in mutant lines with insertions positioned downstream of the *AtTERT* V(18) poly(A) site (Fig. 1C, D). In addition to these 3' gene lines, the position of T-DNA insertions in upstream lines might influence the transcriptional pattern of this variant. The transcription of the alternatively spliced isoform *AtTERT* V(18) was investigated using primers derived from unique features of this variant; a combination of primers designed from spliced borders of exons 5+6 (5-6F), exons 7+8 (7-8R), and forward or reverse primers from intron 6 (6iF, 6iR) was used in qRT-PCR (not shown) and conventional RT-PCR. The respective transcripts were detected using conventional RT-PCR in seedlings and buds in all upstream lines and also in gene lines with the T-DNA insertion located downstream of the putative poly(A) signal of the *AtTERT* V(18) isoform (Fig. 7A, B). However, the amount of alternatively spliced transcript was too low (in the range of a few percent as compared with the full-length transcript in Col and WS4 wts) to perform fully reproducible quantitative assays by the qRT-PCR technique (M Fojtová, unpublished results).

A specific pattern of AtTERT transcription in the 5' gene lines F_385 and F_493

AtTERT transcription in gene lines F_385 and F_493 with T-DNA insertions at the 5' end of the *AtTERT* gene was completely different from that in other gene lines. They showed an ~300- and 30-fold increased transcription, respectively, of exon 1 in G4 seedlings relative to WS4 wt (Fig. 6B; Table 1) and a similar increase in transcription was revealed in G3 seedlings and G4 buds from both lines (Table 1).

Transcription of exon 10 downstream of T-DNA insertions was convincingly reduced in F_493, while in F_385 it was ~3500-fold higher in the G4 seedlings and buds in comparison with the corresponding wt tissues (Fig. 6B; Table 1). RT-PCR and qRT-PCR analyses with primer sets

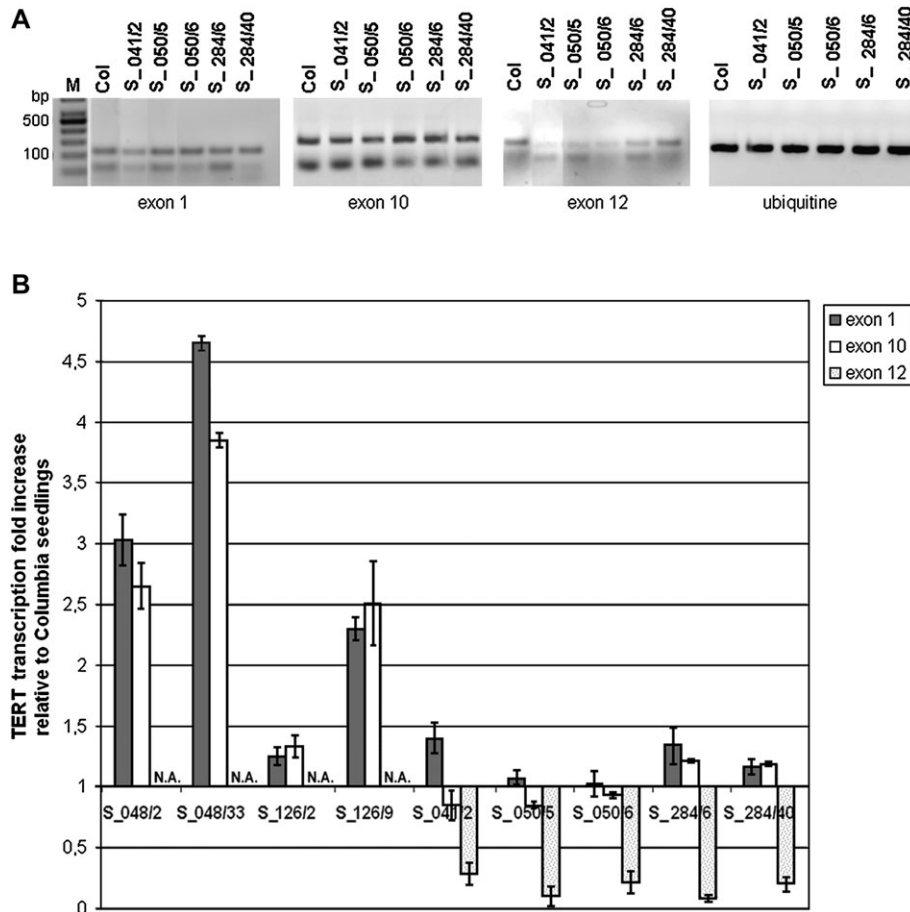


Fig. 5. *AtTERT* transcription in G4 seedlings of T-DNA insertion plant lines of the Columbia background. (A) Analysis by conventional RT-PCR. (B) Analysis by qRT-PCR; at least two individual mutant lines of each accession were analysed. *AtTERT* transcription was slightly increased or was comparable with that in Columbia in upstream lines (S_048 and S_126). The expression levels in other gene lines (S_041, S_050, and S_284) correlated with the position of the T-DNA insertion, i.e. it was comparable with the wt in upstream regions and decreased in the region downstream of the T-DNA insertion. N.A., not analysed.

amplifying regions from exons 4 to 5 and exons 2 to 5 revealed that vigorous transcription had started in exon 2 closely downstream of the T-DNA insertion in the line F_385 (Fig. 6A, B). Moreover, analysis of transcripts downstream of the T-DNA insertion site (primer sets 2F–7,8R and 9F–12R) revealed bands of regular length in G4 seedlings of the F_385 gene line (Fig. 7C), suggesting that splicing of the overexpressed transcripts in both regions is identical to that in wt plants with the functional *AtTERT* mRNA variant. To exclude the possibility that transcription was driven by a strong T-DNA promoter (Supplementary Fig. S1B, C at JXB online), lines F_385 and F_493 were genotyped in more detail. RT-PCRs with T-DNA-specific primers and *AtTERT*-specific primers confirmed that no chimeric transcript was produced, and thus the increased transcription of exons 1 and 10 in line F_385 was not caused by a leaking terminator in the T-DNA in any of these lines (Supplementary Fig. S1C).

In addition, the levels of exon 1 and 10 transcripts were investigated in mature leaves which represent typical telomerase-negative tissue. Surprisingly, the transcription level and expression pattern were similar to those in seedlings and

buds (Fig. 6C; Table 1) in both F_385 and F_493 lines. In other insertion lines, *AtTERT* transcription in mature leaves was under the detection limit (Table 1), i.e. silenced, as expected for plant mature tissues.

Discussion

Two major features of *AtTERT* function were monitored by analysing T-DNA insertion lines of *A. thaliana* for telomerase activity and telomere length. In accordance with previous reports on telomere dynamics in the T-DNA insertion mutant S_061 (Fitzgerald *et al.*, 1999; Ruckova *et al.*, 2008) telomere shortening by 100–500 bp per generation and an absence of telomerase activity was found in lines with a disrupted *AtTERT* gene sequence downstream of the start codon (Fig. 8).

Unchanged telomerase function in upstream lines

Lines with the T-DNA insertion upstream of the start codon showed positive telomerase activity and telomere length

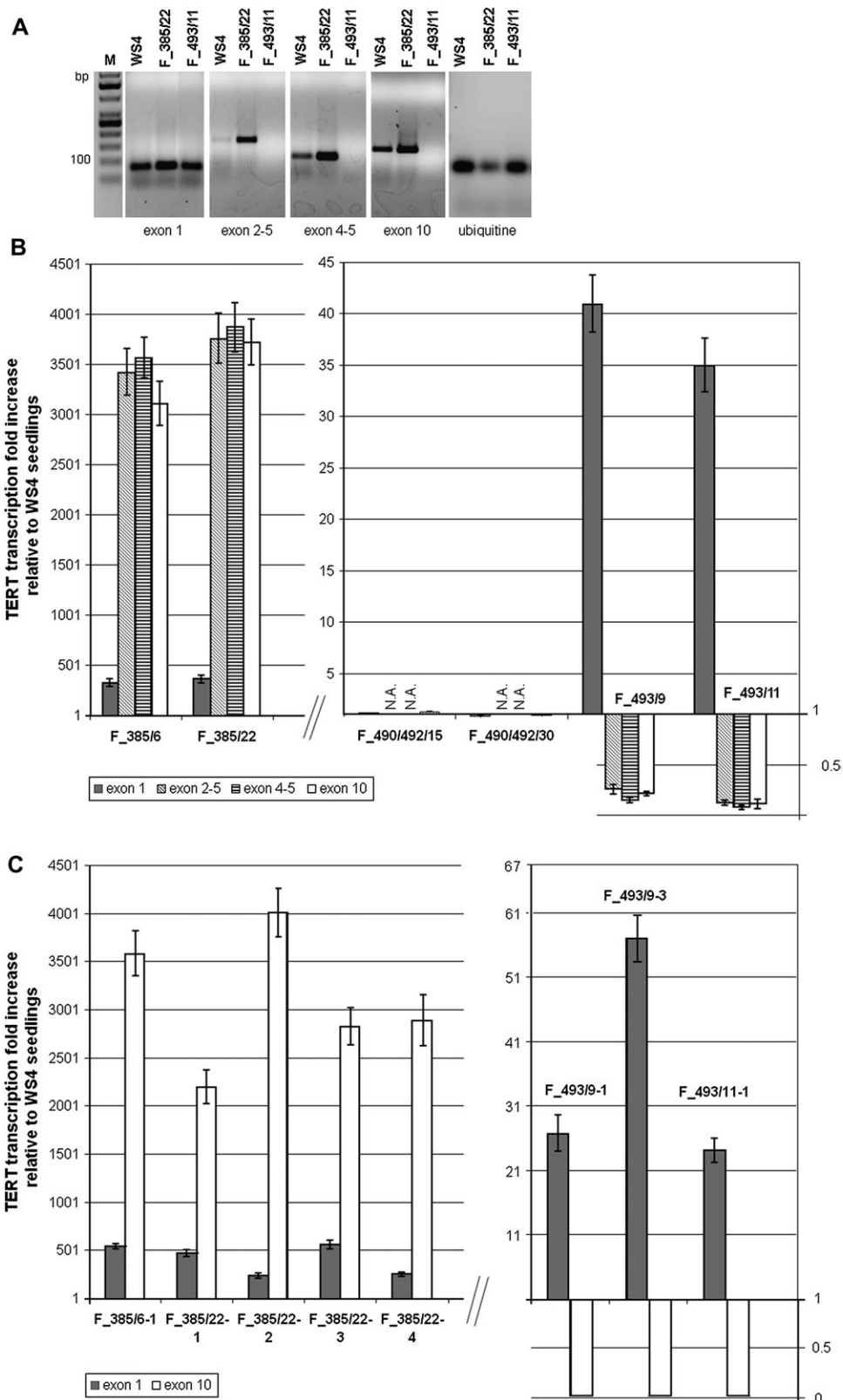


Fig. 6. *AtTERT* transcription in G4 seedlings (A and B) and mature leaves (C) of T-DNA insertion lines of the Wassilevskija background (Ws4). (A) Analysis by conventional RT-PCR. Note the strong bands of PCR products in the F_385/22 individual line in the regions downstream of the T-DNA insertion (exons 2–5, 4–5, and 10) using a marginal amount of cDNA template for amplification (weak ubiquitin band). There is no signal in the F_493/11 individual line in the regions downstream of the T-DNA insertion. (B) Analysis by qRT-PCR. Transcription increased markedly in the regions downstream of the T-DNA insertion in gene line F_385 (left panel). In the upstream line F_490/492 (right panel), expression was comparable with that in the wt in both regions tested (exons 1 and 10). In gene line F_493 (right

comparable with those in wt samples. These results and the position of the T-DNA insertion in the S_126 mutant line suggest that a region as short as 271 bp upstream of ATG can act as a putative ‘minimal promoter’ able to drive sufficient transcription of the telomerase protein subunit gene, resulting in normal telomerase function.

Nevertheless, an increase of *AtTERT* transcription was observed in both seedlings and buds of the S_048 mutant

line, pointing to a possible involvement of a putative regulation element in the region upstream of the minimal promoter. On the other hand, the amount of transcript in mature leaves in upstream lines was reduced convincingly, in contrast to gene lines F_385 and F_493. This suggests that the respective regulatory element may function only at the level of transcription, while it is not involved in tissue-specific regulation.

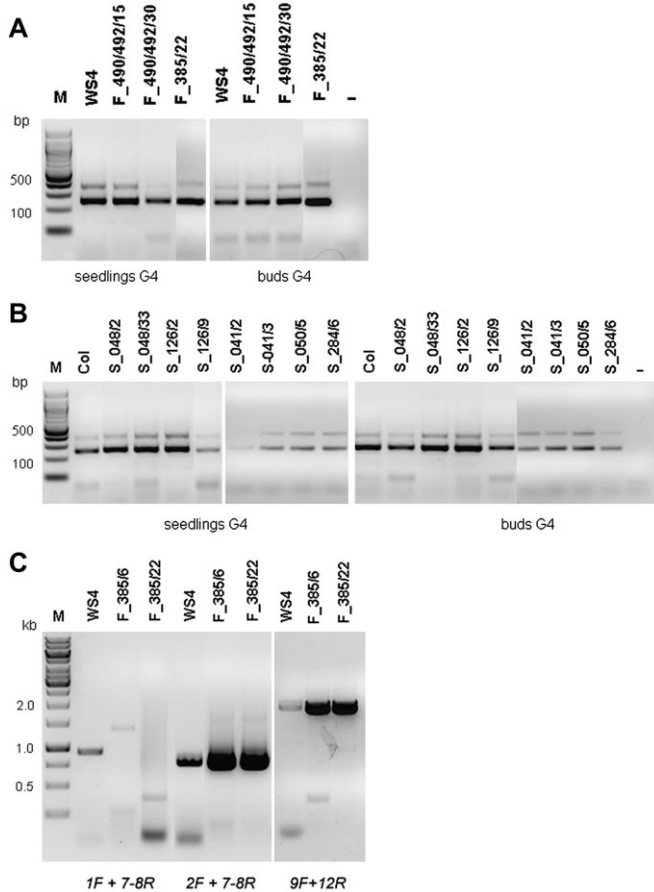


Fig. 7. Presence of the alternatively spliced *AtTERT* variant in seedlings and buds of the fourth generation (G4) of mutant lines of Wassilewskija (A) and Columbia (B) background. A faint band (~500 bp of length) evidencing the presence of an alternatively spliced product was detected in all samples tested (primer set 5-6F and 7-8R). Ws4, Col, wt; –, negative control. (C) Presence of the RT-PCR product of regular length along the *AtTERT* gene in G4 seedlings of the F_385 gene line. No RT-PCR product was obtained using primers surrounding the T-DNA insertion site (1F+7-8R). Strong bands were detected when analysing regions downstream of the T-DNA insertion (2F+7-8R; 9F+12R). The primer 2F is located in a region containing a natural ATG codon inside of exon 2.

Negative telomerase regardless of the position of T-DNA insertion in gene lines

Experiments to determine the minimal length of the telomerase protein subunit which can reconstitute telomerase activity indicated that different regions of *hTERT* are sufficient to function *in vitro* and *in vivo* (Beattie *et al.*, 2000). Deletion of the 20 C-terminal amino acids reduced the activity of human telomerase reconstituted in rabbit reticulocyte lysate (RRL), and truncations of hTERT that lacked the last 205 amino acids (including part of the E motif; see Fig. 1A) remained active when transfected into 293T cells. N-terminal truncations of 300 amino acids were active in both systems, and a truncation spanning amino acids 201–927 was active in 293T cells but not in an RRL. The position of T-DNA insertion in lines S_050 and S_284 (inside exon 11 and 12, respectively) and the unaffected transcription level upstream of the T-DNA insertion might hypothetically give rise to *AtTERT* products containing a ‘minimal length subunit’ analogous to that of *hTERT* which possess all essential enzyme motifs (Figs 1A, C, 8). However, both lines showed telomere shortening and absence of telomerase activity. Similarly, line F_385 with the putative *AtTERT* gene product shortened from the N-terminal end did not show any telomerase activity. There is a possibility that mRNA originating from the gene disrupted by T-DNA insertion is recognized as aberrant and is not effectively translated or produces a non-functional protein, and this could explain the possible absence of translated products of the alternatively spliced isoform *AtTERT* V(I8) in the gene lines S_061, S_041, S_050, and S_284. Also, it is possible that the *AtTERT* V(I8) isoform is not directly involved in telomere maintenance. Unfortunately, these possibilities are difficult to test in plant models because antibodies specific for the respective TERT functional domains are not available.

A putative regulatory element in the region of T-DNA insertion in F_493 and F_385 gene lines

The position of the T-DNA insertion in the *AtTERT* gene could efficiently uncouple the transcription unit from its putative regulatory elements. Delimitation of regulation

panel), an increase of expression was detected in the region upstream of the T-DNA insertion (exon 1), while in the downstream regions the expression is at the limit of detection. N.A., not analysed. (C) *AtTERT* transcription was analysed in mature leaves collected from five individual plants of the F_385 line (left panel) and three individual plants of the F_493 line (right panel). In both mutant lines, the *AtTERT* expression profile in leaves is similar to that in seedlings. Note the relatively high interindividual variability between samples.

Table 1. Summary of analyses of *AtTERT* transcription in T-DNA insertion lines. Transcription in the seedlings (S), buds (B), and old mature leaves (L) is related to that in the respective wt tissue (except for F_385 and F_493 old leaves where transcription is related to Ws-4 seedlings). Data were taken from analyses of at least two individual mutant lines.

NA, not analysed; ND, not detected (expression below the detection limit).

T-DNA insertion line	Tissue/generation	Exon 1	Exon 10	Exon 12
FLAG490F05/FLAG_492C08	SG4	1.04±0.12	0.98±0.22	NA
	BG4	1.13±0.26	1.08±0.17	NA
	LG4	ND	NA	NA
SALK_126201	SG4	1.78±0.73	1.92±0.85	NA
	BG4	2.25±0.21	2.48±0.83	NA
	LG4	ND	NA	NA
SALK_048471 ^a	SG4	3.85±1.21	3.29±0.83	NA
	BG4	4.09±0.86	3.83±0.56	NA
	LG4	ND	NA	NA
FLAG_385G01	SG2	306±32	3417±434	NA
	SG3	331±34	3841±446	NA
	SG4	344±29	3290±560	NA
	BG4	424±53	3541±520	NA
	LG4	440±120	3079±615	NA
FLAG_493F06	SG3	22.5±2.3	0.03±0.01	NA
	SG4	37.8±4.1	0.12±0.02	NA
	BG4	51.1±12.5	0.20±0.05	NA
	LG4	39.3±17.3	ND	NA
SALK_041265 ^b	SG2	1.19±0.32	NA	NA
	SG3	1.12±0.30	NA	0.33±0.11
	SG4	1.42±0.63	0.9±0.29	0.28±0.10
	BG4	1.49±0.22	1.23±0.36	0.21±0.08
	LG4	ND	NA	NA
	SG4	1.05±0.03	0.89±0.05	0.15±0.07
SALK_050921	LG4	ND	NA	NA
	SG4	1.25±0.15	1.2±0.01	0.47±0.07
SAIL_284_B07	SG4	1.25±0.15	1.2±0.01	0.47±0.07
	LG4	N.D.	NA	NA

^a Data shown for individual mutant lines S_048/3, 8, 33; transcription in G4 seedlings of S_048/23 was significantly different from the others (exon 1, 26.3±2.5; exon 10, 21.1±3.8).

^b Complete analysis of the individual mutant line S_041/3 is presented in the Supplementary data at *JXB* online.

elements away from their original positions could provide additional information about their putative role in regulation of transcription, tissue specificity or in collaboration with other regulatory elements (Saracco *et al.*, 2007; Son *et al.*, 2010), as demonstrated here for the lines F_385 and F_493. Interestingly, in these lines and in the S_048 upstream line, the *AtTERT* expression in distinct regions was significantly increased, suggesting a possible disruption of the suppressive function of the putative upstream regulatory elements (Fig. 8). The T-DNA insertions inside intron 1 (F_385) and exon 2 (F_493) revealed several interesting features of these regions. Transcription upstream of both insertion sites was increased, but to different extents: the lines F_385 and F_493 showed a 300- and a 30-fold increase, respectively. Moreover, transcription downstream of the insertion sites revealed completely different patterns: an ~3500-fold increase of *AtTERT* transcription was observed in line F_385, but transcription in line F_493 was completely disrupted similarly to the other gene lines. The differences in *AtTERT* expression in these two lines are probably not related to the T-DNA insertions which both have the same orientation and vector

type, and increased *AtTERT* transcription was not caused by a leaking terminator in the T-DNA (Supplementary Fig. S1B, C at *JXB* online), or to a wt background, because the upstream line F_490/492 showed an expression pattern fully comparable with that of the Wassilevskija wt. These results provide evidence for the presence of a putative regulatory network or at least regulation motifs around the F_385 insertion site. The respective T-DNA insertions are located inside intron 1 (F_385) and exon 2 (F_493) at a distance of 190 bp. The marked differences in *AtTERT* expression both between lines F_385 and F_493 and in comparison with the Wassilevskija wt suggest disruption of some regulatory element in both lines (high expression in the region upstream of T-DNA insertion). This upstream suppressor element could be located (at least partially) between the respective insertion sites (Fig. 8). Nevertheless, the disruption of the putative suppressor function by T-DNA insertion in the second exon in the F_493 mutant line is manifested only by increased transcription in the region upstream of the T-DNA insertion, while T-DNA insertion inside the first intron in the F_385 mutant line resulted in extremely increased transcription of the regions downstream

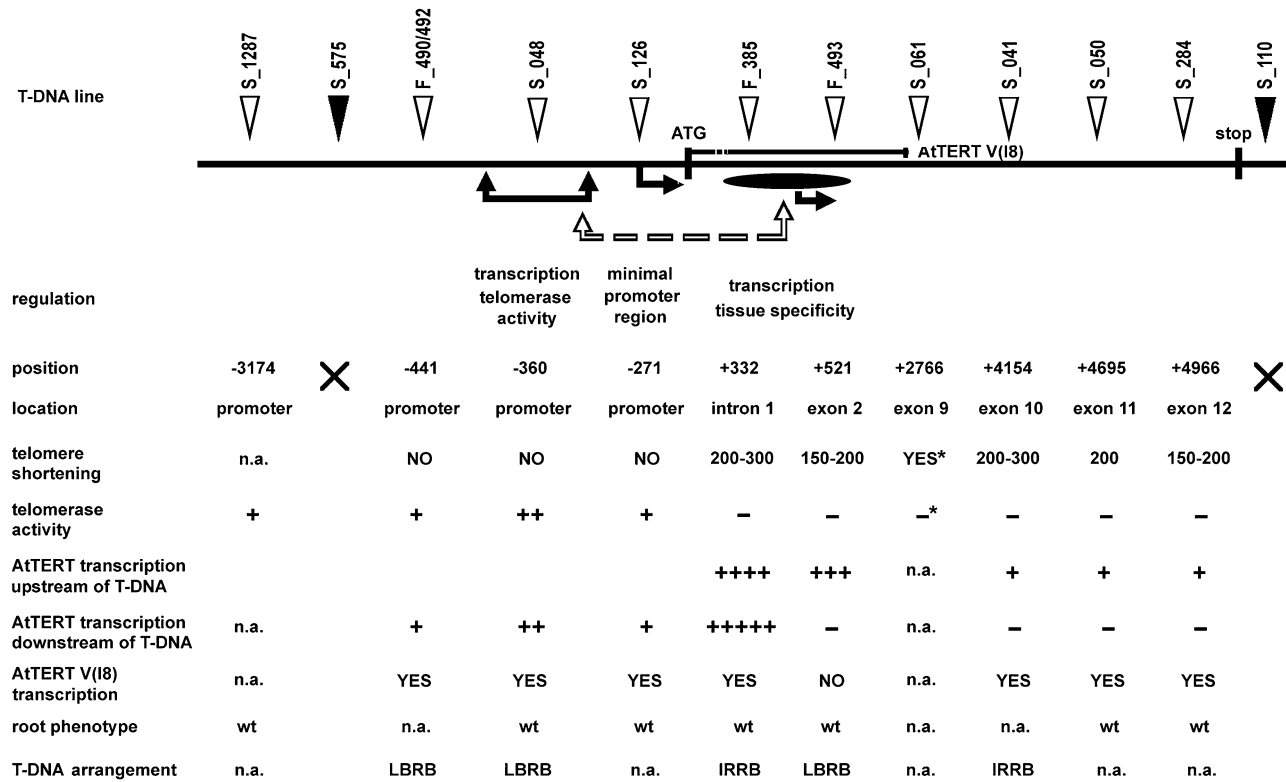


Fig. 8. Overview of results and analyses performed using T-DNA insertion lines. The position and location of T-DNA lines with respect to the ATG start codon and the *AtTERT* gene region are shown in the 5'–3' direction (not to scale). The lines excluded from the study are marked by filled triangles and by a cross (mis-mapping of position); the position of the alternatively spliced isoform *AtTERT V(I8)* is marked above the line representing the genomic *AtTERT* region. Regulatory regions and affected processes are depicted below the line. The minimal promoter region (arrow) is defined by a T-DNA insertion site in the line S_126; the T-DNA insertion line S_048 revealed an increase in transcription and telomerase activity (line with two arrows) in comparison with lines S_126 and F_490/492. Disruption of the regulatory region downstream of the start codon (oval) in lines F_385 and F_493 influenced tissue specificity and the level of *AtTERT* expression upstream of T-DNA insertion in both lines (cooperation with an unknown part of the promoter region, dashed line with arrows) and activated overexpression downstream of the insertion site in F_385 (arrow). The summary of analyses incorporates measurement of telomere shortening and telomerase activity, transcription analyses including the *AtTERT V(I8)* variant, the root phenotype study, and genotyping of T-DNA insertions. The control line S_061 was characterized in detail in Ruckova *et al.* (2008) (asterisk). The T-DNA arrangement is marked as IRRB (inverted repeat along the right border) and LBRB (5'–3' orientation) of T-DNA borders. Note that the arrangement was studied using PCR with the T-DNA primers and specific genotyping primers and it does not exclude the possibility of a tandem repeat in LBRB arrangement. n.a. = not analysed.

of the insertion site. The fate of this *AtTERT* mRNA is unclear; although the extremely up-regulated transcription downstream of T-DNA insertion seems to result in mRNA of regular length (Fig. 7C), there is no active telomerase in this line and telomeres are progressively shortened. This line thus clearly shows disruption of a tight coupling between *AtTERT* transcription and telomerase activity which occurs under natural conditions.

Both gene lines display disruption of the tissue-specific regulation of *AtTERT* transcription (Fig. 8), because a significant increase in the amount of transcripts was observed in telomerase-positive tissues (seedlings and buds) and also in mature leaves (Fig. 6C) which have previously been reported as typical telomerase-negative tissues (Fitzgerald *et al.*, 1996). This specific expression pattern can be attributed to the persisting activity of a strong regulatory element. The 35S enhancer/promoter in the transgenic cassette could be

a promising candidate, but obviously no chimeric transcript is produced (Supplementary Fig. S1C at JXB online), the expression pattern is different among FLAG lines, and the transcription level was unaffected in line F_490/492. The present state of knowledge does not allow determination of whether the putative element involved in the disruption of tissue-specific regulation of telomerase expression in F_493 and F_385 lines is a natural regulatory factor, or a DNA sequence acting as a strong regulatory element in the specific sequence context after the T-DNA insertion was randomly activated (Fig. 8). There are no data available on a possible translation of transcripts in the lines F_385 and F_493; however, the dynamics of telomere shortening and lack of telomerase activity in the F_385 gene line support the hypotheses that the aberrant nature of mRNA prevents its effective translation or results in production of a non-functional protein. It should also be mentioned that this property

of line F_385 might be an example of switching on of a cryptic promoter, and/or of the more general phenomenon termed intron-mediated enhancement (IME; Mascarenhas *et al.*, 1990; E Sýkorová *et al.*, unpublished results). The specific features of line F_385, the position of the T-DNA insertion inside intron 1, and the extremely increased transcription level downstream of T-DNA match features of some IME constructs (Jeon *et al.*, 2000; Chaubet-Gigot *et al.*, 2001) which were used for enhancing transgene expression in crops (Wang *et al.*, 1997; Upadhyaya *et al.*, 2000). Although the mechanism of IME is largely unknown, 5'-proximal introns can increase the expression of transgenes in plants, although at a lower level as observed in line F_385 (for a review, see, for example, Rose *et al.*, 2008). Several reports showed expression downstream of T-DNA in *Arabidopsis* mutant lines which harbour an insertion at the 5' end of the gene (Bertrand *et al.*, 2005; Xu *et al.*, 2007; for a review, see Wang, 2008) but a detailed description of the transcription level and profile is missing in most cases. In conjunction with the present results, these observations suggest a new potential in publicly available T-DNA lines, for example searching for cryptic promoters, regulation sites, or IME elements. Nevertheless, the data presented here reveal additional levels of complexity of the regulation of telomerase activity which form a basis for further research.

Supplementary data

Supplementary data are available at *JXB* online.

Supplementary methods and results.

Table S1. Primers used in analysis of telomerase activity (TRAP), genotyping of mutant lines, and analysis of *AtTERT* transcription.

Table S2. Analysis of *AtTERT* transcription in the individual mutant line S_041/3.

Figure S1. Description of T-DNA lines.

Figure S2. Root growth analysis in S_050/4 (segregated wt) and S_050/13 (gene line).

Figure S3. Root lengths of 13-day-old plants of individual mutant lines.

Figure S4. Sequence alignment of cloned products of the TRAP assay using the CAMV substrate primer in telomerase-negative gene lines.

Figure S5. RNA origin of TRAP products obtained using the CAMV substrate primer in telomerase-negative gene lines.

Figure S6. Detailed analysis of telomerase activity in the individual mutant line S_041/3.

Acknowledgements

We thank Dr Eva Benkova (VIB Ghent, Belgium) for consultations on root elongation analysis. This work was supported by funding to ES and JF from the Academy of Sciences of the Czech Republic (IAA500040801), by funding to JF from the Czech Ministry of Education (LC06004), by

the project CEITEC (CZ.1.05/1.1.00/02.0068) from European Regional Development Fund, and by institutional funding (MSM0021622415, AV0Z50040507, AV0Z50040702). The technical assistance of Jana Kapustová and Marcela Šefčíková is greatly appreciated.

References

- Alonso JM, Stepanova AN, Leisse TJ, *et al.* 2003. Genome-wide insertional mutagenesis of *Arabidopsis thaliana*. *Science* **301**, 653–657.
- Beattie TL, Zhou W, Robinson MO, Harrington L. 2000. Polymerization defects within human telomerase are distinct from telomerase RNA and tep1 binding. *Molecular Biology of the Cell* **11**, 3329–3340.
- Bertrand C, Benhamed M, Li YF, Ayadi M, Lemonnier G, Renou JP, Delarue M, Zhou DX. 2005. *Arabidopsis* HAF2 gene encoding TATA-binding protein (TBP)-associated factor TAF1, is required to integrate light signals to regulate gene expression and growth. *Journal of Biological Chemistry* **280**, 1465–1473.
- Blackburn EH. 2000. Telomere states and cell fates. *Nature* **408**, 53–56.
- Brunaud V, Balergue S, Dubreucq B, *et al.* 2002. T-DNA integration into the *Arabidopsis* genome depends on sequences of pre-insertion sites. *EMBO Report* **3**, 1152–1157.
- Chaubet-Gigot N, Kapros T, Flenet M, Kahn K, Gigot C, Waterborg JH. 2001. Tissue-dependent enhancement of transgene expression by introns of replacement histone H3 genes of *Arabidopsis*. *Plant Molecular Biology* **45**, 17–30.
- Colgin LM, Wilkinson C, Englezou A, Kilian A, Robinson MO, Reddel RR. 2000. The hTERT alpha splice variant is a dominant negative inhibitor of telomerase activity. *Neoplasia* **2**, 426–432.
- Collard BCY, Das A, Virk PS, Mackill DJ. 2007. Evaluation of 'Quick' and 'Dirty' DNA extraction methods for marker-assisted selection in rice (*Oryza sativa* L.). *Plant Breeding* **126**, 47–50.
- Dellaporta SL, Wood J, Hicks JB. 1983. A plant DNA miniprep: version II. *Plant Molecular Biology Reporter* **1**, 19–21.
- Dohmann EM, Kuhnle C, Schwechheimer C. 2005. Loss of the CONSTITUTIVE PHOTOMORPHOGENIC9 signalosome subunit 5 is sufficient to cause the cop/det/fus mutant phenotype in *Arabidopsis*. *The Plant Cell* **17**, 1967–1978.
- Fajkus J, Fulneckova J, Hulanova M, Berkova K, Riha K, Matyasek R. 1998. Plant cells express telomerase activity upon transfer to callus culture, without extensively changing telomere lengths. *Molecular and General Genetics* **260**, 470–474.
- Fitzgerald MS, McKnight TD, Shippen DE. 1996. Characterization and developmental patterns of telomerase expression in plants. *Proceedings of the National Academy of Sciences, USA* **93**, 14422–14427.
- Fitzgerald MS, Riha K, Gao F, Ren S, McKnight TD, Shippen DE. 1999. Disruption of the telomerase catalytic subunit gene from *Arabidopsis* inactivates telomerase and leads to a slow loss of telomeric DNA. *Proceedings of the National Academy of Sciences, USA* **96**, 14813–14818.

- Gallego ME, White CI.** 2001. Rad50 function is essential for telomere maintenance in Arabidopsis. *Proceedings of the National Academy of Sciences, USA* **98**, 1711–1716.
- Grant JD, Broccoli D, Muquit M, Manion FJ, Tisdall J, Ochs MF.** 2001. Telometric: a tool providing simplified, reproducible measurements of telomeric DNA from constant field agarose gels. *Biotechniques* **31**, 1314–1316 1318.
- Heller-Uszynska K, Schnippenkoetter W, Kilian A.** 2002. Cloning and characterization of rice (*Oryza sativa* L) telomerase reverse transcriptase, which reveals complex splicing patterns. *The Plant Journal* **31**, 75–86.
- Henderson IR, Liu F, Drea S, Simpson GG, Dean C.** 2005. An allelic series reveals essential roles for FY in plant development in addition to flowering-time control. *Development* **132**, 3597–3607.
- Herbert BS, Hochreiter AE, Wright WE, Shay JW.** 2006. Nonradioactive detection of telomerase activity using the telomeric repeat amplification protocol. *Nature Protocols* **1**, 1583–1590.
- Jeon JS, Lee S, Jung KH, Jun SH, Kim C, An G.** 2000. Tissue-preferential expression of a rice alpha-tubulin gene, SsTubA1, mediated by the first intron. *Plant Physiology* **123**, 1005–1014.
- Kaneko R, Esumi S, Yagi T, Hirabayashi T.** 2006. Predominant expression of rTERTb, an inactive TERT variant, in the adult rat brain. *Protein and Peptide Letters* **13**, 59–65.
- Kilian A, Bowtell DD, Abud HE, Hime GR, Venter DJ, Keese PK, Duncan EL, Reddel RR, Jefferson RA.** 1997. Isolation of a candidate human telomerase catalytic subunit gene, which reveals complex splicing patterns in different cell types. *Human Molecular Genetics* **6**, 2011–2019.
- Kim TH, Kim BH, Yahalom A, Chamovitz DA, von Arnim AG.** 2004. Translational regulation via 5' mRNA leader sequences revealed by mutational analysis of the Arabidopsis translation initiation factor subunit eif3h. *The Plant Cell* **16**, 3341–3356.
- Liu K, Hodes RJ, Weng N.** 2001. Cutting edge: telomerase activation in human T lymphocytes does not require increase in telomerase reverse transcriptase (hTERT) protein but is associated with hTERT phosphorylation and nuclear translocation. *Journal of Immunology* **166**, 4826–4830.
- Mascarenhas D, Mettler IJ, Pierce DA, Lowe HW.** 1990. Intron-mediated enhancement of heterologous gene expression in maize. *Plant Molecular Biology* **15**, 913–920.
- Meyerson M, Counter CM, Eaton EN, et al.** 1997. Hest2, the putative human telomerase catalytic subunit gene, is up-regulated in tumor cells and during immortalization. *Cell* **90**, 785–795.
- Nakamura TM, Morin GB, Chapman KB, Weinrich SL, Andrews WH, Lingner J, Harley CB, Cech TR.** 1997. Telomerase catalytic subunit homologs from fission yeast and human. *Science* **277**, 955–959.
- Oguchi K, Liu H, Tamura K, Takahashi H.** 1999. Molecular cloning and characterization of AtTERT, a telomerase reverse transcriptase homolog in Arabidopsis thaliana. *FEBS Letters* **457**, 465–469.
- Oguchi K, Tamura K, Takahashi H.** 2004. Characterization of *Oryza sativa* telomerase reverse transcriptase and possible role of its phosphorylation in the control of telomerase activity. *Gene* **342**, 57–66.
- Ohtomo I, Ueda H, Shimada T, Nishiyama C, Komoto Y, Hara-Nishimura I, Takahashi T.** 2005. Identification of an allele of vam3/syp22 that confers a semi-dwarf phenotype in Arabidopsis thaliana. *Plant and Cell Physiology* **46**, 1358–1365.
- Pfaffl MW.** 2004. Quantification strategies in real-time PCR. In: Bustin SA, ed. *A–Z of quantitative PCR*. La Jolla, CA: International University Line, 87–112.
- Podlevsky JD, Bley CJ, Omana RV, Qi X, Chen JJ.** 2008. The telomerase database. *Nucleic Acids Research* **36**, D339–D343.
- Ren S, Johnston JS, Shippen DE, McKnight TD.** 2004. TELOMERASE ACTIVATOR1 induces telomerase activity and potentiates responses to auxin in Arabidopsis. *The Plant Cell* **16**, 2910–2922.
- Riha K, Watson JM, Parkey J, Shippen DE.** 2002. Telomere length deregulation and enhanced sensitivity to genotoxic stress in Arabidopsis mutants deficient in ku70. *EMBO Journal* **21**, 2819–2826.
- Rose AB, Elfersi T, Parra G, Korf I.** 2008. Promoter-proximal introns in Arabidopsis thaliana are enriched in dispersed signals that elevate gene expression. *The Plant Cell* **20**, 543–551.
- Rossignol P, Collier S, Bush M, Shaw P, Doonan JH.** 2007. Arabidopsis POT1a interacts with TERT-V(I8), an N-terminal splicing variant of telomerase. *Journal of Cell Science* **120**, 3678–3687.
- Ruckova E, Friml J, Prochazkova Schrupfova P, Fajkus J.** 2008. Role of alternative telomere lengthening unmasked in telomerase knock-out mutant plants. *Plant Molecular Biology* **66**, 637–646.
- Saracco SA, Miller MJ, Kurepa J, Vierstra RD.** 2007. Genetic analysis of SUMOylation in Arabidopsis: conjugation of SUMO1 and SUMO2 to nuclear proteins is essential. *Plant Physiology* **145**, 119–134.
- Sessions A, Burke E, Presting G, et al.** 2002. A high-throughput Arabidopsis reverse genetics system. *The Plant Cell* **14**, 2985–2994.
- Shakirov EV, Shippen DE.** 2004. Length regulation and dynamics of individual telomere tracts in wild-type Arabidopsis. *The Plant Cell* **16**, 1959–1967.
- Son J, Lee JH, Kim HN, Ha H, Lee ZH.** 2010. cAMP-response-element-binding protein positively regulates breast cancer metastasis and subsequent bone destruction. *Biochemical and Biophysical Research Communications* **398**, 309–314.
- Sykorova E, Fajkus J.** 2009. Structure–function relationships in telomerase genes. *Biology of the Cell* **101**, 375–392.
- Sykorova E, Leitch AR, Fajkus J.** 2006. Asparagales telomerases which synthesize the human type of telomeres. *Plant Molecular Biology* **60**, 633–646.
- Sykorova E, Lim KY, Chase MW, Knapp S, Leitch IJ, Leitch AR, Fajkus J.** 2003. The absence of Arabidopsis-type telomeres in *Cestrum* and closely related genera *Vestia* and *Sessea* (Solanaceae): first evidence from eudicots. *The Plant Journal* **34**, 283–291.
- Tamura K, Liu H, Takahashi H.** 1999. Auxin induction of cell cycle regulated activity of tobacco telomerase. *Journal of Biological Chemistry* **274**, 20997–21002.
- Ulaner GA, Hu JF, Vu TH, Giudice LC, Hoffman AR.** 1998. Telomerase activity in human development is regulated by human telomerase reverse transcriptase (hTERT) transcription and by

alternate splicing of hTERT transcripts. *Cancer Research* **58**, 4168–4172.

Ulaner GA, Hu JF, Vu TH, Giudice LC, Hoffman AR. 2001. Tissue-specific alternate splicing of human telomerase reverse transcriptase (hTERT) influences telomere lengths during human development. *International Journal of Cancer* **91**, 644–649.

Upadhyaya NM, Surin B, Ramm K, Gaudron J, Schunmann PHD, Taylor W, Waterhouse PM, Wang MB. 2000. Agrobacterium-mediated transformation of Australian rice cultivars Jarrah and Amaroo using modified promoters and selectable markers. *Australian Journal of Plant Physiology* **27**, 201–210.

Wang MB, Upadhyaya NM, Brettell RIS, Waterhouse PM. 1997. Intron-mediated improvement of a selectable marker gene for plant transformation using *Agrobacterium tumefaciens*. *Journal of Genetics and Breeding* **513**, 325–334.

Wang YH. 2008. How effective is t-DNA insertional mutagenesis in Arabidopsis? *Journal of Biochemical Technologies* **1**, 11–20.

Wilmoth JC, Wang S, Tiwari SB, Joshi AD, Hagen G, Guilfoyle TJ, Alonso JM, Ecker JR, Reed JW. 2005. Nph4/arf7 and arf19 promote leaf expansion and auxin-induced lateral root formation. *The Plant Journal* **43**, 118–130.

Xu XM, Rose A, Muthuswamy S, Jeong SY, Venkatakrisnan S, Zhao Q, Meier I. 2007. NUCLEAR PORE ANCHOR, the Arabidopsis homolog of Tpr/Mlp1/Mlp2/megator, is involved in mRNA export and SUMO homeostasis and affects diverse aspects of plant development. *The Plant Cell* **19**, 1537–1548.

Yi X, White DM, Aisner DL, Baur JA, Wright WE, Shay JW. 2000. An alternate splicing variant of the human telomerase catalytic subunit inhibits telomerase activity. *Neoplasia* **2**, 433–440.

Hypomethylating drugs efficiently decrease cytosine methylation in telomeric DNA and activate telomerase without affecting telomere lengths in tobacco cells

Eva Majerová, Miloslava Fojtová, Iva Mozgová, Miroslava Bittová & Jiří Fajkus

Plant Molecular Biology

An International Journal on Molecular Biology, Molecular Genetics and Biochemistry

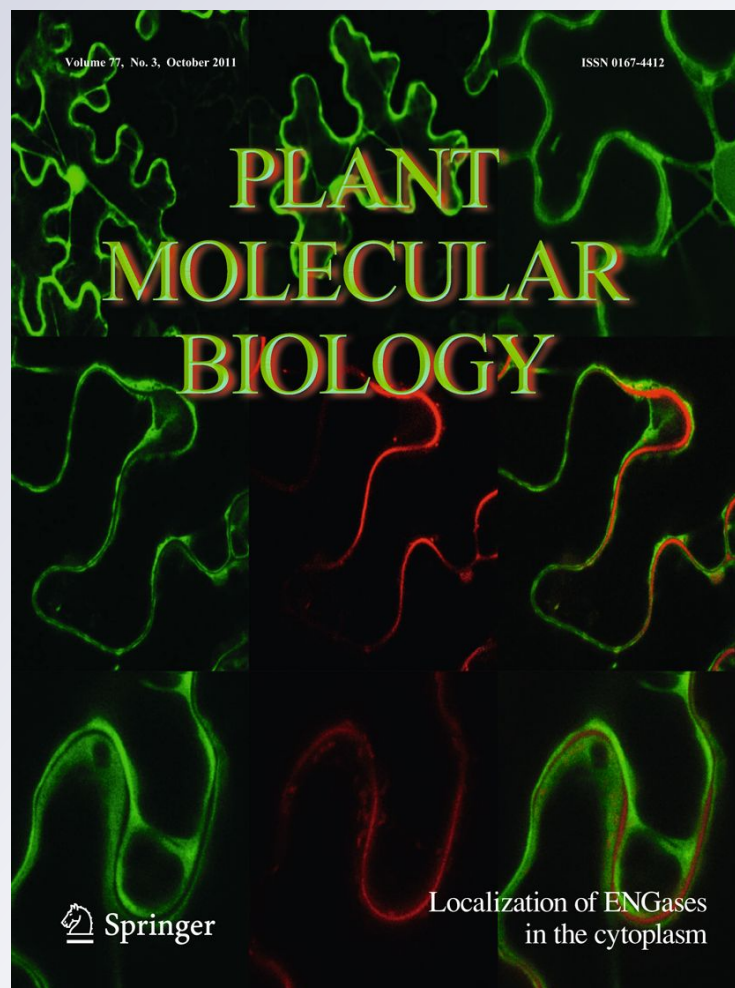
ISSN 0167-4412

Volume 77

Combined 4-5

Plant Mol Biol (2011) 77:371-380

DOI 10.1007/s11103-011-9816-7



Your article is protected by copyright and all rights are held exclusively by Springer Science+Business Media B.V.. This e-offprint is for personal use only and shall not be self-archived in electronic repositories. If you wish to self-archive your work, please use the accepted author's version for posting to your own website or your institution's repository. You may further deposit the accepted author's version on a funder's repository at a funder's request, provided it is not made publicly available until 12 months after publication.

Hypomethylating drugs efficiently decrease cytosine methylation in telomeric DNA and activate telomerase without affecting telomere lengths in tobacco cells

Eva Majerová · Miloslava Fojtová ·
Iva Mozgová · Miroslava Bittová · Jiří Fajkus

Received: 13 April 2011 / Accepted: 11 August 2011 / Published online: 25 August 2011
© Springer Science+Business Media B.V. 2011

Abstract Telomere homeostasis is regulated at multiple levels, including the local chromatin structure of telomeres and subtelomeres. Recent reports demonstrated that a decrease in repressive chromatin marks, such as levels of cytosine methylation in subtelomeric regions, results in telomere elongation in mouse cells. Here we show that a considerable fraction of cytosines is methylated not only in subtelomeric, but also in telomeric DNA of tobacco BY-2 cells. Drug-induced hypomethylation (demonstrated at subtelomeric, telomeric, and global DNA levels) results in activation of telomerase. However, in contrast to mouse cells, the decrease in 5-methylcytosine levels and upregulation of telomerase do not result in any changes of telomere lengths. These results demonstrate the involvement of epigenetic mechanisms in the multilevel process of regulation of telomerase activity in plant cells and, at the same time, they indicate that changes in telomerase activity can be overridden by other factors governing telomere length stability.

Keywords *Nicotiana tabacum* · Cell culture · Telomere · Hypomethylating agents · Zebularine · DNA methylation

Introduction

Telomeres are nucleoprotein complexes forming and protecting the ends of linear eukaryotic chromosomes. They consist of short minisatellite repeats whose sequence is highly conserved through the eukaryotic kingdom, e.g. TTAGGG in vertebrates, and TTTAGGG in most plants. Critical shortening of telomeres, which can occur due to repeated incomplete replication of their 3' end, forces the cell to stop the cell cycle and eventually start apoptotic processes. On the other hand, cells with telomeres that are stably maintained during successive replication cycles become immortal, which is the case of most of cancer cells (Hiyama and Hiyama 2002; Gonzalez-Suarez et al. 2001; Kunicka et al. 2008).

The shortening of telomeres is normally compensated by a specific nucleoprotein complex, telomerase, that is composed of two essential subunits, the catalytic subunit (TERT) and the RNA-subunit (TERC) (Greider and Blackburn 1985; Greider and Blackburn 1987). In human and other mammalian cells, the lack of telomerase in differentiated cells leads to a progressive shortening of telomeres and natural ageing of cells, tissues and organisms (Fajkus et al. 2002; Shay and Wright 2010).

In contrast to humans, plant telomeres are not shortened during ontogenesis (Fajkus et al. 1998; Riha et al. 1998) due to the presence of telomerase activity in dividing meristem cells. Telomerase-deficient *Arabidopsis thaliana* mutants (*Attert-/-*) show surprisingly low rates of telomere shortening per generation (250–500 bp) (Fitzgerald et al. 1996). It was shown recently that these apparently

E. Majerová · M. Fojtová · I. Mozgová · J. Fajkus (✉)
Department of Functional Genomics and Proteomics, Faculty
of Science and Central European Institute of Technology
(CEITEC), Masaryk University, Kamenice 5, 62500 Brno,
Czech Republic
e-mail: fajkus@sci.muni.cz

M. Bittová
Department of Chemistry, Faculty of Science, Masaryk
University, Kotlářská 2, 61137 Brno, Czech Republic

J. Fajkus
Institute of Biophysics, Academy of Sciences of the Czech
Republic, v.v.i., Královopolská 135, 61265 Brno,
Czech Republic

low rates of telomere shortening result from activation of alternative lengthening of telomeres (ALT) which partially compensates for replicative telomere loss in these mutants (Ruckova et al. 2008).

Recent studies showed an involvement of epigenetic mechanisms in regulation of telomere length in mice, where a decrease in DNA and histone methylation marks in mouse embryonic stem cells leads to increased telomere length (Gonzalo et al. 2006; Garcia-Cao et al. 2004). Other experiments revealed that even telomerase-deficient mice with short telomeres exhibit changes in epigenetic pattern of their telomeres and subtelomeres (Benetti et al. 2007).

DNA methylation, historically the first recognized (Doskocil and Sorm 1962) and the first characterized epigenetic modification, plays an important role in regulation of gene expression in eukaryotic cells (for review see Vaillant and Paszkowski (2007); Geiman and Muegge (2010)). Generally, highly methylated blocks in the genome are transcriptionally inactive whereas non-methylated regions are active.

Methylation of cytosines is performed by special enzymes called DNA methyltransferases and is non-random. 5-methylcytosines (5mCs) occur in symmetrical doublet CpGs and, especially in plant DNA, in triplet CpNpG motifs (where N is C, A or T) (Gruenbaum et al. 1981). In addition, methylation of asymmetric CpNpN motifs was observed in plants (Meyer et al. 1994). Methylation in different sequence contexts is known to correspond to different enzymatic activities responsible for “de novo” methylation and for maintenance DNA methylation, respectively (Zhang et al. 2010). De novo methylation occurs at sites that were not methylated before, thus creating new methylation patterns, and the best-known family of de novo DNA methyltransferases in plants is a group of domains rearranged methyltransferases (DRM, homologue to the mammalian Dnmt3 family) (Cao et al. 2000). It was observed that de novo methylation in plants is mediated by an RNA-directed DNA methylation (RdDM) pathway (Cao and Jacobsen 2002b), for review see Chinnusamy and Zhu (2009). Maintenance methylation is targeted to hemi-methylated sequences and conserves already-existing methylation patterns during the replication of DNA. In plants, there are two families of maintenance DNA methyltransferases, the MET1 family (homologues of mammalian Dnmt1), responsible for maintaining the DNA methylation pattern in CpG sequence contexts during the cell cycle (Finnegan and Dennis 1993) and a plant-specific group containing a specific chromodomain, the chromomethyltransferases (CMT) (Henikoff and Comai 1998) that are responsible for stable CpNpG methylation (Cao and Jacobsen 2002a). The latest-known DNA methyltransferase is Dnmt2, but its role in cytosine methylation remains unknown (Zhang et al. 2010).

To study the role of DNA methylation in organisms, targeted gene knock-out of one or more DNA methyltransferases or treatment with hypomethylating drugs (inhibiting methylation) can be used. While genetic modification is usually extensive and permanent, inhibitor treatments allow for transient hypomethylation that can be easily reversed. Among the first discovered hypomethylating drugs were 5-azacytidine and 5-aza-2'-deoxycytidine (Cihak 1974) which are cytidine analogues able to be incorporated into DNA during replication and to influence the DNA methylation level by the formation of a stable complex with DNA methyltransferases. In view of their instability, considerable toxicity and many side-effects (e.g. induction of chromosome breaks) (Beisler 1978; Ghoshal and Bai 2007) they are not very suitable for epigenetic research. The search for a universal hypomethylating drug with a minimum of side-effects brought in another cytidine analogue, zebularine (1-(β -D-ribofuranosyl)-1,2-dihydropyrimidine-2-one) which was synthesized as a cytidine deaminase inhibitor (Kim et al. 1986) and which at present, due to its good stability and low toxicity, is often used in pharmaceutical treatment (for review see Yoo et al. 2004). The effects of zebularine-induced DNA hypomethylation in plants have been described earlier (Baubec et al. 2009).

Besides cytidine analogues, there are drugs that inhibit methylation by different mechanisms. These include DHPA ((S)-9-(2,3-dihydroxypropyl)adenine), first synthesized by Holy (1975) which is a competitive inhibitor of S-adenosyl-L-homocysteine hydrolase, thereby blocking recycling of S-adenosyl-methionine. The depleted pool of this donor of active methyl groups then limits the extent of both DNA- and histone-methyltransferase reactions. DHPA was originally found to have a broad-spectrum antiviral activity (De Clercq et al. 1978) and its hypomethylating impact was discovered only later (Šebestová et al. 1984). At present, a number of experimental studies using this drug are available, including its use in plant systems (Fojtova et al. 1998; Kovarik et al. 2000; Fulnecek et al. 2011).

In 2008, asymmetric methylation of the C-telomeric strand was first detected in *Arabidopsis thaliana* by high-throughput bisulfite sequencing (Cokus et al. 2008), and recently this methylation was shown to be mediated by a siRNA pathway (Vrbsky et al. 2010). Based on these observations and considering the complexity of plant epigenetic pathways, including telomere methylation, questions on a possible role of DNA methylation in telomere maintenance have arisen. Since the *A. thaliana* genome with a low content of heterochromatin may not be a representative model for the plant kingdom (absence of subtelomeric heterochromatin blocks which are typical for most plant genomes, short telomere tracts), an alternative system, the tobacco BY-2 cell line (Nagata et al. 1992), was chosen for

this study. This cell line was successfully used in previous studies of plant telomere biology, including the historically first demonstration of telomerase activity in plant cells (Fajkus et al. 1996). Moreover, telomere-subtelomere junctions (Fajkus et al. 1995b), as well as chromatin structure of telomeres and subtelomeres (Fajkus et al. 1995b; Fajkus et al. 1992; Fajkus and Trifonov 2001) have been characterized in *Nicotiana tabacum*.

In this article we ask whether telomeres in tobacco BY-2 cells are methylated and whether their methylation status can be influenced by hypomethylating agents. We also investigate a possible influence of hypomethylating drugs on telomere maintenance and telomerase activity. Drug-induced DNA hypomethylation is correlated with increased telomerase activity, but in contrast to mouse cells, it does not result in changed telomere lengths.

Materials and methods

Plant material and growth conditions

Nicotiana tabacum BY-2 cells (Nagata et al. 1992) were cultivated in suspension cultures in standard MS medium (Duchefa, M0255.0050) supplemented with sucrose (20 g/l) and 2,4-dichlorophenoxyacetic acid (0.2 mg/l) at 24°C under constant shaking (130 RPM). DHPA and zebularine (5, 10, 25 or 50 µM) were added and cells were cultivated for 1 week. Four ml of the cell culture was then inoculated to fresh media (16 ml) and the remaining cells were harvested using vacuum filtration and used immediately or frozen in liquid nitrogen and stored at –80°C. The morphology of cells was monitored with the phase-contrast microscope.

Analysis of subtelomeric methylation

DNA from plant cells was isolated according to Dellaporta et al. (1983) and 1 µg was cleaved by the methylation-sensitive restriction endonucleases *MspI* or *HpaII* (10 U) overnight and separated in a 1% (w/v) agarose gel. DNA was blotted onto HybondTM-XL membrane (GE Healthcare) and hybridized with a probe for the tobacco subtelomeric satellite repetitive sequence HRS60 (GenBank: X15068.1 (Koukalova et al. 1989)) labelled with α -[³²P]-dATP by random priming (DecaLabelTM DNA labelling kit, MBI Fermentas) and hybridized at 65°C overnight in 0.25 M Na-phosphate pH 7.5, 7% SDS, 0.016 M EDTA. Membranes were washed 3 times in 0.2 × SSC + 0.1% (w/v) SDS for 30 min at 65°C. Hybridization patterns were visualised using a phosphorimager FLA 7000 (FUJI) and analysed by MultiGauge (FujiFilm). The relative level

of cytosine methylation in the HRS60 region was expressed as the ratio of the signal corresponding to bands shorter than 1 kb (the cleaved fraction of DNA with a low content of methylated cytosines) to the total hybridization signal in the lane.

MspI and *HpaII* both recognize the site CCGG and cleave it if completely unmethylated. If the external cytosine is not methylated and the internal remains methylated, *MspI* cleaves the site but not *HpaII*; in all other cases, neither of these enzymes is able to cleave the site. *HpaII* also cleaves under specific conditions when DNA is hemimethylated after replication (Walder et al. 1983).

Whole-genome methylation analysis (according to Havlis et al. 2001)

Forty µg of DNA was cleaved by 100 U of *MspI* or *HpaII* at 37°C and then purified by SDS (0.1%) and NaCl (0.25 M), precipitated by ethanol, and dissolved in TE (1 mM EDTA, 10 mM Tris-HCl). Samples were digested by 500 U of *ExoIII* nuclease and the level of methylated cytosines was evaluated by HPLC using a 10 AVP HPLC system (Shimadzu, Tokyo, Japan) consisting of GT-154 degasser, SCL-10AVP system control unit, LC-10AVP pumps, CTO-10ASVP oven, SPD-M10AVP spectrophotometric detector with diode-array, Class-VP 5.02 software, with 2 × 100 × 4.6 mm hyphenated monolithic columns and Onyx C18 (Phenomenex, USA) columns. The mobile phase was 50 mM phosphate buffer, pH 3, 4% methanol and the flow rate 1.3 ml/min: 10 µl of sample was injected directly and spectra were recorded in the 200–300 nm range.

Analysis of methylation of telomeric DNA (based on Vrbsky et al. 2010)

Genomic DNA was treated by sodium bisulfite (EpiTect Bisulfite Kit, QIAGEN), when non-methylated cytosines are converted to uracils while methylcytosines are resistant to conversion, and transferred onto a nylon membrane by vacuum dot blotting (Bio-Rad Dot Blot). Membranes were hybridized with radioactively-labelled oligonucleotide probes overnight at 42°C in ULTRAhybTM-Oligo Hybridization Buffer (Ambion). The probe AtTR4-C (5'-CCC TAA ACC CTA AAC CCT AAA CCC TAA A 3') was used as the loading normaliser and the probe DEGENER (5' TTA GRR TTT AGR RTT TAG RRT TTA GRR T 3') to detect the fraction of telomeric repeats methylated on the third (inner) cytosine of the (5'-CCCTAAA-3')_n sequence, a major type of telomeric DNA methylation in plants (Cokus et al. 2008); R (i.e. A or G) is used at the complementary positions in the probe because the first and second cytosines

in the repeat are either methylated or non-methylated. Hybridization signals were visualised and evaluated as described above.

Evaluation of TERRA (Telomere Repeat-containing RNA)

Total RNA was isolated using the RNeasy Plant Mini Kit (Qiagen) according to the manufacturer's instructions. The quality and quantity of RNA was checked by electrophoresis on a 1% (w/v) agarose gel and by absorbance measurement (NanoPhotometr IMPLN). Ten µg of RNA were separated by electrophoresis in a 1.2% (w/v) formaldehyde-agarose gel and the gel was washed for 10 min in sterile water to remove formaldehyde. RNA was denatured for 15 min in 0.05 M NaOH and blotted to a Hybond XL membrane in $20 \times$ SSC. The membrane was hybridized with the end-labeled telomeric probe AtTR4-C in ULTRAhyb hybridization buffer (Ambion) for 24 h at 40°C. After washing under low stringency conditions (twice in $2 \times$ SSC + 0.1% (w/v) SDS at 50°C for 15 min), hybridization signals were visualised and evaluated as described above.

Terminal restriction fragment (TRF) analysis

Cells were embedded in agarose blocks as described in Fojtova et al. (2002). The DNA concentration and integrity was checked by a preliminary PFGE (pulsed field gel electrophoresis) using a Gene Navigator (Pharmacia Biotech). Pieces of agarose blocks containing equal amounts of DNA were washed three times in $0.1 \times$ TE (0.1 mM EDTA, 1 mM Tris-HCl, pH 8.0) and digested overnight with 60U of *Hinf*I, *Hae*III or both. DNA was separated by PFGE (pulse times: 2 s for 2 h; ramping 2–20 s for 17 h; and 20 s for 1 h; 180 V; 12°C) in a 1% (w/v) agarose gel in $0.5 \times$ TBE (4.5 mM Tris-HCl, 4.5 mM boric acid, 1.25 mM EDTA). The gel was Southern-blotted onto HybondTM-XL membrane (GE Healthcare) and hybridized with the telomeric oligonucleotide probe AtTR4-C in 0.25 M Na-phosphate pH 7.5, 7% SDS, 0.016 M EDTA at 55°C overnight. The membrane was washed three times in $2 \times$ SSC, 0.5% SDS at 55°C. Hybridization signals were visualised and evaluated as described above and the mean telomere length in a particular lane was defined as the position which corresponded to half of the total peak area. Student's *t* test ($P < 0.05$) was performed to evaluate the data statistically.

Nucleosomal periodicity assay

Nuclei were isolated and nucleosomal digestion was performed as described in (Fajkus et al. 1995a) using three parallel samples for 3, 9 and 27 min. DNA was separated on a 2% (w/v) agarose gel and transferred by Southern blotting

onto HybondTM-XL membranes (GE Healthcare) which were hybridized either with the telomeric oligonucleotide probe AtTR4-G or with a probe for the tobacco subtelomeric satellite repetitive sequence HRS60. Hybridization signals were visualised and evaluated as described above.

Telomere repeat amplification protocol (TRAP and qTRAP)

Protein extracts from cells were isolated following the protocol in Fitzgerald et al. (1996). The TRAP method was performed as described in Fajkus et al. (1998) using TS21 as a substrate primer (5'-GAC AAT CCG TCG AGC AGA GTT-3') and TelPr as a reverse primer (5'-CCG AAT TCA ACC CTA AAA CCC TAA ACC CTA AAC CCC-3'). For qTRAP, the quantitative version of TRAP, the protocol described in Kannan et al. (2008) was followed using the following primers: RRTTRAPfwd (5'-CAC TAT CGA CTA CGC GAT CAG-3') and RRTTRAPrev1 (5'-CCC TAA ACC CTA AAC CCT AAA-3') or RRTTRAPrev2 (5'-CCCTAAACCCTAAACCCTAAACCC-3'), respectively. Two different reverse primers were used to increase the statistical significance and to eliminate possible errors. Relative telomerase activity was calculated as $R = E_{ctrl}^{Ct} / E_{treated}^{Ct}$ (E is the efficiency of the reaction) and all measurements were repeated at least three times using two parallel biological replicates.

Results and discussion

Decreased level of methylcytosines at subtelomeres and at the whole genome level induced by drug treatment

In order to induce hypomethylation of DNA, cells were cultivated in presence of (S)-9-(2,3-dihydroxypropyl)adenine (DHPA) or zebularine in different concentrations (5–50 µM). In view of the cytotoxic effect of both agents (Yoo et al. 2004; Wingard et al. 1983; Jelinek et al. 1981; Baubec et al. 2009) the number of culture passages was limited to three for DHPA and only a single passage for zebularine before the onset of significant growth inhibition. As demonstrated by light microscopy, treated cells showed distinct morphological features including oval shape, markedly reduced protoplasts, and loss of the typical concatenation (Fig. 1).

To evaluate the hypomethylating effect of the drugs, the level of DNA methylation was analysed by three distinct approaches. Firstly, the methylation of the subtelomeric satellite repeat HRS60 was evaluated using the methylation-sensitive restriction endonucleases *Msp*I and *Hpa*II.

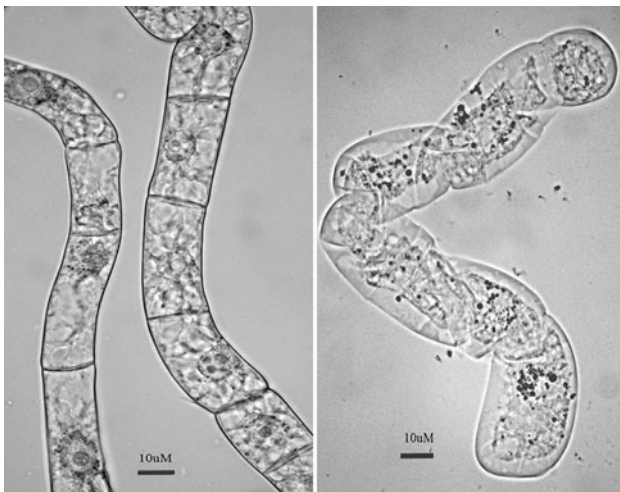


Fig. 1 Morphological difference between control cells and cells treated with 50 μM DHPA at the second passage. Cells were observed using light microscopy without staining. *Left panel* control cells; *right panel* DHPA-treated cells. The bars indicate 10 μm

These both recognize CCGG sites and cleave them if both cytosines are non-methylated, but *MspI* digestion is inhibited by methylation of the outer and *HpaII* is inhibited when either cytosine is methylated.

The results summarized in Fig. 2 demonstrate that both drugs did trigger the hypomethylation of cytosines located in the subtelomeric repeat HRS60, but in different modes. DHPA affected mostly methylation of external cytosines,

as follows from the fact that *MspI* could digest up to almost 60% while differences in *HpaII* digestion between treated and control cells are less pronounced, especially at low DHPA concentration (Fig. 2a–c, e). This DHPA-induced preferential hypomethylation of the external cytosine in CCGG corresponds to previous findings (Kovarik et al. 1994). Although a gradual decrease of methylation during prolonged cultivation in the presence of DHPA was observed, there is no significant dependence of the final maximum extent of hypomethylation on DHPA concentration. This result is evidence for a different sensitivity of genomic loci in tobacco to DHPA-induced hypomethylation, because conspicuous dependence of the level of hypomethylation of 5S rDNA loci on DHPA concentration was reported previously (Fojtova et al. 1998). A fast recovery of the original methylation pattern was observed upon the transfer of cells treated by 5 μM DHPA to DHPA-free medium (4th passage, Fig. 2a), in accordance with the previously-reported reversal of DHPA-induced hypomethylation of cytosines in the CpNpG sequence context in tobacco (Koukalova et al. 2002). A possible hypomethylation of the internal cytosine in the absence of hypomethylation of the external cytosine in the CCGG context cannot be evaluated using this approach.

Zebularine decreased methylation of both cytosines in CCGG sites (Fig. 2d) as shown by the similar extent of DNA digestion by either of the enzymes in the HRS60 repeat in response to the treatment.

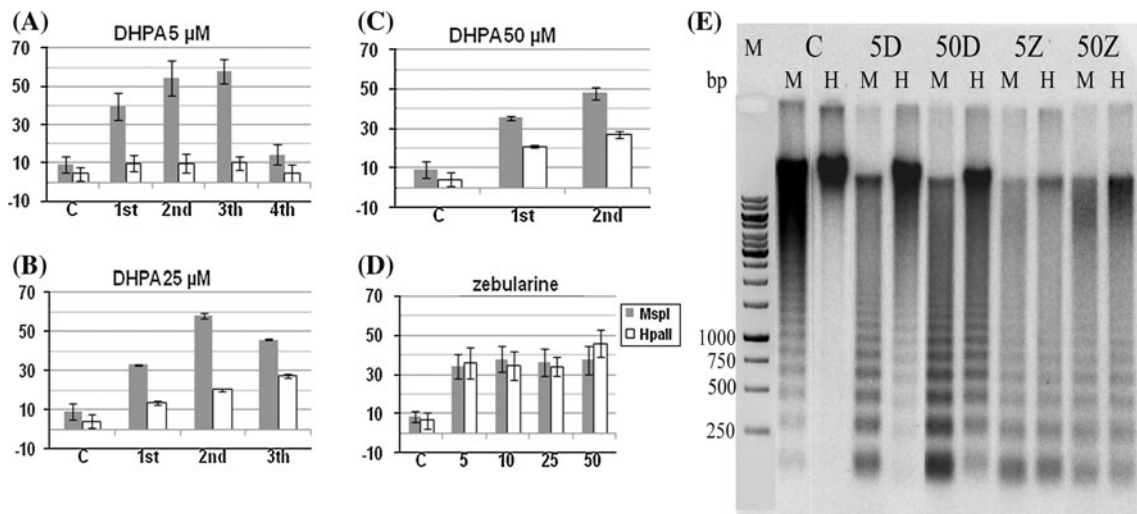


Fig. 2 Drug-induced hypomethylation of cytosines within the CCGG context in the subtelomeric satellite region HRS60. DNA methylation was assayed using methylation-sensitive restriction enzymes followed by Southern hybridization. **a–c** Relative hypomethylation (%) in cells treated by DHPA (up to 3 passages). DHPA concentrations are given above the graphs. The 4th passage in **a** represents recovery of the methylation pattern in cells transferred to DHPA-free medium.

d Relative hypomethylation (%) in cells treated by zebularine at different concentrations (μM) in the first passage. Data were taken from 15 independent analyses (biological and technical repeats included). **e** Southern hybridization of DNA isolated from cells after the 1st passage in the presence of a hypomethylating drug. *Lanes* are labelled as follows: *D* DHPA, *Z* zebularine, 5 and 50 indicate concentration of the drug (μM), *M* *MspI*, *H* *HpaII*

To extend the methylation analysis to the whole genome level, the HPLC method was used. The results showed a rapid decrease of methylated cytosines in the genome during the 1st passage of the treatment by hypomethylating drugs (Fig. 3); while in the control cells the ratio cytosine/methylcytosine was close to 2, in treated cells it reached up to 6.5 and 7.5 for 25 μ M DHPA and all concentrations of zebularine, respectively. Similar analysis was done using *Arabidopsis thaliana* seedlings treated by 20–80 μ M zebularine (Baubec et al. 2009) and a loss of methylcytosines was observed in treated cells, but it was considerably less pronounced compared to the tobacco system. This variation in effects of zebularine on hypomethylation may be related to the significantly different levels of methylated cytosines in the genomes of these two model plants.

Drug-induced hypomethylation of telomeric DNA

To examine the levels of cytosine methylation and induced hypomethylation at tobacco telomeres that contain cytosines only in the asymmetric sequence context (CCCTAAA), DNA was treated by sodium bisulfite. We then measured the relative difference between the hybridization signals of specific oligonucleotides reflecting the total telomeric signal (AtTR4-C probe) and the (partially) methylated fraction (DEGENER probe) in control and treated cells. As shown in Fig. 3b, c, in both DHPA- and zebularine-treated cells the level of methylation of telomeres decreased to 20–26% of that in control cells; both drugs induced a similar extent of hypomethylation and the effect was not dose-dependent under the conditions used.

Comparison of the maximum levels of relative hypomethylation of telomeric (five-fold), subtelomeric (six-fold) and whole-genome DNA (three and a half-fold) shows the more marked response of terminal and subterminal chromosome regions to both drugs, probably

reflecting their naturally heterochromatic character with a high frequency of methylcytosines (Richards and Elgin 2002). The observed hypomethylation of telomeres also shows that both drugs also inhibit methylation of asymmetric cytosines in telomeric (CCCTAAA)_n repeats which is mediated by siRNA (Vrbsky et al. 2010).

Response of TERRA transcription to hypomethylation

Even though the telomeric regions are considered as heterochromatic, they are not transcriptionally silent in control cells. To see whether the level of their transcription was influenced by the epigenetic changes caused by DHPA and zebularine, the level of TERRA was measured. At high concentrations, DHPA influenced the transcription of telomeres negatively (five-fold decrease) whereas zebularine, even at low concentrations (5 μ M), increased it up to three-fold as compared to the control cells (Fig. 4a, b). This difference could be explained by a different mechanism of action of these reagents. As zebularine (as a cytidine analogue) inhibits only methylation of DNA, the rapid hypomethylation causes an increase in transcription at a global scale including telomeres (as shown in Ng et al. (2009)). On the other hand, DHPA inhibits both DNA and histone methyltransferases which brings about potentially ambiguous changes in chromatin structure and in the ratio of euchromatin to heterochromatin (e.g. hypomethylation of H3K9me3 to H3K9me2 leads to heterochromatinization in plants) (Feng and Jacobsen 2011). In this case, subtelomeric regions where TERRA transcription is initiated could be relatively more heterochromatinized and the transcription level would decrease noticeably. Interestingly, telomeric chromatin in *A. thaliana* shows (in addition to the repressive H3K9me2 and H3K27me1 histone H3 marks) also the presence of an “active” mark, H3K4me3 (Vrbsky et al. 2010) whose decrease due to

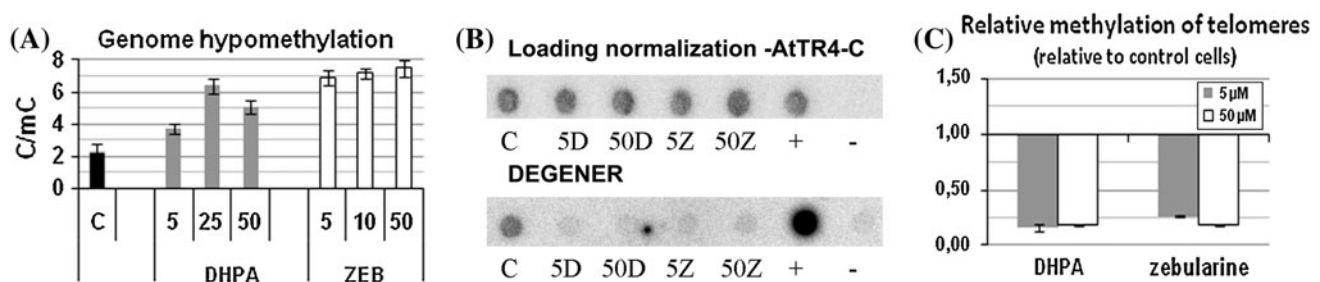


Fig. 3 Drug-induced cytosine hypomethylation at the whole genome level (a) and in telomeric sequences (b, c). **a** Ratio of cytosine to methylcytosine determined by HPLC in the genome of control cells (C) or cells treated by DHPA (grey columns) or by zebularine (white columns). Data were taken from 2 independent analyses (each with three technical repeats). **b** Level of methylated cytosines in telomeric sequences. Cells were cultivated in the presence of the hypomethylating drug at a concentration of 5 or 50 μ M, DNA was treated by bisulfite and

analysed by Southern hybridization using the C-strand telomeric probe (AtTR4-C) as a loading normaliser and the DEGENER probe to determine the level of methylated cytosines. As positive control (+), genomic DNA was loaded and as negative control (-), plasmid pcDNA3 with no insertion was used. **c** Relative methylation of telomeres in treated cells relative to control cells (methylation of control cells has been considered as 1). Grey columns, cells treated with the respective drug at 5 μ M; white columns, cells treated at 50 μ M

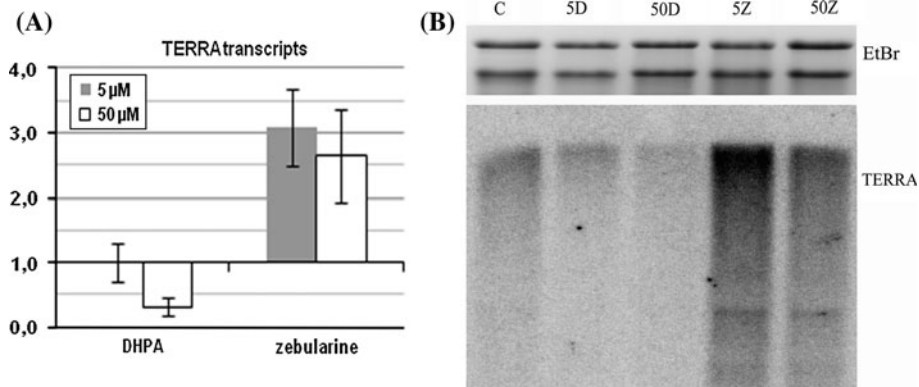


Fig. 4 Transcription of telomeric sequences in cells treated by hypomethylating drugs. **a** Relative level of telomeric transcripts in drug-treated cells relative to control cells (transcription in control cells was considered as 1); drug concentrations are indicated. High concentrations of DHPA (50 μ M) significantly decreased the level of TERRA transcription whereas even low concentration of zebularine

(5 μ M) increased it. Data were taken from 2 independent analyses. **b** Northern hybridization. *Top panel* RNA gel stained with ethidiumbromide; *bottom panel* hybridization with the telomeric probe (AtTR4-C). Abbreviations are the same as in Fig. 2. Note the significant increase of the TERRA signal in cells treated by 5 μ M zebularine

DHPA-induced hypomethylation could contribute to the lower level of TERRA transcription. Surprisingly, in contrast to the negative regulatory effect of TERRA on telomerase activity and telomere length observed in mammals and fungi (reviewed in Feuerhahn et al. 2010), the observed changes of TERRA levels in tobacco cells in response to hypomethylating treatments had no apparent effect on telomerase activity (the activity was increased independently of either decreased or increased TERRA levels in DHPA- and zebularine-treated cells, respectively). Telomere lengths were stable in spite of these changes in telomerase activity (see below) and TERRA levels.

Nucleosome periodicity is maintained in the course of hypomethylation

Along with the changes at the transcription level caused by modified epigenetic regulation, we focused on nucleosome spacing in subtelomeric and telomeric regions in control and treated cells. No significant changes in the nucleosome repeat lengths were observed (data not shown), but a difference was observed between telomeric (repeat length 156 bp) and subtelomeric HRS60 chromatin (180 bp) as described earlier (Fajkus et al. 1995a).

Telomerase activity increases in cells treated by hypomethylating drugs without affecting the length of telomeres

Having confirmed that these drugs induce ongoing hypomethylation, we could approach the main objective of

this work of finding out whether methylation status participates in the regulation of telomere maintenance. For this purpose, the activity of telomerase was measured by TRAP and qTRAP assays and the length of telomeres by TRF analysis. Interestingly, higher concentrations of zebularine and DHPA considerably increased telomerase activity relative to control cells and, in the case of DHPA, it increased further with subsequent passage (Fig. 5b, c). Cells treated with DHPA displayed higher activity of telomerase in comparison with cells treated with the same concentration of zebularine, which presumably can be explained by their different modes of action at promoters of telomerase subunits. Upon transfer of the cells to DHPA-free medium in the 4th passage (Fig. 5b), we could see an immediate reversion of the telomerase activity to the level of control cells (see also the reversal of DNA methylation status in Fig. 2a). DNA hypomethylation thus coincided with increased telomerase activity. As shown in Fig. 5a the pattern of the TRAP assay products in treated cells is very similar to that of control cells and of *Arabidopsis thaliana* seedlings.

Astonishingly, in spite of the activation of telomerase, no corresponding change could be observed in the length of telomeres in treated cells versus control cells (see Fig. 6a–c). This result clearly demonstrates that the activity of telomerase, though necessary for telomere elongation, is just one of many factors involved in regulation of telomere length homeostasis (Fajkus et al. 1998) in addition to, for example, local telomere structure and its accessibility to telomerase. Presumably, specific telomere-binding proteins described earlier in tobacco (Fulneckova and Fajkus 2000; Yang et al. 2004; Lee and Kim 2010) are able to override an increased or aberrant

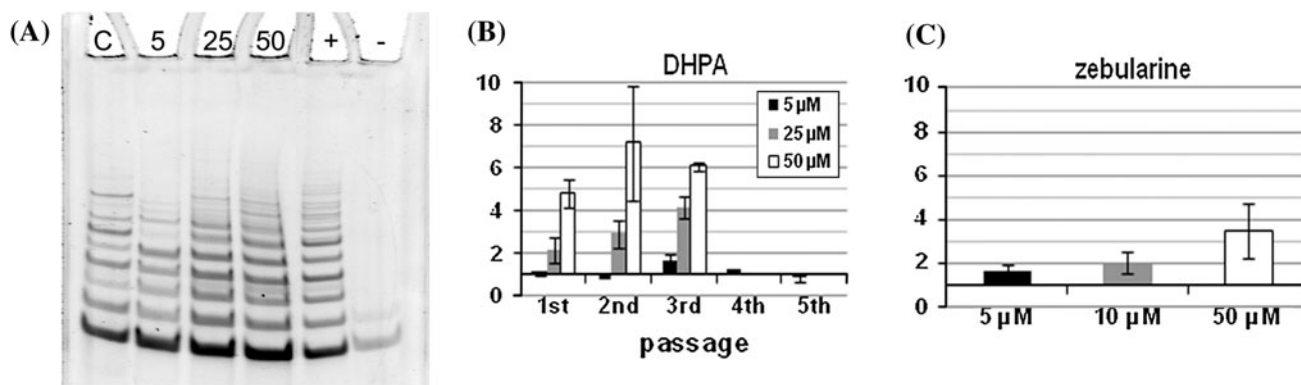
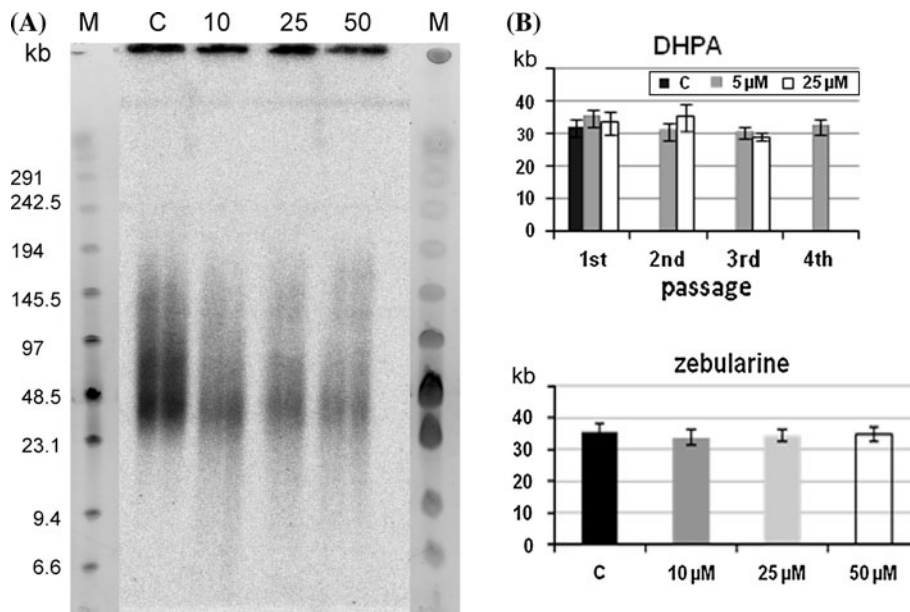


Fig. 5 Activity of telomerase in treated cells. **a** The pattern of TRAP assay products is the same in control and drug-treated cells. The numbers above lanes indicate the concentration of DHPA in the first passage; **D** DHPA; **C** control non-treated cells. Lane (+), positive control, a protein extract from *Arabidopsis* seedlings was used in the TRAP assay; lane (–), negative control, no protein extract in the reaction. **b, c** Activity of telomerase in treated cells relative to control cells as evaluated by a

quantitative (real time) version of TRAP (qTRAP). Telomerase activity in control cells was considered as 1. Treated cells displayed increased activity of telomerase dependent on the concentration of the drug. Transfer of DHPA-treated cells to DHPA-free medium in the 4th passage **b** leads to an immediate decrease of telomerase activity to a level comparable with control non-treated cells

Fig. 6 The length of telomeres in treated cells. **a** Analysis of telomere length by TRF in cells treated by DHPA (1st passage). DHPA concentrations are indicated above the lanes. The telomeric C-strand probe (AtTR4-C) was used for hybridization. **b, c** Telomere length in cells treated by DHPA during 3 passages and after transfer into DHPA-free medium in the 4th passage **b** or in the 1st passage of zebularine treatment (**c**). No significant changes in treated cells were detected for either drug



activity of telomerase by impeding its access to telomeres and thus maintain telomere stability.

Conclusion

Our results show that telomeres in tobacco cells are subject to DNA methylation and that drug-induced DNA hypomethylation results in activation of telomerase. Nevertheless, telomeres maintain their length both during hypomethylation and during the recovery stage (remethylation) after removal of agents which induce hypomethylation.

Acknowledgments This work was supported by the Czech Science Foundation (P501/11/0289, P501/11/0596) the Czech Ministry of Education (MSM0021622415, LC06004 and LC 06035) and by the project “CEITEC—Central European Institute of Technology” (CZ.1.05/1.1.00/02.0068) from European Regional Development Fund. We thank Jana Kapustová for technical assistance, Dr. Ivan Votruba, Institute of Organic Chemistry and Biochemistry ASCR v.v.i., Prague, for providing us with DHPA and Dr. Aleš Kovařík, Institute of Biophysics, ASCR v.v.i., Brno, for providing us with a bacterial clone containing the subtelomeric repeat HRS60.

References

- Baubec T, Pecinka A, Rozhon W, Mittelsten Scheid O (2009) Effective, homogeneous and transient interference with cytosine

- methylation in plant genomic DNA by zebularine. *Plant J* 57(3):542–554. doi:10.1111/j.1365-313X.2008.03699.x
- Beisler JA (1978) Isolation, characterization, and properties of a labile hydrolysis product of the antitumor nucleoside, 5-azacytidine. *J Med Chem* 21(2):204–208
- Benetti R, Garcia-Cao M, Blasco MA (2007) Telomere length regulates the epigenetic status of mammalian telomeres and subtelomeres. *Nat Genet* 39(2):243–250. doi:10.1038/ng1952
- Cao X, Jacobsen SE (2002a) Locus-specific control of asymmetric and CpNpG methylation by the DRM and CMT3 methyltransferase genes. *Proc Natl Acad Sci USA* 99(Suppl 4):16491–16498. doi:10.1073/pnas.162371599
- Cao X, Jacobsen SE (2002b) Role of the *Arabidopsis* DRM methyltransferases in de novo DNA methylation and gene silencing. *Curr Biol* 12(13):1138–1144. doi:S0960982202009259
- Cao X, Springer NM, Muszynski MG, Phillips RL, Kaeppler S, Jacobsen SE (2000) Conserved plant genes with similarity to mammalian de novo DNA methyltransferases. *Proc Natl Acad Sci USA* 97(9):4979–4984. doi:97/9/4979
- Chinnusamy V, Zhu JK (2009) RNA-directed DNA methylation and demethylation in plants. *Sci China C Life Sci* 52(4):331–343. doi:10.1007/s11427-009-0052-1
- Cihak A (1974) Biological effects of 5-azacytidine in eukaryotes. *Oncology* 30(5):405–422
- Cokus SJ, Feng S, Zhang X, Chen Z, Merriman B, Haudenschild CD, Pradhan S, Nelson SF, Pellegrini M, Jacobsen SE (2008) Shotgun bisulphite sequencing of the *Arabidopsis* genome reveals DNA methylation patterning. *Nature* 452(7184):215–219. doi:10.1038/nature06745
- De Clercq E, Descamps J, De Somer P, Holy A (1978) (S)-9-(2,3-Dihydroxypropyl)adenine: an aliphatic nucleoside analog with broad-spectrum antiviral activity. *Science* 200(4341):563–565
- Dellaporta LS, Wood J, Hicks BJ (1983) A plant DNA miniprep: version II. *Plant Mol Biol Repr* 1(4):19–21
- Doskocil J, Sorm F (1962) Distribution of 5-methylcytosine in pyrimidine sequences of deoxyribonucleic acids. *Biochim Biophys Acta* 55:953–959
- Fajkus J, Trifonov EN (2001) Columnar packing of telomeric nucleosomes. *Biochem Biophys Res Commun* 280(4):961–963. doi:10.1006/bbrc.2000.4208
- Fajkus J, Vyskot B, Bezdek M (1992) Changes in chromatin structure due to hypomethylation induced with 5-azacytidine or DL-ethionine. *Febs Lett* 314(1):13–16. doi:0014-5793(92)81449-V
- Fajkus J, Kovarik A, Kralovics R, Bezdek M (1995a) Organization of telomeric and subtelomeric chromatin in the higher plant *Nicotiana tabacum*. *Mol Gen Genet* 247(5):633–638
- Fajkus J, Kralovics R, Kovarik A, Fajkusova L (1995b) The telomeric sequence is directly attached to the HRS60 subtelomeric tandem repeat in tobacco chromosomes. *Febs Lett* 364(1):33–35. doi:0014-5793(95)00347-C
- Fajkus J, Kovarik A, Kralovics R (1996) Telomerase activity in plant cells. *Febs Lett* 391(3):307–309. doi:0014-5793(96)00757-0
- Fajkus J, Fulneckova J, Hulanova M, Berkova K, Riha K, Matyasek R (1998) Plant cells express telomerase activity upon transfer to callus culture, without extensively changing telomere lengths. *Mol Gen Genet* 260(5):470–474
- Fajkus J, Simickova M, Malaska J (2002) Tiptoeing to chromosome tips: facts, promises and perils of today's human telomere biology. *Philos Trans R Soc Lond B Biol Sci* 357(1420):545–562. doi:10.1098/rstb.2001.1053
- Feng S, Jacobsen SE (2011) Epigenetic modifications in plants: an evolutionary perspective. *Curr Opin Plant Biol* 14(2):179–186. doi:10.1016/j.pbi.2010.12.002
- Feuerhahn S, Iglesias N, Panza A, Porro A, Lingner J (2010) TERRA biogenesis, turnover and implications for function. *Febs Lett* 584(17):3812–3818
- Finnegan EJ, Dennis ES (1993) Isolation and identification by sequence homology of a putative cytosine methyltransferase from *Arabidopsis thaliana*. *Nucleic Acids Res* 21(10):2383–2388
- Fitzgerald MS, McKnight TD, Shippen DE (1996) Characterization and developmental patterns of telomerase expression in plants. *Proc Natl Acad Sci USA* 93(25):14422–14427
- Fojtova M, Kovarik A, Votruba I, Holy A (1998) Evaluation of the impact of S-adenosylhomocysteine metabolic pools on cytosine methylation of the tobacco genome. *Eur J Biochem* 252(3):347–352
- Fojtova M, Fulneckova J, Fajkus J, Kovarik A (2002) Recovery of tobacco cells from cadmium stress is accompanied by DNA repair and increased telomerase activity. *J Exp Bot* 53(378):2151–2158
- Fulneckek J, Matyasek R, Votruba I, Holy A, Krizova K, Kovarik A (2011) Inhibition of SAH-hydrolase activity during seed germination leads to deregulation of flowering genes and altered flower morphology in tobacco. *Mol Genet Genomics* 285(3):225–236. doi:10.1007/s00438-011-0601-8
- Fulneckova J, Fajkus J (2000) Inhibition of plant telomerase by telomere-binding proteins from nuclei of telomerase-negative tissues. *Febs Lett* 467(2–3):305–310. doi:S0014-5793(00)01178-9
- Garcia-Cao M, O'Sullivan R, Peters AH, Jenuwein T, Blasco MA (2004) Epigenetic regulation of telomere length in mammalian cells by the Suv39h1 and Suv39h2 histone methyltransferases. *Nat Genet* 36(1):94–99. doi:10.1038/ng1278
- Geiman TM, Muegge K (2010) DNA methylation in early development. *Mol Reprod Dev* 77(2):105–113. doi:10.1002/mrd.21118
- Ghoshal K, Bai S (2007) DNA methyltransferases as targets for cancer therapy. *Drugs Today (Barc)* 43(6):395–422. doi:10.1358/dot.2007.43.6.1062666
- Gonzalez-Suarez E, Samper E, Ramirez A, Flores JM, Martin-Caballero J, Jorcano JL, Blasco MA (2001) Increased epidermal tumors and increased skin wound healing in transgenic mice overexpressing the catalytic subunit of telomerase, mTERT, in basal keratinocytes. *EMBO J* 20(11):2619–2630. doi:10.1093/emboj/20.11.2619
- Gonzalo S, Jaco I, Fraga MF, Chen T, Li E, Esteller M, Blasco MA (2006) DNA methyltransferases control telomere length and telomere recombination in mammalian cells. *Nat Cell Biol* 8(4):416–424. doi:10.1038/ncb1386
- Greider CW, Blackburn EH (1985) Identification of a specific telomere terminal transferase activity in Tetrahymena extracts. *Cell* 43(2 Pt 1):405–413. doi:0092-8674(85)90170-9
- Greider CW, Blackburn EH (1987) The telomere terminal transferase of Tetrahymena is a ribonucleoprotein enzyme with two kinds of primer specificity. *Cell* 51(6):887–898. doi:0092-8674(87)90576-9
- Gruenbaum Y, Stein R, Cedar H, Razin A (1981) Methylation of CpG sequences in eukaryotic DNA. *Febs Lett* 124(1):67–71. doi:0014-5793(81)80055-5
- Havlis J, Madden JE, Revilla AL, Havel J (2001) High-performance liquid chromatographic determination of deoxycytidine monophosphate and methyldeoxycytidine monophosphate for DNA demethylation monitoring: experimental design and artificial neural networks optimisation. *J Chromatogr B Biomed Sci Appl* 755(1–2):185–194
- Henikoff S, Comai L (1998) A DNA methyltransferase homolog with a chromodomain exists in multiple polymorphic forms in *Arabidopsis*. *Genetics* 149(1):307–318
- Hiyama E, Hiyama K (2002) Clinical utility of telomerase in cancer. *Oncogene* 21(4):643–649. doi:10.1038/sj.onc.1205070
- Holy A (1975) Aliphatic analogues of nucleosides, nucleotides and oligonucleotides. *Collect Czech Chem Commun* 40:187–214
- Jelinek R, Holy A, Votruba I (1981) Embryotoxicity of 9-(S)-(2,3-dihydroxypropyl)adenine. *Teratology* 24(3):267–275. doi:10.1002/tera.1420240304

- Kannan K, Nelson AD, Shippen DE (2008) Dyskerin is a component of the *Arabidopsis* telomerase RNP required for telomere maintenance. *Mol Cell Biol* 28(7):2332–2341. doi:[MCB.01490-07](https://doi.org/10.1128/MCB.01490-07)
- Kim CH, Marquez VE, Mao DT, Haines DR, McCormack JJ (1986) Synthesis of pyrimidin-2-one nucleosides as acid-stable inhibitors of cytidine deaminase. *J Med Chem* 29(8):1374–1380
- Koukalova B, Reich J, Matyasek R, Kuhrova V, Bezdek M (1989) A *BamHI* family of highly repetitive DNA sequences of *Nicotiana Tabacum*. *Theor Appl Genet* 78:77–80
- Koukalova B, Votruba I, Fojtova M, Holy A, Kovarik A (2002) Hypomethylation of CNG targets induced with dihydroxypropyladenine is rapidly reversed in the course of mitotic cell division in tobacco. *Theor Appl Genet* 105(6–7):1097–1098. doi:[10.1007/s00122-002-1152-5](https://doi.org/10.1007/s00122-002-1152-5)
- Kovarik A, Koukalova B, Holy A, Bezdek M (1994) Sequence-specific hypomethylation of the tobacco genome induced with dihydroxypropyladenine, ethionine and 5-azacytidine. *Febs Lett* 353(3):309–311
- Kovarik A, Koukalova B, Lim KY, Matyasek R, Lichtenstein CP, Leitch AR, Bezdek M (2000) Comparative analysis of DNA methylation in tobacco heterochromatic sequences. *Chromosom Res* 8(6):527–541
- Kunicka Z, Mucha I, Fajkus J (2008) Telomerase activity in head and neck cancer. *Anticancer Res* 28(5B):3125–3129
- Lee YW, Kim WT (2010) Tobacco GTBP1, a homolog of human heterogeneous nuclear ribonucleoprotein, protects telomeres from aberrant homologous recombination. *Plant Cell* 22(8):2781–2795. doi:[tpc.110.076778](https://doi.org/10.1105/tpc.110.076778)
- Meyer P, Niedenhof I, ten Lohuis M (1994) Evidence for cytosine methylation of non-symmetrical sequences in transgenic *Petunia hybrida*. *EMBO J* 13(9):2084–2088
- Nagata T, Nemoto Y, Hasezawa S (1992) Tobacco BY-2 cell line as the “HeLa” cell in the cell biology of higher plants. *Int Rev Cytol* 112:1–30
- Ng LJ, Cropley JE, Pickett HA, Reddel RR, Suter CM (2009) Telomerase activity is associated with an increase in DNA methylation at the proximal subtelomere and a reduction in telomeric transcription. *Nucleic Acids Res* 37(4):1152–1159. doi:[10.1093/nar/gkn1030](https://doi.org/10.1093/nar/gkn1030)
- Richards EJ, Elgin SC (2002) Epigenetic codes for heterochromatin formation and silencing: rounding up the usual suspects. *Cell* 108(4):489–500. doi:[S009286740200644X](https://doi.org/10.1016/S009286740200644X)
- Riha K, Fajkus J, Siroky J, Vyskot B (1998) Developmental control of telomere lengths and telomerase activity in plants. *Plant Cell* 10(10):1691–1698
- Ruckova E, Friml J, Prochazkova Schrupfova P, Fajkus J (2008) Role of alternative telomere lengthening unmasked in telomerase knock-out mutant plants. *Plant Mol Biol* 66(6):637–646. doi:[10.1007/s11103-008-9295-7](https://doi.org/10.1007/s11103-008-9295-7)
- Šebestová L, Votruba I, Holy A (1984) S-adenosyl-L-homocysteine hydrolase from *Nicotiana tabacum* L.: isolation and properties. *Collect Czech Chem Commun* 49:1543–1551
- Shay JW, Wright WE (2010) Telomeres and telomerase in normal and cancer stem cells. *Febs Lett* 584(17):3819–3825. doi:[10.1016/j.febslet.2010.05.026](https://doi.org/10.1016/j.febslet.2010.05.026)
- Vaillant I, Paszkowski J (2007) Role of histone and DNA methylation in gene regulation. *Curr Opin Plant Biol* 10(5):528–533. doi:[10.1016/j.pbi.2007.06.008](https://doi.org/10.1016/j.pbi.2007.06.008)
- Vrbsky J, Akimcheva S, Watson JM, Turner TL, Daxinger L, Vyskot B, Aufsatz W, Riha K (2010) siRNA-mediated methylation of *Arabidopsis* telomeres. *PLoS Genet* 6(6):e1000986. doi:[10.1371/journal.pgen.1000986](https://doi.org/10.1371/journal.pgen.1000986)
- Walder RY, Langtimm CJ, Chatterjee R, Walder JA (1983) Cloning of the MspI modification enzyme. The site of modification and its effects on cleavage by MspI and HpaII. *J Biol Chem* 258(2):1235–1241
- Wingard JR, Hess AD, Stuart RK, Saral R, Burns WH (1983) Effect of several antiviral agents on human lymphocyte functions and marrow progenitor cell proliferation. *Antimicrob Agents Chemother* 23(4):593–597
- Yang SW, Kim SK, Kim WT (2004) Perturbation of NgTRF1 expression induces apoptosis-like cell death in tobacco BY-2 cells and implicates NgTRF1 in the control of telomere length and stability. *Plant Cell* 16(12):3370–3385. doi:[10.1105/tpc.104.026278](https://doi.org/10.1105/tpc.104.026278)
- Yoo CB, Cheng JC, Jones PA (2004) Zebularine: a new drug for epigenetic therapy. *Biochem Soc Trans* 32(Pt 6):910–912. doi:[10.1042/BST0320910](https://doi.org/10.1042/BST0320910)
- Zhang M, Kimatu JN, Xu K, Liu B (2010) DNA cytosine methylation in plant development. *J Genet Genomics* 37(1):1–12. doi:[10.1016/S1673-8527\(09\)60020-5](https://doi.org/10.1016/S1673-8527(09)60020-5)

Methylation of plant telomeric DNA: what do the results say?

M. I. Vaquero-Sedas and M. A. Vega-Palas: DNA methylation at tobacco telomeric sequences

Eva Majerová · Miloslava Fojtová ·
Terezie Mandáková · Jiří Fajkus

Received: 20 September 2011 / Accepted: 6 October 2011 / Published online: 4 November 2011
© Springer Science+Business Media B.V. 2011

Recently, we reported (Majerova et al. 2011) that hypomethylating drugs efficiently decrease methylation of telomeric DNA and activate telomerase without affecting telomere lengths in tobacco. The key issue of the Letter to Editor written by Vaquero-Sedas and Vega-Palas (2011) is, whether our results demonstrating methylation and drug-induced hypomethylation of tobacco telomeric DNA repeats do correspond to the status of terminal telomeric sequences, or rather to internal telomeric sequences (ITSs) which might exist in tobacco genome as it is the case in *Arabidopsis thaliana*, the model organism which Vaquero-Sedas and Vega-Palas have been working with. They are referring to their recent article (Vaquero-Sedas et al. 2010) in which they conclude that ITSs in *A. thaliana* are heterochromatic, while telomeres are euchromatic. We are pleased that our paper has initiated this debate and take the opportunity to go through the key points of the Letter of Vaquero-Sedas and Vega-Palas.

First, it is important to mention, that the two model genomes *A. thaliana* and *Nicotiana tabacum* differ considerably in the amount of ITSs per genome, and their ratio to the telomeric sequences at chromosome ends. While in *A. thaliana*, terminal (CCCTAA)_n repeats form ca. 30 kb (in the most common Columbia ecotype) per haploid genome, ITSs (including both exact and degenerated

repeats) form 6.3 kb distributed into several blocks of 300–1,200 bp and exhibit a various degree of sequence degeneracy (Uchida et al. 2002). These are termed more appropriately as interstitial telomeric repeats (ITRs) and they are presumably heterochromatic, as would correspond to their subtelomeric or pericentromeric location. They can be detected by Southern hybridization (during terminal restriction fragment analyses) as a signal of about 0.5 kb when the genomic DNA is digested with restriction enzymes of four-nucleotide palindromic recognition sequence, e.g. TruII (MseI) (see e.g. Fojtova et al. (2011)). This signal can also be used as a convenient loading control. Besides ITRs, *A. thaliana* genome contains numerous short ITSs termed as *telo* boxes (AAACCCTA), which in contrast to the ITRs are preferentially located in the 5' flanking regions of genes, mainly in 5' UTR (Gaspin et al. 2010; Regad et al. 1994) and thus are presumably euchromatic. Since these sequences escape detection by Southern blot hybridization, they do not interfere with results obtained using this technique.

Telomeres are 20–160 kb long in *N. tabacum* plant (Fajkus et al. 1995a) and ca. 35 kb in tobacco BY-2 cells (Fajkus et al. 1996; Majerova et al. 2011). Moreover, there was not a significant fraction of ITRs detected by either in situ hybridization (Fig. 1 and Kenton et al. (1993)) or Southern hybridization (as a BAL31-resistant fraction)—as shown by Suzuki et al. (1994), Fig. 5 in that work. Surprisingly, Vaquero-Sedas and Vega-Palas in their Letter cite the same articles in support of their hypothesis. Indeed, no “hybridization signals smaller than 2 kb” are displayed using telomeric probe in HaeIII digestion of tobacco genomic DNA in our work (Fajkus et al. 1995b) quoted by Vaquero-Sedas and Vega-Palas. No ITSs have been revealed in our work dealing with telomere-associated sequences (Horakova and Fajkus 2000). No intercalary ITS

E. Majerová · M. Fojtová · T. Mandáková · J. Fajkus (✉)
Department of Functional Genomics and Proteomics,
Faculty of Science and Central European Institute
of Technology, Masaryk University, Kotlářská 2,
61137 Brno, Czech Republic
e-mail: fajkus@sci.muni.cz

J. Fajkus
Institute of Biophysics, Academy of Sciences of the Czech
Republic v.v.i., Královopolská 135, 61265 Brno, Czech Republic

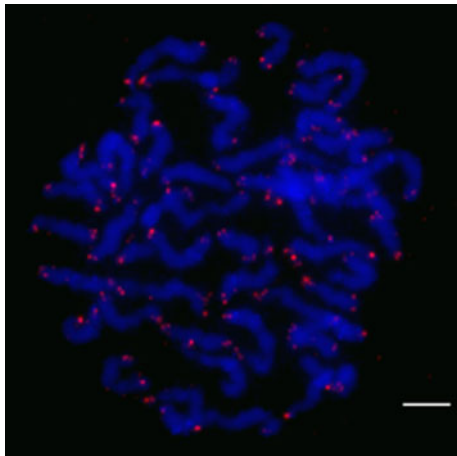


Fig. 1 Fluorescence in situ hybridization of tobacco chromosomes using telomeric probe. Details of the experimental procedure are given in (Mandakova et al. 2010), telomeric probe was prepared according to (Ijdo et al. 1991). Note the terminal location of the hybridization signals. Bar 10 μ m

site was found by cytogenetics either; in fact, Kenton et al. (1993) state that “Sequential in situ hybridization with biotinylated (TTTAGGG)_n and HRS60 showed co-localisation of the two probes only to chromosome ends, indicating that telomere repeated sequence was absent from the intercalary HRS60.1 site.” Suzuki et al. (1994) in his pioneering work observed the presence of a palindrome of telomere-like sequence 5′-TTAGGGTTTTAAACCC TAA-3′ in telomere-associated region of tobacco, and we assume that tobacco genome comprises more of such short telomere-like sequences, similar in size to *A. thaliana* ITSs of the *telo* box-type. These however do not interfere with the results of hybridization experiments due to their short length and detection limit of the technique (see Nepelchova et al. (2005) for a specificity and hybridization conditions for various kinds of telomeric probes).

Specific comments of Vaquero-Sedas and Vega-Palas are focused on chromatin structure of telomeres and ITSs. They refer to their work (Gamez-Arjona et al. 2010) in which a considerable fraction (about 70%) of the total telomere-specific hybridization signal of *Cfo*I-digested DNA was lost after subsequent digestion with frequently cutting restriction enzymes. Part of the signal that disappeared can be found under longer exposure at positions corresponding to 100–500 bp (usual position of *A. thaliana* ITR fragments—see above), but this accounts for only a few percent of the total signal. They speculate, that the disappearing signal represents ITSs and, consequently, ca. 70% of telomere-like hybridization signal in *A. thaliana* corresponds to ITSs. This is, however, in a clear contradiction to the above mentioned data of Uchida et al. (2002) which provide an exact content of interstitial genomic

regions comprising at least 3 telomeric repeats (to exclude random hits) as 20% of the total number telomeric repeats. Thus, according to genomic data, the ratio between terminal and interstitial telomeric repeats is almost reciprocal to that deduced by Gamez-Arjona et al. (2010). This discrepancy calls the results published in Gamez-Arjona et al. (2010) into question. They speculate, that when the majority of telomere probe-specific signal corresponds to ITSs, the results obtained e.g. in analysis of chromatin structure reflect rather chromatin status of ITSs than that of telomeres. However, since this assumption is controversial, as demonstrated above, further implications in that direction are not substantiated.

Vaquero-Sedas and Vega-Palas claim that we refer in Majerova et al. (2011) that “*Arabidopsis* telomeres exhibit high levels of heterochromatic marks like H3K9^{2Me}, H3K27^{Me} and DNA methylation.” This is very imprecise quotation. We, in fact, state [with a reference to Vrbsky et al. (2010)] that “telomeric chromatin in *A. thaliana* shows in addition to the repressive H3K9me2 and H3K27me1 histone H3 marks also the presence of an “active” mark, H3K4me3 whose decrease due to DHPA-induced hypomethylation could contribute to the lower level of TERRA transcription.” More importantly, opinion of Vaquero-Sedas and Vega-Palas that ITSs show heterochromatic structure while telomeres are euchromatic is based on results obtained in Vaquero-Sedas et al. (2010) and the authors are convinced that they are able to analyze histone marks and DNA methylation of ITSs and telomeres independently. Their technique is based on protocol of Lippman et al. (2005) which starts with random fragmentation of a crosslinked chromatin, followed by immunoprecipitation using an appropriate antibody. The immunoprecipitated DNA is either analyzed by two sequential PCR reactions, or amplified by whole genome amplification to increase hybridization sensitivity. Equal amounts of amplified DNA samples are either digested with *Tru*9I or undigested, resolved on agarose gels and hybridized. The first problem of the technique is, of course, the amplification used in both variants of processing, which may considerably change representation of individual genome regions. The other, even more serious problem with the amplification-hybridization technique lies in a fact, that an arbitrary limit of 500 bp is chosen as a boundary between the signal corresponding to telomeres and ITSs. The authors justify this by a Southern hybridization pattern of *A. thaliana* terminal restriction fragments, when genomic DNA is digested with *Tru*9I and hybridized with telomeric probe. In this case, bands corresponding to ITSs are detected below 500 bp indeed, while terminal restriction fragments are 2–5 kb long. However, the authors ignore the fact that in their approach they do not analyze integral genomic DNA,

but—according to the protocol in Lippman et al. (2005)—rather randomly fragmented and amplified DNA sample. The key information—the length span of the resulting fragments used for ChIP—is missing in Vaquero-Sedas et al. (2010). Nevertheless, after subsequent amplification and hybridization to telomeric probe, the input DNA forms a smear starting at 500 bp. The population of these fragments thus inevitably includes (in addition to ITRs/ITSs) telomere fragments of two types: (1) fragments of purely telomeric sequence (from the distal or central part of the telomere), and (2) fragments generated from the proximal telomere region, which comprise, in addition to their telomere part, also an adjacent subtelomeric sequence. Consequently, the latter telomere fragments are shortened by digestion, the hybridization signal of the trimmed telomeric part is moved below the 500 bp limit, and regarded as ITSs. Moreover, it is apparent from the results shown that even with the use of whole genome amplification the results are obtained near to the detection limit of hybridization, which raises further doubts about validity and quantitative precision of the results.

The Letter by Vaquero-Sedas and Vega-Palas apparently contains incorrect and imprecise quotations. Nevertheless, they in fact have made a very positive contribution by drawing more attention to the ITSs and problems connected with their possible influence on results of telomere analysis. Therefore, we appreciate these comments as well as the possibility to respond to them.

In summary, although it is not our intention to arbitrate the conflicting interpretation of results obtained in *Arabidopsis* (Vaquero-Sedas et al. 2010; Vrbsky et al. 2010), a more appropriate approach is still required to address the problem of independent analysis of chromatin structure of ITSs and telomeres. The data referred to above suggest that at least two kinds of ITSs exist in the *Arabidopsis* genome, the ITRs with presumably heterochromatic structure, and the short telobox-type ITSs dispersed in euchromatin. In our work, we take advantage of using tobacco cells which do not constitute the problem of any considerable fraction of ITRs in genomic DNA, which would be of at least similar order of magnitude as the amount of telomeric repeats comprised in extra-long tobacco telomeres. Consequently, our results obtained in tobacco are easier to interpret. However, we can envisage, that many other interesting problems are yet to be solved in connection with telomere chromatin structure (and tobacco could again be an appropriate model to do it): for example, chromatin structure of the distal and proximal part of telomeres, especially in case of the long telomeres occurring at mouse or tobacco chromosomes, may be as different as the chromatin structure of different types of ITSs. Why some telomeres exhibit telomere position effect while the others do not? In other words, chromatin, including chromatin of

telomeres, has probably more colours than just black and white, as was shown recently (Riddle et al. 2011; Roudier et al. 2011). Let us look forward to further surprises at chromosome ends.

Acknowledgments This work was supported by the Czech Science Foundation (P501/11/0289, P501/11/0596), the Czech Ministry of Education (MSM0021622415) and by the project “CEITEC—Central European Institute of Technology” (CZ.1.05/1.1.00/02.0068) from European Regional Development Fund.

References

- Fajkus J, Kovarik A, Kralovics R, Bezdek M (1995a) Organization of telomeric and subtelomeric chromatin in the higher plant *Nicotiana tabacum*. *Mol Gen Genet* 247(5):633–638
- Fajkus J, Kralovics R, Kovarik A, Fajkusova L (1995b) The telomeric sequence is directly attached to the HRS60 subtelomeric tandem repeat in tobacco chromosomes. *FEBS Lett* 364(1):33–35
- Fajkus J, Kovarik A, Kralovics R (1996) Telomerase activity in plant cells. *FEBS Lett* 391(3):307–309
- Fojtova M, Peska V, Dobsakova Z, Mozgova I, Fajkus J, Sykorova E (2011) Molecular analysis of the T-DNA insertion mutants identified putative regulatory elements in the AtTERT gene. *J Exp Bot*. doi:10.1093/jxb/err235
- Gamez-Arjona FM, Lopez-Lopez C, Vaquero-Sedas M, Vega-Palas MA (2010) On the organization of the nucleosomes associated with telomeric sequences. *Biochim Biophys Acta* 1803(9):1058–1061
- Gaspin C, Rami JF, Lescure B (2010) Distribution of short interstitial telomere motifs in two plant genomes: putative origin and function. *BMC Plant Biol* 10:283
- Horakova M, Fajkus J (2000) TAS49-a dispersed repetitive sequence isolated from subtelomeric regions of *Nicotiana tomentosiformis* chromosomes. *Genome* 43(2):273–284
- Ijdo JW, Wells RA, Baldini A, Reeders ST (1991) Improved telomere detection using a telomere repeat probe (TTAGGG)_n generated by PCR. *Nucl Acids Res* 19(17):4780
- Kenton A, Parokony AS, Gleba YY, Bennett MD (1993) Characterization of the *Nicotiana tabacum* L. genome by molecular cytogenetics. *Mol Gen Genet* 240(2):159–169
- Lippman Z, Gendrel AV, Colot V, Martienssen R (2005) Profiling DNA methylation patterns using genomic tiling microarrays. *Nat Methods* 2(3):219–224
- Majerova E, Fojtova M, Mozgova I, Bittova M, Fajkus J (2011) Hypomethylating drugs efficiently decrease cytosine methylation in telomeric DNA and activate telomerase without affecting telomere lengths in tobacco cells. *Plant Mol Biol*. doi:10.1007/s11103-011-9816-7
- Mandakova T, Joly S, Krzywinski M, Mummenhoff K, Lysak MA (2010) Fast diploidization in close mesopolyploid relatives of *Arabidopsis*. *Plant Cell* 22(7):2277–2290
- Neplechova K, Sykorova E, Fajkus J (2005) Comparison of different kinds of probes used for analysis of variant telomeric sequences. *Biophys Chem* 117(3):225–231
- Regad F, Lebas M, Lescure B (1994) Interstitial telomeric repeats within the *Arabidopsis thaliana* genome. *J Mol Biol* 239(2):163–169
- Riddle NC, Minoda A, Kharchenko PV, Alekseyenko AA, Schwartz YB, Tolstorukov MY, Gorchakov AA, Jaffe JD, Kennedy C, Linder-Basso D, Peach SE, Shanower G, Zheng H, Kuroda MI, Pirrotta V, Park PJ, Elgin C, Karpen GH (2011) Plasticity in patterns of histone modifications and chromosomal proteins in *Drosophila* heterochromatin. *Genome Res* 21(2):147–163

- Roudier F, Ahmed I, Berard C, Sarazin A, Mary-Huard T, Cortijo S, Bouyer D, Caillieux E, Duvernois-Berthet E, Al-Shikhley L, Giraut L, Despres B, Drevensek S, Barneche F, Derozier S, Brunaud V, Aubourg S, Schnittger A, Bowler C, Martin-Magniette ML, Robin S, Caboche M, Colot V (2011) Integrative epigenomic mapping defines four main chromatin states in *Arabidopsis*. *EMBO J* 30(10):1928–1938
- Suzuki K, Yamagiwa Y, Matsui T, Yoshida K (1994) Restriction enzyme-resistant high molecular weight telomeric DNA fragments in tobacco. *DNA Res* 1(3):129–138
- Uchida W, Matsunaga S, Sugiyama R, Kawano S (2002) Interstitial telomere-like repeats in the *Arabidopsis thaliana* genome. *Genes Genet Syst* 77(1):63–67
- Vaquero-Sedas MI, Vega-Palas MA (2011) DNA methylation at tobacco telomeric sequences. *Plant Mol Biol*. doi:[10.1007/s11103-011-9833-6](https://doi.org/10.1007/s11103-011-9833-6)
- Vaquero-Sedas MI, Gamez-Arjona FM, Vega-Palas MA (2010) *Arabidopsis thaliana* telomeres exhibit euchromatic features. *Nucl Acids Res* 39(6):2007–2017
- Vrbsky J, Akimcheva S, Watson JM, Turner TL, Daxinger L, Vyskot B, Aufsatz W, Riha K (2010) siRNA-mediated methylation of *Arabidopsis* telomeres. *PLoS Genet* 6(6):e1000986

Role of HMGB Proteins in Chromatin Dynamics and Telomere Maintenance in *Arabidopsis thaliana*

Petra Procházková Schrumpfová^{1,*}, Miloslava Fojtová^{1,2}, Petr Mokroš¹, Klaus D. Grasser³ and Jiří Fajkus^{1,2}

¹Department of Functional Genomics and Proteomics, Faculty of Science and Central European Institute of Technology, Masaryk University, Kotlářská 2, CZ-61137 Brno, Czech Republic; ²Institute of Biophysics, Academy of Sciences of the Czech Republic, v.v.i., Královopolská 135, CZ-61265 Brno, Czech Republic; ³Cell Biology & Plant Physiology, Regensburg University, Universitätsstr. 31, D-93053 Regensburg, Germany

Abstract: Chromosome stability is conditioned by functional chromatin structure of chromosome ends – telomeres. Organisation and regulation of telomere maintenance represent a complex process whose details still remain enigmatic, especially in plants. Several telomere-binding or telomere-associated proteins and distinct epigenetic marks have been shown to influence telomere length and telomerase activity. HMGB proteins play important role in dynamic changes of chromatin structure and are involved in regulation of cellular processes of key importance, such as replication, transcription, recombination and DNA-repair. HMGB proteins in plants are more diversified than in other eukaryotes. Here, we summarise the roles of plant HMGB proteins in regulation of chromatin structure and dynamics and report on the newly identified role of AtHMGB1 protein in the regulation of plant telomere length. Astonishingly, contrary to mice mHMGB1 homologue, AtHMGB1 does not affect telomerase activity and AtHMGB1 loss or overexpression does not cause any obvious changes in chromatin architecture.

Keywords: HMGB, telomere shortening/elongation, plants, chromatin, epigenetics.

HMGB PROTEINS: THEIR ROLES IN CHROMATIN STRUCTURE AND DYNAMICS

High mobility group (HMG) proteins represent a heterogeneous group of small and relatively abundant non-histone proteins associated with the chromatin of eukaryotic organisms [1]. There are three structurally distinct classes of HMG proteins: the HMG-nucleosome binding family (HMGN), the HMG-AT-hook family (HMGA) and the HMG-box family (HMGB). Proteins belonging to the family of HMGB proteins act as architectural factors, facilitating the assembly of nucleoprotein complexes, which are involved in the regulation of DNA-dependent processes [2-4]. As a distinctive feature, the HMGB proteins contain a ~75-amino acid residue DNA-binding domain, termed the HMG-box domain. The three-dimensional fold of this domain, consisting essentially of three α -helices which are arranged in an L-shape, is well conserved [4].

Members of the HMGB family of proteins (~13-27 kDa) have been characterised from various plant species, revealing that they share many properties with their counterparts from other eukaryotic organisms, and that they are different in some respects [5]. In contrast to mammalian HMGB proteins, which contain two HMG-box domains, the typical plant HMGB-type proteins have a single HMG-box domain, which is flanked by a basic N-terminal domain and an acidic

C-terminal domain. The HMG-box domains of the various plant HMGB proteins are relatively conserved, but compared to the mammalian homologues the basic and acidic flanking regions vary considerably in length and sequence [5, 6]. According to results of *in vitro* studies, plant HMGB proteins bind linear DNA non-sequence-specifically with moderate affinity, but recognise specifically certain DNA structures such as minicircles and four-way junctions, and they severely bend linear DNA upon binding [7-10]. Possible structural similarity of four-way junctions to the linker DNA located near the entrance and exit of nucleosomes has been discussed [11]. Moreover, maize HMGB proteins were found to assist the formation of specific nucleoprotein complexes involved in transcription and recombination [12-14]. In this context, HMGB proteins do not act as classical transcriptional regulators, but they mediate the function in transcription *via* interactions with different sequence-specific transcriptional regulators; for example, with Dof [5] and bZIP [15] in plants, and p53 [16], Rel [17], HOX [18], SREBP families [19] or TFIID/TFIIA [20] in mammals. In the cell nucleus, the HMGB proteins display a high dynamics, interacting with DNA/chromatin only transiently before moving on to the next binding site, thereby scanning the nuclear space for binding sites [21].

TELOMERES AS HETEROCHROMATIC STRUCTURES

The terminal parts of chromosomes in higher eukaryotes, telomeres, are folded into nucleosomal chromatin structure similarly to the other chromosome domains. This structure, however, shows some specific features. It displays short nu-

*Address correspondence to this author at the Department of Functional Genomics and Proteomics, Faculty of Science and Central European Institute of Technology, Masaryk University, Kotlářská 2, CZ-61137 Brno, Czech Republic; Tel: +420-549494003 Fax: +420-549492654; E-mail: schpetra@centrum.cz

cleosomal spacing (usually 30-40 bp less than the bulk chromatin) and extensive subnucleosomal fragmentation of mononucleosomes and dinucleosomes, while longer chromatin stretches are stable with regularly spaced nucleosomes [22, 23]. Thus it appears that telomere has a specific chromatin structure, distinct from the subtelomere and the other constitutively heterochromatic loci. The available experimental data and structural considerations were incorporated into the columnar model of telomere nucleosome arrangement [24], in which the DNA is wound round the column of stacked histone octamers.

The telomeric nucleosomes are further organised – together with specific proteins such as TRF1 or TRF2 in mammalian cells [25] and their myb-like counterparts in plants [26, 27] (see also the review of Peška *et al.* in this issue) into terminal chromatin loops. In particular, TRF1 was recently shown to induce mobility of telomeric nucleosomes and their telomere-specific compaction [28]. TRF2 also plays a role in nucleosome assembly and, interestingly, its overexpression leads to the increased spacing of telomeric nucleosomes, the loss of heterochromatic marks at telomeric repeats, and telomere shortening [29]. Recent results obtained in *Arabidopsis* reveal that telomeric nucleosomes contain a mixture of active and inactive chromatin marks on histone H3 [30]. Moreover, telomeric DNA in plants is modified by methylation of cytosines, preferentially of the third cytosine in the CCCTAAA telomeric repeat sequence [31]. This kind of methylation in asymmetric sequence context (no CpG or CpHpG are present in canonical telomere sequence) is dependent on plant-specific RNA-dependent DNA methylation (RdDM) pathway and 24 nt siRNA. The siRNA molecules targeting telomere sequences are derived from telomeric repeat-containing RNAs (TERRA) first observed in mammals and *Drosophila* [32, 33] and now reported also in plants [30].

Role of epigenetic factors in telomere maintenance has been studied extensively in mammalian cells, where the loss of heterochromatic marks resulted in telomere elongation and increase in telomere recombination. This relationship between telomere length and chromatin structure acts in both directions, since the progressive telomere loss reduces chromatin compaction at telomeric and subtelomeric domains (reviewed in [34]).

It appears that situation in plants may be quite different from mouse or human models, as exemplified by a contradictory sense of some histone epigenetic marks (e.g. H3K9me3, reviewed in [35]) or the presence of cytosine methylation in plant telomeric DNA. In our recent results (Majerova *et al.*, in preparation) it appears that inhibition of DNA methylation does not affect telomere lengths in plants, thus contrasting to the previous results in mammalian telomeres where the loss of function of DNA and histone methyltransferases lead to the extensive telomere elongation (reviewed in [36]).

HMGB IS INVOLVED IN TELOMERE MAINTENANCE IN MICE. WHAT ABOUT PLANTS?

As described in the previous paragraph, epigenetic phenomena play important roles in telomere maintenance and regulation. Besides DNA and histone epigenetic marks, an

other important epigenetic process is chromatin remodelling. It has been described that a number of HMG proteins play role in dynamic changes of chromatin structure. In particular, the C-terminal acidic tail of HMGB1 protein may interact with basic domains of histones, resulting in the weakening of their binding (or in the case of histone H1 in its displacement) in the nucleosomes (reviewed by [37]). Accordingly, the acidic tail of HMG-box proteins is essential for their function in promoting nucleosome mobility and chromatin remodelling. In current model, HMGB binds at the edge of the nucleosome, thereby displacing H1. HMGB binding results in DNA bending and formation of DNA loop, which then functions as anchoring site for the remodelling complex. HMGB dissociates from the loop upon binding of the remodelling complex which then propagates the looped DNA around the histone octamer. Nucleosome remodelling exposes a transcription factor (TF) binding sequence (inaccessible under the former nucleosome position). This site is present by HMGB and bound by TF. In some cases, HMGB can facilitate binding of TF also by direct interaction with TF, followed by binding of TF-HMGB complex to DNA [37].

Since the processes of telomere repeat transcription and chromatin condensation are involved in regulation of telomere length, investigation of possible role of HMGB proteins could be of high interest.

In our results obtained in mouse embryonic fibroblast cells, knockout of *mHMGB1* resulted in marked decrease in telomerase activity, telomere shortening and increase in chromosome instability. However, this effect was not due to changes in expression of either of the telomerase subunits, but rather through the involvement of the HMGB1 in assembly of telomerase nucleoprotein complex. Accordingly, interaction between the HMG box B and the catalytic telomerase subunit mTERT was observed (Polanska, Kunická *et al.*, unpublished results).

To examine whether a similar effect occurs also in the model plant organism *Arabidopsis thaliana*, we took advantage of existence of T-insertion lines with *athmgb1* gene knockout [SAIL_261_B02, ecotype Col-0], and the Col-0 plants overexpressing the introduced *AtHMGB1* gene under the control of 35S promoter (pGII0179-35S-HMGB1). As described above, situation in *Arabidopsis* is complicated by the existence of seven proteins [38] that contain HMG-box domain flanked by a basic and acidic domain and thus can be classified as HMGB-type proteins. *AtHMGB1* protein appears as a typical member of the plant HMGB-type proteins in *A. thaliana* and could be regarded as the ortholog of mammalian HMGB1, but not necessarily performing the equivalent functions.

ATHMGB1 PARTICIPATES IN TELOMERE MAINTENANCE, BUT DOES NOT AFFECT TELOMERASE ACTIVITY IN ARABIDOPSIS

Similarly to mammals, general telomere lengths were significantly shortened in mutant *athmgb1* plants compared to Col-0 plants. In accordance to this observation we have detected marked telomere elongation in plants overexpressing *AtHMGB1* protein *AtHMGB1*^{OE}, see Fig. (1). Interestingly, elongated telomeres in *AtHMGB1*^{OE} plants are not dispersed continuously but they rather migrate on agarose

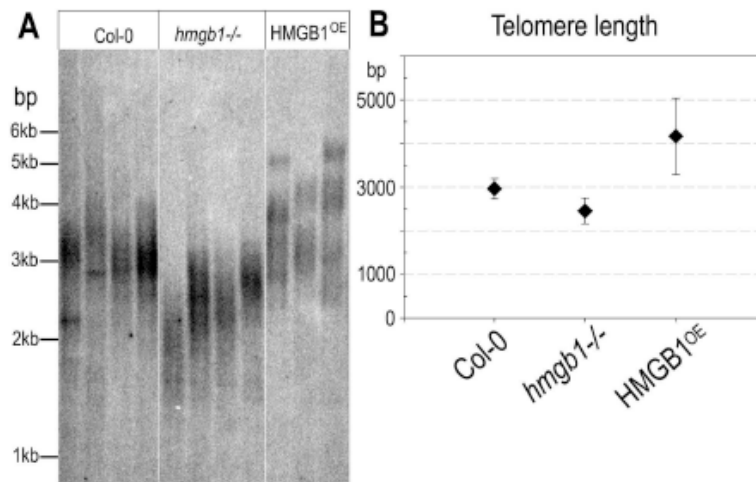


Fig. (1). Changes in telomere lengths in response to *AtHMGB1* knockout or overexpression. A) An example of analysis of telomere lengths using TRF (*Terminal Restriction Fragment*) assay. Genomic DNA was digested with restriction enzyme (*Tru*II) which cuts genomic DNA into short fragments, but does not cleave telomeric sequence lacking any cutting sites. DNA was then separated on agarose gel, blotted to the nylon membrane and hybridised against radioactively end-labelled telomeric probe (CCCTAAA)₄. Signals were visualised using phosphorimager FLA7000 (FUJIFILM). Compared to wild type plants (Col-0 lanes), telomeres of *athmgb1* mutant plants display telomere shortening, while enormous telomere lengthening and a heterogeneous pattern of telomeres is observed in plants overexpressing *AtHMGB1* protein. B) Graphical representation of the mean telomere lengths evaluated from TRF patterns. Data were taken from 3 independent analyses.

gel as discrete bands, which is typical for telomeres generated by alternative telomere lengthening (ALT). The expansion of telomeres was also proven at the level of the individual chromosome arms Fig. (2). Both the chromosome arms with huge clusters of heterochromatin (45S rDNA tandem repeats) in subtelomeric regions (2L, 4L), and the arms with transcribed genes in telomere-associated regions (3L, 2R) showed similar telomere elongation in *AtHMGB1*^{OE} plants. Neither of these revealed the population of the longest telomeres. Since the analysis of individual telomeres is able to detect only a subset of telomeres possessing a single-stranded G-overhang, it is possible that the extensively elongated telomeres do not possess the G-overhangs, as would correspond to their ALT origin. On the other hand, fluorescence *in situ* hybridisation on metaphase chromosomes revealed the moderate but significant increase of telomeric signal in the *AtHMGB1*^{OE} line samples as compared to Col-0 wild type $P < 0.0001$, Fig. (3) thus supporting independently the above results of telomere length analysis Fig. (1).

The relative telomere shortening observed in *athmgb1* mutant plants is similar to that observed in mice indicating a general role of HMGB1 protein in telomere maintenance across the kingdoms. However, the pathway mediating this effect seems to be different. While the telomere shortening in mouse cells lacking mHMGB1 can be attributed to the insufficient telomerase activity (five- to tenfold decrease compared to normal cells), no changes in telomerase activity (the intensity of bands obtained by Telomere Repeat Amplification Protocol, TRAP) and telomerase processivity (extension of TRAP products ladder) could be observed in either *A. thaliana athmgb1* or *AtHMGB1*^{OE} plants Fig. (4). These results were confirmed by quantitative analysis of telomerase activity (not shown).

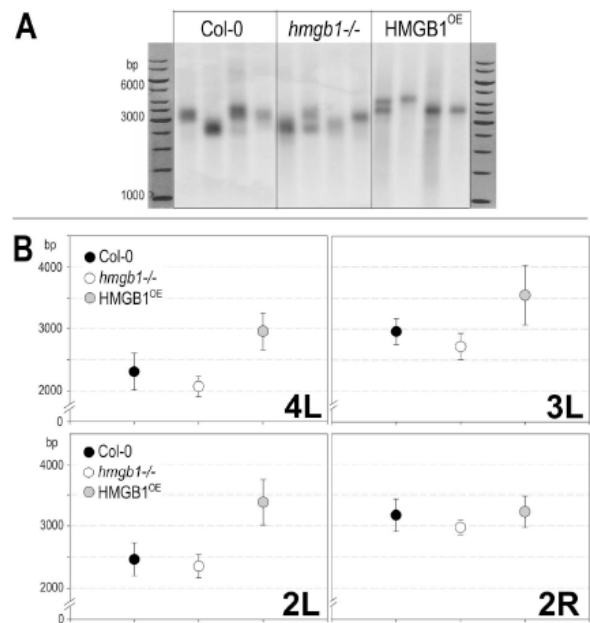


Fig. (2). Telomere length at individual chromosome arms. A) Example of PETRA analysis (*Primer Extension Telomere Repeat Amplification*) which is based on extension of a primer annealed to the telomeric G-overhang towards the subtelomeric region, and subsequent amplification of the primary extension product using a second primer derived from a unique subtelomeric sequence (primer from the 4L arm has been used in the example shown here). Products were separated on agarose gel, Southern-hybridised to telomeric probe and visualised as described in Fig. (1). B) Results of analysis of telomeres at four different chromosome arms (4L, 3L, 2L and 2R). Distances between the telomere-subtelomere junction and the position of a given subtelomeric primer were subtracted from the total size of the PCR product.

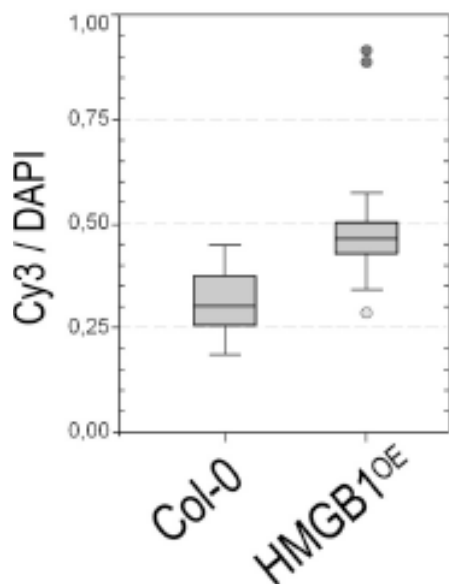


Fig. (3). Graphical evaluation of the fluorescence in situ (FISH) analysis of the telomeric tracts. In nuclei of Col-0 and AtHMGB1^{OE} plants, the telomere-specific signal (PNA probe with Cy3 dye) was related to that of DAPI and processed using the ISIS imaging software. Terms were evaluated with paired-t-test with statistical significance at alpha 0.05; dots represent outlying samples.

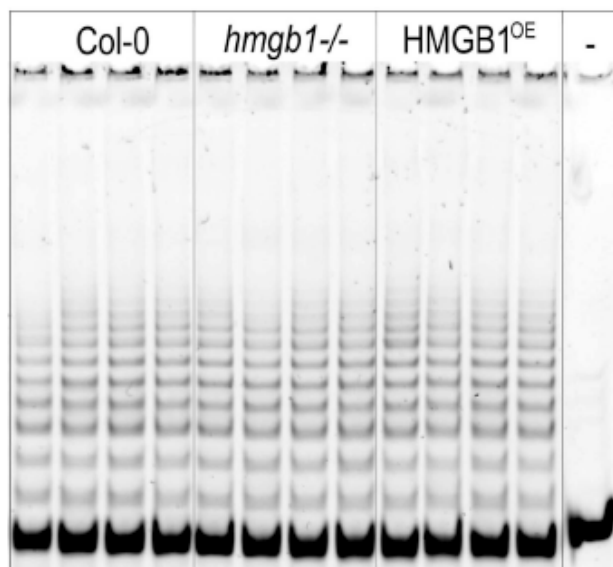


Fig. (4). Telomerase activity. Ladder of telomeric repeats produced in TRAP assay (*Telomere Repeat Amplification Protocol*). No differences in the AtHMGB1 null or overexpressing lines were observed in comparison to wild-type (Col-0) plants in either telomerase processivity or activity. - Negative control: - line; no protein extract in the reaction.

HMGB PROTEINS PARTICIPATE IN THE RESPONSE TO STRESS STIMULI

HMGB proteins in plants apparently exert their assistant role in gene expression by influencing stress- and stimulus-responsive pathways [38]. Plants with altered levels of HMGB proteins were found to be affected in their responses to abiotic stress treatments. Compared to control plants,

transgenic *Arabidopsis* plants overexpressing *AtHMGB2*, under salt and drought stress display retarded germination and subsequent growth. Overexpression of *AtHMGB4* did not influence seed germination and plant growth under stress condition [39]. While *Arabidopsis* plants overexpressing *AtHMGB5* behave like wild type, plants lacking *AtHMGB5* under stress conditions show retarded germination and subsequent growth. Overexpression of *AtHMGB2* did not affect the expression of a selection of stress-related genes, whereas the expression of several germination-responsive genes was altered [39]. Both the absence and overexpression of *AtHMGB1* in *Arabidopsis* resulted in an increased sensitivity towards the genotoxic agent methyl methane sulphonate. When exposed to elevated NaCl concentrations, the germination of AtHMGB1-overexpressors was reduced, whereas the *athmgb1* mutant germinated normally [38].

In tobacco BY-2 culture cells, significant increase of telomerase activity during cadmium-induced genotoxic stress and recovery stage was described [40]. Based on these particular results, changes in telomerase activity in *athmgb1* or AtHMGB^{OE} plants under cadmium-induced stress conditions could be expected. However, in *A. thaliana* seedlings, no significant and reproducible response of telomerase activity to the cadmium treatment (up to 50 μ M CdSO₄) was detected either in wild type Col-0 or in *athmgb1* and AtHMGB1^{OE} lines (data not shown). Similarly, no signs of increased genomic instability (chromosome bridges, fusions etc.) were observed using the chromosome staining with 4',6-diamidino-2-phenylindole (DAPI). In contrast to AtHMGB1^{OE} plants exposed to salinity (NaCl) or other type of genotoxic stress (MMS) where seeds germination is retarded [38], no similar effect of cadmium treatment on seed germination was observed in *athmgb1* and AtHMGB1^{OE} lines.

EMERGING CONNECTION BETWEEN HMGB1 AND TRANSCRIPTION OF TELOMERE REPEATS?

TERRA transcripts, non-coding RNA molecules derived from telomeric repeats, represent another level of regulation of telomerase activity and telomere homeostasis. In mammals, the presence of telomeric and subtelomeric heterochromatin-specific epigenetic marks was shown to influence telomerase activity, telomere length and level of TERRA [36, 41]. Moreover, TERRA transcripts are able to inhibit telomerase activity *in vitro* [42]; recently, direct binding of TERRA to human telomerase subunits in cell extract resulting in inhibition of telomerase activity was reported [43]. Complexity of plant-specific epigenetic pattern including massive methylation of cytosines outside CpG sequence context (reviewed in [44]), DNA methylation pathway directed by non-coding RNA molecules [45], active DNA demethylation [46] and the existence of specific RNA polymerases IV and V [47], are also reflected in the pattern of TERRA transcripts. While in mammals most of TERRA consists of UUAGGG repeats (which means that they are transcribed from C-rich telomeric strand in centromere to telomere direction), in plants both TERRA (UUUAGGG) and ARRET (antisense telomeric transcripts, AAAUCCC) were detected. These transcripts arise either directly from telomeres or are generated from the relatively abundant telomeric tracts located near the centromeres; their processing into siRNA molecules was demonstrated [30].

Analysis of TERRA transcript by northern blot which was followed by hybridisation against radioactively labelled telomeric probe showed a slight increase of TERRA level in AtHMGB1-deficient line, and a decrease in the overexpressing line Fig. (5). This observation may reflect local changes in chromatin structure and accessibility. AtHMGB1, acting as general co-regulator of transcription, may in this context facilitate “normal” transcription of coding genes located in subtelomeric regions, thus impairing transcription of the non-coding TERRA. However, the observed differences in TERRA levels (increase to about 1.8 fold in *athmgb1*, decrease to about 0.7 fold in AtHMGB1^{OE} as compared to Col-0) are relatively moderate. In plants, any influence of telomerase activity by TERRA transcripts has not been reported yet. Based on the studies in mammalian models showing a direct association of TERRA to telomeric sequences [32, 42] and inhibition of telomerase activity by TERRA [43], it is possible to assume that changes of TERRA transcript levels in *athmgb1* and AtHMGB1^{OE} plant lines are not marked enough to be reflected in the alteration of telomerase activity and the observed changes in telomere length are induced independently of telomerase. In this context, the increased and decreased accessibility of chromosome ends to telomerase in AtHMGB1^{OE} and *athmgb1* plants, respectively, may be a prospective possibility.

HMGB AS AN ENIGMATIC EPIGENETIC PLAYER

Despite of the documented effect of AtHMGB1 on telomere maintenance, a detailed mechanism of its involvement is far from being clear. In the meantime, we can at least draw a couple of various conclusions that could slightly elucidate this issue:

1) **AtHMGB1 does not exert its effect on telomere length via direct regulation of telomerase.** We cannot exclude a possibility that the effect on telomerase assembly/activity observed in mammalian cells is mediated by another member of HMGB protein family in *Arabidopsis* due to possible functional overlaps among the different HMGB-type proteins found in plants: the process of their sub-functionalisation. Another possibility is the indirect effect of AtHMGB1 on TERRA levels, which escapes detection by the *in vitro* TRAP assay, but can occur *in vivo*.

2) **AtHMGB1 loss or overexpression do not cause any massive/general changes in chromatin architecture.** (e.g., at the level of nucleosome spacing or size of chromocenters [38]). This would correspond to the proposed role of HMGB proteins as specific co-factors of transcriptional regulators. Increased occurrence of chromosome fusions and other cytogenetic abnormalities due to the loss of AtHMGB1 were also not observed in *Arabidopsis*, in contrast to mammalian cells. *Arabidopsis* telomeres thus appear to remain functional despite of shortening in *athmgb1* mutants [38].

3) **AtHMGB1 is involved in the stress- or stimulus-responsive pathways.** Most of the AtHMGB proteins were shown to be involved in various stress-response pathways and it seems that different types of stress could initialise distinct paths containing an appropriate AtHMGB member. E.g. the expression of AtHMGB2 and AtHMGB3 was up/down regulated by cold and salt treatment and dehydration, while AtHMGB1 expression is affected only by the salt stress [38,

39]. Response to the genotoxic stress could also vary according to the type of genotoxic agents; AtHMGB1 is involved in the response to MMS [38] but not to cadmium ions. Recent data indicate that HMGB proteins also affect efficient DNA repair in various organisms, including human [48, 49]. Similarly, diverse expression of DNA repair-related factor in *athmgb1* mutant compared to Col-0 plants denotes that AtHMGB proteins could be involved in DNA-repair machinery in plant model [38].

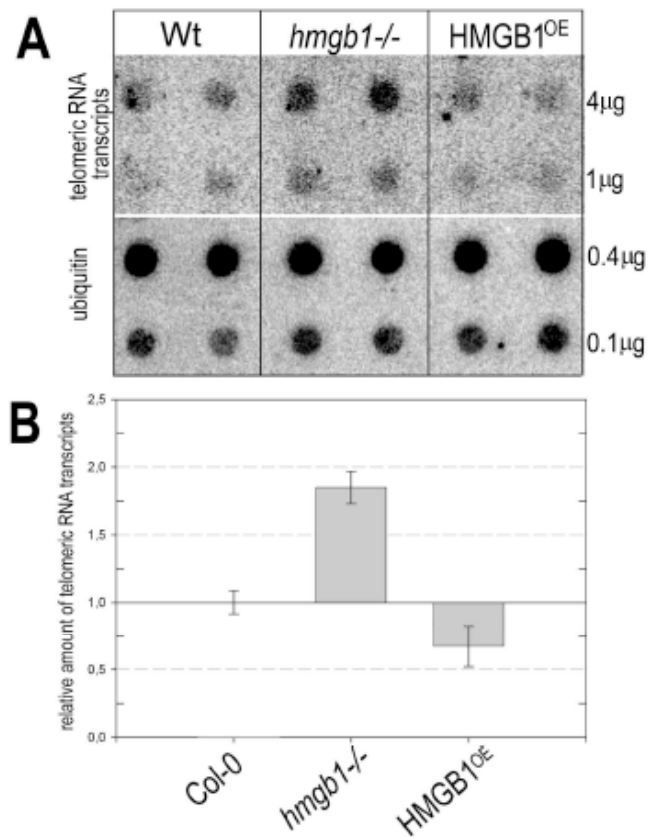


Fig. (5). Telomeric transcripts. A) RNA isolated from 7-day seedlings was transferred to the nylon membrane using vacuum and hybridised with radioactively labelled telomeric oligonucleotide (CCCTAAA)₄ and ubiquitin probes. The amount of RNA loaded on the membrane is given on the right. B) The intensity of hybridisation signal for telomeric RNA was determined and expressed relative to the ubiquitin to eliminate possible inaccuracy in loading. Slight increase of telomeric transcript levels in *athmgb1* mutants and decrease in overexpressing lines (as compared to the Col-0 wild type) was observed.

ACKNOWLEDGEMENT

This work was supported by the Grant Agency of the Czech Republic (521/08/P452, 204/08/1530) and the institutional funding (MSM0021622415, AV0Z50040507, AV0Z50040702). We thank Terezie Mandaková for assistance with statistical analysis. Technical support of Jana Kapustová and Marcela Šefčíková is highly appreciated.

REFERENCES

- [1] Reeves, R. Nuclear functions of the HMG proteins. *Biochim. Biophys. Acta.*, **2010**, *1799*, 3- 14.

- [2] Agresti, A.; Bianchi, M. E. HMGB proteins and gene expression. *Curr. Opin. Genet. Dev.*, **2003**, *13*, 170-178.
- [3] Bustin, M. Regulation of DNA-dependent activities by the functional motifs of the high-mobility-group chromosomal proteins. *Mol. Cell. Biol.*, **1999**, *19*, 5237-5246.
- [4] Thomas, J. O.; Travers, A. A. HMGI and 2, and related 'architectural' DNA-binding proteins. *Trends Biochem. Sci.*, **2001**, *26*, 167-174.
- [5] Grasser, M.; Christensen, J. M.; Peterhansel, C.; Grasser, K. D. Basic and acidic regions flanking the HMG-box domain of maize HMGB1 and HMGB5 modulate the stimulatory effect on the DNA binding of transcription factor Dof2. *Biochemistry*, **2007**, *46*, 6375-6382.
- [6] Pedersen, D. S.; Grasser, K. D. The role of chromosomal HMGB proteins in plants. *Biochim. Biophys. Acta.*, **2010**, *1799*, 171-174.
- [7] Grasser, K. D.; Krech, A. B.; Feix, G. The maize chromosomal HMGA protein recognizes structural features of DNA and increases DNA flexibility. *Plant J.*, **1994**, *6*, 351-358.
- [8] Webster, C. I.; Packman, L. C.; Pwee, K. H.; Gray, J. C. High mobility group proteins HMGI and HMGI/Y bind to a positive regulatory region of the pea plastocyanin gene promoter. *Plant J.*, **1997**, *11*, 703-715.
- [9] Wu, Q.; Zhang, W.; Pwee, K. H.; Kumar, P. P. Rice HMGB1 protein recognizes DNA structures and bends DNA efficiently. *Arch. Biochem. Biophys.*, **2003**, *411*, 105-111.
- [10] Zhang, W.; Wu, Q.; Pwee, K. H.; Jois, S. D.; Kini, R. M. Characterization of the interaction of wheat HMGA with linear and four-way junction DNAs. *Biochemistry*, **2003**, *42*, 6596-6607.
- [11] Varga-Weisz, P.; van Holde, K.; Zlatanova, J. Competition between linker histones and HMGI for binding to four-way junction DNA: implications for transcription. *Biochem. Biophys. Res. Commun.*, **1994**, *203*, 1904-1911.
- [12] Grasser, K. D.; Launholt, D.; Grasser, M. High mobility group proteins of the plant HMGB family: dynamic chromatin modulators. *Biochim. Biophys. Acta.*, **2007**, *1769*, 346-357.
- [13] Krohn, N. M.; Yanagisawa, S.; Grasser, K. D. Specificity of the stimulatory interaction between chromosomal HMGB proteins and the transcription factor Dof2 and its negative regulation by protein kinase CK2-mediated phosphorylation. *J. Biol. Chem.*, **2002**, *277*, 32438-32444.
- [14] Stemmer, C.; Fernandez, S.; Lopez, G.; Alonso, J. C.; Grasser, K. D. Plant chromosomal HMGB proteins efficiently promote the bacterial site-specific beta-mediated recombination *in vitro* and *in vivo*. *Biochemistry*, **2002**, *41*, 7763-7770.
- [15] Schultz, T. F.; Spiker, S.; Quatrano, R. S. Histone H1 enhances the DNA binding activity of the transcription factor EmbP-1. *J. Biol. Chem.*, **1996**, *271*, 25742-25745.
- [16] Jayaraman, L.; Moorthy, N. C.; Murthy, K. G.; Manley, J. L.; Bustin, M.; Prives, C. High mobility group protein-1 (HMGI) is a unique activator of p53. *Genes Dev.*, **1998**, *12*, 462-472.
- [17] Decoville, M.; Giraud-Panis, M. J.; Mosrin-Huaman, C.; Leng, M.; Locker, D. HMG boxes of DSP1 protein interact with the rel homology domain of transcription factors. *Nucleic Acids Res.*, **2000**, *28*, 454-462.
- [18] Zappavigna, V.; Falciola, L.; Helmer-Citterich, M.; Mavilio, F.; Bianchi, M. E. HMGI interacts with HOX proteins and enhances their DNA binding and transcriptional activation. *EMBO J.*, **1996**, *15*, 4981-4991.
- [19] Najima, Y.; Yahagi, N.; Takeuchi, Y.; Matsuzaka, T.; Sekiya, M.; Nakagawa, Y.; Amemiya-Kudo, M.; Okazaki, H.; Okazaki, S.; Tamura, Y.; Iizuka, Y.; Ohashi, K.; Harada, K.; Gotoda, T.; Nagai, R.; Kadowaki, T.; Ishibashi, S.; Yamada, N.; Osuga, J.; Shimano, H. High mobility group protein-B1 interacts with sterol regulatory element-binding proteins to enhance their DNA binding. *J. Biol. Chem.*, **2005**, *280*, 27523-27532.
- [20] Shykind, B. M.; Kim, J.; Sharp, P. A. Activation of the TFIID-TFIIA complex with HMGI-2. *Genes Dev.*, **1995**, *9*, 1354-1365.
- [21] Launholt, D.; Merkle, T.; Houben, A.; Schulz, A.; Grasser, K. D. Arabidopsis chromatin-associated HMGA and HMGB use different nuclear targeting signals and display highly dynamic localization within the nucleus. *Plant Cell*, **2006**, *18*, 2904-2918.
- [22] Fajkus, J.; Kovarik, A.; Kralovics, R.; Bezdek, M. Organization of Telomeric and Subtelomeric Chromatin in the Higher-Plant *Nicotiana-Tabacum*. *Mol. Gen. Genet.*, **1995**, *247*, 633-638.
- [23] Sykorova, E.; Fajkus, J.; Ito, M.; Fukui, K. Transition between two forms of heterochromatin at plant subtelomeres. *Chromosome Res.*, **2001**, *9*, 309-323.
- [24] Fajkus, J.; Trifonov, E. N. Columnar packing of telomeric nucleosomes. *Biochem. Biophys. Res. Commun.*, **2001**, *280*, 961-963.
- [25] Palm, W.; de Lange, T. How shelterin protects mammalian telomeres. *Annu. Rev. Genet.*, **2008**, *42*, 301-334.
- [26] Mozgova, I.; Schrumpfova, P. P.; Hofr, C.; Fajkus, J. Functional characterization of domains in AtTRB1, a putative telomere-binding protein in Arabidopsis thaliana. *Phytochemistry*, **2008**, *69*, 1814-1819.
- [27] Schrumpfova, P. P.; Kuchar, M.; Palecek, J.; Fajkus, J. Mapping of interaction domains of putative telomere-binding proteins AtTRB1 and AtPOT1b from Arabidopsis thaliana. *FEBS Lett.*, **2008**, *582*, 1400-1406.
- [28] Pisano, S.; Leoni, D.; Galati, A.; Rhodes, D.; Savino, M.; Caccione, S. The human telomeric protein hTRF1 induces telomere-specific nucleosome mobility. *Nucleic Acids Res.*, **2010**, *38*, 2247-2255.
- [29] Benetti, R.; Schoeftner, S.; Munoz, P.; Blasco, M. A. Role of TRF2 in the assembly of telomeric chromatin. *Cell Cycle*, **2008**, *7*, 3461-3468.
- [30] Vrbsky, J.; Akimcheva, S.; Watson, J. M.; Turner, T. L.; Daxinger, L.; Vyskot, B.; Aufsatz, W.; Riha, K. siRNA-mediated methylation of Arabidopsis telomeres. *PLoS Genet.*, **2010**, *6*, e1000986.
- [31] Cokus, S. J.; Feng, S. H.; Zhang, X. Y.; Chen, Z. G.; Merriman, B.; Haudenschild, C. D.; Pradhan, S.; Nelson, S. F.; Pellegrini, M.; Jacobsen, S. E. Shotgun bisulphite sequencing of the Arabidopsis genome reveals DNA methylation patterning. *Nature*, **2008**, *452*, 215-219.
- [32] Azzalin, C. M.; Reichenbach, P.; Khoriauli, L.; Giulotto, E.; Lingner, J. Telomeric repeat-containing RNA and RNA surveillance factors at mammalian chromosome ends. *Science*, **2007**, *318*, 798-801.
- [33] Savitsky, M.; Kwon, D.; Georgiev, P.; Kalmykova, A.; Gvozdev, V. Telomere elongation is under the control of the RNAi-based mechanism in the Drosophila germline. *Genes Dev.*, **2006**, *20*, 345-354.
- [34] Schoeftner, S.; Blasco, M. A. A 'higher order' of telomere regulation: telomere heterochromatin and telomeric RNAs. *EMBO J.*, **2009**, *28*, 2323-2336.
- [35] Fransz, P.; ten Hoopen, R.; Tessadori, F. Composition and formation of heterochromatin in Arabidopsis thaliana. *Chromosome Res.*, **2006**, *14*, 71-82.
- [36] Blasco, M. A. The epigenetic regulation of mammalian telomeres. *Nat. Rev. Genet.*, **2007**, *8*, 299-309.
- [37] Stros, M. HMGB proteins: Interactions with DNA and chromatin. *Biochim. Biophys. Acta.-Gene Regul. Mech.*, **2010**, *1799*, 101-113.
- [38] Lildballe, D. L.; Pedersen, D. S.; Kalamajka, R.; Emmersen, J.; Houben, A.; Grasser, K. D. The expression level of the chromatin-associated HMGB1 protein influences growth, stress tolerance, and transcriptome in Arabidopsis. *J. Mol. Biol.*, **2008**, *384*, 9-21.
- [39] Kwak, K. J.; Kim, J. Y.; Kim, Y. O.; Kang, H. Characterization of transgenic Arabidopsis plants overexpressing high mobility group B proteins under high salinity, drought or cold stress. *Plant Cell. Physiol.*, **2007**, *48*, 221-231.
- [40] Fojtova, M.; Fulneckova, J.; Fajkus, J.; Kovarik, A. Recovery of tobacco cells from cadmium stress is accompanied by DNA repair and increased telomerase activity. *J. Exp. Bot.*, **2002**, *53*, 2151-2158.
- [41] Ng, L. J.; Copley, J. E.; Pickett, H. A.; Reddel, R. R.; Suter, C. M. Telomerase activity is associated with an increase in DNA methylation at the proximal subtelomere and a reduction in telomeric transcription. *Nucleic Acids Res.*, **2009**, *37*, 1152-1159.
- [42] Schoeftner, S.; Blasco, M. A. Developmentally regulated transcription of mammalian telomeres by DNA-dependent RNA polymerase II. *Nat. Cell Biol.*, **2008**, *10*, 228-236.
- [43] Redon, S.; Reichenbach, P.; Lingner, J. The non-coding RNA TERRA is a natural ligand and direct inhibitor of human telomerase. *Nucleic Acids Res.*
- [44] Bird, A. DNA methylation patterns and epigenetic memory. *Genes Dev.*, **2002**, *16*, 6-21.
- [45] Wassenegger, M.; Heimes, S.; Riedel, L.; Sanger, H. L. RNA-directed de novo methylation of genomic sequences in plants. *Cell*, **1994**, *76*, 567-576.

- [46] Penterman, J.; Zilberman, D.; Huh, J. H.; Ballinger, T.; Henikoff, S.; Fischer, R. L. DNA demethylation in the Arabidopsis genome. *Proc. Natl. Acad. Sci. U S A*, **2007**, *104*, 6752-6757.
- [47] Onodera, Y.; Haag, J. R.; Ream, T.; Nunes, P. C.; Pontes, O.; Pikaard, C. S. Plant nuclear RNA polymerase IV mediates siRNA and DNA methylation-dependent heterochromatin formation. *Cell*, **2005**, *120*, 613-622.
- [48] Prasad, R.; Liu, Y.; Deterding, L. J.; Poltoratsky, V. P.; Kedar, P. S.; Horton, J. K.; Kanno, S.; Asagoshi, K.; Hou, E. W.; Khodyreva, S. N.; Lavrik, O. I.; Tomer, K. B.; Yasui, A.; Wilson, S. H. HMGB1 is a cofactor in mammalian base excision repair. *Mol. Cell*, **2007**, *27*, 829-841.
- [49] Yuan, F.; Gu, L.; Guo, S.; Wang, C.; Li, G. M. Evidence for involvement of HMGB1 protein in human DNA mismatch repair. *J. Biol. Chem.*, **2004**, *279*, 20935-20940.

Received: ?????????????????? Revised: ?????????????????? Accepted: ??????????????????

RESEARCH PAPER

Developmental silencing of the *AtTERT* gene is associated with increased H3K27me3 loading and maintenance of its euchromatic environment

Anna Ogrocká¹, Eva Sýkorová^{1,2}, Jiří Fajkus^{1,2} and Miloslava Fojtová^{1,*}

¹ CEITEC – Central European Institute of Technology, Masaryk University, Kamenice 5, 625 00 Brno, Czech Republic

² Institute of Biophysics, Academy of Sciences of the Czech Republic v.v.i., Královopolská 65, 612 65 Brno, Czech Republic

* To whom correspondence should be addressed. E-mail: fojtova@sci.muni.cz

Received 12 December 2011; Revised 26 February 2012; Accepted 19 March 2012

Abstract

Telomerase, an enzyme responsible for the maintenance of linear chromosome ends, is precisely regulated during plant development. In animals, involvement of the epigenetic state of the telomerase reverse transcriptase (*TERT*) gene in the complex regulation of telomerase activity has been reported. To reveal whether epigenetic mechanisms participate in the regulation of plant telomerase, the relationship between telomerase activity in tissues of *Arabidopsis thaliana* and DNA methylation and histone modifications in the *A. thaliana TERT (AtTERT)* upstream region was studied. As expected, a gradual decrease of telomerase activity during leaf maturation was observed. A different pattern with a more progressive loss of telomerase activity and *AtTERT* transcription during leaf development was revealed in *MET1* gene-knockout mutants. Analysis of DNA methylation in the *AtTERT* upstream region showed low levels of methylated cytosines without notable differences between telomerase-positive and telomerase-negative wild-type tissues. Surprisingly, a high level of CG methylation was found in the *AtTERT* coding region, although this type of methylation is a characteristic attribute of constitutively expressed genes. Analysis of chromatin modifications in the *AtTERT* upstream region and in exon 5 showed increased loading of the H3K27me3 mark in the telomerase-negative mature leaf compared to telomerase-positive seedlings, whereas H3K4me3, H3K9Ac, and H3K9me2 were approximately at the same level. Consistently, the chromatin structure of the *AtTERT* gene was maintained. These results are discussed in the context of the general involvement of epigenetic mechanisms in the regulation of gene expression and with respect to similar studies performed in animal models.

Key words: *Arabidopsis thaliana*, developmental regulation, DNA methylation, histone modifications, telomerase.

Introduction

Telomerase is a ribonucleoprotein enzyme complex responsible for the synthesis of telomeres, specialized nucleoprotein structures at the ends of linear eukaryotic chromosomes. Telomerase consists of a catalytic subunit, telomerase reverse transcriptase (TERT), and a telomerase RNA (TR) subunit which serves as a template for the elongation of the telomere motif. Telomerase activity is strictly regulated during plant development. Analysis of model plants including *Arabidopsis* (Fitzgerald *et al.*, 1996), *Silene latifolia* (Riha *et al.*, 1998), tobacco (Fajkus *et al.*, 1998), barley (Heller *et al.*, 1996),

soybean (Fitzgerald *et al.*, 1996), and tomato (Broun *et al.*, 1992) has revealed active telomerase in organs and tissues containing dividing meristem cells (seedlings, root tips, blossoms, floral buds) and in cell cultures (Fajkus *et al.*, 1996). On the other hand, telomerase activity was abolished in organs formed by terminally differentiated cells, e.g. stems or mature leaves. In this respect, the pattern of telomerase activity in plants resembles that in humans, but with a notable difference: telomerase down-regulation in terminally differentiated plant cells is reversible and highly dynamic, as is their differentiation

Abbreviations: *AtTERT*, *A. thaliana TERT*; ChIP, chromatin immunoprecipitation; *hTERT*, human *TERT*; TERT, telomerase reverse transcriptase; TR subunit, telomerase RNA subunit.

© 2012 The Author(s).

This is an Open Access article distributed under the terms of the Creative Commons Attribution Non-Commercial License (<http://creativecommons.org/licenses/by-nc/3.0/>), which permits unrestricted non-commercial use, distribution, and reproduction in any medium, provided the original work is properly cited.

status itself, and reflects the totipotent character of plant cells (Fajkus *et al.*, 1998). Nevertheless, the general pattern of telomerase activity is different even among mammalian model species; while in most human adult somatic tissues telomerase expression and activity are undetectable or very low, mouse somatic tissue cells express a detectable amount of the *TERT* mRNA (Horikawa *et al.*, 2005). This indicates that developmental regulation of telomerase is not driven by simple and generally valid mechanisms.

In plants, the molecular mechanisms of telomerase regulation at both the cellular and organism levels are far from being elucidated. These processes include regulation of telomerase transcription (Fitzgerald *et al.*, 1996; Oguchi *et al.*, 1999), alternative splicing of *TERT* gene transcripts (Heller-Uszynska *et al.*, 2002; Rossignol *et al.*, 2007), and post-translational modifications of telomerase (Oguchi *et al.*, 2004). A recent description of the *Arabidopsis* TR subunit suggested a possible involvement of two variant RNA subunits in formation of telomerase nucleoprotein complexes, yielding telomerases of different activity (Cifuentes-Rojas *et al.*, 2011). Moreover, strong regulatory elements downstream of the transcription start site were identified in our previous study (Fojtova *et al.*, 2011), demonstrating an enormous complexity of the plant telomerase regulation process.

The involvement of the chromatin state and epigenetic mechanisms in regulation of the *TERT* gene were demonstrated in animal models (reviewed in (Zhu *et al.*, 2011)). Hyperacetylated and H3K4-methylated histones were associated with human *TERT* (*hTERT*) expression in telomerase-positive cells, while H3K9 and H3K20 methylation marked histones in telomerase-negative cells. Although the sequence of the *hTERT* locus including the promoter region meets parameters for the CpG islands, no unambiguous correlation between promoter methylation and activity exists. Association of *hTERT* promoter methylation with the loss of its activity is evidenced by the demethylation-induced increase of *hTERT* transcription in immortalized fibroblasts (Devereux *et al.*, 1999) and binding of methyl-CpG-binding domain protein 2 (MBD 2) to the hypermethylated *hTERT* promoter in HeLa cells (Chatagnon *et al.*, 2009). On the other hand, demethylation in tumour cell lines with high telomerase activity was correlated with a significant reduction of *hTERT* transcription (Guilleret and Benhattar, 2003). It is supposed that in this case methylation prevents the transcriptional repressors from binding, but a small methylation-free region near the transcription start site is able to ensure *hTERT* transcription. Nevertheless, in most normal somatic cells with a basal level of telomerase activity the *hTERT* promoter is hypomethylated (Dessain *et al.*, 2000). As regards chromatin structure, it was shown that cell differentiation was associated with the loss of DNaseI-hypersensitive sites in the human and mouse *TERT* promoters and their upstream regions (Wang *et al.*, 2009), showing that changes of chromatin structure leading to its more condensed state are connected with *hTERT* transcriptional silencing.

In this work, telomerase activity during *Arabidopsis thaliana* development was correlated with the *A. thaliana*

TERT (*AtTERT*) epigenetic pattern. While DNA methylation did not seem to be involved in the gradual attenuation of telomerase transcription during leaf maturation, the repressive chromatin modification signal – trimethylation of lysine 27 in histone H3 (H3K27me3) – was installed in the *AtTERT* upstream and gene body regions in telomerase-negative tissue. Nevertheless, no significant change in the general chromatin structure accompanied the H3K27me3 loading, and developmentally silenced *AtTERT* maintained the euchromatin-specific modifications.

Materials and methods

Plant material

A. thaliana seedlings of the Columbia-0 ecotype and a *ddm1* (*At5g66750*) mutant (*ddm1-8* strain, SALK000590) were purchased from the Nottingham *Arabidopsis* Stock Centre (Alonso *et al.*, 2003), and seedlings of the mutant plant with a T-DNA insertion in the *MET1* gene (*At5g49160*, *met1-3* strain; Saze *et al.*, 2003) were kindly provided by Dr Ales Pecinka (GMI, Vienna, Austria). Primers for genotyping are described in Supplementary Table S1. Seeds were placed on half-strength Murashige-Skoog (Duchefa Biochemie, Haarlem, The Netherlands) agar plates and grown under cycles of 8 h light (illumination $100 \mu\text{mol m}^{-2} \text{s}^{-1}$), at 21 °C and 16 h dark at 19 °C. After 7 days, seedlings were collected for analyses. Plants were grown in soil from 2 week-old seedlings under the same light/dark conditions favouring leaf growth. Leaves were harvested from 6–8 week-old plants as depicted in Fig. 1A.

Analysis of telomerase activity (TRAP assay)

Telomerase extracts from *Arabidopsis* tissues were prepared as described (Fitzgerald *et al.*, 1996; Sykorova *et al.*, 2003). Telomerase activity was analysed according to the protocol in (Fajkus *et al.*, 1998). First, 1 μl of 10 μM TS21 substrate primer (Supplementary Table S1) was mixed with 1 μl of telomerase extract (protein concentration 50 $\text{ng } \mu\text{l}^{-1}$). Primer elongation proceeded in 25 μl of the reaction buffer at 26 °C for 45 min. After extension, telomerase was heat-inactivated and samples were cooled to 80 °C. Then, 1 μl of 10 μM TELPR reverse primer (Supplementary Table S1) and 2 units of DyNAzymeII DNA polymerase (Finnzymes, Espoo, Finland) were added to start PCR amplification of telomerase extension products (35 cycles of 95 °C/30 s, 65 °C/30 s, 72 °C/30 s) followed by a final extension (72 °C/5 min). Products of TRAP reactions were analysed by electrophoresis on a 12.5% polyacrylamide gel in 0.5 \times TBE buffer; the gel was stained with GelStar Nucleic Acid Gel Stain (LONZA, Basel, Switzerland) and signals were visualized using the LAS-3000 system (FujiFilm, Tokyo, Japan). Telomerase activity and processivity were deduced from the intensity and extension of the TRAP products ladder, respectively.

The quantitative version of the TRAP assay was performed as described in Herbert *et al.* (2006) using FastStart SYBR Green Master (Roche, Basel, Switzerland) and TS21 and TELPR primers. Samples were analysed in triplicates in a 20 μl reaction mix. Ct values were determined using Rotorgene6000 (Qiagen, Hilden, Germany) software and relative telomerase activity was calculated by the ΔCt method (Pfaffl, 2004).

RNA isolation and RT-PCR analysis

Total RNA was isolated from *Arabidopsis* tissues using the RNeasy Plant Mini Kit (Qiagen) followed by DNase I treatment (TURBO DNA-free; Applied Biosystems/Ambion, Foster City, CA, USA) according to the manufacturer's instructions. The quality and quantity of RNA was checked by electrophoresis on 1% (w/v) agarose gels and by absorbance measurements

(NanoPhotometr IMPLEN). cDNA was prepared by reverse transcription of 1 µg of RNA using M-MuLV reverse transcriptase (New England Biolabs, Hitchin, Herts, UK) and Random Nonamers (Sigma-Aldrich, St Louis, MO, USA). Quantification of the *AtTERT* transcript relative to the ubiquitin reference transcript was done using FastStart SYBR Green Master (Roche) on the Rotorgene6000 (Qiagen). One µl of five-times-diluted cDNA was added to the 20 µl reaction mix; the final concentration of each forward and reverse primer was 0.25 µM (Supplementary Table S1). Reactions were done in triplicates; the PCR programme consisted of 15 min of initial denaturation at 94 °C followed by 40 cycles of 30 s at 94 °C, 30 s at 56 °C, and 30 s at 72 °C. Analyses were performed for at least two biological replicates in three technical replicates. Transcription in the respective tissue was calculated as the fold increase/decrease relative to wild-type 7 day seedlings ($\Delta\Delta C_t$ method (Pfaffl, 2004)).

DNA isolation and analysis of DNA methylation

Total genomic DNA was isolated from 1 g of 7 day seedlings and 6–8 week-old leaves by the cetyltrimethylammonium bromide method as described in Kovarik *et al.* (2000).

Bisulphite conversion of genomic DNA was done by the EpiTect Bisulphite Kit (Qiagen) in which non-methylated cytosines are converted to uracils and amplified as thymines in the subsequent PCR, while 5-methylcytosines are resistant in this reaction (Clark *et al.*, 1994). Sequences of primers for amplification of the *AtTERT* upstream region (284 bp fragment) and *AtTERT* exon 5 (476 bp fragment) are listed in Supplementary Table S1. PCR was done using DyNAzymeII DNA polymerase in a programme consisting of initial denaturation (2 min) and 40 cycles of 30 s at 94 °C, 30 s at 56 °C and 40 s at 72 °C followed by a final extension (72 °C/5 min). PCR products were cloned using a TOPO TA cloning kit (Invitrogen, Carlsbad, CA, USA) and sequenced (Macrogen, Seoul, South Korea). Methylation of cytosines located in the respective sequence context was analysed by CyMATE software (Hetzl *et al.*, 2007) in the 224 bp *AtTERT* upstream region (close to the ATG site) where the sequencing signals were convincingly seen, and in the *AtTERT* exon 5.

Analysis of histone modifications by chromatin immunoprecipitation

Histone modifications by chromatin immunoprecipitation (ChIP) were analysed using the EpiQuik™ Plant Chip Kit (Epigentek, Farmingdale, NY, USA). Chromatin was crosslinked for 15 min in 1% formaldehyde (Sigma-Aldrich), fragmented by sonication (Bioruptor; Diagenode, Liège, Belgium) to an average fragment length of 500 bp, and immunoprecipitated by antibodies against H3K9me2 (Abcam, Cambridge, UK), H3K4me3 (Abcam), H3K9Ac (Abcam), or H3K27me3 (Millipore, Billerica, MA, USA). A total of 20 ng of purified DNA from the immunoprecipitated fractions was subjected to PCR using primers for the *AtTERT* upstream region and the exon 5 (Supplementary Table S1) and DyNAzymeII DNA polymerase with the same PCR programme as described for analysis of DNA methylation. Quantitative PCR was performed as described for RT-PCR analysis. Results were evaluated statistically using the two-tailed Student's *t* test; a *P* value of <0.05 was considered as statistically significant.

Results

Gradual decrease of telomerase activity during leaf maturation

Telomerase activity was determined by the TRAP assay in *A. thaliana* 7 day seedlings and leaves of different ages (Fig. 1A). A gradual decrease of telomerase activity during

leaf maturation was observed (Fig. 1B, 1C). Telomerase activity comparable to or even higher than that in 7 day seedlings was observed in young leaves (leaf A, Fig. 1A). In a so-called middle-aged leaf (leaf B), telomerase activity was

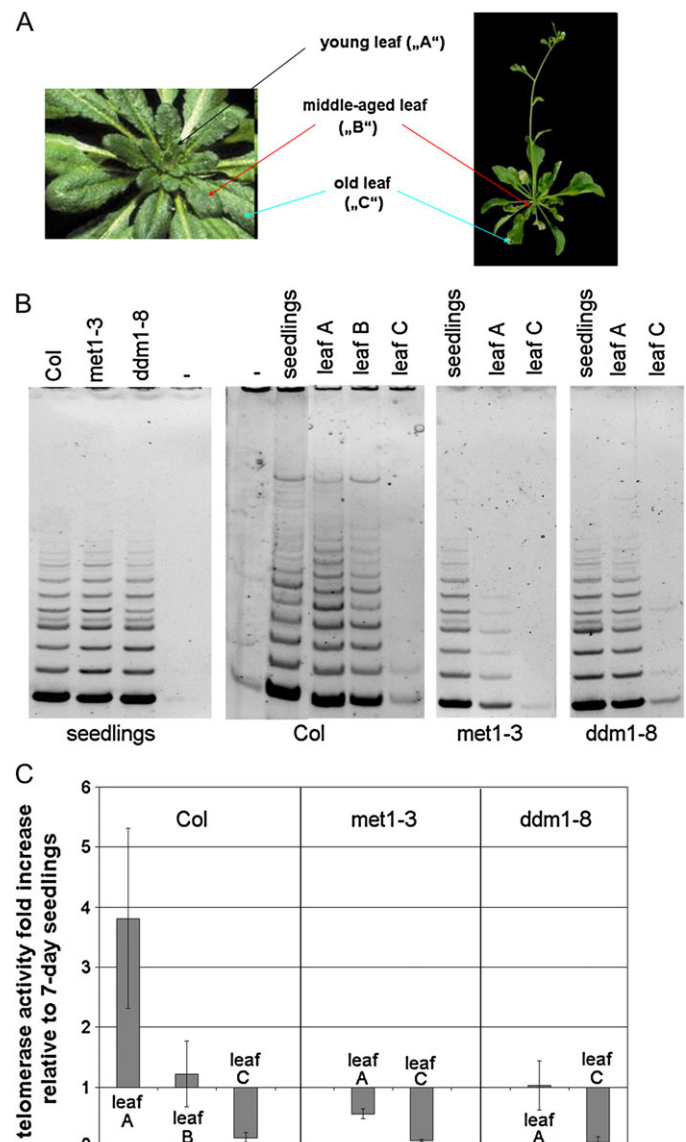


Fig. 1. Telomerase activity dynamics in *Arabidopsis* wild-type and methylation mutant tissues. (A) Strategy for collection of leaves at different developmental stages. (B) *In vitro* telomerase activity assays. Telomerase activity was determined in extracts from 7 day seedlings and from leaves collected from the Columbia wild-type (Col), *met1-3*, and *ddm1-8* plants using the TS21 and TELPR primers (Supplementary Table S1). Lanes show: –, negative controls (no protein extract in the reaction); leaf A, young leaf; leaf B, middle-aged leaf; leaf C, mature leaf. (C) Quantitative analysis of telomerase activity in leaves. Analysis was based on SYBR Green I fluorescence detection and was performed using at least two biological replicates (three technical replicates for each). The ΔC_t method (Pfaffl, 2004) was used to calculate relative telomerase activity. Analyses were done for two biological replicates in three technical replicates; error bars show SD.

around the level in seedlings and was absent or very low in mature leaves (leaf C).

The dynamics of telomerase activity during plant development are believed to be correlated with *TERT* promoter activity, i.e. with the level of the transcript for the telomerase protein subunit. A good correlation between *AtTERT* transcription and telomerase activity was observed (Supplementary Fig. S1).

Telomerase dynamics is affected in leaves of the met1-3 mutant

Numerous studies have shown that DNA methylation plays an important role in the modulation of promoter activity. Although the precise range of the *AtTERT* promoter has not been characterized yet, a minimal telomerase promoter has recently been identified using a collection of T-DNA insertion lines as a sequence 271 bp upstream of the ATG signal (Fojtova *et al.*, 2011). To investigate cytosine methylation in this putative promoter, primers delimiting the region from position -284 to the ATG codon (Supplementary Table S1) were designed to amplify sodium bisulphite-modified DNA templates. The number of methylated cytosines is very low in this region and there is no notable difference in cytosine methylation between telomerase-positive (7 day seedlings) and -negative (mature leaves) tissues (Supplementary Fig. S2). Based on these results, DNA methylation in the putative promoter region is not a dominant factor in the regulation of *AtTERT* transcription.

The above results were complemented by an analysis of mutant plants defective in pathways crucial for the maintenance of cytosine methylation. Analysis of telomerase activity in seedlings of *met1-3* and *ddm1-8* mutants revealed patterns fully comparable to the wild type (Fig. 1B, left panel), and no significant changes in *AtTERT* transcription were detected (Fig. 2A).

The *ddm1-8* mutant plants showed telomerase activities in young (leaf A) and old (leaf C) leaves to be more or less comparable to those in leaves of the corresponding developmental stage in wild-type plants (Fig. 1B), although – according to the results of quantitative assays (Fig. 1C) – telomerase activity in the *ddm1-8* young leaf is lower than in wild-type Columbia tissues, approaching the value observed in the middle-aged wild-type leaves (leaf B). Surprisingly, in repeated analyses *met1-3* mutants revealed considerably lower telomerase activity in young leaves (Fig. 1B, 1C). The amounts of *AtTERT* transcript in young leaves of one plant heterozygous for a T-DNA insertion in the *MET1* gene and of two plants homozygous for this insertion were close to the detection limit (Fig. 2B), i.e. significantly lower than in the corresponding wild-type samples, in which *AtTERT* transcription was even higher as compared to that in 7 day seedlings (Supplementary Fig. S1). Based on these analyses, it is possible to hypothesize that a complex pattern of phenotypic defects connected to the loss of *MET1* function (Mathieu *et al.*, 2007) encompasses disruption of telomerase developmental regulation, leading to an early loss of telomerase expression and activity in the mutant leaves. But in contrast

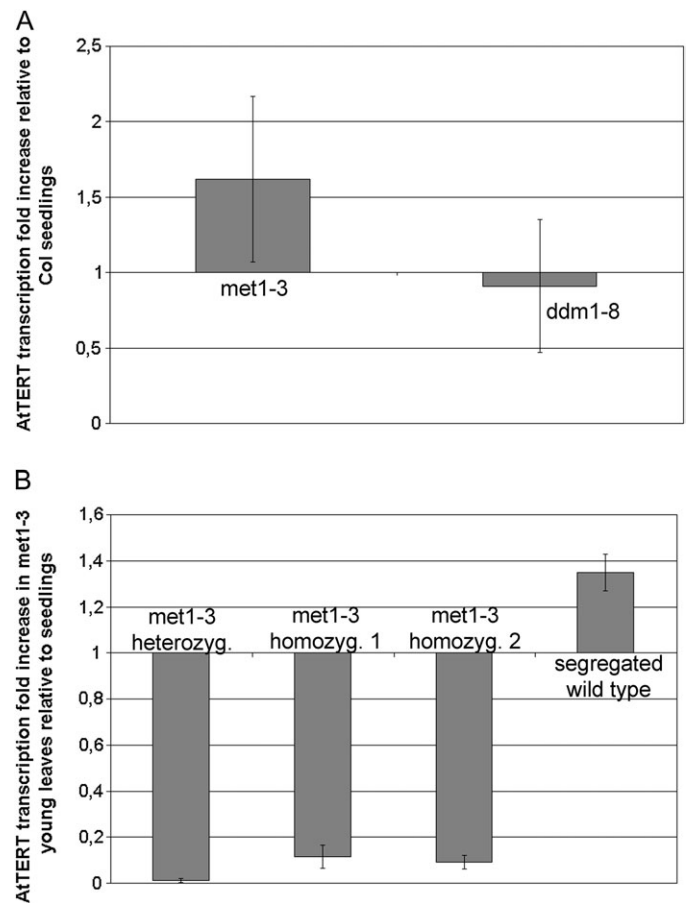


Fig. 2. Analysis of *AtTERT* transcription in methylation mutants. (A) *AtTERT* transcription in 7 day seedlings from methylation mutants. Analysis was done using four biological replicates of seedlings from four *ddm1-8* homozygous plants and from four *met1-3* heterozygous plants. Amplification of a 110 bp fragment of the *AtTERT* exon 1 was expressed relative to the ubiquitin endogenous control. The $\Delta\Delta Ct$ method (Pfaffl, 2004) was used to calculate *AtTERT* transcription. Error bars show SD. No significant change of the *AtTERT* transcript level as compared to wild-type seedlings was observed. Col, Columbia wild-type. (B) *AtTERT* transcription in young leaves from *met1-3* plants (one heterozygous and two homozygous representatives; homozygous plants were selected with extremely low frequency and did not grow up to the reproductive stage, as previously reported by Saze *et al.*, 2003) and from segregated wild-type plants. *AtTERT* transcription in *met1-3* young leaves was significantly lower compared to wild-type samples (Supplementary Fig. S1).

to observations suggesting that the phenotypic consequences of CG methylation erasure are not simply overcome by the reintroduction of the function of both *MET1* alleles, *AtTERT* transcription (Fig. 2B) and telomerase activity (not shown) are fully reverted in plants segregated from the mutant background.

AtTERT is CG-methylated in the gene body region

Although the *AtTERT* putative promoter region is not methylated in either of the tissues tested, methylation in exon 5 in *Arabidopsis* was detected by high-throughput methylation

analysis (<http://signal.salk.edu/cgi-bin/methylome?GENE=At5g16850>) (Zhang *et al.*, 2006). In agreement with this report, a relatively high level of CG methylation was detected in 7 day seedlings and mature leaves of wild-type plants using a primer set delimiting a 476 bp region of the *AtTERT* fifth exon (Fig. 3). CHG and CHH methylations were low and close to the average levels reported for the whole *A. thaliana* genome (6.7 and 1.7%, respectively). A significant decrease of methylation in CG doublets was observed in *met1-3* and *ddm1-8* tissues, which was more pronounced in *met1-3* mutants where CG methylation dropped to a level comparable to those of CHG and CHH. As in the wild type, the amount of methylated cytosines was comparable in different tissues of both mutant plants (Fig. 3).

AtTERT gene silencing is accompanied by increased loading of the H3K27me3 epigenetic mark, but the region maintains its euchromatic nature

Modifications of histone amino acid residues represent crucial determinants of chromatin structure and activity of the corresponding DNA regions. We analysed the distribution of four selected chromatin epigenetic marks in the *AtTERT* upstream region and in exon 5 of telomerase-positive (7 day seedlings) and telomerase-negative (mature leaf) tissues. Crosslinked and sonicated chromatin was immunoprecipitated using antibodies against H3K4me3 (a euchromatin-specific epigenetic mark), H3K9me2 (heterochromatin, mainly constitutive), H3K27me3 (heterochromatin in developmentally silenced regions), and H3K9Ac (euchromatin). Primers for PCR covered the region from -336 bp to the ATG position and 476 bp region of exon 5 (Supplementary Table S1).

AtTERT upstream and exon 5 regions are clearly associated with the euchromatin-specific histone modifications H3K4me3 and H3K9Ac in both telomerase-positive and telomerase-negative tissues, while levels of H3K9me2 are low (Fig. 4). These results suggest that the general chromatin environment in the *AtTERT* gene is not markedly altered during plant development. Correspondingly, the pattern of micrococcal nuclease digestion of *AtTERT* chromatin is comparable in nuclei isolated from 7 day seedlings and from mature leaves (Supplementary Fig. S3). In agreement with previously published results obtained from analysis of 10 day seedlings (Turck *et al.*, 2007; Zhang *et al.*, 2007; Roudier *et al.*, 2011), low signals for the H3K27me3 fraction were detected in 7 day seedlings. In the mature leaf, the intensity of this signal increased significantly in both analysed regions (Fig. 4). A similar pattern of distribution of chromatin marks was observed in 7 day seedlings and mature leaves of *met1-3* mutant plants (Supplementary Fig. S4).

Discussion

Epigenetic modifications of promoter sequences are strong determinants of their transcriptional potency. While promoter-associated DNA methylation is generally consid-

ered as a silencing mark, the pattern of histone modifications is more complex and displays both organism- and locus-specific features (Fransz *et al.*, 2006; Hon *et al.*, 2009).

A detailed methylation map of the *A. thaliana* genome was obtained using high-throughput sequencing approaches (Zhang *et al.*, 2006), and the low level of methylated cytosines observed in the *AtTERT* upstream region (Supplementary Fig. S2) is in accordance with this map. Using mammalian models, convincing data showing involvement of epigenetic mechanisms in telomerase developmental regulation have been reported. While the function of *TERT* promoter methylation was rather ambiguous, as an increase of promoter activity was observed to accompany both hypo- and hypermethylated states, the role of native chromatin environment including histone modifications for tight *hTERT* gene regulation was clearly demonstrated (reviewed in Zhu *et al.*, 2011). In our study, no correlation was observed between *AtTERT* transcription and methylation of the putative minimal promoter. Nevertheless, based on the conclusions of Vaughn *et al.* (2007), methylation of promoters in *Arabidopsis* is a relatively rare event and in this respect DNA methylation is not broadly involved in the regulation of gene expression.

Interestingly, along the *AtTERT* gene methylation in the CG sequence context was detected in the fifth exon (Fig. 3). This type of methylation, termed gene body methylation, has been found in both plant and mammalian genomes (Lorincz *et al.*, 2004; Cokus *et al.*, 2008; Lunerova-Bedrichova *et al.*, 2008). In *Arabidopsis*, genes methylated in transcribed regions are generally constitutively expressed and display lower tissue specificity compared to genes with methylated promoters (Zhang *et al.*, 2006). In a more detailed study (Aceituno *et al.*, 2008) gene body methylation was negatively correlated with gene responsiveness, i.e. capacity to change expression under developmental and environmental stimuli. The protein subunit of telomerase does not fit this general rule, because its expression changes significantly during plant development and the function of the gene body methylation in the *AtTERT* locus remains enigmatic. A connection between *AtTERT* gene methylation and alternative splicing of the *AtTERT* transcript (Rossignol *et al.*, 2007) may be a promising possibility. Unfortunately, testing of this hypothesis is methodically rather difficult due to the very low level of the alternatively spliced *AtTERT* transcript which reduces the reproducibility of quantitative RT-PCR assays (M. Fojtová, unpublished results).

Interesting findings arise from the analysis of the *AtTERT* transcription in *met1-3* mutant leaves. Low levels of *AtTERT* transcripts and telomerase activity were found in developing leaves of *met1-3* mutants (Fig. 1B, 1C, 2B), while in wild-type young leaves both values were even higher as compared to seedlings (Supplementary Fig. S1). This observation might indicate impaired developmental regulation of the *AtTERT* gene in *met1* mutants. We should however be careful about drawing such conclusions, and take into consideration possible moderate variations in the leaf developmental stage (although in all cases, leaves of approximately the same age were collected for analyses), and the very small size (due to their retarded growth) of *met1-3* mutants leaves considered as

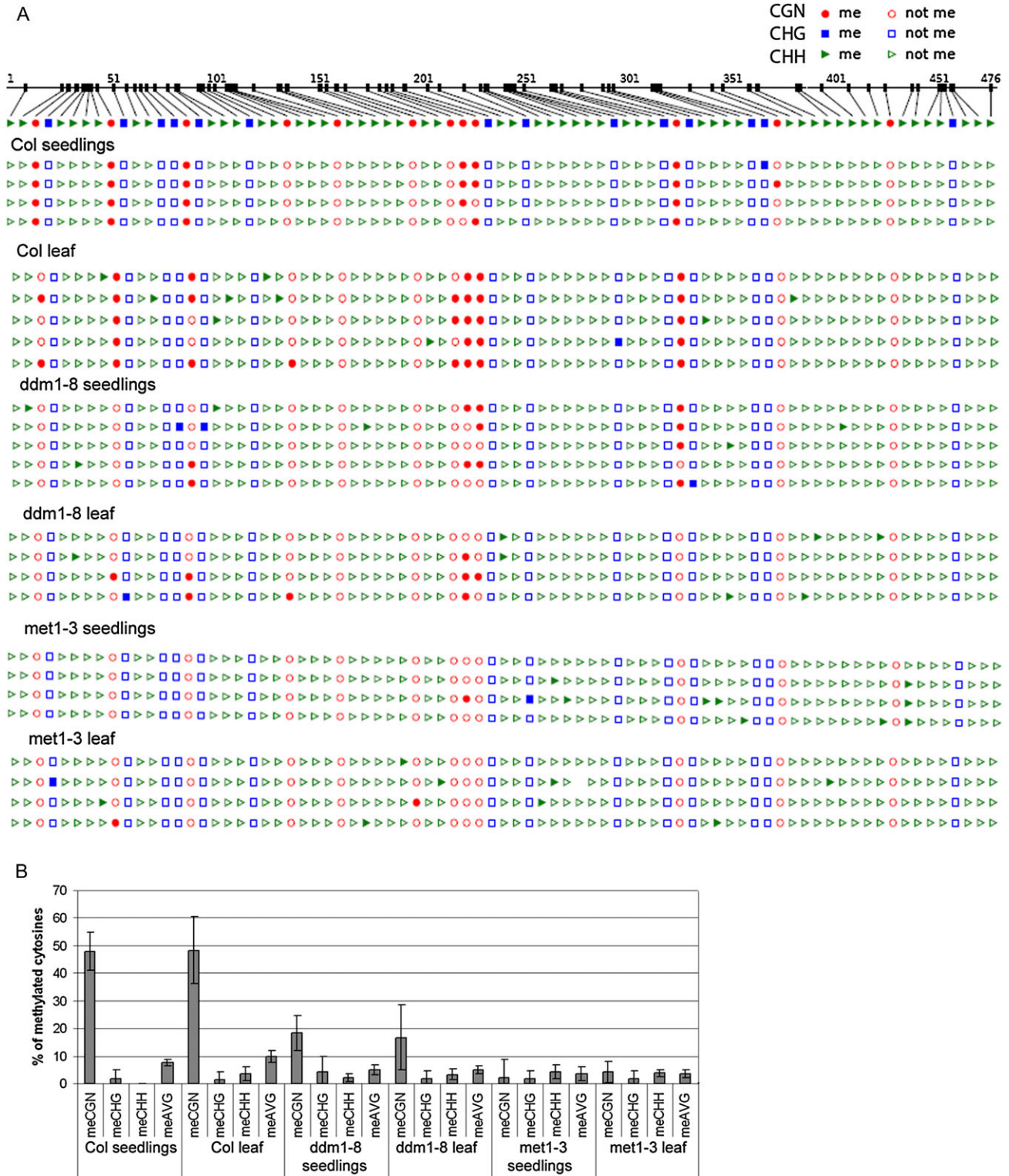


Fig. 3. Analysis of DNA methylation in *AtTERT* exon 5 by bisulphite genomic sequencing. (A) Distribution of methylated cytosines along the 476 bp region of exon 5. Seven day seedlings and mature leaves (leaf C, Fig. 1A) from wild-type and methylation mutants were subjected to analysis. Col, Columbia wild-type; CG methylation, red circles; CHG methylation, blue squares; methylation of cytosines in a non-symmetrical sequence context, green triangles; filled symbols, methylated cytosine; empty symbols, non-methylated cytosine. Twelve cytosines in CG, 14 cytosines in CHG, and 53 cytosines in CHH were evaluated. (B) Graphical representation of the methylated cytosine content in the respective sequence context in tissues of wild-type and methylation mutant plants. Note the comparable level of methylated cytosines in tissues of the same genotype. In all *met1-3* and *ddm1-8* clones, the level of methylated cytosines in a CG sequence context was decreased significantly, and this drop was more pronounced in the *met1-3* mutant background. meAVG, average cytosine methylation.

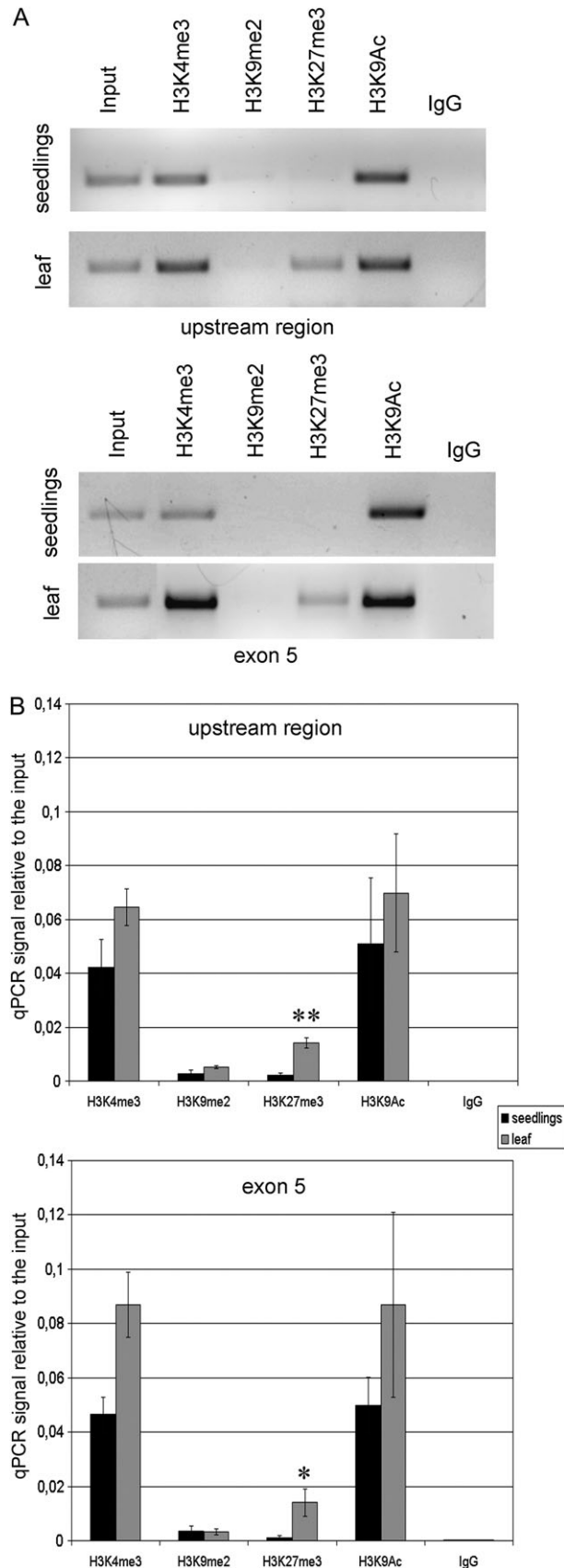


Fig. 4. Analysis of histone modifications in the *AtTERT* upstream region and in exon 5 by ChIP. DNAs from immunoprecipitated fractions of chromatin were purified and a 336 bp region upstream of the ATG signal and a 476 bp region of the fifth exon were

young leaves. Further comprehensive research including analysis of other crucial mutations in related pathways is necessary to clarify this topic definitely.

The recently published map of the main epigenetic states in *Arabidopsis* chromatin revealed distinct combinations of 12 chromatin marks defining active genes, repressed genes, silent repeat elements, and intergenic regions (Roudier *et al.*, 2011). According to the present data, *AtTERT* chromatin was associated with the histone marks H3K4me3, H3K4me2, H3K36me3, and H3K27me1 in 10-day seedlings. Except for the H3K27me1 modification which is prevalent in silent transposable elements, the other modifications are convincingly linked with transcriptionally active genes, in accordance with our result demonstrating enrichment of *AtTERT* chromatin in H3K4me3 and H3K9Ac marks in 7 day seedlings. In telomerase-negative samples, increased H3K27me3 loading in the *AtTERT* upstream and exon 5 regions was observed (Fig. 4) while signals for the other modifications (H3K4me3, H3KAc, and H3K9me2) were more or less comparable in both telomerase-positive and telomerase-negative tissues. The simultaneous presence of H3K4me3 and H3K27me3 in this locus seems to be rather contradictory with the data of Roudier *et al.* (2011) and Ha *et al.* (2011), which show low association of these marks. Because the levels of H3K4me3 and H3K9Ac remained reproducibly high in both regions analysed and based on results of micrococcal nuclease digestion (Supplementary Fig. S3), one can speculate that – despite the increased H3K27me3 loading – the *AtTERT* chromatin maintained the euchromatin state in telomerase-negative tissue. Moreover, silencing of *FLC* gene transcription during the plant transition to flowering – representing a typical example of developmental gene regulation – is accompanied, besides distinctive H3K27me3 loading, by a significant decrease of H3K4me3 and H3KAc and even an increase of H3K9me2 (see Bastow *et al.*, 2004; reviewed by Deal and Henikoff, 2011). To verify the necessity of H3K27me3 for the *AtTERT* silencing, analysis of telomerase dynamics in plants with loss of function of terminal flower 2 (TFL2)/like heterochromatin protein 1 (LHP1) might be informative. TFL2/LHP1 is essential for the establishment of the H3K27me3 repressive modification at developmentally regulated genes (Turck *et al.*, 2007) and loss of its

amplified using classical (A) or quantitative (B) PCR (qPCR). (A) A representative example of PCR amplification of the *AtTERT* upstream region and of exon 5 in immunoprecipitated fractions. Signals of euchromatin-specific marks (H3K4me2, H3K9Ac) were strong in both tissues analysed; signals for the modification typical for constitutive heterochromatin (H3K9me2) were below the detection limit. Note the distinct H3K27me3 band in the leaf samples. (B) Two biological replicates of wild-type seedlings and mature leaves were immunoprecipitated and subjected to quantitative PCR. Signal from the immunoprecipitated fractions was expressed relative to that from the total input chromatin. The amount of the H3K27me3 mark increased in the telomerase-negative tissue (leaf) in both regions analysed ($P < 0.01$ in the *AtTERT* upstream region; $P < 0.05$ in the exon 5).

function leads to a broad range of developmental defects (Gaudin *et al.*, 2001).

In recent reports, independence of H3K27me3 and DNA methylation (Zhang *et al.*, 2007) and even mutual exclusivity of these modifications (Weinhofer *et al.*, 2010) were demonstrated. In this context, essentially the same patterns of histone modifications, including increased H3K27me3 loading in telomerase-negative tissue in the methylation-free upstream region and in exon 5 with an increased level of methylated cytosines, are very interesting. Since histone modifications are comparable in mature leaves of the *met1-3* mutant (Supplementary Fig. S4) and of the wild type (Fig. 4), it seems that H3K27me3 loading is in no way affected by cytosine methylation in exon 5.

Taken together, our analysis of the epigenetic states of the *TERT* gene in telomerase-positive and telomerase-negative *Arabidopsis* tissues reveals differential levels of H3K27me3 modification. Nevertheless, in contrast to the situation in mammalian cells where chromatin surrounding the active *TERT* gene is associated with euchromatin-specific histone modifications (hyperacetylation and H3K4 methylation), while chromatin of the silenced *hTERT* gene is marked by H3K9 methylation and H4K20 methylation (i.e. modifications typical for silenced and even heterochromatic regions; Wang *et al.*, 2009), such notable changes of native chromatin environment are not associated with *TERT* gene silencing in *Arabidopsis*. Although immediate promoter status generally results from a complex interplay of many cellular factors, the observed differences between animal and plant cells in the mechanisms involved in developmental regulation of *TERT* may reflect a unique attribute of plants – their totipotency – which accords with a reversible and dynamic character of telomerase silencing (Fajkus *et al.*, 1998).

Supplementary material

Supplementary material is available at *JXB* online.

Supplementary Table S1. Sequences of primers used in genotyping the mutant lines, telomerase activity assay, quantitative analysis of transcription, analysis of methylation by bisulphite genomic sequencing (BGS), and analysis of chromatin modifications (ChIP).

Supplementary Fig. S1. *AtTERT* transcription in wild-type leaves.

Supplementary Fig. S2. Analysis of DNA methylation in *AtTERT* upstream region by bisulphite genomic sequencing.

Supplementary Fig. S3. Micrococcal nuclease digestion of nuclei isolated from *Arabidopsis* seedlings and leaves.

Supplementary Fig. S4. Analysis of histone modifications in the *met1-3* seedlings and mature leaves.

Acknowledgements

This work was supported by the Czech Science Foundation (P501/11/0596), the Grant Agency of the AS CR (IAA50 0040801), and the project 'CEITEC – Central European

Institute of Technology' (CZ.1.05/1.1.00/02.0068) from the European Regional Development Fund.

References

- Aceituno FF, Moseyko N, Rhee SY, Gutierrez RA.** 2008. The rules of gene expression in plants: organ identity and gene body methylation are key factors for regulation of gene expression in *Arabidopsis thaliana*. *BMC Genomics* **9**, 438.
- Alonso JM, Stepanova AN, Leisse TJ, Kim CJ, Chen H, Shinn P, Stevenson DK, Zimmerman J, Barajas P, Cheuk R, *et al.*** 2003. Genome-wide insertional mutagenesis of *Arabidopsis thaliana*. *Science* **301**, 653–657.
- Bastow R, Mylne JS, Lister C, Lippman Z, Martienssen RA, Dean C.** 2004. Vernalization requires epigenetic silencing of FLC by histone methylation. *Nature* **427**, 164–167.
- Broun P, Ganai MW, Tanksley SD.** 1992. Telomeric arrays display high levels of heritable polymorphism among closely related plant varieties. *Proceedings of the National Academy of Sciences, USA* **89**, 1354–1357.
- Chatagnon A, Bougel S, Perriaud L, Lachuer J, Benhattar J, Dante R.** 2009. Specific association between the methyl-CpG-binding domain protein 2 and the hypermethylated region of the human telomerase reverse transcriptase promoter in cancer cells. *Carcinogenesis* **30**, 28–34.
- Cifuentes-Rojas C, Kannan K, Tseng L, Shippen DE.** 2011. Two RNA subunits and POT1a are components of *Arabidopsis* telomerase. *Proceedings of the National Academy of Sciences, USA* **108**, 73–78.
- Clark SJ, Harrison J, Paul CL, Frommer M.** 1994. High sensitivity mapping of methylated cytosines. *Nucleic Acids Research* **22**, 2990–2997.
- Cokus SJ, Feng S, Zhang X, Chen Z, Merriman B, Haudenschild CD, Pradhan S, Nelson SF, Pellegrini M, Jacobsen SE.** 2008. Shotgun bisulphite sequencing of the *Arabidopsis* genome reveals DNA methylation patterning. *Nature* **452**, 215–219.
- Deal RB, Henikoff S.** 2011. Histone variants and modifications in plant gene regulation. *Current Opinion in Plant Biology* **14**, 116–122.
- Dessain SK, Yu H, Reddel RR, Beijersbergen RL, Weinberg RA.** 2000. Methylation of the human telomerase gene CpG island. *Cancer Research* **60**, 537–541.
- Devereux TR, Horikawa I, Anna CH, Annab LA, Afshari CA, Barrett JC.** 1999. DNA methylation analysis of the promoter region of the human telomerase reverse transcriptase (*hTERT*) gene. *Cancer Research* **59**, 6087–6090.
- Fajkus J, Kovarik A, Kralovics R.** 1996. Telomerase activity in plant cells. *FEBS Letters* **391**, 307–309.
- Fajkus J, Fulneckova J, Hulanova M, Berkova K, Riha K, Matyasek R.** 1998. Plant cells express telomerase activity upon transfer to callus culture, without extensively changing telomere lengths. *Molecular and General Genetics* **260**, 470–474.
- Fitzgerald MS, McKnight TD, Shippen DE.** 1996. Characterization and developmental patterns of telomerase expression in plants.

Proceedings of the National Academy of Sciences, USA **93**, 14422–14427.

- Fojtova M, Peska V, Dobsakova Z, Mozgova I, Fajkus J, Sykorova E.** 2011. Molecular analysis of the T-DNA insertion mutants identified putative regulatory elements in the *AtTERT* gene. *Journal of Experimental Botany* **62**, 5531–5545.
- Fransz P, ten Hoopen R, Tessadori F.** 2006. Composition and formation of heterochromatin in *Arabidopsis thaliana*. *Chromosome Research* **14**, 71–82.
- Gaudin V, Libault M, Pouteau S, Juul T, Zhao G, Lefebvre D, Grandjean O.** 2001. Mutations in LIKE HETEROCHROMATIN PROTEIN 1 affect flowering time and plant architecture in *Arabidopsis*. *Development* **128**, 4847–4858.
- Guillemet I, Benhattar J.** 2003. Demethylation of the human telomerase catalytic subunit (hTERT) gene promoter reduced hTERT expression and telomerase activity and shortened telomeres. *Experimental Cell Research* **289**, 326–334.
- Ha M, Ng DW, Li WH, Chen ZJ.** 2011. Coordinated histone modifications are associated with gene expression variation within and between species. *Genome Research* **21**, 590–598.
- Heller K, Kilian A, Piatyszek MA, Kleinhofs A.** 1996. Telomerase activity in plant extracts. *Molecular and General Genetics* **252**, 342–345.
- Heller-Uszynska K, Schnippenkoetter W, Kilian A.** 2002. Cloning and characterization of rice (*Oryza sativa* L) telomerase reverse transcriptase, which reveals complex splicing patterns. *Plant Journal* **31**, 75–86.
- Herbert BS, Hochreiter AE, Wright WE, Shay JW.** 2006. Nonradioactive detection of telomerase activity using the telomeric repeat amplification protocol. *Nature Protocols* **1**, 1583–1590.
- Hetzl J, Foerster AM, Raidl G, Mittelsten Scheid O.** 2007. CyMATE: a new tool for methylation analysis of plant genomic DNA after bisulphite sequencing. *The Plant Journal* **51**, 526–536.
- Hon G, Wang W, Ren B.** 2009. Discovery and annotation of functional chromatin signatures in the human genome. *PLoS Computational Biology* **5**, e1000566.
- Horikawa I, Chiang YJ, Patterson T, Feigenbaum L, Leem SH, Michishita E, Larionov V, Hodes RJ, Barrett JC.** 2005. Differential cis-regulation of human versus mouse TERT gene expression in vivo: identification of a human-specific repressive element. *Proceedings of the National Academy of Sciences, USA* **102**, 18437–18442.
- Kovarik A, Van Houdt H, Holy A, Depicker A.** 2000. Drug-induced hypomethylation of a posttranscriptionally silenced transgene locus of tobacco leads to partial release of silencing. *FEBS Letters* **467**, 47–51.
- Lorincz MC, Dickerson DR, Schmitt M, Groudine M.** 2004. Intragenic DNA methylation alters chromatin structure and elongation efficiency in mammalian cells. *Nature Structural and Molecular Biology* **11**, 1068–1075.
- Lunerova-Bedrichova J, Bleys A, Fojtova M, Khaitova L, Depicker A, Kovarik A.** 2008. Trans-generation inheritance of methylation patterns in a tobacco transgene following a post-transcriptional silencing event. *Plant Journal* **54**, 1049–1062.
- Mathieu O, Reinders J, Caikovski M, Smathajitt C, Paszkowski J.** 2007. Transgenerational stability of the *Arabidopsis* epigenome is coordinated by CG methylation. *Cell* **130**, 851–862.
- Oguchi K, Liu H, Tamura K, Takahashi H.** 1999. Molecular cloning and characterization of *AtTERT*, a telomerase reverse transcriptase homolog in *Arabidopsis thaliana*. *FEBS Letters* **457**, 465–469.
- Oguchi K, Tamura K, Takahashi H.** 2004. Characterization of *Oryza sativa* telomerase reverse transcriptase and possible role of its phosphorylation in the control of telomerase activity. *Gene* **342**, 57–66.
- Pfaffl MW.** 2004. Quantification strategies in real-time PCR. In: S.A. Bustin, ed. *A-Z of Quantitative PCR*. International University Line, La Jolla, CA, 87–112.
- Riha K, Fajkus J, Siroky J, Vyskot B.** 1998. Developmental control of telomere lengths and telomerase activity in plants. *The Plant Cell* **10**, 1691–1698.
- Rossignol P, Collier S, Bush M, Shaw P, Doonan JH.** 2007. *Arabidopsis* POT1A interacts with TERT-V(18), an N-terminal splicing variant of telomerase. *Journal of Cellular Sciences* **120**, 3678–3687.
- Roudier F, Ahmed I, Berard C, Sarazin A, Mary-Huard T, Cortijo S, Bouyer D, Caillieux E, Duvernois-Berthet E, Al-Shikhley L, et al.** 2011. Integrative epigenomic mapping defines four main chromatin states in *Arabidopsis*. *EMBO Journal* **30**, 1928–1938.
- Saze H, Mittelsten Scheid O, Paszkowski J.** 2003. Maintenance of CpG methylation is essential for epigenetic inheritance during plant gametogenesis. *Nature Genetics* **34**, 65–69.
- Sykorova E, Lim KY, Chase MW, Knapp S, Leitch IJ, Leitch AR, Fajkus J.** 2003. The absence of *Arabidopsis*-type telomeres in *Cestrum* and closely related genera *Vestia* and *Sessea* (Solanaceae): first evidence from eudicots. *Plant Journal* **34**, 283–291.
- Turck F, Roudier F, Farrona S, Martin-Magniette ML, Guillaume E, Buisine N, Gagnot S, Martienssen RA, Coupland G, Colot V.** 2007. *Arabidopsis* TFL2/LHP1 specifically associates with genes marked by trimethylation of histone H3 lysine 27. *PLoS Genetics* **3**, e86.
- Wang S, Zhao Y, Hu C, Zhu J.** 2009. Differential repression of human and mouse TERT genes during cell differentiation. *Nucleic Acids Research* **37**, 2618–2629.
- Weinhofer I, Hehenberger E, Roszak P, Hennig L, Kohler C.** 2010. H3K27me3 profiling of the endosperm implies exclusion of polycomb group protein targeting by DNA methylation. *PLoS Genetics* **6**, e1001152.
- Vaughn MW, Tanurdzic M, Lippman Z, Jiang H, Carrasquillo R, Rabinowicz PD, Dedhia N, McCombie WR, Agier N, Bulski A, Colot V, Doerge RW, Martienssen RA.** 2007. Epigenetic natural variation in *Arabidopsis thaliana*. *PLoS Biology* **5**, e174.
- Zhang X, Yazaki J, Sundaresan A, Cokus S, Chan SW, Chen H, Henderson IR, Shinn P, Pellegrini M, Jacobsen SE, et al.** 2006. Genome-wide high-resolution mapping and functional analysis of DNA methylation in *Arabidopsis*. *Cell* **126**, 1189–1201.
- Zhang X, Clarenz O, Cokus S, Bernatavichute YV, Pellegrini M, Goodrich J, Jacobsen SE.** 2007. Whole-genome analysis of histone H3 lysine 27 trimethylation in *Arabidopsis*. *PLoS Biology* **5**, e129.
- Zhu J, Zhao Y, Wang S.** 2011. Chromatin and epigenetic regulation of the telomerase reverse transcriptase gene. *Protein Cell* **1**, 22–32.

Three *TERT* genes in *Nicotiana tabacum*

Eva Sýkorová · Jana Fulnečková · Petr Mokroš ·
Jiří Fajkus · Miloslava Fojtová · Vratislav Peška

Received: 13 December 2011 / Revised: 15 March 2012 / Accepted: 29 March 2012
© Springer Science+Business Media B.V. 2012

Abstract Telomerase is essential for proper functioning of telomeres in eukaryotes. We cloned and characterised genes for the protein subunit of telomerase (TERT) in the allotetraploid *Nicotiana tabacum* (tobacco) and its diploid progenitor species *Nicotiana sylvestris* and *Nicotiana tomentosiformis* with the aim of determining if allopolyploidy (hybridisation and genome duplication) influences TERT activity and divergence. Two of the three sequence variants present in the tobacco genome (*NtTERT-C/s* and *NtTERT-D*) revealed similarity to two sequence variants found in *N. sylvestris* and another variant (*NtTERT-C/t*) was similar to *TERT* of *N. tomentosiformis*. Variants of *N. sylvestris* origin showed less similarity to each other

(80.5 % in the genomic region; 90.1 % in the coding sequence) than that between the *NtTERT-C/s* and *NtTERT-C/t* variants (93.6 and 97.2 %, respectively). The *NtTERT-D* variant was truncated at the 5' end, and indels indicated that it was a pseudogene. All tobacco variants were transcribed and alternatively spliced sequences were detected. Analysis of gene arrangements uncovered a novel exon in the N-terminal domain of *TERT* variants, a feature that is likely to be commonly found in Solanaceae species. In addition, species-specific duplications were observed within exon 5. The putative function, copy number and evolutionary origin of these *NtTERT* sequence variants are discussed.

Keywords telomerase · telomere · TERT · evolution · Solanaceae · polyploidy

Responsible Editor: Pat Heslop-Harrison.

Electronic supplementary material The online version of this article (doi:10.1007/s10577-012-9282-3) contains supplementary material, which is available to authorized users.

E. Sýkorová (✉) · J. Fulnečková · J. Fajkus · M. Fojtová ·
V. Peška
Institute of Biophysics,
Academy of Sciences of the Czech Republic, v.v.i.,
Královopolská 135,
61265 Brno, Czech Republic
e-mail: evin@ibp.cz

E. Sýkorová · P. Mokroš · J. Fajkus · M. Fojtová · V. Peška
Faculty of Science, and CEITEC-Central European
Institute of Technology, Masaryk University,
Kamenice 5,
62500 Brno, Czech Republic

Abbreviations

BLAST	Basic Local Alignment Search Tool
DAPI	4',6-Diamidino-2-phenylindole
EST	Expressed Sequence Tags
FISH	Fluorescence in situ hybridization
GISH	Genome in situ hybridization
GRS	Gazdová repetitive sequence
gss	Genome Survey Sequences
HRS	highly repetitive sequence
MITE	Miniature inverted-repeat transposable element
MS	Murashige – Skoog
NLS	Nuclear localization signal
PCR	Polymerase chain reaction

rDNA	ribosomal DNA
RT-PCR	Reverse transcriptase polymerase chain reaction
SDS	Sodium dodecyl sulfate
SINE	Short interspersed nuclear elements
SSC	Saline-Sodium Citrate
TAE	Tris-acetate-EDTA
TERT	Telomerase reverse transcriptase
UTR	Untranslated region
wgs	whole-genome-shotgun

chromosomes (Blackburn and Gall 1978). Telomerase consists of a protein subunit with reverse transcriptase motifs (telomerase reverse transcriptase (TERT)) and an RNA subunit which provides a template for synthesis of telomere repeat DNA. *Nicotiana tabacum* (tobacco) has been used in pioneering research on telomere and subtelomere structure (Koukalova et al. 1989; Fajkus et al. 1995a, b) and for detection of telomerase activity in plant cells (Fajkus et al. 1996). Stable telomere maintenance and reversible up- and down-regulation of telomerase during plant development was first described in tobacco (Fajkus et al. 1998), as well as telomere-binding proteins that influence the accessibility of telomeres to telomerase (Fulneckova and Fajkus 2000). Tobacco BY-2 cells have also been used to describe cell-cycle-dependent regulation of

Introduction

Telomeres are maintained by a special enzyme, telomerase, which adds telomeric repeats to the ends of linear

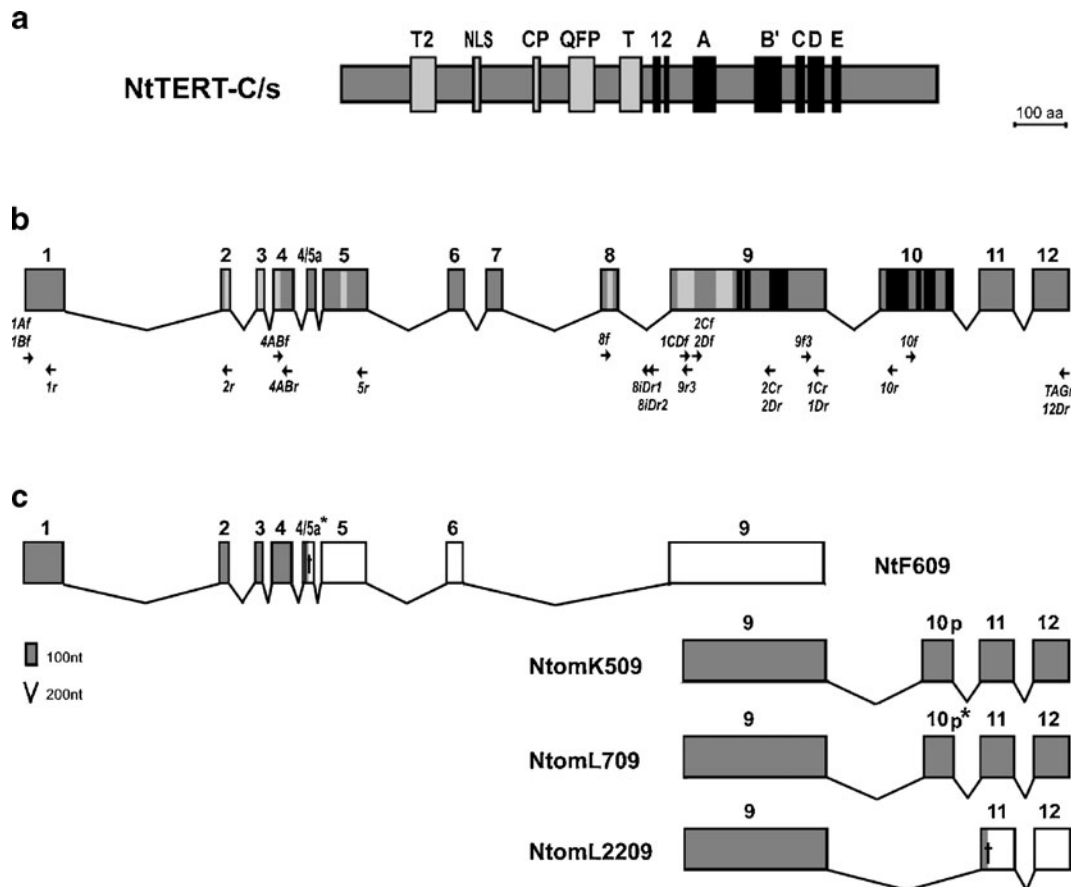


Fig. 1 Arrangement of the *C/s* variant of *NtTERT*. **a** The conserved regions of the NtTERT protein (telomerase specific motifs—*T2*, *CP*, *QFP*, and *T*; reverse transcriptase motifs—*1*, *2*, *A–E*; nuclear localisation-like signal—*NLS* (Sykorova et al. 2006)) are highlighted. **b** The exon/intron arrangement of the *NtTERT* gene sequence is shown including the position of conserved

regions as in (a); positions of PCR primers (Table S2) are marked by arrows. **c** Arrangement of clones with alternatively spliced sequences from *N. tabacum* (*Nt*) and *N. tomentosiformis* (*Ntom*). Putative translated regions are shaded, dagger premature stop codon, 10p and 10p*—two different alternative splicing sites inside exon 10

telomerase activity and its response to plant hormones (Tamura et al. 1999) or abiotic stress (Fojtova et al. 2002). These cells have also been used to demonstrate that tobacco telomeres are methylated and that drug-induced hypomethylation increases telomerase activity, without a change in telomere length (Majerova et al. 2011a, b).

Genes coding the plant TERT subunit have been identified experimentally and characterised in model species *Arabidopsis thaliana*, *Oryza sativa* (Fitzgerald et al. 1999; Heller-Uszynska et al. 2002; Oguchi et al. 2004), *Zea mays* and in Asparagales (Sykorova et al. 2006). The *TERT* gene structure of 12 exons was revealed in plants with typical plant-type telomeres and those with human-type telomeres (reviewed in Sykorova and Fajkus 2009). The telomerase-specific motifs (T2, CP, QFP and T) important for binding the telomerase RNA subunit are localised in the N-terminal part of TERT comprising exons 2–9, and the reverse transcriptase motifs (1, 2 and A–E) essential for enzyme activity are located inside exons 9 and 10 (Fig. 1). Alternatively spliced variants of *TERT* transcripts with out-of-frame and/or in-frame mutations were identified in all studied species. In particular, in vitro interaction of the protein product of AtTERT V(I8) splicing variant with the putative telomere binding protein AtPOT1a suggests its putative function in telomere maintenance (Rossignol et al. 2007). The role of the other splicing variants in plants has not been elucidated yet, but analogous to human splicing variants, they could be involved in tissue specific regulation of TERT transcription (reviewed in Sykorova and Fajkus 2009).

Tobacco is an allopolyploid species that formed within the last 200,000 years from the diploid progenitors of *N. sylvestris* (the maternally derived *S*-genome donor of tobacco) and *N. tomentosiformis* (the paternally derived *T*-genome donor of tobacco) (Murad et al. 2002; Lim et al. 2004; Clarkson et al. 2010). In genomes of higher eukaryotes, including that of the most common model plant *A. thaliana*, a paleotetraploid species, a parallel existence of two or more variants of the *TERT* gene has not been described, suggesting that some unknown restrictions control the number of copies of this particular gene per genome. We have therefore analysed the *TERT* genes in *N. tabacum* and in its diploid progenitors *N. sylvestris*

and *N. tomentosiformis*, to reveal the outcome of the allopolyploidisation process in the case of the *TERT* gene.

Materials and methods

Plant material, DNA and RNA extraction

N. tabacum L. (cv. Vielblättriger, line T3 and cv. Petit Havana SR1), *N. sylvestris* (Speg. & Comes) and *Nicotiana tomentosiformis* (Goodsp.) plants were grown from seeds in the greenhouse. Genomic DNA was extracted from leaves following the protocol from Dellaporta et al. (1983). Total RNA was isolated from seedlings grown on agar plates supplemented with Murashige–Skoog media (1/2 MS, Duchefa, Haarlem, The Netherlands) for two weeks. RNA was prepared and purified using NucleoSpin® RNA Plant kits (Machery Nagel) followed by treatment by Turbo DNA-free kits (Ambion).

PCR, RT-PCR and cloning

PCR reaction conditions were based on the manufacturer recommendations. We used a highly precise Phusion® High-Fidelity DNA Polymerase (error rate, 4.4×10^{-7} , Finnzymes) for cloning of genomic DNA sequences (e.g. sequences linking exons 1 and 4, 4 and 9, 9 and 12, see also Appendix S1), a one-step protocol with Transcriptor reverse transcriptase and Expand System (error rate, 4.6×10^{-6} , Transcriptor One-Step RT-PCR Kit, Roche) for RT-PCR, and short-distance PCR amplification (analysis of exons 4+5, intron 8 and exon 9) was performed by DyNazyme™ DNA Polymerase (error rate, 2.28×10^{-4} , Finnzymes). The PCR products were cloned into TOPO vectors according to type of PCR products produced by polymerases (pCR®II-TOPO® and pCR®-Blunt II-TOPO®, respectively, Invitrogen) and sequenced (Cogenics Ltd., UK). Initial thermocycler conditions for most PCR reactions were as follows: (1) DyNazyme II—35 cycles of 94°C/30 s, 56°C/30 s and 72°C/1 min, (2) Phusion—35 cycles of 98°C/10 s, 56°C/10 s and 68°C/2 min30 s. RT-PCR reactions were performed using Transcriptor One-Step RT-PCR Kit (Roche) and products were sequenced directly and/or cloned into pCR®II-TOPO® vector. PCR and RT-PCR reactions were optimised using temperature gradient and time extension

(see [Electronic supplementary material](#)). TERT sequences were deposited in GenBank (Table S3).

Primer design and sequence analysis

Candidate *TERT* sequences from plants (see Table S1) were identified in the GenBank database using BLAST searches and aligned manually. Prediction of exon/intron boundaries was done manually using consensus AG/GT borders. The BLAST search was performed repetitiously using our cloned sequences as queries to identify sequences from low conserved regions (Fig. S1). The presence of sequence motifs like repeats was analysed by DNasis software, and sequence alignments and similarity calculations were done by Winstar software (WINSTAR, Inc.) or manually. Primers (Fig. 1) were designed using Winstar software or manually; all primer sequences are listed in Table S2.

Restriction digestion and Southern hybridisation

Genomic DNA samples (*N. tabacum* cv. T3, *N. sylvestris* and *N. tomentosiformis*) were digested by *MspI* and/or *EcoRI* restriction endonucleases cutting inside the *TERT* gene and run using conventional electrophoresis on 0.9 % agarose gels in TAE. Gels were alkali blotted and hybridised at 65°C (Fajkus et al. 1995a) with a probe derived from the clone 1CDTAG35 (Table S3). The probe was radioactively labelled using the DecaPrime kit (MBI Fermentas GMBH, St. Leon-Rot, Germany). The membrane was washed under high stringency conditions (0.2× SSC, 0.1 % SDS at 65°C) and signals were visualised by the FLA7000 phosphoimager (FujiFilm). Densitometry and pixel intensities were evaluated by MultiGauge software (FujiFilm).

Fluorescent in situ hybridisation

Chromosome preparations and squashes were performed as published previously (Lim et al. 1998, 2000). DNA probes were labelled with AlexaFluor488-dUTP (Molecular Probes) or Cy3-dUTP (Amersham Pharmacia Biotech) by nick translation and the concentration of *NtTERT* probes for visualisation was optimised. The hybridisation mix (30 µl/slide) contained 40, 100, 160 or 500 ng of each labelled DNA probe (signals were visible from 100 ng, and 160 ng was used

finally), 10 % dextran sulphate and 50 % formamide in 2× SSC. The probe and chromosomes were denatured together on a hot plate at 80°C for 2 min and incubated in a moist chamber at 37°C for 18 h. After hybridisation slides were washed in 35 % formamide in 2× SSC at 42°C and mounted in Vectashield (Vector Laboratories) with 1 µg/ml 4',6-diamidino-2-phenylindole (DAPI; Sigma-Aldrich) as DNA stain. For rehybridisation, the slides were washed twice with 2× SSC and postfixed in 4 % formaldehyde.

Fluorescence signals were analysed with an Olympus BX-61 epifluorescence microscope equipped with an AxioCam CCD camera (Zeiss). Images were captured and processed with ISIS imaging software (MetaSystems). Images were manipulated using Adobe Photoshop by changing the colour balance, contrast, and brightness uniformly across the image.

For localisation of the *NtTERT* gene loci, the clones 1B4AB-1, 4AB1C-28 and 1CDTAG-35 from *N. tabacum* representing the C/s variant of *NtTERT*, or alternatively the clone 4AB1C-9 from *N. tomentosiformis*, were used separately or in various combinations as described in Results. The S-genome-specific probe of the HRS60 repeat is a 183-bp monomeric unit organised in a tandem array, localised in heterochromatic blocks of chromosomes of *N. sylvestris* and *N. tabacum* (Koukalova et al. 1989). The plasmid pGRS1.3 (GenBank X78263.1, kindly provided by Dr. A. Kovarik, Institute of Biophysics, Czech Republic) was used for preparation of a probe for the GRS satellite (Gazdova et al. 1995) which has a 180- to 182-bp monomeric unit organised in a tandem array and occurring as heterochromatic blocks on *N. tabacum* and *N. tomentosiformis* chromosomes. For visualisation of the 45S rDNA loci, an internal 2,478 bp (*EcoRI*) fragment of the 25S rRNA gene was used (Kiss et al. 1989). The clone pCT4.2 (Mozgova et al. 2010), corresponding to a 500-bp 5S rRNA repeat (GenBank M65137), was used for localisation of 5S rDNA loci.

Results

The *N. tabacum* genome contains three variants of the *NtTERT* gene

Using our knowledge about conserved protein regions of plant telomerases (Sykorova et al. 2006; Sykorova

and Fajkus 2009), we searched public databases for candidate *TERT* sequences from plants, especially from Solanaceae. Our BLAST search revealed EST sequences from *Ipomoea nil* and several other sequences from Solanaceae and gss sequences from *N. tabacum* and *Solanum tuberosum* (GenBank ER831256) that we identified as candidate *TERT* sequences (Table S1). The gss sequences were highly similar, especially in putative exon regions, but they contained nucleotide (nt) polymorphisms and insertions/deletions (indels) across aligned regions. The variant sequences occurred in three regions identified by putative exon/intron boundaries in *TERT* (see [Electronic supplementary material](#), Fig. S1 and Table S1). These were between: (1) exon 1 to intron 4 including upstream of the ATG start codon, (2) exon 9 to intron 9 and (3) exons 10 to 12 including a sequence downstream of the stop codon (the nomenclature follows Fitzgerald et al. (1999)). Analysis of polymorphisms showed that several indels found within putative exons were out-of-frame mutations leading to premature stop codons. This finding suggested the presence of a pseudogene variant in addition to a functional gene variant. We hypothesised that one copy had come from each of the diploid progenitors, but that one had become nonfunctional during the evolution of divergence in the allopolyploid *N. tabacum*. Such a view was supported also by the gss sequence (GenBank ET861330) of putative pseudogene exon 12, which contained a highly divergent sequence including a premature stop codon; however, this hypothesis turned out to be too simplistic.

To test the hypothesis, we designed specific primers against the putative exon 9 for candidate *NtTERT* variants named C (coding putative functional variant)

and D (putative pseudogene variant) and also primers from homologous regions of both variants (Fig. 1; Table S2). Surprisingly, sequencing of cloned PCR products revealed three *NtTERT* sequence variants in *N. tabacum* (see [Electronic supplementary material](#) and Appendix S1 for details). The same experimental design using a genomic DNA template of *N. sylvestris* and *N. tomentosiformis* revealed two variants in *N. sylvestris* and one variant in *N. tomentosiformis*. In summary, a comparison of these sequences revealed that the genomic variants found in putative ancestral species corresponded to variants identified in tobacco, resulting in two C variants (named C/t for putative *T*-genome origin and C/s for putative *S*-genome origin) and one D variant (found also in *N. sylvestris*).

Nicotiana TERT-C variants represent full length sequences, while the *TERT-D* variants show truncation at the 5' end

Because alignments of gss sequences showed only two variants in all three partially contiguous regions, there was a question to which variant they belong. In attempt to cover the whole gene sequence and to link together regions (1), (2) and (3) identified in silico (see above and Fig. S1), we performed PCR reactions on genomic DNA of *N. tabacum* with primers designed to amplify the regions between exons 1 and 4, exons 4 and 9 and between exon 9 and the stop codon (Fig. 1b; Appendix S1). Sequencing of genomic and RT-PCR clones (Table S3, see below) enabled us to link all regions and to determine that the contiguous C/s variant of the *NtTERT* genomic sequence was 11.7 kb long (Fig. 1b). The *NtTERT-C/t* variant includes

Table 1 Similarity among *Nicotiana TERT* variants analysed by ClustalW

cDNA ^a vs. gene		cDNA similarity					
		Ntab-C/t	Ntom-C	Ntab-C/s	Nsyl-C	Ntab-D	Nsyl-D
Gene similarity	Ntab-C/t	X	98.7	97.2	96.9	90.3	90.3
	Ntom-C	98.8	X	97.1	96.8	90	90
	Ntab-C/s	93.6	93.5	X	99.4	90.1	90.1
	Nsyl-C	93.4	93.4	99.7	X	89.8	89.8
	Ntab-D	77.3	77.2	80.5	80.6	X	99.9
	Nsyl-D	77.4	77.3	80.7	80.7	99.3	X

Exon 9 to stop codon (1CDf x12Dr primers)

^a Putative exon regions of D variants for analysis corresponded to C variants

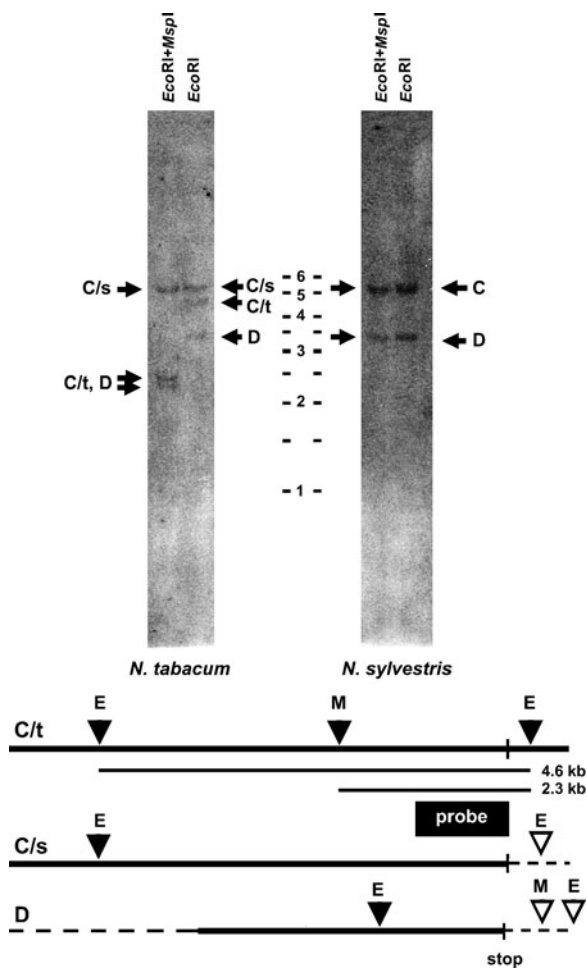


Fig. 2 Restriction digestion of *N. tabacum* and *N. sylvestris* genomic DNA and Southern hybridisation. Three and two variant-specific bands (arrows) of the predicted length were identified in *N. tabacum* and *N. sylvestris*, respectively (above). Schematic diagram of variant-specific genomic sequences (*NtTERT-C/t*, *C/s*, *D*) showing the positions of *EcoRI* (E) and *MspI* (M) cutting sites derived from cloned sequences or predicted from in silico sequences (closed triangles) and length of restriction fragments. Putative positions of the cutting sites (open triangles) in unknown parts of the variants (dashed line) were deduced from the hybridisation patterns when the probe covered exon 10 to the stop codon

several insertions/deletions in exon and intron regions caused mainly by the presence of repetitive sequences (see below). Comparison with the gss sequences identified in silico from contig (1) (exon 1 to 4) confirmed that they represent only the *NtTERT-C/s* and *NtTERT-C/t* variants. The gss sequences corresponding to the *NtTERT-D* variant were found only in contigs (2) and (3) that cover regions from exons 9 to 12. Moreover,

the gss sequence upstream of exon 9 (GenBank FH054998, D variant including the putative intron 8, see [Electronic supplementary material](#) and Table S1) showed no similarity with any of the C-variant gss sequences, suggesting the truncation of the putative pseudogene variant at the 5' end. Also, attempts to amplify the D-variant-specific region upstream of exon 9 using different combinations of primers were not successful (not shown, see additional information in Appendix S1).

A comparison of *N. tabacum TERT* genomic sequences with *N. sylvestris* and *N. tomentosiformis* sequences revealed a high similarity among variants from all three species (Table 1). The highest similarity in the corresponding coding regions exists between the D variants of *N. tabacum* and *N. sylvestris* (99.9 %) and between the *NtTERT-C/s* and the C variant from *N. sylvestris* (99.4 %), and a slightly lower similarity is seen between the *NtTERT-C/t* and the C variant from *N. tomentosiformis* (98.7 %). A notably low similarity is seen between the C and D variants from *N. sylvestris* (or C/s and D from *N. tabacum*, Table 1).

We also examined the arrangement of *NtTERT* variants in the tobacco genome with a special focus on the D-variant, using restriction digestion of genomic DNA by enzymes specific for variants (*EcoRI* or double digestion with *EcoRI* and *MspI*, Fig. 2) and long template PCR (additional information in Appendix S1). We used a radioactively labelled probe specific for the region from exons 10 to 12 which allowed us to identify all three variants. *EcoRI* cuts specifically inside intron 9 of the D variant and both C variants have the *EcoRI* site inside intron 7. Using our gss sequence alignment, we identified another *EcoRI* site in the 3' UTR region of the *NtTERT-C/t* variant but we did not have sequence information on other variants. *MspI* cuts the *NtTERT-C/t* variant specifically inside intron 9 and in theory, its combination with *EcoRI* would shorten the *EcoRI* product to distinguish *NtTERT-C/t* and *NtTERT-C/s* variants. Southern hybridisation showed three bands in the *EcoRI* digest of tobacco genomic DNA corresponding to the *NtTERT* variants, and two bands from restriction digestion of *N. sylvestris* genomic DNA which confirmed the inheritance of tobacco *NtTERT-C/s* and *NtTERT-D* variants from the *N. sylvestris* progenitor. The double digest clearly identified the *NtTERT-C/t* variant and revealed the presence of the second *MspI* site in the 3' UTR region in the tobacco D variant that

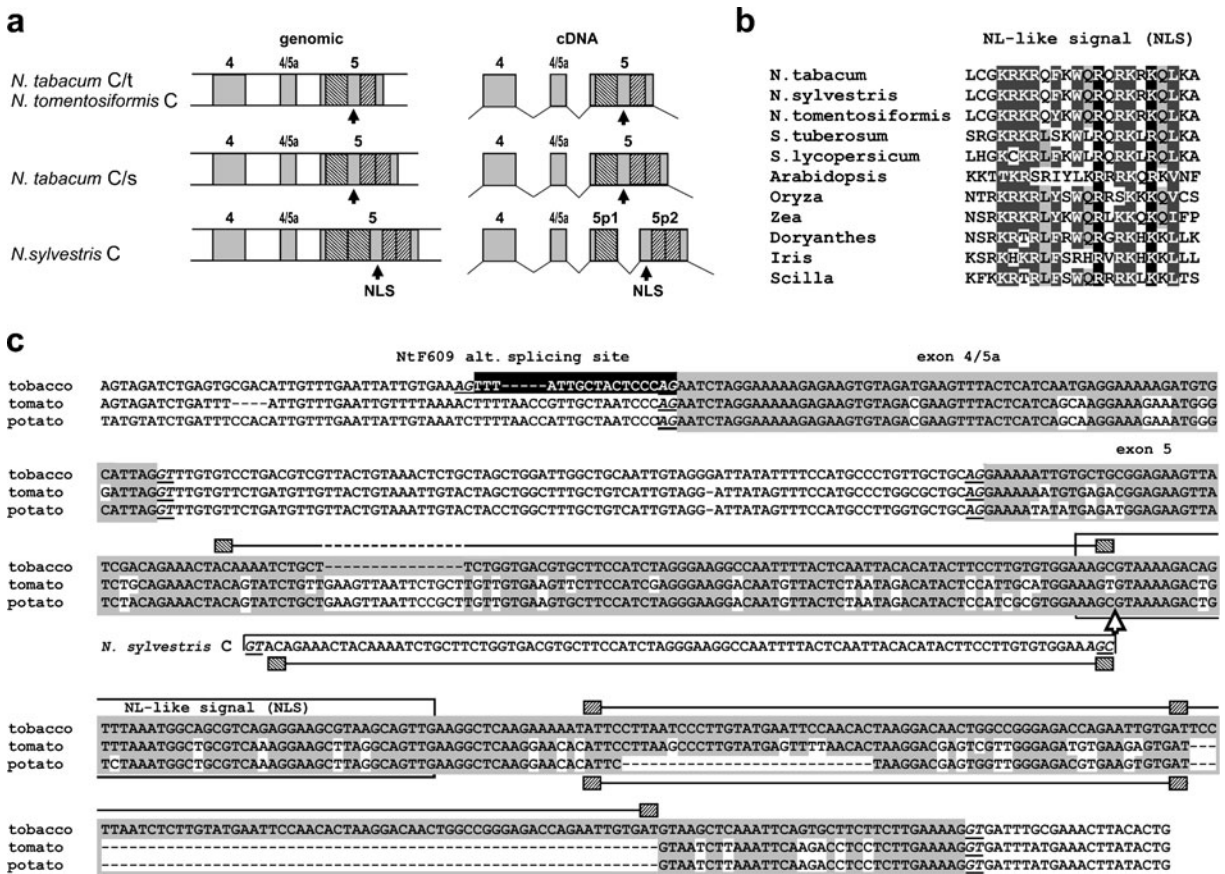


Fig. 3 Arrangement of the exon 4/5a and adjacent regions. **a** Variant-specific organisation of genomic and cDNA sequences from *Nicotiana* species. Repeats inside exon 5 are highlighted. **b** Conserved nuclear localisation-like signal (NLS, arrows in (a) and boxed in (c)) identified inside exon 5 in plant TERT sequences. **c** Alignment of candidate *TERT* sequences from

Solanaceae model species shows the presence of the conserved exon 4/5a region, the tobacco specific alternative splicing site upstream of exon 4/5a and repetitive sequences (boxed as in (a)). The insertion of the repetitive sequence specific for the C variant of *N. sylvestris* is marked by the arrow and boxed as in (a)

illustrates a difference in the genome vicinity of the D variant in tobacco and *N. sylvestris*.

Variants of *NtTERT*, including pseudogene variants, are transcribed

Telomerase is active in meristemic tissues (e.g. seedlings and buds) where its protein subunit is transcribed, as shown for model plants (Fitzgerald et al. 1999; Heller-Uszynska et al. 2002; Fojtova et al. 2011), reviewed in Sykorova and Fajkus (2009). Direct sequencing and cloning of RT-PCR products from seedlings allowed us to define exon/intron borders and to estimate the length of the entire cDNA of the *NtTERT-C/s* variant from *N. tabacum* (3,687 nt), the C variant from *N. sylvestris* (3,687 nt), a partial cDNA

sequence of the C-variant from *N. tomentosiformis* (3,126 nt, from exon 4 to stop), and the *NtTERT-C/t* variant from *N. tabacum* (2,023 nt, from exon 9 to stop). In addition, the RT-PCR clones from amplification of the 5' and 3' part of *TERT* revealed several alternatively spliced isoforms (Fig. 1c; Table S3). Comparison of sequences from *N. tabacum* and its progenitor diploids using different primer combinations revealed that the same alternative splicing as in the *NtTERT-F609* isoform (Figs. 1c and 3c) is utilised by all three species. This alternative splice site is 17 nucleotides upstream of exon 4/5 and results in out-of-frame mutations leading to a premature stop codon, and lack of exons 7 and 8 (Fig. 3c). In the 3' part of the *TERT*, three splicing isoforms were identified among *N. tomentosiformis* clones (Fig. 1c), two of them being

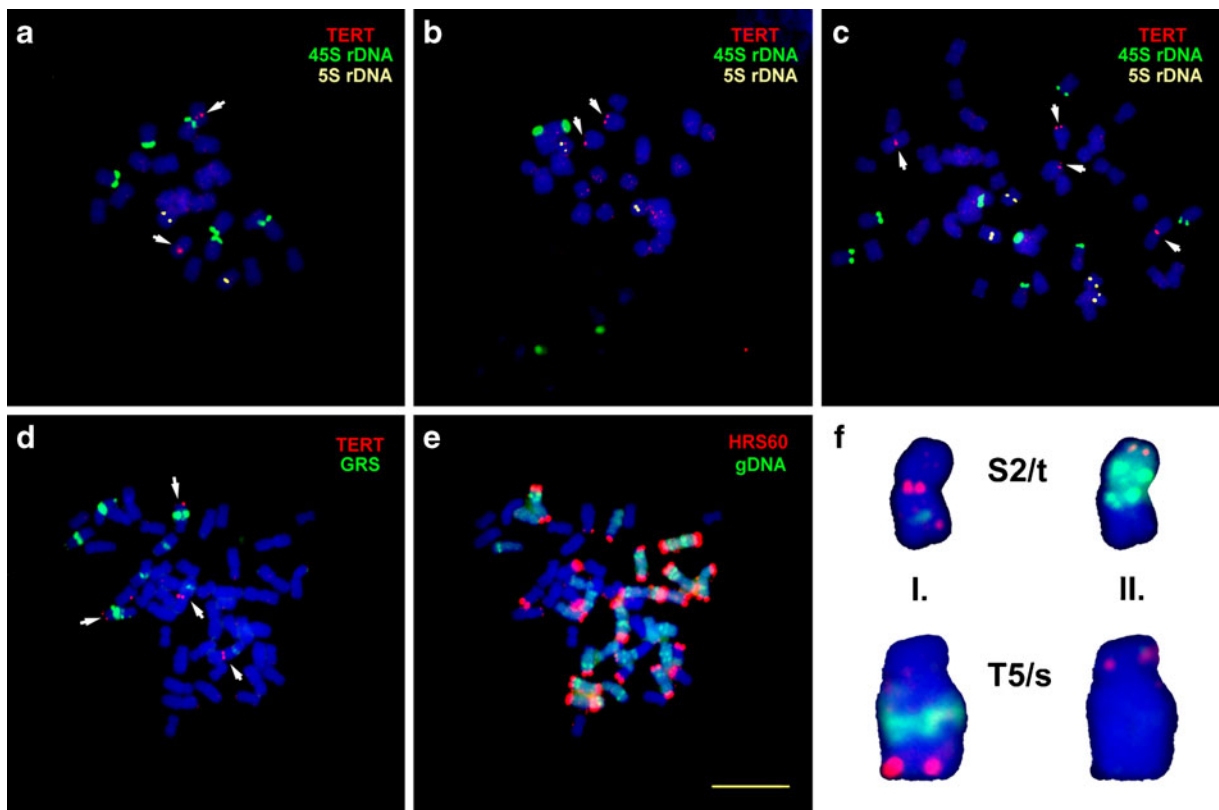


Fig. 4 Localisation of the *NiTERT* gene in *Nicotiana* species by FISH. Mitotic chromosomes of *N. sylvestris* (a), *N. tomentosiformis* (b) and *N. tabacum* (c) labelled with a probe for *NiTERT* (red) and overlaid with DAPI staining for DNA (blue). The rDNA loci are labelled with probes for 45S rDNA (green) and 5S rDNA (yellow). The positions of *TERT* loci are marked by arrows. Two rounds of FISH were used to identify *N. tabacum* chromosomes bearing *NiTERT* loci (d, e). The chromosomes of *N. tabacum* were labelled with probes for *NiTERT* (red, d) and

the tandem repeat GRS (green, d) and counterstained with DAPI (d, f). After stripping of probes, the slides were hybridised in a second round to show the *S*-genome specific translocations by GISH using total genomic DNA from *N. sylvestris* (e, green) and the tandem repeat HRS60 (red, e). f Detail of identified chromosomes S2/t and T5/s showing alternation of signals after two rounds of FISH. Note the small HRS60 signal at the chromosome tip specific for the T5/s chromosome. The nomenclature follows (Lim et al. 2000). Bar=10 μ m

in-frame mutations with partial deletion of exon 10 (*Ntom*-K509 and *Ntom*-L709) and one lacking exon 10 (*Ntom*-L2209).

Next, we analysed which variants are transcribed and may be translated to a functional protein. We first analysed the presence of transcribed sequence variants in *N. tabacum* using RT-PCR primer sets from exon 9. Direct sequencing of the RT-PCR products confirmed the transcription of both C variants (Fig. S4). Surprisingly, RT-PCR products were observed also in control reactions with the primer set specific for the D variant. Sequencing of the cloned products revealed that the D variant is transcribed in *N. tabacum* and *N. sylvestris*. Furthermore, we used primer sets spanning introns to exclude false positives due to genomic DNA contamination. Results from one-step RT-PCR clearly showed that the

D variant is transcribed and utilises the same alternative splicing site inside exon 10 as the *N. tomentosiformis* splicing isoform *NtomL709* (Table S3 and Fig. 1c).

Fluorescent in situ hybridisation shows two loci for the *NiTERT* gene

For localisation of *NiTERT* variants, we used three genomic clones (Table S3) covering the entire length of the *NiTERT*-C/s variants 1B4AB1 (3.25 kb, exons 1 to 4), 4AB1C28 (6.08 kb, exons 4 to 9), and 1CDTAG35 (3.36 kb, exon 9 to stop), separately or in combinations. The longest clone 4AB1C28 showed four strong signals on *N. tabacum* chromosomes (Fig. 4c, d) and two signals on *N. sylvestris* and *N. tomentosiformis* chromosomes (Fig. 4a, b).

Alternatively, we used a genomic clone from *N. tomentosiformis* covering the same region as the *N. tabacum* clone 4AB1C28 with the same result (not shown). The clones 1B4AB1 and 1CDTAG35 did not show signals when used separately, and in combination they showed signals at the same positions as the clone 4AB1C28 when a high amount of probe (500 ng/slide) was applied (not shown). The absence of additional signal representing the *Ni*TERT-D variant could be caused by technical reasons, e.g. short probe length and limited similarity to the *Ni*TERT-C/s variant, or the *Ni*TERT-D variant could be located proximal to the *Ni*TERT-C/s variant and below the detection limit on mitotic chromosomes. In attempt to specify *Ni*TERT chromosomal locations, we used combinations of rDNA-specific probes, genome in situ hybridisation (GISH), and the tobacco *S*- and *T*-genome-specific satellite probes HRS60 and GRS. Hybridisation with the 5S and 45S rDNA probes clearly excluded several chromosomes (Fig. 4a-c). GISH using a *N. sylvestris* DNA probe labelled the *S*-genome in tobacco and clearly distinguished the *Ni*TERT locus near the centromere on the short arm of chromosome S2/t bearing a large translocation from the *T*-genome (Fig. 4e, f; the nomenclature follows (Lim et al. 2000)). The second *Ni*TERT locus was identified using a combination of clone 4AB1C28 and GRS probes, which localised both sequences on the chromosome with the strongest GRS signal in the *T*-genome (Fig. 4d, f). To confirm its chromosomal position, we re-probed the slide with the HRS60 probe which showed signals only on four *T*-genome chromosomes bearing small *S*-genome translocations (Fig. 4e, f). Comparison of these signals identified the second *Ni*TERT locus in the terminal part of the long arm of chromosome T5/s. The *N. sylvestris* and *N. tomentosiformis* TERT signals showed similar locations near the centromere and near the terminus (probably of chromosomes 2 and 5, respectively; Fig. 4a, b) confirming the additive character of *Ni*TERT variants in the evolution of the tobacco genome.

Exon/intron arrangement of the *Ni*TERT gene reveals the presence of a novel exon 4/5a and repeat motifs inside exon 5

Plant TERT genes characterised previously using molecular biology methods contain conserved protein motifs, useful for identification of candidate sequences, and a conserved gene structure of 12 exons (see Sykorova and Fajkus 2009 for a review). Generally, plant

TERT gene structure is characterised by long exons in the 3' region and relatively short exons in the 5' region (see Fig. 1a, b). Several exons in the 5' part of the TERT gene code for linker regions with low similarity in TERT protein sequences, making it difficult to predict exon/intron boundaries for exons 4, 5, 6 and 7. We performed RT-PCR reactions using the same primer sets as for gene cloning (see above) to identify coding regions of the *Ni*TERT gene. Alignment of genomic and cDNA sequences showed the presence of a new exon (4/5a) between exons 4 and 5 (Figs. 1b, 3). The exon 4/5a is 64 bp long, the introns upstream and downstream of the exon 4/5a in *N. tabacum* are short (148 and 89 bp, respectively), and the same arrangement is present in *N. sylvestris* and *N. tomentosiformis*. Because of the low protein similarity common for this TERT region, we are unable to determine if the evolutionary origin of exon 4/5a is by insertion of a novel exon or by the splitting of an existing ancestral exon.

Further detailed analysis revealed other unexpected features inside exon 5. We found a 63-bp duplication resulting in the repetition of 21 amino acids (aa) in the protein sequence. To examine the whole region, we performed PCR and RT-PCR reactions to amplify sequences from exon 4 to the end of exon 5 (Figs. 1b, 3) of *N. sylvestris* and *N. tomentosiformis* TERTs. The results clearly showed that the 21aa duplication inside exon 5 is not present in *N. tomentosiformis* (Fig. 3, Table 2, also [Electronic supplementary material](#) and [Appendix S1](#)). Moreover, another 93 bp duplication within exon 5 was found in *N. sylvestris* but surprisingly, this duplication was not present in cloned RT-PCR products from *N. sylvestris* (Fig. 3; Table 2) suggesting a possible alternative splicing event. However, the borders of the duplicated region do not precisely follow the AG/GT splice site consensus, suggesting that more than one C variant may be present in *N. sylvestris* (Fig. 3; see also "Discussion"). Examination of the protein sequences of exons 5 from all species revealed that both tandem repeats occur in positions outside of the nuclear localisation signal (NLS)-like motif conserved in plant TERTs (Sykorova et al. 2006; Figs. 1a, b and 3).

Repetitive sequences reflect evolutionary genome changes

In addition to the repeats described within exon 5, several other repetitive sequences were identified inside the tobacco TERT genes (Table 2):

Table 2 Repetitive sequences in Solanaceae *TERT* gene variants

Region	Length (bp)	<i>N. tabacum</i> C/t	<i>N. tomentosiformis</i> C	<i>N. tabacum</i> C/s	<i>N. sylvestris</i> C	<i>N. tabacum</i> D	<i>N. sylvestris</i> D	Description	<i>S. tuberosum</i> ^a	<i>S. lycopersicum</i> ^a
Exon 4/5a	64	1x	1x	1x	1x	n.d.	n.d.	Novel exon	1x	1x
Exon 5	63	1x	1x	2x	2x	n.d.	n.d.	Tandem repeat	0.5x	1x
Exon 5	93	1x	1x	1x	2x	n.d.	n.d.	Tandem repeat	1x	1x
Intron 7	102	n.a.	2x	2x	2x	n.d.	n.d.	Tandem repeat with linker 24 bp	1x	1x
Intron 7	175	n.a.	1x	1x	1x	n.d.	n.d.	Repetitive sequence with similarity to other sequences from databases	0x	0x
Intron 8	17	1x	1x	2x	2x	n.d.	n.d.	Tandem repeat embedding 64 bp long indel	1x	1x
Intron 8	222	0x	0x	1x	1x	n.d.	n.d.	MITE, Stonaway-like superfamily	0x	0x
Intron 9	101	2x	2x	2x	2x	2x	2x	Tandem repeat with linker 41 bp	2x ^b	2x ^b
Intron 9	94	2x	2x	1x	1x	1x	1x	Tandem repeat with linker 3 bp	1x ^b	1x ^b
Intron 9	506	0x	0x	0x	0x	1x	1x	Repetitive sequence with similarity to other sequences from databases	0x	0x

n.d. not determined, *n.a.* not analysed

^a *S. tuberosum* sequence is derived from 3 scaffolds and *S. lycopersicum* sequence is derived from single scaffold

^b Low sequence similarity

1. A variant specific repeat, e.g. a putative DNA transposon inside intron 8 found in *N. sylvestris* and the *NtTERT-C/s* variant. This is 222 bp long and has characteristic features of SINE (short interspersed nuclear elements), specifically of the *Stonaway*-like MITE superfamily (miniature inverted-repeat transposable element (Schenke et al. 2003; Kuang et al. 2009)). These non-autonomous transposable elements are characterised by the presence of 32-bp long inverted repeats at the borders, TA target site duplication, and lack of an open reading frame. BLAST (Fig. S1) revealed this MITE could be found in many sequences from Solanaceae including genes, e.g. *MADSI* (Kelly et al. 2010).
2. A 64-bp long indel within intron 8 was identified by sequencing of RT-PCR products. This sequence is framed by a duplication of 17 bp including a splice site-like sequence, AG/GT. Perhaps this generates an alternatively spliced variant or represents a target sequence duplication site differing between genomic sequence variants. To examine the intron 8 region in detail, we sequenced PCR products from genomic DNA of *N. sylvestris* and *N. tomentosiformis* (Fig. 1b, see [Electronic supplementary material](#), Table S2 and Appendix S1). We found that both features (MITE and indel) are present in *N. sylvestris* but not in *N. tomentosiformis*, and so are probably inherited in *N. tabacum* from a *N. sylvestris* progenitor (Table 2).
3. BLAST searches identified two other regions with similarity to many plant DNA sequences from the est and nr databases within introns 7 and 9 (Fig. S1). A 175-bp long sequence from intron 7 is present in all the *Nicotiana TERT* variants examined, indicating its ancient origin.
4. A 506-bp long sequence within intron 9 is specific to the D variants of *N. tabacum* and *N. sylvestris* (see Table 2), suggesting that it was introduced to a pseudogene variant in the *N. sylvestris* ancestor before the formation of *N. tabacum*.
5. Intron 9 also contains two more tandem repeats—a 101-bp repeat present in all *Nicotiana TERTs*, and a 94-bp sequence with two copies in *N. tomentosiformis TERT* and the *NtTERT-C/t* variant (Table 2). None of these sequences showed similarity to other sequences accessible in public databases.

Discussion

Studies of telomerase evolution are linked to fundamental questions addressing the regulation of telomere length, arrangement of telomere and subtelomere regions, and the relation between genome size and chromatin structure. The data suggest a high rate of sequence divergence in *TERT* during the evolution of species in the genus *Nicotiana*. Experimental data, analysis *in silico*, and BLAST searches revealed several specific features of *Nicotiana TERT* sequences: (1) the presence of three *NtTERT* gene variants inherited by *N. tabacum* from the progenitor diploids; (2) transcription of all variants, including a processed pseudogene found in *N. tabacum* and *N. sylvestris*; (3) a novel arrangement of the *TERT* genes with the presence of an additional exon (exon 4/5a), compared with other published *TERTs* (Figs. 1 and 3; Fig. S2); and (4) the presence of repetitive sequences with tandem duplications, including variant-specific repeats within exon 5 (Fig. 3; Table 2).

As described for other tobacco genes, the *NtTERT-C/s* variant is more similar to the *N. sylvestris C* variant than the *NtTERT-C/t* variant to the *N. tomentosiformis C* variant. The D variant from the *N. sylvestris* progenitor is interesting; it has indels within exon regions, leading to premature stop codons and putative gene truncation at the 5' end, suggestive of a pseudogene. However, the variant is transcribed, and so may be involved in the regulation of *TERT* expression, presumably via RNA interference mechanism. Pseudogenes may act in two ways here. First, pseudogene genomic sequences can encode siRNAs. Second, pseudogene transcripts can act as indirect post-transcriptional regulators decoying ncRNA, in particular miRNAs that target the parental gene (reviewed in Muro et al. 2011). Several scenarios are possible for its origin, e.g. from ancient gene/genome duplication, from recombination between separate alleles, and/or maybe from another diploid donor genome (Kelly et al. 2010). Several studies of nuclear genes in *N. tabacum* reveal that parental homologues are maintained (Fulnecek et al. 2009; Clarkson et al. 2010), as observed here for *TERT* sequences, despite apparent gene redundancy in this allopolyploid species for up to 200,000 years (Lim et al. 2004). Using simple approaches of sequence comparison (see [Electronic supplementary material](#), Appendix S1 and Fig. S3), it is difficult to decide if the difference between the C

and the D variants could originate from different selective pressure in these two regions or from another donor species. To evaluate these hypotheses, it will be necessary to perform cloning and analysis of more *Nicotiana* *TERT* genomic sequences including those from other polyploid species with *N. sylvestris* progenitors as ancestral genome donors. Such a series exists in *Nicotiana* in the polyploid section Repandae, formed ~5 million years ago, and in the polyploid section Suaveolentes, formed 10 million years ago (Lim et al. 2004).

Several interesting features specific for *TERT* were revealed. The novel exon 4/5a, which was identified in RT-PCR products, occurs in a region of low protein sequence conservation. Experimentally characterised plant *TERTs* have 12 exons, although a discrepancy in this number had been predicted from in silico analyses of genome sequencing datasets (reviewed in Sykorova and Fajkus 2009). The structures of *TERT* genes are largely conserved (e.g. among vertebrates), although differences were reported in related urochordates, e.g. two species of *Ciona*; *Ciona intestinalis* has 17 exons and a gene structure similar to vertebrate *TERT*, while an intronless *TERT* was found in *Ciona savignyi* (Li et al. 2007). The discovery of exon 4/5a in all three *Nicotiana* species shows the need to experimentally validate predicted gene structures.

The duplication within exon 5, resulting in a tandem repeat in the protein sequence, was identified in a region outside of the conserved NLS signal position, confirming its potential importance for the *TERT* protein. The translated 63-bp-long duplication possesses strongly acidic and polar amino acid residues which contribute negative charges to the basic amino acid composition of exon 5 (not shown). This duplication has no obvious function. The exon 5 codes for the linker sequence between the telomerase-specific T2 (exons 2, 3 and 4) and CP motifs (exon 8), and this region has not been analysed in structural studies of *TERT* from *Tetrahymena* and *Tribolium* (Rouda and Skordalakes 2007; Gillis et al. 2008). The function of this region (except for the predicted NLS signal) and its importance for the structure of the *TERT* protein are unknown. The exon 4/5a, which precedes exon 5, codes for part of the protein linker without any conserved features. Its origin and functional importance cannot be assessed, but it would be interesting to examine Solanaceae/Solanales relatives to track its evolutionary past.

Our experimental data revealed the possibility that the *TERT* gene may be present in *Nicotiana* genomes in several copies. Southern hybridisation showed three bands corresponding to three *TERT* variants from *N. tabacum* DNA digest, and two signals as expected for two variants in *N. sylvestris* (Fig. 2). Quantitative evaluation of the signal of the *N. tabacum* and *N. sylvestris* bands showed the tobacco bands as equal, but the band corresponding to the *N. sylvestris* C variant was twice as strong as the D variant band (not shown). This leaves open the question about the copy number of *TERT* variants in the *N. sylvestris* genome and underlines the need to investigate other *Nicotiana* polyploids. Nevertheless, it is also possible that there is another gene variant differing, e.g. by the number of tandem repeats of the 31 amino acid motif in exon 5, as previously shown for the putrescine *N*-methyltransferase genes (Hashimoto et al. 1998).

Genome sequences of *Solanum lycopersicum* (tomato) and *S. tuberosum* (potato) have been released in the GenBank database, although neither is fully assembled. Nevertheless, they enabled us to compare our findings about the *Nicotiana* *TERT* gene structure with other species from Solanaceae (Fig. 3; Table 2). The data analysed are derived from three scaffold sequences of *S. tuberosum* and one of *S. lycopersicum* (wgs GenBank database, whole-genome-shotgun sequences), although these might change in subsequent genome assembly releases. Nevertheless, comparison with the *N. tabacum* *TERT* sequence showed that both *Solanum* species contain a *TERT* region corresponding to exon 4/5a (Fig. 3), and thus this may originate in the deep past of Solanaceae *TERTs*. Alignments to other regions showed that the highly repetitive sequences from introns, e.g. the putative *Stonaway*-like MITE and the 506-bp long D-variant specific sequence (Table 2), are absent in these *Solanum* species. Other repetitive sequences forming tandem duplications in *Nicotiana* *TERTs* are present only in one copy in *Solanum* *TERTs* (except the 101-bp tandem repeat, Table 2, see also [Electronic supplementary material](#), Appendix S1, Fig. S2) and show a low similarity. The alternative splice site upstream of the exon 4/5a which is utilised in the abundant transcript *NtTERT-F609* (Figs. 1c, 3) and the tandem duplications inside exon 5 are not present in *Solanum* *TERT* sequences (Fig. 3). The alternative splice sites inside exon 10 identified in the isoforms *NtomTERT-K509*, *NtomTERT-L709* and in the D-variant transcript are

present and might be utilised also in *Solanum* transcripts. The fact that we were not able to link potato scaffolds containing *TERT* sequences leaves open the similar question about the number of *TERT* copies in the *S. tuberosum* genome, as discussed above.

Interspecific hybridisation and genome multiplication have been considered to be major forces in the evolution of angiosperms (Soltis and Soltis 1995; Leitch and Leitch 2008). Polyploidy is associated with changes in gene copy number, reflecting genome duplication and the subsequent fate of genes associated with inherent gene redundancy. The protein subunit of human telomerase has been shown to regulate telomerase action at the transcriptional level, and *TERT* genes from model organisms have been described as single copy genes (with the exception of developmentally regulated *TERT* genes in *Euplotes* (Karamysheva et al. 2003)). Increases of the copy number of human *TERT* and *TERC* (coding the RNA subunit) genes have been reported in cancer cells (Cao et al. 2008). Our study reveals the transcription of three *TERT* genes in *N. tabacum* and at least two genes in *N. sylvestris*. It remains to be determined how these multiple *TERT* alleles influence telomere activity and telomere maintenance.

Acknowledgements This work was supported by the Grant Agency of the Academy of Sciences of the Czech Republic (IAA500040801), the Grant agency of the Czech Republic (501/11/0596), the project “CEITEC—Central European Institute of Technology” (CZ.1.05/1.1.00/02.0068) from European Regional Development Fund and institutional funding. We would like to thank Mrs. Jedličková and Mrs. Šípková for technical help and Dr. A. Kovařík (Institute of Biophysics) for providing plasmid pGRS1.3.

References

- Blackburn EH, Gall JG (1978) Tandemly repeated sequence at termini of extrachromosomal ribosomal RNA genes in *Tetrahymena*. *J Mol Biol* 120:33–53
- Cao Y, Bryan TM, Reddel RR (2008) Increased copy number of the *TERT* and *TERC* telomerase subunit genes in cancer cells. *Cancer Sci* 99:1092–1099
- Clarkson JJ, Kelly LJ, Leitch AR, Knapp S, Chase MW (2010) Nuclear glutamine synthetase evolution in *Nicotiana*: phylogenetics and the origins of allotetraploid and homoploid (diploid) hybrids. *Mol Phylogenet Evol* 55:99–112
- Dellaporta SL, Wood J, Hicks JB (1983) A plant DNA mini-preparation: version II. *Plant Mol Biol Rep* 1:19–21
- Fajkus J, Kovarik A, Kralovics R, Bezdek M (1995a) Organization of telomeric and subtelomeric chromatin in the higher-plant *Nicotiana-Tabacum*. *Mol Gen Genet* 247:633–638
- Fajkus J, Kralovics R, Kovarik A, Fajkusova L (1995b) The telomeric sequence is directly attached to the HRS60 subtelomeric tandem repeat in tobacco chromosomes. *FEBS Lett* 364:33–35
- Fajkus J, Kovarik A, Kralovics R (1996) Telomerase activity in plant cells. *FEBS Lett* 391:307–309
- Fajkus J, Fulneckova J, Hulanova M, Berkova K, Riha K, Matyasek R (1998) Plant cells express telomerase activity upon transfer to callus culture, without extensively changing telomere lengths. *Mol Gen Genet* 260:470–474
- Fitzgerald MS, Riha K, Gao F, Ren S, McKnight TD, Shippen DE (1999) Disruption of the telomerase catalytic subunit gene from *Arabidopsis* inactivates telomerase and leads to a slow loss of telomeric DNA. *Proc Natl Acad Sci USA* 96:14813–14818
- Fojtova M, Fulneckova J, Fajkus J, Kovarik A (2002) Recovery of tobacco cells from cadmium stress is accompanied by DNA repair and increased telomerase activity. *J Exp Bot* 53:2151–2158
- Fojtova M, Peska V, Dobsakova Z, Mozgova I, Fajkus J, Sykorova E (2011) Molecular analysis of T-DNA insertion mutants identified putative regulatory elements in the *AtTERT* gene. *J Exp Bot* 62:5531–5545
- Fulneckek J, Matyasek R, Kovarik A (2009) Faithful inheritance of cytosine methylation patterns in repeated sequences of the allotetraploid tobacco correlates with the expression of DNA methyltransferase gene families from both parental genomes. *Mol Genet Genomics* 281:407–420
- Fulneckova J, Fajkus J (2000) Inhibition of plant telomerase by telomere-binding proteins from nuclei of telomerase-negative tissues. *FEBS Lett* 467:305–310
- Gazdova B, Siroky J, Fajkus J et al (1995) Characterization of a new family of tobacco highly repetitive DNA, GRS, specific for the *Nicotiana tomentosiformis* genomic component. *Chromosome Res* 3:245–254
- Gillis AJ, Schuller AP, Skordalakes E (2008) Structure of the *Tribolium castaneum* telomerase catalytic subunit TERT. *Nature* 455:633–637
- Hashimoto T, Shoji T, Mihara T et al (1998) Intraspecific variability of the tandem repeats in *Nicotiana putrescens* *N*-methyltransferases. *Plant Mol Biol* 37:25–37
- Heller-Uszynska K, Schnippenkoetter W, Kilian A (2002) Cloning and characterization of rice (*Oryza sativa* L) telomerase reverse transcriptase, which reveals complex splicing patterns. *Plant J* 31:75–86
- Karamysheva Z, Wang L, Shrode T, Bednenko J, Hurley LA, Shippen DE (2003) Developmentally programmed gene elimination in *Euplotes crassus* facilitates a switch in the telomerase catalytic subunit. *Cell* 113:565–576
- Kelly LJ, Leitch AR, Clarkson JJ, Hunter RB, Knapp S, Chase MW (2010) Intragenic recombination events and evidence for hybrid speciation in *Nicotiana* (Solanaceae). *Mol Biol Evol* 27:781–799
- Kiss T, Kis M, Solymosy F (1989) Nucleotide sequence of a 25S rRNA gene from tomato. *Nucleic Acids Res* 17:796
- Koukalova B, Reich J, Matyasek R, Kuhrova V, Bezdek M (1989) A *bam*HI family of highly repeated DNA-sequences of *Nicotiana tabacum*. *Theor Appl Genet* 78:77–80

- Kuang H, Padmanabhan C, Li F et al (2009) Identification of miniature inverted-repeat transposable elements (MITEs) and biogenesis of their siRNAs in the Solanaceae: new functional implications for MITEs. *Genome Res* 19:42–56
- Leitch AR, Leitch IJ (2008) Genomic plasticity and the diversity of polyploid plants. *Science* 320:481–483
- Li Y, Yates JA, Chen JJ (2007) Identification and characterization of sea squirt telomerase reverse transcriptase. *Gene* 400:16–24
- Lim KY, Leitch IJ, Leitch AR (1998) Genomic characterisation and the detection of raspberry chromatin in polyploid *Rubus*. *Theor Appl Genet* 97:1027–1033
- Lim KY, Matyasek R, Lichtenstein CP, Leitch AR (2000) Molecular cytogenetic analyses and phylogenetic studies in the *Nicotiana* section Tomentosae. *Chromosoma* 109:245–258
- Lim KY, Matyasek R, Kovarik A, Leitch AR (2004) Genome evolution in allotetraploid *Nicotiana*. *Biol J Linn Soc* 82:599–606
- Majerova E, Fojtova M, Mandakova T, Fajkus J (2011a) Methylation of plant telomeric DNA: what do the results say?: M. I. Vaquero-Sedas and M. A. Vega-Palas: DNA methylation at tobacco telomeric sequences. *Plant Mol Biol* 77:533–536
- Majerova E, Fojtova M, Mozgova I, Bittova M, Fajkus J (2011b) Hypomethylating drugs efficiently decrease cytosine methylation in telomeric DNA and activate telomerase without affecting telomere lengths in tobacco cells. *Plant Mol Biol* 77:371–380
- Mozgova I, Mokros P, Fajkus J (2010) Dysfunction of chromatin assembly factor I induces shortening of telomeres and loss of 45S rDNA in *Arabidopsis thaliana*. *Plant Cell* 22:2768–2780
- Murad L, Lim KY, Christodoulou V et al (2002) The origin of tobacco's T genome is traced to a particular lineage within *Nicotiana tomentosiformis* (Solanaceae). *Am J Bot* 89:921–928
- Muro EM, Mah N, Andrade-Navarro MA (2011) Functional evidence of post-transcriptional regulation by pseudogenes. *Biochimie* 93:1916–21
- Oguchi K, Tamura K, Takahashi H (2004) Characterization of *Oryza sativa* telomerase reverse transcriptase and possible role of its phosphorylation in the control of telomerase activity. *Gene* 342:57–66
- Rossignol P, Collier S, Bush M, Shaw P, Doonan JH (2007) Arabidopsis POT1A interacts with TERT-V(I8), an N-terminal splicing variant of telomerase. *J Cell Sci* 120:3678–87
- Rouda S, Skordalakes E (2007) Structure of the RNA-binding domain of telomerase: implications for RNA recognition and binding. *Structure* 15:1403–1412
- Schenke D, Sasabe M, Toyoda K, Inagaki YS, Shiraishi T, Ichinose Y (2003) Genomic structure of the NtPDR1 gene, harboring the two miniature inverted-repeat transposable elements, NtToya1 and NtStowaway101. *Genes Genet Syst* 78:409–418
- Soltis DE, Soltis PS (1995) The dynamic nature of polyploid genomes. *Proc Natl Acad Sci USA* 92:8089–8091
- Sykorova E, Leitch AR, Fajkus J (2006) Asparagales telomerases which synthesize the human type of telomeres. *Plant Mol Biol* 60:633–646
- Sykorova E, Fajkus J (2009) Structure-function relationships in telomerase genes. *Biol Cell* 101(375–392):371–392
- Tamura K, Liu H, Takahashi H (1999) Auxin induction of cell cycle regulated activity of tobacco telomerase. *J Biol Chem* 274:20997–21002

Structure-function relationships during transgenic telomerase expression in *Arabidopsis*

Dagmar Zachová^a, Miloslava Fojtová^{a,b}, Martina Dvořáčková^{a,b}, Iva Mozgová^{a,†}, Inna Lermontova^c, Vratislav Peška^{a,b}, Ingo Schubert^{a,c}, Jiří Fajkus^{a,b} and Eva Sýkorová^{a,b,*}

^aFaculty of Science and Central European Institute of Technology, Masaryk University, CZ-61137, Brno, Czech Republic

^bInstitute of Biophysics, Academy of Sciences of the Czech Republic, CZ-61265, Brno, Czech Republic

^cLeibniz Institute of Plant Genetics and Crop Plant Research, D-06466, Gatersleben, Germany

Correspondence

*Corresponding author,
e-mail: evin@ibp.cz

Received 24 September 2012;
revised 13 December 2012

doi:10.1111/ppl.12021

Although telomerase (EC 2.7.7.49) is important for genome stability and totipotency of plant cells, the principles of its regulation are not well understood. Therefore, we studied subcellular localization and function of the full-length and truncated variants of the catalytic subunit of *Arabidopsis thaliana* telomerase, *AtTERT*, in planta. Our results show that multiple sites in *AtTERT* may serve as nuclear localization signals, as all the studied individual domains of the *AtTERT* were targeted to the nucleus and/or the nucleolus. Although the introduced genomic or cDNA *AtTERT* transgenes display expression at transcript and protein levels, they are not able to fully complement the lack of telomerase functions in *tert* $-/-$ mutants. The failure to reconstitute telomerase function in planta suggests a more complex telomerase regulation in plant cells than would be expected based on results of similar experiments in mammalian model systems.

Introduction

Telomerase is a hot topic of research in molecular, cellular, developmental and cancer biology since its discovery (Greider and Blackburn 1985) and especially, upon finding of its association with cellular immortalization and cancer (Counter et al. 1992, Kim et al. 1994, Bodnar et al. 1998). Plant systems proved to be particularly useful in telomere research as they are telomerase-competent, i.e. their telomerase activity is downregulated during differentiation, but can be upregulated again in response to induction of cell division. Therefore, plant cells are able to maintain stable telomeres

during development and germ cells possess unshortened telomeres although these cells differentiate only late in development (Fajkus et al. 1996, Fajkus et al. 1998, Riha et al. 1998, Holt et al. 1999, Fojtova et al. 2002). Several factors involved in telomerase regulation have been reported, including changes in accessibility of telomeres to telomerase caused by telomere-binding proteins (Fulneckova and Fajkus 2000), regulation of transcription and alternative splicing of the catalytic telomerase subunit TERT (Fitzgerald et al. 1999, Oguchi et al. 1999, Heller-Uszynska et al. 2002), regulation of the phosphorylation state of TERT induced by phytohormones (Tamura et al. 1999; Yang et al. 2002) or association

Abbreviations – Ct, cycle threshold; CTE, C-terminal-extension domain; DMSO, dimethylsulfoxide; GFP, green fluorescent protein; HRP, horseradish peroxidase; NES, nuclear export signal; NLS, nuclear localization signal; PCR, polymerase chain reaction; RID1, RNA-interacting domain 1; RIPA, radio-immuno-precipitation-assay; RT, reverse transcriptase; TEN, telomerase essential N-terminal domain; TERT, telomerase reverse transcriptase; TRAP, telomere-repeat amplification protocol; TRBD, telomerase RNA binding domain; TRF, terminal restriction fragment; wt, wild type.

[†]Present address: Department of Plant Biology and Forest Genetics, Uppsala BioCenter, Swedish University of Agricultural Sciences and Linnean Center for Plant Biology, Box 7080, SE-75007 Uppsala, Sweden

of TERT with alternative RNA subunits (Cifuentes-Rojas et al. 2011). In analogy with mammalian systems, subcellular trafficking of telomerase components and their assembly into the functional nucleoprotein holoenzyme complex promoted by distinct molecular chaperones might represent another important level of telomerase regulation (Holt et al. 1999, Collins 2008, Woo et al. 2009).

Here, we report on telomerase regulation at the level of expression of the *Arabidopsis thaliana* gene encoding the catalytic subunit of telomerase (*AtTERT*), and its individual domains. Functional importance and subcellular localization of the *AtTERT* protein domains were tested by expression in wild-type (wt) and mutant plants and transiently in protoplasts or *Nicotiana benthamiana* leaves. The ability of distinct domains to reconstitute telomerase activity and to maintain telomeres was analyzed in parallel.

Materials and methods

Plant material, *Agrobacterium*-mediated transformation and transient expression

The *Agrobacterium tumefaciens* hypervirulent strain LBA4404. pBR1MCS-virGN54D (van der Fits et al. 2000) was used for transformation of *A. thaliana* wt plants (Col-0, C24) and of the homozygous *tert* $-/-$ T-DNA insertion line (FLAG_493F07, Versailles INRA collection, <http://dbsgap.versailles.inra.fr/portail/>) (for detailed description see Fojtova et al. 2011) by the flower-dip method. Due to the original *bar* resistance gene within the T-DNA insertion (Brunaud et al. 2002; Samson et al. 2002), the *tert* $-/-$ line could be transformed only using vectors with hygromycin resistance. Cultures of *Agrobacterium* strain LBA4404 with *AtTERT* constructs (in ratio 1:1 with a culture strain containing the p19 to prevent gene silencing; Voinnet et al. 2000) were used for transient expression in *N. benthamiana* leaves via syringe infiltration. The construct 35S::YFP in the pC-TAP Gateway vector (Rubio et al. 2005) was used as a positive control. For transient expression in protoplasts, 1 μ g of plasmid DNA of pBM35s-YFP constructs (see below and Table S2, Supporting information) was electroporated into *A. thaliana* protoplasts according to Schallau et al. (2008).

Generation of partial and full-length *AtTERT* constructs

The cloned cDNA sequence of *AtTERT* (Oguchi et al. 1999; GenBank AF135454) was used as a template for preparation of constructs (Fig. 1) via polymerase

chain reaction (PCR) with specific primers (1) containing restriction sites for ligation into pBM35s-C-YFP (Lermontova et al. 2006) or pBM35s-N6xHis+2xc-myc (see Appendix S1 and Fig. S1, Supporting Information) vectors or (2) containing recombination sites for cloning into the Gateway[®] entry vector (pDONRTM/Zeo, Invitrogen, Carlsbad, CA) according to manufacturer's instruction. The full-length genomic *AtTERT* insert was amplified by PCR from genomic DNA and cloned into the pDONRTM/Zeo entry vector. All Gateway entry clones and cassettes in pBM35s vectors were sequenced before the construction of destination binary vectors. Cassettes with *AtTERT* constructs were inserted either into pLH binary vectors (www.dna-cloning-service.de) or Gateway destination vectors. The used Gateway destination vectors (obtained from ABRC stock center; www.arabidopsis.org) were (1) pMDC32 (no tag), pMDC43 (N-GFP), pMDC83 (C-GFP) (Curtis and Grossniklaus 2003); (2) pEarleyGate101 (C-YFP), pEarleyGate103 (C-GFP) (Earley et al. 2006); (3) pGWB20 (C-fused 10x c-myc), pGWB21 (N-fused 10x c-myc) (Nakagawa et al. 2007). Primer sequences and cloning procedures are described in Supporting Information. A description of vector/insert combinations is given in Table S2.

Microscopic analysis of fluorescent signals

Fluorescent signals of green/yellow fluorescent protein (GFP)/YFP in GFP/YFP-*AtTERT* fusion constructs were analyzed using an epifluorescence microscope Olympus BX-61 (www.olympus-global.com) equipped with a DP70 CCD camera using appropriate excitation and emission filter for GFP/YFP (AHF Analysentechnik, Tübingen, Germany) and bright field to detect subcellular structures. Non-transformed plants were taken as a negative control and background fluorescence was determined by using the same exposure time for the wt and transformed plants. Fluorescence images were processed using ADOBE PHOTOSHOP. The proteasome inhibitor MG132 was used to prevent degradation and to increase accumulation of transgenic proteins in plants. One-week-old transgenic *Arabidopsis* seedlings were incubated in liquid Murashige and Skoog (Duchefa Biochemie, Haarlem, The Netherlands) medium with either 50 μ M MG132 (Calbiochem, Merck Millipore, Billerica, MA; dissolved in DMSO, dimethylsulfoxide) or 50 μ M DMSO solution (mock treatment) for 10–16 h. The fusion proteins were detected microscopically. As positive controls we used 35S::YFP or 35S::GFP constructs for transient transformations and *A. thaliana* stable transformants bearing a 35S::GFP construct obtained from Keke Yi (Zhejiang University, Hangzhou, China) were used.

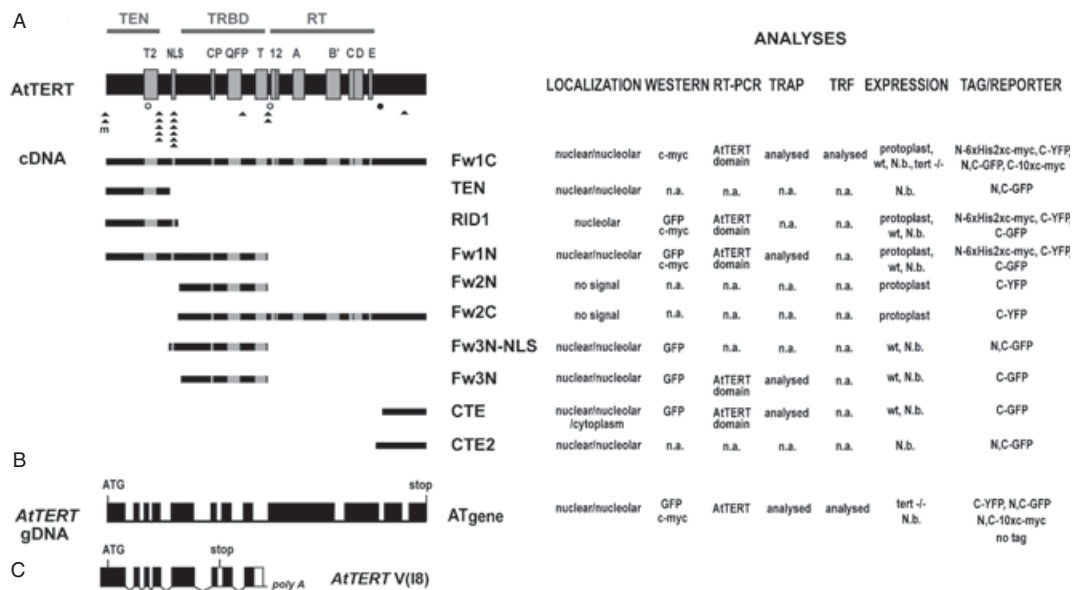


Fig. 1. Overview of the *AtTERT* genomic and cDNA constructs (on left) and experimental approaches (on right). (A) Composition of the *AtTERT* constructs derived from full-length cDNA and positions of functional motifs along the *AtTERT* protein are shown. The regions of structural domains TEN, TRBD and RT are depicted above the conserved RT motifs (1, 2, A, B', C, D and E), telomerase-specific motifs (T2, CP, QFP and T) and a NLS, nucleus localization-like signal. A mitochondrial target signal (m) and further NLS positions predicted in silico per site (triangles) are shown below the *AtTERT* protein. Positions of a region bearing a NES and a nucleolar targeting signal identified in C-terminal hTERT (closed circles, see Fig. S5) and the putative NES sequences identified in silico in *AtTERT* (open circles, Table S3) are indicated. The analyses performed are summarized in right columns: transient expression in *Arabidopsis thaliana* protoplasts (protoplast), in *Nicotiana benthamiana*-infiltrated leaves (N.b.) and stable expression in transformed wt or mutant (*tert* $-/-$) *A. thaliana* plants; expression of transgenes was tested also on Western blots using tag-specific antibodies. Microscopic studies comprise reporter subcellular localizations. RT-PCR analyses include natural *AtTERT* transcription; over-expression of *AtTERT* domains and analysis of splicing (ATgene) in combination with telomerase activity assay (TRAP). The *tert* $-/-$ mutant transformed by full-length *AtTERT* constructs was analyzed for telomere length (TRF) and reconstitution of telomerase activity. The composition of the *AtTERT* genomic construct and performed analyses are shown in (B) and the structure of alternatively spliced variant *AtTERT* V(I8) in (C). Full details about expression systems using specific combinations of constructs and vectors, including results; and of localization-signal predictions in silico are given in Tables S2 and S3. n.a., not analyzed.

Western blot analysis

Total proteins from one mature leaf of *A. thaliana* transformants, from three leaf discs of infiltrated *N. benthamiana* or approximately 200 mg of *Arabidopsis* seedlings were extracted using extraction buffer (20 mM Tris-Cl, pH 8, 300 mM NaCl, 5 mM MgCl₂, 0.1% NP-40, 5 mM dithiothreitol, 5 mM EDTA, protease inhibitor; Roche), or the RIPA (radio-immuno-precipitation-assay) extraction buffer (50 mM Tris-Cl, 150 mM NaCl, 1% NP-40, 0.5% Na deoxycholate, 0.1% SDS, 5 mM dithiothreitol, protease inhibitor). Alternatively, homogenization of the plant tissue was performed directly in loading buffer for sodium dodecylsulphate polyacrylamide gel electrophoresis (SDS-PAGE). The protein concentration was measured according to Bradford (1976). Samples (30 µg of total protein) were heat denatured in Laemmli buffer (Laemmli 1970), separated in 8–12.5% SDS-PAGE gel and proteins were transferred onto a nitrocellulose membrane (Hybond ECL, Amersham Biosciences, GE Healthcare, Little

Chalfont, UK). Membranes were blocked using 5% powdered milk in 1 × TBS/(Tris-Buffered Saline, 20 mM Tris, 137 mM NaCl, pH 7.4) supplemented with 0.5% Tween for 2 h. Then the primary antibody was added and incubated with the membrane for 2 h (anti-GFP Roche, Basel, Switzerland, 1181446001, 1:3000 dilution or anti-myc clone 9E10, Sigma, St. Louis, MO, 1:1000). After washing 3 × 10 min in 1 × TBS/0.5% Tween, membranes were incubated with the secondary antibody for 30 min and washed again. Secondary antibody conjugated to horseradish peroxidase (HRP, Sigma, 1:10 000) was applied and detected using ECL West Dura (Pierce Biotechnology, Rockford, IL) as a substrate for HRP. Chemiluminescence signals were detected using Las3000 (Fujifilm, Tokyo, Japan). To confirm the antibody created no background signal and reliably recognized GFP transgene protein, we used non-transformed *N. benthamiana* leaves as a negative control and our previously defined construct GFP-TRB1 (Dvořáčková et al. 2010) as a positive control.

RNA isolation and analysis of *AtTERT* transcription

Total RNA was isolated from 7-day-old seedlings and separately from roots and shoots of the seedlings, mature rosette leaves of *A. thaliana* plants and from transformed leaf discs of *N. benthamiana* with the RNeasy Plant Mini Kit (Qiagen, Hilden, Germany) followed by the DNaseI treatment (TURBO DNA-free; Applied Biosystems/Ambion, Austin, TX) according to manufacturer's instruction. Quality and quantity of RNA were checked by electrophoresis on 1% (w/v) agarose gels and by absorbance measurement (NanoPhotometr IMPLN, München, Germany). For reverse transcription polymerase chain reaction (RT-PCR) analysis of transient expression, cDNA was prepared using the EP0451 kit (MBI Fermentas, Vilnius, Lithuania) and PCR was run with Go-Tag DNA Polymerase (Promega, Madison, WI) according to manufacturer's recommendation. Primer sequences are given in Table S1.

cDNA for quantitative RT-PCR assays (qRT-PCR) was prepared by reverse transcription of 1 µg of RNA using the M-MuLV (New England Biolabs, Ipswich, MA) RT and Random Nonamers (Sigma). Quantification of the *AtTERT* transcript level related to the *UBIQUITINE-10* (*UBQ-10*) reference gene was done using FastStart SYBR Green Master (Roche) and the ROTORGENE3000 (Qiagen) machine. One microliter of cDNA was added to the 20-µl reaction mix. The final concentration of each primer was 0.25 µM (sequences are given in Table S1). Reactions were done in triplicates. The PCR cycle was 15 min initial denaturation followed by 40 cycles of 20 s at 94°C, 20 s at 56°C and 20 s at 72°C. Sybr Green I fluorescence was monitored consecutively after the extension step. The amount of the respective transcript was determined for at least two individuals of each transgenic line. The *AtTERT* expression was calculated as a fold increase or decrease relative to the wt tissue ($\Delta\Delta C_t$ method; Pfaffl 2004).

Analysis of telomerase activity (TRAP assay)

Protein extracts from 7-day-old seedlings of *A. thaliana*, shoot and root parts of the seedlings were prepared as described (Fitzgerald et al. 1999; Sykorova et al. 2003) and tested for telomerase activity according to the protocol of Fajkus et al. (1998). Briefly, 1 µl of 10 µM TS21 substrate primer (Table S1) was mixed with 1 µl of telomerase extract (protein concentration 50 ng µl⁻¹). Primer elongation proceeded in 25 µl of reaction buffer at 26°C for 45 min. After extension, telomerase was heat-inactivated for 10 min at 95°C and cooled to 80°C. One microliter of 10 µM of the TELPR reverse primer (Table S1) and two units of DyNAzyme DNA Polymerase (Finnzymes, Espoo, Finland) were added to start the PCR

step of the telomere-repeat amplification protocol (TRAP) assay (35 cycles of 95°C/30 s, 65°C/30 s, 72°C/30 s) followed by a final extension (72°C/5 min). Products of the TRAP reaction were analyzed by electrophoresis on a 12.5% polyacrylamide gel in 0.5 × TBE buffer. Gels were stained with GelStar Nucleic Acid Gel Stain (LONZA, Rockland, ME) and signals were visualized using the LAS-3000 system (Fujifilm). The quantitative variant of the TRAP analysis was performed as described (Herbert et al. 2006) using FastStart SYBR Green Master (Roche, Mannheim, Germany) and TS21 and TELPR primers. Samples were analyzed in triplicates. One microliter protein extract diluted to 50 ng/µl protein was added to the 20-µl reaction mix. Cycle threshold (C_t) values were determined using the ROTORGENE3000 (Qiagen) machine software and the relative telomerase activity was calculated by the ΔC_t method (Pfaffl 2004).

Analysis of telomere lengths using TRF analysis

Terminal restriction fragment (TRF) analysis in *tert* $-/-$ transformants was performed as described in Fojtova et al. 2011. Briefly, genomic DNA samples from two individual plants homozygous for each transgene construct (Fig. S4) were digested by *Tru11* cutting near (but not inside) telomeres, separated on 0.8% agarose gel and alkali-blotted onto Hybond-XL (Amersham Biosciences) membrane. The membrane was hybridized with telomeric probe (Table S1) at 55°C overnight. After washing, the signals were visualized by the FLA7000 phosphoimager (FujiFilm) and the grayscale intensity profile of telomeric signals was generated by MULTIGAUGE software (FujiFilm). The unweighted mean TRF length (Fig. 5A) was calculated as $\sum(OD_i \times L_i) / \sum(OD_i)$, where OD_i is the signal intensity above background within intervals i , and L_i is the molecular weight (kb) at the mid-point of interval i .

Results

Experimental strategy and description of *AtTERT* constructs used for the transformation of the wt and *tert* $-/-$ *Arabidopsis* lines

The constructs summarized in Fig. 1 were used to study (1) subcellular localization of *AtTERT* domains and of the full-length *AtTERT* gene in vivo and (2) the influence of over-expressed partial *AtTERT* cDNA constructs on natural telomerase activity. In addition, we investigated the potential of the full-length *AtTERT* constructs to reconstitute telomerase (3) in mature leaves (i.e. telomerase-negative tissue) of *A. thaliana* wt and (4) in seedlings and leaves of *tert* $-/-$ mutant plants. For these purposes, we generated constructs with full-length

and partial cDNA *AtTERT* sequences, and with the full-length genomic *AtTERT* sequence (from start to stop codon). The cDNA constructs and the genomic construct were used to stably transform wt (Col0 and C-24) or *tert* $-/-$ mutant plants (WS4 ecotype). Transient expression of selected constructs was performed in *N. benthamiana* leaves or *A. thaliana* protoplasts. All cDNA and full-length genomic *AtTERT* constructs with or without tags (c-myc-, His- and fluorescent proteins) were controlled by the 35S promoter (see section Materials and methods, Figs 1 and S1, Table S2). Expression of constructs was monitored on Western blots using antibodies against the corresponding tag and/or by RT-PCR. Expression of GFP/YFP-fused constructs was investigated in vivo by fluorescence microscopy (all analyses are specified in Table S2).

AtTERT protein and its domains localize mainly within the nucleus and the nucleolus

Transient expression of the full-length *AtTERT* cDNA fragment Fw1C (Fig. 1) in *N. benthamiana* leaves was microscopically detected using N-GFP as well as C-GFP-fused constructs, i.e. vector pMDC43 (stronger signal, Fig. 2A) and vector pMDC83 (weaker signal), respectively. Both GFP constructs showed signals within the nucleus and the nucleolus. Signals of the *AtTERT* cDNA construct Fw1C were generally weaker (Fig. 2A) than that of the full-length *AtTERT* genomic construct ATgene (Fig. 2B). Next, we studied the localization of truncated *AtTERT* cDNA variants to assess which part of the protein is responsible for the nuclear localization. Plant telomerases contain a conserved nuclear localization signal (NLS) within their N-terminal part (Sykorova et al. 2006, Fig. 1). *Arabidopsis thaliana* transformants stably over-expressing *AtTERT* (over-expression confirmed by qRT-PCR, Fig. 3B) revealed no detectable signals except seedlings treated by proteasome inhibitor MG132 (Fig. 2C–F). This finding is consistent with our observation that *AtTERT* fragments co-purify with proteasome components during tandem affinity purification (Majerská et al., manuscript in preparation). We also experienced problems with RID1 (RNA-interacting domain 1) transformants tagged with GFP/YFP that displayed no signals (C-GFP and C-YFP tag) or no transformants were selected (C-GFP); thus, finally only transient expression in *A. thaliana* protoplasts was successful (Fig. 2H). Transient expression in *N. benthamiana* leaves (Fig. 2A, B, I–O, Table 1) and *A. thaliana* protoplasts (Fig. 2G, H) yielded signals with most constructs within the nucleus and the nucleolus, including the cDNA fragments possessing the designated NLS (Fig. 1, RID1, Fw1N and Fw3N-NLS)

as well as fragments without the NLS [TEN (telomerase essential N-terminal domain) and Fw3N]. Comparison of localization patterns showed a preferential localization in nucleolus for Fw3N (Fig. 2J) and Fw3N-NLS (Fig. 2I) fragments while the N-terminal fragment TEN localized more evenly within nucleus and nucleolus (Fig. 2K, L, Table 1). Transiently expressed fragments showed nuclear speckles (Fig. 2L) which were occasionally visible also in stably transformed *A. thaliana* plants. Two fragments of the telomerase C-terminus – CTE, CTE2 (Fig. 2M–O) – localize to the nucleus and nucleolus. CTE displayed additional signals in cytoplasm of *N. benthamiana* cells (Fig. 2O, Table 1). Apparently, the preferential localization of telomerase within nucleolus and nucleus is mediated through several localization signals in various domains.

AtTERT genomic constructs display correct mRNA splicing and protein translation

The ATgene insert represents full-length genomic DNA with exons and introns (Fig. 1). Its mRNA is spliced. Among all samples bearing the ATgene insert, only the construct in pMDC43 (N-fused with GFP) was microscopically detectable after transient expression in *N. benthamiana* leaves (Figs 2B and S2). Fluorescence signals in lines harboring the ATgene construct within the pMDC43 vector were found to be dispersed in the nucleus, in nuclear speckles and in the nucleolus (Fig. S2A, D–F). The same localization was observed in *tert* $-/-$ plants for the ATgene construct (Fig. 2C).

A successful expression of ATgene constructs at mRNA level was confirmed by RT-PCR including a splicing of the sixth intron typical for the *AtTERT* V(18) isoform (Rossignol et al. 2007). A qualitatively similar pattern of RT-PCR products was detected in all samples with or without tag (Fig. 4A, C). The samples from transiently transformed *N. benthamiana* leaves showed a quantitative imbalance of splicing products in comparison to wt *A. thaliana* plants (Fig. 4A) and contrary to stably transformed *tert* $-/-$ mutant plants over-expressing ATgene constructs (Fig. 4C). Western blot analyses confirmed expression of a protein of the expected size using C-GFP- (pEarleyGate 103) and C-YFP- (pEarleyGate 101) fused constructs (Fig. 4B). Altogether, these results suggest correct mRNA splicing and translation of *AtTERT* (Fig. 4). The protein derived from the N-GFP-fused construct (in pMDC43, microscopically detectable) was slightly shorter than expected (Fig. 4b), and proteins extracted in RIPA buffer (see Materials and methods) contained strong additional short bands (Fig. 4B, right panel). RIPA buffer contains the ionic detergent sodium deoxycholate as an

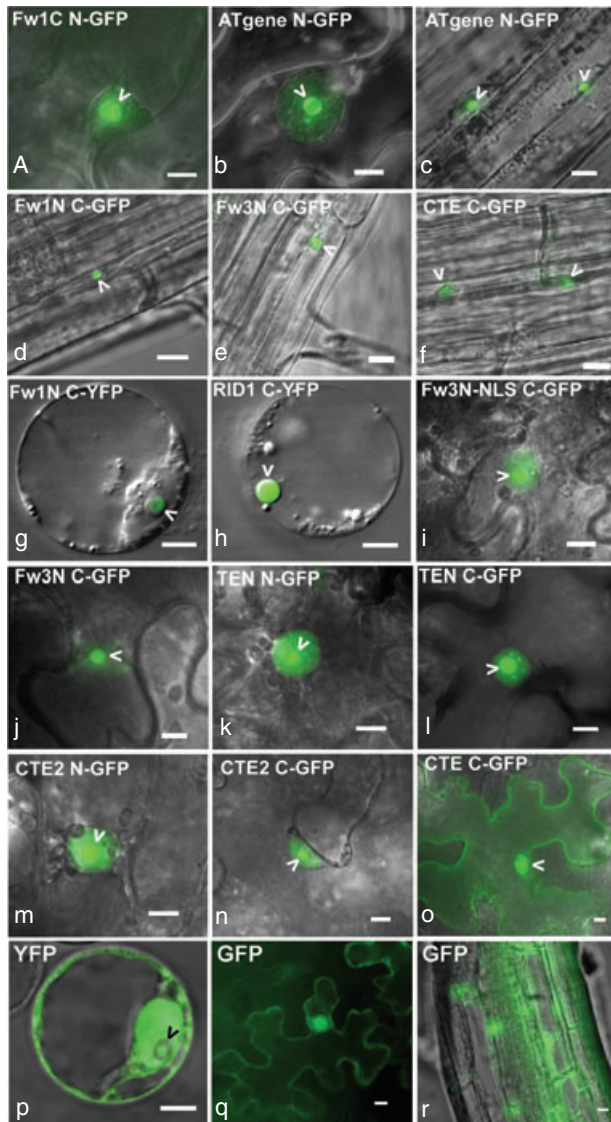


Fig. 2. Localization of AtTERT domains and of a full-length AtTERT genomic construct in stable *Arabidopsis thaliana* transformants and in transiently expressing *Nicotiana benthamiana* leaves. Localization of a representative set of the AtTERT constructs including the full-length cDNA (Fw1C, A) or genomic AtTERT (ATgene, B, C) constructs and the partial cDNA constructs – Fw1N (D, G), RID1 (H), Fw3N-NLS (I), Fw3N (E, J), CTE2 (M, N), CTE (F, O), TEN (K–L) is shown after transient expression in *Arabidopsis* protoplasts (G, H), *N. benthamiana* leaves (A, B, I–O), or in seedlings of stable transformants of wt *A. thaliana* (D–F) or *tert* $-/-$ mutant (C) plants visualized after MG132 treatment. The constructs were C-terminally fused with YFP (G, H), GFP (D–F, I, J, L, N, O) or N-terminally fused with GFP (A–C, K, M). Signals appear in nuclei and nucleoli (white arrow). Localization of unfused YFP protein in *Arabidopsis* protoplasts (I), and unfused GFP in *N. benthamiana* leaves (Q) or *A. thaliana* stable transformant (R). Bar = 10 μ m.

Table 1. Localization pattern of AtTERT constructs transiently expressed in *Nicotiana benthamiana* leaves. N.D., not detected.

Construct	Tag	Nucleoli			Nuclei			Cytoplasm			Number of examined cells of <i>N. benthamiana</i> (100%)	
		Strong (%)	Detectable (%)	N.D. (%)	Strong (%)	Detectable (%)	N.D. (%)	Strong (%)	Detectable (%)	N.D. (%)		Speckles (%)
AtCTE	C-GFP	77	23	0	52	48	0	87	10	3	23	31
AtCTE2	N-GFP	61	39	0	59	41	0	0	14	86	26	74
AtCTE2	C-GFP	70	30	0	69	31	0	0	30	70	13	67
Fw3N NLS	N-GFP	95	5	0	5	94	2	0	20	80	14	133
Fw3N	C-GFP	93	7	0	4	80	15	0	0	100	41	46
TEN	N-GFP	96	4	0	72	26	2	0	0	100	9	47
TEN	C-GFP	89	11	0	25	72	3	0	0	100	25	76
Atgene	N-GFP	70	30	0	22	78	0	0	0	100	26	46

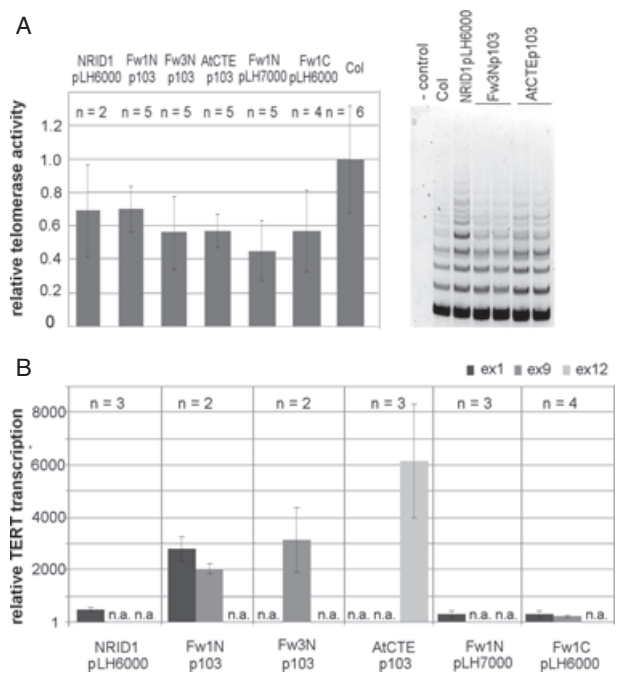


Fig. 3. Analysis of telomerase activity (A) and *AtTERT* expression (B) in wt plants transformed by *AtTERT* constructs. (A) Telomerase activity was analyzed by quantitative (left panel) and conventional (right panel) TRAP assay in 7-day-old seedlings of stable *Arabidopsis* transformants. Telomerase activity in Col0 seedlings was arbitrarily set as 1. (B) *AtTERT* transcription was analyzed for exon 1, exon 9 and exon 12 regions, according to the type of construct used for transformation of *Arabidopsis* Col0 wt and related to the transcription level in Col0 seedlings which was arbitrarily set as 1. n, number of individuals analyzed; n.a., not analyzed.

active constituent and is particularly used for nuclear membrane disruption in nuclear extracts. Because of nuclear and nucleolar localization of telomerase in our experiments, we have chosen RIPA buffer to increase the nuclear and nucleolar protein fraction in the protein extracts. Because we could not detect C-terminal telomerase GFP/YFP microscopically whereas the N-terminal fusion proteins were clearly visible, we presume that the majority of microscopically detected signals might correspond to shorter proteins representing C-terminally truncated variants and/or products of alternatively spliced mRNA, e.g. the *AtTERT* V(I8) isoform. Thus, fluorescent protein at the N-terminus is not affected by splicing while the tag might be cut off if C-terminally located.

Telomerase activity is not significantly affected in transformed wt *Arabidopsis* plants

Telomerase activity and *AtTERT* transcription were investigated in seedlings (telomerase positive tissue)

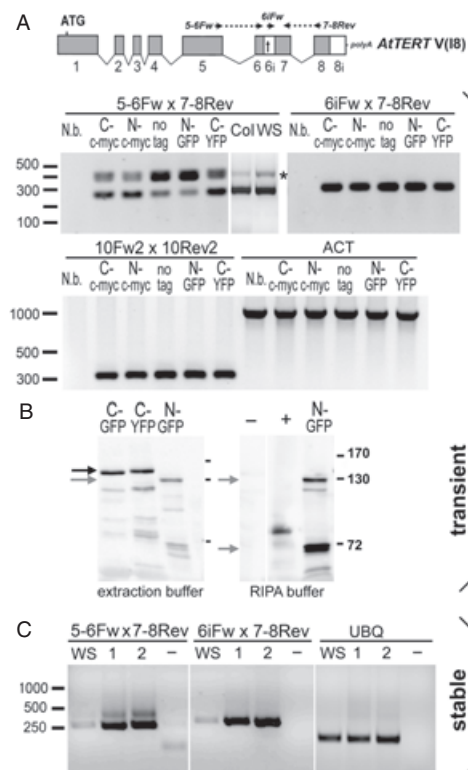


Fig. 4. Transient and stable expression of the full-length genomic *AtTERT* transgene (ATgene) (A) RT-PCR analysis of transient expression in *Nicotiana benthamiana* leaves and (B) Western blot of full-length genomic *AtTERT*-GFP/YFP constructs, (C) stable expression in seedlings of *tert*^{-/-} *Arabidopsis thaliana* mutant plants. (A) ATgene construct examined for presence of alternatively spliced *AtTERT* variants showed two products in RT-PCR with primers 5-6Fw and 7-8Rev indicative of alternative splicing (marked by asterisk) reported in the *AtTERT* V(I8) variant (Rossignol et al. 2007, schema above panels shows position of primers); retention of intron 6 specific for alternatively spliced variant was detected using primers surrounding intron 6 to exon 8 region (primer set 6iFw × 7-8Rev); control of *AtTERT* transcription with primer set amplifying exon 10 (10Fw2 × 10Rev2); control of cDNA quality with primer set amplifying tobacco actin gene (ACT). ATgene transgenes are marked according to the fusion with protein tag (N, C-terminal, c-myc, GFP, YFP, no tag); controls – *N. benthamiana* leaf (N.b.), seedlings of wt ecotypes Columbia and Wassilewskija (Col and WS), marker in bp. (B) GFP antibody was used to detect telomerase-GFP/YFP fusions in transiently transformed *N. benthamiana* leaves. The same pattern was detected for the full-length construct ATgene C-terminally fused with GFP or YFP (black arrow), the N-terminally GFP-fused ATgene construct displayed C-terminally truncated proteins (gray arrows) suggesting predominant expression of alternatively spliced isoforms, different protein extraction efficiency in standard protein extraction buffer (left panel) and in RIPA buffer (right panel) is shown. Positive control (+, GFP-TRB1, Dvořáčková et al. 2010) and negative control (–, N.b. leaf) confirmed antibody specificity and low background, protein marker ladder in kDa. (C) Seedlings of two independent lines (1, 2) of *A. thaliana tert*^{-/-} mutant transformed with ATgene construct without tag and wt seedlings (WS) were analyzed for presence of the alternatively spliced *AtTERT* variant using primer combinations as in (A), control of cDNA quality with primer set amplifying *A. thaliana* ubiquitin gene (UBQ), negative control (–, no-template).

and mature leaves (telomerase-negative tissue) of *Arabidopsis* transformants bearing cDNA constructs with AtTERT domains to reveal possible effects of over-expressed transgenes. In addition to GFP-fused constructs, we used constructs N-terminally fused to a short tag (6xHis, 2xc-myc, see Appendix S1 and Table S2). The transcription of the introduced *AtTERT* fragments was markedly increased in transformants (Fig. 3B). Despite this observation, drop of telomerase activity was detected in seedlings of all transformed plants in comparison to wt (Fig. 3A). Nevertheless, this decrease of activity was not considered as significant for the following reasons: (1) quantification of the telomerase activity is related only to the total protein amount in the extracts, which is less convincing and reproducible as compared to the reference genes used routinely in standard quantitative PCR analyses; (2) standard deviation in Columbia samples (six independent biological replicates, i.e. 7-day seedling germinated from the seeds collected from six Columbia plants) is relatively high and (3) the pattern of the conventional TRAP is similar in all samples tested (Fig. 3A, right panel).

We also addressed the question of how *AtTERT* transcription and telomerase activity differ in separate parts of seedlings of *A. thaliana* wt (ecotype Columbia – Col0) and transformants. Shoots and roots of 7-day seedlings were separated and root tips containing the meristematic region were further dissected from the upper part of the root (Fig. S3A, right panel). Results of qRT-PCR and quantitative TRAP showed that *AtTERT* transcription and telomerase activity are located mainly in the root and especially the root tip in wt *A. thaliana* seedlings (Fig. S3). Also, two *A. thaliana* transformants with different expression level of the same transgene (fragment Fw1N, Fig. 3B) were investigated for telomerase activity and natural *AtTERT* transcription pattern (analyzing exon 10 transcription, which is not present in the Fw1N fragment, Fig. 1) in separate parts of seedlings. No difference compared to wt plants was detected, suggesting the regulation of the natural *AtTERT* gene is not affected by the introduced *AtTERT* constructs.

In analogy to the observation in humans, over-expressed full-length AtTERT construct is supposed to interact with the natural telomerase RNA subunit constitutively expressed in *Arabidopsis* tissues (Cifuentes-Rojas et al. 2011) including telomerase-negative leaves. However, neither the full-length cDNA (Fw1C) nor genomic *AtTERT* (ATgene) constructs led to reconstitution of telomerase activity in leaves. Similarly, none of the investigated partial cDNA constructs (Table S2) over-expressing AtTERT domains switched on telomerase activity in leaves.

Full-length genomic constructs partially restored telomerase activity in *tert* $-/-$ mutants but did not restore telomerase function on telomeres

Full-length protein-expressing constructs are often used to complement mutations in a gain-of-function approach. Human telomerase activity is fully restored to immortalize telomerase-inactive cell lines using constructs of coding DNA sequence (Bodnar et al. 1998, Bachand and Autexier 1999). We took advantage of flexibility of the Gateway system and employed a similar strategy using the full-length cDNA (Fw1C), and additionally, the full-length genomic (ATgene) *AtTERT* constructs with or without tags (Fig. 1 and Table S2). We used for transformation a *tert* $-/-$ mutant line in which T-DNA insertion disrupted the *AtTERT* gene sequence resulting in loss of telomerase activity and shortening of telomeres (Fojtova et al. 2011). The expression of *AtTERT* constructs was monitored by Western blot and/or by qRT-PCR, and reconstruction of telomerase activity was investigated by the TRAP assay (scheme of the experiment in Fig. 5D). The majority of genomic *AtTERT* constructs showed an *AtTERT* transcription increased by more than three orders of magnitude compared to wt, independently of the vector used (Fig. 5). Nevertheless, we did not detect the corresponding transgenic proteins on Western blots using tag-specific antibodies, and telomerase activity was not detected in whole seedlings of any transformed mutant plants. Analysis of root tips (tissue with high telomerase activity in wt seedlings; see Fig. S3) revealed low but detectable telomerase activity in *tert* $-/-$ mutants transformed with the full-length genomic construct in contrary to those transformed with the cDNA construct (Fig. 5C). The telomeres remained significantly shortened in all transformants (Figs 5A and S4) despite their telomerase activity status in root tips, displaying a pattern of TRFs similar to that of the *tert* $-/-$ mutant used for transformation and no reversal of telomere length to that of wt was observed (Fojtova et al. 2011).

Discussion

In this study we addressed questions regarding relationship between the function and the structure of *A. thaliana TERT* gene by (1) identification of signals in AtTERT protein important for its nuclear localization; (2) monitoring of natural telomerase activity for potential impact of over-expressed *AtTERT* cDNA and genomic constructs; (3) investigation of transcription and translation pattern of artificial genomic *AtTERT* constructs after transient transformation and in mutant plants and (4) testing for complementation of AtTERT in *tert* $-/-$

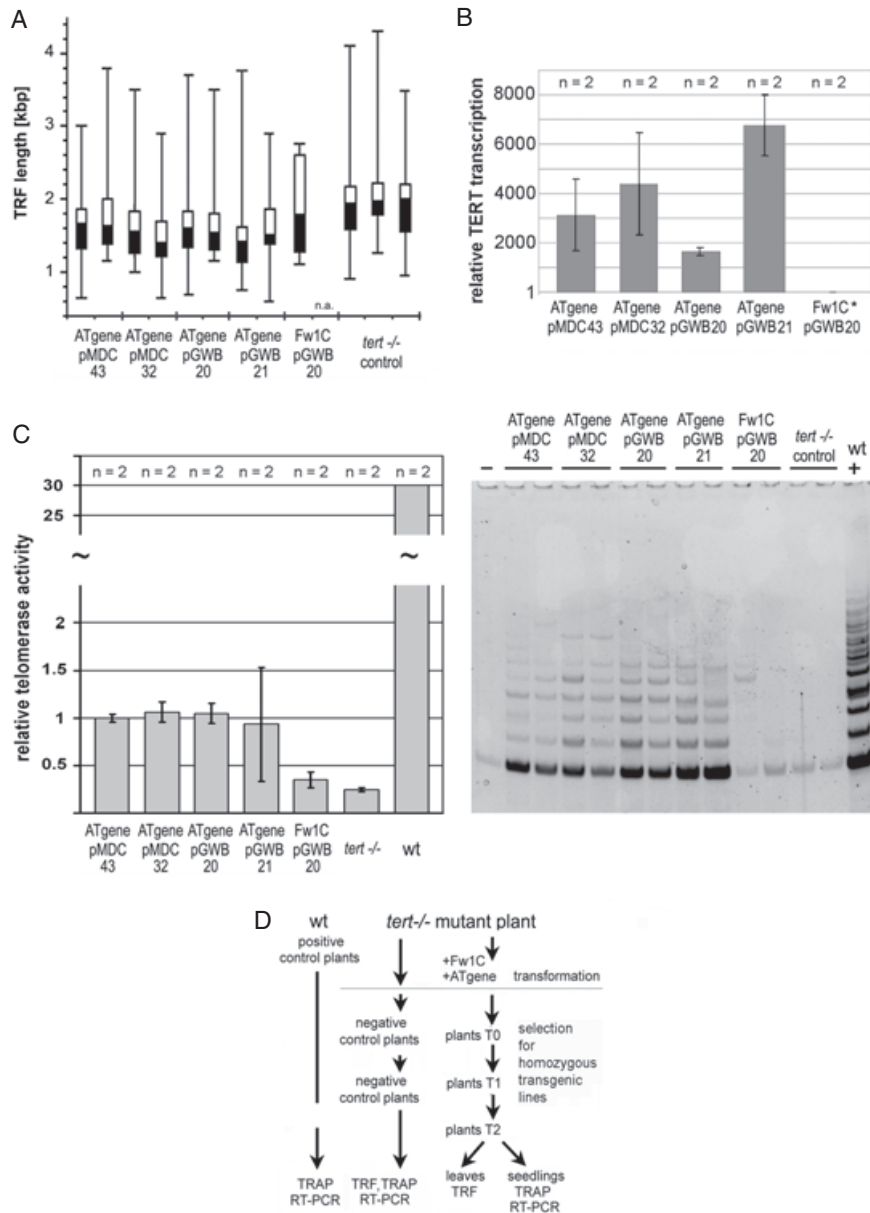


Fig. 5. Analysis of TRF lengths and *AtTERT* transcription in *tert*^{-/-} plants transformed by full-length *AtTERT* constructs. (A) The TRF lengths in *tert*^{-/-} plants non-transformed (control, three individuals) or transformed (two individuals) with full-length cDNA (Fw1C) or genomic (ATgene) *AtTERT* constructs. Vectors without tag (pMDC32), with N-terminal GFP tag (pMDC43) and with N- or C-terminal c-myc tags (pGWB20 and pGWB21) were compared. The TRF lengths of individual plants are presented using box-and-whisker plot where the bottom part (black) and the top (white) of the box are the lower and upper quartiles, respectively, separated by the median. The ends of the whiskers represent the minimum and maximum of TRF lengths (see also Fig. S4), outliers are not indicated in the plot. The third subsequent generation of *tert*^{-/-} plants transformed by *AtTERT* constructs (T2) was analyzed and compared to the second subsequent generation of *tert*^{-/-} control plants as shown in (D). Expression levels of the *AtTERT* constructs were monitored (using exon 9 transcription) in 7-day-old seedlings of *tert*^{-/-} transformants (B), *the relative *AtTERT* transcription of the Fw1C construct was 9.0 ± 5.0 as compared to wt (WS) tissue. (C) Restoration of telomerase activity was analyzed by quantitative (left) and conventional (right panel) TRAP assay in root tips of 7-day-old seedlings of *tert*^{-/-} transformants. In the quantitative assay, telomerase activity was expressed relatively to ATgene in pMDC43. Telomerase activity was detectable in samples transformed by full-length genomic construct. (D) Schematic diagram of experimental approach and analyses.

mutants and in wt tissues lacking telomerase activity by full-length genomic and cDNA constructs.

AtTERT possesses multiple nucleus/nucleolus localization signals

TERT undergoes a dynamic subnuclear shuttling between the nucleoli and nucleoplasm that depends on the cell cycle, DNA damage or cellular transformation in human cells (Tomlinson et al. 2006). Studies of human TERT showed nuclear localization of C-terminally and N-terminally truncated fragments and exclusively nucleolar localization of the TRBD (telomerase RNA binding domain) (Etheridge et al. 2002). Human telomerase was also detected in nuclear speckles due to interaction with other proteins (Oh et al. 2009) or assembly of telomerase holoenzyme (Li et al. 2010, Zhong et al. 2012). We were searching for AtTERT structural motifs responsible for subcellular localizations. Transient expression of full-length *AtTERT* cDNA in *N. benthamiana* leaves showed localization within nucleus and nucleolus independently of the vector used (Fw1C, Fig. 2A). The C-terminally truncated fragments RID1 and Fw1N yielded signals predominantly in the nucleolus, consistent with a previous report (Rossignol et al. 2007), suggesting a nucleus/nucleolus targeting sequence in the N-terminal part of AtTERT. The most conserved NLS motif in this AtTERT region represents a bipartite NLS identified in silico in other plants' TERT (Sykorova et al. 2006, Sykorova and Fajkus 2009) and described in hTERT (Chung et al. 2012). All AtTERT fragments possessing this signal were localized within nucleus and/or nucleolus. However, our in silico analysis identified further protein motifs with similarity to the NLS-like consensus sequence scattered along AtTERT (Fig. 1, see Table S3 for details) which might be responsible for nuclear localization of recombinant proteins lacking the most conserved NLS sequence. The TEN fragment includes the predicted bipartite NLS in the linker region adjacent to the T2 motif and another protein motif which, based on its similarity to an N-terminal motif of human TERT (Santos et al. 2004), is considered to encode a mitochondrial leader sequence (Fig. 1). The latter motif was present in several cDNA fragments, but we did not observe any mitochondrial localization of the encoded proteins. Another NLS-like sequence occurs inside the highly conserved QFP motif (Sykorova et al. 2006) which may function as nucleus targeting signal in the Fw3N construct. All constructs containing a putative TRBD (Fw3N, Fw3N-NLS, Fw1N, Fig. 1) localized predominantly to nucleolus. So far, motifs directing proteins to the nucleolus are not known. Preferential nucleolar localization of proteins was shown to occur via interaction with rRNA and/or

with known nucleolar proteins (Becherel et al. 2006). The TRBD (Fig. 1A) is crucial for binding the telomerase RNA subunit (Lai et al. 2001, Rouda and Skordalakes 2007). One region responsible for nucleolar localization in human TERT was mapped to the RNA-binding domain (Etheridge et al. 2002) roughly corresponding to the Fw3N fragment of AtTERT. Another nucleolar targeting signal was suggested in C terminus of hTERT (Fig. S5; Lin et al. 2008). Human TERT also interacts with nucleolin (Khurts et al. 2004). Localization within nucleus and nucleolus was observed also for two fragments of the AtTERT C-terminus (CTE and CTE2) without a previously identified NLS-like sequence. However, the NLS Mapper predicted a bipartite NLS in this region too (Fig. 1, see Supporting Information for detail). Cytoplasmic localization of the CTE fragment was detected when transiently expressed in *N. benthamiana* leaves but not in seedlings of stable *A. thaliana* transformants. This discrepancy is most likely caused by over-expression during transient transformation. Nevertheless, interaction of the At4g33945 and At5g10350 proteins with the CTE2 fragment was found in cytoplasm and nucleus, respectively, of tobacco BY-2 protoplasts confirming potential localization of AtTERT in different subcellular compartments (Lee et al. 2012). An N-terminally truncated fragment of hTERT corresponding to the AtTERT CTE2 region was located in nuclei and nucleoli of HeLa cells. Lin et al. (2008) suggested the presence of a specific nucleolus targeting signal (Figs 1 and S5) in the hTERT region with a nuclear export signal (NES; Seimiya et al. 2000), indicating that this region has multiple functions. Comparison of hTERT and AtTERT proteins reveals some sequence similarities in this region (Fig. S5) but we found neither exclusive nucleolar localization nor exclusion from the nucleus of the CTE2 protein in comparison to the CTE. As also in silico prediction localized a putative NES within a different part of AtTERT (Fig. 1 and Table S3, Supporting information), this problem needs further investigation. In conclusion, we presume the nucleolar localization of different AtTERT fragments may have different further reasons, e.g. interaction with telomerase RNA or with nucleolar proteins (e.g. nucleolin).

AtTERT gene regulation requires complex functional elements

In analogy to previous studies in human, we used full-length cDNA (Fw1C) and a genomic *AtTERT* construct (ATgene) to reconstitute telomerase function in *tert* $-/-$ mutants. To prevent a possible loss of function by C-terminal protein tagging reported previously for hTERT in vivo (Ouellette et al. 1999, Banik et al. 2002), constructs with an N-terminal tag (functional with

hTERT) or without any tag were chosen for reconstitution experiments. The transcription level of both *AtTERT* constructs was high and the genomic construct displayed functional and alternatively spliced isoforms as expected (Fig. 4). The expression at the protein level was confirmed by Western blot and by microscopic analysis of transient expression of tagged *AtTERT* in *N. benthamiana* leaves (Figs 2 and 4). No case of telomerase activation or telomere elongation was observed in leaves of wt plants, and the low telomerase activity detected in root tips of *tert* $-/-$ mutants transformed by genomic *AtTERT* constructs did not restore sufficiently telomerase function on telomeres (Figs 5 and S4).

The fact that transgene products were not detected in stable *Arabidopsis* transformants by Western blot analysis (see Table S2), and microscopic detection was possible only after MG132 proteasome inhibitor treatment indicates that TERT protein level in *Arabidopsis* is regulated post-translationally via proteasome pathway. It might be that in stably transformed *Arabidopsis* plants exogenous TERT protein cannot be protected from proteasome degradation, because it cannot be recognized by molecular chaperones required for the assembly of active telomerase (Holt et al. 1999, Lee et al. 2010). This can be due to asynchronized expression of TERT and its stabilizing chaperones due to the 35S promoter present in all *TERT* constructs. Our study of *tert* mutant lines bearing T-DNA insertion inside and outside of *AtTERT* suggested regulatory elements upstream and downstream of the ATG start codon (Fojtova et al. 2011). The downstream regions of the genomic construct are not sufficient for successful functional *AtTERT* complementation and apparently the natural genomic context of the *AtTERT* gene is necessary for its correct function.

In summary, we conclude that a crosstalk between regulatory elements located downstream and upstream of the start codon might be essential for effective expression and correct function of the *AtTERT*, and that plant TERT expression differs from that of the human enzyme by a complex multi-level regulation.

Acknowledgements – We thank Ms Jana Kapustová and Ms Kateřina Šípková for technical assistance, Jan Hapala, MSc, for help with TRF quantification and Jana Majerská, MSc, for consultation of proteasome. We thank the anonymous reviewers for their constructive comments and suggestions that helped to improve manuscript. This work was supported by the institutional support (Institute of Biophysics ASCR, AV0Z50040702), the internal support of international collaboration by the Academy of Sciences of the Czech Republic (M200040903), the Grant Agency of Academy of Sciences of the Czech Republic (IAA500040801), the

project CEITEC from European Regional Development Fund (CZ.1.05/1.1.00/02.0068) and the European Social Fund (CZ.1.07/2.3.00/20.0189).

References

- Bachand F, Autexier C (1999) Functional reconstitution of human telomerase expressed in *Saccharomyces cerevisiae*. *J Biol Chem* 274: 38027–38031
- Banik SS, Guo C, Smith AC, Margolis SS, Richardson DA, Tirado CA, Counter CM (2002) C-terminal regions of the human telomerase catalytic subunit essential for in vivo enzyme activity. *Mol Cell Biol* 22: 6234–6246
- Becherel OJ, Gueven N, Birrell GW, Schreiber V, Suraweera A, Jakob B, Taucher-Scholz G, Lavin MF (2006) Nucleolar localization of aprataxin is dependent on interaction with nucleolin and on active ribosomal DNA transcription. *Hum Mol Genet* 15: 2239–2249
- Bodnar AG, Ouellette M, Frolkis M, Holt SE, Chiu CP, Morin GB, Harley CB, Shay JW, Lichtsteiner S, Wright WE (1998) Extension of life-span by introduction of telomerase into normal human cells. *Science* 279: 349–352
- Bradford MM (1976) A rapid and sensitive method for the quantitation of microgram quantities of protein utilizing the principle of protein-dye binding. *Anal Biochem* 72: 248–254
- Brunaud V, Balzergue S, Dubreucq B, Aubourg S, Samson F, Chauvin S, Bechtold N, Cruaud C, DeRose R, Pelletier G, Lepiniec L, Caboche M, Lecharny A (2002) T-DNA integration into the *Arabidopsis* genome depends on sequences of pre-insertion sites. *EMBO Rep* 3: 1152–1157
- Chung J, Khadka P, Chung IK (2012) Nuclear import of hTERT requires a bipartite nuclear localization signal and Akt-mediated phosphorylation. *J Cell Sci* 125: 2684–2697
- Cifuentes-Rojas C, Kannan K, Tseng L, Shippen DE (2011) Two RNA subunits and POT1a are components of *Arabidopsis* telomerase. *Proc Natl Acad Sci USA* 108: 73–78
- Collins K (2008) Physiological assembly and activity of human telomerase complexes. *Mech Ageing Dev* 129: 91–98
- Counter CM, Avilion AA, LeFeuvre CE, Stewart NG, Greider CW, Harley CB, Bacchetti S (1992) Telomere shortening associated with chromosome instability is arrested in immortal cells which express telomerase activity. *EMBO J* 11: 1921–1929
- Curtis MD, Grossniklaus U (2003) A gateway cloning vector set for high-throughput functional analysis of genes in planta. *Plant Physiol* 133: 462–469
- Dvořáčková M, Rossignol P, Shaw PJ, Koroleva OA, Doonan JH, Fajkus J (2010) AtTRB1, a telomeric

- DNA-binding protein from Arabidopsis, is concentrated in the nucleolus and shows highly dynamic association with chromatin. *Plant J* 61: 637–649
- Earley KW, Haag JR, Pontes O, Opper K, Juehne T, Song K, Pikaard CS (2006) Gateway-compatible vectors for plant functional genomics and proteomics. *Plant J* 45: 616–629
- Etheridge KT, Banik SS, Armbruster BN, Zhu Y, Terns RM, Terns MP, Counter CM (2002) The nucleolar localization domain of the catalytic subunit of human telomerase. *J Biol Chem* 277: 24764–24770
- Fajkus J, Kovarik A, Kralovics R (1996) Telomerase activity in plant cells. *FEBS Lett* 391: 307–309
- Fajkus J, Fulneckova J, Hulanova M, Berkova K, Riha K, Matyasek R (1998) Plant cells express telomerase activity upon transfer to callus culture, without extensively changing telomere lengths. *Mol Gen Genet* 260: 470–474
- van der Fits L, Deakin EA, Hoge JH, Memelink J (2000) The ternary transformation system: constitutive virG on a compatible plasmid dramatically increases *Agrobacterium*-mediated plant transformation. *Plant Mol Biol* 43: 495–502
- Fitzgerald MS, Riha K, Gao F, Ren S, McKnight TD, Shippen DE (1999) Disruption of the telomerase catalytic subunit gene from Arabidopsis inactivates telomerase and leads to a slow loss of telomeric DNA. *Proc Natl Acad Sci USA* 96: 14813–14818
- Fojtova M, Fulneckova J, Fajkus J, Kovarik A (2002) Recovery of tobacco cells from cadmium stress is accompanied by DNA repair and increased telomerase activity. *J Exp Bot* 53: 2151–2158
- Fojtova M, Peska V, Dobsakova Z, Mozgova I, Fajkus J, Sykorova E (2011) Molecular analysis of T-DNA insertion mutants identified putative regulatory elements in the AtTERT gene. *J Exp Bot* 62: 5531–5545
- Fulneckova J, Fajkus J (2000) Inhibition of plant telomerase by telomere-binding proteins from nuclei of telomerase-negative tissues. *FEBS Lett* 467: 305–310
- Greider CW, Blackburn EH (1985) Identification of a specific telomere terminal transferase activity in *Tetrahymena* extracts. *Cell* 43: 405–413
- Heller-Uszynska K, Schnippenkoetter W, Kilian A (2002) Cloning and characterization of rice (*Oryza sativa* L) telomerase reverse transcriptase, which reveals complex splicing patterns. *Plant J* 31: 75–86
- Herbert BS, Hochreiter AE, Wright WE, Shay JW (2006) Nonradioactive detection of telomerase activity using the telomeric repeat amplification protocol. *Nat Protoc* 1: 1583–1590
- Holt SE, Aisner DL, Baur J, Tesmer VM, Dy M, Ouellette M, Trager JB, Morin GB, Toft DO, Shay JW, Wright WE, White MA (1999) Functional requirement of p23 and Hsp90 in telomerase complexes. *Genes Dev* 13: 817–826
- Khurts S, Masutomi K, Delgermaa L, Arai K, Oishi N, Mizuno H, Hayashi N, Hahn WC, Murakami S (2004) Nucleolin interacts with telomerase. *J Biol Chem* 279: 51508–51515
- Kim NW, Piatyszek MA, Prowse KR, Harley CB, West MD, Ho PL, Coviello GM, Wright WE, Weinrich SL, Shay JW (1994) Specific association of human telomerase activity with immortal cells and cancer. *Science* 266: 2011–2015
- Laemmli UK (1970) Cleavage of structural proteins during the assembly of the head of bacteriophage T4. *Nature* 227: 680–685
- Lai CK, Mitchell JR, Collins K (2001) RNA binding domain of telomerase reverse transcriptase. *Mol Cell Biol* 21: 990–1000
- Lee JH, Khadka P, Baek SH, Chung IK (2010) CHIP promotes human telomerase reverse transcriptase degradation and negatively regulates telomerase activity. *J Biol Chem* 285: 42033–42045
- Lee LY, Wu FH, Hsu CT, Shen SC, Yeh HY, Liao DC, Fang MJ, Liu NT, Yen YC, Dokládal L, Sykorová E, Gelvin SB, Lin CS (2012) Screening a cDNA library for protein-protein interactions directly in planta. *Plant Cell* 24: 1746–1759
- Lermontova I, Schubert V, Fuchs J, Klatter S, Macas J, Schubert I (2006) Loading of Arabidopsis centromeric histone CENH3 occurs mainly during G2 and requires the presence of the histone fold domain. *Plant Cell* 18: 2443–2451
- Li ZH, Tomlinson RL, Terns RM, Terns MP (2010) Telomerase trafficking and assembly in *Xenopus* oocytes. *J Cell Sci* 123: 2464–2472
- Lin J, Jin R, Zhang B, Chen H, Bai YX, Yang PX, Han SW, Xie YH, Huang PT, Huang C, Huang JJ (2008) Nucleolar localization of TERT is unrelated to telomerase function in human cells. *J Cell Sci* 121: 2169–2176
- Nakagawa T, Kurose T, Hino T, Tanaka K, Kawamukai M, Niwa Y, Toyooka K, Matsuoka K, Jinbo T, Kimura T (2007) Development of series of gateway binary vectors, pGWBs, for realizing efficient construction of fusion genes for plant transformation. *J Biosci Bioeng* 104: 34–41
- Oguchi K, Liu H, Tamura K, Takahashi H (1999) Molecular cloning and characterization of AtTERT, a telomerase reverse transcriptase homolog in *Arabidopsis thaliana*. *FEBS Lett* 457: 465–469
- Oh W, Ghim J, Lee EW, Yang MR, Kim ET, Ahn JH, Song J (2009) PML-IV functions as a negative regulator of telomerase by interacting with TERT. *J Cell Sci* 122: 2613–2622
- Ouellette MM, Aisner DL, Savre-Train I, Wright WE, Shay JW (1999) Telomerase activity does not always imply

- telomere maintenance. *Biochem Biophys Res Commun* 254: 795–803
- Pfaffl MW (2004) Quantification strategies in real-time PCR. In: Bustin SA (ed) *A-Z of Quantitative PCR*. International University Line, La Jolla, pp 87–112
- Riha K, Fajkus J, Siroky J, Vyskot B (1998) Developmental control of telomere lengths and telomerase activity in plants. *Plant Cell* 10: 1691–1698
- Rossignol P, Collier S, Bush M, Shaw P, Doonan JH (2007) Arabidopsis POT1A interacts with TERT-V(18), an N-terminal splicing variant of telomerase. *J Cell Sci* 120: 3678–3687
- Rouda S, Skordalakes E (2007) Structure of the RNA-binding domain of telomerase: implications for RNA recognition and binding. *Structure* 15: 1403–1412
- Rubio V, Shen Y, Saijo Y, Liu Y, Gusmaroli G, Dinesh-Kumar SP, Deng XW (2005) An alternative tandem affinity purification strategy applied to Arabidopsis protein complex isolation. *Plant J* 41: 767–778
- Samson F, Brunaud V, Balzergue S, Dubreucq B, Lepiniec L, Pelletier G, Caboche M, Lecharny A (2002) FLAGdb/FST: a database of mapped flanking insertion sites (FSTs) of *Arabidopsis thaliana* T-DNA transformants. *Nucleic Acids Res* 30: 94–97
- Santos JH, Meyer JN, Skovvaga M, Annab LA, Van Houten B (2004) Mitochondrial hTERT exacerbates free-radical-mediated mtDNA damage. *Aging Cell* 3: 399–411
- Schallau A, Kakhovskaya I, Tewes A, Czihal A, Tiedemann J, Mohr M, Grosse I, Manteuffel R, Baumlein H (2008) Phylogenetic footprints in fern spore- and seed-specific gene promoters. *Plant J* 53: 414–424
- Seimiya H, Sawada H, Muramatsu Y, Shimizu M, Ohko K, Yamane K, Tsuruo T (2000) Involvement of 14-3-3 proteins in nuclear localization of telomerase. *EMBO J* 19: 2652–2661
- Sykorova E, Fajkus J (2009) Structure-function relationships in telomerase genes. *Biol Cell* 101: 375–392
- Sykorova E, Lim KY, Kunicka Z, Chase MW, Bennett MD, Fajkus J, Leitch AR (2003) Telomere variability in the monocotyledonous plant order Asparagales. *Proc R Soc Lond B Biol Sci* 270: 1893–1904
- Sykorova E, Leitch AR, Fajkus J (2006) Asparagales telomerases which synthesize the human type of telomeres. *Plant Mol Biol* 60: 633–646
- Tamura K, Liu H, Takahashi H (1999) Auxin induction of cell cycle regulated activity of tobacco telomerase. *J Biol Chem* 274: 20997–21002
- Tomlinson RL, Ziegler TD, Supakorndej T, Terns RM, Terns MP (2006) Cell cycle-regulated trafficking of human telomerase to telomeres. *Mol Biol Cell* 17: 955–965
- Voinnet O, Lederer C, Baulcombe DC (2000) A viral movement protein prevents spread of the gene silencing signal in *Nicotiana benthamiana*. *Cell* 103: 157–167
- Woo SH, An S, Lee HC, Jin HO, Seo SK, Yoo DH, Lee KH, Rhee CH, Choi EJ, Hong SI, Park IC (2009) A truncated form of p23 down-regulates telomerase activity via disruption of Hsp90 function. *J Biol Chem* 284: 30871–30880
- Yang SW, Jin E, Chung IK, Kim WT (2002) Cell cycle-dependent regulation of telomerase activity by auxin, abscisic acid and protein phosphorylation in tobacco BY-2 suspension culture cells. *Plant J* 29: 617–626
- Zhong FL, Batista LF, Freund A, Pech MF, Venteicher AS, Artandi SE (2012) TPP1 OB-fold domain controls telomere maintenance by recruiting telomerase to chromosome ends. *Cell* 150: 481–494

Supporting Information

Additional Supporting Information may be found in the online version of this article:

Table S1. Primer sequences.

Table S2. Description of T-DNA constructs and performed analyses.

Table S3. Prediction of subcellular localization in silico.

Fig. S1. Preparation of modified pBM-35 s vector and ligation of *AtTERT* constructs.

Fig. S2. Localization pattern of *AtTERT* genomic DNA in *Nicotiana benthamiana* leaves.

Fig. S3. *AtTERT* gene transcription and telomerase activity in separate parts of wt plants.

Fig. S4. Southern hybridization of genomic DNA from *tert* $-/-$ plants transformed by full-length *AtTERT* constructs.

Fig. S5. Motifs involved in subnuclear shuttling of hTERT.

Appendix S1. Supplementary methods and results.

Edited by E. Scarpella



Completion of cell division is associated with maximum telomerase activity in naturally synchronized cultures of the green alga *Desmodesmus quadricauda*



Tereza Ševčíková^{a,e}, Kateřina Bišová^b, Miloslava Fojtová^{a,c}, Alena Lukešová^d, Kristýna Hřčková^d, Eva Sýkorová^{a,c,*}

^aInstitute of Biophysics, Academy of Sciences of the Czech Republic, v.v.i., 612 65 Brno, Czech Republic

^bLaboratory of Cell Cycles of Algae, Institute of Microbiology, Academy of Sciences of the Czech Republic, v.v.i., 379 81 Třeboň, Czech Republic

^cFaculty of Science and CEITEC – Central European Institute of Technology, Masaryk University, Kamenice 5, 625 00 Brno, Czech Republic

^dInstitute of Soil Biology, Biology Centre Academy of Sciences of the Czech Republic, v.v.i., Na Sádkách 7, 370 05 České Budějovice, Czech Republic

^eLife Science Research Center, Department of Biology and Ecology, Faculty of Science, University of Ostrava, Chittussiho 10, 710 00 Ostrava, Czech Republic

ARTICLE INFO

Article history:

Received 20 December 2012

Revised 17 January 2013

Accepted 23 January 2013

Available online 8 February 2013

Edited by Varda Rotter

Keywords:

Desmodesmus quadricauda

Telomere repeat amplification protocol

Cell cycle

Telomerase

ABSTRACT

Telomerase maintains the ends of eukaryotic chromosomes, and its activity is an important parameter correlating with the proliferative capacity of cells. We have investigated cell cycle-specific changes in telomerase activity using cultures of *Desmodesmus quadricauda*, a model alga naturally synchronized by light/dark entrainment. A quantitative telomerase assay revealed high activity in algal cultures, with slight changes during the light period. Significantly increased telomerase activity was observed at the end of the dark phase, when cell division was complete. In contrast to other models, a natural separation between nuclear and cellular division typical for the cell cycle in *D. quadricauda* made this observation possible.

© 2013 Federation of European Biochemical Societies. Published by Elsevier B.V. All rights reserved.

1. Introduction

The ends of eukaryotic linear chromosomes are protected from degradation and fusion by telomeres. The maintenance of telomeres is effected in most eukaryotic organisms by telomerase, a special reverse transcriptase that elongates telomeres, solving the so-called end-replication problem (see [1] and references herein). In multicellular organisms, telomerase is predominantly active in regenerative and stem cell populations, but not in fully differentiated tissues [2,3] where telomeres are shortened after each round of DNA replication. Renewal of telomerase activity frequently

accompanies tumour progression. Telomerase activity and its regulation during the cell cycle has been investigated in several studies of vertebrate, yeast, slime mold and plant cells with different outcomes. Human and hamster cell lines showed a tight regulation of telomerase activity, with a peak in S phase [4,5]. These findings, however, were questioned and revised by Holt et al. [6] who did not find any cell-cycle related changes in telomerase activity in human cells sorted by flow cytometry [2], in contrast to those synchronized using biochemical inhibitors of the cell cycle [4–6]. Increased telomerase activity occurred in tobacco BY-2 cells in early S phase [7], but in late S phase for yeasts (see [1] for review) and slime mold [8].

Synchronization of cell cultures is mainly achieved by metabolic agents that block the cell cycle at a particular phase, disturbing the cell's physiology. Thus, using model systems or synchronization protocols that better reflect natural processes is preferred. Naturally synchronized cells of the slime mold *Physarum polycephalum* offer an uncomplicated cell cycle comprising only S, M and G2 phases [8]. A missing G1 phase and cellular division are advantageous for studies of DNA replication but this system hardly reflects all biological processes. Synchronization protocols of most green

Abbreviations: CDK, cyclin dependent kinase; CP, commitment point; Ct, cycle threshold; FACS, fluorescence-activated cell sorting; ND, nuclear division; PEG, polyethylene glycol; PD, protoplast division; pS, pre-S phase; qTRAP, quantitative telomere repeat amplification protocol; TRAP, telomere repeat amplification protocol

* Corresponding author at: Institute of Biophysics, Academy of Sciences of the Czech Republic, v.v.i., Královopolská 135, CZ-61265 Brno, Czech Republic. Fax: +420 541211293.

E-mail address: evin@ibp.cz (E. Sýkorová).

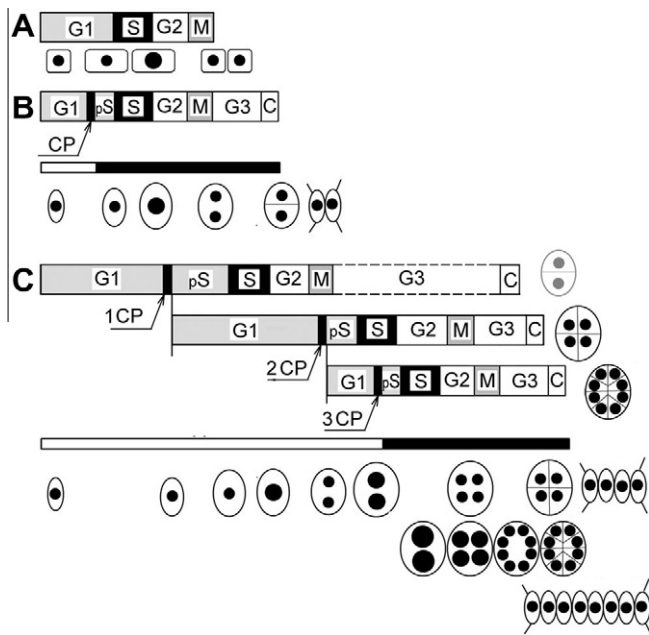


Fig. 1. Schematic comparison of classical and multiple fission cell cycle of *Desmodesmus quadricauda*. The classical model (A) describes G1 (growth phase), S (DNA replication), G2 and M phases (nuclear division closely followed by cellular division). The cell cycle of *D. quadricauda* (B, C) consists of G1, S, G2 and M phases as a classical cell cycle but nuclear (M) and cellular divisions (C) are separated by a G3 phase. Progression of a simple binary fission sequence of growth and reproductive events and light-dependency of key processes is illustrated in (B) with the light/dark period indicated by white/black bars under the scheme of the DNA-division sequence (B, C). The synchronized cell cycle is initiated by a light switch and during the G1 phase the cell grows until its threshold size is attained (marked CP). CP points to the stage in the cell cycle at which the cell becomes committed to triggering and terminating the sequence of processes leading to the duplication of reproductive structures (formally equivalent to start in yeast and the restriction point in mammalian cells). The processes before attainment of CP are light and growth dependent while the rest of the cell cycle after CP is light independent. After CP, the pre-replication phase (pS, syn. late G1 phase) starts and the processes required for the initiation of DNA replication are assumed to happen during this phase. The S phase and G2 phase are the same as in the classical model comprising DNA replication and activation of processes leading to the initiation of mitosis, respectively. The M phase, during which nuclear division occurs, is followed by the G3 phase which activates the processes leading to cellular division and finally, by the C phase during which, cell cleavage produces daughter cells. The multiple fission cell cycle of *D. quadricauda* shown in (C) illustrates overlapping sequences of these events that occur within a single cell (see also Appendix S1 for details). Depending on the length of illumination and light intensity, the cells can attain one, two or three CPs for final division into 2, 4 or 8 daughter cells. In experiments presented in this work, all cells completed the first M phase during the light period and the final cell population contained only 4- or 8-celled daughter coenobia (illustrated by dashed line of the first G3 phase and cell dividing to two daughter cells shown in grey). Modified after [13].

algae use a physiological alternation of light and dark periods as is present in nature and their telomeres are maintained by telomerase [9].

The *Arabidopsis*-type telomeric repeat forms telomeres of the green nonplastidic alga *Desmodesmus quadricauda* (Sphaeropleales, Chlorophyceae), an organism that has a long established history in cell cycle research [10,11]. In contrast to other model green algae, progression of the *D. quadricauda* cell cycle more closely resembles that of other eukaryotes (Fig. 1) and is regulated by the activities of CDK-like kinases and a histone H1 kinase [12,13]. *D. quadricauda* divides by multiple fission cell cycles (Fig. 1) into 2, 4, or 8 daughter cells [10,11]. The newly formed cells from a single mother stay connected together in coenobia. The multiple fission cell cycle consists of several overlapping sequences of G1, S, G2 and M phases followed by a *D. quadricauda*-specific G3 phase (separating nuclear and cellular divisions) and

cytokinesis. Thus in *D. quadricauda* cells, nuclear and cellular division are naturally separated. Synchronization of *D. quadricauda* cell cultures is achieved by the physiological process of alternating light/dark periods. During the light period, the cells grow and progress through the cell cycle. During the dark phase, all light-independent processes (DNA replication, nuclear and cellular divisions) are completed and cells enter the subsequent G1 phase (designated here as G1'). The dark period ensures that no cells can grow after finishing cell division and therefore serves as a major synchronizing factor. Properly synchronized cultures contain cell populations with 100% of the cells entering the cell cycle and undergoing mitosis within 2–3 h (time ratio of mitosis to cell cycle is 1:10). The three cell divisions are completed within 4 h (Fig. 1) [10,11,14]. This is in contrast to synchronization procedures of human or plant cells, during which a limited number of cells (40–60%) enter the cell cycle and the progression of such cells through a single mitosis (quantified by mitotic index) takes 3–5 h [15].

In the present work, we analyzed telomerase dynamics during the cell cycle of highly synchronized *D. quadricauda* cultures. Exceptionally high telomerase activity was detected in algal cultures, with small changes occurring during the light period of the cell cycle. A marked increase in telomerase activity was observed during the dark period of culture when cell division of coenobia was completed, suggesting a link between the regulation of telomerase activity and the cell cycle.

2. Materials and methods

2.1. Culture growth conditions and cell cycle synchronization

The chlorococcal alga *Desmodesmus quadricauda* (Turpin) Hegevald (syn. *Scenedesmus quadricauda* (Turp.) Bréb.), strain Greifswald/15 (CCALA 463) was obtained from the Culture Collection of Autotrophic Microorganisms maintained at the Institute of Botany ASCR, Třeboň, Czech Republic. The cultures were grown at 30 °C in the inorganic nutrient medium described by Ref. [16], aerated with air containing 2% (v/v) CO₂, and illuminated by OSRAM L36/41 fluorescent tubes; the light intensity at the surface of the culture vessels was 490 μmol m⁻² s⁻¹. During the synchronization procedure (at least three consecutive cycles of alternating 15/9 h of light/dark) preceding the experiment, the cell concentration was maintained at ~1 × 10⁶ cells ml⁻¹ during the light phase in order to retain cellular synchrony. To initiate the experiment, the culture was initially diluted to ~2 × 10⁶ cells ml⁻¹ to maximize the amount of material available for biochemical analyses. During the experiments, the synchronized cultures were either grown under the same conventional conditions, or were exposed to different light/dark cycles (for details see Section 3).

2.2. Assessment of cell cycle progression

2.2.1. Commitment point curves

Samples were taken hourly or bi-hourly from a synchronous culture during the light period and incubated under aeration at 30 °C in the dark. At the end of the cell cycle, the proportions of binuclear daughter cells, 4- and 8-celled daughter coenobia, and undivided mother cells were assessed and plotted against the time of transfer to darkness [10,17].

2.2.2. Nuclear divisions

Nuclei were stained by SYBR Green I dye (Molecular Probes) and the percentages of mono-, bi-, tetra- and octonuclear cells were estimated using fluorescence microscopy technique developed by Vítová et al. [18].

2.2.3. Cell division curves

Hourly taken Samples were fixed in 0.25% glutaraldehyde. The percentage of undivided mother cells, mother cells divided into two, four, or eight protoplasts, and daughter coenobia were determined.

2.3. Determination of total DNA, RNA, and protein levels

Total nucleic acids and proteins from control samples were extracted and measured as described by Zachleder et al. [19].

2.4. Preparation of telomerase extracts

Telomerase activity was determined using a protocol developed for plant telomerases [3,20] and modified for use with algae [9,21]. Briefly, 20 ml of culture was centrifuged at 5000×g for 5 min, and cell pellets were disrupted by vortexing with zirconic beads (1 mm diameter) in extraction buffer [3]. After centrifugation at 100000×g for 15 min, the telomerase-containing fraction was enriched from 500 µl of supernatant solution (crude protein extract) by precipitation with PEG 8000 (10% final concentration) and the pellet was dissolved in 30 µl of extraction buffer. Alternatively, samples of crude protein extracts (without PEG precipitation) were used in a TRAP assay. The amount of total protein in extracts was determined using the Bradford method [22] or by the Bicinchoninic Acid Kit for Protein Determination (Sigma Aldrich).

2.5. TRAP assay

The telomere repeat amplification protocol (TRAP) assay was performed using protein extracts containing 50 ng of total protein and combination of a substrate primer TS21 and reverse primer (TELPR30-3A) according protocol described in [9]. Products were analyzed by polyacrylamide gel electrophoresis (PAGE), stained by GelStar(R) Nucleic Acid Gel Stain (LONZA) and visualized on a LAS3000 (FujiFilm). The quantitative version of the TRAP assay was performed as described by Herbert et al. [23] using FastStart SYBR Green Master (Roche) using the same primers. Samples were analyzed in triplicate in a 20 µl reaction mix. Ct values were determined using RotorGene6000 (Qiagen) software and relative telomerase activity was calculated by the Δ Ct method [24].

3. Results

3.1. Optimization of the telomerase purification procedure and qTRAP analysis

D. quadricauda possesses an *Arabidopsis*-type telomere and protocols for telomerase activity, detection and quantification could be adapted from existing plant telomerase protocols. Telomerase extracts were prepared from algal samples, roughly corresponding to G1, S, M, M/D and G1' phases (Figs. S1 and S2). We tested telomerase activity in a pilot experiment by a standard in vitro TRAP assay using the same input protein level. In the first step of this assay, telomerase adds telomeric repeats to non-telomeric substrates (substrate primer). An extension product is then PCR-amplified in the second step using the same non-telomeric substrate primer and a telomeric oligonucleotide as a reverse primer. Telomerase activity was demonstrated in all samples investigated (Figs. S1 and S2). To determine the conditions for the quantitative analysis of telomerase activity (qTRAP) in *D. quadricauda* samples, we optimized the preparation of protein samples (material disruption, protein extraction, centrifugation, see Section 2) and performed control qTRAP experiments (see Supplementary material). Finally, the PEG-precipitation protocol was found suitable for preparation

of telomerase extracts, including efficient removal of inhibitors (Figs. S1 and S2, Supplementary material).

3.2. Telomerase activity during the multiple fission cell cycle of *D. quadricauda*

Pilot experiments (see above) were performed using samples roughly corresponding to different phases of the cell cycle and showed a slight increase in telomerase activity during the S phase (Fig. S1B). A partially different outcome was observed in parallel experiments (Figs. S1, S2) suggesting a necessity to investigate changes in telomerase activity in more detail, and also because each biological replica had its own growth characteristic. Another pilot experiment was performed under standard conditions (15/9 h of light/dark) and with hourly collected samples from two biological replicates, two sub-replicates of the latter also served as a technical replicate (Fig. 2). Very high synchrony was well documented by progression through cell division; the cells underwent two or three rounds of cell division within 3 h (Figs. 2 and S2). However in several PEG-purified telomerase extracts from the hourly collected replicates, the protein concentration required for establishing a qTRAP assay was not determined (the protein level was below our detection limit), and thus were omitted from the qTRAP analyses. These excluded samples were collected at the beginning of the cycle and after the 8th hour, when algal cultures were diluted to maintain optimal growth conditions. For qTRAP analysis of other hourly collected samples, results were normalized to the 7th hour of the cell cycle (before dilution of the culture) and the relative telomerase activity (increase/decrease) was determined (Fig. 2A). Generally, absolute telomerase activity in *D. quadricauda* samples was very high (see Section 4) and small changes observed during the light period were not significant. However, telomerase activity was notably increased during the dark period after cell division of coenobia was complete (Figs. 2A and S2C). Changes in telomerase activity were different in the biological replicas (Figs. 2, S1 and S2) in last 2 h of the experiment, showing either a constant level or a mild decrease, thus provoking the question of how telomerase activity is equalized at the beginning of a new cell cycle.

3.3. Increased telomerase activity during the dark phase corresponds to completion of cell division

We conducted a modified experiment (i) to verify the telomerase activity pattern during the dark period; and (ii) to determine whether lower telomerase activity at the beginning of the cell cycle might be a light-generated or dilution-generated stress response. The experimental design was modified as follows – (1) the cultures were followed during a prolonged dark period after cell division was completed and during the early hours of the light period of a new cell cycle, (2) dilution in the 8th hour was omitted and (3) the initial concentration of cells was 4×10^6 cells ml⁻¹. Two experiments were conducted differing only in the timing of the onset of the light period (Fig. 3A) allowing identification of any light-dependent and/or synchronization regime-dependent changes in telomerase activity. Samples from the two experiments (with two technical replicas each) were collected at distinct time points as described in Fig. 3. Progression through the cell division within the population was calculated for both biological replicas as the division index that sums the numbers of cells divided into 2, 4, and 8 daughter cells respectively. It confirmed the highly synchronous cell cycle progression because 100% of the cells underwent two or three nuclear divisions within 4 h (Fig. 3A, see also above). Telomerase activity in samples from hours 0, 4, and 14 (the end of light period) of the first cell cycle confirmed telomerase activity levels similar to those of the previous standard experiment

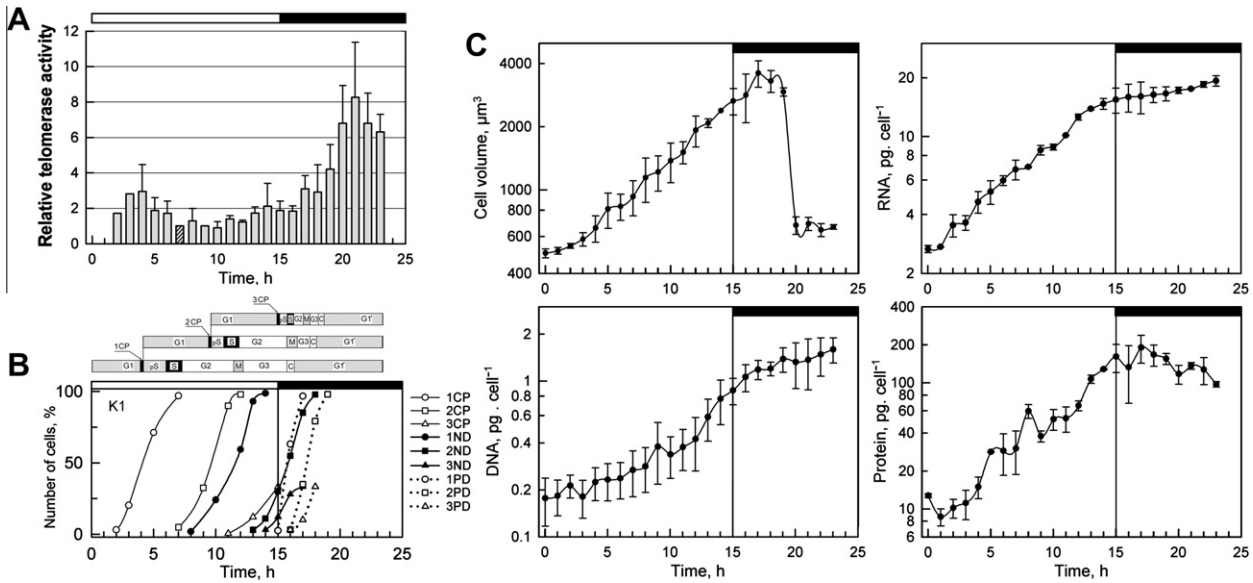


Fig. 2. Telomerase activity analysed by qTRAP in synchronized algal cultures during cell cycle progression. Increased relative telomerase activity (A) in the dark period during and after cellular division was observed. The quantitative analysis was related to the 7 h sample (hatched box) which was analysed in all replicas and was collected before culture dilution. Several samples were omitted from qTRAP due to their low protein concentration (see Section 3) and data from individual replicas are shown at 2, 3 and 9 h. Progress of the cell cycle in a population of a representative replica (B) is documented by cellular characteristics of commitment points (CP), nuclear division (ND) and protoplast division (PD) with a schema of multiple fission cell cycle progression within a single cell related to completion of individual processes in 50% of the population above the curves. The molecular changes (C) are reflected by curves showing accumulation of RNA, DNA and protein (calculated in pg per mother cell), the mean cell volume curve clearly shows that most of the cells divided at hour 20. The bars above graphs mark light conditions.

(Fig. 2A). During a prolonged dark period, we again observed an increase in telomerase activity in the hours following completion of cell division (Fig. 3A). Control measurements of DNA (Fig. 3C) confirmed that this increase in telomerase activity was not connected to DNA replication. No further nuclear division or growth was observed (Figs. 3C and S3). Telomerase activity remained elevated during the entire dark period and persisted into the light period; it gradually decreased during the early light period but the decrease was not directly linked to the light switch. When compared to the results of the standard experiments (Fig. 2A), there was a good agreement in the general pattern of telomerase activity. High telomerase activity accompanied the completion of cell division and the activity gradually decreased but stayed elevated until the attainment of the first CP. Thereafter, it declined until the next cell division.

4. Discussion

Telomerase regulation during the cell cycle is of longstanding interest in telomere biology. Telomerase needs to be active in maintaining telomere length either prior to or early in S phase. Surprisingly, we observed increased telomerase activity concomitant with and after completion of cellular division (Figs. 2 and 3). In contrast to other model systems used for studying cell-cycle dependent telomerase regulation, the *D. quadricauda* cell cycle naturally separates nuclear and cellular division so our results indicate a new connection between telomerase regulation and cell cycle control. Detailed studies of telomerase action on yeast telomeric ends showed that high telomerase activity in vitro does not necessarily lead to telomere repeat synthesis in vivo (see [1] and references herein). As no telomere-specific cellular process is assigned for cellular division or the subsequent G1 phase of the cell cycle (designated here as G1'), the increase in telomerase activity may be connected to non-telomeric functions as was presumed for a human telomerase role in signalling pathways, transcription or in mitochondria (see [25] for review). Concomitant with cell division in green algae are chloroplast and mitochondrial divisions [26,27]

which are not fully described yet and might be alternative targets for telomerase non-telomeric functions. The phase-specific metabolic processes connected to cell cycle progression in the G1 phase during the dark period or the light period should be technically identical, except for photosynthesis; however, no systematic studies of this cell cycle phase have been published. Thus, a connection between the regulation of telomerase activity and the start of a new cell cycle is of interest. Assembly of the telomerase complex is not sufficient to initiate the synthesis of telomeres until other critical factors are supplied, such as cyclin/cdk activity [28] and accessibility of telomeric ends (see [1] and references herein). A complete transit across the G1 phase is governed by the presence of extracellular growth factors and biochemical processes that allow the cell to bypass the restriction point. These include hyperphosphorylation of Rb protein, the functional activation of E2F-1, loss of several cyclin-dependent kinase inhibitors and subsequent accumulation of a threshold level of cyclin/CDK activity [29], the homologs of which are present in green algae [30–33]. Telomerase interacts with the Rb pathway (see [34] for review); its overexpression caused increased cyclin D1 expression and consequently hyperphosphorylation of Rb [35]. It is conceivable that these molecules are also one of the targets of telomerase during the G1 phase. The interaction between telomerase and the Rb pathway seems to work both ways as functional Rb down-regulates telomerase activity [29]. Therefore the two activities could be counteracting each other until some cell cycle event (attainment of restriction point) favours one of them.

Analysis of *D. quadricauda* telomerase activity by qTRAP revealed high telomerase activity throughout the multiple fission cell cycle. Although no direct comparison of telomerase activity in cells of different models (algae, plants) has been made, there were striking differences between Ct values obtained in our analyses with *D. quadricauda* (Ct values in the range of 9–10) extracts diluted to a protein concentration of 50 ng/ml compared with other models. For comparison, analysis of telomerase activity of *Arabidopsis thaliana* telomerase positive tissues (buds, 7-day old seedlings), showed Ct values in the range of 18–20 and ~15 in *A. thaliana* cell

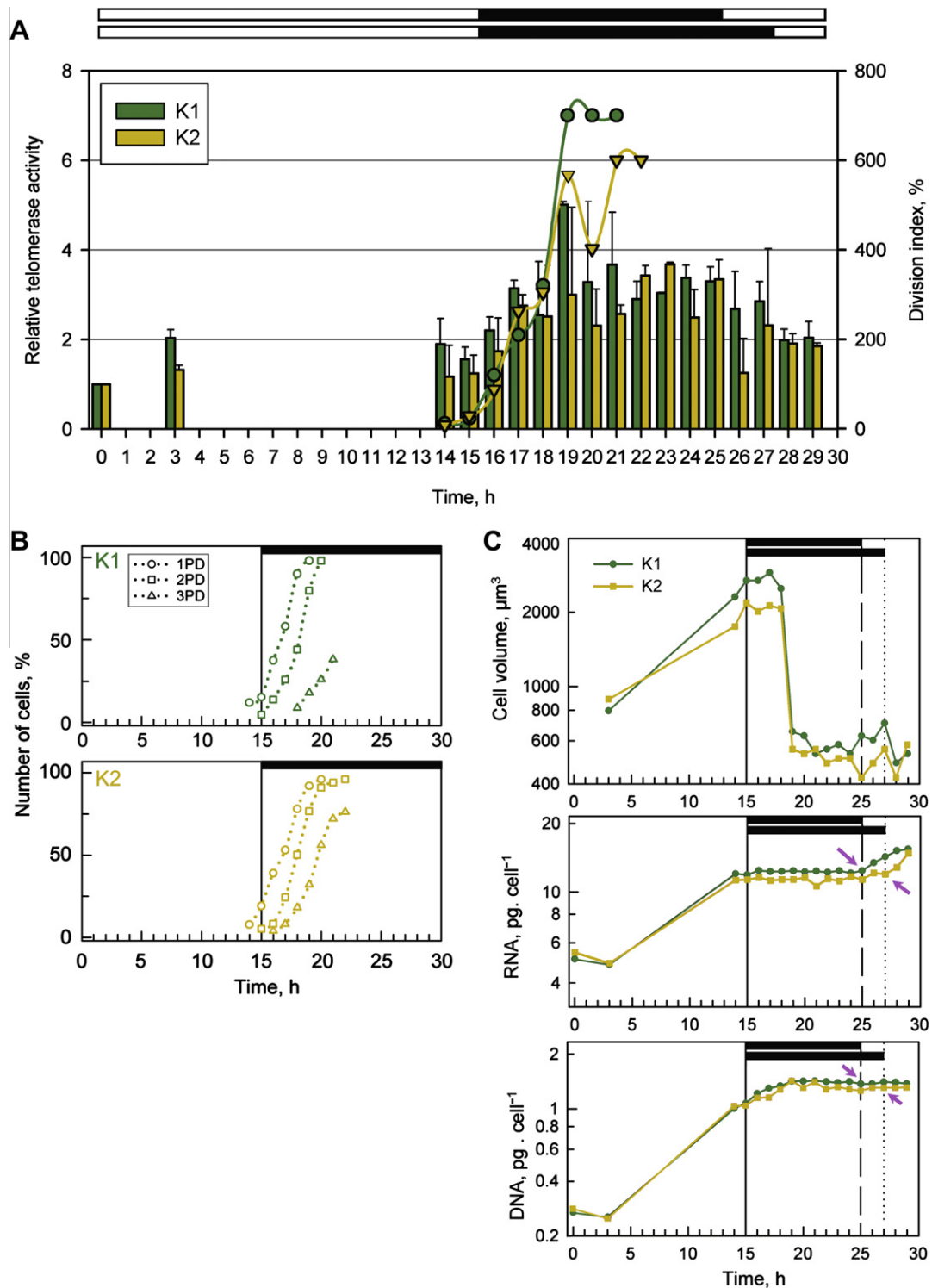


Fig. 3. Telomerase activity during experiments with prolonged dark periods. Relative telomerase activity (A, related to the 0 h samples) in two biological replicas (K1, K2) with different light conditions (marked by bars above graphs) was elevated during and after cellular division, depicted as division index curves (also compare with protoplast division curves in B) and slightly decreased during a prolonged dark period. Other cell cycle processes (attainment of CP and ND) are not depicted in the graph since the culture was not sampled during the time at which they usually occur. Progression of the last ND was masked by concurrently undergoing PD. However, the timing and progression through PD suggests that other cell cycle processes run similarly to the previous experiments. A light switch at hour 25 (replica K1) and hour 27 (replica K2) did not significantly influence telomerase activity. (C) Cell growth arrest in the dark and progression through cellular division in the population is illustrated by changes in the mean cell volume; the DNA level in both replicas was not changed after the light switch (grey arrows) but the RNA level was elevated in response to light (both calculated in pg per mother cell).

cultures, which are the most telomerase-active *Arabidopsis* systems. Telomerase activity in crude extracts of cultured dinoflagellates was reflected in a Ct value of 25 (Fojtová, M., unpublished

results). Ct is the number of PCR cycles in quantitative assay, when the fluorescence of SYBR Green I dye increases above a threshold; in fact Ct reflects the amount of template in the reaction mixture,

i.e. lower Ct indicates higher template concentration. Thus difference in Ct values by 1, 2, 3 reflects 2, 4, 8 times higher/lower relative telomerase activity. In this respect, the extremely high telomerase activity in PEG-precipitated extracts from *D. quadricauda* suggests that this is a good model system for further studies, where changes in telomerase activity (e.g. following various treatments, changed living conditions etc.) can be precisely determined.

Acknowledgements

We would like to thank Mrs. Jedličková, Mrs. Šipková and Mrs. Jana Kapustová for excellent technical help. This work was supported by the GACR [521/09/1912], by the project “CEITEC—Central European Institute of Technology” [CZ.1.05/1.1.00/02.0068], by grant from the Ministry of Education, Youth and Sports of the Czech Republic [LH12145 to K.B.] and by institutional funding [AVOZ50040702].

Appendix A. Supplementary data

Supplementary data associated with this article can be found, in the online version, at <http://dx.doi.org/10.1016/j.febslet.2013.01.058>.

References

- Wellinger, R.J. and Zakian, V.A. (2012) Everything you ever wanted to know about *Saccharomyces cerevisiae* telomeres: beginning to end. *Genetics* 191, 1073–1105.
- Holt, S.E., Wright, W.E. and Shay, J.W. (1996) Regulation of telomerase activity in immortal cell lines. *Mol. Cell. Biol.* 16, 2932–2939.
- Fitzgerald, M.S., McKnight, T.D. and Shippen, D.E. (1996) Characterization and developmental patterns of telomerase expression in plants. *Proc. Natl. Acad. Sci. USA* 93, 14422–14427.
- Zhu, X., Kumar, R., Mandal, M., et al. (1996) Cell cycle-dependent modulation of telomerase activity in tumor cells. *Proc. Natl. Acad. Sci. USA* 93, 6091–6095.
- Kruk, P.A., Orren, D.K. and Bohr, V.A. (1997) Telomerase activity is elevated in early S phase in hamster cells. *Biochem. Biophys. Res. Commun.* 233, 717–722.
- Holt, S.E., Aisner, D.L., Shay, J.W., et al. (1997) Lack of cell cycle regulation of telomerase activity in human cells. *Proc. Natl. Acad. Sci. USA* 94, 10687–10692.
- Tamura, K., Liu, H. and Takahashi, H. (1999) Auxin induction of cell cycle regulated activity of tobacco telomerase. *J. Biol. Chem.* 274, 20997–21002.
- Shimada, Y., Nakano, M., Kanda, N., et al. (1997) Cell cycle-dependent activation of telomerase in naturally synchronized culture of a true slime mold, *Physarum polycephalum*. *Biochem. Biophys. Res. Commun.* 232, 492–496.
- Fulnečková, J., Hasíková, T., Fajkus, J., et al. (2012) Dynamic evolution of telomeric sequences in the green algal order Chlamydomonadales. *Genome Biol. Evol.* 4, 248–264.
- Šetlík, I. and Zachleder, V. (1984) The multiple fission cell reproductive patterns in algae in: *The Microbial Cell Cycle* (Nurse, P. and Streiblová, E., Eds.), pp. 253–279, CRC Press Inc., Boca Raton, FL.
- Zachleder, V. and Šetlík, I. (1988) Distinct controls of DNA-replication and of nuclear division in the cell-cycles of the chlorococcal alga *Scenedesmus quadricauda*. *J. Cell Sci.* 91, 531–539.
- Bišová, K., Vítová, M. and Zachleder, V. (2000) The activity of total histone H1 kinases is related to growth and commitment points while the p13(suc1)-bound kinase activity relates to mitoses in the alga *Scenedesmus quadricauda*. *Plant Physiol. Biochem.* 38, 755–764.
- Hlavová, M., Čížková, M., Vítová, M., et al. (2011) DNA damage during G2 phase does not affect cell cycle progression of the green alga *Scenedesmus quadricauda*. *PLoS ONE* 6, e19626.
- Komárek, J., Růžička, J. and Simmer, J. (1968) Synchronization of the cultures of *Scenedesmus* by optimizing the length of the light period. *Biol. Plantarum* 10, 177–189.
- Kumagai-Sano, F., Hayashi, T., Sano, T., et al. (2007) Cell cycle synchronization of tobacco BY-2 cells. *Nat. Protoc.* 1, 2621–2627.
- Zachleder, V. and Šetlík, I. (1982) Effect of irradiance on the course of RNA-synthesis in the cell-cycle of *Scenedesmus quadricauda*. *Biol. Plantarum* 24, 341–353.
- Zachleder, V., Schläfli, O. and Boschetti, A. (1997) Growth-controlled oscillation in activity of histone H1 kinase during the cell cycle of *Chlamydomonas reinhardtii* (Chlorophyta). *J. Phycol.* 33, 673–681.
- Vítová, M., Hendrychová, J., Čížková, M., et al. (2008) Accumulation, activity and localization of cell cycle regulatory proteins and the chloroplast division protein FtsZ in the alga *Scenedesmus quadricauda* under inhibition of nuclear DNA replication. *Plant Cell Physiol.* 49, 1805–1817.
- Zachleder, V., Bišová, K., Vítová, M., et al. (2002) Variety of cell cycle patterns in the alga *Scenedesmus quadricauda* (Chlorophyta) as revealed by application of illumination regimes and inhibitors. *Eur. J. Phycol.* 37, 361–371.
- Sýkorová, E., Lim, K.Y., Kunická, Z., et al. (2003) Telomere variability in the monocotyledonous plant order Asparagales. *Proc. R. Soc. Lond. B, Biol. Sci.* 270, 1893–1904.
- Fojtová, M., Wong, J.T., Dvořáčková, M., et al. (2010) Telomere maintenance in liquid crystalline chromosomes of dinoflagellates. *Chromosoma* 119, 485–493.
- Bradford, M.M. (1976) A rapid and sensitive method for the quantitation of microgram quantities of protein utilizing the principle of protein-dye binding. *Anal. Biochem.* 72, 248–254.
- Herbert, B.S., Hochreiter, A.E., Wright, W.E., et al. (2006) Nonradioactive detection of telomerase activity using the telomeric repeat amplification protocol. *Nat. Protoc.* 1, 1583–1590.
- Pfaffl, M.W. (2004) Quantification strategies in real-time PCR in: *A-Z of Quantitative PCR* (Bustin, S.A., Ed.), pp. 87–112, International University Line, La Jolla, CA, USA.
- Majerská, J., Sýkorová, E. and Fajkus, J. (2011) Non-telomeric activities of telomerase. *Mol. Biosyst.* 7, 1013–1023.
- Goodenough, U.W. (1970) Chloroplast division and pyrenoid formation in *Chlamydomonas reinhardtii*. *J. Phycol.* 6, 1–6.
- Zachleder, V., Kawano, S. and Kuroiwa, T. (1996) Uncoupling of chloroplast reproductive events from cell cycle division processes by 5-fluorodeoxyuridine in the alga *Scenedesmus quadricauda*. *Protoplasma* 192, 228–234.
- Collins, K. (2008) Physiological assembly and activity of human telomerase complexes. *Mech. Ageing Dev.* 129, 91–98.
- Crowe, D.L. and Nguyen, D.C. (2001) Rb and E2F-1 regulate telomerase activity in human cancer cells. *Biochim. Biophys. Acta* 1518, 1–6.
- Robbins, S., Khadaroo, B., Camasses, A., et al. (2005) Genome-wide analysis of core cell cycle genes in the unicellular green alga *Ostreococcus tauri*. *Mol. Biol. Evol.* 22, 589–597.
- Merchant, S.S., Prochnik, S.E., Vallon, O., et al. (2007) The *Chlamydomonas* genome reveals the evolution of key animal and plant functions. *Science* 318, 245–250.
- Umen, J.G. and Goodenough, U.W. (2001) Control of cell division by a retinoblastoma protein homolog in *Chlamydomonas*. *Genes Dev.* 15, 1652–1661.
- Olson, B.J., Oberholzer, M., Li, Y., et al. (2010) Regulation of the *Chlamydomonas* cell cycle by a stable, chromatin-associated retinoblastoma tumor suppressor complex. *Plant Cell* 22, 3331–3347.
- Alonso, M.M., Fueyo, J., Yung, W.K., et al. (2006) E2F1 and telomerase: alliance in the dark side. *Cell Cycle* 5, 930–935.
- Yang, J., Song, K., Krebs, T.L., et al. (2008) Rb/E2F4 and Smad2/3 link survivin to TGF-beta-induced apoptosis and tumor progression. *Oncogene* 27, 5326–5338.



Chromatin features of plant telomeric sequences at terminal vs. internal positions

Eva Majerová¹, Terezie Mandáková¹, Giang T. H. Vu^{2†}, Jiří Fajkus^{1,3}, Martin A. Lysak¹ and Miloslava Fojtová^{1*}

¹ Mendel Centre for Plant Genomics and Proteomics, Central European Institute of Technology and Faculty of Science, Masaryk University, Brno, Czech Republic

² Max Planck Institute for Plant Breeding Research, Cologne, Germany

³ Institute of Biophysics, Academy of Sciences of the Czech Republic v.v.i., Brno, Czech Republic

Edited by:

Scott Jackson, University of Georgia, USA

Reviewed by:

Kyung Do Kim, University of Georgia, USA

Chad Niederhuth, University of Georgia, USA

*Correspondence:

Miloslava Fojtová, Central European Institute of Technology and Faculty of Science, Masaryk University, Kamenice 5, 625 00 Brno, Czech Republic
e-mail: fojtova@sci.muni.cz

† Present address:

Giang T. H. Vu, Leibniz Institute of Plant Genetics and Crop Plant Research, Gatersleben, Stadt Seeland, Germany

Epigenetic mechanisms are involved in regulation of crucial cellular processes in eukaryotic organisms. Data on the epigenetic features of plant telomeres and their epigenetic regulation were published mostly for *Arabidopsis thaliana*, in which the presence of interstitial telomeric repeats (ITRs) may interfere with genuine telomeres in most analyses. Here, we studied the epigenetic landscape and transcription of telomeres and ITRs in *Nicotiana tabacum* with long telomeres and no detectable ITRs, and in *Ballantinia antipoda* with large blocks of pericentromeric ITRs and relatively short telomeres. Chromatin of genuine telomeres displayed heterochromatic as well as euchromatic marks, while ITRs were just heterochromatic. Methylated cytosines were present at telomeres and ITRs, but showed a bias with more methylation toward distal telomere positions and different blocks of *B. antipoda* ITRs methylated to different levels. Telomeric transcripts TERRA (G-rich) and ARRET (C-rich) were identified in both plants and their levels varied among tissues with a maximum in blossoms. Plants with substantially different proportions of internally and terminally located telomeric repeats are instrumental in clarifying the chromatin status of telomeric repeats at distinct chromosome locations.

Keywords: telomere, chromatin, epigenetics, *Nicotiana tabacum*, *Ballantinia antipoda*, histone modifications, DNA methylation

INTRODUCTION

Epigenetic mechanisms are involved in the regulation of crucial cellular processes such as gene expression, replication timing, and cell cycle control. Epigenetic regulation is mediated by changes in chromatin structure induced by chromatin remodeling complexes, DNA methylation, posttranslational modifications of histones, or *via* non-coding RNA molecules. As shown previously, telomeres, complex nucleoprotein structures located at the ends of linear eukaryotic chromosomes, are subjects of epigenetic control and their maintenance is influenced by changes in telomeric and subtelomeric chromatin (reviewed in Galati et al., 2013; Fojtova and Fajkus, 2014). In human cells, proper telomere function is crucial for healthy development. Pathological shortening of telomeres leads to genomic instability and serious malfunctions or premature death, such as in dyskeratosis congenita, aplastic anemia, or immunodeficiency centromere instability and facial anomalies (ICF) syndrome. Reactivation of telomere maintenance in terminally differentiated cells is one of the basic premises for cellular immortalization and cancerogenesis.

In epigenetic analyses of telomeric chromatin, it is important to distinguish between terminal and interstitial telomeric repeats (ITRs), i.e., telomeric repeats without a chromosome capping function, since their chromatin states may differ. In *A. thaliana*, 8 regions of ITRs were described on three chromosomes, ranging from 300 bp to 1.2 kb (Uchida et al., 2002). Large blocks of

telomeric repeats were recently found in pericentromeric regions of some chromosomes in representatives of the Solanaceae family (He et al., 2012). Interestingly, the most recent findings revealed large blocks of imperfect telomeric repeats in the proximity of centromeres of all *Ballantinia antipoda* (Brassicaceae) chromosomes (Mandaková et al., 2010). In *Nicotiana tabacum*, no detectable ITR regions were observed (Majerova et al., 2011a) while telomere lengths ranged from 20 to 160 kb (Fajkus et al., 1995a; Kovarik et al., 1996).

Methods used for analyses of telomeric chromatin usually cannot distinguish between ITRs and telomeres. Cytosines in CCCTAAA telomeric repeats have been reported to be partially methylated in *A. thaliana*, suggesting their heterochromatic nature (Cokus et al., 2008). In contrast, telomeric chromatin of *A. thaliana* seems relatively “open,” displaying euchromatic histone modifications such as H3K4me3 (Vrbsky et al., 2010). Nevertheless, the epigenetic state of telomeric chromatin in *A. thaliana* is far from being elucidated because, in contrast to results demonstrating the existence of intermediate heterochromatin at telomeres (Vrbsky et al., 2010), the heterochromatic character of ITRs (including cytosine methylation) and the euchromatic nature of genuine telomeres were also reported (Vaquero-Sedas et al., 2011). Our recent findings show that in tobacco cell cultures, disruption of DNA and histone methylation *via* drug treatment does not influence telomere length

(Majerová et al., 2011b), while hypomethylation of the *A. thaliana* genome either by genetic manipulation or by drugs leads to significantly shortened telomeres (Ogrocka et al., 2014). Methylation of telomeric DNA thus apparently represents an additional layer of epigenetic regulation of plant telomere maintenance that is absent in yeast and animal models (reviewed in Fojtova and Fajkus, 2014).

To address open questions regarding the nature of plant telomeric chromatin, we have expanded the research to plant models that differ markedly in their telomere/ITR ratios. Here, we compare the epigenetic state and transcription of telomeric repeats of *N. tabacum* with no detectable ITRs and extra-long telomeres, and of *B. antipoda* with a major fraction of telomeric repeats present as ITRs, forming large centromeric blocks, and short terminal blocks of telomeres. These plants with substantially different fractions of internally and terminally located telomeric repeats facilitate studies on the epigenetic status of plant chromatin with telomeric repeats at terminal or interstitial position.

MATERIALS AND METHODS

PLANT GROWTH

N. tabacum and *N. tomentosiformis* seeds were surface sterilized with 90% bleach SAVO (Biochemie group, a.s., active substance: NaClO), and germinated on plates with Murashige–Skoog (MS) medium (Duchefa Biochemicals) supplemented with 1% sucrose and 0.8% plant agar. After 10 days, seedlings were potted into soil and grown under short day conditions (light, 150 mmolm⁻²s⁻¹ for 8 h at 21°C; darkness for 16 h at 19°C) for 1 month. Plants were then planted into a greenhouse until they produced seeds. Plants of *B. antipoda* were grown from seeds that originated from Mount Alexander Regional Park, Victoria, Australia (herbarium sheet no. MEL 2280901). *B. antipoda* seeds were surface sterilized with 0.5% NaOCl and germinated on plates with MS medium in 0.8% plant agar. Then seedlings were put into soil and cultivated in a growth chamber under long day conditions (16 h light, 8 h dark).

FLUORESCENCE *IN SITU* HYBRIDIZATION (FISH) OF A TELOMERIC PROBE

Actively growing, young roots of *N. tabacum* were pretreated with ice-cold water for 12 h and fixed in ethanol:acetic acid (3:1) at 4°C for 24 h. Entire inflorescences of *B. antipoda* were fixed in ethanol:acetic acid (3:1) at 4°C overnight and stored in 70% ethanol at -20°C until use. Preparation of mitotic and stretched pachytene chromosomes from *N. tabacum* root tips and *B. antipoda* anthers was as described (Mandaková et al., 2010). A telomeric FISH probe was prepared (Ijdo et al., 1991), labeled with biotin-dUTP by nick translation and ethanol precipitated (Mandaková et al., 2010). Probes and chromosomes were denatured together on a hot plate at 80°C for 2 min and incubated in a moist chamber at 37°C overnight. The hybridized probe was detected by avidin–Texas Red (Vector Laboratories) and amplified by goat anti-avidin–biotin (Vector Laboratories) and avidin–Texas Red (Mandaková et al., 2010, 2013). Chromosomes were counterstained with 4',6-diamidino-2-phenylindole (2 µg/ml) in Vectashield (Vector Laboratories). Fluorescence signals were

analyzed and photographed using an Olympus BX-61 epifluorescence microscope and a CoolCube camera (MetaSystems), and pseudocolored/inverted/merged using Adobe Photoshop CS2 software (Adobe Systems).

ANALYSIS OF TERMINAL POSITION OF TELOMERIC REPEATS AND TELOMERE LENGTHS

The length of telomeres was analyzed by the terminal restriction fragment (TRF) method, which is based on digestion of genomic DNA by frequently cutting restriction enzyme(s) having no recognition site within the telomeric repeats. Plant tissues were embedded in agarose blocks and high molecular weight DNA was purified as described (Fojtova et al., 2002). Samples were digested by Bal31 nuclease (NEB) to degrade terminal telomeric sequences and then by a mix of restriction enzymes *Nla*IV, *Hae*III, *Hinf*I (all purchased from NEB) to delimit telomeric regions (Fajkus et al., 1998). High molecular weight DNA in agarose blocks was analyzed by pulse field gel electrophoresis and subsequent Southern hybridization with a radioactively labeled pTel-C probe, see below. For *B. antipoda* samples, low molecular weight DNA in solution was ethanol-precipitated and analyzed by conventional agarose electrophoresis followed by Southern hybridization.

RELATIVE METHYLATION OF TELOMERS IN NICOTIANA SPECIES

Protoplasts of young leaves of *N. tabacum* and *N. tomentosiformis* were isolated (Yoo et al., 2007). Cells were exposed to a mixture of 0.125 g Cellulase R10 (Serva); 0.025 g Macerozyme R10 (Serva) and 0.025 g Pectolyase Y-23 (Duchefa Biochemicals) in 10 ml digestion buffer (0.4 M mannitol, 20 mM KCl, 20 mM MES pH 5.7, 10 mM CaCl₂, 0.1% BSA) for 4 h. Fresh protoplasts were embedded into agarose blocks and processed as described (Fojtova et al., 2002). DNA in agarose blocks was digested with Bal31 nuclease (1U per block) for 15, 45, and 90 min in a total volume of 300 µl. One third of the sample was used for the TRF analysis to check the extent of telomere shortening by Bal31 cleavage. DNA from the rest of the agarose block was isolated using a QIAEX II Gel Extraction Kit (Qiagen). Four hundred ng of DNA was treated with sodium bisulfite (EpiTect Bisulfite Kit, Qiagen) to convert non-methylated cytosine into uracil (Clark et al., 1994) and transferred onto a Hybond XL nylon membrane (GE Healthcare) by vacuum dot blotting (Bio-Rad Dot Blot). As positive hybridization control untreated tobacco DNA, and as negative control pUC19 plasmid DNA were loaded onto the membrane. Membranes were hybridized with radioactively labeled oligonucleotide probes as follows: (i) overnight at 55°C in 0.25 M Na-phosphate pH 7.5, 7% SDS (w/v), 0.016 M EDTA for the probe pTel-C (CCCTAAA)₄ that was used as the loading normalizer; (ii) overnight at 42°C in ULTRAhyb™–Oligo Hybridization Buffer (Ambion) for the probe DEGENER (TTAGRRT)₄, R = G or A, to detect the methylated or partially methylated fraction of telomeric repeats (for details see Majerová et al., 2011b). The membrane was washed 3 times in 2 × SSC and 0.1% (w/v) SDS. Hybridization signals were visualized on a FLA-7000 phosphorimager (FujiFilm) and the signal intensity was evaluated by MultiGauge Analysis Software (FujiFilm). To express the relative methylation of cytosines located in the proximal telomere region vs. the whole length

telomere, the ratio of DEGENER/loading hybridization signals in Bal31-digested samples was normalized to that of intact telomeres ($(\text{Bal31}^{\text{DEGENER}}/\text{Bal31}^{\text{ptelC}})/(\text{intact}^{\text{DEGENER}}/\text{intact}^{\text{ptelC}})$).

ANALYSIS OF CYTOSINE METHYLATION IN *B. ANTIPODA* ITRs BY BISULFITE SEQUENCING

Two repetitive sequences, Ba493 and Ba576, found in intra-chromosomal regions of *B. antipoda* and containing perfect and degenerated telomeric repeats, were chosen for analysis of the level of methylated cytosines in ITRs. Identification of these sequences was based on *B. antipoda* preliminary whole genome sequencing data (A. Pecinka laboratory, Max Planck Institute for Plant Breeding Research, Cologne, Germany; unpublished results). DNA was isolated from *B. antipoda* leaves, flower buds and blossoms (Dellaporta et al., 1983), converted by sodium bisulfite (EpiTect Bisulfite Kit, Qiagen) and amplified by PCR using 493 and 576 primers (Table S1) and MyTaq DNA Polymerase (Bioline) in a program consisting of initial denaturation (94°C, 2 min) and 35 cycles of 15 s at 94°C, 15 s at 47°C for 493 primers and at 52°C for 576 primers, and 10 s at 72°C followed by a final extension (72°C/10 min). PCR products 251 and 264 bp for Ba493 and Ba576, respectively, were cloned using a TOPO TA cloning kit (Invitrogen) and sequenced (Macrogen). Methylation of cytosines located in the respective sequence context was analyzed by the CyMATE software (Hetzl et al., 2007). Statistical evaluation of the data was carried out using a One-Way independent ANOVA test. Seven clones for each tissue were analyzed. To take in account natural repeat sequence variability with respect to consensus sequences, native DNA (without bisulfite treatment) was PCR amplified using 493 and 576 primers (Table S1) and 15 clones per primer pair were sequenced (Figure S1; GenBank accession numbers KJ922958—KJ922987). Results of cytosine methylation analyses were compared with the consensus sequence of clones obtained by PCR using the same primer pairs and unmodified DNA (Figure S1).

ANALYSIS OF HISTONE MODIFICATIONS BY CHROMATIN IMMUNOPRECIPITATION (ChIP)

Chromatin of *N. tabacum* and *B. antipoda* (0.9 g) was cross-linked with 1% formaldehyde (Sigma) and ChIP was carried out using the EpiQuik™ Plant ChIP Kit (Epigentek) with the antibodies against H3K9me3 (Millipore), H3K9me2 (Abcam), H3K4me3 (Abcam), H4K20me1 (Millipore), and H3K27me3 (Millipore). Two different conditions were used for sonication of plant material in a Diagenode sonicator (Bioruptor)—13 rounds of pulses (15 s at 160 W, 60 s off) for *B. antipoda*; and 13 rounds of pulses (15 s at 160 W, 60 s off) and 7 rounds of pulses (15 s at 200 W, 60 s off) for tobacco. Immunoprecipitated DNA was dot-blotted on a Hybond XL nylon membrane (GE Healthcare) and hybridized with the radioactively labeled probes ptel-C, Ba493 ITR region BAC clone, and Ba576 ITR region PCR product (the same primers as for bisulfite sequencing analysis were used, Table S1). The ptel-C probe was labeled with γ -³²P ATP by T4 Polynucleotide Kinase (NEB) and hybridized for 24 h at 55°C. Ba493 and Ba576 probes were labeled with α -³²P dATP by a DecaLabel DNA Labeling Kit (Fermentas) and hybridized for 24 h at 65°C. After washing the membranes (3 × 30 min in 2 × SSC + 0.1% (w/v) SDS at 55°C

for the ptel-C probe; 3 × 30 min in 0.2 × SSC + 0.1% (w/v) SDS at 65°C for Ba493 and Ba576 probes), hybridization signals were visualized on FLA-7000 (FujiFilm).

ANALYSIS OF TELOMERIC TRANSCRIPTS TERRA AND ARRET

Total RNA was isolated from plant tissues using the RNeasy Plant Mini Kit (Qiagen) according to manufacturer's instructions. Quality and quantity of RNA were checked by electrophoresis on a 1% (w/v) agarose gel and by UV-absorbance (NanoPhotometr IMPLen). Five μ g of RNA were transferred to the Hybond-N membrane (GE Healthcare) and fixed for 15 min by UV-crosslinking and subsequently for 2 h at 80°C. Membranes were hybridized with the end-labeled telomeric probes ptel-C (CCCTAAA)₄ and ptel-G (TTTAGGG)₄ for 24 h at 50°C. After washing under low stringency conditions (3 × 15 min in 2 × SSC + 0.1% (w/v) SDS at 50°C), hybridization signals were visualized using a FLA-7000 phosphorimager (FujiFilm) and evaluated using MultiGauge (Fuji Film) software. Then, membranes were re-hybridized with Ba493 and Ba576 probes, respectively, as described above. Before re-hybridization, the radioactive telomeric probe was removed by 0.1% SDS (90°C for 5 min) and membranes were exposed overnight to ensure that there is no residual signal.

RESULTS AND DISCUSSION

DISTINCT LOCALIZATION OF TELOMERIC REPEATS AT *N. TABACUM* AND *B. ANTIPODA* CHROMOSOMES

In our previous cytogenetic study we showed for *B. antipoda*, an endemic Australian cruciferous species (Brassicaceae) with six chromosome pairs ($2n = 12$), that *Arabidopsis*-like telomeric repeats hybridized to chromosome termini and to all centromeres (Mandaková et al., 2010).

To specify the localization of ITRs in *B. antipoda*, we performed FISH on extended meiotic pachytene chromosomes. FISH analysis corroborated the previous report (Mandaková et al., 2010) and showed that ITRs localized to highly condensed centromeric heterochromatin of all chromosomes (Figures 1A,B). Bal31 digestion of high molecular weight DNA confirmed the presence of large Bal31-resistant blocks comprising *Arabidopsis*-like TTTAGGG telomeric repeats in the *B. antipoda* genome (Figure 2A). Approximately 750 bp units of these ITRs were separated by *NlaIV*, *HaeIII*, and *HinfI* recognition sites (Figure 2B), but a considerable fraction of ITR units was not digested, forming DNA clusters of ca. 20 kb (Figure 2B). Previous cytogenetic and phylogenetic analyses showed that the *B. antipoda* genome has descended from eight ancestral chromosomes ($n = 8$) through an allopolyploid whole-genome duplication event. Due to the extensive reduction of chromosome number (presumably from $n = 16$ to $n = 6$), the six *B. antipoda* chromosomes represent complex mosaics of duplicated ancestral genomic blocks, reshuffled by numerous chromosome rearrangements. Based on knowledge of the exact karyotype structure of *B. antipoda* (Mandaková et al., 2010), we can exclude large ITR tracts as being relics of chromosome rearrangements bringing telomeres into centromere regions.

N. tabacum was characterized as a species with long genuine telomeres of relatively heterogeneous length (Fajkus et al., 1995a;

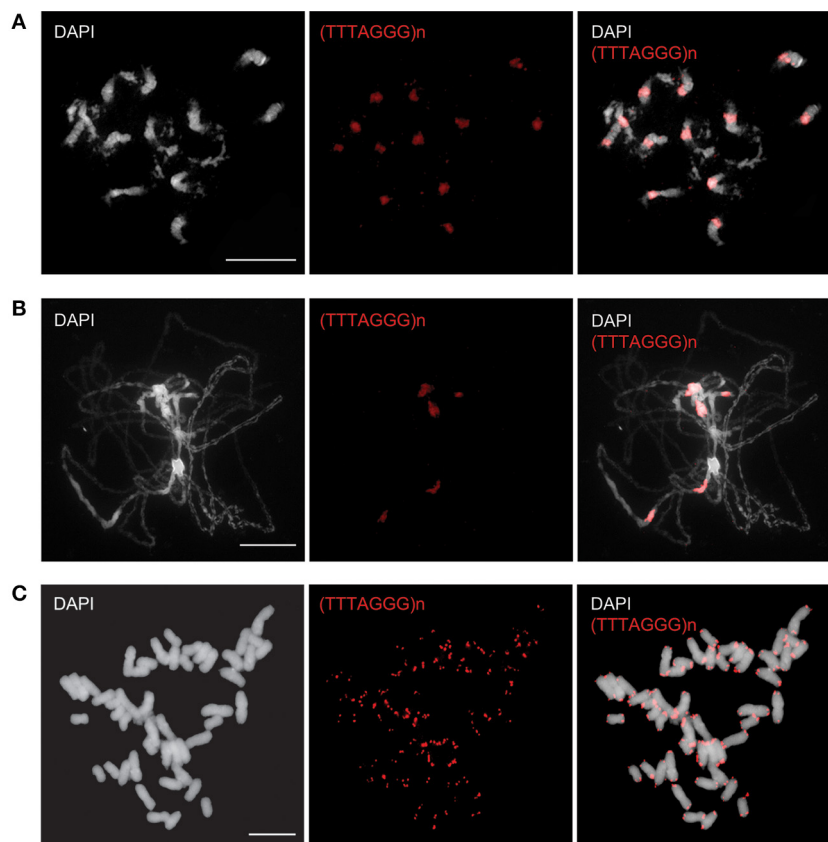


FIGURE 1 | Fluorescence *in situ* localization of the telomeric repeats in *B. antipoda* and *N. tabacum*. In *B. antipoda*, the telomere repeats (red) hybridize preferentially to centromeres, whereas minor signals at

chromosome termini are less prominent on mitotic (A) and pachytene (B) chromosomes. The exclusive terminal location of the telomere repeats was detected on mitotic chromosomes of *N. tabacum* (C).

Kovarik et al., 1996) and no detectable fraction of internally located telomeric repeats (Figure 1C; Majerova et al., 2011a). In this context, tobacco may be considered as an appropriate model for analysis of epigenetic properties of plant telomeric chromatin, because the content of ITRs in its genome is by orders in magnitude lower (if any) compared to the genuine telomeres and thus allows more straightforward interpretation of results.

METHYLATION OF CYTOSINES IN NICOTIANA TELOMERES SHOWS BIAS WITH MORE METHYLATION TOWARD DISTAL TELOMERE POSITION

Methylated cytosines in plant telomeres were detected by whole-genome bisulfite shotgun sequencing (Cokus et al., 2008). Since telomeres are most frequently methylated at the third (inner) cytosine of the CCCTAAA repeat, we designed a degenerate oligonucleotide probe (termed DEGENER) that hybridizes to telomeric sequences methylated at the third cytosine in bisulfite-modified DNA, while the remaining two (outer) cytosines can be either methylated or non-methylated (Majerova et al., 2011b). To evaluate relative telomere methylation in different samples, we normalized the signal obtained with the DEGENER probe to the signal generated by a loading probe (pltel-C) that hybridizes to the G-rich telomeric strand.

Since telomeres in *Nicotiana* species are relatively long (20–160 kb in *N. tabacum* and 20–50 kb in *N. tomentosiformis* Fajkus et al., 1995a; Kovarik et al., 1996) we studied the 5-methylcytosines (5mC) distribution along these telomere repeat tracts. For this purpose, high molecular weight DNA was progressively digested with Bal31 exonuclease. Efficient degradation of telomeres in Bal31-digested samples was checked by (i) TRF analysis that showed loss of the telomere-specific hybridization signal (Figure 3A) and by (ii) hybridization using the loading pltel-C probe. Similarly as in TRF analysis, the telomere-specific signal in Bal31-digested samples was markedly reduced (Figure 3B).

From the ratio of hybridization signals using DEGENER and loading probes (Figures 3B,C), it became evident that in *Nicotiana* species, 5mCs were not uniformly distributed along the telomeres. There was a difference in methylation level at the proximal part of the telomere relative to the whole telomere. In *N. tabacum*, after 90 min of Bal31 digestion, telomeres were degraded to ca. 2/3 of their initial amount, as determined by comparing loading signal intensities in the dot blot analysis (Figure 3B). In this sample, the relative density of methylated cytosines decreased to ~80% (Figure 3C), demonstrating that the level of methylated cytosines is slightly lower in the proximal part of the telomere compared to the average value along the whole telomere.

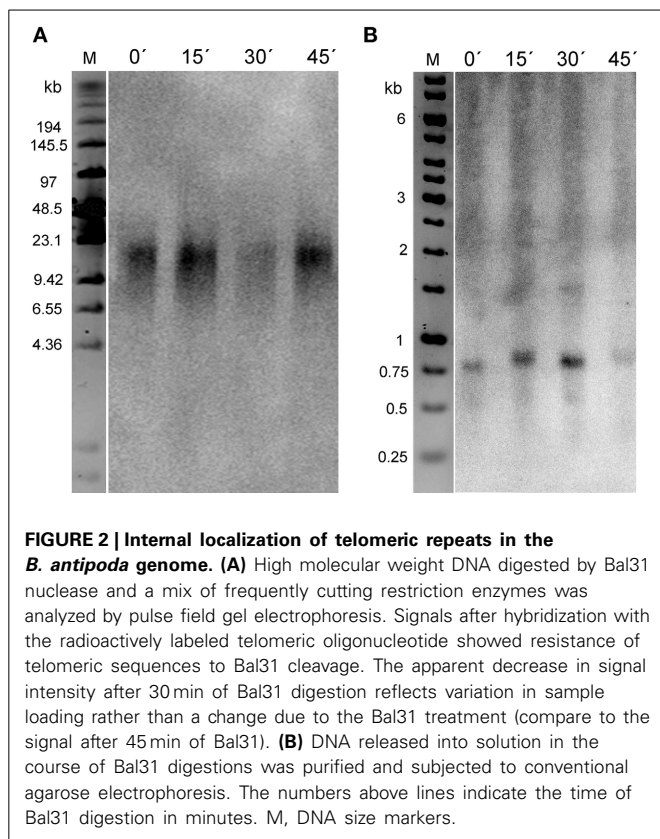


FIGURE 2 | Internal localization of telomeric repeats in the *B. antipoda* genome. (A) High molecular weight DNA digested by Bal31 nuclease and a mix of frequently cutting restriction enzymes was analyzed by pulse field gel electrophoresis. Signals after hybridization with the radioactively labeled telomeric oligonucleotide showed resistance of telomeric sequences to Bal31 cleavage. The apparent decrease in signal intensity after 30 min of Bal31 digestion reflects variation in sample loading rather than a change due to the Bal31 treatment (compare to the signal after 45 min of Bal31). **(B)** DNA released into solution in the course of Bal31 digestions was purified and subjected to conventional agarose electrophoresis. The numbers above lines indicate the time of Bal31 digestion in minutes. M, DNA size markers.

In *N. tomentosiformis*, the relative decrease in 5mC density toward the proximal part of the telomere was similar as in *N. tabacum* but shifted toward higher relative values corresponding to the shorter total telomere lengths in *N. tomentosiformis*. After 90 min of Bal31 digestion, telomeres were degraded by ~40% (Figure 3B) and the relative density of 5mC in remaining parts of telomeres was ~50% compared to the sample with intact telomeres (Figure 3C). The level of 5mC in *N. tomentosiformis* is thus markedly higher at the distal part of telomeres.

We conclude that both *Nicotiana* species show remarkable similarities in increased relative methylation density at distal telomere regions. Strikingly, in tobacco chromosomes, the distal telomere domain, which is maintained by the combined action of telomerase and the conventional replication machinery, showed a higher 5mC level than the proximal telomere domain which is (i) adjacent to the densely methylated subtelomeric heterochromatin (Fajkus et al., 1995b), is (ii) replicated in a conventional way and is (iii) closer to the presumed transcription start site of TERRA transcripts (see below). According to recent findings, transcribed DNA regions with asymmetry in C/G distribution between the strands (e.g., telomeres) can be protected from methylation by formation of RNA-DNA hybrids (R-loops) when the C-rich DNA strand is transcribed and G-rich RNA is produced (Ginno et al., 2012). This situation could happen in the case of telomeres producing TERRA transcripts (G-rich). These transcripts elongate toward distal parts of telomeres and may not span the entire telomere length.

INTERSTITIAL TELOMERIC REPEATS IN THE *B. ANTIPODA* GENOME ARE METHYLATED TO A DIFFERENT EXTENT

No unequivocal data about methylation are available for ITRs. The pilot analysis of *A. thaliana* telomeric chromatin (Vrbsky et al., 2010) did not, *a priori*, distinguish between terminal and ITRs. However, high stringency hybridization conditions during their analyses of telomeric cytosine methylation suggested a predominant detection of perfect repeats in genuine telomeres. In another study, methylated cytosines were detected only at ITRs (Vaquero-Sedas et al., 2011). Here, we used two methods to evaluate general and specific patterns of methylation of cytosines located at internal telomeric repeats of *B. antipoda*: (i) hybridization of bisulfite-modified DNA with the DEGENER probe, and (ii) bisulfite sequencing of selected telomeric repeat-containing intrachromosomal regions.

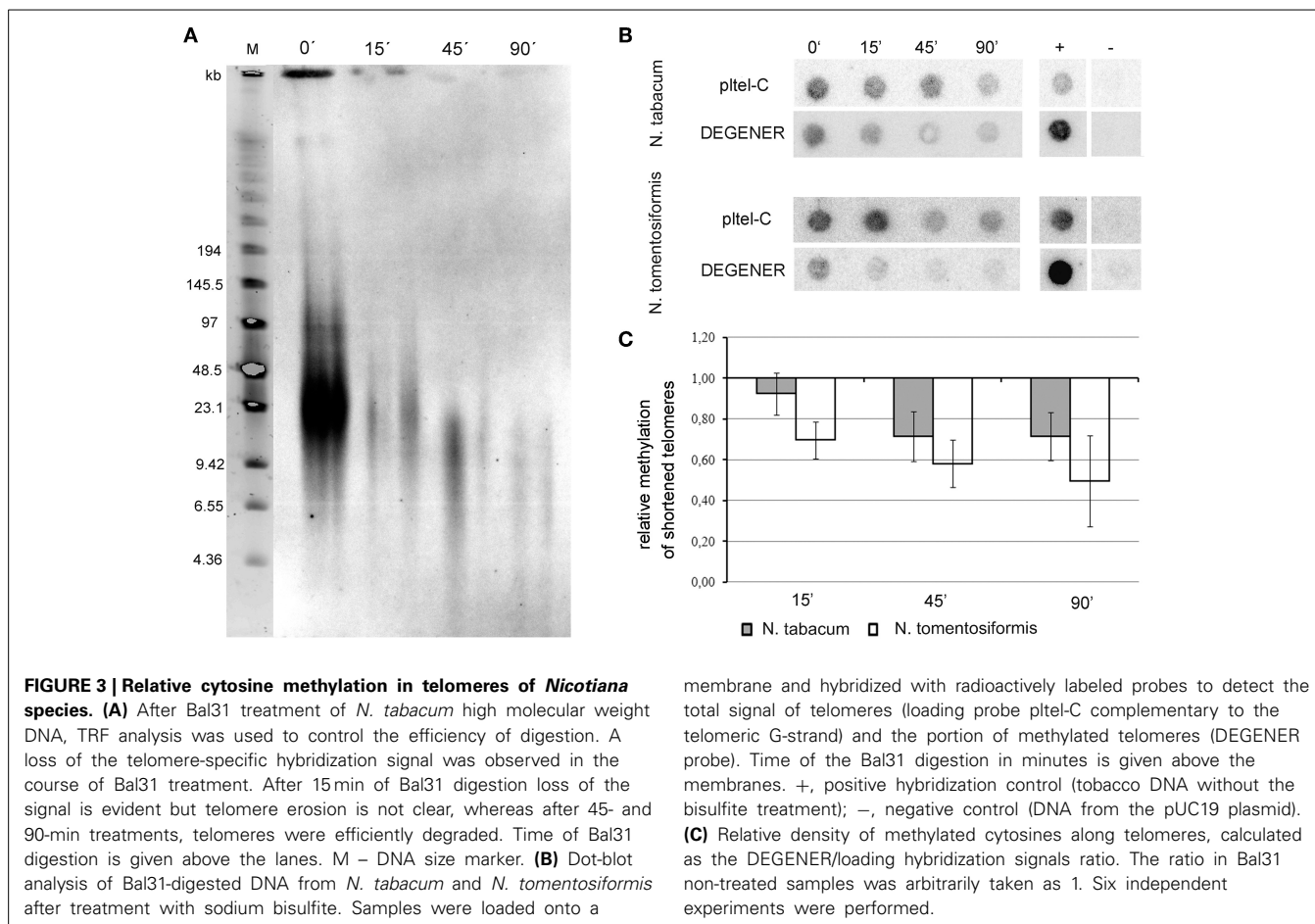
Dot blot analyses using bisulfite-treated DNA and radioactively labeled DEGENER and loading probes clearly showed that cytosines of *B. antipoda* telomeric repeats were methylated (Figure 4A). The hybridization signal using the DEGENER probe was persistent after extensive Bal31 digestion, implying the presence of methylated cytosines in internally located telomeric repeats that were resistant to the Bal31 treatment. In addition, the intensities of hybridization signals using the p1tel-C probe were maintained in Bal31-digested samples, which is in agreement with the data presented in the Figure 2 and confirms localization of a majority of telomeric repeats at internal positions.

We carried out bisulfite sequencing of two ITR regions—Ba493 and Ba576. DNAs from leaves, flower buds, and blossoms were converted by sodium bisulfite and PCR amplified. We found that 87, 96, and 82% of cytosines of telomeric repeats located in the Ba493 region were methylated in leaves, flower buds, and blossoms, respectively (Figures 4B,C), while 24% of cytosines of telomeric sequences of the Ba576 region were methylated in leaves and flower buds and 56% in blossoms (Figures 4B,C). Thus, internal telomeric repeats in *B. antipoda* are methylated and the level of 5mC varies considerably between Ba493 and Ba576 regions which were subjected to the detailed analysis.

CHROMATIN OF INTERNAL AND TERMINAL TELOMERIC REPEATS SHOWS DISTINCT HISTONE MARKS

Few studies were focused on chromatin features of plant telomeres. In one study, the dual character of *A. thaliana* telomeres with prevalent heterochromatic histone modifications, but clearly detectable euchromatic mark was reported (Vrbsky et al., 2010), and in another, analysis using different techniques demonstrated the predominantly euchromatic character of genuine telomeres and the heterochromatic nature of ITRs (Vaquero-Sedas et al., 2011). We approached this problem from a new perspective and compared histone modifications at terminal and internal telomeric repeats using plants with a different distribution of telomeric repeats between ITRs and genuine telomeres.

To investigate the epigenetic patterns of telomere repeat-containing chromatin at distinct genomic locations, ChIP analyses were carried out using antibodies against five specific histone modifications: H3K4me3 and H3K9me3 as euchromatic marks in plants, H4K20me1 and H3K9me2 as heterochromatic marks, and H3K27me3 as mark of developmentally silenced genes



(reviewed in Berr et al., 2011). The telomere-specific probe pتل-C was applied for hybridization to address telomeric sequences; in *B. antipoda* additionally, Ba493 and Ba576 were used to address ITR regions. In accordance with the previous results for *A. thaliana* (Vrbsky et al., 2010), we found that tobacco telomeres were significantly enriched in H3K9me2 and H3K27me3 modifications, with a contribution of euchromatic H3K4me3 (Figure 5). Telomeric repeats of *B. antipoda* showed predominantly the heterochromatic mark H3K9me2, and a minor signal for H3K4me3. No H3K27me3 was detected within telomeric chromatin of *B. antipoda*. Hybridization with the ITR-specific probes Ba493 and Ba576 revealed only signals for H3K9me2 (Figure 5). Extensive mapping of chromatin states in *A. thaliana* showed that H3K9me2 and H3K4me3 marks are, in essence, mutually exclusive (Roudier et al., 2011). In this context, the association of both modifications with plant telomeres may indicate the existence of two distinct fractions of telomeric chromatin; the dominant heterochromatic fraction associated with H3K9me2 and the second one that is more euchromatin-like. We did not find any H3K9me3 signal suggesting different roles for H3K9 and H3K4 trimethylations at plant telomeres, although both these modifications frequently co-localized at euchromatic genes in *A. thaliana* (Roudier et al., 2011). Moreover, we did not detect H4K20me1 at tobacco telomeres, which is astonishing because the dominant plant telomeric mark H3K9me2 was found mainly

at heterochromatic transposable elements and other repeats, and overlaps significantly with H4K20me1 in *A. thaliana* (Roudier et al., 2011). The high density of H3K9me2 (Roudier et al., 2011) suggests that these marks may occur independently of each other in distinct chromosome regions, and telomeres may represent such regions.

Our results support the hypothesis that genuine telomeres exhibit a dual epigenetic character, with H3K9me2 as the prevalent mark while ITRs are exclusively heterochromatic. The presence of the H3K27me3 at genuine telomeres in tobacco [and its association with telomeric repeats in *A. thaliana* and rice (Vaquero-Sedas et al., 2012)] represents an interesting feature. Its functional significance remains to be elucidated.

TELOMERES AND INTERNAL TELOMERIC REPEATS ARE BOTH TRANSCRIBED

In 2007, subtelomere-originated RNA repeats UUAGGG, called TERRA (telomere repeat-containing RNA), were detected in human cells, proving that telomeres are actively transcribed (Azzalin et al., 2007). Since then, TERRA transcripts have been found in birds, budding yeast, fission yeast, *A. thaliana* and tobacco (Vrbsky et al., 2010; Majerova et al., 2011b; Bah and Azzalin, 2012). TERRA is believed to associate directly with telomeres and to regulate the maintenance of telomere length in humans *via* negative control of telomerase activity

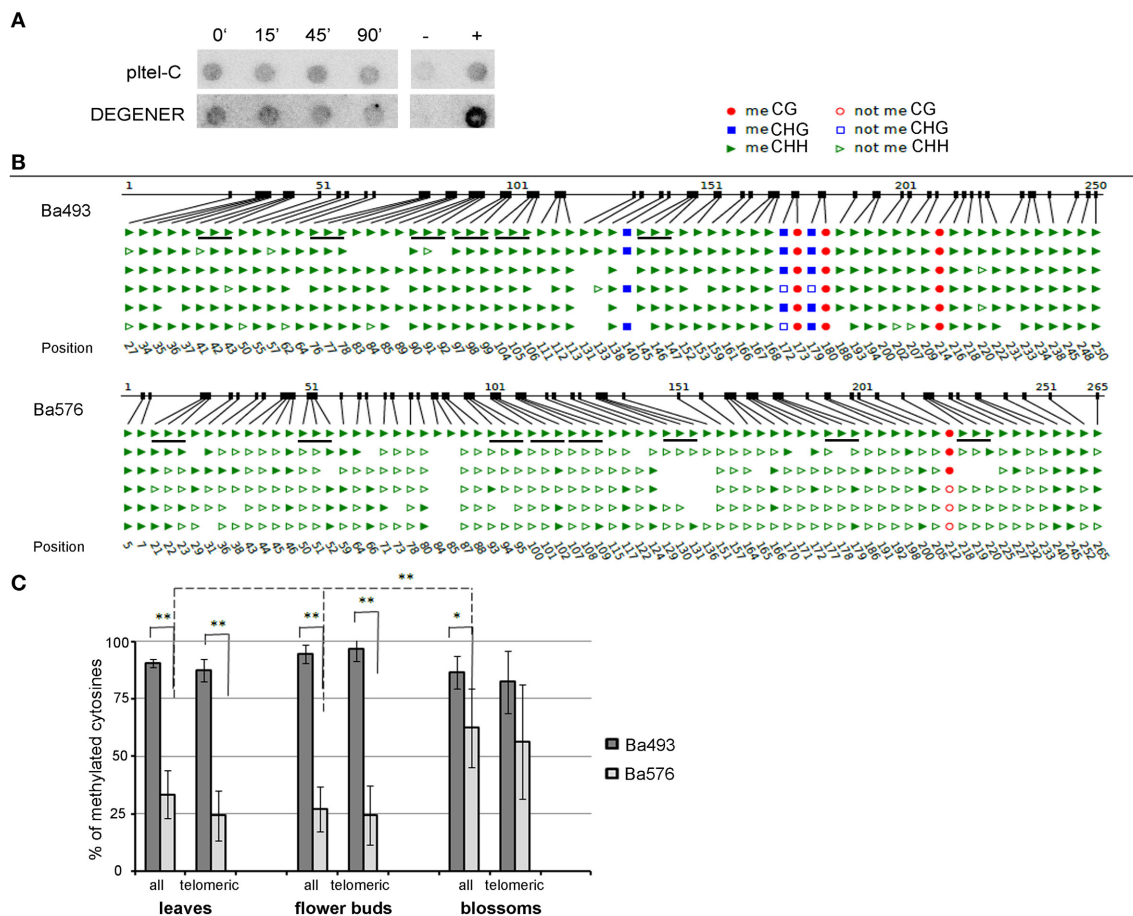


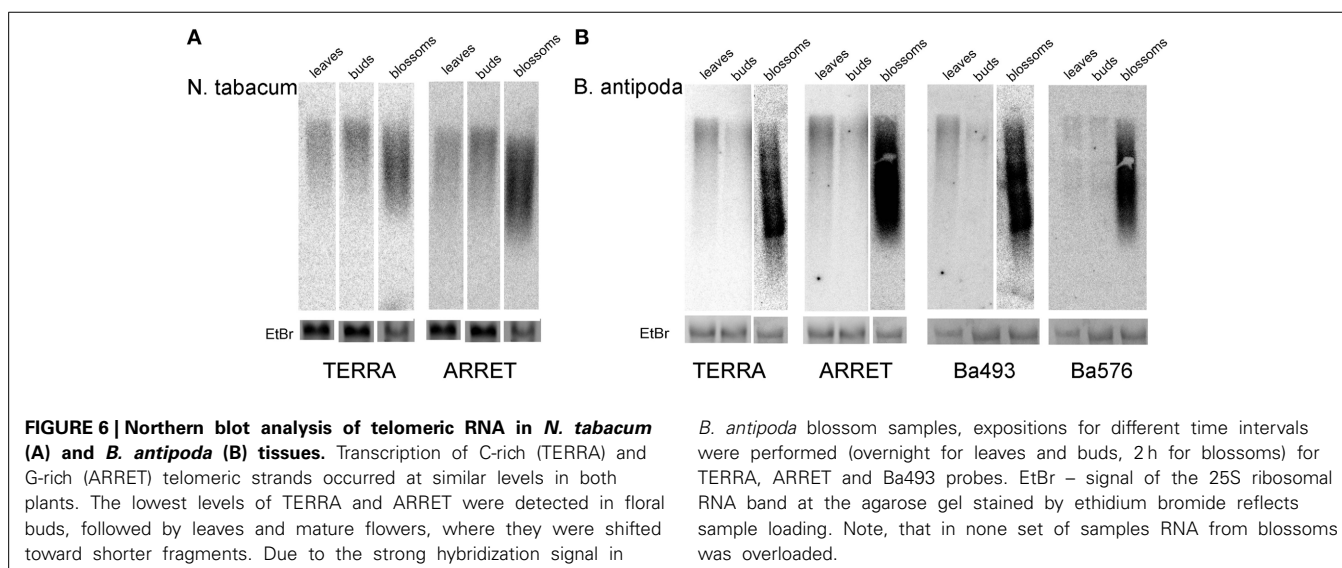
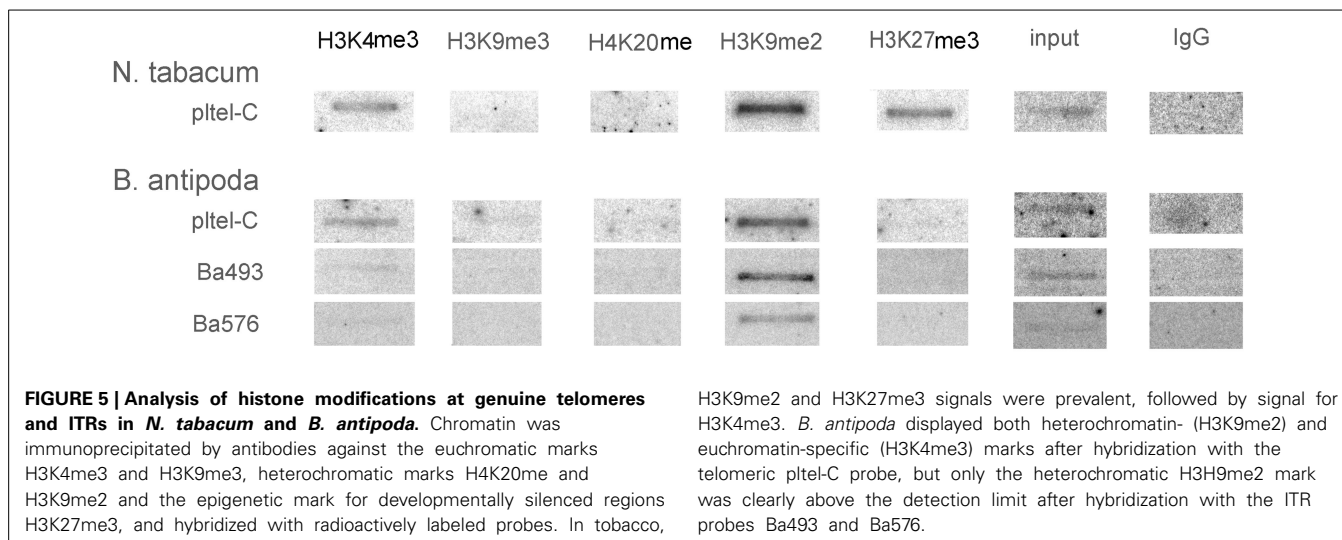
FIGURE 4 | Methylation of cytosines of *B. antipoda* telomeric repeats.

(A) Analysis of global methylation of cytosines in telomeric repeats of *B. antipoda*. High molecular weight DNA was treated with Bal31, converted with bisulfite and analyzed by Southern hybridization against loading and DEGENER probes. Signals with the DEGENER probe indicating methylated cytosines in telomeric repeats were obtained in all samples. The time of Bal31 digestion is given above the membranes. +, positive hybridization control (tobacco DNA without the bisulfite treatment); –, negative control (DNA from pUC19 plasmid). **(B)** An example of bisulfite sequencing data for Ba493 and Ba576 regions in adult leaves. Non-symmetrically located cytosines are depicted as green

triangles; full triangle, methylated; empty triangle, non-methylated cytosine. Cytosines located in perfect telomeric repeats are underlined. The first line of the scheme where all cytosines in all sequence contexts are presented as full figures represents position of respective cytosine. **(C)** Graphical representation of telomeric cytosine methylation within the ITR-containing sequences Ba493 and Ba576. Three tissues were analyzed to reveal possible tissue-specific methylation pattern. “all,” all cytosines located in non-symmetrical sequence context; “telomeric,” cytosines located in perfect telomeric repeats. Data were processed by One-Way independent ANOVA test with standard weighted-means, * is used for $P < 0.05$, ** for $P < 0.01$.

(Azzalin et al., 2007; Ng et al., 2009). Surprisingly, in yeast cells, a different scenario was recently described; telomeric transcripts are preferentially derived from short telomeres and guide telomerase to the chromosome ends from which they originated (Cusanelli et al., 2013). Transcription of the telomeric G-strand is generally less abundant. In humans, a very faint signal of these transcripts was found, in contrast to fission yeast, where C-strand-rich telomeric RNAs were described and named ARIA and antisense ARRET (α ARRET) (Bah et al., 2012). In *A. thaliana*, telomere C-strand (ARRET) transcripts were detected and found to be transcribed mostly from ITRs (Vrbsky et al., 2010). Tobacco and *B. antipoda* allow a comparative analysis of telomere repeat transcripts derived from genuine telomeres vs. ITRs.

RNA isolated from leaves of *B. antipoda* and *N. tabacum* plants was analyzed by northern blotting. Membranes were hybridized either with a radioactively labeled pltel-C probe (CCCTAAA)₄, which hybridizes to the G-rich telomeric strand and detects TERRA, or a pltel-G probe (TTTAGGG)₄, which hybridizes to the C-rich telomeric strand and detects ARRET. In tobacco, both C-rich and G-rich telomeric transcripts were detected at similar levels (Figure 6A, left lines). Taking into consideration that tobacco has no detectable ITRs (Majerová et al., 2011a), transcription of the G-rich telomeric strand (resulting in ARRET transcripts) can be generated by two possible pathways. According to the first scenario, transcription of the G-rich telomeric strand starts within the telomeres using telomeric repeats or hidden non-telomeric sequences as transcription start sites (TSSs). The second



hypothesis assumes synthesis of ARRET directly from TERRA by RNA-dependent RNA polymerases.

To analyze the level of telomeric transcripts in *B. antipoda*, besides ptel-C and ptel-G telomeric probes, specific probes for Ba493 and Ba576 ITR regions were used. No cross-hybridization was detected between Ba493 and Ba576 probes under high stringency conditions (Figure S2A). Therefore, these probes detect the intracellular levels of transcripts derived specifically from the corresponding ITR. Also with tobacco RNA Ba493 and Ba576 probes yielded no signal (Figure S2B). Thus, the probes for *B. antipoda* ITR did not hybridize to telomeres in general.

Both TERRA and ARRET transcripts were detected in *B. antipoda* leaves, at approximately the same level (Figure 6B, left lines). Re-hybridization of membranes with Ba493 and Ba576 probes revealed the presence of transcripts derived from ITR regions. These results imply that a detectable fraction of TERRA and ARRET in *B. antipoda* is transcribed from ITRs. This

corresponds with previous results showing that a relevant fraction of telomeric transcripts in *A. thaliana* is derived from ITRs (Vrbsky et al., 2010). We suggest that in plants with a considerable proportion of ITRs in the genome, the telomere repeat-containing RNA originates mostly from the ITRs and only a small fraction of RNA may come from genuine telomeres. Nevertheless, in plants without detectable ITRs, e.g., tobacco, telomeric transcripts must originate from genuine telomeres and, in the case of ARRET, transcription must start within the telomere itself. Whether there is a functional difference between TERRA and ARRET remains to be explored, but a possible role of ARRET may be plant-specific as ARRET was not detected in mammals (Azzalin et al., 2007). In this context, in *A. thaliana*, telomeric transcripts were shown to be involved in RNA-directed methylation of asymmetrically located telomeric cytosines (Vrbsky et al., 2010), and double-stranded RNA molecules participated in this process.

THE LEVEL OF TELOMERE REPEAT-CONTAINING RNA IS TISSUE-SPECIFIC AND NOT CORRELATED WITH METHYLATION OF CYTOSINES IN ITRs

To quantify transcripts from telomeric repeats in different tissues, RNA samples isolated from leaves, flower buds, and blossoms were analyzed by northern hybridization. Our results showed that the level of telomere repeat-derived RNAs was tissue-specific in both species and no significant differences were found when comparing different transcripts in the same tissue (TERRA vs. ARRET, Ba493 vs. Ba576, Ba576 vs. TERRA, etc., **Figure 6**). The amount of telomeric RNA in blossoms was an order of magnitude higher than in leaves. Relatively low levels of telomeric transcripts detected in leaves are surprising because similar analyses of *A. thaliana* tissues yielded the highest TERRA level in leaves (Vrbsky et al., 2010). The amount of Ba493 and Ba576 ITR-derived RNA is very similar (**Figure 6B**) although DNA methylation in these regions differs markedly (see **Figures 4B,C**). The Ba493 ITR region was shown to be highly methylated (~85% of cytosines are methylated), whereas Ba576 ITR is methylated to about 25% in leaves and floral buds and 56% in blossoms. Differences in levels of telomeric RNA in different tissues are thus not correlated with the level of DNA methylation. The different amounts of RNA could be caused by RNA decay that may vary in different tissues, but no relevant analyses have been done, to our knowledge. Another possibility would be a DNA methylation-independent tissue-specific transcription at the ITR. In tobacco culture cells, the TERRA level was increased in cells with hypomethylated DNA but slightly decreased in cells treated with a general inhibitor of methylation, i.e., in cells with impaired DNA and histone methylation, indicating that the level of TERRA is sensitive to changes in the global methylation pattern (Majerová et al., 2011b). In this context, TSSs located in tobacco genuine telomeres may be more sensitive to DNA methylation [DNA hypomethylation thus increases transcription from tobacco telomeres (Majerová et al., 2011b)], while ITRs in the *B. antipoda* genome are covered with 5mC that do not affect transcript elongation. This hypothesis is testable by further studies, especially in the light of our assumption that tobacco telomeres contain TSSs of unknown sequence(s).

CONCLUSION

Localization of telomeric repeats in both terminal and internal chromosomal positions in common model plants significantly complicates interpretation of analyses of epigenetic status of telomeric chromatin, and separate analyses of telomeres and ITRs are methodically not trivial. Our data using model plants with dominant fraction of telomeric repeats at different chromosomal positions revealed that (i) cytosines located in genuine telomeres and ITRs are methylated with the gradient toward distal part of telomeres and different level of methylation in different ITRs, respectively; (ii) telomeres are associated with histones with both euchromatin- and heterochromatin-specific modifications with yet unknown importance for telomere proper structure and function while ITRs are exclusively heterochromatic; and (iii) telomeres and ITRs are transcribed, the level of telomeric transcripts is tissue-dependent, peaks in blossoms and is not correlated with ITRs methylation. These results are beneficial

for confirmation and refining of the data obtained using common model plants where the unambiguous interpretation may be influenced by the presence of telomeric repeats at both chromosomal locations. In addition, results demonstrate the usefulness of less common plant models for epigenetic studies.

AUTHOR CONTRIBUTIONS

Eva Majerová analyzed cytosine methylation, histone modifications, and telomeric transcripts level; Terezie Mandáková performed FISH analyses; Giang T. H. Vu carried out preparation of *B. antipoda* samples for next generation sequencing and participated at the data evaluation; Miloslava Fojtová, Jiří Fajkus, and Martin A. Lysak designed research; Miloslava Fojtová, Jiří Fajkus, Eva Majerová, and Terezie Mandáková evaluated data and wrote the manuscript. All authors read and approved the final version of the manuscript.

ACKNOWLEDGMENTS

We thank Ingo Schubert (The Leibniz Institute of Plant Genetics and Crop Plant Research, Gatersleben, Germany) for reading the manuscript and critical discussions, Jiri Macas (Institute of Plant Molecular Biology, Biology Centre ASCR, České Budějovice, Czech Republic) and Ales Pecinka (Max Planck Institute for Plant Breeding Research, Cologne, Germany) for sequence processing and valuable comments. Seeds of *N. tomentosiformis* were kindly provided by Sandra Knapp (Natural History Museum, London, UK). This work was supported by the Czech Science Foundation (P501/11/0596), by the project “CEITEC - Central European Institute of Technology” (CZ.1.05/1.1.00/02.0068) from the European Regional Development Fund and by the European Social Fund (CZ.1.07/2.3.00/20.0189, CZ.1.07/2.3.00/30.0037).

SUPPLEMENTARY MATERIAL

The Supplementary Material for this article can be found online at: <http://www.frontiersin.org/journal/10.3389/fpls.2014.00593/abstract>

REFERENCES

- Azzalin, C. M., Reichenbach, P., Khoraiuli, L., Giulotto, E., and Lingner, J. (2007). Telomeric repeat containing RNA and RNA surveillance factors at mammalian chromosome ends. *Science* 318, 798–801. doi: 10.1126/science.1147182
- Bah, A., and Azzalin, C. M. (2012). The telomeric transcriptome: from fission yeast to mammals. *Int. J. Biochem. Cell Biol.* 44, 1055–1059. doi: 10.1016/j.biocel.2012.03.021
- Bah, A., Wischniewski, H., Shchepachev, V., and Azzalin, C. M. (2012). The telomeric transcriptome of *Schizosaccharomyces pombe*. *Nucleic Acids Res.* 40, 2995–3005. doi: 10.1093/nar/gkr1153
- Berr, A., Shafiq, S., and Shen, W. H. (2011). Histone modifications in transcriptional activation during plant development. *Biochim. Biophys. Acta* 1809, 567–576. doi: 10.1016/j.bbagr.2011.07.001
- Clark, S. J., Harrison, J., Paul, C. L., and Frommer, M. (1994). High-sensitivity mapping of methylated cytosines. *Nucleic Acids Res.* 22, 2990–2997. doi: 10.1093/nar/22.15.2990
- Cokus, S. J., Feng, S. H., Zhang, X. Y., Chen, Z. G., Merriman, B., Haudenschild, C. D., et al. (2008). Shotgun bisulphite sequencing of the Arabidopsis genome reveals DNA methylation patterning. *Nature* 452, 215–219. doi: 10.1038/nature06745
- Cusanelli, E., Romero, C. A., and Chartrand, P. (2013). Telomeric noncoding RNA TERRA is induced by telomere shortening to nucleate telomerase molecules at short telomeres. *Mol. Cell* 51, 780–791. doi: 10.1016/j.molcel.2013.08.029
- Dellaporta, L. S., Wood, J., and Hicks, B. J. (1983). A plant DNA miniprep: version II. *Plant Mol. Biol. Rep.* 1, 19–21. doi: 10.1007/BF02712670

- Fajkus, J., Fulneckova, J., Hulanova, M., Berkova, K., Riha, K., and Matyasek, R. (1998). Plant cells express telomerase activity upon transfer to callus culture, without extensively changing telomere lengths. *Mol. Gen. Genet.* 260, 470–474. doi: 10.1007/s004380050918
- Fajkus, J., Kovarik, A., Kralovics, R., and Bezdek, M. (1995a). Organization of telomeric and subtelomeric chromatin in the higher plant *Nicotiana tabacum*. *Mol. Gen. Genet.* 247, 633–638. doi: 10.1007/BF00290355
- Fajkus, J., Kralovics, R., Kovarik, A., and Fajkusova, L. (1995b). The telomeric sequence is directly attached to the HRS60 subtelomeric tandem repeat in tobacco chromosomes. *FEBS Lett.* 364, 33–35. doi: 10.1016/0014-5793(95)00347-C
- Fojtova, M., and Fajkus, J. (2014). Epigenetic regulation of telomere maintenance. *Cytogenet. Genome Res.* 143, 125–135. doi: 10.1159/000360775
- Fojtova, M., Fulneckova, J., Fajkus, J., and Kovarik, A. (2002). Recovery of tobacco cells from cadmium stress is accompanied by DNA repair and increased telomerase activity. *J. Exp. Bot.* 53, 2151–2158. doi: 10.1093/jxb/erf080
- Galati, A., Micheli, E., and Cacchione, S. (2013). Chromatin structure in telomere dynamics. *Front. Oncol.* 3:46. doi: 10.3389/fonc.2013.00046
- Ginno, P. A., Lott, P. L., Christensen, H. C., Korf, I., and Chedin, F. (2012). R-loop formation is a distinctive characteristic of unmethylated human CpG island promoters. *Mol. Cell* 45, 814–825. doi: 10.1016/j.molcel.2012.01.017
- He, L., Liu, J., Torres, G. A., Zhang, H., Jiang, J., and Xie, C. (2012). Interstitial telomeric repeats are enriched in the centromeres of chromosomes in *Solanum* species. *Chromosome Res.* 21, 5–13. doi: 10.1007/s10577-012-9332-x
- Hetzl, J., Foerster, A. M., Raidl, G., and Mittelsten Scheid, O. (2007). CyMATE: a new tool for methylation analysis of plant genomic DNA after bisulphite sequencing. *Plant J.* 51, 526–536. doi: 10.1111/j.1365-313X.2007.03152.x
- Ijdo, J. W., Wells, R. A., Baldini, A., and Reeders, S. T. (1991). Improved telomere detection using a telomere repeat probe (TTAGGG)_n generated by PCR. *Nucleic Acids Res.* 19, 4780–4780. doi: 10.1093/nar/19.17.4780
- Kovarik, A., Fajkus, J., Koukalova, B., and Bezdek, M. (1996). Species-specific evolution of telomeric and rDNA repeats in the tobacco composite genome. *Theor. Appl. Genet.* 92, 1108–1111. doi: 10.1007/BF00224057
- Majerova, E., Fojtova, M., Mandaková, T., and Fajkus, J. (2011a). Methylation of plant telomeric DNA: what do the results say? *Plant Mol. Biol.* 77, 533–536. doi: 10.1007/s11103-011-9834-5
- Majerova, E., Fojtova, M., Mozgova, I., Bittova, M., and Fajkus, J. (2011b). Hypomethylating drugs efficiently decrease cytosine methylation in telomeric DNA and activate telomerase without affecting telomere lengths in tobacco cells. *Plant Mol. Biol.* 77, 371–380. doi: 10.1007/s11103-011-9816-7
- Mandaková, T., Joly, S., Krzywinski, M., Mummenhoff, K., and Lysak, M. A. (2010). Fast diploidization in close mesopolyploid relatives of *Arabidopsis*. *Plant Cell* 22, 2277–2290. doi: 10.1105/tpc.110.074526
- Mandaková, T., Kovarik, A., Zozomova-Lihova, J., Shimizu-Inatsugi, R., Shimizu, K. K., Mummenhoff, K., et al. (2013). The more the merrier: recent hybridization and polyploidy in *Cardamine*. *Plant Cell* 25, 3280–3295. doi: 10.1105/tpc.113.114405
- Ng, L. J., Cropley, J. E., Pickett, H. A., Reddel, R. R., and Suter, C. M. (2009). Telomerase activity is associated with an increase in DNA methylation at the proximal subtelomere and a reduction in telomeric transcription. *Nucleic Acids Res.* 37, 1152–1159. doi: 10.1093/nar/gkn1030
- Ogrocka, A., Polanska, P., Majerova, E., Janeba, Z., Fajkus, J., and Fojtova, M. (2014). Compromised telomere maintenance in hypomethylated *Arabidopsis thaliana* plants. *Nucleic Acids Res.* 42, 2919–2931. doi: 10.1093/nar/gkt1285
- Roudier, F., Ahmed, I., Berard, C., Sarazin, A., Mary-Huard, T., Cortijo, S., et al. (2011). Integrative epigenomic mapping defines four main chromatin states in *Arabidopsis*. *EMBO J.* 30, 1928–1938. doi: 10.1038/emboj.2011.103
- Uchida, W., Matsunaga, S., Sugiyama, R., and Kawano, S. (2002). Interstitial telomere-like repeats in the *Arabidopsis thaliana* genome. *Genes Genet. Syst.* 77, 63–67. doi: 10.1266/ggs.77.63
- Vaquero-Sedas, M. I., Gamez-Arjona, F. M., and Vega-Palas, M. A. (2011). *Arabidopsis thaliana* telomeres exhibit euchromatic features. *Nucleic Acids Res.* 39, 2007–2017. doi: 10.1093/nar/gkq1119
- Vaquero-Sedas, M. I., Luo, C. Y., and Vega-Palas, M. A. (2012). Analysis of the epigenetic status of telomeres by using ChIP-seq data. *Nucleic Acids Res.* 40:e163. doi: 10.1093/nar/gks730
- Vrbysky, J., Akimcheva, S., Watson, J. M., Turner, T. L., Daxinger, L., Vyskot, B., et al. (2010). siRNA-mediated methylation of *Arabidopsis* telomeres. *PLoS Genet.* 6:e1000986. doi: 10.1371/journal.pgen.1000986
- Yoo, S. D., Cho, Y. H., and Sheen, J. (2007). *Arabidopsis* mesophyll protoplasts: a versatile cell system for transient gene expression analysis. *Nat. Protoc.* 2, 1565–1572. doi: 10.1038/nprot.2007.199

Conflict of Interest Statement: The authors declare that the research was conducted in the absence of any commercial or financial relationships that could be construed as a potential conflict of interest.

Received: 26 August 2014; accepted: 11 October 2014; published online: 04 November 2014.

Citation: Majerová E, Mandáková T, Vu GTH, Fajkus J, Lysak MA and Fojtová M (2014) Chromatin features of plant telomeric sequences at terminal vs. internal positions. *Front. Plant Sci.* 5:593. doi: 10.3389/fpls.2014.00593

This article was submitted to *Plant Genetics and Genomics*, a section of the journal *Frontiers in Plant Science*.

Copyright © 2014 Majerová, Mandáková, Vu, Fajkus, Lysak and Fojtová. This is an open-access article distributed under the terms of the Creative Commons Attribution License (CC BY). The use, distribution or reproduction in other forums is permitted, provided the original author(s) or licensor are credited and that the original publication in this journal is cited, in accordance with accepted academic practice. No use, distribution or reproduction is permitted which does not comply with these terms.

Compromised telomere maintenance in hypomethylated *Arabidopsis thaliana* plants

Anna Ogrocká^{1,2,†}, Pavla Polanská^{1,2,†}, Eva Majerová^{1,2}, Zlatko Janeba³, Jiří Fajkus^{1,2,4} and Miloslava Fojtová^{1,2,*}

¹Mendel Centre for Plant Genomics and Proteomics, Central European Institute of Technology (CEITEC), Masaryk University, Kamenice 5, 62500 Brno, Czech Republic, ²Functional Genomics and Proteomics, National Centre for Biomolecular Research, Faculty of Science, Masaryk University, Kotlářská 2, 611 37 Brno, Czech Republic, ³Institute of Organic Chemistry and Biochemistry, Academy of Sciences of the Czech Republic v.v.i., Flemingovo nám. 2, 166 10, Prague, Czech Republic and ⁴Institute of Biophysics, Academy of Sciences of the Czech Republic v.v.i., Královopolská 135, 612 65 Brno, Czech Republic

Received July 10, 2013; Revised October 30, 2013; Accepted November 19, 2013

ABSTRACT

Telomeres, nucleoprotein structures at the ends of linear eukaryotic chromosomes, are important for the maintenance of genomic stability. Telomeres were considered as typical heterochromatic regions, but in light of recent results, this view should be reconsidered. Asymmetrically located cytosines in plant telomeric DNA repeats may be substrates for a DNA methyltransferase enzyme and indeed, it was shown that these repeats are methylated. Here, we analyse the methylation of telomeric cytosines and the length of telomeres in *Arabidopsis thaliana* methylation mutants (*met 1-3* and *ddm 1-8*), and in their wild-type siblings that were germinated in the presence of hypomethylation drugs. Our results show that cytosine methylation in telomeric repeats depends on the activity of MET1 and DDM1 enzymes. Significantly shortened telomeres occur in later generations of methylation mutants as well as in plants germinated in the presence of hypomethylation drugs, and this phenotype is stably transmitted to the next plant generation. A possible role of compromised *in vivo* telomerase action in the observed telomere shortening is hypothesized based on telomere analysis of hypomethylated telomerase knockout plants. Results are discussed in connection with previous data in this field obtained using different model systems.

INTRODUCTION

Telomeres are specialized nucleoprotein structures, usually formed by minisatellite DNA repeat sequences located at the ends of linear eukaryotic chromosomes. Telomeres are essential for maintenance of genomic integrity, compensating for the replicative loss of DNA at chromosomal termini and distinguishing natural chromosome ends from chromosome breaks [reviewed in (1)]. The basic functions of telomeres are performed in chromatin context. Telomere repeats and adjacent subtelomeric regions are associated with histones and non-histone proteins, including a number of telomere-specific proteins.

Regulation of gene expression and chromatin structure via epigenetic mechanisms has been convincingly documented using many model organisms [reviewed in (2)]. Two kinds of modifications of macromolecules are crucial for epigenetic regulation: DNA methylation and modifications of histone proteins [reviewed in (3)]. Furthermore, regulatory roles of small and non-coding RNAs have been established (4). These mechanisms modulate the dynamics of chromatin structure governing activation/repression of resident genes, e.g. in response to developmental and environmental stimuli. The general epigenetic landscape in plants is considerably more varied compared with that in animals. (i) Cytosines located in CG, CHG (H = A, T, C) and asymmetrical CHH sequences can be methylated in plant genomes, while predominantly CG methylation and a lower level of non-CG methylation during specific developmental phases were reported in animal cells [(5), reviewed in (6)]. Methylation of asymmetrically localized cytosines in plant telomeric CCCTAAA sequences was reported in

*To whom correspondence should be addressed. Tel: +420 549 495 601; Fax: +420 549 492 654; Email: fojtova@sci.muni.cz

†These authors contributed equally to the paper as first authors.

Arabidopsis thaliana (7,8) and in tobacco (9). (ii) Genes encoding enzymes catalysing DNA demethylation during specific developmental phases and at specific genomic loci were identified in *Arabidopsis* (10,11), while in mammalian cells, demethylation is linked to base excision repair processes (12). (iii) The plant-specific RNA polymerases IV and V (13,14) catalyse the synthesis of RNA molecules involved in RNA-directed DNA methylation pathways.

The involvement of epigenetic mechanisms in the regulation of telomere homeostasis is a popular research topic and studies in this field have been carried out using various animal models. In these cells, telomeric tracts, as well as adjacent subtelomeric regions, are maintained in a heterochromatic state associated with heterochromatin-specific histone modification. Nevertheless, in recent studies using mouse embryonic fibroblasts, association of telomeres with both the heterochromatin-specific (H3K9me3) and the euchromatin-specific (H3K4me3) epigenetic marks were reported, although the H3K4me3 loading was lower than that of H3K9me3 (15), and the level of heterochromatic marks was surprisingly low at telomeres in human fibroblasts (16) and T-cells (17). While mammalian telomeres lack CG sequences, the natural substrate of known mammalian DNA methyltransferases, in human somatic cells, the subtelomeric repeats are CG-rich and methylated (18,19). The importance of subtelomeric DNA methylation and heterochromatin-specific modifications of telomeric histones for telomere homeostasis was reported in both human and mouse cells, where loss of heterochromatin-specific modifications led to significant lengthening of telomeres and in some cases, to an increase in telomere recombination (20–25). In contrast to these studies, Roberts *et al.* (26) reported that telomere lengths were not affected in mouse epigenetic mutants, challenging the idea of epigenetic control of telomere homeostasis in mammalian cells.

In the classic model, and similarly as in mammalian cells, plant telomeres were viewed as heterochromatic loci (27). A more recent study, however, characterized *A. thaliana* telomeric chromatin as an intermediate heterochromatin possessing both hetero- and euchromatin-specific histone modifications (8). Vaquero-Sedas *et al.* (28) even concluded that telomeres of *A. thaliana* exhibit predominantly euchromatic features, while subtelomeres and interstitial telomeric sequences are of a heterochromatic nature.

Other factors possibly involved in telomere homeostasis are telomeric transcripts [telomeric repeat containing RNA (TERRA)], the discovery of which has challenged the long-standing opinion that telomeres are transcriptionally inert (29). Although intensively studied, connections between TERRA and telomerase activity/telomere homeostasis are far from clear. TERRA and transcription of telomeres do not affect telomere lengths, and TERRA does not inhibit telomerase activity *in vivo* in human cancer cells (30). Conversely, telomere length-dependent inhibition of telomerase activity *in vitro* by TERRA (31), binding of TERRA to the RNA subunit of telomerase (hTR) and partially to the telomerase catalytic subunit (hTERT) in human cells (32), and telomerase-independent telomere shortening induced by

up-regulation of TERRA in *Saccharomyces cerevisiae* (33), have been reported. In plants, the presence of TERRA transcripts has been reported in *Arabidopsis* (8) and in tobacco BY-2 cells (9).

Here, we examine the length and methylation of telomeres in *A. thaliana* methylation mutants (*met 1-3* and *ddm 1-8*), and in wild-type (wt) plants that were germinated in the presence of hypomethylation agents. The *MET1* gene encodes the DNA methyltransferase (34) responsible for maintaining methylation of cytosines located in CG sequences. Proper *MET1* gene function is crucial for the maintenance of the general epigenetic pattern, including CG and non-CG methylation, histone modifications and chromatin structure (35). The *DDM1* gene encodes a protein with similarities to the SWI/SNF family of chromatin remodelling factors (36). A mutation in this gene leads to a significant decrease in the overall level of DNA methylation (37).

Zebularine [1-(β-D-ribofuranosyl)-1,2-dihydropyrimidine-2-one, ZEB] is a cytidine analogue (38) that is stable in aqueous solution and has relatively low toxicity [reviewed in (39)]. Its hypomethylation effect is similar to that of the traditionally used cytidine analogues, 5-azacytidine and 5-aza-2'-deoxycytidine (40). These compounds are incorporated into DNA during replication and form stable complexes with DNA methyltransferases, thereby reducing their methylation activity. In the model plants *A. thaliana* (41), and *Nicotiana tabacum* (9), ZEB-induced loss of DNA methylation was described.

DHPA [(*S*)-9-(2,3-dihydroxypropyl)adenine] (42) is a competitive inhibitor of *S*-adenosyl-L-homocysteine hydrolase, the enzyme that degrades *S*-adenosyl-L-homocysteine, a by-product of transmethylation reactions and a potent inhibitor of all methyltransferases, to homocysteine and adenosine. A number of experimental studies have been carried out using this drug for epigenetic modifications, including its application in plant systems (9,43–46).

We observe distinct telomere shortening in chemically hypomethylated plants and in later generations of methylation mutants. The shortening of telomeres neither correlates with the change in transcription of the telomerase reverse transcriptase (*AtTERT*) gene nor with telomerase activity assayed *in vitro*. Hypotheses considering *in vivo* processes involved in telomere shortening and the role of telomerase in the maintenance of shortened telomeres are presented.

MATERIALS AND METHODS

Plant material

Arabidopsis thaliana seeds of the Columbia-0 ecotype, *DDM1* (At5g66750) mutant (*ddm1-8* strain, SALK000590) and *TERT* (At5g16850) mutant (*tert-/-*, SALK061434) were purchased from the Nottingham Arabidopsis Stock Centre (47); seeds of the mutant plant with a T-DNA insertion in the *MET1* gene [At5g49160, *met1-3* strain, (48)] were kindly provided by Dr Ales Pecinka (GMI, Vienna, Austria). Primers for genotyping are shown in Supplementary Table S1. Seeds were placed on half strength Murashige–Skoog (½ MS, Duchefa) agar

plates and grown under cycles of 8 h light (illumination $100\text{ mmol m}^{-2}\text{ s}^{-1}$), 21°C and 16 h dark, 19°C. Plants were grown in soil under the same light/dark conditions favouring leaf growth; 1-month-old plants were then cultivated using 16 h/8 h light/dark cycles, accelerating flowering and seed development. Leaves were harvested from 2-month-old plants.

Arabidopsis thaliana Columbia-0 and *tert*-/- seeds were germinated for 7 days on agar plates containing ½ MS medium supplemented with ZEB (Sigma) or DHPA at concentrations of 100 and 250 µM. Plants were then grown in soil as described earlier.

Analysis of telomere lengths by the terminal restriction fragment method

Analysis of telomere length by the terminal restriction fragment (TRF) method is based on the digestion of genomic DNA by a frequently cutting restriction endonuclease without a recognition site in the G-rich telomeric sequences. After hybridization with a radioactively labelled telomeric oligonucleotide probe, the signal corresponds to non-digested telomeric tracts (plus subtelomeric regions up to the first restriction site upstream of the telomeres). Analyses were performed as previously described (49,50).

Analysis of cytosine methylation in telomeric repeats

Bisulfite conversion of genomic DNA was carried out using the EpiTect Bisulfite Kit (Qiagen). During the bisulfite treatment, non-methylated cytosines are converted to uracils and amplified as thymines in the subsequent PCR, while 5-methylcytosines are resistant to this reaction (51). To analyse the methylation of all cytosines located in telomeric repeats, we followed the protocol described in (8), with modifications (9). Bisulfite-modified DNA (300 ng) was transferred to a Hybond XL membrane (GE Healthcare) by vacuum dot blotting (Bio-Rad Dot Blot). Membranes were hybridized overnight at 42°C with [³²P] labelled oligonucleotide probes in ULTRAhyb™-Oligo Hybridization Buffer (Ambion). A 'loading' probe (CCCTAAA)₄ was used as a loading normalizer, and the 'degener' probe (TTAGRRT)₄, where R = A or G, detected telomeres where the third cytosine of the (ACCCTAA)_n repeat was methylated, and other cytosines were either methylated or non-methylated. After washing under low stringency conditions (twice at 50°C for 30 min in 2× SSC, 0.1% SDS), hybridization signals were visualized using the FLA7000 phosphoimager (FujiFilm) and analysed using the MultiGauge software (FujiFilm).

Methylation of telomeric cytosines located in the proximal part of the 1L chromosome arm telomere was analysed as described in (8). PCR primer sequences for amplification of the fragment containing telomeric repeats are shown in Supplementary Table S1. PCR was carried out using DyNAzymeII DNA Polymerase (Finnzymes) in a cycle consisting of initial denaturation (2 min), 30 cycles of 30 s at 94°C, 30 s at 56°C and 30 s at 72°C, followed by final extension (72°C/8 min). PCR products were cloned using a TOPO TA Cloning Kit

(Invitrogen) and sequenced (Macrogen). Methylation of cytosines was analysed by CyMATE software (52) in lengths of ~390 bp, where the sequencing signals were clear. Statistical evaluation was done by one-way weighted analysis of variance (ANOVA), a statistical tool used for simultaneous analysis of differences between two or more means. Seventeen clones from three Columbia plants, 11 clones from two *ddm1-8* G2 plants, 12 clones from two *met1-3* G2 plants and 4 clones from a segregated wt plant were analysed. Samples were taken as independent.

To analyse relative methylation of cytosines located in terminal and internal telomeric repeats, high-molecular weight DNA was isolated and digested by Bal31 nuclease as described (53,54). DNA in agarose plugs was either digested by TruI (MseI) restriction endonuclease (Fermentas/Thermo Fisher Scientific) and analysed by TRF, or isolated by QIAEX II Gel extraction Kit (Qiagen), modified by sodium bisulfite, spotted by vacuum blotting onto nylon membrane and hybridized with radioactively labelled 'loading' and 'degener' probes as described earlier.

RESULTS

Methylation of cytosines in telomeric repeats is significantly lower in hypomethylated plants

Telomere length and methylation of cytosines in telomeric repeats were assayed in hypomethylated *A. thaliana* var. Columbia-0 plants in which hypomethylation was induced by (i) loss of function of the gene essential for the maintenance of a stable methylation pattern in *met1-3* and *ddm1-8* mutants and (ii) germinating seeds of wt plants in the presence of the hypomethylation drugs, ZEB or DHPA (Figure 1). To verify the loss of DNA methylation in mutant plants and in seedlings germinated in the presence of hypomethylation drugs, methylation of cytosines in a 180-bp centromeric repeat was investigated using the methylation-sensitive restriction endonuclease HpaII (see Supplementary Methods). Methylation was significantly lower in leaves of mutant plants and in seedlings germinated in the presence of hypomethylation drugs (Supplementary Figure S1), as previously reported (41,48). In leaves of wt plants segregated from the *met1-3* mutant background, the methylation was almost comparable to samples without a mutant history, although in some individuals bands evidencing the non-methylated cytosines in the CCGG sequence motif were visible (Supplementary Figure S1A). In mature leaves of DHPA-treated plants that were grown in soil without the drugs, methylation returned to control levels (Supplementary Figure S1B), consistent with the transient hypomethylation effect described for this drug (44). Variable patterns of centromeric repeat methylations were observed in plants germinated in the presence of ZEB and even in the progenies of plants affected by 250 µM ZEB, although in these cases, the levels of non-methylated cytosines in CCGG sequences were significantly lower than those in ZEB-treated seedlings (Supplementary Figure S1B).

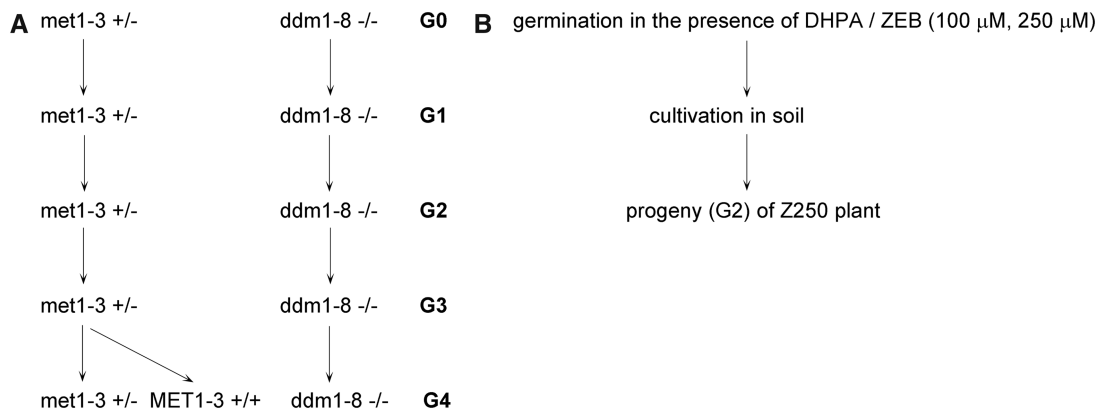


Figure 1. Schematic picture of the experimental strategy. (A) *met1-3* and *ddm1-8* mutant plants were propagated and genotyped in each generation. Material for analyses was collected from *ddm1-8*^{-/-} homozygous individuals and *met1-3*^{+/-} heterozygous plants; *met1-3*^{-/-} homozygous mutants were selected with extremely low frequency and did not grow to the reproductive stage (48). G0 of *ddm1-8* plants represents the T3 progeny of the original accession. In the fourth generation (G4), segregated wt plants (*MET1-3*^{+/+}) were selected for analysis of telomere length. (B) *Arabidopsis thaliana* seedlings were germinated in the presence of hypomethylation drugs DHPA or ZEB for 7 days. Plants were then cultivated in soil, and after 9 weeks, leaves were collected for analysis. Progenies (G2) of plants that had been treated with 250 μ M ZEB (Z250) were grown for telomere length analysis.

To analyse cytosine methylation in telomeric repeats regardless of their chromosomal position, bisulfite-converted DNA was spotted onto nylon membrane and hybridized with a radioactively labelled probe that detected methylated and partially methylated telomeric repeats ('degener' probe). Relative differences between signals from *A. thaliana* wt plants compared with methylation mutants demonstrated a loss of methylated telomeric cytosines within the mutant background (Figure 2). A similar pattern was observed when populations of seedlings germinated in the presence of 250 μ M DHPA and 250 μ M ZEB were analysed—a distinctly lower hybridization signal using the 'degener' probe in hypomethylated seedlings as compared with the control non-treated sample. Hypomethylation did not persist in mature leaves of drug-germinated plants or in wt plants segregated from the *met1-3* mutant background; in these samples, methylation of telomeric cytosines recovered to the level of control/wt plants (Figure 2).

Results obtained from the above analyses provide information about methylation of cytosines in telomeric repeats in terminal (in telomeres) and internal (in ITSs) chromosomal locations within the *A. thaliana* genome. Because ITSs represent a relatively large proportion of all telomeric repeats [20–70%, depending on the methodology used and sequence accuracy, (55,56)], we followed the approach described in (8) and carried out a detailed analysis of methylation in a specific telomeric region; the proximal part of the 1L chromosome arm telomere. According to bisulfite genomic sequencing data from wt Columbia leaves, almost 60% of all asymmetrically located cytosines and >60% of cytosines located in perfect telomeric repeats are methylated (Figure 3A and B). These data demonstrate, at least for this specific region, the presence of methylated cytosines in *A. thaliana* telomeres. In both *met1-3* and *ddm1-8* methylation mutants, the number of methylated cytosines in asymmetrical sequences, within and outside of telomeric repeats, is significantly lower compared with Columbia wt leaves (Figure 3). In wt segregated from the *met1-3*

mutant, methylation recovered almost to the Columbia wt level, although a reduced level of methylation was observed in cytosines located outside of perfect telomeric repeats. Based on these data, methylation of cytosines in telomeric repeats appears to be dependent on the activity of enzymes that maintain a stable methylation pattern.

Although dot-blot analyses revealed cytosine hypomethylation in telomeric repeats of DHPA- and ZEB-treated seedlings (Figure 2, middle panel), no such trend was observed for cytosines located in the proximal 1L chromosome arm telomere; methylation patterns of asymmetrically located cytosines within and outside of perfect telomeric repeats, in treated seedlings (Supplementary Figure S2) and in leaves of plants germinated in the presence of drugs (not shown), were similar to controls.

Bearing in mind previous contradictory data revealing the presence (7,8) or absence (28) of methylation of telomeric cytosines in *A. thaliana*, we aimed to determine the relative level of methylation at terminally located telomeric repeats. To selectively degrade telomeres, high-molecular weight DNA from *A. thaliana* leaves was digested by Bal31 exonuclease. Telomere shortening by Bal31 was verified by TRF analysis (Figure 4A); a significant loss of the telomere-specific signal during Bal31 digestion was observed, while signals from ITSs were comparable in Bal31-treated and non-treated samples. DNA was isolated from agarose plugs, modified by sodium bisulfite, spotted onto nylon membrane and hybridized with radioactively labelled 'loading' and 'degener' probes (Figure 4B). The reduction in the telomere-specific signal from the loading probe in Bal31-digested samples (to about one half as compared with the non-digested control) demonstrated the loss of terminal telomeric repeats. Comparison of the hybridization signals obtained using the 'degener' probe relative to the 'loading' probe did not reveal any statistically significant differences and showed a relatively stable methylation of telomeric cytosines during BAL31 digestion (Figure 4C); this demonstrated that methylation of cytosines in telomeres and in interstitial telomeric repeats was similar.

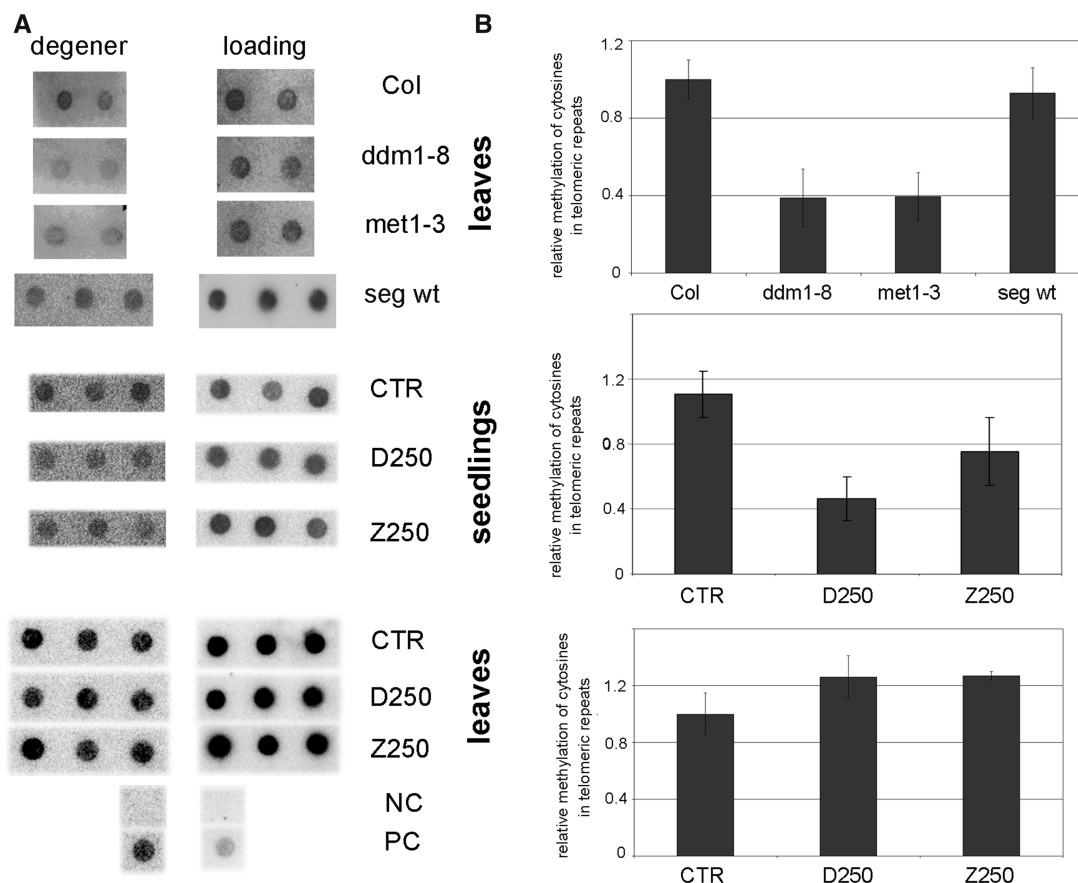


Figure 2. Analysis of general methylation of telomeric cytosines. (A) About 300 ng of bisulfite modified DNA isolated from plant tissues was spotted onto the membrane and hybridized with the radioactively labelled ‘degener’ probe (TTAGRR_T)₄, R = A or G, which generated a signal from methylated and partially methylated fractions, and the ‘loading’ probe (CCCTAAA)₄ complementary to the G-strand of telomeres, which was used for normalization. Top panel: for analysis of *ddm1-8* and *met1-3* methylation mutants, leaves of G2 plants were collected from 10 individuals, two representatives are presented; 10 Columbia wt (Col; two presented) and 7 wt plants segregated from the *met1-3* mutant (seg wt; three presented) were analysed. Middle panel: analysis of seedlings grown on control medium (CTR), medium supplemented with 250 μM DHPA (D250) and 250 μM ZEB (Z250); three biological replicates were analysed. Bottom panel: analysis of mature leaves from three representative plants grown from drug-treated seedlings. NC, negative control, DNA from the plasmid pUC19; PC, positive control, non-converted genomic DNA isolated from *A. thaliana* leaves. (B) Relative methylation of telomeric cytosines in hypomethylated *A. thaliana* tissues. Hybridization signals were evaluated by the MultiGauge software (FujiFilm), and expressed as the ‘degener’/‘loading’ ratio. Signals of Columbia leaves and control non-treated samples (CTR) were arbitrary taken as 1 in respective analyses.

Telomere shortening in hypomethylated *A. thaliana* plants and in plants with a history of hypomethylation

Stable telomere length is important for genomic stability. We determined the lengths of telomeric repeats to establish whether *A. thaliana* genomic hypomethylation influences telomere homeostasis. In Columbia wt plants, telomeres were ~3 kb long with some variations between individuals (Figure 5). Up to the second generation (G2) of methylation mutants, telomeres were maintained at about wt lengths, although some individuals with shorter telomeres were observed, even in G1 and G2. In G3, telomeres of mutants were markedly shortened by ~500–700 bp in *met1-3* plants and even more than 1 kb in some *ddm1-8* individuals. Telomere shortening continued into the next generation (G4) although in this case, plants with shortened telomeres as distinct as in G3 were not observed (Figure 5A).

Telomeres in plants that had been treated by hypomethylation drugs during germination were also distinctly shorter, and the shortening was more

pronounced in ZEB-treated plants. While telomeres of plants germinated in the presence of DHPA were ~500 bp shorter compared with non-treated controls, in ZEB-treated individuals, shortening by more than 1 kb was observed (Figure 5B). Telomere shortenings in plants that were grown in the presence of different concentrations of methylation inhibitors (100 and 250 μM) were similar, thus independent of the drug concentrations used.

To investigate possible recovery from telomere shortening induced by genome hypomethylation, telomere lengths were analysed in wt plants segregated from the *met1-3* mutant background, and in the progenies of plants treated with 250 μM ZEB (Figure 1). Telomeres in both groups remained markedly shorter (Figure 5A and B), demonstrating meiotic stability of this phenotype.

Involvement of telomerase in telomere shortening of hypomethylated *A. thaliana* plants

Telomerase is an enzyme responsible for the elongation of telomeres, and loss of its function leads to progressive

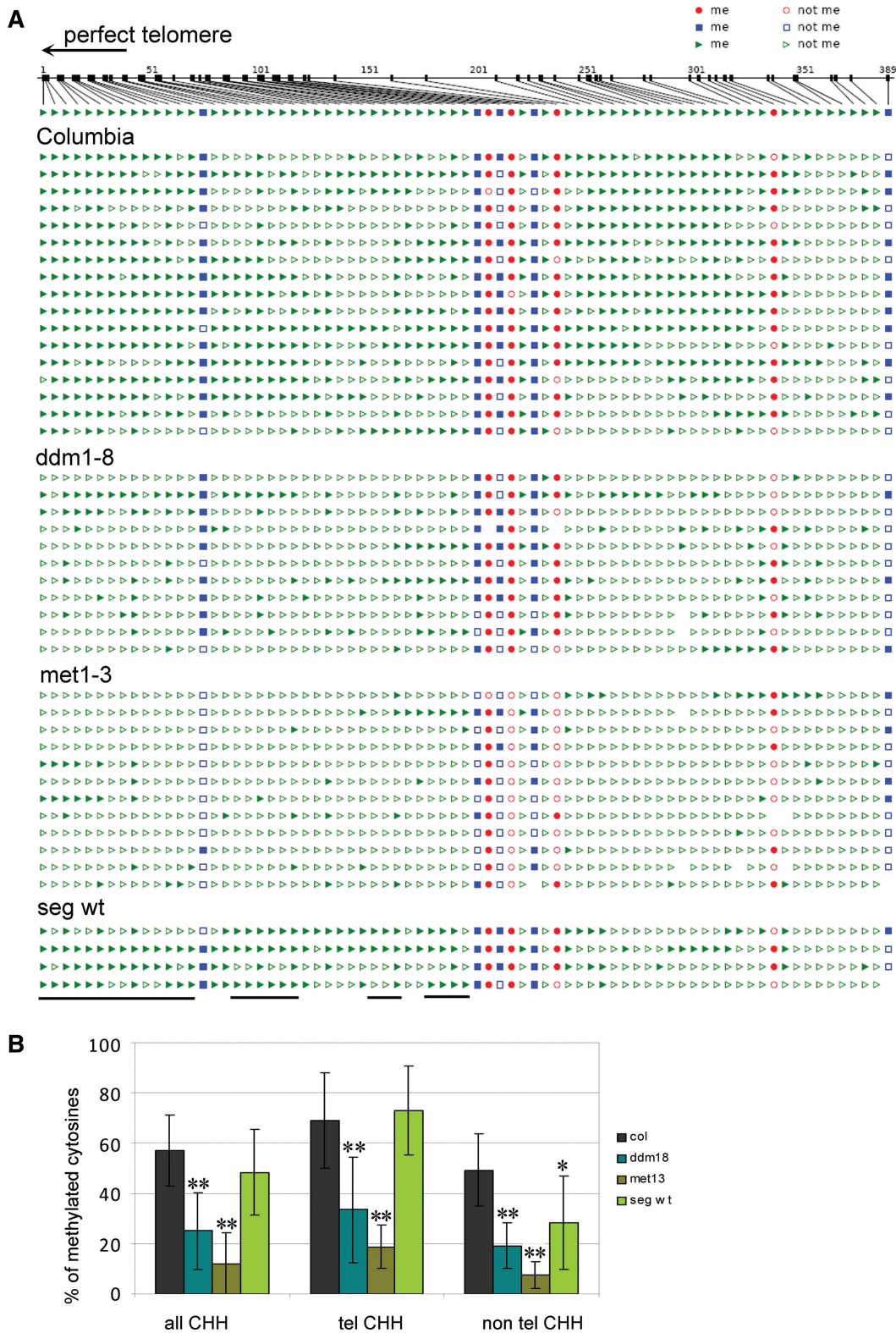


Figure 3. Analysis of cytosine methylation in the proximal part of the 1L telomere arm. (A) Distribution of methylated cytosines along the 389-bp region, which is delimited by primers derived from the subtelomeric region and a specific insertion into the 1L telomere (8). Seventeen clones from three Columbia plants, 11 clones from two *ddm1-8* G2 plants, 12 clones from two *met1-3* G2 plants and 4 clones from a segregated wt plant (seg wt) were analysed. Red circles, CG methylation; blue squares, CHG methylation; green triangles, CHH methylation; filled symbols, methylated cytosine; empty symbols, non-methylated cytosine. Positions of cytosines located in perfect telomeric repeats are delimited by the black lines below the figure. The arrowhead determines the direction to the perfect telomere. (B) Graphical representation of the level of all methylated cytosines located in non-symmetrical sequences (all CHH), in perfect telomeric repeats (tel CHH) and outside these repeats (non-tel CHH). Standard deviations reflect variability between clones. The level of methylated cytosines is significantly lower in methylation mutant clones (** $P < 0.01$ for all sequence contexts). In the segregated wt, methylation of cytosines outside of telomeric repeats (non-tel CHH) is reduced (* $P < 0.05$).

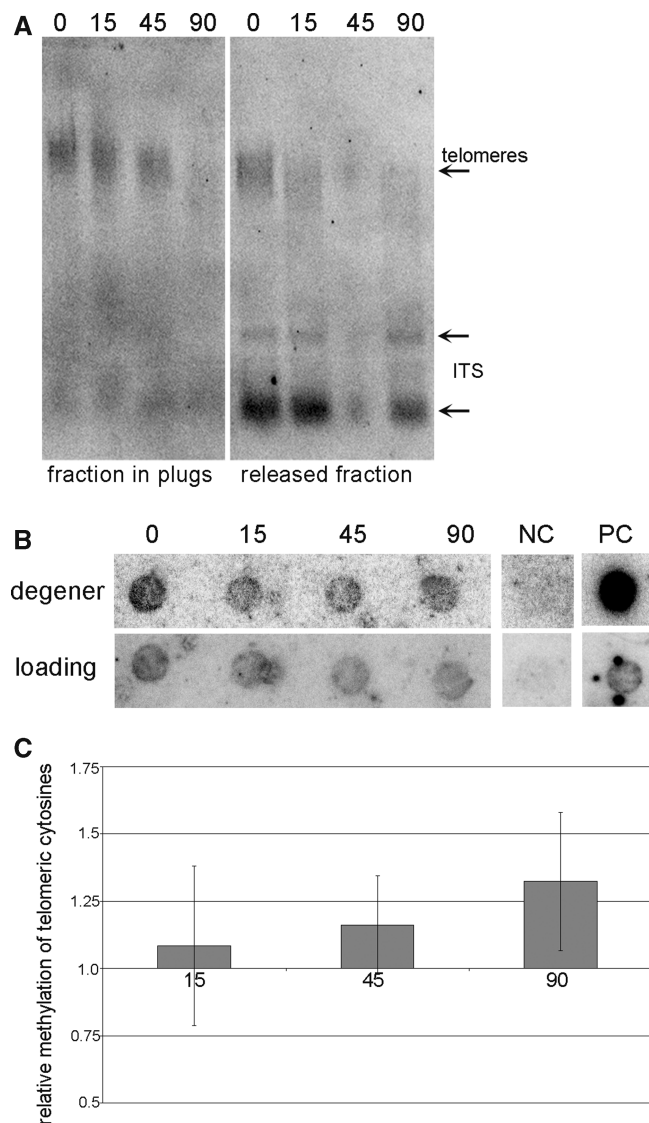


Figure 4. Analysis of relative methylation of cytosines in telomeric repeats. **(A)** High-molecular weight DNA in agarose plugs was digested by Bal31 exonuclease and analysed by TRF. The fraction retained in agarose plugs and the fraction released into the solution were analysed separately. The time of Bal31 digestion (in min) is marked above the lines. The positions of telomeres and ITSs are depicted by arrowheads. **(B)** DNA isolated from agarose plugs was modified by sodium bisulfite and analysed by Southern hybridization with radioactively labelled 'loading' and 'degener' probes. The time of BAL31 digestion (in min) is depicted. NC, negative control, DNA from the plasmid pUC19; PC, positive control, non-modified genomic DNA isolated from *A. thaliana* leaves. **(C)** Relative methylation of telomeric cytosines in Bal31-digested samples. Hybridization signals were evaluated by the MultiGauge software (FujiFilm), and expressed as the 'degener'/'loading' ratio. The ratio in BAL31 non-digested samples was arbitrary taken as 1. Five independent experiments were evaluated.

telomere shortening during subsequent plant generations (50,57). To determine whether telomerase dysfunction is involved in the process of telomere shortening observed in later generations of *met1-3* and *ddm1-8* mutants, and in plants germinated in the presence of hypomethylation drugs, telomerase activity and transcription of the gene encoding the telomerase protein subunit (*AtTERT*) were

analysed in buds, i.e. in tissue with high telomerase activity (58). Telomerase activity and *AtTERT* gene transcription were assayed in generations G2 and G4 of *met1-3* and *ddm1-8* relative to the wt (see Supplementary Methods). Neither telomerase activity nor *AtTERT* transcription was significantly affected in any of the mutants (Supplementary Figure S3). Correspondingly, in plants germinated in the presence of hypomethylation drugs, telomerase activity and transcription were at control levels in telomerase-positive tissues investigated, in 7-day seedlings and in buds (data not shown). Therefore, in *A. thaliana* plants, neither *AtTERT* transcription nor telomerase activity (as examined by assay *in vitro*) was sensitive to hypomethylation.

In addition to telomerase, other proteins involved in telomere homeostasis in *A. thaliana* have been described. Nevertheless, transcription of six selected genes coding for such proteins [telomerase RNA subunits *AtTER1*, *AtTER2* (59), *AtPOT1a* (60), *ATPOT1b* (61,62), *AtTRB1* (63), *AtCTC1* (60)] was at wt levels in buds collected from G2 and G4 generations of *met1-3* and *ddm1-8* mutants, as well as in buds of plants treated with hypomethylation drugs (data not shown). In addition, analysis of TERRA transcripts (see Supplementary Methods) using primers specific for 2R, 3L and 5L chromosome arms (8) did not reveal significant differences between individuals germinated in the presence of 250 μ M DHPA or 250 μ M ZEB, except for slightly elevated levels of TERRA derived from the 3L chromosome arm (Supplementary Figure S4).

Due to the complexity of the process of telomere maintenance, it is tricky to obtain unambiguous information on possible *in vivo* involvement of telomerase in telomere shortening. We analysed telomere lengths in plants with loss of telomerase function; in *tert-/-* mutants (50,57), germinated in the presence and absence of 250 μ M ZEB. According to the working hypothesis, if telomere shortening in hypomethylated *A. thaliana* plants is dependent on telomerase action, then the lengths of telomeres in hypomethylated *tert-/-* mutants would be similar to those in *tert-/-* mutants germinated in control medium because active telomerase is entirely absent here and therefore cannot be modified by hypomethylation during germination. If any telomerase-independent factor participates in telomere shortening, both effects will be additive and presumably telomeres will be even shorter in hypomethylated *tert-/-* mutant plants. As shown in the TRF profiles in Figure 6, telomere lengths in hypomethylated *tert-/-* plants remained the same as those in mutants germinated in control medium. Although these experiments suggest involvement of telomerase in the observed telomere shortening in hypomethylated plants, they do not identify directly a specific underlying step in telomerase *in vivo* regulation.

DISCUSSION

The long-established view of plant telomeres as heterochromatic loci was challenged by the recent data

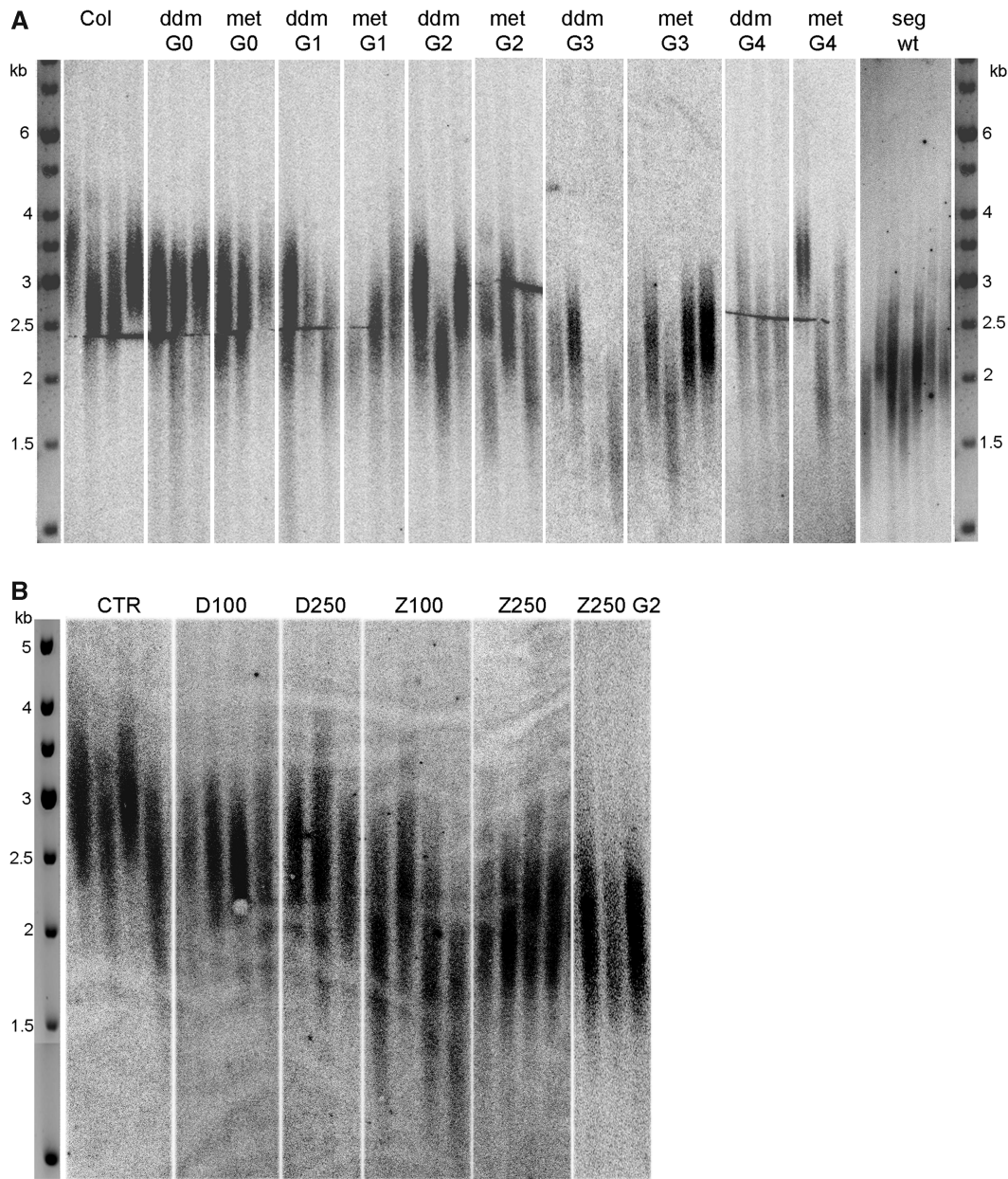


Figure 5. Telomere lengths in hypomethylated *A. thaliana* plants. Lengths of telomeres were analysed by the TRF method in methylation mutants (A) and in plants germinated in the presence of hypomethylation drugs (B). (A) G0–G4 generations of *ddm1-8* and *met1-3* mutant plants and plants without T-DNA insertion segregated from *met1-3* G3 mutants (seg wt, for details, see Figure 1) were analysed. (B) CTR, control non-treated *A. thaliana* plants; D100, plants germinated in the presence of 100 μ M DHPA; D250, plants germinated in the presence of 250 μ M DHPA; Z100, plants germinated in the presence of 100 μ M ZEB; Z250, plants germinated in the presence of 250 μ M ZEB; Z250 G2, progenies of plants germinated in the presence of 250 μ M ZEB.

demonstrating the presence of both heterochromatin- and euchromatin-specific epigenetic modifications of telomeric histones in *A. thaliana* (8). Following an independent study by another group (28), telomeric sequences were hypothesized to have a euchromatic character for *A. thaliana* telomeres and a heterochromatic character for interstitial telomeric sequences. Even in the field of mammalian telomeric chromatin, where data on the importance of heterochromatin-specific modifications for telomere stability were collected mainly using mouse models [reviewed in (64)], the general doctrine of telomeric heterochromatin was challenged by observations in

human cells (16,17). Contrary to the universality of the genetic code, there is no unique or generally valid epigenetic code, and data obtained in different model systems are required to shed more light on the epigenetic nature of telomeric chromatin and to distinguish between specific features of a model system and more general principles.

Methylation of telomeric cytosines is dependent on the activity of MET1 and DDM1 enzymes

Arabidopsis thaliana is an excellent model organism for epigenetic studies due to the accessibility of mutant line

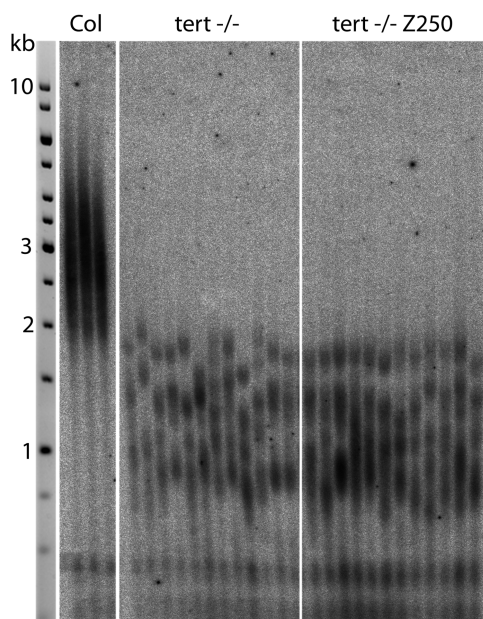


Figure 6. Telomere lengths in hypomethylated telomerase mutant (*tert-/-*) plants. Lengths of telomeres were analysed by TRF in leaves of *tert-/-* plants and *tert-/-* plants germinated for 7 days in the presence of 250 μ M ZEB (*tert-/-* Z250).

collections, including lines with loss-of-function of important epigenetic factors. On the other hand, hypomethylation induced by chemical drugs may be a relatively easy way to disturb an established epigenetic landscape in a broad range of model organisms. Such compounds were used in a pilot study analysing the epigenetic regulation of telomeres in cultured cells of *N. tabacum* (9).

In our experiments, cytosine methylation, including cytosines in telomeric repeats, was significantly lower in mutant plants with loss of function of enzymes (MET1 and DDM1) that are essential for the maintenance of a stable pattern of methylation. After restoration of the wt allele in a *met1-3* mutant background the methylation in both symmetrically (centromeric repeat; Supplementary Figure S1A) and asymmetrically (telomeres; Figures 2 and 3) located cytosines returned almost to the wt pattern. This agrees with a recent observation that loss of methylation in genic regions is persistent in segregated wt while methylation in another type of sequence, transposable elements, recovers to wt level, suggesting site-specific regulation of DNA methylation (65). Similarly, treatment of *A. thaliana* plants with hypomethylation drugs during germination led to a decreased level of telomeric and centromeric cytosine methylation in seedlings, i.e. during the developmental stage when plant tissue is in direct contact with the drug (Figure 2; Supplementary Figure S1B). During cultivation of plants in soil without drugs, DHPA-induced hypomethylation was completely reversed (Figure 2; Supplementary Figure S1B), as was observed in previous experiments using tobacco plants and cell cultures (44,45). Although the hypomethylating effect of ZEB was also reported as transient (41), in our experiments, distinct

hypomethylation of cytosines located in CCGG sequences was detectable even in the next plant generation (Supplementary Figure S1B). This may be due to a higher concentration of ZEB or a different *A. thaliana* ecotype used in our study. Nevertheless, our data agree with that of 5-azacytidine-induced stable hypomethylation of symmetrically located cytosines, as observed in repetitive sequences in tobacco plants (66). This is also consistent with similar hypomethylation mechanisms of both 5-azacytidine and ZEB drugs.

Although in the leaves of methylation mutants loss of methylation of asymmetrically located cytosines in the proximal part of the 1L telomere arm was demonstrated (Figure 3), no changes were detected in drug-treated seedlings (Supplementary Figure S2). This difference may be attributed to different methods of induction of the hypomethylation state (chemical versus genetic).

Even though it was demonstrated that cytosines located in perfect telomeric repeats in the proximal part of the telomere on the 1L chromosome arm are methylated [(8) and Figure 3; Supplementary Figure S2], and that the extent of this methylation is dependent on the activity of MET1 and DDM1 enzymes (Figure 3), questions remain about the level of true (terminal) telomere methylation in *A. thaliana* (28). Our analyses of the relative methylation of cytosines located in CCCTAAA sequences of Bal-31 digested DNA, i.e. in samples depleted of telomeres (Figure 4), demonstrated that cytosines in telomeres and in interstitial telomeric sequences are methylated to similar extents. The finding that cytosines in *A. thaliana* true telomeres are methylated is consistent with the data on drug-induced hypomethylation of telomeric cytosines in tobacco (9) where significant levels of intrachromosomal telomeric repeats were not found (67).

Compromised telomere maintenance in hypomethylated plants raises questions on underlying mechanism

In our previous work, we demonstrated that in *Arabidopsis*, DNA methylation was not significantly involved in the developmental regulation of transcription of the telomerase catalytic subunit (68). Correspondingly, transcription of the telomerase catalytic subunit and telomerase activity *in vitro* were not affected in later generations of *met1-3* and *ddm1-8* mutants nor in plants treated with hypomethylation drugs during germination (Supplementary Figure S3). Analysis of telomerase activity by *in vitro* TRAP assay only provides information on whether active telomerase is present in the extracted material. The absence of an additive effect of hypomethylation and disruption of telomerase activity (Figure 6) suggests (though indirectly) a possible involvement of telomerase in the observed telomere shortening. Although telomerase activity is essential for telomere elongation, the complex process of telomere maintenance involves numerous factors participating in regulation of telomerase activity *in vivo* which cannot be reflected by the used *in vitro* assays. In principle, the genome hypomethylation may affect telomere homeostasis by three ways: (i) directly via modulation of telomerase

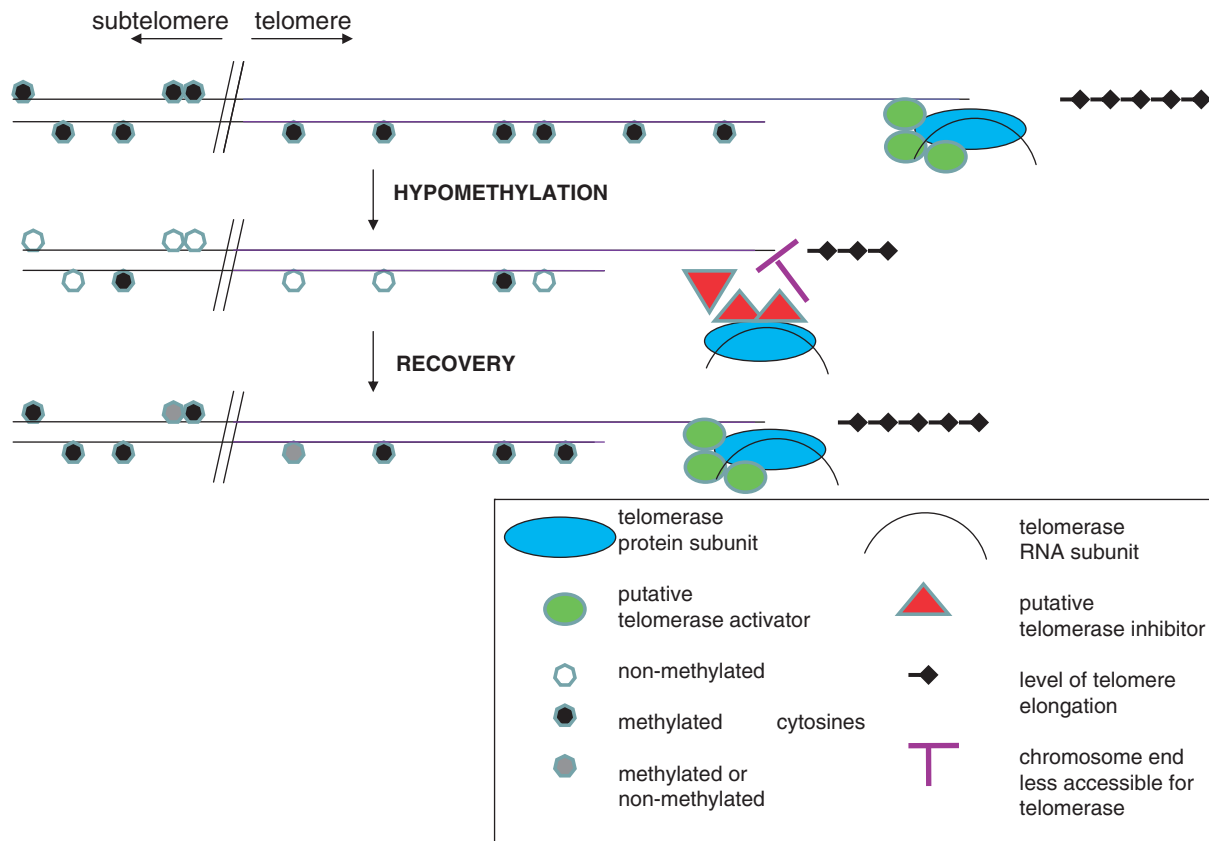


Figure 7. Schematic depiction of the role of telomerase in the process of telomere shortening and in the subsequent propagation of telomeres. Under normal circumstances (top), telomerase is active in telomerase-positive tissues and maintains the length of telomeres. Complex changes in hypomethylated genomes (middle) lead to compromised telomere maintenance (manifested as telomere shortening), which may be caused either by factors modulating telomerase action *in vivo* (e.g. the restricted accessibility of chromosome ends or the absence/presence of not yet-identified telomerase activators/inhibitors) or by telomerase-independent process(es). In wt segregated from the *met1-3* mutant and in the progenies of plants germinated in the presence of ZEB (bottom), telomeres remain shortened and are maintained at the stable length sufficient for normal cell functions by telomerase. The interface between telomeric and subtelomeric regions is marked by an oblique double line.

transcription (and consequently activity)—which was ruled out [Supplementary Figure S3; (68)]; (ii) by compromised function of telomerase ‘holoenzyme’ complex, which includes, in addition to both core telomerase subunits, a group of telomerase-associated protein factors affecting, e.g. telomerase recruitment, intracellular trafficking and localization and (iii) indirectly by a restricted accessibility of telomere chromatin to telomerase.

In animal models, telomere lengthening and increased recombination of telomeres were observed as consequences of the loss of heterochromatin-specific epigenetic modifications, including DNA methylation [(22) and reviewed in (64)]. On the other hand, the presence of critically short telomeres was correlated with hypomethylation of subtelomeric regions (20) or hypomethylation throughout the genome (69). Varied effects described in different animal model systems, and strikingly, quite opposite effects observed between plant and animal systems, are remarkable. Nevertheless, in telomere/telomerase biology and in epigenetics, considerable differences between plant and animal models do exist at many levels, and epigenetic modulation of telomere length—interlinking these two fields—thus logically reflects organism-specific features of both.

In our previous study, telomere lengths were stable, and telomerase activity was elevated in cultured tobacco cells treated with ZEB or DHPA (9), contrary to the observations in *Arabidopsis* where telomerase activity *in vitro* is not changed but telomeres are significantly shorter. These results suggest distinctions in pathways of epigenetic regulation of telomeres and telomerase, even between different model plants. The observed differences may be associated with distinct features of genomes and epigenomes of these plants, in particular a high content of ITSs, a lower global methylation and heterochromatin level (e.g. the absence of subtelomeric chromatin blocks), and a short telomere size in *A. thaliana* compared with *N. tabacum*.

Shortened telomeres are maintained over plant generations

Analysis of telomere lengths in wt plants segregated from the *met1-3* mutant, and in progenies of plant germinated in the presence of 250 μ M ZEB reveals that shorter telomeres are maintained through meiosis. Similar results were obtained using mouse embryonic stem cells impaired in DNA methyltransferases function, but with elongated telomeres (22); a partial increase in subtelomeric DNA methylation was observed after re-introduction of the

methyltransferase gene, but the telomeres remained long. These data indicate that epigenetic stress—loss of DNA methylation—is necessary for implementation of telomere length change, but not for its maintenance. Moreover, telomere shortening in hypomethylated *A. thaliana* is not too dramatic or critical, and very probably does not lead to genomic or chromosomal instabilities (70). Thus telomerase simply maintains the same telomere length as present in parental cells (Figure 7). This scenario is supported by the considerable variability in telomere length, not only between different plant species [i.e. *A. thaliana* ecotype Columbia 3–5 kb, and *N. tabacum* 20–150 kb (71)] but also between different ecotypes of *A. thaliana*; striking variations in telomere length between individuals of the Wassilewskija ecotype have been documented. Crossings between Wassilewskija plants with short and long telomeres showed that telomere length in the progeny was determined by the parental telomere length (72).

Our data demonstrate that similarly to the other repetitive sequences in the plant genome, telomeres are under epigenetic control. Continuation of these studies using different model plants with distinctive telomeric distributions (i.e. *A. thaliana* with a significant proportion of telomeric repeats in interstitial telomeric sequences versus *N. tabacum* with a predominant fraction of telomeric repeats located in telomeres) may reveal new knowledge about specific and general features of plant telomeric chromatin.

SUPPLEMENTARY DATA

Supplementary Data are available at NAR Online.

ACKNOWLEDGEMENTS

Technical assistance of Mrs Jana Kapustova is highly appreciated.

FUNDING

Czech Science Foundation [P501/11/0596], the project ‘CEITEC—Central European Institute of Technology’ [CZ.1.05/1.1.00/02.0068] from the European Regional Development Fund, and the research project RVO61388963 (to Z.J.). Funding for open access charge: the project ‘CEITEC—Central European Institute of Technology’ [CZ.1.05/1.1.00/02.0068].

Conflict of interest statement. None declared.

REFERENCES

- Blackburn,E.H. (2001) Switching and signaling at the telomere. *Cell*, **106**, 661–673.
- Bird,A. (2007) Perceptions of epigenetics. *Nature*, **447**, 396–398.
- Martin,C. and Zhang,Y. (2007) Mechanisms of epigenetic inheritance. *Curr. Opin. Cell Biol.*, **19**, 266–272.
- Mattick,J.S. and Makunin,I.V. (2006) Non-coding RNA. *Hum. Mol. Genet.*, **15**(Spec No 1), R17–R29.
- Lister,R., Pelizzola,M., Dowen,R.H., Hawkins,R.D., Hon,G., Tonti-Filippini,J., Nery,J.R., Lee,L., Ye,Z., Ngo,Q.M. *et al.* (2009) Human DNA methylomes at base resolution show widespread epigenomic differences. *Nature*, **462**, 315–322.
- Zhang,X. (2008) The epigenetic landscape of plants. *Science*, **320**, 489–492.
- Cokus,S.J., Feng,S., Zhang,X., Chen,Z., Merriman,B., Haudenschild,C.D., Pradhan,S., Nelson,S.F., Pellegrini,M. and Jacobsen,S.E. (2008) Shotgun bisulphite sequencing of the *Arabidopsis* genome reveals DNA methylation patterning. *Nature*, **452**, 215–219.
- Vrbsky,J., Akimcheva,S., Watson,J.M., Turner,T.L., Daxinger,L., Vyskot,B., Aufsatz,W. and Riha,K. (2010) siRNA-mediated methylation of *Arabidopsis* telomeres. *PLoS Genet.*, **6**, e1000986.
- Majerova,E., Fojtova,M., Mozgova,I., Bittova,M. and Fajkus,J. (2011) Hypomethylating drugs efficiently decrease cytosine methylation in telomeric DNA and activate telomerase without affecting telomere lengths in tobacco cells. *Plant Mol. Biol.*, **77**, 371–380.
- Penterman,J., Zilberman,D., Huh,J.H., Ballinger,T., Henikoff,S. and Fischer,R.L. (2007) DNA demethylation in the *Arabidopsis* genome. *Proc. Natl Acad. Sci. U.S.A.*, **104**, 6752–6757.
- Zheng,X., Pontes,O., Zhu,J., Miki,D., Zhang,F., Li,W.X., Iida,K., Kapoor,A., Pikaard,C.S. and Zhu,J.K. (2008) ROS3 is an RNA-binding protein required for DNA demethylation in *Arabidopsis*. *Nature*, **455**, 1259–1262.
- Hajkova,P., Jeffries,S.J., Lee,C., Miller,N., Jackson,S.P. and Surani,M.A. (2010) Genome-wide reprogramming in the mouse germ line entails the base excision repair pathway. *Science*, **329**, 78–82.
- Onodera,Y., Haag,J.R., Ream,T., Costa Nunes,P., Pontes,O. and Pikaard,C.S. (2005) Plant nuclear RNA polymerase IV mediates siRNA and DNA methylation-dependent heterochromatin formation. *Cell*, **120**, 613–622.
- Wierzbicki,A.T., Haag,J.R. and Pikaard,C.S. (2008) Noncoding transcription by RNA polymerase Pol IVb/Pol V mediates transcriptional silencing of overlapping and adjacent genes. *Cell*, **135**, 635–648.
- Cao,F., Li,X., Hiew,S., Brady,H., Liu,Y. and Dou,Y. (2009) Dicer independent small RNAs associate with telomeric heterochromatin. *RNA*, **15**, 1274–1281.
- O’Sullivan,R.J., Kubicek,S., Schreiber,S.L. and Karlseder,J. (2010) Reduced histone biosynthesis and chromatin changes arising from a damage signal at telomeres. *Nat. Struct. Mol. Biol.*, **17**, 1218–1225.
- Rosenfeld,J.A., Wang,Z., Schones,D.E., Zhao,K., DeSalle,R. and Zhang,M.Q. (2009) Determination of enriched histone modifications in non-genic portions of the human genome. *BMC Genomics*, **10**, 143.
- Brock,G.J., Charlton,J. and Bird,A. (1999) Densely methylated sequences that are preferentially localized at telomere-proximal regions of human chromosomes. *Gene*, **240**, 269–277.
- de Lange,T., Shiue,L., Myers,R.M., Cox,D.R., Naylor,S.L., Killery,A.M. and Varmus,H.E. (1990) Structure and variability of human chromosome ends. *Mol. Cell. Biol.*, **10**, 518–527.
- Benetti,R., Garcia-Cao,M. and Blasco,M.A. (2007) Telomere length regulates the epigenetic status of mammalian telomeres and subtelomeres. *Nat. Genet.*, **39**, 243–250.
- Benetti,R., Gonzalo,S., Jaco,I., Schotta,G., Klatt,P., Jenuwein,T. and Blasco,M.A. (2007) Suv4-20h deficiency results in telomere elongation and derepression of telomere recombination. *J. Cell Biol.*, **178**, 925–936.
- Gonzalo,S., Jaco,I., Fraga,M.F., Chen,T., Li,E., Esteller,M. and Blasco,M.A. (2006) DNA methyltransferases control telomere length and telomere recombination in mammalian cells. *Nat. Cell Biol.*, **8**, 416–424.
- Ng,L.J., Cropley,J.E., Pickett,H.A., Reddel,R.R. and Suter,C.M. (2009) Telomerase activity is associated with an increase in DNA methylation at the proximal subtelomere and a reduction in telomeric transcription. *Nucleic Acids Res.*, **37**, 1152–1159.
- Palacios,J.A., Herranz,D., De Bonis,M.L., Velasco,S., Serrano,M. and Blasco,M.A. (2011) SIRT1 contributes to telomere maintenance and augments global homologous recombination. *J. Cell Biol.*, **191**, 1299–1313.
- Vera,E., Canela,A., Fraga,M.F., Esteller,M. and Blasco,M.A. (2008) Epigenetic regulation of telomeres in human cancer. *Oncogene*, **27**, 6817–6833.

26. Roberts, A.R., Blewitt, M.E., Youngson, N.A., Whitelaw, E. and Chong, S. (2011) Reduced dosage of the modifiers of epigenetic reprogramming Dnmt1, Dnmt3L, SmcHD1 and Foxo3a has no detectable effect on mouse telomere length in vivo. *Chromosoma*, **120**, 377–385.
27. Kavi, H.H., Xie, W., Fernandez, H.R. and Birchler, J.A. (2005) Global analysis of siRNA-mediated transcriptional gene silencing. *Bioessays*, **27**, 1209–1212.
28. Vaquero-Sedas, M.I., Gamez-Arjona, F.M. and Vega-Palas, M.A. (2010) *Arabidopsis thaliana* telomeres exhibit euchromatic features. *Nucleic Acids Res.*, **39**, 2007–2017.
29. Azzalin, C.M., Reichenbach, P., Khoriavali, L., Giulotto, E. and Lingner, J. (2007) Telomeric repeat containing RNA and RNA surveillance factors at mammalian chromosome ends. *Science*, **318**, 798–801.
30. Farnung, B.O., Brun, C.M., Arora, R., Lorenzi, L.E. and Azzalin, C.M. (2012) Telomerase efficiently elongates highly transcribing telomeres in human cancer cells. *PLoS One*, **7**, e35714.
31. Schoeftner, S. and Blasco, M.A. (2008) Developmentally regulated transcription of mammalian telomeres by DNA-dependent RNA polymerase II. *Nat. Cell Biol.*, **10**, 228–236.
32. Redon, S., Reichenbach, P. and Lingner, J. (2010) The non-coding RNA TERRA is a natural ligand and direct inhibitor of human telomerase. *Nucleic Acids Res.*, **38**, 5797–5806.
33. Pfeiffer, V. and Lingner, J. (2012) TERRA promotes telomere shortening through exonuclease 1-mediated resection of chromosome ends. *PLoS Genet.*, **8**, e1002747.
34. Ronemus, M.J., Galbiati, M., Ticknor, C., Chen, J. and Dellaporta, S.L. (1996) Demethylation-induced developmental pleiotropy in *Arabidopsis*. *Science*, **273**, 654–657.
35. Mathieu, O., Reinders, J., Caikovski, M., Smathajitt, C. and Paszkowski, J. (2007) Transgenerational stability of the *Arabidopsis* epigenome is coordinated by CG methylation. *Cell*, **130**, 851–862.
36. Jeddleloh, J.A., Stokes, T.L. and Richards, E.J. (1999) Maintenance of genomic methylation requires a SWI2/SNF2-like protein. *Nat. Genet.*, **22**, 94–97.
37. Vongs, A., Kakutani, T., Martienssen, R.A. and Richards, E.J. (1993) *Arabidopsis thaliana* DNA methylation mutants. *Science*, **260**, 1926–1928.
38. Kim, C.H., Marquez, V.E., Mao, D.T., Haines, D.R. and McCormack, J.J. (1986) Synthesis of pyrimidin-2-one nucleosides as acid-stable inhibitors of cytidine deaminase. *J. Med. Chem.*, **29**, 1374–1380.
39. Yoo, C.B., Cheng, J.C. and Jones, P.A. (2004) Zebularine: a new drug for epigenetic therapy. *Biochem. Soc. Trans.*, **32**, 910–912.
40. Cihak, A. (1974) Biological effects of 5-azacytidine in eukaryotes. *Oncology*, **30**, 405–422.
41. Baubec, T., Pecinka, A., Rozhon, W. and Mittelsten Scheid, O. (2009) Effective, homogeneous and transient interference with cytosine methylation in plant genomic DNA by zebularine. *Plant J.*, **57**, 542–554.
42. Holy, A. (1975) Aliphatic analogues of nucleosides, nucleotides and oligonucleotides. *Collect. Czech. Chem. C.*, **40**, 187–214.
43. Kovarik, A., Van Houdt, H., Holy, A. and Depicker, A. (2000) Drug-induced hypomethylation of a posttranscriptionally silenced transgene locus of tobacco leads to partial release of silencing. *FEBS Lett.*, **467**, 47–51.
44. Koukalova, B., Votruba, I., Fojtova, M., Holy, A. and Kovarik, A. (2002) Hypomethylation of CNG targets induced with dihydroxypropyladenine is rapidly reversed in the course of mitotic cell division in tobacco. *Theor. Appl. Genet.*, **105**, 796–801.
45. Fulnecek, J., Matyasek, R., Votruba, I., Holy, A., Krizova, K. and Kovarik, A. (2011) Inhibition of SAH-hydrolase activity during seed germination leads to deregulation of flowering genes and altered flower morphology in tobacco. *Mol. Genet. Genomics*, **285**, 225–236.
46. Fojtova, M., Kovarik, A., Votruba, I. and Holy, A. (1998) Evaluation of the impact of S-adenosylhomocysteine metabolic pools on cytosine methylation of the tobacco genome. *Eur. J. Biochem.*, **252**, 347–352.
47. Alonso, J.M. and Stepanova, A.N. (2003) T-DNA mutagenesis in *Arabidopsis*. *Methods Mol. Biol.*, **236**, 177–188.
48. Saze, H., Mittelsten Scheid, O. and Paszkowski, J. (2003) Maintenance of CpG methylation is essential for epigenetic inheritance during plant gametogenesis. *Nat. Genet.*, **34**, 65–69.
49. Jaske, K., Mokros, P., Mozgova, I., Fojtova, M. and Fajkus, J. (2013) A telomerase-independent component of telomere loss in chromatin assembly factor 1 mutants of *Arabidopsis thaliana*. *Chromosoma*, **122**, 285–293.
50. Ruckova, E., Friml, J., Prochazkova Schrupfova, P. and Fajkus, J. (2008) Role of alternative telomere lengthening unmasked in telomerase knock-out mutant plants. *Plant Mol. Biol.*, **66**, 637–646.
51. Clark, S.J., Harrison, J., Paul, C.L. and Frommer, M. (1994) High sensitivity mapping of methylated cytosines. *Nucleic Acids Res.*, **22**, 2990–2997.
52. Hetzl, J., Foerster, A.M., Raidl, G. and Mittelsten Scheid, O. (2007) CyMATE: a new tool for methylation analysis of plant genomic DNA after bisulphite sequencing. *Plant J.*, **51**, 526–536.
53. Fojtova, M., Fulneckova, J., Fajkus, J. and Kovarik, A. (2002) Recovery of tobacco cells from cadmium stress is accompanied by DNA repair and increased telomerase activity. *J. Exp. Bot.*, **53**, 2151–2158.
54. Sykora, E., Fajkus, J., Meznikova, M., Lim, K.Y., Neplechova, K., Blattner, F.R., Chase, M.W. and Leitch, A.R. (2006) Minisatellite telomeres occur in the family Alliaceae but are lost in Allium. *Am. J. Bot.*, **93**, 814–823.
55. Uchida, W., Matsunaga, S., Sugiyama, R. and Kawano, S. (2002) Interstitial telomere-like repeats in the *Arabidopsis thaliana* genome. *Genes Genet. Syst.*, **77**, 63–67.
56. Gamez-Arjona, F.M., Lopez-Lopez, C., Vaquero-Sedas, M.I. and Vega-Palas, M.A. (2010) On the organization of the nucleosomes associated with telomeric sequences. *Biochim. Biophys. Acta*, **1803**, 1058–1061.
57. Fitzgerald, M.S., Riha, K., Gao, F., Ren, S., McKnight, T.D. and Shippen, D.E. (1999) Disruption of the telomerase catalytic subunit gene from *Arabidopsis* inactivates telomerase and leads to a slow loss of telomeric DNA. *Proc. Natl Acad. Sci. U.S.A.*, **96**, 14813–14818.
58. Fitzgerald, M.S., McKnight, T.D. and Shippen, D.E. (1996) Characterization and developmental patterns of telomerase expression in plants. *Proc. Natl Acad. Sci. U.S.A.*, **93**, 14422–14427.
59. Cifuentes-Rojas, C., Kannan, K., Tseng, L. and Shippen, D.E. (2011) Two RNA subunits and POT1a are components of *Arabidopsis* telomerase. *Proc. Natl Acad. Sci. U.S.A.*, **108**, 73–78.
60. Surovtseva, Y.V., Shakirov, E.V., Vespa, L., Osbun, N., Song, X. and Shippen, D.E. (2007) *Arabidopsis* POT1 associates with the telomerase RNP and is required for telomere maintenance. *EMBO J.*, **26**, 3653–3661.
61. Kuchar, M. and Fajkus, J. (2004) Interactions of putative telomere-binding proteins in *Arabidopsis thaliana*: identification of functional TRF2 homolog in plants. *FEBS Lett.*, **578**, 311–315.
62. Shakirov, E.V., Surovtseva, Y.V., Osbun, N. and Shippen, D.E. (2005) The *Arabidopsis* Pot1 and Pot2 proteins function in telomere length homeostasis and chromosome end protection. *Mol. Cell. Biol.*, **25**, 7725–7733.
63. Mozgova, I., Schrupfova, P.P., Hofr, C. and Fajkus, J. (2008) Functional characterization of domains in AtTRB1, a putative telomere-binding protein in *Arabidopsis thaliana*. *Phytochemistry*, **69**, 1814–1819.
64. Blasco, M.A. (2007) The epigenetic regulation of mammalian telomeres. *Nat. Rev. Genet.*, **8**, 299–309.
65. Stroud, H., Greenberg, M.V., Feng, S., Bernatavichute, Y.V. and Jacobsen, S.E. (2013) Comprehensive analysis of silencing mutants reveals complex regulation of the *Arabidopsis* methylome. *Cell*, **152**, 352–364.
66. Vyskot, B., Koukalova, B., Kovarik, A., Sachambula, L., Reynolds, D. and Bezdek, M. (1995) Meiotic transmission of a hypomethylated repetitive DNA family in tobacco. *Theor. Appl. Genet.*, **91**, 659–664.
67. Majerova, E., Fojtova, M., Mandakova, T. and Fajkus, J. (2011) Methylation of plant telomeric DNA: what do the results say?

- (Vaquero-Sedas, M.I. and Vega-Palas, M.A.: DNA methylation at tobacco telomeric sequences). *Plant Mol. Biol.*, **77**, 533–536.
68. Ogrocka, A., Sykorova, E., Fajkus, J. and Fojtova, M. (2012) Developmental silencing of the AtTERT gene is associated with increased H3K27me3 loading and maintenance of its euchromatic environment. *J. Exp. Bot.*, **63**, 4233–4241.
69. Pucci, F., Gardano, L. and Harrington, L. (2013) Short telomeres in ESCs lead to unstable differentiation. *Cell Stem Cell*, **12**, 479–486.
70. Riha, K., McKnight, T.D., Griffing, L.R. and Shippen, D.E. (2001) Living with genome instability: plant responses to telomere dysfunction. *Science*, **291**, 1797–1800.
71. Fajkus, J., Kovarik, A., Kralovics, R. and Bezdek, M. (1995) Organization of telomeric and subtelomeric chromatin in the higher plant *Nicotiana tabacum*. *Mol. Gen. Genet.*, **247**, 633–638.
72. Shakirov, E.V. and Shippen, D.E. (2004) Length regulation and dynamics of individual telomere tracts in wild-type *Arabidopsis*. *Plant Cell*, **16**, 1959–1967.

Epigenetic Regulation of Telomere Maintenance

Miloslava Fojtová Jiří Fajkus

Central European Institute of Technology (CEITEC) and Faculty of Science, Masaryk University, and Institute of Biophysics, Academy of Sciences of the Czech Republic, v.v.i., Brno, Czech Republic

Key Words

Chromatin · DNA methylation · Epigenetics · Histone modifications · Telomerase · Telomere · Telomeric transcripts

Abstract

As chromatin structures, telomeres undergo epigenetic regulation of their maintenance and function. In plants, these processes are likely of a higher complexity than in animals or yeasts, as exemplified by methylation of cytosines in plant telomeric DNA or reversible developmental regulation of plant telomerase. We highlight the dual role of telomeres from the epigenetic point of view: (i) as chromatin structures that are the subject of epigenetic regulation (e.g. DNA and histone modifications), and (ii) as chromosome domains acting themselves as epigenetic regulatory elements (e.g. in the telomere position effect). Possibly, some molecular tools (e.g. telomeric transcripts) are common to both these aspects of telomere epigenetics. We further discuss the justification for the classical textbook view of telomeres as heterochromatic structures.

© 2014 S. Karger AG, Basel

Merging Epigenetics with Telomere Biology

Epigenetics is apparently approaching (if not already passing) its zenith these years. Its importance for shaping cellular phenotypes – programming and possible re-pro-

gramming of the developmental fate of cells – is currently widely recognised, and consequently, this field of research has become rather crowded. As a result of this effort of the large international community, the molecular mechanisms responsible for epigenetic phenomena have been clarified in considerable details, and applications of this knowledge (slowly but surely) are entering practise, e.g. in medicine [reviewed in Bojang and Ramos, 2013], namely in the form of epigenetic drugs [Nebbio et al., 2012].

Epigenetics is beyond doubt the field in which plant model systems have played a dominant role – because of the unmatched richness and diversity of epigenetic tools found in plants. Epigenetic molecular mechanisms including methylation of cytosines in DNA, covalent modifications of histones and RNA interference (RNAi) pathways are involved in regulation of pivotal cellular processes such as gene expression, replication timing, differentiation, and adaptation of the organism to changing environmental conditions. Plants, as sessile organisms, have developed a complex set of epigenetic tools to cope with suboptimal living conditions and adapt to environmental changes. Some of these mechanisms are unique to plants, the striking example being a motley pattern of cytosine methylation. In contrast, in animals methylated cytosines are located almost exclusively in a CG sequence context, although more recent studies have revealed a fraction of methylated cytosines in non-CG motives in de-differentiated human cells [Ramsahoye et al., 2000; Lister

et al., 2009], and 5-methylcytosines in CHG triplets (where H indicates non-G nucleotides) were detected in genes containing trinucleotide repeats in human normal and tumour tissues [Lee et al., 2010]. The functional significance of these modifications remains elusive.

In plants, methylated cytosines are frequently located in symmetric CG doublets and CHG triplets, as well as in non-symmetric CHH sequences, and correspondingly, 3 plant methyltransferase enzymes have been identified. MET1, a dominant plant methyltransferase, is responsible not only for the maintenance of CG methylation (like its mammalian homolog DNMT1) but also for the stability of the general epigenetic pattern including non-CG methylation, histone modifications and chromatin structure [Mathieu et al., 2007]. Methylation of cytosines in symmetric CHG sites is driven by the plant-specific enzyme CHROMOMETHYLASE 3 (CMT3). DOMAINS REARRANGED METHYLTRANSFERASES 1/2 (DRM1/2), orthologs of mammalian DNMT3a/b, cooperate with CMT3 in maintenance of non-symmetric CHH methylation and in de novo methylation of cytosines in all sequence contexts in the process of RNA-directed DNA methylation (RdDM) [Henderson et al., 2010]. RdDM was also originally described in plants and considered as a plant-specific mechanism. Correspondingly, plant-specific RNA polymerases IV and V participating in this process were described [Herr et al., 2005; Wierzbicki et al., 2012]. Inspired by these discoveries in plants, the involvement of RdDM in gene silencing was then demonstrated in human cells [Kawasaki and Taira, 2004; Morris et al., 2004].

Differences have also been described between plant and animal kingdoms in the other type of epigenetic marks – covalent modifications of histone proteins. The pattern of histone modifications is extremely complex, and its combinatorial character in histone amino acids of a particular nucleosome constitutes the basis of the so-called histone code. This code, as well as the other epigenetic codes, does not show universality comparable to the genetic code. A typical example of the striking differences between plants and animals is methylation of lysine 9 of histone H3 and lysine 20 of histone H4: whereas in *Arabidopsis thaliana* mono-methylated lysine residues are associated predominantly with heterochromatic loci and tri-methylated with euchromatin, the situation in mouse is the opposite, with H3K9me and H4K20me present mainly in euchromatin, and H3K9me3 and H4K20me3 in heterochromatin [reviewed in Fransz et al., 2006].

The last epigenetic mechanism briefly mentioned in this introduction is RNAi. In the breakthrough discovery

of this process, plant models played an important role, too. Although the mechanism of RNAi was elucidated using *Caenorhabditis elegans* in 1998 [Fire et al., 1998], several years earlier posttranscriptional silencing of gene expression – at that time called co-suppression – was described (but not explained) in *Petunia hybrida* [Napoli et al., 1990] and has been shown to have the same mechanistic base as RNAi. Among other RNAi processes studied and unravelled using plant models let us mention, for example, the discovery of RNA-dependent RNA polymerase [Dalmay et al., 2000; Mourrain et al., 2000] (this enzyme activity was detected in humans only recently as a specific pathway for double-stranded RNA production [Maida et al., 2009]), the involvement of small RNA molecules in defence processes against viral infection [Waterhouse et al., 1998], and the direct connection between small RNA molecules, DNA methylation and gene silencing [Jones et al., 1998; Mette et al., 2000].

The control of gene activity, and subsequently, of gene expression networks, which establish the cell phenotype (through their impact on the proteome and, ultimately, the metabolome), occurs at the level of chromatin structure. Therefore, the epigenetic landscape, a term used originally by Conrad H. Waddington as a metaphor to express the interconnected roles of stochastic and deterministic events in cell differentiation, can also be understood (in a narrow sense) as a chromatin landscape. Nucleosomal and higher-order-levels of chromatin structure regulate, for example, the accessibility of DNA to transcription factors, the timing of replication, the activity of transposable elements, and the dynamics of DNA repair, utilising the above-mentioned molecular epigenetic mechanisms as well as additional ones like chromatin remodelling or deposition of variant histones to nucleosomes [Zhu et al., 2012]. It is thus evident that epigenetic processes are not limited only to the gene expression level. For example, the process of nucleosome assembly on newly replicated DNA (i.e. an epigenetic process) is tightly connected with maintenance of genome integrity: in chromatin assembly factor 1 mutants of *A. thaliana* (*fas* mutants), a progressive and specific loss of telomeres and rDNA was observed [Mozgova et al., 2010; Jaske et al., 2013].

Telomeres are terminal, but nevertheless integral parts of chromosomes, and as such they are also formed and function as supramolecular nucleoprotein (chromatin) structures. Their DNA component is usually formed by repetitive DNA whose incomplete end-replication by the conventional replication machinery can be compensated by elongation via a specific ribonucleoprotein com-

plex with RNA-dependent DNA polymerase activity – the telomerase. Besides preventing the replicative shortening, telomeres also protect chromosome ends from being mistaken for unrepaired chromosome breaks. For the latter function, protein components of telomeres are responsible (see below). Whereas nucleotide sequences of telomeres are usually homogeneous, of a low degeneracy (as a result of precise synthesis by telomerase and protection of telomeres against recombination), and the same at all chromosome ends, their adjacent proximal sequences (telomere-associated or subtelomeric), forming a boundary region between a telomere and a distal-most gene, are frequently composed of highly degenerated telomere-like motifs, satellite repeats, and single- or low-copy sequences. These may combine in complex subtelomeric arrays [Fajkus et al., 1995a, b; Sykorova et al., 2001, 2003a].

With the exception of some lower organisms with short telomeres (e.g. budding yeasts and some protozoa), the major part of telomeres is folded into nucleosomes [Makarov et al., 1993; Tommerup et al., 1994; Fajkus et al., 1995a] which are regularly spaced but show a 30–40 bp shorter periodicity than the bulk chromatin in the same organism [Lejnine et al., 1995]. All chromatin repeat length values – 156, 166 and 177 bp – observed in telomeres of various eukaryotes [Fajkus and Trifonov, 2001] are multiples of the nucleosome DNA helical repeat of 10.4 bp [Cohan et al., 2006], representing 15–17 times this value. Digestion of telomeric chromatin with micrococcal nuclease results in extensive subnucleosomal cleavage of short (mono- and di-nucleosomal) chromatin fragments [Makarov et al., 1993; Tommerup et al., 1994; Fajkus et al., 1995a]. This likely reflects interplay between telomeric DNA and histones: while wrapping of DNA around histone octamers is intrinsically determined by DNA bendability [Trifonov, 2010], telomeric repeats (mostly 6–8 bp long) do not fit the nucleosome DNA helical repeat of 10.4 bp. Weak nucleosome positioning then results in sliding and lower thermodynamic stability of telomeric nucleosomes [Fajkus et al., 1995a]. Sliding between multiple isoenergetic positions results in high mobility of telomeric nucleosomes under in vitro conditions [Rossetti et al., 1998]. However, the observations of tight and regular nucleosome packing in micrococcal nuclease digestion experiments [Fajkus et al., 1995a], as well as by electron microscopy [Nikitina and Woodcock, 2004], atomic force microscopy, and in reconstitution experiments under near-physiological conditions [Galati et al., 2012] rather point to a stable and periodic structure under in vivo conditions. A possible explanation of the ap-

parent contradiction between the lack of nucleosome positioning signals in telomere DNA sequences and yet their regular chromatin structure was provided by the so-called columnar model [Fajkus and Trifonov, 2001] in which the DNA is continuously wound around columns of histone octamers which are stabilised by interactions between them. Octamer-to-octamer stacking contacts stabilize the overall structure cooperatively, preventing the whole nucleosome structure from sliding.

Recent results show that non-histone chromatin proteins also participate in regulation of telomere homeostasis. Loss of the high mobility group protein HMGB1 results in telomere shortening in *Arabidopsis* [Prochazkova Schrupfova et al., 2011] and mice [Polanska et al., 2012]. In mouse embryonic fibroblasts, HMGB1 interacts with telomerase reverse transcriptase (TERT) and telomerase RNA (TR) subunits, and its loss resulted in a marked decrease in telomerase activity and in the level of TR. Interestingly, loss of the closely related protein HMGB2 showed opposite effects [Polanska et al., 2012].

The functionally best characterised components of mammalian telomeric chromatin are telomere-specific proteins, which are the key performers of basic telomere roles – to distinguish between natural chromosome ends and unrepaired chromosome breaks and the corresponding inhibition of the DNA damage response at telomeres, and to ensure chromosome end-replication via recruitment of telomerase and by facilitating progress of replication forks through telomeres [Palm and de Lange, 2008; de Lange, 2009; Sfeir et al., 2009; Nandakumar et al., 2012; Sfeir and de Lange, 2012]. It is not quite clear whether telomere-specific proteins are able to bind telomeric nucleosomes, or whether they compete with histones for binding to telomeric DNA. The rare contributions to this field deal with the proteins TRF1 and TRF2, which are able to bind the duplex part of vertebrate telomeres and are components of the telomeric complex called shelterin [de Lange, 2005]. TRF1 is able to specifically recognize telomeric binding sites located within nucleosomes, forming a ternary complex. The formation of this complex is strongly dependent on the orientation of binding sites on the nucleosome surface, rather than on the location of the binding sites with respect to the nucleosome dyad [Galati et al., 2006]. The telomeric protein TRF2 negatively regulates nucleosome density during nucleosome assembly by a cell cycle-dependent mechanism that increases internucleosomal distance [Galati et al., 2012]. Chromatin structure thus participates in the establishment of a telomeric capping complex in the nucleosomal context.

In plants, a telomeric complex analogous to shelterin awaits full description in spite of many candidate proteins [for reviews see Rotkova et al., 2009; Peska et al., 2011] and promising recent results of functional and interaction assays of telomere repeat binding proteins [Prochazkova Schrupfova et al., 2014]. Motivation to study telomere protein complements in plants, and plant telomere biology in general, arises from the peculiarities of the plant model system. Among these, the developmental plasticity of plant cells, reflected by their totipotency, is most notable. This implicates reversible regulation of telomerase activity – which we actually demonstrated some time ago [Fajkus et al., 1998; Riha et al., 1998]. Molecular players responsible for reversible telomerase regulation in plant cells pose an attractive target for possible biomedical applications of telomere biology and are sought primarily at the levels of protein components of plant telomeres and regulation of the basic telomerase subunits – TERT and TR.

Plant Telomeres as Subjects of Epigenetic Regulation

As chromatin structures, telomeres pose targets for epigenetic molecular mechanisms including DNA methylation, histone modification, chromatin remodelling or RNAi. In the case of telomeres, however, the ultimate result of these processes is not a change in expression of a target gene, but rather a change of telomere length or structure which may be reflected in modulation of telomere protective function.

Methylation of Cytosines in Plant Telomeres

Telomeric DNA is composed of short tandem repetitive sequences, the primary structure of which is relatively conserved. In vertebrates, telomeres consist of TTAGGG repeats, while in most plants the telomeric repeat has one more T (TTTAGGG). Nevertheless, sequence variability of plant telomeres is relatively high, as the vertebrate telomeric sequence has also been identified in species of the order Asparagales [Adams et al., 2001; Sykorova et al., 2003c]. Plants of the genus *Allium* even lack canonical telomeric sequences at chromosome termini [Pich et al., 1996; Sykorova et al., 2006], and a similar pattern was also observed in representatives of the genera *Cestrum*, *Vestia* and *Sessea* (family Solanaceae) [Sykorova et al., 2003b]. Telomere sequence diversity has been described also in algae [Fulneckova et al., 2012, 2013].

As mentioned above, plant cells possess an enzymatic machinery which enables them to methylate cytosines in all sequence contexts, and thus non-symmetrically located cytosines in CCCTAAA telomeric repeats are potential targets for methylation. The first evidence for telomeric methylcytosines in *A. thaliana* was presented in 2008 [Cokus et al., 2008]. In that study, bisulfite-converted DNA was analysed by shotgun sequencing, and this sensitive high-throughput approach revealed a pattern of DNA methylation in so far inaccessible genome regions including telomeres. According to this data, telomeric cytosines are methylated to a level dependent on the cooperative activities of the enzymes DRM1, DRM2 and CMT3. Moreover, there is an evident preference for methylation among telomeric cytosines: the third (inner) cytosine in the CCCTAAA sequence is methylated most frequently (to about 10%), while methylation of the other cytosines is significantly lower (less than 1%). The presence of methylated cytosines in telomeric repeats in *A. thaliana* leaves and in *Nicotiana tabacum* cells in culture was confirmed by an independent approach based on the hybridisation of membrane-bound bisulfite-converted DNA with radioactively labelled probes. In the *Arabidopsis* study [Vrbsky et al., 2010], a TTTAGGG probe homologous to the telomeric repeat with all cytosines methylated (and thus resistant to bisulfite treatment) was used. In tobacco cells, methylation of telomeric cytosines was determined by a degenerate probe TTTAGRR (R = A or G) better reflecting the pattern of methylation (this probe hybridised with bisulfite-treated telomeric repeats in which the inner cytosine was methylated and the outer cytosines were either methylated or non-methylated) [Majerova et al., 2011b].

In many organisms including plants and humans, telomeric repeats are located not only at the chromosome termini but even inside chromosomes, forming so-called interstitial telomeric sequences (ITSs). These sequences are relatively abundant in the *A. thaliana* genome, encompassing 20–70% of total telomeric repeats (the estimation is dependent on the methodology used and the conditions applied for sequence filtering) [Uchida et al., 2002; Gamez-Arjona et al., 2010]. While genuine telomeric repeats are relatively perfect, ITSs and telomere-associated sequences show high levels of imprecise (degenerated) repeats, and can thus be distinguished by the stringency of hybridisation conditions or directly from DNA sequencing data. Definitely, the presence of a significant amount of telomeric repeats outside the chromosome termini complicates analysis of telomeric DNA methylation and chromatin properties and interpretation of data (see

below). To distinguish between genuine telomeres and ITSs in *A. thaliana*, the restriction endonuclease *Tru1I* (recognition site TTAA) was used leaving telomeres intact but cutting in ITSs, and subsequent analysis using an antibody against methylcytosine revealed methylation only in ITSs [Vaquero-Sedas et al., 2011], conflicting with previous observations [Cokus et al., 2008; Vrbsky et al., 2010]. Nevertheless, methylation of telomeric cytosines in the study of Vrbsky et al. [2010] was verified by hybridization under high stringency conditions, and sequencing data were presented which demonstrated directly the presence of methylated cytosines in 13 perfect telomeric repeats in the centromere-proximal part of the 1L chromosome arm telomere. Further, the pattern of methylation density was the same as that described by Cokus et al. [2008], i.e. with the inner cytosine as the most frequently methylated. Essentially the same results were obtained in our independent study [Ogrocka et al., 2014]. In this context, *N. tabacum* and *Nicotiana* species generally seem to be very useful models for analyses of the epigenetic properties of plant telomeric chromatin for several reasons: (i) to our knowledge, no significant fraction of ITSs is present in the tobacco genome [Majerova et al., 2011a]; (ii) tobacco plants and cell cultures are amenable to most molecular biology approaches; (iii) tobacco is a plant well established in telomere biology, and some fundamental findings such as the first evidence of telomerase activity in plants [Fajkus et al., 1996], characterization of telomeric nucleosomes [Fajkus and Trifonov, 2001] and mapping of telomere-subtelomere junctions [Fajkus et al., 1995b] have been made using this model. In the future, utilization of other methodical approaches and analysis of telomeric cytosine methylation in a broader set of plant models is necessary to make unambiguous and generally applicable conclusions in this field.

Epigenetics of Plant Telomeric Histones

Analysis of epigenetic modifications of telomeric histones faces the same difficulties as studies of DNA methylation – hybridization of immunoprecipitated chromatin fractions (ChIP) with telomeric probes provides aggregated information on marks located at both telomeres and ITSs. For mammalian (especially mouse) models, there are papers reporting the heterochromatin-specific histone marks associated with telomeric and subtelomeric chromatin and their importance for telomere maintenance and stability [reviewed in Blasco, 2007]. Several recent reports dealing with human telomeres, however, question the unequivocal view of telomeres as heterochromatic structures: (i) the level of heterochromatic

marks was surprisingly low in human fibroblast telomeres [O’Sullivan et al., 2010], and (ii) the telomeres of human T-cells were associated with euchromatic marks while heterochromatic H3K9me3 was under-represented [Rosenfeld et al., 2009]. Nevertheless, further data were recently presented supporting the significance of the heterochromatic character of human telomeres for proper telomere function and genome integrity [Canudas et al., 2011; Postepska-Igielska et al., 2013].

In the *A. thaliana* model, hybridisation of ChIP fractions under stringent conditions – to suppress signals from ITSs – revealed both types of epigenetic modification at telomeric chromatin which manifests its dual (bivalent) character termed by the authors ‘intermediate heterochromatin’ [Vrbsky et al., 2010]. On the other hand, in separate analyses of *Tru1I*-sensitive (enriched in ITSs) and -resistant (enriched in genuine telomeres) fractions, telomeric histones were associated with euchromatin-specific modifications while ITSs were marked like heterochromatin [Vaquero-Sedas et al., 2011]. Abundant euchromatic marks at *A. thaliana* telomeres were confirmed by the same group by processing of available ChIP-sequencing data for sequence precision [Vaquero-Sedas et al., 2012]. Since only a limited number of reports are available dealing with the epigenetic analyses of plant telomeric chromatin, mostly using only a single model plant, *A. thaliana*, this topic is open and waiting for new comprehensive data.

Telomere Maintenance in Organisms with a Changed Epigenetic Status

The influence of modulation of the epigenetic pattern on telomere stability and protective function has been studied extensively in mammalian models. Results of Maria Blasco’s group showed that loss of heterochromatin-specific epigenetic modifications, including DNA methylation, resulted in telomere elongation and increased telomere recombination in mouse and human cells [reviewed in Blasco, 2007], and conversely, in cells with loss of telomerase function (thus with shorter telomeres) reduced H3K9me3 loading at telomeres and subtelomeres was detected [Benetti et al., 2007]. These data support an interconnection between the heterochromatic character of telomeres and their correct operation. Nevertheless, in a similar study with mouse epigenetic mutants no change of telomere length was detected [Roberts et al., 2011].

In plants, telomere homeostasis was analysed in hypomethylated *N. tabacum* culture cells and in *A. thaliana* plants. Telomeres of tobacco cells cultivated in the presence of hypomethylation-inducing drugs maintained

their lengths despite significantly increased telomerase activity and both global and telomere hypomethylation [Majerova et al., 2011b]. On the other hand, in *A. thaliana* plants hypomethylated either genetically (mutants with loss of function of enzymes essential for the maintenance of a stable DNA methylation pattern) or chemically (via germination in the presence of hypomethylation drugs), telomerase transcription and activity were at wild type levels, but telomeres were significantly shorter. This short telomere phenotype was stably transmitted to the plants segregated from the mutant background and to the next generation of plants influenced by the hypomethylation drugs during germination [Ogrocka et al., 2014]. These results illustrate the differences in epigenetic regulation of telomere homeostasis not only between animal and plant models, but even among plant species.

Telomeric Transcripts I

Discoveries following the elucidation of the crucial role of RNA molecules in regulation of processes via RNAi mechanisms have transformed the general view of chromatin function. Heterochromatin was traditionally considered as an inactive part of the genome encompassing silent transposons, repetitive elements and inactive genes. Telomeres belonged to this category. Like a bolt from the blue, the report of Volpe et al. [2002] showed that components of the RNAi pathway are essential for proper heterochromatin formation in fission yeast because this requires transcription of heterochromatin. Five years later, it was established that mammalian telomeres are transcribed from subtelomeric regions toward telomeres and that these TERRA transcripts (telomeric repeat-containing RNA) associate with the chromosome termini [Azzalin et al., 2007], thus identifying telomeric RNA as a novel functional component of telomeric chromatin [Schoeftner and Blasco, 2008]. This work is now considered as the first proof of transcription of telomeres, but even earlier reports indicated this possibility [Morcillo et al., 1988; Rudenko and Van der Ploeg, 1989; Solovei et al., 1994]. TERRA, like other long, non-coding transcripts, is believed to have the capacity to epigenetically influence the sequences from which it arose, telomeres and telomeric chromatin.

A positive correlation between telomere length and TERRA transcription was presented by Schoeftner and Blasco [2008]. According to their observations, loss of heterochromatin-specific epigenetic marks in mouse cells led to a long telomere phenotype accompanied by an increased level of TERRA transcripts. On the other hand,

telomere elongation repressed TERRA transcription by increased H3K9me3 density in telomeric chromatin and by heterochromatin protein HP1 α in human cells lines, although the length of TERRA molecules increased upon telomere elongation [Arnoult et al., 2012]. TERRA transcription accelerated telomere shortening in *Saccharomyces cerevisiae* [Pfeiffer and Lingner, 2012], and high TERRA levels were detected in patients suffering from ICF (immunodeficiency, centromeric instability, facial anomalies) syndrome with short telomeres [Yehezkel et al., 2008].

Data reporting the influence of TERRA transcripts on telomeric chromatin and telomere homeostasis in plants are limited, but a complex pattern was observed in *A. thaliana*. While in mammals telomeric transcripts arising only from the subtelomeric region were found, in *Arabidopsis* transcripts originated in both subtelomeres (TERRA) and telomeres (ARRET, antisense telomeric transcripts) were detected – at least at some chromosome termini [Vrbsky et al., 2010]. Moreover, a significant – maybe dominant – fraction of TERRA and ARRET is transcribed from ITSs. A portion of the telomeric transcripts is processed to small RNA molecules which are crucial for the maintenance of methylation of telomeric cytosines via the RdDM pathway (see above). Such processing of telomeric transcripts to small RNAs is not a plant-specific phenomenon; in mouse embryonic stem cells, 24-nt long telomeric transcript molecules were found to be involved in formation of the telomeric heterochromatin [Cao et al., 2009]. Regarding telomeric chromatin structure, the pattern of telomeric histone modifications was essentially the same in *A. thaliana* wild type plants and in mutants with a loss of function of RNA-dependent RNA polymerase in which the level of telomeric siRNAs and telomeric cytosine methylation were significantly reduced. More detailed analysis revealed that close to the telomere-subtelomere boundary, the loading of heterochromatin-specific marks was significantly reduced in the mutant background [Vrbsky et al., 2010], providing evidence for the cooperation of multiple epigenetic mechanisms in the maintenance of plant telomeric and subtelomeric chromatin structure.

Telomeres as Epigenetic Agents

Telomeres are not only targets for epigenetic processes such as DNA methylation and histone modifications, but themselves exert effects on other chromatin domains both in *cis*- and *trans*-positions.

Telomere Position Effect

As a classical example in this direction, the telomere position effect (TPE) should be mentioned. The silencing effect of telomeres on transcriptional activity of adjacent genes (or transgenes) has been first described in the yeast *S. cerevisiae* [Gottschling et al., 1990]; when a gene was placed near a telomere, its transcription was repressed. Genes under the influence of these TPEs can switch between repressed and transcriptionally active states, each of which is quasi-stable for many cell generations. In fact, TPE can be considered as a specific case of the so-called position-effect variegation described in *Drosophila* as the mosaic expression of genes juxtaposed to heterochromatin [Henikoff, 1992]. Yeast telomeres exert TPE not only at the level of gene transcription, but also on the timing of replication origin activation [Ferguson and Fangman, 1992]. Early experiments further showed that TPE could be alleviated by transcription of a telomere, using an inducible promoter which was introduced adjacent to a telomere of a single chromosome arm such that transcription could be induced toward the end of the chromosome. Transcription proceeded through the entire length of the telomeric tract and caused a modest reduction in the average length of the transcribed telomere. Transcription of the telomere substantially reduced the frequency of cells in which an adjacent reporter gene was subject to TPE, without compromising the stability of the chromosome [Sandell et al., 1994]. The importance of this result became evident only recently in connection with the observation of TERRA telomeric transcripts (see above). Besides yeasts and *Drosophila*, TPE has been identified in several other organisms, including mammals. The first systematic study of TPE in human cells showed that HeLa clones containing a reporter gene adjacent to a newly-formed telomere showed 10 times lower expression of the reporter gene than control clones generated by random integration [Baur et al., 2001]. Expression could be restored by trichostatin A, a histone deacetylase inhibitor. Overexpression of hTERT (human telomerase reverse transcriptase) cDNA resulted in telomere elongation and an additional decrease in expression of the reporter gene in telomeric clones. This dependence of TPE on telomere length suggested a novel mechanism modifying gene expression throughout the replicative life-span of human cells, suggesting that telomere shortening could be involved in human diseases not only as a barrier against tumour progression (by generating DNA damage signals which induce replicative senescence), but also as an age-dependent regulator of subtelomeric gene expression. Among natural human subtelomeric genes, however,

only the interferon-stimulated gene 15 (*ISG15*), located 1 Mb from the end of chromosome 1p, has been found to be regulated by telomere length, while the other genes distal to *ISG15* did not show any TPE [Lou et al., 2009]. A role for increased *ISG15* expression in increased inflammatory response in aging was hypothesized, but not demonstrated. The loss of TPE, however, was recently found to contribute to the pathogenesis of facio-scapulo-humeral dystrophy (FSHD), a disease associated with the contraction of a D4Z4 tandem repeat array at the 4q subtelomere. This D4Z4 array functions as an insulator and repressor that interferes with enhancer-promoter communication and protects transgenes from position effects [Ottaviani et al., 2009, 2010], and upon contraction of the array this insulator function is lost. Furthermore, it was found that the *DUX4* (double homeobox 4) gene, located within each of the D4Z4 units, is the primary candidate for FSHD pathogenesis [Jones et al., 2012]; it is upregulated over 10-fold in FSHD myoblasts and myotubes with short telomeres, and its expression is inversely proportional to telomere length [Stadler et al., 2013]. Thus, FSHD may be the first known human disease in which TPE contributes to an age-related phenotype.

At the molecular level, the features of TPE are dependent on a specific higher-order organization of the telomeric chromatin and chromatin-associated proteins. For example, repression of a subtelomeric reporter gene in human cells was alleviated by increasing the dosage of the TRF1 protein or by trichostatin A. Derepression upon trichostatin A treatment correlated with the delocalization of HP1 α and HP1 β proteins. In contrast, 5-azacytidine, a demethylating agent, or sirtinol, an inhibitor of the Sir2 family of deacetylases, had no apparent effect on telomeric repression [Koering et al., 2002]. Contrary to the results of studies with human cell lines, TPE in mouse ES cells was not reversed by trichostatin A, and prolonged culturing resulted in extensive DNA methylation and complete silencing of telomeric transgenes which could be reversed by treatment with 5-azacytidine. Thus, TPE appears to involve a 2-step process in which the initial repression is subsequently reinforced by DNA methylation [Pedram et al., 2006]. TPE – as an epigenetic phenomenon – is dependent on genetic background, as was nicely illustrated by introduction of the same linear human artificial chromosome into genetically distinct cell lines and animal models [Weuts et al., 2012]. Telomere lengths and de novo subtelomeric DNA methylation in this construct adapted to distinct genetic backgrounds, and expression of subtelomeric genes was inversely correlated with telomere length and subtelomeric methylation.

In contrast to many other organisms with extensive gene-poor subtelomeric regions, telomeres in *A. thaliana* are directly adjacent to transcriptionally active genes. In this configuration, telomeres are more similar to silenced transposons inserted in gene-rich regions than to pericentromeric heterochromatin [Vrbsky et al., 2010]. This is also reflected in the intermediate heterochromatin features of telomeres and the very limited expansion of repressive histone H3 modifications to telomere-associated regions [Bernatavichute et al., 2008; Vrbsky et al., 2010]. Correspondingly, TPE has not been observed in *A. thaliana*. Also, the absence of replicative telomere shortening during plant development [Fajkus et al., 1998; Riha et al., 1998] probably excludes the possibility of a modulation of subtelomeric gene activity by telomere truncation similar to that observed for human *ISG15* or *DUX4* genes (see above). *A. thaliana* with its relatively short telomeres of intermediate heterochromatin character may, of course, represent a specific case and not provide general conclusions. TPE could possibly be present in plants with long telomeres and large subtelomeric heterochromatin blocks, like e.g. tobacco [Fajkus et al., 1995a, b]. Although very limited information is available here, a stable maintenance and expression of subtelomeric insertions has been demonstrated in tobacco [Iglesias et al., 1997], without any marks of TPE. The question of TPE in plants thus requires further investigation.

In addition to TPE, a recent report suggests that short telomeres can affect transgene expression at non-telomeric sites in the mouse [Roberts et al., 2013]. Using multiple generations of *Terc* knockout mice (lacking a functional gene coding for the RNA subunit of telomerase), the authors showed that inheriting shorter telomeres from one parent increased the likelihood of transcriptional silencing at a non-telomeric transgene inherited from the other parent, and that reduced transgene expression during embryonic development was associated with the inheritance of shorter telomeres rather than lack of *Terc*. The activity of a non-telomeric transgene further decreased in the next generations and was associated with increased DNA methylation and also with genetic changes, including variations in copy number at the transgene array. Although the mechanism of this *in trans* effect of short telomeres is unknown, it apparently involves both genetic and epigenetic pathways.

Telomeric Transcripts II

Considering the functions of telomeric transcripts, we could find ourselves in a vicious circle: telomeric transcripts as epigenetic factors may modulate the struc-

ture of telomeric chromatin and influence telomere homeostasis, as discussed in the preceding paragraphs, while on the other hand TERRA transcripts are derived from telomeres and in this context may represent a tool for telomere-mediated epigenetic regulation. A striking example is an interconnection between TERRA level and telomerase activity. Inhibition of telomerase by TERRA was observed in in-vitro experiments in human [Redon et al., 2010] and in mouse [Schoeftner and Blasco, 2008] cells. On the other hand, telomerase activity was not dependent on the TERRA level in vivo in yeast [Pfeiffer and Lingner, 2012] or in human cancer cells [Farnung et al., 2012]. Recent experiments demonstrated that heterogeneous nuclear ribonucleoprotein A1 (hnRNPA1), which is involved in RNA biogenesis and telomere maintenance, may alleviate inhibition of telomerase by TERRA, providing a possible explanation for the contradiction between the in vitro and in vivo data [Redon et al., 2013].

To our knowledge, only one report dealt with the connection between TERRA and telomerase activity in plants. In tobacco suspension culture cells cultivated in the presence of hypomethylation drugs, a decrease or an increase of TERRA levels was observed depending on the drug used, while in both cases telomerase activity increased significantly [Majerova et al., 2011b]. These results suggest that factors other than changed TERRA transcription are involved in modulation of telomerase activity in this system. Plant models would offer possibilities to study the potential influence of elongated or shortened telomeres on TERRA transcription because *Arabidopsis* mutants exhibiting these phenotypes – long or short telomeres – are available. However, there is an obstacle which is common in plant telomere biology: transcripts are derived from both genuine telomeres and from ITSs, and although it is possible to analyse transcription from the respective telomeres specifically by PCR [Vrbsky et al., 2010], evaluation and interpretation of the data would be complicated. Promising results in this field will likely depend on novel approaches and studies of other model species.

Conclusions

The epigenetics of telomeres associates problems of both epigenetics and telomere biology, but – due to the relative universality and essentiality of telomeres – provides findings and perspective discoveries of fundamental importance. We are already aware of the variety of

colours (or flavours) of plant chromatin, as well as of the alternative telomeres and variant telomere-maintenance mechanisms in plants. So the coming steps will not be simple but surely exciting.

Acknowledgement

This work was supported by the Czech Science Foundation (P501/11/0596, P501/11/0289), by the project 'CEITEC – Central European Institute of Technology' (CZ.1.05/1.1.00/02.0068) from the European Regional Development Fund, and by projects CZ.1.07/2.3.00/20.0189 and CZ.1.07/2.3.00/20.0043 from the European Social Fund.

References

- Adams SP, Hartman TP, Lim KY, Chase MW, Bennett MD, et al: Loss and recovery of *Arabidopsis*-type telomere repeat sequences 5'-(TTTAGGG)_n-3' in the evolution of a major radiation of flowering plants. *Proc Biol Sci* 268:1541–1546 (2001).
- Arnoult N, Van Beneden A, Decottignies A: Telomere length regulates TERRA levels through increased trimethylation of telomeric H3K9 and HP1α. *Nat Struct Mol Biol* 19:948–956 (2012).
- Azzalin CM, Reichenbach P, Khoraiuli L, Giulotto E, Lingner J: Telomeric repeat containing RNA and RNA surveillance factors at mammalian chromosome ends. *Science* 318:798–801 (2007).
- Baur JA, Zou Y, Shay JW, Wright WE: Telomere position effect in human cells. *Science* 292:2075–2077 (2001).
- Benetti R, Garcia-Cao M, Blasco MA: Telomere length regulates the epigenetic status of mammalian telomeres and subtelomeres. *Nat Genet* 39:243–250 (2007).
- Bernatavichute YV, Zhang X, Cokus S, Pellegrini M, Jacobsen SE: Genome-wide association of histone H3 lysine nine methylation with CHG DNA methylation in *Arabidopsis thaliana*. *PLoS One* 3:e3156 (2008).
- Blasco MA: The epigenetic regulation of mammalian telomeres. *Nat Rev Genet* 8:299–309 (2007).
- Bojang P Jr, Ramos KS: The promise and failures of epigenetic therapies for cancer treatment. *Cancer Treat Rev* 40:153–169 (2013).
- Canudas S, Houghtaling BR, Bhanot M, Sasa G, Savage SA, et al: A role for heterochromatin protein 1γ at human telomeres. *Genes Dev* 25:1807–1819 (2011).
- Cao F, Li X, Hiew S, Brady H, Liu Y, Dou Y: Dicer independent small RNAs associate with telomeric heterochromatin. *RNA* 15:1274–1281 (2009).
- Cohananim AB, Kashi Y, Trifonov EN: Three sequence rules for chromatin. *J Biomol Struct Dyn* 23:559–566 (2006).
- Cokus SJ, Feng S, Zhang X, Chen Z, Merriman B, et al: Shotgun bisulphite sequencing of the *Arabidopsis* genome reveals DNA methylation patterning. *Nature* 452:215–219 (2008).
- Dalmay T, Hamilton A, Rudd S, Angell S, Baulcombe DC: An RNA-dependent RNA polymerase gene in *Arabidopsis* is required for posttranscriptional gene silencing mediated by a transgene but not by a virus. *Cell* 101:543–553 (2000).
- de Lange T: Shelterin: the protein complex that shapes and safeguards human telomeres. *Genes Dev* 19:2100–2110 (2005).
- de Lange T: How telomeres solve the end-protection problem. *Science* 326:948–952 (2009).
- Fajkus J, Trifonov EN: Columnar packing of telomeric nucleosomes. *Biochem Biophys Res Commun* 280:961–963 (2001).
- Fajkus J, Kovarik A, Kralovics R, Bezdek M: Organization of telomeric and subtelomeric chromatin in the higher-plant *Nicotiana tabacum*. *Mol Gen Genet* 247:633–638 (1995a).
- Fajkus J, Kralovics R, Kovarik A, Fajkusova L: The telomeric sequence is directly attached to the HRS60 subtelomeric tandem repeat in tobacco chromosomes. *FEBS Lett* 364:33–35 (1995b).
- Fajkus J, Kovarik A, Kralovics R: Telomerase activity in plant cells. *FEBS Lett* 391:307–309 (1996).
- Fajkus J, Fulneckova J, Hulanova M, Berkova K, Riha K, Matyasek R: Plant cells express telomerase activity upon transfer to callus culture, without extensively changing telomere lengths. *Mol Gen Genet* 260:470–474 (1998).
- Farnung BO, Brun CM, Arora R, Lorenzi LE, Azzalin CM: Telomerase efficiently elongates highly transcribing telomeres in human cancer cells. *PLoS One* 7:e35714 (2012).
- Ferguson BM, Fangman WL: A position effect on the time of replication origin activation in yeast. *Cell* 68:333–339 (1992).
- Fire A, Xu S, Montgomery MK, Kostas SA, Driver SE, Mello CC: Potent and specific genetic interference by double-stranded RNA in *Caenorhabditis elegans*. *Nature* 391:806–811 (1998).
- Franz P, ten Hoopen R, Tessadori F: Composition and formation of heterochromatin in *Arabidopsis thaliana*. *Chromosome Res* 14:71–82 (2006).
- Fulneckova J, Hasikova T, Fajkus J, Lukesova A, Elias M, Sykora E: Dynamic evolution of telomeric sequences in the green algal order Chlamydomonadales. *Genome Biol Evol* 4:248–264 (2012).
- Fulneckova J, Sevcikova T, Fajkus J, Lukesova A, Lukes M, et al: A broad phylogenetic survey unveils the diversity and evolution of telomeres in eukaryotes. *Genome Biol Evol* 5:468–483 (2013).
- Galati A, Rossetti L, Pisano S, Chapman L, Rhodes D, et al: The human telomeric protein TRF1 specifically recognizes nucleosomal binding sites and alters nucleosome structure. *J Mol Biol* 360:377–385 (2006).
- Galati A, Magdiniere F, Colasanti V, Bauwens S, Pinte S, et al: TRF2 controls telomeric nucleosome organization in a cell cycle phase-dependent manner. *PLoS One* 7:e34386 (2012).
- Gamez-Arjona FM, Lopez-Lopez C, Vaquero-Sedas MI, Vega-Palas MA: On the organization of the nucleosomes associated with telomeric sequences. *Biochim Biophys Acta* 1803:1058–1061 (2010).
- Gottschling DE, Aparicio OM, Billington BL, Zakian VA: Position effect at *S. cerevisiae* telomeres: reversible repression of Pol II transcription. *Cell* 63:751–762 (1990).
- Hendersson IR, Deleris A, Wong W, Zhong X, Chin HG, et al: The de novo cytosine methyltransferase DRM2 requires intact UBA domains and a catalytically mutated paralog DRM3 during RNA-directed DNA methylation in *Arabidopsis thaliana*. *PLoS Genet* 6:e1001182 (2010).
- Henikoff S: Position effect and related phenomena. *Curr Opin Genet Dev* 2:907–912 (1992).
- Herr AJ, Jensen MB, Dalmay T, Baulcombe DC: RNA polymerase IV directs silencing of endogenous DNA. *Science* 308:118–120 (2005).
- Iglesias VA, Moscone EA, Papp I, Neuhuber F, Michalowski S, et al: Molecular and cytogenetic analyses of stably and unstably expressed transgene loci in tobacco. *Plant Cell* 9:1251–1264 (1997).
- Jaske K, Mokros P, Mozgova I, Fojtova M, Fajkus J: A telomerase-independent component of telomere loss in chromatin assembly factor 1 mutants of *Arabidopsis thaliana*. *Chromosome* 122:285–293 (2013).
- Jones AL, Thomas CL, Maule AJ: De novo methylation and co-suppression induced by a cytoplasmically replicating plant RNA virus. *EMBO J* 17:6385–6393 (1998).

- Jones TI, Chen JCJ, Rahimov F, Homma S, Arashiro P, et al: Facioscapulohumeral muscular dystrophy family studies of *DUX4* expression: evidence for disease modifiers and a quantitative model of pathogenesis. *Hum Mol Genet* 21:4419–4430 (2012).
- Kawasaki H, Taira K: Induction of DNA methylation and gene silencing by short interfering RNAs in human cells. *Nature* 431:211–217 (2004).
- Koering CE, Pollice A, Zibella MP, Bauwens S, Puisieux A, et al: Human telomeric position effect is determined by chromosomal context and telomeric chromatin integrity. *EMBO Rep* 3:1055–1061 (2002).
- Lee J, Jang SJ, Benoit N, Hoque MO, Califano JA, et al: Presence of 5-methylcytosine in CpNpG trinucleotides in the human genome. *Genomics* 96:67–72 (2010).
- Lejnine S, Makarov VL, Langmore JP: Conserved nucleoprotein structure at the ends of vertebrate and invertebrate chromosomes. *Proc Natl Acad Sci USA* 92:2393–2397 (1995).
- Lister R, Pelizzola M, Dowen RH, Hawkins RD, Hon G, et al: Human DNA methylomes at base resolution show widespread epigenomic differences. *Nature* 462:315–322 (2009).
- Lou ZJ, Wei J, Riethman H, Baur JA, Voglauer R, et al: Telomere length regulates ISG15 expression in human cells. *Aging* 1:608–621 (2009).
- Maida Y, Yasukawa M, Furuuchi M, Lassmann T, Possemato R, et al: An RNA-dependent RNA polymerase formed by TERT and the *RMRP* RNA. *Nature* 461:230–235 (2009).
- Majerova E, Fojtova M, Mandakova T, Fajkus J: Methylation of plant telomeric DNA: What do the results say? (author reply). *Plant Mol Biol* 77:533–536 (2011a).
- Majerova E, Fojtova M, Mozgova I, Bittova M, Fajkus J: Hypomethylating drugs efficiently decrease cytosine methylation in telomeric DNA and activate telomerase without affecting telomere lengths in tobacco cells. *Plant Mol Biol* 77:371–380 (2011b).
- Makarov VL, Lejnine S, Bedoyan J, Langmore JP: Nucleosomal organization of telomere-specific chromatin in rat. *Cell* 73:775–787 (1993).
- Mathieu O, Reinders J, Caikovski M, Smathajitt C, Paszkowski J: Transgenerational stability of the *Arabidopsis* epigenome is coordinated by CG methylation. *Cell* 130:851–862 (2007).
- Mette MF, Aufsatz W, van der Winden J, Matzke MA, Matzke AJ: Transcriptional silencing and promoter methylation triggered by double-stranded RNA. *EMBO J* 19:5194–5201 (2000).
- Morcillo G, Barettono D, Carmona MJ, Carretero MT, Diez JL: Telomeric DNA sequences differentially activated by heat shock in two *Chironomus* subspecies. *Chromosoma* 96:139–144 (1988).
- Morris KV, Chan SW, Jacobsen SE, Looney DJ: Small interfering RNA-induced transcriptional gene silencing in human cells. *Science* 305:1289–1292 (2004).
- Mourrain P, Beclin C, Elmayan T, Feuerbach F, Godon C, et al: *Arabidopsis* *SGS2* and *SGS3* genes are required for posttranscriptional gene silencing and natural virus resistance. *Cell* 101:533–542 (2000).
- Mozgova I, Mokros P, Fajkus J: Dysfunction of chromatin assembly factor 1 induces shortening of telomeres and loss of 45S rDNA in *Arabidopsis thaliana*. *Plant Cell* 22:2768–2780 (2010).
- Nandakumar J, Bell CF, Weidenfeld I, Zaug AJ, Leinwand LA, Cech TR: The TEL patch of telomere protein TPP1 mediates telomerase recruitment and processivity. *Nature* 492:285–289 (2012).
- Napoli C, Lemieux C, Jorgensen R: Introduction of a chimeric chalcone synthase gene into *Petunia* results in reversible co-suppression of homologous genes *in trans*. *Plant Cell* 2:279–289 (1990).
- Nebbioso A, Carafa V, Benedetti R, Altucci L: Trials with ‘epigenetic’ drugs: an update. *Mol Oncol* 6:657–682 (2012).
- Nikitina T, Woodcock CL: Closed chromatin loops at the ends of chromosomes. *J Cell Biol* 166:161–165 (2004).
- Ogrocka A, Polanska P, Majerova E, Janeba Z, Fajkus J, Fojtova M: Compromised telomere maintenance in hypomethylated *Arabidopsis thaliana* plants. *Nucleic Acids Res* 42:2919–2931 (2014).
- O’Sullivan RJ, Kubicek S, Schreiber SL, Karlseder J: Reduced histone biosynthesis and chromatin changes arising from a damage signal at telomeres. *Nat Struct Mol Biol* 17:1218–1225 (2010).
- Ottaviani A, Rival-Gervier S, Boussouar A, Foerster AM, Rondier D, et al: The D4Z4 macrosatellite repeat acts as a CTCF and A-type lamins-dependent insulator in facio-scapulo-humeral dystrophy. *PLoS Genet* 5:e1000394 (2009).
- Ottaviani A, Schluth-Bolard C, Gilson E, Magdiner F: D4Z4 as a prototype of CTCF and lamins-dependent insulator in human cells. *Nucleus* 1:30–36 (2010).
- Palm W, de Lange T: How shelterin protects mammalian telomeres. *Annu Rev Genet* 42:301–334 (2008).
- Pedram M, Sprung CN, Gao Q, Lo AWI, Reynolds GE, Murnane JP: Telomere position effect and silencing of transgenes near telomeres in the mouse. *Mol Cell Biol* 26:1865–1878 (2006).
- Peska V, Prochazkova Schruppova P, Fajkus J: Using the telobox to search for plant telomere binding proteins. *Curr Protein Pept Sci* 12:75–83 (2011).
- Pfeiffer V, Lingner J: TERRA promotes telomere shortening through exonuclease 1-mediated resection of chromosome ends. *PLoS Genet* 8:e1002747 (2012).
- Pich U, Fuchs J, Schubert I: How do Alliaceae stabilize their chromosome ends in the absence of TTTAGGG sequences? *Chromosome Res* 4:207–213 (1996).
- Polanska E, Dobsakova Z, Dvorackova M, Fajkus J, Stros M: HMGB1 gene knockout in mouse embryonic fibroblasts results in reduced telomerase activity and telomere dysfunction. *Chromosoma* 121:419–431 (2012).
- Postepska-Igielska A, Krunic D, Schmitt N, Greulich-Bode KM, Boukamp P, Grummt I: The chromatin remodelling complex NoRC safeguards genome stability by heterochromatin formation at telomeres and centromeres. *EMBO Rep* 14:704–710 (2013).
- Prochazkova Schruppova P, Fojtova M, Mokros P, Grasser KD, Fajkus J: Role of HMGB proteins in chromatin dynamics and telomere maintenance in *Arabidopsis thaliana*. *Curr Protein Pept Sci* 12:105–111 (2011).
- Prochazkova Schruppova P, Vychodilova I, Dvorackova M, Majerska J, Dokladal L, et al: Telomere repeat binding proteins are functional components of *Arabidopsis* telomeres and interact with telomerase. *Plant J* 77:770–781 (2014).
- Ramsahoye BH, Binizkiewicz D, Lyko F, Clark V, Bird AP, Jaenisch R: Non-CpG methylation is prevalent in embryonic stem cells and may be mediated by DNA methyltransferase 3a. *Proc Natl Acad Sci USA* 97:5237–5242 (2000).
- Redon S, Reichenbach P, Lingner J: The non-coding RNA TERRA is a natural ligand and direct inhibitor of human telomerase. *Nucleic Acids Res* 38:5797–5806 (2010).
- Redon S, Zemp I, Lingner J: A three-state model for the regulation of telomerase by TERRA and hnRNPA1. *Nucleic Acids Res* 41:9117–9128 (2013).
- Riha K, Fajkus J, Siroky J, Vyskot B: Developmental control of telomere lengths and telomerase activity in plants. *Plant Cell* 10:1691–1698 (1998).
- Roberts AR, Blewitt ME, Youngson NA, Whitelaw E, Chong S: Reduced dosage of the modifiers of epigenetic reprogramming *Dnmt1*, *Dnmt3L*, *SmcHD1* and *Foxo3a* has no detectable effect on mouse telomere length *in vivo*. *Chromosoma* 120:377–385 (2011).
- Roberts AR, Huang E, Jones L, Daxinger L, Chong S, Whitelaw E: Non-telomeric epigenetic and genetic changes are associated with the inheritance of shorter telomeres in mice. *Chromosoma* 122:541–554 (2013).
- Rosenfeld JA, Wang Z, Schones DE, Zhao K, DeSalle R, Zhang MQ: Determination of enriched histone modifications in non-genic portions of the human genome. *BMC Genomics* 10:143 (2009).
- Rossetti L, Cacchione S, Fua M, Savino M: Nucleosome assembly on telomeric sequences. *Biochemistry* 37:6727–6737 (1998).
- Rotkova G, Sykorova E, Fajkus J: Protect and regulate: recent findings on plant POT1-like proteins. *Biol Plantarum* 53:1–4 (2009).
- Rudenko G, Van der Ploeg LH: Transcription of telomere repeats in protozoa. *EMBO J* 8:2633–2638 (1989).

- Sandell LL, Gottschling DE, Zakian VA: Transcription of a yeast telomere alleviates telomere position effect without affecting chromosome stability. *Proc Natl Acad Sci USA* 91:12061–12065 (1994).
- Schoeftner S, Blasco MA: Developmentally regulated transcription of mammalian telomeres by DNA-dependent RNA polymerase II. *Nat Cell Biol* 10:228–236 (2008).
- Sfeir A, de Lange T: Removal of shelterin reveals the telomere end-protection problem. *Science* 336:593–597 (2012).
- Sfeir A, Kosiyatrakul ST, Hockemeyer D, MacRae SL, Karlseder J, et al: Mammalian telomeres resemble fragile sites and require TRF1 for efficient replication. *Cell* 138:90–103 (2009).
- Solovei I, Gaginskaya ER, Macgregor HC: The arrangement and transcription of telomere DNA sequences at the ends of lampbrush chromosomes of birds. *Chromosome Res* 2:460–470 (1994).
- Stadler G, Rahimov F, King OD, Chen JCJ, Robin JD, et al: Telomere position effect regulates *DUX4* in human facioscapulohumeral muscular dystrophy. *Nat Struct Mol Biol* 20:671–678 (2013).
- Sykorova E, Fajkus J, Ito M, Fukui K: Transition between two forms of heterochromatin at plant subtelomeres. *Chromosome Res* 9:309–323 (2001).
- Sykorova E, Cartagena J, Horakova M, Fukui K, Fajkus J: Characterization of telomere-subtelomere junctions in *Silene latifolia*. *Mol Genet Genomics* 269:13–20 (2003a).
- Sykorova E, Lim KY, Chase MW, Knapp S, Leitch IJ, et al: The absence of *Arabidopsis*-type telomeres in *Cestrum* and closely related genera *Vestia* and *Sessea* (Solanaceae): first evidence from eudicots. *Plant J* 34:283–291 (2003b).
- Sykorova E, Lim KY, Kunicka Z, Chase MW, Bennett MD, et al: Telomere variability in the monocotyledonous plant order Asparagales. *Proc Biol Sci* 270:1893–1904 (2003c).
- Sykorova E, Fajkus J, Meznikova M, Lim KY, Neplechova K, et al: Minisatellite telomeres occur in the family Alliaceae but are lost in *Allium*. *Am J Bot* 93:814–823 (2006).
- Tommerup H, Dousmanis A, de Lange T: Unusual chromatin in human telomeres. *Mol Cell Biol* 14:5777–5785 (1994).
- Trifonov EN: Nucleosome positioning by sequence, state of the art and apparent finale. *J Biomol Struct Dyn* 27:741–746 (2010).
- Uchida W, Matsunaga S, Sugiyama R, Kawano S: Interstitial telomere-like repeats in the *Arabidopsis thaliana* genome. *Genes Genet Syst* 77:63–67 (2002).
- Vaquero-Sedas MI, Gamez-Arjona FM, Vega-Palás MA: *Arabidopsis thaliana* telomeres exhibit euchromatic features. *Nucleic Acids Res* 39:2007–2017 (2011).
- Vaquero-Sedas MI, Luo C, Vega-Palás MA: Analysis of the epigenetic status of telomeres by using ChIP-seq data. *Nucleic Acids Res* 40:e163 (2012).
- Volpe TA, Kidner C, Hall IM, Teng G, Grewal SI, Martienssen RA: Regulation of heterochromatic silencing and histone H3 lysine-9 methylation by RNAi. *Science* 297:1833–1837 (2002).
- Vrbsky J, Akimcheva S, Watson JM, Turner TL, Daxinger L, et al: siRNA-mediated methylation of *Arabidopsis* telomeres. *PLoS Genet* 6:e1000986 (2010).
- Waterhouse PM, Graham MW, Wang MB: Virus resistance and gene silencing in plants can be induced by simultaneous expression of sense and antisense RNA. *Proc Natl Acad Sci USA* 95:13959–13964 (1998).
- Weuts A, Voet T, Verbeeck J, Lambrechts N, Wirix E, et al: Telomere length homeostasis and telomere position effect on a linear human artificial chromosome are dictated by the genetic background. *Nucleic Acids Res* 40:11477–11489 (2012).
- Wierzbicki AT, Cocklin R, Mayampurath A, Lister R, Rowley MJ, et al: Spatial and functional relationships among Pol V-associated loci, Pol IV-dependent siRNAs, and cytosine methylation in the *Arabidopsis* epigenome. *Genes Dev* 26:1825–1836 (2012).
- Yehezkel S, Segev Y, Viegas-Pequignot E, Skorecki K, Selig S: Hypomethylation of subtelomeric regions in ICF syndrome is associated with abnormally short telomeres and enhanced transcription from telomeric regions. *Hum Mol Genet* 17:2776–2789 (2008).
- Zhu Y, Dong AW, Shen WH: Histone variants and chromatin assembly in plant abiotic stress responses. *Biochim Biophys Acta* 1819:343–348 (2012).

SI CHROMATIN AND DEVELOPMENT

Chromatin dynamics of plant telomeres and ribosomal genes

Martina Dvořáčková^{1,2,3}, Miloslava Fojtová^{1,2,3} and Jiří Fajkus^{1,2,3,*}¹Mendel Centre for Plant Genomics and Proteomics, Central European Institute of Technology, Kamenice 5, 62500 Brno, Czech Republic²Faculty of Science, Masaryk University, Kamenice 5, 62500 Brno, Czech Republic, and³Institute of Biophysics, Academy of Sciences of the Czech Republic, Královopolská 135, 61265 Brno, Czech Republic

Received 28 January 2015; revised 3 March 2015; accepted 3 March 2015.

*For correspondence (e-mail fajkus@sci.muni.cz).

SUMMARY

Telomeres and genes encoding 45S ribosomal RNA (rDNA) are frequently located adjacent to each other on eukaryotic chromosomes. Although their primary roles are different, they show striking similarities with respect to their features and additional functions. Both genome domains have remarkably dynamic chromatin structures. Both are hypersensitive to dysfunctional histone chaperones, responding at the genomic and epigenomic levels. Both generate non-coding transcripts that, in addition to their epigenetic roles, may induce gross chromosomal rearrangements. Both give rise to chromosomal fragile sites, as their replication is intrinsically problematic. However, at the same time, both are essential for maintenance of genomic stability and integrity. Here we discuss the structural and functional inter-connectivity of telomeres and rDNA, with a focus on recent results obtained in plants.

Keywords: telomere, rDNA, *Arabidopsis thaliana*, *Nicotiana tabacum*, chromatin, epigenetics.

TELOMERES, rDNA REPETITIVE SEQUENCES AND GENOME STABILITY

Specific genomic elements have been shown to be crucial for maintenance of genome integrity. Telomeres, complex nucleoprotein structures forming the physical ends of linear eukaryotic chromosomes, represent such genomic regions, and, in some organisms, are considered as a part of the cellular clock machinery determining the life span of the cell. Due to the intrinsic properties of the DNA replication process, telomeres are shortened during each cell division, and act as a physical barrier to protect genetic information inside the chromosomes. Shortening of telomeres to a critical level is a signal to stop the cell cycle and start the processes of cellular senescence. Elongation of telomere repeats may be accomplished by telomerase (Greider and Blackburn, 1985), a specific ribonucleoprotein enzyme complex. In humans, telomerase activity is repressed in most somatic tissues during development. Loss of telomerase activity in terminally differentiated human tissues leads to a short-telomere phenotype and natural ageing at the level of cells and the whole organism (Hayflick, 1982; Greider, 1990; Harley *et al.*, 1990). The progress of developmental silencing of telomerase activity

differs among mammalian model organisms, e.g. telomerase expression and activity have been detected in mouse somatic tissues (Horikawa *et al.*, 2005). In plants, telomerase is not silenced during embryogenesis, and remains active in organs and tissues containing dividing meristematic cells (seedlings, root tips, floral buds, blossom) throughout plant ontogenesis; telomerase becomes silenced only in terminally differentiated organs (mature leaves). Correspondingly, the lengths of telomeres are maintained during plant development, and remain stable even in tissues with inactive telomerase. Moreover, telomerase silencing in differentiated cells is reversible, and telomerase may be re-activated, for example upon initiation of cell division during plant regeneration from leaf mesophyll cells, reflecting the totipotent character of plant cells (Fajkus *et al.*, 1998).

In mammalian tissues with inactive telomerase, telomeres are inevitably shortened in the course of cell division. De-regulation of telomere lengths is a reliable marker of genomic instability (Banerjee and Myung, 2004; Hong *et al.*, 2007). In human cells, proper telomere function is crucial for healthy development, and pathological shortening of telomeres leads to genomic instability and serious malfunctions, such as in dyskeratosis congenita, aplastic

anaemia, or immunodeficiency, centromere instability and facial anomalies syndrome. On the other hand, re-activation of telomere maintenance in terminally differentiated cells is one of the basic premises with respect to cellular immortalization and cancer development. Telomere erosion in *Arabidopsis thaliana* mutants lacking telomerase is relatively mild, as only 250–500 bp of telomeric repeats are lost in each plant generation, without apparent phenotypic defects in early plant generations (Fitzgerald *et al.*, 1999; Riha *et al.*, 2001). A plausible explanation for this effect is that a recombination-based process of alternative lengthening of telomeres (ALT), which is active during early plant development, may partially compensate for the loss of telomerase function (Ruckova *et al.*, 2008).

Apart from telomeres (and of course centromeres; Lerontova *et al.*, in this issue), other elements may also be associated with genomic stability. Recently, a hypothesis was discussed suggesting that, in budding yeast, the stability of rDNA loci (DNA coding for ribosomal RNA) has a clear effect on cellular life span, as extra copies of rDNA were shown to protect budding yeast from sensitivity to the DNA-damaging agents methyl methane sulfonate and UV irradiation (Ide *et al.*, 2010; Ganley and Kobayashi, 2011). Ribosomal genes belong to the category of housekeeping genes. Unlike telomeres, rDNA does not experience an end-replication problem that leads to its shortening with each cell division, and is present in the genome as a multi-copy gene family encompassing long (frequently sub-telomeric) chromosomal segments. However, the instability of rDNA originates from the requirement for its transcriptional activity during almost the entire cell cycle, including S phase. Due to these transcriptional requirements, extra copies of rDNA are required for proper rDNA cohesion during DNA damage repair processes (Ide *et al.*, 2010). Moreover, many DNA breaks are introduced into rDNA during replication by protein machinery present at the replication fork barrier (RFB) site, which initiates controlled replication fork stalling to allow replication only in the direction of transcription (Kobayashi and Horiuchi, 1996; Banerjee and Myung, 2004; Sofueva *et al.*, 2011). Breaks within rDNA due to the activity of FOB1 (fork blocking less) may be repaired by equal or unequal sister chromatid recombination, which leads to the rDNA copy number maintenance or rDNA copy number changes, respectively (Ganley *et al.*, 2009). In budding yeast, many factors influencing rDNA copy number have been described, and are summarized in Table 1. Altogether, the intrinsically unstable character of rDNA requires a demanding quality check system to maintain rDNA integrity and appropriate copy number (Kobayashi, 2014). The instability of rDNA caused by malfunction of the replication fork blocking system may thus play a role as a sensor of genome instability, even in the absence of critical telomere shortening.

STRUCTURE OF TELOMERIC AND rDNA CHROMATIN

In eukaryotes, the majority of the genome is arranged in nucleosomes, which are basic structural units of chromatin. Nucleosomes not only have a fundamental structural role in the multi-level processes of DNA compaction, but represent dynamic functional units modulating DNA accessibility. Crucial metabolic pathways such as gene expression, DNA repair and replication, and cell-cycle progression are affected through histone post-translational modifications, the presence of histone variants and ATP-dependent remodelling (reviewed in Saha *et al.*, 2006).

From a cytological point of view, *A. thaliana* telomeres and 45S rDNA are close neighbours. In all ecotypes of *A. thaliana* so far studied, the 45S rDNA loci are positioned sub-terminally, at the distal ends of the short arms of chromosomes 2 and 4 (Figure 1a) (Kaul *et al.*, 2000). In some organisms, telomeres and rDNA even show an intermingled arrangement. For example, in the flagellated unicellular eukaryote *Giardia lamblia*, short tandem repeats of telomere-like sequences are present in the distal-most rRNA genes (Le Blancq *et al.*, 1991). In the *Tetrahymena* thermophila macronucleus, telomeric sequences in rDNA mini-chromosomes partially overlap with non-transcribed spacers of rDNA. While the bulk rDNA of this ciliate is packed with histones in typical nucleosomes (Piper *et al.*, 1976), the part adjacent to telomeres is packed into three specifically positioned nucleosomes, and non-nucleosomal organization is present at the transcription termination site (Budarf and Blackburn, 1986).

Telomeres in lower eukaryotes are usually short and are associated with specific proteins in non-nucleosomal structures, termed telosomes. Telomeres of higher eukaryotes are organized in nucleosomes, displaying an unusual repeat length of approximately 157 bp, i.e. 20–40 bp shorter than the bulk chromatin (Makarov *et al.*, 1993; Tommerup *et al.*, 1994; Fajkus *et al.*, 1995; as reviewed in Pisano *et al.*, 2008). Based on analyses of short human telomeres, a hypothesis regarding the non-nucleosomal structure of distal telomere ends has been presented (Tommerup *et al.*, 1994). It is important to consider the complex structural pattern of telomeric chromatin, which is essential for the telomere protective functions in which many proteins (largely uncharacterized in the case of plants) participate (Table 2). Most telomeres possess a single-stranded DNA overhang formed by a G-rich strand that is required to form a specific structure termed a telomeric loop (t-loop) (Griffith *et al.*, 1999). The t-loop is believed to be essential for telomere capping (reviewed in de Lange, 2004). Another specific local DNA structure that may be formed by the G-rich strand of telomeres is a four-stranded structure (G quadruplex, G4), whose various topology variants have been demonstrated to form *in vitro* (reviewed in Burge *et al.*, 2006) and *in vivo* (Paeschke

Table 1 Factors involved in rDNA stability in *S. cerevisiae*

Factor	Full name	Function within the rDNA locus	rDNA-related phenotype in mutants	References
Replication and transcription-related elements				
ARS	Autonomously replicating sequence	Initiation of replication	Inability to amplify copies	Ganley <i>et al.</i> (2009)
E-pro	EXP promoter (RNA polymerase II promoter)	Initiation of IGS transcription, removal of cohesin, stimulation of unequal sister chromatid exchange	Inability to amplify copies	Kobayashi and Ganley (2005); Kobayashi <i>et al.</i> (2001)
FOB1	Fork blocking less 1	RFB protein, inhibition of bi-directional replication, induction of double-stranded DNA breaks, rDNA silencing through recruitment of the RENT complex (regulator of nucleolar silencing and telophase)	Decreased recombination, inability to amplify copies	Houseley and Tollervey (2011); Huang and Moazed (2003); Kobayashi (2006)
RPA135	RNA Polymerase A 135	Subunit of RNA polymerase I, transcription of rDNA	Copy number reduction	Kobayashi <i>et al.</i> (1998)
POL32	Polymerase 32	Subunit of DNA polymerase δ , DNA replication, DNA repair	Reduced ability to amplify copies, reduced copy number	Houseley and Tollervey (2011)
POL2	Polymerase	Subunit of DNA polymerase ϵ , involved in break induced replication	Inability to amplify copies, copy number fluctuation and reduction	Houseley and Tollervey (2011)
DNA repair proteins				
MRE11	Meiotic recombination homologue 11	Endonuclease, subunit of the MRX complex (MRE11 RAD50 XRS2), DNA double-strand break repair, resection of DNA at broken sites	Inability to amplify copies	Bentsen <i>et al.</i> (2013); Kobayashi <i>et al.</i> (2004)
RAD52	DNA repair and recombination protein 52	Annealing of complementary single-stranded DNA, stimulation of the RAD51 recombinase, break induced replication	Inability to amplify copies	Kobayashi <i>et al.</i> (2004)
Histone-modifying enzymes and silencing factors				
RTT109	Regulator of Ty1 transposition	Histone acetyl transferase, maintenance of chromatin structure, prevention of break induced replication	Large copy number expansion	Houseley and Tollervey (2011)
ASF1	Anti-silencing factor 1	Acetylation of H3K56, nucleosome assembly and remodelling	Copy number expansion	Houseley and Tollervey (2011)
SIR2	Silent information regulator 2	Histone deacetylase of the Sirtuin family, subunit of the RENT complex, silencing of rDNA, suppression of E-pro transcription, prevention of unequal sister chromatid exchange, association with RFB, repression of rDNA origins, regulation of rDNA cohesion	Increased frequency of repeat contraction and expansion leading to higher heterogeneity within the rDNA locus, increased recombination, decreased cohesion	Gottlieb and Esposito (1989); Huang and Moazed (2003); Kobayashi <i>et al.</i> (1998, 2004); Yoshida <i>et al.</i> (2014)
JHD2	Jumonji C domain-containing histone demethylase 2	SIR2-independent rDNA silencing, telomere silencing, H3K4 demethylase	Hypercondensation during mitosis	Ryu and Ahn (2014)
NSI1	NTS1 silencing protein 1	Interaction with RENT and FOB1, rDNA silencing	Increased recombination	Ha <i>et al.</i> (2012)

(continued)

Table 1. (continued)

Factor	Full name	Function within the rDNA locus	rDNA-related phenotype in mutants	References
Other factors				
SMC1	Stability of mini-chromosomes 1	Cohesin, chromosome segregation, double-stranded DNA break repair	Increased unequal recombination within rDNA	Kobayashi <i>et al.</i> (2004); Strunnikov <i>et al.</i> (1993)
SMC2 SMC4	Structural maintenance of chromosomes 2 and 4	Condensin, correct separation of rDNA during M phase, association upstream of ARS, binding to RFB and polymerase I promoter	Increased mitotic recombination, absence of sister chromatid separation, rDNA decondensation	Bhalla <i>et al.</i> (2002); Freeman <i>et al.</i> (2000)
TOP1	Topoisomerase 1	Relaxation of positively and negatively supercoiled DNA, regulation of RNA polymerase I transcription	Increased recombination, R-loop formation, inhibition of rDNA transcription	El Hage <i>et al.</i> (2010)
TRF4/ PAP2	Poly(A) polymerase 2	Subunit of the TRAMP complex (TRF4/AIR2/MTR4 polyadenylation), polyadenylation of hypomodified tRNAs, snoRNA and rRNA precursors, degradation of IGS transcripts	Copy number fluctuation	Houseley <i>et al.</i> (2007)

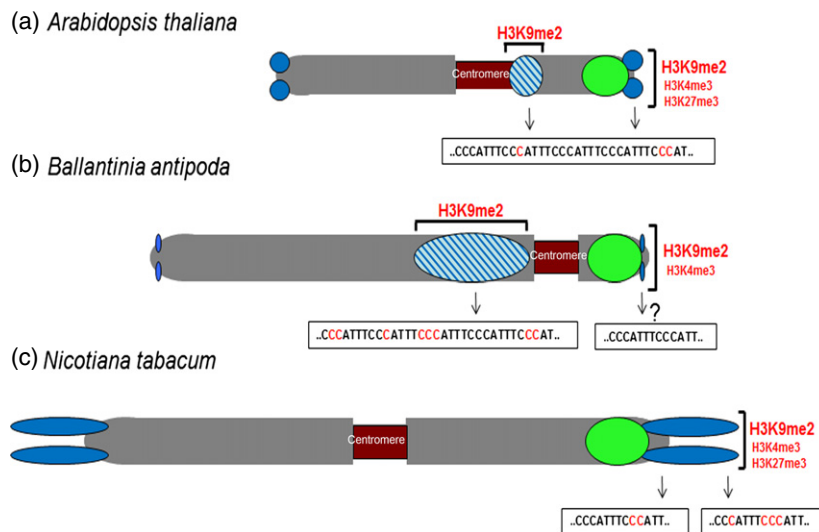


Figure 1. Arrangement of telomeres (blue circles/ellipses at chromosome ends), ITRs (light blue shaded circle/ellipse inside chromosomes) and rDNA loci (green ellipses) on chromosomes of model species *Arabidopsis thaliana* (a), *Ballantinia antipoda* (b) and *Nicotiana tabacum* (c).

In *A. thaliana* (a), length of telomeres ranges between 2 and 9 kb, depending on ecotype (Shakirov and Shippen, 2004); ITRs are located close to the centromere on the short arm of chromosome 1 (Richards *et al.*, 1991), and other ITR loci are located around the centromeres on chromosomes 2 and 3 and close to the telomere on chromosome 2 (Uchida *et al.*, 2002). Blocks of rDNA are located in sub-telomeric regions of the short arms of chromosomes 2 and 4 (Kaul *et al.*, 2000; Siroky, 2008). Cytosines in telomeres and ITRs are methylated (red Cs) to approximately the same extent (Ogrocka *et al.*, 2014), the chromatin of telomeres exhibits dual character with the prevalence of the heterochromatic H3K9me2 histone mark (Vrbsky *et al.*, 2010), and the chromatin of ITRs is largely heterochromatic. In *B. antipoda* (b), genuine telomeres are relatively short, and large blocks of ITRs are located in pericentromeric regions of all chromosomes (Mandakova *et al.*, 2010; Majerova *et al.*, 2014). 45S rDNA loci are located at the distal ends of chromosomes 2 and 5 (Mandakova *et al.*, 2010). Cytosines in ITRs are methylated, and the level of methylation varies between ITR loci, and the nature of telomeric and ITRs chromatin is essentially the same as in *A. thaliana* (Majerova *et al.*, 2014). *N. tabacum* (c) has long (60–160 kb) and heterogeneous telomeres (Fajkus *et al.*, 1995), and no ITR fraction was found in its genome (Majerova *et al.*, 2011b, 2014). Blocks of rDNA are located at the distal ends of chromosomes 10, 11 and 12 from the S parental genome (*Nicotiana sylvestris*) and chromosome 3 from the T parental genome (*Nicotiana tomentosiformis*) (Lim *et al.*, 2000). The level of heterochromatin-specific modifications at telomeric histones is greater than that of euchromatin-specific modifications, and, as in *A. thaliana*, the H3K27me3 mark was associated with telomeres. Telomeric cytosines are methylated, with a higher density in the distal parts of telomeres (Majerova *et al.*, 2014).

Table 2 Proteins involved in telomere length maintenance in plants. Proteins with the telomere phenotype are referenced

Protein	Function	Telomere phenotype in mutant plants ^a	References
Telomere-binding proteins			
TBP1	Telomere-binding protein; telomeric DNA <i>in vitro</i> binding	Telomere elongation in <i>A. thaliana</i>	Hwang and Cho (2007)
TRB1	Telomere repeat-binding protein; co-localization with telomeres, interaction with telomerase	Telomere shortening in <i>A. thaliana</i>	Schrumpfova <i>et al.</i> (2014)
WHY1	Binding of telomeric single-stranded DNA	Telomere elongation via the telomerase pathway in <i>A. thaliana</i>	Yoo <i>et al.</i> (2007)
GTBP1	G-strand-specific single-stranded telomere-binding protein	Telomere elongation, increased level of extra-chromosomal telomeric circles, chromosome fusions in <i>N. tabacum</i>	Lee and Kim (2010)
TRF1	Binding of telomeric double-stranded DNA in tobacco	Suppression results in telomere elongation; over-expression results in telomere shortening in <i>N. tabacum</i> cell culture	Yang <i>et al.</i> (2004)
Proteins involved in the telomerase pathway			
POT1 ^b in <i>Physcomitrella patens</i>	Telomere protection and binding to telomeric single-stranded DNA	Telomere shortening, increased level of G overhangs, chromosome fusions	Shakirov <i>et al.</i> (2005); Surovtseva <i>et al.</i> (2007); Shakirov <i>et al.</i> (2010)
POT1a in <i>A. thaliana</i>	No telomeric DNA binding, involvement in the telomerase pathway	Loss causes progressive telomere shortening	
POT1b in <i>A. thaliana</i>	Role in chromosome end protection	Over-expression causes telomere shortening and fusions	
NAP57 (dyskerin)	Component of active telomerase ribonucleoprotein	Null mutation lethal in <i>A. thaliana</i> ; mutated allele results in telomere shortening via the telomerase pathway	Kannan <i>et al.</i> (2008)
Telomere protection complexes			
CST	Telomere protection complex comprising CTC1, STN1 and TEN1	Telomere shortening, increased telomere recombination and chromosome fusions in <i>A. thaliana</i>	Song <i>et al.</i> (2008); Surovtseva <i>et al.</i> (2009); Leehey <i>et al.</i> (2013)
KU70/80	Component of non-homologous end-joining DNA repair pathway; association with chromosome ends, protection from nucleolysis	Telomere elongation in <i>A. thaliana</i> and <i>Oryza sativa</i> ; increased level of extra-chromosomal telomeric circles in <i>A. thaliana</i> KU70 mutants	Bundock and Hooykaas (2002); Riha <i>et al.</i> (2002); Gallego <i>et al.</i> (2003); Riha and Shippen (2003); Hong <i>et al.</i> (2010)
MRN	Protein complex comprising MRE11, RAD50 and NBS1; involved in recognition and signalling of double-stranded DNA breaks	MRE11 loss of function results in telomere elongation in <i>A. thaliana</i> ; RAD50 loss of function results in telomere shortening in <i>A. thaliana</i>	Gallego and White (2001); Bundock and Hooykaas (2002)
Proteins involved in DNA replication and chromatin structure maintenance			
HMG-B	High-mobility group protein B; modulation of chromatin architecture, involvement in DNA-related processes (transcription, replication, repair, recombination)	Telomere shortening in <i>A. thaliana</i>	Schrumpfova <i>et al.</i> (2011)
CAF1	Chromatin assembly factor 1; H3/H4 histone chaperone, replication-dependent nucleosome assembly	Progressive telomere shortening in <i>A. thaliana</i>	Mozgova <i>et al.</i> (2010)

(continued)

Table 2. (continued)

Protein	Function	Telomere phenotype in mutant plants ^a	References
DDM1	Decrease of DNA methylation, chromatin remodelling factor	Telomere shortening in <i>A. thaliana</i>	Ogrocka <i>et al.</i> (2014)
MET1	Dominant DNA methyltransferase, CG methylation	Telomere shortening in <i>A. thaliana</i>	Ogrocka <i>et al.</i> (2014)
DRM1,2/CMT3	Non-CG DNA methyltransferases	Telomere shortening in <i>A. thaliana</i>	Vaquero-Sedas and Vega-Palas (2014)
RPA1	Replication protein A1; component of a protein complex involved in DNA-related processes	Telomere elongation in <i>A. thaliana</i>	Takashi <i>et al.</i> (2009)

^aAlternative functional studies are described when loss-of-function mutants were not available.

^bIn addition to the results shown, detailed biochemical analysis across the plant kingdom revealed *in vitro* binding of *Z. mays* POT1b paralogue and POT1 proteins from *Asparagus officinalis* and green algae *Ostreococcus lucimarinus* to telomeric single-stranded DNA (Shakirov *et al.*, 2009).

et al., 2005; reviewed in Lipps and Rhodes, 2009). In addition to telomeres, G4 structures have been reported to form at a number of gene promoters, e.g. of the MYCC gene (Simonsson *et al.*, 1998).

Complexity of processes taking place at chromosomal ends has dramatically increased with the discovery of telomeric repeat-containing RNA (TERRA), which is thought to play a significant role in the regulation of telomere maintenance. As TERRA is formed by the G-rich strand, it is able to form G quadruplexes (Phan, 2010), although the functional consequences of this arrangement remain to be elucidated. The potential of G4 structures to prevent access of telomerase to chromosomal ends is being examined with respect to the design of anticancer drugs (Crees *et al.*, 2014), because telomerase is involved in cell proliferation in approximately 85% of cancers.

Despite their presumed importance, the existence of G overhangs at telomeres is not generally conserved. A detailed analysis of *A. thaliana* telomeres revealed that approximately half of the chromosomal ends are blunt-ended, or contain very short 1–3 nt G overhangs, but the functional integrity of these telomeres is maintained (Riha *et al.*, 2000; Kazda *et al.*, 2012). In organisms that typically use telomerase for telomere extension (including humans), replacement of 3' G-rich overhangs by 5' C-rich overhangs is the mark of the recombination-dependent process of ALT (Oganesian and Karlseder, 2011). Interestingly, in *Caenorhabditis elegans*, both C and G overhangs are present at chromosomal ends (Raices *et al.*, 2008).

Importantly, rDNA in many organisms, including budding yeast and human, shows a number of G-rich elements with high quadruplex-forming potential (Hershman *et al.*, 2008). In particular, there are 11 sequences with quadruplex-forming potential in the sense strand of human 25S rDNA locus and 4 sequences in 18S rDNA locus. These sequences with potential to form quadruplex are also

present in rRNA products (Hanakahi *et al.*, 1999). Thus, enrichment in quadruplex-forming potential is an interesting feature common to telomeres and rDNA. Another remarkable aspect of the quadruplex-forming potential of budding yeast and human rDNA is that it is restricted to one DNA strand. Because the RFB of each rDNA repeat ensures that most replication occurs in the same direction as rRNA transcription, it follows that the strand with quadruplex-forming potential will usually be replicated by the lagging-strand DNA replication machinery (Linskens and Huberman, 1988). Strikingly, this is the same arrangement that is present at telomeres, where the G-rich strands run 5'→3' towards the chromosome termini, and are thus copied by lagging strand synthesis from sub-telomeric origins (Hershman *et al.*, 2008).

Nucleosomes are formed on the basis of electrostatic interactions between negatively charged phosphates in DNA and positively charged amino acids in histones. Intrinsic properties of DNA, such as bendability, establish the susceptibility of particular DNA sequences to form nucleosomes (Anselmi *et al.*, 1999; Trifonov, 2010). Among many DNA sequences analysed so far, telomeric repeats exhibit the lowest nucleosome positioning signals (Fajkus *et al.*, 1995; Cacchione *et al.*, 1997; Rossetti *et al.*, 1998). In agreement with this, telomeric nucleosomes are highly mobile, as shown by experiments *in vitro* (Pisano *et al.*, 2007), because their sliding energy is relatively low. Accordingly, profiles of micrococcal nuclease digestion of telomeric chromatin depend on the length of chromatin fibres. While short mono- and dinucleosomal fragments of telomeric chromatin are hypersensitive to micrococcal nuclease treatment in both mammals and plants (Tommerup *et al.*, 1994; Fajkus *et al.*, 1995), in longer chromatin fibres, telomeric nucleosomes show higher resistance to micrococcal nuclease cleavage and shorter and more regular nucleosome spacing than bulk chromatin. These features are

reflected by a columnar model of telomeric chromatin in which telomeric DNA is evenly wound along stacked histone octamers into a tightly packed polynucleosomal structure (Fajkus and Trifonov, 2001). In agreement with this model, *in vitro* reconstitution of nucleosomes on telomere repeats shows random spacing that is shifted to a shorter periodicity (157 bp) as the concentration of nucleosomes in the reaction increases. No such effect was observed for rDNA sequences (Mechelli *et al.*, 2004). In addition, a reduced level of histone H1 in telomeric chromatin was found in different organisms (Ascenzi and Gantt, 1999; Par-seghian *et al.*, 2001). Relative H1 depletion of telomeric nucleosomes may be directly connected to their short spacing, which is below the value of 166 bp for a chromatosome (core particle size plus an approximately 20 bp region protected by H1) (Zlatanova *et al.*, 1999). The lower H1 content at telomeres may also be related to the presence of H3.3 (see below) that prevents association with the linker histone H1 (Braunschweig *et al.*, 2009).

Regular telomeric repeats assemble into short-spaced nucleosomal structures, no matter whether they are positioned terminally or interstitially, i.e. as interstitial telomeric repeats (ITRs), such as in the Chinese hamster ovary cells (Revaud *et al.*, 2009). However, ITRs containing degenerated telomeric repeats form ordinary nucleosomes with a spacing corresponding to bulk chromatin (Gamez-Arjona *et al.*, 2010). Bulk chromatin features were also observed in telomeres of plants of the order Asparagales, where the ancestral, Arabidopsis-type of telomeric repeats (TTTAGGG)_n has been predominantly (but not fully) replaced by the human-type telomeric sequence (TTAGGG)_n and the motifs are intermingled irregularly (Rotkova *et al.*, 2004).

In addition to histones, numerous other proteins are required to perform telomeric functions such as inhibition of the DNA damage response at telomeres (de Lange, 2009), recruitment of telomerase to chromosome ends, or facilitating telomere replication (Sfeir *et al.*, 2009). These proteins are currently thought to assemble into two distinct complexes known as shelterin (de Lange, 2005) and CST complexes (Surovtseva *et al.*, 2009).

The CST complex was originally described in budding yeast (Gao *et al.*, 2007) as a telomere-specific replication protein A-like complex comprising three subunits (CDC13, STN1 and TEN1). This complex is involved in protection of single-stranded chromosomal termini, and regulates telomere replication. The complex is conserved in higher eukaryotes, including plants and humans, and contributes to telomere replication and protection (see Price *et al.*, 2010 for review).

The other complex - shelterin - has been described in detail in mammalian cells (de Lange, 2005). It consists of six core components: TRF1 (telomeric repeat binding factor 1), TRF2 (telomeric repeat binding factor 2), RAP1

(repressor activator protein 1), TIN2 (TRF1-interacting nuclear factor 2), TPP1 (TIN2 interacting protein 1) and POT1 (protection of telomeres 1). Two of the shelterin proteins, TRF1 and TRF2, bind double-stranded telomeric DNA using a specific Myb-like motif termed telobox (Bilaud *et al.*, 1996), and negatively regulate telomere length. TRF1 and TRF2 are involved in the formation of capping structures that prevent access of telomerase to the chromosomal ends (de Lange, 2005). Two recent reports have shown that both of these proteins influence nucleosomal organization, directly connecting this process with telomere protective function. In the first study, a negative correlation between telomeric nucleosomal density and the TRF2 level, due to alterations in the inter-nucleosomal distance, was demonstrated (Galati *et al.*, 2012). In the second study, TRF1 was reported to induce sliding of telomeric histones *in vitro*. The process was ATP-independent and specific for telomeric sequences (Pisano *et al.*, 2010). These results demonstrate another level at which telomeric proteins may modulate the structure of telomeric chromatin. TRF1 and TRF2 recruit two other shelterin components - RAP1 and TIN2 - to telomeres. TIN2 further interacts with TPP1 protein, which binds the last shelterin component, POT1. POT1 also binds to the G-rich strand of telomeric DNA from either the single-stranded G overhang or the displacement loop (D-loop) at the base of the t-loop. In this way, shelterin may bridge the double- and single-stranded parts of telomeric DNA.

In contrast to the CST complex, the existence of a shelterin equivalent in plants has not been demonstrated, although many (perhaps too many) putative shelterin components have been found in plants (reviewed in Peska *et al.*, 2011). An overview of plant proteins with a known effect on telomere maintenance is given in Table 2. Among the most promising candidates are proteins of the single myb histone family. This plant-specific group of proteins has been described in *A. thaliana*, maize (*Zea mays*) and parsley (*Petroselinum crispum*). Their Myb-like telomere-binding domain is similar to the Myb domain in shelterin proteins TRF1 and TRF2, but the middle H1/H5 part resembles more general chromatin factors (Marian *et al.*, 2003). Members of this family in Arabidopsis (AtTRB proteins) are spread throughout the nucleus and nucleolus during G₁, S and G₂ phases. AtTRB1 forms nuclear speckles that co-localize with telomeres (Dvorackova *et al.*, 2010; Schrupfova *et al.*, 2014). Additionally, AtTRB1 is a dynamic factor with high turnover on the chromatin (Dvorackova *et al.*, 2010), suggesting that, similarly to TRF1 and TRF2, this protein may be involved in modulating the nucleosomal structure of *A. thaliana* telomeres (Hofr *et al.*, 2009). The description of AtTRB1 interactions with telomeric DNA, both *in vitro* (Schrumpfova *et al.*, 2004; Mozgova *et al.*, 2008) and *in vivo* (Schrumpfova *et al.*, 2014), as well as with the telomerase terminal transferase (AtTERT)

subunit, and AtPOT1B, one of the paralogues of the POT1 shelterin component in Arabidopsis (Kuchar and Fajkus, 2004; Schrupfova *et al.*, 2008), supports a role of AtTRB other functions in non-telomeric chromatin.

The organization of ribosomal chromatin is quite different from that at telomeres. 45S rDNA of *A. thaliana* forms tandemly repeated 10 kb units, of which approximately 5.5 kb represents a coding region for 18S, 5.8S and 25S rRNAs separated from each other by the short internal transcribed spacers ITS1 and ITS2. These gene clusters are joined to neighbouring clusters by a 4.5 kb intergenic spacer (IGS). Non-transcribed part of IGS constitutes a non-transcribed spacer. The IGS contains regulatory elements of transcription and replication, and, in contrast to the rRNA genes, its sequence is not homogeneous. rDNA units are usually repeated hundreds to thousands of times, and approximately 570 copies occur per haploid Arabidopsis genome. The chromatin state of individual rDNA units varies significantly, with only approximately 10% of copies usually being active and decondensed, while the rest of the rDNA is more compacted in inactive DNA loci. There is controversy regarding the presence of nucleosomes on the RNA polymerase I-transcribed fraction of rDNA (Hamperl *et al.*, 2013). While classical electron microscopic studies suggest complete removal of nucleosomes at the actively transcribed fraction of rDNA (Miller and Beatty, 1969), other reports have shown a remodelled, dynamic, but still nucleosomal arrangement of the transcribed rDNA fraction (Jones *et al.*, 2007), with lower nucleosome occupancy in the coding region compared with the IGS (Zentner *et al.*, 2011).

MODULATION OF TELOMERE AND rDNA CHROMATIN BY HISTONE VARIANTS AND HISTONE CHAPERONES

Based on ChIP data (Stroud *et al.*, 2012; Vaquero-Sedas and Vega-Palas, 2013), Arabidopsis telomeres are enriched in the histone H3.3 variant, while ITRs are occupied by the canonical H3.1.

H3.3 is a histone variant that creates a balance between open and closed chromatin (Ahmad and Henikoff, 2002; Lin *et al.*, 2013). Loss of H3.3 led to increased chromatin condensation in mouse embryos (Lin *et al.*, 2013). In *Xenopus* oocytes, H3.3 deposition consistently induced re-programming of normally silent embryonic genes (Ng and Gurdon, 2008; Goldberg *et al.*, 2010; Jullien *et al.*, 2012). In contrast, the presence of H3.3 at telomeres of mammalian embryonic stem cells is required for transcriptional repression of telomeric repeats (Goldberg *et al.*, 2010). In Arabidopsis, genome-wide ChIP sequencing data in dividing and non-dividing tissues confirmed enrichment of H3.3 at transcriptionally active sites (Stroud *et al.*, 2012; Wollmann *et al.*, 2012).

Association of Arabidopsis telomeres with the H3.3 variant (which generally compromises the heterochromatic

nature of chromatin) makes the reported presence of a H3K27me3 histone mark at plant telomeres rather surprising (Vaquero-Sedas *et al.*, 2012; Majerova *et al.*, 2014), because the occurrence of H3.3 and H3K27me3 marks was shown to be mutually exclusive in the genome-wide study (Stroud *et al.*, 2012). These data suggest specific properties of plant telomeric chromatin that are to some extent apparently similar to those of 'bivalent' chromatin domains in developmental regulatory genes in mammalian embryonic stem cells (Sachs *et al.*, 2013). The 'intermediate' or 'bivalent' character of plant telomeric chromatin may be the reason why the so-called telomere position effect, i.e. silencing of genes adjacent to telomeres, has not been demonstrated in plants (reviewed in Fojtova and Fajkus, 2014).

rDNA loci (and often also telomeres) are excluded from genome-wide analyses due to difficulties in their assembly. Knowledge about rDNA chromatin structure in particular is limited despite its high abundance in the genome. Actively transcribed rDNA associates with the nucleolus, often forming bright nucleolar foci that are sensitive to treatment with the transcription inhibitor actinomycin D. Such foci were shown to associate with the H3.3 histone variant in *Nicotiana benthamiana* leaves (Shi *et al.*, 2011). In support of these observations, Arabidopsis nucleolar foci co-localized with the histone chaperone HIRA (histone regulator A) (Nie *et al.*, 2014). *Drosophila* rDNA also associates with H3.3 (Ahmad and Henikoff, 2002), and dynamic exchanges between canonical H3.1 and H3.3 were detected during rDNA gene activation in *Drosophila*, as well as in a mouse model (Lin *et al.*, 2013).

Histone occupation directly regulates the dynamics of both telomeric and rDNA chromatin, and correct incorporation of variant histones and their chromatin marks precisely determines in which state chromatin persists (Roudier *et al.*, 2011; Sequeira-Mendes *et al.*, 2014). Histone assembly itself is performed by multi-functional protein complexes called histone chaperones, either during replication (Smith and Stillman, 1989; Verreault *et al.*, 1996) or in a replication-independent fashion during transcription, homologous recombination or DNA repair (Endo *et al.*, 2006; Kim and Haber, 2009; Hoek *et al.*, 2011; Frey *et al.*, 2014). An ATRX-DAXX (an alpha thalassemia-mental retardation syndrome X-linked; death-associated protein 6) protein complex (Lewis *et al.*, 2010) participates in telomeric chromatin remodelling and H3.3 loading to telomeres during mid-late S phase (Wong *et al.*, 2010). Disruption of this process severely affects telomere integrity, as indicated by the increased number of phosphorylated γ H2AX foci and telomere dysfunction-induced foci, or telomere fragile phenotypes (Wong *et al.*, 2010; Ivanauskiene *et al.*, 2014). Interestingly, DAXX has been described as an interacting component of telomerase (Tang *et al.*, 2015), and several cancer cell lines showing alternative lengthening of

telomeres (without active telomerase) were shown to have defects in ATRX or DAXX functions (Heaphy *et al.*, 2011). A complex similar to DAXX has not yet been identified in the Arabidopsis genome, and there are presumably other factors involved in histone loading to telomeres that substitute for the specific function of the ATRX–DAXX complex. Other known histone chaperones usually have more conserved functions across species, although the mechanisms by which they participate in different cellular pathways often differ (Kaul *et al.*, 2000; Galvani *et al.*, 2008).

There are two major H3/H4 histone chaperones: chromatin assembly factor 1 (CAF1), consisting of three subunits: fasciata 1 and 2 (FAS1, FAS2) and multicopy suppressor of IRA 1 (MSI1) in plants; chromatin assembly complex (CAC1, CAC2, CAC3) in budding yeast; p150, p60 and p48 in mammals (Smith and Stillman, 1989; Kaufman *et al.*, 1997), and anti-silencing factor 1 (ASF1), comprising one protein in budding or fission yeast and two paralogues (ASF1A and ASF1B) in plants and mammals (Kaul *et al.*, 2000). These chaperones incorporate canonical H3.1/H4 into DNA during replication, and ASF1 also collaborates with HIRA to exchange H3.1 for H3.3 at transcriptionally active sites. Processes of H3/H4 histone loading require a specific conformation that is facilitated by histone chaperones FACT facilitates chromatin transcription 1 or NAP1 nucleosome assembly protein 1 (Bowman *et al.*, 2011; McCullough *et al.*, 2013). These factors are primarily involved in deposition of the other core histone components (H2A/H2B dimers) (Ishimi *et al.*, 1985; Ito *et al.*, 1996; Hondele *et al.*, 2013).

As many genes in Arabidopsis are duplicated, if one copy is deleted, its function may be taken over by its homologue. That is why the phenotype of single mutants is often masked; for example, Arabidopsis *asf1* single mutants do not show a strong phenotype compared with *asf1ab* mutants (Zhu *et al.*, 2011). Simultaneous *ASF1A* and *ASF1B* deletions cause a growth defect associated with abnormal development, cell number reduction and delayed S phase, as well as increased expression of S-phase checkpoint and DNA repair genes.

The situation for CAF1 is quite different. There are clear effects in mutants lacking either of the two main subunits of the chromatin assembly factor (FAS1 or FAS2), while deletion of the smallest subunit MSI1 is lethal for plants (Kohler *et al.*, 2003). Arabidopsis *fas* mutants, much like *asf1ab*, show growth defects with abnormal development of meristem and up-regulated DNA repair genes, together with an increased level of homologous recombination (Endo *et al.*, 2006; Kirik *et al.*, 2006).

On the other hand, loss of function of budding yeast CAF1 is quite well tolerated and its function may be replaced by HIRA or ASF1 chaperones (Kaufman *et al.*, 1998; Duc *et al.*, 2015). Deletion of the *S. cerevisiae* *CAC1* gene causes effects such as reduced telomere silencing,

mis-localization of the telomere-binding protein RAP1, markedly increased gross chromosomal rearrangements with *de novo* telomere additions or translocations, but maintenance of telomere length is not affected (Enomoto *et al.*, 1997; Kaufman *et al.*, 1997; Myung *et al.*, 2003).

In contrast, Arabidopsis CAF1 mutants have defects in telomere length and 45S rDNA stability (Figure 2). Both regions are progressively lost over plant generations (Mozgova *et al.*, 2010). Loss of telomeres is more profound in the double mutant *fas1tert*, thus demonstrating that CAF1 and telomerase dysfunctions shorten telomeres through independent pathways (Jaske *et al.*, 2013). In terms of rDNA dynamics, the loss of rDNA (but not telomeres) is slower when *RAD51B* is dysfunctional, suggesting involvement of homologous recombination, probably of a single-strand annealing type (Muchova *et al.*, 2015). The contribution of the homologous recombination machinery to the *fas* phenotype has also been shown (Gao *et al.*, 2012); deletion of the NAP-related proteins NRP1 and NRP2 resulted in complementation of the hyper-recombinogenic phenotype without recovery of telomere length. These two results suggest that the mechanisms causing loss of telomeres and rDNA in *fas* mutants are different. A contribution of ASF1 or HIRA to maintenance of the repeats has not yet been determined.

It is known that *S. cerevisiae* ASF1 maintains the activity of telomere-proximal genes on a subset of telomeres (Lu and Kobor, 2014), and rDNA copy number balance is maintained by the activity of ASF1 together with the histone deacetylase SIR2 (Table 1) (Houseley and Tollervey, 2011). Mutants lacking ASF1 and SIR2 proteins show amplified rDNA copy number, independently of the homologous recombination machinery (Houseley and Tollervey, 2011). Depletion of ASF1A and ASF1B leads to rapid induction of ALT in human fibroblasts or cancer cells, associated with other telomere dysfunction phenotypes, e.g. a higher level of telomere sister chromatid exchange, the presence of extra-chromosomal telomeric DNA or inter-telomeric exchange (O'Sullivan *et al.*, 2014).

INVOLVEMENT OF EPIGENETIC MECHANISMS IN TELOMERE MAINTENANCE

Maintenance of telomere length is a complex process, with many factors being involved, including epigenetic regulatory mechanisms. Telomeres, due to their repetitive character, have traditionally been considered as heterochromatic regions. This assumption is supported by convincing data from mammalian studies. The presence of heterochromatin-specific histone modifications at telomeres and sub-telomeres was shown to be essential for the proper structure and function of telomeres, and loss of these marks correlated with disruption of telomere maintenance and genomic instability in mouse cells (reviewed in Blasco, 2007; Galati *et al.*, 2013). Telomeric

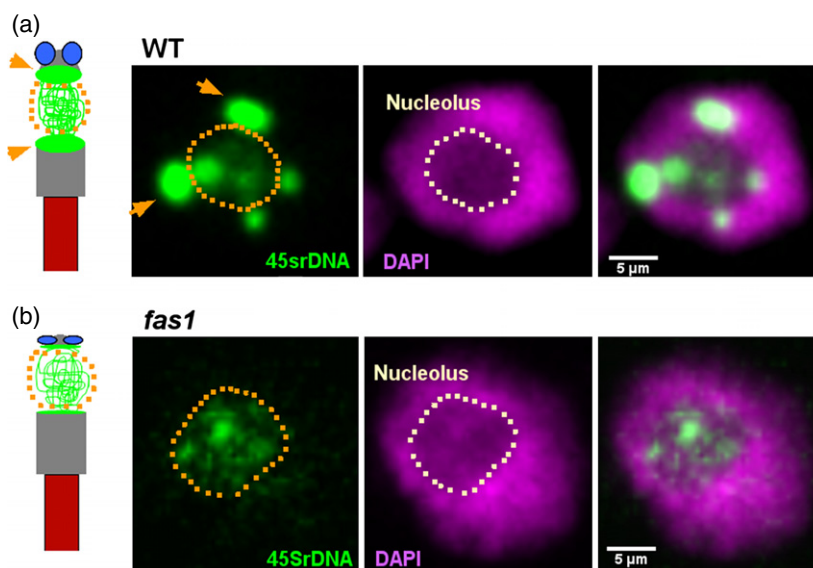


Figure 2. Distribution of 45S ribosomal DNA within Arabidopsis root nuclei.

(a) Wild-type nucleus: rDNA (green); DNA (magenta, stained with DAPI - 4',6-diamidin-2-fenylindol). The 45S rDNA cluster in the wild-type is organized into condensed foci (transcriptionally inactive fraction), and more decondensed, transcriptionally active parts, as shown schematically on the left: green circles represent the inactive fraction, green fibres represent the active part. As shown in the microscope images, inactive rDNA is found in large foci outside the nucleolus (a region with less DAPI staining), while the active part is in a more decondensed state, with several small foci or uniform labelling within the nucleolus.

(b) *fas1* G6 nucleus: rDNA (green); DNA (magenta, stained with DAPI). In *fas* mutants, 45S rDNA is systematically lost, thus only the active fraction remains. A significant reduction in rDNA copy number may be seen in the microscopic image; the remaining 45S rDNA is localized in the nucleolus.

and sub-telomeric chromatin in telomerase-deficient mice with eroded telomeres was depleted of heterochromatic H3K9me3 and H4K20me3 modifications (Benetti *et al.*, 2007). In addition, genome-wide hypomethylation was observed as a consequence of the critically short telomeres in telomerase-negative embryonic stem cells (Pucci *et al.*, 2013), demonstrating the mutual relationship between stability and the epigenetic pattern of telomeres.

In contrast to the number of studies dealing with epigenetic properties of mammalian telomeres and the correlation between the epigenetic state of telomeric chromatin and telomere homeostasis, significantly less effort has been expended on an analogous analysis in plants, although plants as model organisms are no less interesting in this respect, in fact quite the opposite. A good example of this is that plant cells possess an enzymatic apparatus that enables methylation of cytosines in all sequence contexts, while methylated cytosines in mammals are localized predominantly in CpG symmetrical doublets. Cytosines in the C-rich strand of the telomeric repeat (CCCTAAA) are natural targets for plant methyltransferases, and data from the whole-genome *A. thaliana* methylation study confirmed this (Cokus *et al.*, 2008).

In a pilot study of the epigenetic properties of *A. thaliana* telomeric chromatin, its dual character was reported, as both heterochromatin- and euchromatin-specific histone modifications were found to be associated with telomeric DNA, and a proportion of the telomeric cytosines was

methylated (Vrbsky *et al.*, 2010). The presence of a considerable proportion of ITRs in the *A. thaliana* genome (Figure 1a) complicates unambiguous interpretation of epigenetic analyses of telomeric chromatin. Indeed, these results were challenged, and the euchromatic nature of *A. thaliana* telomeres was reported (Vaquero-Sedas *et al.*, 2011). Nevertheless, analysis of telomeres in *Nicotiana tabacum* (tobacco), a species with long telomeres and no detectable ITR fraction (Figure 1c) (Majerova *et al.*, 2011b), demonstrated that telomeric histones were associated with both heterochromatin- and euchromatin-specific marks, with a clear prevalence of the heterochromatic H3K9me2 mark (Majerova *et al.*, 2014). Interestingly, in accordance with a previous observation (Vaquero-Sedas *et al.*, 2012), H3K27me3, a chromatin mark found on developmentally silenced genes, was present on telomeric histones (Figure 1a,c). The significance of this modification, and the general significance of all histone marks, with respect to the proper structure and function of plant telomeres remains to be determined.

Hypomethylation of the *A. thaliana* genome, induced either chemically (seedlings germinated in the presence of hypomethylation drugs) or genetically [mutants with impaired function of the MET1 DNA methyltransferase (Mathieu *et al.*, 2007) or the DDM1 chromatin remodelling factor (Vongs *et al.*, 1993)], led to a significant decrease in methylated telomeric cytosines (Ogrocka *et al.*, 2014). Surprisingly, while overall genome hypomethylation in

mammalian cells led to telomere elongation (Gonzalo *et al.*, 2006), telomeres in leaves of hypomethylated plants were significantly shortened, and the short-telomere phenotype was stably transmitted to the progeny, without any signs of genomic instability. Loss of methylation of cytosines in telomeric repeats was also observed in plants lacking RNA-dependent RNA polymerase 2 (Vrbsky *et al.*, 2010), an essential component of the plant-specific RNA-directed DNA methylation pathway. It would be interesting to analyse telomere lengths in these mutants to determine whether the loss of methylation of non-symmetrically located telomeric cytosines represents a necessary and sufficient condition for induction of telomere instability. This seems plausible, because telomeres of *A. thaliana* mutants with loss of function of non-CpG DNA methyltransferases were significantly shorter (Vaquero-Sedas and Vega-Palas, 2014). The differences in telomere lengths in hypomethylated *A. thaliana* plants were not correlated with changes in the activity and expression of telomerase (Ogrocka *et al.*, 2014). Accordingly, no significant contribution of DNA methylation to the developmental silencing of telomerase transcription and activity was observed in terminally differentiated *A. thaliana* tissues. Furthermore, the euchromatic nature of the region encompassing the gene encoding the catalytic subunit of telomerase was maintained in both telomerase-positive and telomerase-negative tissues (Ogrocka *et al.*, 2012). As mentioned above, the process of telomere maintenance is rather complex, and many factors participating in it may be under epigenetic control. These factors may influence the formation of a fully functional telomerase complex or the accessibility of telomeres to telomerase, important factors that it is not possible to assess by *in vitro* analysis of telomerase activity.

The stability of telomeres was also analysed in a hypomethylated tobacco cell culture (Majerova *et al.*, 2011a). Cultivation in the presence of hypomethylation drugs caused genome-wide cytosine hypomethylation, including a significant decrease in the level of methylated cytosines located in telomeric repeats. As tobacco does not contain a significant ITR fraction (Majerova *et al.*, 2011b), the results of this study only reflect changes in the methylation level of genuine telomeres. In contrast to analyses of *A. thaliana* hypomethylated plants, the lengths of telomeres in hypomethylated tobacco cells were unaffected, despite markedly increased telomerase activity (Majerova *et al.*, 2011a). Similarly, our preliminary unpublished data indicate that more pronounced changes in the chromatin structure accompany telomerase developmental silencing in tobacco leaves.

The differing involvement of epigenetic mechanisms in telomere and telomerase regulation in *A. thaliana* and *N. tabacum* may be understandable given the dissimilarities in composition of the genomes and epigenomes of

these two model plants. Compared to *N. tabacum*, *A. thaliana* has a significantly smaller genome with a low content of repetitive sequences and also a low level of heterochromatic regions. Correspondingly, overall DNA methylation in *A. thaliana* is significantly lower, methylated cytosines are located preferentially in CpG doublets, and even the general methylation landscape differs between these plants (reviewed in Suzuki and Bird, 2008).

As in mammalian cells, plant telomeres appear to be under epigenetic control, at least in the model plants investigated. The opposite effects of hypomethylation stress on telomere stability and telomerase activity in *A. thaliana* and tobacco may indicate different involvement of epigenetic mechanisms in regulating crucial cellular processes (including telomere maintenance) in these species (Vaughn *et al.*, 2007). Analyses of other plants with genomes/epigenomes similar to those of either *A. thaliana* or *N. tabacum* are essential to identify generally valid and species-specific aspects of epigenetic regulation of plant telomeres.

The epigenetic status of rDNA and its regulation are currently understood considerably better than for telomeres, and are important for the general understanding of epigenetic processes. This is beyond the scope of this review, but has been discussed elsewhere (Preuss and Pikaard, 2007; McStay and Grummt, 2008; Guetg and Santoro, 2012).

GENOME FRAGILITY ASSOCIATED WITH TELOMERES AND rDNA

As discussed above, telomeres as well as rDNA are loci that affect genomic stability. rDNA (and sometimes telomeric DNA) also forms so-called genome fragile sites that, once activated, are hotspots for chromosomal fragmentation and gross chromosomal rearrangements (Mondello *et al.*, 2000; Ruiz-Herrera *et al.*, 2008; d'Alcontres *et al.*, 2014; Rocha *et al.*, 2015).

In most eukaryotic genomes, telomeric repeats are located not only at chromosomal ends, forming genuine telomeres, but also internally as ITRs, and are found within sub-telomeric, centromeric and pericentromeric regions (Meyne *et al.*, 1990; Richards *et al.*, 1991; He *et al.*, 2013). Apart from typical ITRs, there are other types of short interstitial telomeric sequences such as telomere-associated sequences that form an important component of plant sub-telomeres (Suzuki *et al.*, 1994; Mao *et al.*, 1997), and the so-called telo-boxes, AAACCCTA motifs in the 5' upstream regions of many genes, including the promoters of genes involved in ribosome biogenesis (Gaspin *et al.*, 2010). Epigenetic states of these elements reflect the general character of the region in which they occur, i.e. telomere-associated sequences are present in heterochromatic sub-telomeres and telo-boxes are present in the proximity of euchromatic active promoters. ITRs may have arisen (i)

from telomere–telomere fusions of ancestral chromosomes (a striking example of such an event is the fusion of two ancestral ape chromosomes during evolution of human chromosome 2; Ijdo *et al.*, 1991), (ii) from microsatellite expansion (considering the ITRs as a class of hexameric microsatellite) due to DNA polymerase slippage, resulting in insertion (or deletion) of a certain number of repeat units, or (iii) by repair of DNA breaks by ‘chromosome healing’, which is contributed to by telomerase (reviewed in Lin and Yan, 2008).

While the functional importance and evolutionary exigency of genuine telomeres is obvious, the role of ITRs is the subject of hypotheses. The biological relevance of ITRs is mainly connected to their fragility, and, in mammals, even very short ITRs induce unstable genomic sites, leading to DNA breakage, genomic rearrangements or recombination. In this respect, ITRs are targets of common mutagens and carcinogens, and are correlated with cancer breakpoints (Mondello *et al.*, 2000). An interesting observation was made in *S. cerevisiae*, where a telomeric sequence was inserted *de novo* into an intron of the reporter gene. The locus then showed a quite high rate of contraction and deletion, and even inversions involving interactions between ITRs and the natural telomere (Akse-nova *et al.*, 2013). In plants, genomic fragility was correlated with ITRs in the genomes of the grass *Phleum echinatum*. Moreover, in *P. echinatum*, rDNA and ITRs overlap, forming a hyper-fragile spot (Grabowska-Joachimak *et al.*, 2015). In *A. thaliana*, sequences encompassing telomeric repeats were detected in centromeric region of chromosome 1 (Richards *et al.*, 1991), and six other regions ranging from 300 bp to 1.2 kb were found in another study (Uchida *et al.*, 2002). Recently, a specific genomic arrangement was described in another Brassicaceae species *Ballantinia antipoda*, where the proportion of telomeric repeats in ITRs significantly exceeded those in genuine telomeres (Mandakova *et al.*, 2010; Figure 1b). A similar intriguing genomic organization was also observed in Chinese hamster, where a telomeric probe revealed strong signals in centromeric regions and only faint terminal spots on genuine telomeres (Simi *et al.*, 1998).

The reason for the fragility of ITRs is not known. Moreover, some ITRs manifest themselves as hotspots while others do not (reviewed in Bolzan, 2012). In this context, the high AT content of ITRs pre-determines them as unstable sequences. Furthermore, tetraplex structures potentially formed by the G-rich strand have been reported as prospective sites of chromosomal recombination (Azzalin *et al.*, 2001). Higher levels of telomeric repeat degeneracy may therefore be assumed to contribute to increased genomic stability of ITRs.

The fragility of rDNA, which is well described in budding yeast, relates to the problematic replication of this locus. rDNA fragility is increased by repetitiveness of the locus

itself, representing a recombination hotspot. In *Lolium perenne*, fragile sites, visible as chromosomal gaps, were found within the 45S rDNA locus (Huang *et al.*, 2008). Inhibition of replication by aphidicolin or of transcription by actinomycin D increased the level of lesions within rDNA, and induced formation of visible fragile sites in *L. perenne* as well as in barley (*Hordeum vulgare*) and maize (Huang *et al.*, 2012). A study supporting these findings was recently performed in mammals, showing that approximately nine sites within the IGS, where the CCCTC-binding factor is bound, correlate with DNA double-strand break hotspots and a more open chromatin state, associated with the H3K4me3 histone mark. In addition, use of the circular chromosome conformation capture technique revealed physical attachment of rDNA fragile sites with other pericentromeric loci that are prone to DNA double-strand break formation (Tchurikov *et al.*, 2014). As a fragile locus, rDNA has its own specific features. It has to be stable enough to supply cells with ribosomes, but, on the other hand, rDNA loci variation, as well as changes in gene copy number within the rDNA locus, are quite common during plant evolution (Khaitova *et al.*, 2010; Malinska *et al.*, 2010; Guo and Han, 2014). This is partially due to iter-recombinogenic character, and its ability to behave as a jumping element (Schubert and Wobus, 1985; Huang *et al.*, 2008; Singh and Barman, 2013).

Intriguingly, possible functional complementation between telomeres and rDNA has been discussed in plants lacking typical telomeres and telomerase (Sykorova *et al.*, 2003, 2006). In representatives of the genus *Allium*, rDNA appears to be a promising candidate to substitute for canonical telomeric repeats (Pich *et al.*, 1996). Another interesting phenomenon was described in the fission yeast *Schizosaccharomyces pombe*, in which, upon deletion of telomerase, rDNA spread to the chromosome ends to protect them (Jain *et al.*, 2010). A similar effect was observed in calli of *A. thaliana* mutants with loss of telomerase function, in which amplification of rDNA occurs in response to the lack of telomeres (Siroky *et al.*, 2003).

Therefore, dynamic changes in rDNA loci paradoxically generate both genomic instabilities as well as conferring genome stabilization when re-located to chromosomal termini. For telomeres, the situation is quite similar; they are protective at chromosome ends while potentially fragile and dangerous when located internally as ‘telomere rene-gades’. Thus the two loci, which occur frequently as close chromosome neighbours, show a striking dependence on chromosome position for their stability.

REPLICATION ISSUES FOR rDNA AND TELOMERES

Replication of repeats is quite challenging, and contributes to the instability of telomeres and rDNA. A common defect within rDNA and telomeres may be increased polymerase slippage (or slipped strand mis-pairing) caused by the

presence of direct repeats at the site of replication. This leads to polymerase disassociation from the replicating strand, and binding to another upstream sequence, resulting in insertions or deletions. The phenomenon has been described as repeat-induced mutagenesis (Aksenova *et al.*, 2013), and is another mechanism by which genomic content may be altered, similar to the DNA repair-created insertions and deletions described in budding yeast and plants (Yu and Gabriel, 1999; Vu *et al.*, 2014).

Telomeres, as chromosomal ends, are not replicated completely due to their inability to replicate the most distal landing sites for RNA primers initiating synthesis of Okazaki fragments during lagging-strand replication. If telomerase does not complete telomere replication in actively proliferating cells, telomeres erode. Components of the telomeric protective complex shelterin are known to actively participate in the regulation of telomere replication. For example, TRF1 prevents replication fork stalling, and its deficiency induces a telomere fragility phenotype in mouse embryonic fibroblasts (Sfeir *et al.*, 2009). In addition, for the proper progress of replication, unwinding of local telomeric structures such as G quadruplexes or t-loops is required (Rizzo *et al.*, 2009). For this purpose, bloom syndrome (BLM) and regulator of telomere elongation 1 (RTEL1) helicases are recruited through TRF1 for further telomere processing. Homologues of RTEL1 and BLM helicases were recently identified in the Arabidopsis genome (Hartung *et al.*, 2007; Recker *et al.*, 2014) but *rte1* plants did not show telomere loss (Hu *et al.*, 2015).

The current model of telomere replication speculates that the *S. pombe* telomeric proteins RAP1, RAP1 (repressor activator protein 1), TAZ1 (telomere length regulator 1 - taz 1), POZ1 (pot1 associated protein 1 - poz1) or components of the CST complex, in addition to telomerase recruitment, directly regulate loading of polymerases to the telomeric leading and lagging strands (Chang *et al.*, 2013; Lue *et al.*, 2014). For example, RIF1 (a RAP1-interacting factor) in *Saccharomyces cerevisiae* and TAZ1 in *S. pombe*, control firing of late replication origins (Tazumi *et al.*, 2012; Peace *et al.*, 2014). Deletion of these telomeric proteins alters telomere lengths, indicating that aberrant replication is one of the causes of telomere abnormalities (Chang *et al.*, 2013).

In rDNA, quite complex mechanisms have been established to prevent collision between replication and transcription, as their overlap is inevitable. These mechanisms are based on the presence of the RFB, as mentioned above. This element maintains replication only in the direction of rDNA transcription. In *S. cerevisiae*, a replication origin and RFB lie within the non-transcribed spacer, between the 35S and 5S gene units (Skryabin *et al.*, 1984). Budding yeast RFB maintains rDNA copy number through the protein FOB1, a necessary component for correct RFB and recombination hotspot sites functions (Kobayashi

et al., 1998). Recently, the the SUUR protein (the suppressor of underreplication), which blocks replication fork progression, was shown to regulate gene copy number in *Drosophila* (Nordman *et al.*, 2014). In Arabidopsis, the RFB sequence is not known. In *Pisum sativum*, RFB was identified at the 3' end of the 25S rRNA gene (Lopez-Estrano *et al.*, 1999). An interesting observation was made in Arabidopsis plants containing a marker to check the level of recombination and expressing the *S. cerevisiae* RFB region. In such transformants, the presence of the budding yeast non-transcribed spacer of RFB stimulated homologous recombination, and might possibly even function as a real RFB (Urawa *et al.*, 2001). Another element functioning in regulation of *S. cerevisiae* rDNA gene copy number is E-pro, a promoter for RNA polymerase II transcription. E-pro activity induces cohesin dissociation from rDNA, followed by unequal recombination and changes in rDNA copy number (Kobayashi and Ganley, 2005).

EFFECT OF NON-CODING TRANSCRIPTS ON GENOMIC INSTABILITY

Budding yeast E-pro is a promoter located in the non-transcribed region, corresponding to the IGS region in Arabidopsis. The IGS in Arabidopsis starts with a 3' external transcribed spacer, a 700 bp region containing at least four sequence variants (VAR1-VAR4; Pontvianne *et al.*, 2010) followed by repetitive blocks of approximately 22 bp with *SalI* restriction sites (Sal boxes), and a 5' untranslated region. Usually two or three TATA box binding sequences are found in the IGS: one for the gene promoter and the rest being spacer promoters (Doelling and Pikaard, 1995). Spacer promoters are able to bind RNA polymerase II, but it was unclear whether transcription is activated throughout the IGS or not.

While the importance of rRNA gene transcription for ribosome biogenesis seems clear, the relevance of IGS transcription in Arabidopsis was only recently clarified in studies on *hda6* histone deacetylase mutants (Earley *et al.*, 2010). Chromatin immunoprecipitation experiments showed that the whole 45S rDNA, including the IGS, is associated with RNA polymerase II, and the IGS partially associates with RNA polymerase I also. In the *hda6* mutant, increased levels of IGS sense and antisense transcripts were detected, inducing *de novo* asymmetric siRNA-directed methylation. Interestingly, *hda6* mutants were not able to silence the normally inactive rDNA variant 1, VAR1. These data suggest that IGS expression represents an important step in rDNA regulation, via DNA methylation. In *fas* mutants, VAR1 expression correlates with hypomethylation of the promoter region and subsequent erosion of rDNA repeats (Pontvianne *et al.*, 2013). Under physiological conditions, hypomethylation of the rDNA promoter occurs in the active/nucleolar fraction of rDNA genes, but not in the inactive/nuclear fraction. In WT, active

as well as inactive rDNA copies are present (Figure 2a), while in *fas* mutants, only the nucleolar/active rDNA fraction remains (Figure 2b).

As the rDNA must be transcribed even during replication, increased transcription may cause replication fork collisions. Recent studies in mammals show that cells can deal with this problem by separation of replication and transcription processes which is more accurate in the nucleolus compared to the nucleus (Smirnov *et al.*, 2014). Surprisingly, in mammals, replicating active rDNA copies are removed from the nucleolus, while silent copies were found to replicate inside the nucleolus (Dimitrova, 2011). A hypothesis developed by Kobayashi predicts that non-transcribed rDNA copies are important to enable the DNA damage repair machinery to proceed with damaged rDNA (Kobayashi 2011). When rDNA copy number is low, ongoing transcription interferes with the correct cohesion of sister chromatids required for efficient DNA repair (Ide *et al.*, 2010).

Another potential threat to genomic stability is formation of RNA:DNA hybrids. These are associated with DNA double-strand break formation, and are followed by gross chromosomal rearrangements (Wahba *et al.*, 2011). The sites of hybrid formation, termed R-loops, block replication fork progression (Dominguez-Sanchez *et al.*, 2011; Gan *et al.*, 2011). Accumulation of RNA:DNA hybrids has been detected at rDNA, telomeres, transposons or transcribed loci, and DNA instabilities induced by transcription were mediated through hybrid formation (Huertas and Aguilera, 2003; Wahba *et al.*, 2011; Lin *et al.*, 2014). For example, budding yeast *sin3* mutant, which is unable to repress transcription, accumulates RNA:DNA hybrids in rDNA loci. Such sites stimulated formation of RAD52 foci (Wahba *et al.*, 2011).

In telomeres, RNA:DNA hybrid formation arises from TERRA transcripts. In mammalian cells, TERRA preferentially comprises G-rich telomeric RNA strands (UUAGGG repeats), thus originating in sub-telomeric regions (Azzalin *et al.*, 2007). In *A. thaliana* (Vrbsky *et al.*, 2010) and *N. tabacum* (Majerova *et al.*, 2014), not only TERRA but also the complementary C-rich telomeric transcripts ARRET (nomenclature here is still chaotic, see below), were detected at comparable levels. Similarly, C-rich telomeric transcripts have been detected in *S. pombe* (Bah *et al.*, 2012). The telomeric transcriptome in *S. pombe* is even more complex, as, in addition to the G-rich telomeric transcripts TERRA and the C-rich telomeric transcripts (here termed ARIA), two other RNAs were described: sub-telomeric RNA complementary to the sub-telomeric part of TERRA and lacking the perfect telomeric repeats (here termed ARRET), and its complementary strand α ARRET (Bah *et al.*, 2012).

TERRA induced instability in ALT cells, leading to unwanted recombination of telomeres. Correspondingly,

RNase H1, an enzyme that is able to degrade RNA:DNA hybrids, is associated with telomeres in ALT cells. Increased levels of RNase H1 lead to telomere shortening in ALT cells, but had no effect on telomere homeostasis in telomerase-positive cells (Arora *et al.*, 2014).

Due to the apparent universal presence of RNA:DNA hybrids at telomeres and rDNA, and their huge effect on genomic stability, further research in this field is clearly required.

CONCLUSION

It is apparent from this review that telomeres and rDNA, occurring frequently as adjacent chromatin domains in eukaryotic genomes, are highly dynamic loci. In addition to their apparent essential roles (protection of genome integrity in the case of telomeres, and delivery of rRNA components of ribosomes in the case of rDNA), they show a remarkably wide spectrum of effects on essential cellular processes. Our knowledge in this area has progressed through study of many model organisms, including plants. However, there are many open questions regarding these two loci, as exemplified by non-coding transcripts of telomeres or rDNA IGS. These transcripts result in accumulation of RNA:DNA hybrids, which may initiate gross chromosomal rearrangements and interfere with ongoing replication of these loci, or even directly collide with the replication machinery. Similarly, ITRs act as fragile sites in the genome but are nevertheless tolerated in the long term. Why do cells undergo these risks? What benefits balance these risks? Are there alternative solutions to these problems in less-studied model systems that may be used in therapy or prevention of human diseases associated with genomic instability? Hopefully, the rapid pace of progress in this field will answer these questions, and generate many more.

ACKNOWLEDGEMENTS

Eva Sýkorová (Institute of Biophysics, Academy of Sciences of the Czech Republic, Brno) is acknowledged for fruitful discussions and valuable comments. This work was supported by the Czech Science Foundation (P501/11/0289, 13-06943S and 13-11563P), the project 'CEITEC – Central European Institute of Technology' (CZ.1.05/1.1.00/02.0068) from the European Regional Development Fund, and the European Social Fund (CZ.1.07/2.3.00/20.0189 and CZ.1.07/2.3.00/30.0009).

REFERENCES

- Ahmad, K. and Henikoff, S. (2002) Histone H3 variants specify modes of chromatin assembly. *Proc. Natl Acad. Sci. USA*, **99**, 16477–16484.
- Aksenova, A.Y., Greenwell, P.W., Dominska, M., Shishkin, A.A., Kim, J.C., Petes, T.D. and Mirkin, S.M. (2013) Genome rearrangements caused by interstitial telomeric sequences in yeast. *Proc. Natl Acad. Sci. USA*, **110**, 19866–19871.
- d'Alcontres, M.S., Palacios, J.A., Mejias, D. and Blasco, M.A. (2014) TopoII-alpha prevents telomere fragility and formation of ultra thin DNA bridges during mitosis through TRF1-dependent binding to telomeres. *Cell Cycle*, **13**, 1463–1481.

- Anselmi, C., Bocchinfuso, G., De Santis, P., Savino, M. and Scipioni, A. (1999) Dual role of DNA intrinsic curvature and flexibility in determining nucleosome stability. *J. Mol. Biol.* **286**, 1293–1301.
- Arora, R., Lee, Y., Wischnewski, H., Brun, C.M., Schwarz, T. and Azzalin, C.M. (2014) RNaseH1 regulates TERRA-telomeric DNA hybrids and telomere maintenance in ALT tumour cells. *Nat. Commun.* **5**, 5220.
- Ascenzi, R. and Gant, J.S. (1999) Subnuclear distribution of the entire complement of linker histone variants in *Arabidopsis thaliana*. *Chromosoma*, **108**, 345–355.
- Azzalin, C.M., Nergadze, S.G. and Giulotto, E. (2001) Human intrachromosomal telomeric-like repeats: sequence organization and mechanisms of origin. *Chromosoma*, **110**, 75–82.
- Azzalin, C.M., Reichenbach, P., Khoriaili, L., Giulotto, E. and Lingner, J. (2007) Telomeric repeat containing RNA and RNA surveillance factors at mammalian chromosome ends. *Science*, **318**, 798–801.
- Bah, A., Wischnewski, H., Shchepachev, V. and Azzalin, C.M. (2012) The telomeric transcriptome of *Schizosaccharomyces pombe*. *Nucleic Acids Res.* **40**, 2995–3005.
- Banerjee, S. and Myung, K. (2004) Increased genome instability and telomere length in the *elg1*-deficient *Saccharomyces cerevisiae* mutant are regulated by S-phase checkpoints. *Eukaryot. Cell*, **3**, 1557–1566.
- Benetti, R., Garcia-Cao, M. and Blasco, M.A. (2007) Telomere length regulates the epigenetic status of mammalian telomeres and subtelomeres. *Nat. Genet.* **39**, 243–250.
- Bentsen, I.B., Nielsen, I., Lisby, M., Nielsen, H.B., Gupta, S.S., Mundbjerg, K., Andersen, A.H. and Bjergbaek, L. (2013) MRX protects fork integrity at protein-DNA barriers, and its absence causes checkpoint activation dependent on chromatin context. *Nucleic Acids Res.* **41**, 3173–3189.
- Bhalla, N., Biggins, S. and Murray, A.W. (2002) Mutation of YCS4, a budding yeast condensin subunit, affects mitotic and nonmitotic chromosome behavior. *Mol. Biol. Cell*, **13**, 632–645.
- Bilaud, T., Koering, C.E., Binet-Brasselet, E., Ancelin, K., Pollice, A., Gasser, S.M. and Gilson, E. (1996) The telobox, a Myb-related telomeric DNA binding motif found in proteins from yeast, plants and human. *Nucleic Acids Res.* **24**, 1294–1303.
- Blasco, M.A. (2007) The epigenetic regulation of mammalian telomeres. *Nat. Rev. Genet.* **8**, 299–309.
- Bolzan, A.D. (2012) Chromosomal aberrations involving telomeres and interstitial telomeric sequences. *Mutagenesis*, **27**, 1–15.
- Bowman, A., Ward, R., Wiechens, N., Singh, V., El-Mkami, H., Norman, D.G. and Owen-Hughes, T. (2011) The histone chaperones Nap1 and Vps75 bind histones H3 and H4 in a tetrameric conformation. *Mol. Cell*, **41**, 398–408.
- Braunschweig, U., Hogan, G.J., Pagie, L. and van Steensel, B. (2009) Histone H1 binding is inhibited by histone variant H3.3. *EMBO J.* **28**, 3635–3645.
- Budarf, M.L. and Blackburn, E.H. (1986) Chromatin structure of the telomeric region and 3'-nontranscribed spacer of Tetrahymena ribosomal RNA genes. *J. Biol. Chem.* **261**, 363–369.
- Bundock, P. and Hooykaas, P. (2002) Severe developmental defects, hypersensitivity to DNA-damaging agents, and lengthened telomeres in *Arabidopsis* MRE11 mutants. *Plant Cell*, **14**, 2451–2462.
- Burge, S., Parkinson, G.N., Hazel, P., Todd, A.K. and Neidle, S. (2006) Quadruplex DNA: sequence, topology and structure. *Nucleic Acids Res.* **34**, 5402–5415.
- Cacchione, S., Cerone, M.A. and Savino, M. (1997) *In vitro* low propensity to form nucleosomes of four telomeric sequences. *FEBS Lett.* **400**, 37–41.
- Chang, Y.T., Moser, B.A. and Nakamura, T.M. (2013) Fission yeast shelterin regulates DNA polymerases and Rad3(ATR) kinase to limit telomere extension. *PLoS Genet.* **9**, e1003936.
- Cokus, S.J., Feng, S., Zhang, X., Chen, Z., Merriman, B., Haudenschild, C.D., Pradhan, S., Nelson, S.F., Pellegrini, M. and Jacobsen, S.E. (2008) Shotgun bisulphite sequencing of the *Arabidopsis* genome reveals DNA methylation patterning. *Nature*, **452**, 215–219.
- Crees, Z., Girard, J., Rios, Z. *et al.* (2014) Oligonucleotides and G-quadruplex stabilizers: targeting telomeres and telomerase in cancer therapy. *Curr. Pharm. Des.* **20**, 6422–6437.
- Dimitrova, D.S. (2011) DNA replication initiation patterns and spatial dynamics of the human ribosomal RNA gene loci. *J. Cell Sci.* **124**, 2743–2752.
- Doelling, J.H. and Pikaard, C.S. (1995) The minimal ribosomal RNA gene promoter of *Arabidopsis thaliana* includes a critical element at the transcription initiation site. *Plant J.* **8**, 683–692.
- Dominguez-Sanchez, M.S., Barroso, S., Gomez-Gonzalez, B., Luna, R. and Aguilera, A. (2011) Genome instability and transcription elongation impairment in human cells depleted of THO/TREX. *PLoS Genet.* **7**, e1002386.
- Duc, C., Benoit, M., Le Goff, S., Simon, L., Poulet, A., Cotterell, S., Tatout, C. and Probst, A.V. (2015) The histone chaperone complex HIR maintains nucleosome occupancy and counterbalances impaired histone deposition in CAF-1 complex mutants. *Plant J.* **81**, 707–722.
- Dvorackova, M., Rossignol, P., Shaw, P.J., Koroleva, O.A., Doonan, J.H. and Fajkus, J. (2010) AtTRB1, a telomeric DNA-binding protein from *Arabidopsis*, is concentrated in the nucleolus and shows highly dynamic association with chromatin. *Plant J.* **61**, 637–649.
- Earley, K.W., Pontvianne, F., Wierzbicki, A.T., Blevins, T., Tucker, S., Costanunes, P., Pontes, O. and Pikaard, C.S. (2010) Mechanisms of HDA6-mediated rRNA gene silencing: suppression of intergenic Pol II transcription and differential effects on maintenance versus siRNA-directed cytosine methylation. *Genes Dev.* **24**, 1119–1132.
- El Hage, A., French, S.L., Beyer, A.L. and Tollervey, D. (2010) Loss of topoisomerase I leads to R-loop-mediated transcriptional blocks during ribosomal RNA synthesis. *Genes Dev.* **24**, 1546–1558.
- Endo, M., Ishikawa, Y., Osakabe, K. *et al.* (2006) Increased frequency of homologous recombination and T-DNA integration in *Arabidopsis* CAF-1 mutants. *EMBO J.* **25**, 5579–5590.
- Enomoto, S., McCuneZierath, P.D., GeramiNejad, M., Sanders, M.A. and Berman, J. (1997) RLF2, a subunit of yeast chromatin assembly factor-I, is required for telomeric chromatin function *in vivo*. *Genes Dev.* **11**, 358–370.
- Fajkus, J. and Trifonov, E.N. (2001) Columnar packing of telomeric nucleosomes. *Biochem. Biophys. Res. Commun.* **280**, 961–963.
- Fajkus, J., Kovarik, A., Kralovics, R. and Bezdek, M. (1995) Organization of telomeric and subtelomeric chromatin in the higher plant *Nicotiana tabacum*. *Mol. Gen. Genet.* **247**, 633–638.
- Fajkus, J., Fulneckova, J., Hulanova, M., Berkova, K., Riha, K. and Matyasek, R. (1998) Plant cells express telomerase activity upon transfer to callus culture, without extensively changing telomere lengths. *Mol. Gen. Genet.* **260**, 470–474.
- Fitzgerald, M.S., Riha, K., Gao, F., Ren, S.X., McKnight, T.D. and Shippen, D.E. (1999) Disruption of the telomerase catalytic subunit gene from *Arabidopsis* inactivates telomerase and leads to a slow loss of telomeric DNA. *Proc. Natl Acad. Sci. USA*, **96**, 14813–14818.
- Fojtova, M. and Fajkus, J. (2014) Epigenetic regulation of telomere maintenance. *Cytogenet. Genome Res.* **143**, 125–135.
- Freeman, L., Aragon-Alcaide, L. and Strunnikov, A. (2000) The condensin complex governs chromosome condensation and mitotic transmission of rDNA. *J. Cell Biol.* **149**, 811–824.
- Frey, A., Listovsky, T., Guilbaud, G., Sarkies, P. and Sale, J.E. (2014) Histone H3.3 is required to maintain replication fork progression after UV damage. *Curr. Biol.* **24**, 2195–2201.
- Galati, A., Magdinier, F., Colasanti, V. *et al.* (2012) TRF2 controls telomeric nucleosome organization in a cell cycle phase-dependent manner. *PLoS ONE*, **7**, e34386.
- Galati, A., Micheli, E. and Cacchione, S. (2013) Chromatin structure in telomere dynamics. *Front. Oncol.* **3**, 46.
- Gallego, M.E. and White, C.I. (2001) RAD50 function is essential for telomere maintenance in *Arabidopsis*. *Proc. Natl Acad. Sci. USA*, **98**, 1711–1716.
- Gallego, M.E., Jalut, N. and White, C.I. (2003) Telomerase dependence of telomere lengthening in ku80 mutant *Arabidopsis*. *Plant Cell*, **15**, 782–789.
- Galvani, A., Courbeyrette, R., Agez, M., Ochsnein, F., Mann, C. and Thuret, J.Y. (2008) *In vivo* study of the nucleosome assembly functions of ASF1 histone chaperones in human cells. *Mol. Cell Biol.* **28**, 3672–3685.
- Gamez-Arjona, F.M., Lopez-Lopez, C., Vaquero-Sedas, M.I. and Vega-Palas, M.A. (2010) On the organization of the nucleosomes associated with telomeric sequences. *Biochim. Biophys. Acta*, **1803**, 1058–1061.
- Gan, W., Guan, Z., Liu, J., Gui, T., Shen, K., Manley, J.L. and Li, X. (2011) R-loop-mediated genomic instability is caused by impairment of replication fork progression. *Genes Dev.* **25**, 2041–2056.
- Ganley, A.R. and Kobayashi, T. (2011) Monitoring the rate and dynamics of concerted evolution in the ribosomal DNA repeats of *Saccharomyces cerevisiae* using experimental evolution. *Mol. Biol. Evol.* **28**, 2883–2891.
- Ganley, A.R., Ide, S., Saka, K. and Kobayashi, T. (2009) The effect of replication initiation on gene amplification in the rDNA and its relationship to aging. *Mol. Cell*, **35**, 683–693.

- Gao, H., Cervantes, R.B., Mandell, E.K., Otero, J.H. and Lundbland, V. (2007) RPA-like proteins mediate yeast telomere function. *Nat. Struct. Mol. Biol.* **14**, 208–214.
- Gao, J., Zhu, Y., Zhou, W.B., Molinier, J., Dong, A.W. and Shen, W.H. (2012) NAP1 family histone chaperones are required for somatic homologous recombination in Arabidopsis. *Plant Cell*, **24**, 1437–1447.
- Gaspin, C., Rami, J.F. and Lescure, B. (2010) Distribution of short interstitial telomere motifs in two plant genomes: putative origin and function. *BMC Plant Biol.* **10**, 283.
- Goldberg, A.D., Banaszynski, L.A., Noh, K.M. et al. (2010) Distinct factors control histone variant H3.3 localization at specific genomic regions. *Cell*, **140**, 678–691.
- Gonzalo, S., Jaco, I., Fraga, M.F., Chen, T.P., Li, E., Esteller, M. and Blasco, M.A. (2006) DNA methyltransferases control telomere length and telomere recombination in mammalian cells. *Nat. Cell Biol.* **8**, 416–424.
- Gottlieb, S. and Esposito, R.E. (1989) A new role for a yeast transcriptional silencer gene, SIR2, in regulation of recombination in ribosomal DNA. *Cell*, **56**, 771–776.
- Grabowska-Joachimiak, A., Kula, A., Gernard-Kliefoth, D. and Joachimiak, A.D. (2015) Karyotype structure and chromosome fragility in the grass *Pleum echinatum* Ghost. *Protoplasma*, **252**, 301–306.
- Greider, C.W. (1990) Telomeres, telomerase and senescence. *BioEssays*, **12**, 363–369.
- Greider, C.W. and Blackburn, E.H. (1985) Identification of a specific telomere terminal transferase activity in Tetrahymena extracts. *Cell*, **43**, 405–413.
- Griffith, J.D., Comeau, L., Rosenfield, S., Stansel, R.M., Bianchi, A., Moss, H. and de Lange, T. (1999) Mammalian telomeres end in a large duplex loop. *Cell*, **97**, 503–514.
- Guettig, C. and Santoro, R. (2012) Formation of nuclear heterochromatin. The nucleolar point of view. *Epigenetics*, **7**, 811–814.
- Guo, X. and Han, F. (2014) Asymmetric epigenetic modification and elimination of rDNA sequences by polyploidization in wheat. *Plant Cell*, **26**, 4311–4327.
- Ha, C.W., Sung, M.K. and Huh, W.K. (2012) Nsi1 plays a significant role in the silencing of ribosomal DNA in *Saccharomyces cerevisiae*. *Nucleic Acids Res.* **40**, 4892–4903.
- Hamperl, S., Wittner, M., Babl, V., Perez-Fernandez, J., Tschochner, H. and Griesenbeck, J. (2013) Chromatin states at ribosomal DNA loci. *Biochim. Biophys. Acta*, **1829**, 405–417.
- Hanakahi, L.A., Sun, H. and Maizels, N. (1999) High affinity interactions of nucleolin with G-G-paired rDNA. *J. Biol. Chem.* **274**, 15908–15912.
- Harley, C.B., Futcher, A.B. and Greider, C.W. (1990) Telomeres shorten during ageing of human fibroblasts. *Nature*, **345**, 458–460.
- Hartung, F., Suer, S. and Puchta, H. (2007) Two closely related RecQ helicases have antagonistic roles in homologous recombination and DNA repair in *Arabidopsis thaliana*. *Proc. Natl Acad. Sci. USA*, **104**, 18836–18841.
- Hayflick, L. (1982) Biological aspects of human ageing. *Br. J. Hosp. Med.* **27**, 366–368, passim.
- He, L., Liu, J., Torres, G.A., Zhang, H.Q., Jiang, J.M. and Xie, C.H. (2013) Interstitial telomeric repeats are enriched in the centromeres of chromosomes in *Solanum* species. *Chromosome Res.* **21**, 5–13.
- Heaphy, C.M., de Wilde, R.F., Jiao, Y. et al. (2011) Altered telomeres in tumors with ATRX and DAXX mutations. *Science*, **333**, 425.
- Hershman, S.G., Chen, Q., Lee, J.Y., Kozak, M.L., Yue, P., Wang, L.S. and Johnson, F.B. (2008) Genomic distribution and functional analyses of potential G-quadruplex-forming sequences in *Saccharomyces cerevisiae*. *Nucleic Acids Res.* **36**, 144–156.
- Hoek, M., Myers, M.P. and Stillman, B. (2011) An analysis of CAF-1-interacting proteins reveals dynamic and direct interactions with the KU complex and 14-3-3 proteins. *J. Biol. Chem.* **286**, 10876–10887.
- Hofr, C., Sultesova, P., Zimmermann, M., Mozgova, I., Schrupfova, P.P., Wimmerova, M. and Fajkus, J. (2009) Single-Myb-histone proteins from *Arabidopsis thaliana*: a quantitative study of telomere-binding specificity and kinetics. *Biochem. J.* **419**, 221–228.
- Hondele, M., Stuwe, T., Hassler, M. et al. (2013) Structural basis of histone H2A-H2B recognition by the essential chaperone FACT. *Nature*, **499**, 111–114.
- Hong, J.P., Byun, M.Y., Koo, D.H., An, K., Bang, J.W., Chung, I.K., An, G. and Kim, W.T. (2007) Suppression of RICE TELOMERE BINDING PROTEIN 1 results in severe and gradual developmental defects accompanied by genome instability in rice. *Plant Cell*, **19**, 1770–1781.
- Hong, J.P., Byun, M.Y., An, K., Yang, S.J., An, G. and Kim, W.T. (2010) OsKu70 is associated with developmental growth and genome stability in rice. *Plant Physiol.* **152**, 374–387.
- Horikawa, L., Chiang, Y.J., Patterson, T., Feigenbaum, L., Leem, S.H., Michishita, E., Larionov, V., Hodes, R.J. and Barrett, J.C. (2005) Differential cis-regulation of human versus mouse TERT gene expression *in vivo*: identification of a human-specific repressive element. *Proc. Natl Acad. Sci. USA*, **102**, 18437–18442.
- Houseley, J. and Tollervey, D. (2011) Repeat expansion in the budding yeast ribosomal DNA can occur independently of the canonical homologous recombination machinery. *Nucleic Acids Res.* **39**, 8778–8791.
- Houseley, J., Kotovic, K., El Hage, A. and Tollervey, D. (2007) Trf4 targets ncRNAs from telomeric and rDNA spacer regions and functions in rDNA copy number control. *EMBO J.* **26**, 4996–5006.
- Hu, Z., Cools, T., Kalhorzadeh, P., Heyman, J. and De Veyder, L. (2015) Deficiency of the Arabidopsis helicase RTEL1 triggers a SOG1-dependent replication checkpoint in response to DNA cross-links. *Plant Cell*, **27**, 149–161.
- Huang, J. and Moazed, D. (2003) Association of the RENT complex with nontranscribed and coding regions of rDNA and a regional requirement for the replication fork block protein Fob1 in rDNA silencing. *Genes Dev.* **17**, 2162–2176.
- Huang, J., Ma, L., Yang, F., Fei, S.Z. and Li, L. (2008) 45S rDNA regions are chromosome fragile sites expressed as gaps *in vitro* on metaphase chromosomes of root-tip meristematic cells in *Lolium* spp. *PLoS ONE*, **3**, e2167.
- Huang, M., Li, H., Zhang, L. et al. (2012) Plant 45S rDNA clusters are fragile sites and their instability is associated with epigenetic alterations. *PLoS ONE*, **7**, e35139.
- Huertas, P. and Aguilera, A. (2003) Cotranscriptionally formed DNA:RNA hybrids mediate transcription elongation impairment and transcription-associated recombination. *Mol. Cell*, **12**, 711–721.
- Hwang, M.G. and Cho, M.H. (2007) *Arabidopsis thaliana* telomeric DNA-binding protein 1 is required for telomere length homeostasis and its Myb-extension domain stabilizes plant telomeric DNA binding. *Nucleic Acids Res.* **35**, 1333–1342.
- Ide, S., Miyazaki, T., Maki, H. and Kobayashi, T. (2010) Abundance of ribosomal RNA gene copies maintains genome integrity. *Science*, **327**, 693–696.
- Ijdo, J.W., Baldini, A., Ward, D.C., Reeders, S.T. and Wells, R.A. (1991) Origin of human chromosome 2 - an ancestral telomere-telomere fusion. *Proc. Natl Acad. Sci. USA*, **88**, 9051–9055.
- Ishimi, Y., Sato, W., Kojima, M., Sugawara, K., Hanaoka, F. and Yamada, M. (1985) Rapid purification of nucleosome assembly protein (AP-I) and production of monoclonal antibodies against it. *Cell Struct. Funct.* **10**, 373–382.
- Ito, T., Bulger, M., Kobayashi, R. and Kadonaga, J.T. (1996) *Drosophila* NAP-1 is a core histone chaperone that functions in ATP-facilitated assembly of regularly spaced nucleosomal arrays. *Mol. Cell Biol.* **16**, 3112–3124.
- Ivanauskienė, K., Delbarre, E., McGhie, J.D., Kuntziger, T., Wong, L.H. and Collas, P. (2014) The PML-associated protein DEK regulates the balance of H3.3 loading on chromatin and is important for telomere integrity. *Genome Res.* **24**, 1584–1594.
- Jain, D., Hebden, A.K., Nakamura, T.M., Miller, K.M. and Cooper, J.P. (2010) HAATI survivors replace canonical telomeres with blocks of generic heterochromatin. *Nature*, **467**, 223–227.
- Jaske, K., Mokros, P., Mozgova, I., Fojtova, M. and Fajkus, J. (2013) A telomerase-independent component of telomere loss in chromatin assembly factor 1 mutants of *Arabidopsis thaliana*. *Chromosoma*, **122**, 285–293.
- Jones, H.S., Kawachi, J., Braglia, P., Alen, C.M., Kent, N.A. and Proudfoot, N.J. (2007) RNA polymerase I in yeast transcribes dynamic nucleosomal rDNA. *Nat. Struct. Mol. Biol.* **14**, 123–130.
- Jullien, J., Astrand, C., Szenker, E., Garrett, N., Almouzni, G. and Gurdon, J.B. (2012) HIRA dependent H3.3 deposition is required for transcriptional reprogramming following nuclear transfer to *Xenopus* oocytes. *Epigenetics Chromatin*, **5**, 17.
- Kannan, K., Nelson, A.D.L. and Shippen, D.E. (2008) Dyskerin is a component of the Arabidopsis telomerase RNP required for telomere maintenance. *Mol. Cell Biol.* **28**, 2332–2341.
- Kaufman, P.D., Kobayashi, R. and Stillman, B. (1997) Ultraviolet radiation sensitivity and reduction of telomeric silencing *Saccharomyces cerevisiae* cells lacking chromatin assembly factor-I. *Genes Dev.* **11**, 345–357.
- Kaufman, P.D., Cohen, J.L. and Osley, M.A. (1998) Hir proteins are required for position-dependent gene silencing in *Saccharomyces cerevisiae* in the absence of chromatin assembly factor I. *Mol. Cell Biol.* **18**, 4793–4806.

- Kaul, S., Koo, H.L., Jenkins, J. *et al.* (2000) Analysis of the genome sequence of the flowering plant *Arabidopsis thaliana*. *Nature*, **408**, 796–815.
- Kazda, A., Zellinger, B., Rossler, M., Derboven, E., Kusenda, B. and Riha, K. (2012) Chromosome end protection by blunt-ended telomeres. *Genes Dev.* **26**, 1703–1713.
- Khaitova, L., Werlemark, G., Nybom, H. and Kovarik, A. (2010) Frequent silencing of rDNA loci on the univalent-forming genomes contrasts with their stable expression on the bivalent-forming genomes in polyploid dogroses (*Rosa* sect. *Caninae*). *Heredity*, **104**, 113–120.
- Kim, J.A. and Haber, J.E. (2009) Chromatin assembly factors Asf1 and CAF-1 have overlapping roles in deactivating the DNA damage checkpoint when DNA repair is complete. *Proc. Natl Acad. Sci. USA*, **106**, 1151–1156.
- Kirik, A., Pecinka, A., Wendeler, E. and Reiss, B. (2006) The chromatin assembly factor subunit FASCIATA1 is involved in homologous recombination in plants. *Plant Cell*, **18**, 2431–2442.
- Kobayashi, T. (2006) Strategies to maintain the stability of the ribosomal RNA gene repeats—collaboration of recombination, cohesion, and condensation. *Genes Genet. Syst.* **81**, 155–161.
- Kobayashi, T. (2011) How does genome instability affect lifespan?: roles of rDNA and telomeres. *Genes Cells*, **16**, 617–624.
- Kobayashi, T. (2014) Ribosomal RNA gene repeats, their stability and cellular senescence. *Proc. Jpn. Acad., Ser. B, Phys. Biol. Sci.* **90**, 119–129.
- Kobayashi, T. and Ganley, A.R. (2005) Recombination regulation by transcription-induced cohesin dissociation in rDNA repeats. *Science*, **309**, 1581–1584.
- Kobayashi, T. and Horiuchi, T. (1996) A yeast gene product, Fob1 protein, required for both replication fork blocking and recombinational hotspot activities. *Genes Cells*, **1**, 465–474.
- Kobayashi, T., Heck, D.J., Nomura, M. and Horiuchi, T. (1998) Expansion and contraction of ribosomal DNA repeats in *Saccharomyces cerevisiae*: requirement of replication fork blocking (Fob1) protein and the role of RNA polymerase I. *Genes Dev.* **12**, 3821–3830.
- Kobayashi, T., Nomura, M. and Horiuchi, T. (2001) Identification of DNA cis elements essential for expansion of ribosomal DNA repeats in *Saccharomyces cerevisiae*. *Mol. Cell. Biol.* **21**, 136–147.
- Kobayashi, T., Horiuchi, T., Tongaonkar, P., Vu, L. and Nomura, M. (2004) SIR2 regulates recombination between different rDNA repeats, but not recombination within individual rRNA genes in yeast. *Cell*, **117**, 441–453.
- Kohler, C., Hennig, L., Bouveret, R., Gheyselinck, J., Grossniklaus, U. and Grissem, W. (2003) Arabidopsis MSI1 is a component of the MEA/FIE Polycomb group complex and required for seed development. *EMBO J.* **22**, 4804–4814.
- Kuchar, M. and Fajkus, J. (2004) Interactions of putative telomere-binding proteins in *Arabidopsis thaliana*: identification of functional TRF2 homolog in plants. *FEBS Lett.* **578**, 311–315.
- de Lange, T. (2004) T-loops and the origin of telomeres. *Nat. Rev. Mol. Cell Biol.* **5**, 323–329.
- de Lange, T. (2005) Shelterin: the protein complex that shapes and safeguards human telomeres. *Genes Dev.* **19**, 2100–2110.
- de Lange, T. (2009) How telomeres solve the end-protection problem. *Science*, **326**, 948–952.
- Le Blancq, S.M., Kase, R.S. and Van der Ploeg, L.H. (1991) Analysis of a *Giardia lamblia* rRNA encoding telomere with [TAGGG]_n as the telomere repeat. *Nucleic Acids Res.* **19**, 5790.
- Lee, Y.W. and Kim, W.T. (2010) Tobacco GTBP1, a homolog of human heterogeneous nuclear ribonucleoprotein, protects telomeres from aberrant homologous recombination. *Plant Cell*, **22**, 2781–2795.
- Leehy, K.A., Lee, J.R., Song, X.Y., Renfrew, K.B. and Shippen, D.E. (2013) MERISTEM DISORGANIZATION1 encodes TEN1, an essential telomere protein that modulates telomerase processivity in Arabidopsis. *Plant Cell*, **25**, 1343–1354.
- Lermontova, I., Sandmann, M., Mascher, M., Schmit, A.-C. and Chabouté, M.-E. Centromere chromatin and its dynamics in plants; in this issue.
- Lewis, P.W., Elsaesser, S.J., Noh, K.M., Stadler, S.C. and Allis, C.D. (2010) Daxx is an H3.3-specific histone chaperone and cooperates with ATRX in replication-independent chromatin assembly at telomeres. *Proc. Natl Acad. Sci. USA*, **107**, 14075–14080.
- Lim, K.Y., Matyasek, R., Lichtenstein, C.P. and Leitch, A.R. (2000) Molecular cytogenetic analyses and phylogenetic studies in the Nicotiana section Tomentosae. *Chromosoma*, **109**, 245–258.
- Lin, K.W. and Yan, J. (2008) Endings in the middle: current knowledge of interstitial telomeric sequences. *Mutation Res.* **658**, 95–110.
- Lin, C.J., Conti, M. and Ramalho-Santos, M. (2013) Histone variant H3.3 maintains a decondensed chromatin state essential for mouse preimplantation development. *Development*, **140**, 3624–3634.
- Lin, C.J., Koh, F.M., Wong, P., Conti, M. and Ramalho-Santos, M. (2014) Hira-mediated H3.3 incorporation is required for DNA replication and ribosomal RNA transcription in the mouse zygote. *Dev. Cell*, **30**, 268–279.
- Linskens, M.H.K. and Huberman, J.A. (1988) Organization of replication of ribosomal DNA in *Saccharomyces cerevisiae*. *Mol. Cell. Biol.* **8**, 4927–4935.
- Lipps, H.J. and Rhodes, D. (2009) G-quadruplex structures: *in vivo* evidence and function. *Trends Cell Biol.* **19**, 414–422.
- Lopez-Estrano, C., Schvartzman, J.B., Krimer, D.B. and Hernandez, P. (1999) Characterization of the pea rDNA replication fork barrier: putative cis-acting and trans-acting factors. *Plant Mol. Biol.* **40**, 99–110.
- Lu, P.Y. and Kobor, M.S. (2014) Maintenance of heterochromatin boundary and nucleosome composition at promoters by the Asf1 histone chaperone and SWR1-C chromatin remodeler in *Saccharomyces cerevisiae*. *Genetics*, **197**, 133–145.
- Lue, N.F., Chan, J., Wright, W.E. and Hurwitz, J. (2014) The CDC13-STN1-TEN1 complex stimulates Pol alpha activity by promoting RNA priming and primase-to-polymerase switch. *Nat. Commun.* **5**, 5762.
- Majerova, E., Fojtova, M., Mozgova, I., Bittova, M. and Fajkus, J. (2011a) Hypomethylating drugs efficiently decrease cytosine methylation in telomeric DNA and activate telomerase without affecting telomere lengths in tobacco cells. *Plant Mol. Biol.* **77**, 371–380.
- Majerova, E., Fojtova, M., Mandakova, T. and Fajkus, J. (2011b) Methylation of plant telomeric DNA: what do the results say? (Vaquero-Sedas, M.I. and Vega-Palas, M.A.: DNA methylation at tobacco telomeric sequences). *Plant Mol. Biol.* **77**, 533–536.
- Majerova, E., Mandakova, T., Vu, G.T.H., Fajkus, J., Lysak, M.A. and Fojtova, M. (2014) Chromatin features of plant telomeric sequences at terminal vs. internal positions. *Front. Plant Sci.* **5**, 593.
- Makarov, V.L., Lejnine, S., Bedoyan, J. and Langmore, J.P. (1993) Nucleosomal organization of telomere-specific chromatin in rat. *Cell*, **73**, 775–787.
- Malinska, H., Tate, J.A., Matyasek, R., Leitch, A.R., Soltis, D.E., Soltis, P.S. and Kovarik, A. (2010) Similar patterns of rDNA evolution in synthetic and recently formed natural populations of *Tragopogon* (*Asteraceae*) allotetraploids. *BMC Evol. Biol.* **10**, 291.
- Mandakova, T., Joly, S., Krzywinski, M., Mummenhoff, K. and Lysak, M.A. (2010) Fast diploidization in close mesopolyploid relatives of Arabidopsis. *Plant Cell*, **22**, 2277–2290.
- Mao, L., Devos, K.M., Zhu, L. and Gale, M.D. (1997) Cloning and genetic mapping of wheat telomere-associated sequences. *Mol. Gen. Genet.* **254**, 584–591.
- Marian, C.O., Bordoli, S.J., Goltz, M., Santarella, R.A., Jackson, L.P., Danilevskaia, O., Beckstette, M., Meeley, R. and Bass, H.W. (2003) The maize Single myb histone 1 gene, Smh1, belongs to a novel gene family and encodes a protein that binds telomere DNA repeats *in vitro*. *Plant Physiol.* **133**, 1336–1350.
- Mathieu, O., Reinders, J., Caikovski, M., Smathajitt, C. and Paszkowski, J. (2007) Transgenerational stability of the Arabidopsis epigenome is coordinated by CG methylation. *Cell*, **130**, 851–862.
- McCullough, L., Poe, B., Connell, Z., Xin, H. and Formosa, T. (2013) The FACT histone chaperone guides histone H4 into its nucleosomal conformation in *Saccharomyces cerevisiae*. *Genetics*, **195**, 101–113.
- McStay, B. and Grummt, I. (2008) The epigenetics of rRNA genes: from molecular to chromosome biology. *Annu. Rev. Cell Dev. Biol.* **24**, 131–157.
- Mechelli, R., Anselmi, C., Cacchione, S., De Santis, P. and Savino, M. (2004) Organization of telomeric nucleosomes: atomic force microscopy imaging and theoretical modeling. *FEBS Lett.* **566**, 131–135.
- Meyne, J., Baker, R.J., Hobart, H.H., Hsu, T.C., Ryder, O.A., Ward, O.G., Wiley, J.E., Wurster-Hill, D.H., Yates, T.L. and Moyzis, R.K. (1990) Distribution of nontelomeric sites of the (TTAGGG)_n telomeric sequence in vertebrate chromosomes. *Chromosoma*, **99**, 3–10.
- Miller, O.L. Jr and Beatty, B.R. (1969) Visualization of nucleolar genes. *Science*, **64**, 955–957.
- Mondello, C., Pirzio, L., Azzalin, C.M. and Giulotto, E. (2000) Instability of interstitial telomeric sequences in the human genome. *Genomics*, **68**, 111–117.

- Mozgova, I., Schruppova, P.P., Hofr, C. and Fajkus, J. (2008) Functional characterization of domains in AtTRB1, a putative telomere-binding protein in *Arabidopsis thaliana*. *Phytochemistry*, **69**, 1814–1819.
- Mozgova, I., Mokros, P. and Fajkus, J. (2010) Dysfunction of chromatin assembly factor 1 induces shortening of telomeres and loss of 45S rDNA in *Arabidopsis thaliana*. *Plant Cell*, **22**, 2768–2780.
- Muchova, V., Amiard, S., Mozgova, I., Dvorackova, M., Gallego, M.E., White, C. and Fajkus, J. (2015) Homology-dependent repair is involved in 45S rDNA loss in plant CAF-1 mutants. *Plant J.* **81**, 198–209.
- Myung, K., Pennaneach, V., Kats, E.S. and Kolodner, R.D. (2003) *Saccharomyces cerevisiae* chromatin-assembly factors that act during DNA replication function in the maintenance of genome stability. *Proc. Natl Acad. Sci. USA*, **100**, 6640–6645.
- Ng, R.K. and Gurdon, J.B. (2008) Epigenetic memory of an active gene state depends on histone H3.3 incorporation into chromatin in the absence of transcription. *Nat. Cell Biol.* **10**, 102–109.
- Nie, X., Wang, H., Li, J., Holec, S. and Berger, F. (2014) The HIRA complex that deposits the histone H3.3 is conserved in *Arabidopsis* and facilitates transcriptional dynamics. *Biol. Open*, **3**, 794–802.
- Nordman, J.T., Kozhevnikova, E.N., Verrijzer, C.P., Pindyurin, A.V., Andreyeva, E.N., Shloma, V.V., Zhimulev, I.F. and Orr-Weaver, T.L. (2014) DNA copy-number control through inhibition of replication fork progression. *Cell Rep.* **9**, 841–849.
- Oganesian, L. and Karlseder, J. (2011) Mammalian 5' C-rich telomeric overhangs are a mark of recombination-dependent telomere maintenance. *Mol. Cell*, **42**, 224–236.
- Ogrocka, A., Sykorova, E., Fajkus, J. and Fojtova, M. (2012) Developmental silencing of the AtTERT gene is associated with increased H3K27me3 loading and maintenance of its euchromatic environment. *J. Exp. Bot.* **63**, 4233–4241.
- Ogrocka, A., Polanska, P., Majerova, E., Janeba, Z., Fajkus, J. and Fojtova, M. (2014) Compromised telomere maintenance in hypomethylated *Arabidopsis thaliana* plants. *Nucleic Acids Res.* **42**, 2919–2931.
- O'Sullivan, R.J., Arnoult, N., Lackner, D.H., Oganesian, L., Haggblom, C., Corpet, A., Almouzni, G. and Karlseder, J. (2014) Rapid induction of alternative lengthening of telomeres by depletion of the histone chaperone ASF1. *Nat. Struct. Mol. Biol.* **21**, 167–174.
- Paeschke, K., Simonsson, T., Postberg, J., Rhodes, D. and Lipps, H.J. (2005) Telomere end-binding proteins control the formation of G-quadruplex DNA structures *in vivo*. *Nat. Struct. Mol. Biol.* **12**, 847–854.
- Parseghian, M.H., Newcomb, R.L. and Hamkalo, B.A. (2001) Distribution of somatic H1 subtypes is non-random on active vs. inactive chromatin II: distribution in human adult fibroblasts. *J. Cell. Biochem.* **83**, 643–659.
- Peace, J.M., Ter-Zakarian, A. and Aparicio, O.M. (2014) Rif1 regulates initiation timing of late replication origins throughout the *S. cerevisiae* genome. *PLoS ONE*, **9**, e98501.
- Peska, V., Schruppova, P.P. and Fajkus, J. (2011) Using the telobox to search for plant telomere binding proteins. *Curr. Protein Pept. Sci.* **12**, 75–83.
- Phan, A.T. (2010) Human telomeric G-quadruplex: structures of DNA and RNA sequences. *FEBS J.* **277**, 1107–1117.
- Pich, U., Fuchs, J. and Schubert, I. (1996) How do Alliaceae stabilize their chromosome ends in the absence of TTTAGG sequences? *Chromosome Res.* **4**, 207–213.
- Piper, P.W., Celis, J., Kaltoft, K., Leer, J.C., Nielsen, O.F. and Westergaard, O. (1976) Tetrahymena ribosomal RNA gene chromatin is digested by micrococcal nuclease at sites which have the same regular spacing on the DNA as corresponding sites in the bulk nuclear chromatin. *Nucleic Acids Res.* **3**, 493–505.
- Pisano, S., Marchioni, E., Galati, A., Mechelli, R., Savino, M. and Cacchione, S. (2007) Telomeric nucleosomes are intrinsically mobile. *J. Mol. Biol.* **369**, 1153–1162.
- Pisano, S., Galati, A. and Cacchione, S. (2008) Telomeric nucleosomes: forgotten players at chromosome ends. *Cell. Mol. Life Sci.* **65**, 3553–3563.
- Pisano, S., Leoni, D., Galati, A., Rhodes, D., Savino, M. and Cacchione, S. (2010) The human telomeric protein hTRF1 induces telomere-specific nucleosome mobility. *Nucleic Acids Res.* **38**, 2247–2255.
- Pontvianne, F., Abou-Elail, M., Douet, J. et al. (2010) Nucleolin is required for DNA methylation state and the expression of rRNA gene variants in *Arabidopsis thaliana*. *PLoS Genet.* **6**, e1001225.
- Pontvianne, F., Blevins, T., Chandrasekhara, C. et al. (2013) Subnuclear partitioning of rRNA genes between the nucleolus and nucleoplasm reflects alternative epiallelic states. *Genes Dev.* **27**, 1545–1550.
- Preuss, S. and Pikaard, C.S. (2007) RRNA gene silencing and nucleolar dominance: insights into a chromosome-scale epigenetic on/off switch. *Biochim. Biophys. Acta*, **1769**, 383–392.
- Price, C.M., Boltz, K.A., Chaiken, M.F., Stewart, J.A., Beilstein, M.A. and Shippen, D.E. (2010) Evolution of CST function in telomere maintenance. *Cell Cycle*, **9**, 3157–3165.
- Pucci, F., Gardano, L. and Harrington, L. (2013) Short telomeres in ESCs lead to unstable differentiation. *Cell Stem Cell*, **12**, 479–486.
- Raices, M., Verdun, R.E., Compton, S.A., Haggblom, C.I., Griffith, J.D., Dillin, A. and Karlseder, J. (2008) *C. elegans* telomeres contain G-strand and C-strand overhangs that are bound by distinct proteins. *Cell*, **132**, 745–757.
- Recker, J., Knoll, A. and Puchta, H. (2014) The *Arabidopsis thaliana* homolog of the helicase RTEL1 plays multiple roles in preserving genome stability. *Plant Cell*, **26**, 4889–4902.
- Revaud, D., Mozziconacci, J., Sabatier, L., Desmaze, C. and Lavelle, C. (2009) Sequence-driven telomeric chromatin structure. *Cell Cycle*, **8**, 1099–1100.
- Richards, E.J., Goodman, H.M. and Ausubel, F.M. (1991) The centromere region of *Arabidopsis thaliana* chromosome 1 contains telomere-similar sequences. *Nucleic Acids Res.* **19**, 3351–3357.
- Riha, K. and Shippen, D.E. (2003) Ku is required for telomeric C-rich strand maintenance but not for end-to-end chromosome fusions in *Arabidopsis*. *Proc. Natl Acad. Sci. USA*, **100**, 611–615.
- Riha, K., McKnight, T.D., Fajkus, J., Vyskot, B. and Shippen, D.E. (2000) Analysis of the G-overhang structures on plant telomeres: evidence for two distinct telomere architectures. *Plant J.* **23**, 633–641.
- Riha, K., McKnight, T.D., Griffing, L.R. and Shippen, D.E. (2001) Living with genome instability: plant responses to telomere dysfunction. *Science*, **291**, 1797–1800.
- Riha, K., Watson, J.M., Parkey, J. and Shippen, D.E. (2002) Telomere length deregulation and enhanced sensitivity to genotoxic stress in *Arabidopsis* mutants deficient in Ku70. *EMBO J.* **21**, 2819–2826.
- Rizzo, A., Salvati, E., Porru, M., D'Angelo, S., Stevens, M.F., D'Incalci, M., Leonetti, C., Gilson, E., Zupi, G. and Biroccio, A. (2009) Stabilization of quadruplex DNA perturbs telomere replication leading to the activation of an ATR-dependent ATM signaling pathway. *Nucleic Acids Res.* **37**, 5353–5364.
- Rocha, L.C., de Oliveira Bustamante, F., Silveira, R.A., Torres, G.A., Mittelmann, A. and Techio, V.H. (2015) Functional repetitive sequences and fragile sites in chromosomes of *Lolium perenne* L. *Protoplasma*, **252**, 451–460.
- Rossetti, L., Cacchione, S., Fua, M. and Savino, M. (1998) Nucleosome assembly on telomeric sequences. *Biochemistry*, **37**, 6727–6737.
- Rotkova, G., Sklenickova, M., Dvorackova, M., Sykorova, E., Leitch, A.R. and Fajkus, J. (2004) An evolutionary change in telomere sequence motif within the plant section Asparagales had significance for telomere nucleoprotein complexes. *Cytogenet. Genome Res.* **107**, 132–138.
- Roudier, F., Ahmed, I., Berard, C. et al. (2011) Integrative epigenomic mapping defines four main chromatin states in *Arabidopsis*. *EMBO J.* **30**, 1928–1938.
- Ruckova, E., Friml, J., Prochazkova Schruppova, P. and Fajkus, J. (2008) Role of alternative telomere lengthening unmasked in telomerase knock-out mutant plants. *Plant Mol. Biol.* **66**, 637–646.
- Ruiz-Herrera, A., Nergadze, S.G., Santagostino, M. and Giulotto, E. (2008) Telomeric repeats far from the ends: mechanisms of origin and role in evolution. *Cytogenet. Genome Res.* **122**, 219–228.
- Ryu, H.Y. and Ahn, S. (2014) Yeast histone H3 lysine 4 demethylase Jhd2 regulates mitotic rDNA condensation. *BMC Biol.* **12**, 75.
- Sachs, M., Onodera, C., Blaschke, K., Ebata, K.T., Song, J.S. and Ramalho-Santos, M. (2013) Bivalent chromatin marks developmental regulatory genes in the mouse embryonic germline *in vivo*. *Cell Rep.* **3**, 1777–1784.
- Saha, A., Wittmeyer, J. and Cairns, B.R. (2006) Chromatin remodelling: the industrial revolution of DNA around histones. *Nat. Rev. Mol. Cell Biol.* **7**, 437–447.
- Schrumpfova, P., Kuchar, M., Mikova, G., Skrisovska, L., Kubiarova, T. and Fajkus, J. (2004) Characterization of two *Arabidopsis thaliana* myb-like proteins showing affinity to telomeric DNA sequence. *Genome*, **47**, 316–324.

- Schrumpfova, P.P., Kuchar, M., Palecek, J. and Fajkus, J. (2008) Mapping of interaction domains of putative telomere-binding proteins AtTRB1 and AtPOT1b from *Arabidopsis thaliana*. *FEBS Lett.* **582**, 1400–1406.
- Schrumpfova, P.P., Fojtova, M., Mokros, P., Grasser, K.D. and Fajkus, J. (2011) Role of HMGB proteins in chromatin dynamics and telomere maintenance in *Arabidopsis thaliana*. *Curr. Protein Pept. Sci.* **12**, 105–111.
- Schrumpfova, P.P., Vychodilova, I., Dvorackova, M., Majerska, J., Dokladal, L., Schorova, S. and Fajkus, J. (2014) Telomere repeat binding proteins are functional components of *Arabidopsis* telomeres and interact with telomerase. *Plant J.* **77**, 770–781.
- Schubert, I. and Wobus, U. (1985) *In situ* hybridization confirms jumping nucleolus organizing regions in *Allium*. *Chromosoma*, **92**, 143–148.
- Sequeira-Mendes, J., Araguez, I., Peiro, R., Mendez-Giraldez, R., Zhang, X., Jacobsen, S.E., Bastolla, U. and Gutierrez, C. (2014) The functional topography of the *Arabidopsis* genome is organized in a reduced number of linear motifs of chromatin states. *Plant Cell*, **26**, 2351–2366.
- Sfeir, A., Kosiyatrakul, S.T., Hockemeyer, D., MacRae, S.L., Karlseeder, J., Schildkraut, C.L. and de Lange, T. (2009) Mammalian telomeres resemble fragile sites and require TRF1 for efficient replication. *Cell*, **138**, 90–103.
- Shakirov, E.V. and Shippen, D.E. (2004) Length regulation and dynamics of individual telomere tracts in wild-type *Arabidopsis*. *Plant Cell*, **16**, 1959–1967.
- Shakirov, E.V., Surovtseva, Y.V., Osbun, N. and Shippen, D.E. (2005) The *Arabidopsis* Pot1 and Pot2 proteins function in telomere length homeostasis and chromosome end protection. *Mol. Cell. Biol.* **25**, 7725–7733.
- Shakirov, E.V., Song, X.Y., Joseph, J.A. and Shippen, D.E. (2009) POT1 proteins in green algae and land plants: DNA-binding properties and evidence of co-evolution with telomeric DNA. *Nucleic Acids Res.* **37**, 7455–7467.
- Shakirov, E.V., Perroud, P.F., Nelson, A.D., Cannell, M.E., Quatrano, R.S. and Shippen, D.E. (2010) Protection of Telomeres 1 is required for telomere integrity in the moss *Physcomitrella patens*. *Plant Cell*, **22**, 1838–1848.
- Shi, L., Wang, J., Hong, F., Spector, D.L. and Fang, Y. (2011) Four amino acids guide the assembly or disassembly of *Arabidopsis* histone H3.3-containing nucleosomes. *Proc. Natl Acad. Sci. USA*, **108**, 10574–10578.
- Simi, S., Attolini, C. and Giulotto, E. (1998) Intrachromosomal telomeric repeats and stabilization of truncated chromosomes in V79 Chinese hamster cells. *Mutat. Res.* **397**, 229–233.
- Simonsson, T., Pecinka, P. and Kubista, M. (1998) DNA tetraplex formation in the control region of c-myc. *Nucleic Acids Res.* **26**, 1167–1172.
- Singh, M. and Barman, A.S. (2013) Chromosome breakages associated with 45S ribosomal DNA sequences in spotted snakehead fish *Channa punctatus*. *Mol. Biol. Rep.* **40**, 723–729.
- Siroky, J. (2008) Chromosome landmarks as tools to study the genome of *Arabidopsis thaliana*. *Cytogenet. Genome Res.* **120**, 202–209.
- Siroky, J., Zluvova, J., Riha, K., Shippen, D.E. and Vyskot, B. (2003) Rearrangements of ribosomal DNA clusters in late generation telomerase-deficient *Arabidopsis*. *Chromosoma*, **112**, 116–123.
- Skryabin, K.G., Eldarov, M.A., Larionov, V.L., Bayev, A.A., Klootwijk, J., de Regt, V.C., Veldman, G.M., Planta, R.J., Georgiev, O.I. and Hadjiolov, A.A. (1984) Structure and function of the nontranscribed spacer regions of yeast rDNA. *Nucleic Acids Res.* **12**, 2955–2968.
- Smirnov, E., Borkovec, J., Kovacic, L. et al. (2014) Separation of replication and transcription domains in nucleoli. *J. Struct. Biol.* **188**, 259–266.
- Smith, S. and Stillman, B. (1989) Purification and characterization of Caf-1, a human cell factor required for chromatin assembly during DNA replication *in vitro*. *Cell*, **58**, 15–25.
- Sofueva, S., Osman, F., Lorenz, A., Steinacher, R., Castagnetti, S., Ledesma, J. and Whitby, M.C. (2011) Ultrafine anaphase bridges, broken DNA and illegitimate recombination induced by a replication fork barrier. *Nucleic Acids Res.* **39**, 6568–6584.
- Song, X.Y., Leehy, K., Warrington, R.T., Lamb, J.C., Surovtseva, Y.V. and Shippen, D.E. (2008) STN1 protects chromosome ends in *Arabidopsis thaliana*. *Proc. Natl Acad. Sci. USA*, **105**, 19815–19820.
- Stroud, H., Otero, S., Desvoyes, B., Ramirez-Parra, E., Jacobsen, S.E. and Gutierrez, C. (2012) Genome-wide analysis of histone H3.1 and H3.3 variants in *Arabidopsis thaliana*. *Proc. Natl Acad. Sci. USA*, **109**, 5370–5375.
- Strunnikov, A.V., Larionov, V.L. and Koshland, D. (1993) SMC1: an essential yeast gene encoding a putative head-rod-tail protein is required for nuclear division and defines a new ubiquitous protein family. *J. Cell Biol.* **123**, 1635–1648.
- Surovtseva, Y.V., Shakirov, E.V., Vespa, L., Osbun, N., Song, X.Y. and Shippen, D.E. (2007) *Arabidopsis* POT1 associates with the telomerase RNP and is required for telomere maintenance. *EMBO J.* **26**, 3653–3661.
- Surovtseva, Y.V., Churikov, D., Boltz, K.A., Song, X.Y., Lamb, J.C., Warrington, R., Leehy, K., Heacock, M., Price, C.M. and Shippen, D.E. (2009) Conserved telomere maintenance component 1 interacts with STN1 and maintains chromosome ends in higher eukaryotes. *Mol. Cell*, **36**, 207–218.
- Suzuki, M.M. and Bird, A. (2008) DNA methylation landscapes: provocative insights from epigenomics. *Nat. Rev. Genet.* **9**, 465–476.
- Suzuki, K., Yamagawa, Y., Matsui, T. and Yoshida, K. (1994) Restriction enzyme-resistant high molecular weight telomeric DNA fragments in tobacco. *DNA Res.* **1**, 129–138.
- Sykorova, E., Lim, K.Y., Chase, M.W., Knapp, S., Leitch, I.J., Leitch, A.R. and Fajkus, J. (2003) The absence of *Arabidopsis*-type telomeres in *Cestrum* and closely related genera *Vestia* and *Sessea* (Solanaceae): first evidence from eudicots. *Plant J.* **34**, 283–291.
- Sykorova, E., Fajkus, J., Meznikova, M., Lim, K.Y., Neplechova, K., Blattner, F.R., Chase, M.W. and Leitch, A.R. (2006) Minisatellite telomeres occur in the family Alliaceae but are lost in *Allium*. *Am. J. Bot.* **93**, 814–823.
- Takashi, Y., Kobayashi, Y., Tanaka, K. and Tamura, K. (2009) *Arabidopsis* replication protein A 70a is required for DNA damage response and telomere length homeostasis. *Plant Cell Physiol.* **50**, 1965–1976.
- Tang, M., Li, Y., Zhang, Y. et al. (2015) Disease mutant analysis identifies a novel function of DAXX in telomerase regulation and telomere maintenance. *J. Cell Sci.* **15**, 331–341.
- Tazumi, A., Fukuura, M., Nakato, R. et al. (2012) Telomere-binding protein Taz1 controls global replication timing through its localization near late replication origins in fission yeast. *Genes Dev.* **26**, 2050–2062.
- Tchurikov, N.A., Fedoseeva, D.M., Sosin, D.V., Snezhkina, A.V., Melnikova, N.V., Kudryavtseva, A.V., Kravatsky, Y.V. and Kretova, O.V. (2014) Hot spots of DNA double-strand breaks and genomic contacts of human rDNA units are involved in epigenetic regulation. *J. Mol. Cell. Biol.*, pii: mju038.
- Tommerup, H., Dousmanis, A. and de Lange, T. (1994) Unusual chromatin in human telomeres. *Mol. Cell. Biol.* **14**, 5777–5785.
- Trifonov, E.N. (2010) Nucleosome positioning by sequence, state of the art and apparent finale. *J. Biomol. Struct. Dyn.* **27**, 741–746.
- Uchida, W., Matsunaga, S., Sugiyama, R. and Kawano, S. (2002) Interstitial telomere-like repeats in the *Arabidopsis thaliana* genome. *Genes Genet. Syst.* **77**, 63–67.
- Urawa, H., Hidaka, M., Ishiguro, S., Okada, K. and Horiuchi, T. (2001) Enhanced homologous recombination caused by the non-transcribed spacer of the rDNA in *Arabidopsis*. *Mol. Genet. Genomics*, **266**, 546–555.
- Vaquero-Sedas, M.I. and Vega-Palas, M.A. (2013) Differential association of *Arabidopsis* telomeres and centromeres with histone H3 variants. *Sci. Rep.* **3**, 1202.
- Vaquero-Sedas, M.I. and Vega-Palas, M.A. (2014) Determination of *Arabidopsis thaliana* telomere length by PCR. *Sci. Rep.* **4**, 5540.
- Vaquero-Sedas, M.I., Gamez-Arjona, F.M. and Vega-Palas, M.A. (2011) *Arabidopsis thaliana* telomeres exhibit euchromatic features. *Nucleic Acids Res.* **39**, 2007–2017.
- Vaquero-Sedas, M.I., Luo, C. and Vega-Palas, M.A. (2012) Analysis of the epigenetic status of telomeres by using ChIP-seq data. *Nucleic Acids Res.* **40**, e163.
- Vaughn, M.W., Tanurdzic, M., Lippman, Z. et al. (2007) Epigenetic natural variation in *Arabidopsis thaliana*. *PLoS Biol.* **5**, 1617–1629.
- Verreault, A., Kaufman, P.D., Kobayashi, R. and Stillman, B. (1996) Nucleosome assembly by a complex of CAF-1 and acetylated histones H3/H4. *Cell*, **87**, 95–104.
- Vongs, A., Kakutani, T., Martienssen, R.A. and Richards, E.J. (1993) *Arabidopsis thaliana* DNA methylation mutants. *Science*, **260**, 1926–1928.
- Vrbsky, J., Akimcheva, S., Watson, J.M., Turner, T.L., Daxinger, L., Vyskot, B., Aufsatz, W. and Riha, K. (2010) siRNA-mediated methylation of *Arabidopsis* telomeres. *PLoS Genet.* **6**, e1000986.
- Vu, G.T.H., Cao, H.X., Watanabe, K., Hensel, G., Blattner, F.R., Kumlehn, J. and Schubert, I. (2014) Repair of site-specific DNA double-strand breaks

- in barley occurs via diverse pathways primarily involving the sister chromatid. *Plant Cell*, **26**, 2156–2167.
- Wahba, L., Amon, J.D., Koshland, D. and Vuica-Ross, M.** (2011) RNase H and multiple RNA biogenesis factors cooperate to prevent RNA:DNA hybrids from generating genome instability. *Mol. Cell*, **44**, 978–988.
- Wollmann, H., Holec, S., Alden, K., Clarke, N.D., Jacques, P.E. and Berger, F.** (2012) Dynamic deposition of histone variant H3.3 accompanies developmental remodeling of the Arabidopsis transcriptome. *PLoS Genet.* **8**, e1002658.
- Wong, L.H., McGhie, J.D., Sim, M., Anderson, M.A., Ahn, S., Hannan, R.D., George, A.J., Morgan, K.A., Mann, J.R. and Choo, K.H.** (2010) ATRX interacts with H3.3 in maintaining telomere structural integrity in pluripotent embryonic stem cells. *Genome Res.* **20**, 351–360.
- Yang, S.W., Kim, S.K. and Kim, W.T.** (2004) Perturbation of NgTRF1 expression induces apoptosis-like cell death in tobacco BY-2 cells and implicates NgTRF1 in the control of telomere length and stability. *Plant Cell*, **16**, 3370–3385.
- Yoo, H.H., Kwon, C., Lee, M.M. and Chung, I.K.** (2007) Single-stranded DNA binding factor AtWHY1 modulates telomere length homeostasis in Arabidopsis. *Plant J.* **49**, 442–451.
- Yoshida, K., Bacal, J., Desmarais, D. et al.** (2014) The histone deacetylases sir2 and rpd3 act on ribosomal DNA to control the replication program in budding yeast. *Mol. Cell* **54**, 691–697.
- Yu, X. and Gabriel, A.** (1999) Patching broken chromosomes with extranuclear cellular DNA. *Mol. Cell*, **4**, 873–881.
- Zentner, G.E., Saiakhova, A., Manaenkov, P., Adams, M.D. and Scacheri, P.C.** (2011) Integrative genomic analysis of human ribosomal DNA. *Nucleic Acids Res.* **39**, 4949–4960.
- Zhu, Y., Weng, M., Yang, Y., Zhang, C., Li, Z., Shen, W.H. and Dong, A.** (2011) Arabidopsis homologues of the histone chaperone ASF1 are crucial for chromatin replication and cell proliferation in plant development. *Plant J.* **66**, 443–455.
- Zlatanova, J., Leuba, S.H. and van Holde, K.** (1999) Chromatin structure revisited. *Crit. Rev. Eukaryot. Gene Expr.* **9**, 245–255.

Telomere dynamics in the lower plant *Physcomitrella patens*

Miloslava Fojtová, Eva Sýkorová, Lucie Najdekrová, Pavla Polanská, Dagmar Zachová, Radka Vagnerová, Karel J. Angelis, et al.

Plant Molecular Biology

An International Journal on Molecular Biology, Molecular Genetics and Biochemistry

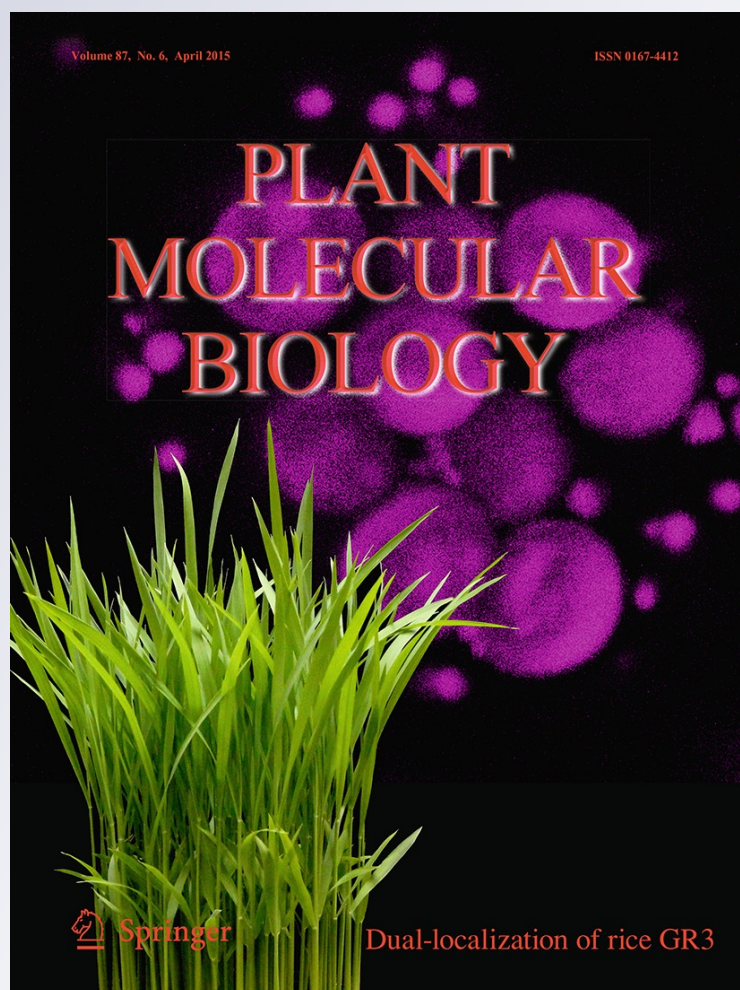
ISSN 0167-4412

Volume 87

Number 6

Plant Mol Biol (2015) 87:591-601

DOI 10.1007/s11103-015-0299-9



Your article is protected by copyright and all rights are held exclusively by Springer Science +Business Media Dordrecht. This e-offprint is for personal use only and shall not be self-archived in electronic repositories. If you wish to self-archive your article, please use the accepted manuscript version for posting on your own website. You may further deposit the accepted manuscript version in any repository, provided it is only made publicly available 12 months after official publication or later and provided acknowledgement is given to the original source of publication and a link is inserted to the published article on Springer's website. The link must be accompanied by the following text: "The final publication is available at link.springer.com".

Telomere dynamics in the lower plant *Physcomitrella patens*

Miloslava Fojtová · Eva Sýkorová · Lucie Najdekrová ·
Pavla Polanská · Dagmar Zachová · Radka Vagnerová ·
Karel J. Angelis · Jiří Fajkus

Received: 6 January 2015 / Accepted: 16 February 2015 / Published online: 21 February 2015
© Springer Science+Business Media Dordrecht 2015

Abstract A comparative approach in biology is needed to assess the universality of rules governing this discipline. In plant telomere research, most of the key principles were established based on studies in only single model plant, *Arabidopsis thaliana*. These principles include the absence of telomere shortening during plant development and the corresponding activity of telomerase in dividing (meristem) plant cells. Here we examine these principles in *Physcomitrella patens* as a representative of lower plants. To follow telomerase expression, we first characterize the gene coding for the telomerase reverse transcriptase subunit *PpTERT* in *P. patens*, for which only incomplete prediction has been

available so far. In protonema cultures of *P. patens*, growing by filament apical cell division, the proportion of apical (dividing) cells was quantified and telomere length, telomerase expression and activity were determined. Our results show telomere stability and demonstrate proportionality of telomerase activity and expression with the number of apical cells. In addition, we analyze telomere maintenance in *mre11*, *rad50*, *nbs1*, *ku70* and *lig4* mutants of *P. patens* and compare the impact of these mutations in double-strand-break (DSB) repair pathways with earlier observations in corresponding *A. thaliana* mutants. Telomere phenotypes are absent and DSB repair kinetics is not affected in *P. patens* mutants for DSB factors involved in non-homologous end joining (NHEJ). This is compliant with the overall dominance of homologous recombination over NHEJ pathways in the moss, contrary to the inverse situation in flowering plants.

Miloslava Fojtová, Eva Sýkorová and Lucie Najdekrová have contributed equally to this study.

During manuscript preparation the pre-release of the new moss genome annotation V3.1 was made available at cosmoss.org. Our experimental results define the prediction Pp3c1_42700V1.1 as a correct gene model for the *PpTERT*.

Electronic supplementary material The online version of this article (doi:10.1007/s11103-015-0299-9) contains supplementary material, which is available to authorized users.

M. Fojtová · E. Sýkorová · L. Najdekrová · P. Polanská ·
D. Zachová · J. Fajkus (✉)
Faculty of Science and CEITEC – Central European Institute
of Technology, Masaryk University, Kamenice 5, 62500 Brno,
Czech Republic
e-mail: fajkus@sci.muni.cz

M. Fojtová · E. Sýkorová · J. Fajkus
Institute of Biophysics, Czech Academy of Sciences, v.v.i.,
Královopolská 135, 61265 Brno, Czech Republic

R. Vagnerová · K. J. Angelis
Institute of Experimental Botany, Czech Academy of Sciences,
v.v.i., Na Karlovce 1, 16000 Prague 6, Czech Republic

Keywords *Physcomitrella patens* · Telomere maintenance · Telomerase · *PpTERT* structure · DSB repair mutants

Introduction

Telomeres are the conserved terminal domains of linear chromosomes, which are essential for protection of chromosome integrity. Telomeres are chromatin structures and as such they are formed by telomeric DNA and numerous protein components (reviewed in Fajkus et al. 2005). Telomeres serve multiple roles, but their fundamental functions include demarcation of natural chromosome ends to distinguish them from unrepaired chromosome breaks and prevent telomeres from unwanted repair (the so called end-protection problem) (de Lange 2009). Failure in this

function results in chromosome fusions and subsequent genome instability [breakage–fusion–bridge cycle, BFB (McClintock 1941)]. This function is dependent on specific telomeric proteins, as well as the protective secondary structures (such as G-quadruplexes or t-loops) of telomeric DNA itself (de Lange 2009). The second major role of telomeres is to solve the end-replication problem, i.e. to ensure stable maintenance of themselves, as the conventional semiconservative replication is not able to replicate completely the 3'-end of the parental DNA strand synthesized by lagging strand synthesis (Olovnikov 1971). The most common mechanism to counteract this replicative telomere shortening is telomere elongation by a specific ribonucleoprotein complex called telomerase (Greider and Blackburn 1985, 1987). Telomerase replenishes telomeres by a reverse transcription mechanism using its catalytic protein subunit (Telomerase Reverse Transcriptase, TERT) and template RNA subunit (Telomerase RNA, TR) (Greider and Blackburn 1989) for synthesis of tandem repeats of $T_xA_yG_z$ units as TTAGGG in vertebrates or TTTAGGG in most land plants and algae (Sykorova et al. 2003b; Fulneckova et al. 2013).

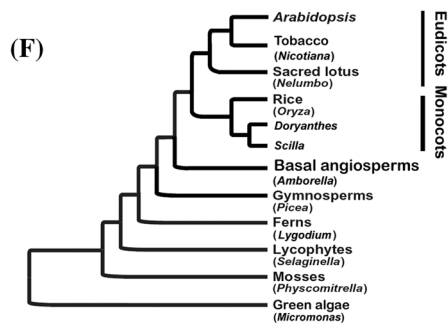
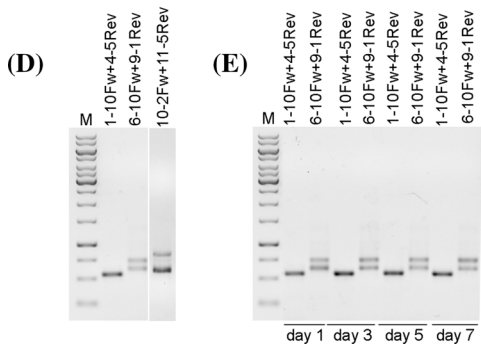
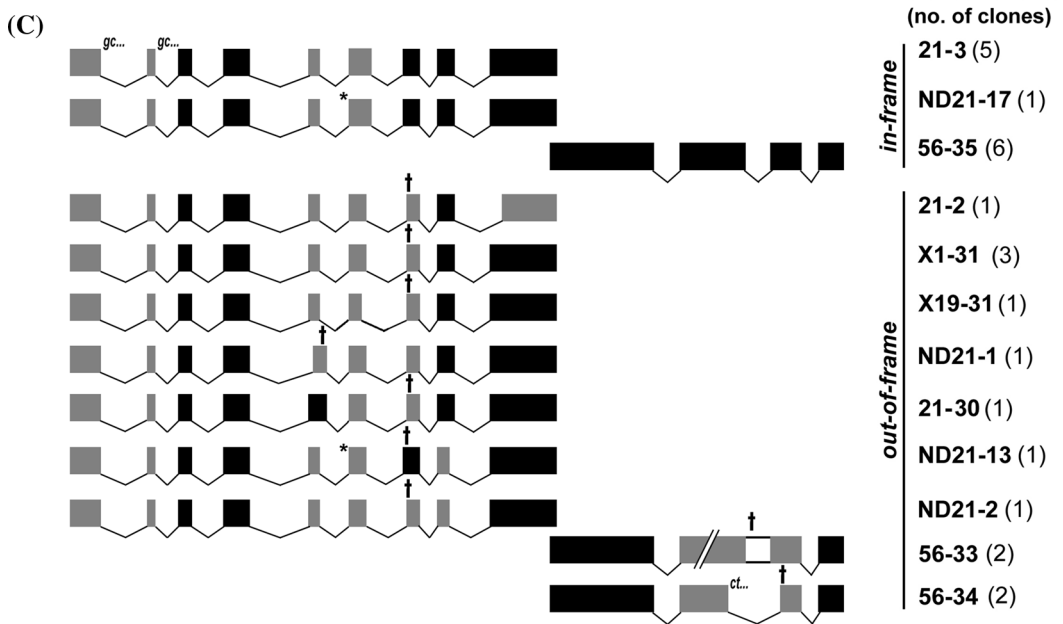
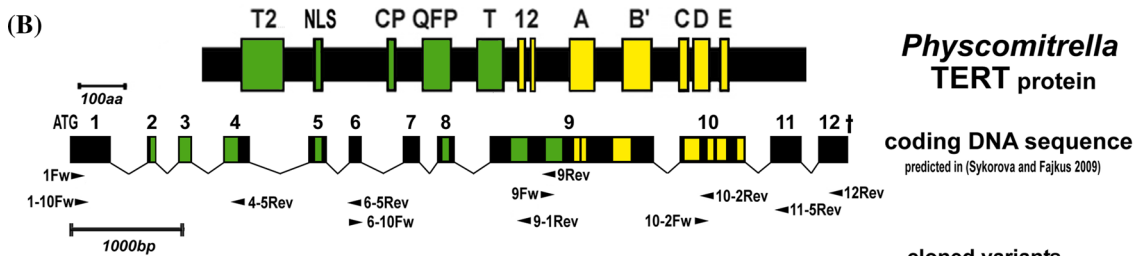
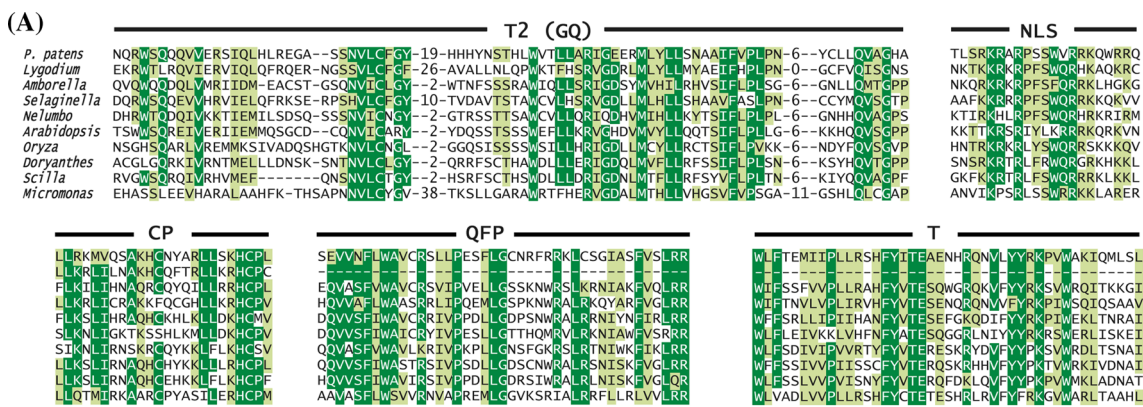
Telomere and telomerase functions are highly conserved among yeasts, protozoans, plants and animals, although exceptions were described which show a telomere sequence different from its phylogenetic position (Sykorova et al. 2003a, b) or even a different (telomerase-independent) mechanism of telomere synthesis (Pich et al. 1996; Sykorova et al. 2006a). In plants, telomere biology has been studied mostly in classical model species such as *Arabidopsis thaliana* or *Nicotiana tabacum* (Fajkus et al. 1995, 1996; Fitzgerald et al. 1996) and compared to flowering plants, much less information is available in lower plants like moss and algae species (Suzuki 2004; Shakirov et al. 2010; Fulneckova et al. 2012, 2013).

Physcomitrella patens is a species of moss (bryophytes) which is a basal lineage of land plants, having diverged before the acquisition of well-developed vasculature (Fig. 1f). As the oldest living branch in land plant evolution, it stands in an important phylogenetic position for comparative studies to illuminate the evolution of the mechanisms behind the complexity of modern plants, including model organisms, such as *Arabidopsis*, and crop plants (Rensing et al. 2008). The body plans of all land plants are shaped through the actions of apical meristems, tissues composed of self-renewing stem cells that provide daughter cells for subsequent differentiation (Graham et al. 2000; Friml et al. 2006; Benkova et al. 2009) and some common pathways of apical meristem regulation may be conserved between ancestral plants and present day mosses (Prigge and Bezanilla 2010; Viaene et al. 2014).

Unlike its 450 million years younger land plant relatives, *Physcomitrella* is one of a few known multicellular

Fig. 1 PpTERT protein, gene, expression and mRNA splicing variants. **a, b** The *Physcomitrella* (Bryophytes) telomerase reverse transcriptase (TERT) subunit comprises conserved N-terminal telomerase specific regions [T2(GQ), NLS, CP, QFP, T] and reverse transcriptase motifs (1, 2, A–E) similar to other TERTs. The predicted PpTERT coding DNA sequence (**b**) from the start (ATG) to the stop (†) codon was revised and detailed analysis of cloned cDNA sequences (**c**) confirmed the existence of 12 exons in the *PpTERT* gene and a high number of splicing events leading mostly to out-of-frame variants with premature stop codons. Detailed RT-PCR analysis (primer positions shown in **b**) and sequencing of purified RT-PCR products (representative combinations obtained in RNA from 7 day protonemata shown in **d**) demonstrated the major splicing pattern in the exon 1–4 region (1–10Fw and 4–5Rev primers) which confirms data from all cloned cDNA sequences. In addition, the presence of two abundant mRNA variants corresponding to the in-frame representative clone 21–3 and the out-of-frame representative clone X1–31 (compare primer combination 6–10Fw and 9–1Rev in **d**) was revealed during protonema development (**e**). The major splicing variant of the 3'/region is represented by the in-frame clone 56–35. Besides that, a low abundance of the out-of-frame variant 56–33 was observed (10–2Fw and 11–5Rev primers, shown in **d**). Phylogeny position of *Physcomitrella* (**f**) as a basal plant lineage indicates that its 12 exon TERT structure as ancestral to plant telomerase TERT genes. An overview of land plant phylogeny including the relationship among major lineages of angiosperms was adapted and modified from (Albert et al. 2013) (scientific names in parentheses). **a** Aligned sequences (phylogeny relationship shown in **f**) were (i) experimentally verified TERT sequences from *Arabidopsis* (Genbank AAD54276.1), rice (*Oryza sativa*, AAM21641.1), *Doryanthes excelsa* (AAX19887.1), *Scilla peruviana* (both Asparagales, AAX21217.1); (ii) transcriptome isotig from fern (*Lygodium japonicum*, isotig24217, <http://bioinf.mind.meiji.ac.jp/kanikusa/>) (iii) predicted TERT sequences from green alga (*Micromonas* sp. RCC299, Mamiellales, Genbank XP_002505190.1), sacred lotus (*Nelumbo nucifera*, Proteales, Genbank XP_010257254.1); (iv) revised TERT prediction from *Amborella trichopoda* (basal Magnoliophyta, AmTr_v1.0_scaffold00007, NW_006498404) and *Selaginella moellendorffii* (Lycopodiidae, SELMOscaffold_16, NW_003314277). **b** Positions of telomerase specific motifs are highlighted in the PpTERT protein and predicted coding DNA sequence. **c** Cloned cDNA sequences (clone names on right with the number of corresponding sequenced clones given in brackets) show usage of the alternative splice donor sites (*gc...*, *ct...*), and a high number of splicing events either corresponding (*black*) or not corresponding (*grey*) to predicted exon–intron borders illustrated in part (**b**). The alternative splice donor site in exon 6 (*) was found in two clones and it differs in three nucleotides from the major splice site

organisms with a highly efficient system of homologous recombination (Schaefer 2002; Kamisugi et al. 2006). Consequently, gene targeting in *Physcomitrella* is five orders of magnitude more efficient than in angiosperms and two orders of magnitude more efficient than in mouse embryonic stem cells, thus being comparable with that observed in *Saccharomyces cerevisiae* (Kamisugi et al. 2006). In contrast to seed plants, the dominating generation in the moss life cycle is the haploid gametophyte and the regenerating moss filaments (protonemata) can be directly assayed using PCR methods without complex back-crosses (Kamisugi et al. 2006; Smidkova et al. 2010).



In this paper, we take advantage of the use of *P. patens* to perform a comparative investigation of telomere dynamics between this species representing lower plants, and flowering plants. In contrast to animals, telomerase is not developmentally silenced during embryogenesis in flowering plants, but remains active throughout entire plant life in dividing meristem cells (Fajkus et al. 1996; Fitzgerald et al. 1996). This results in the absence of replicative telomere shortening during individual plant development in contrast to animals (Fajkus et al. 1998; Riha et al. 1998). However, experimental support for these conclusions has been only indirect so far since plant samples used for telomere and telomerase analyses always contain unknown proportions of meristem cells in great excess of other cells. In contrast, the filaments of *P. patens* protonema grows by apical cell division and represents a perfect cell-lineage and, therefore, plant development can be pinpointed to the differentiation of a single cell. Most importantly, the percentage of apical cells can be quantified exactly, depending on the days of protonema cultivation (total cell number) and the level of protonema branching, and thus it is possible to tackle the telomere and telomerase dynamics experimentally. To do this, we characterise here the gene coding for telomerase reverse transcriptase, *PpTERT*, in *P. patens* that we have predicted previously from genome sequencing data (Sykorova and Fajkus 2009). We further perform analyses of *PpTERT* expression, telomerase activity and telomere lengths, in samples with a varying percentage of apical cells during protonema growth. Finally, we examine telomerase activity and telomere lengths in selected mutants for DNA repair factors which are potentially involved in *P. patens* telomere structure, function and maintenance, as inferred from the corresponding results obtained in land plants.

Materials and methods

Plant material

Physcomitrella patens (Hedw.) B.S.G. “Gransden 2004” wild type and the mutants *pprad50*, *ppmre11*, *ppnbs1* and *pplig4* were described previously (Kamisugi et al. 2012; Hola et al. 2013). The *pplig4* and *ppku70* mutants in the C-NHEJ repair pathway were generated by D. G. Schaefer, Neuchatel University, Switzerland and F. Nogue, INRA, Paris, France as gene replacement mutants, and were kindly provided to us by the authors.

Cultivation of *P. patens*

P. patens wild type and mutants were propagated vegetatively as described by (Knight et al. 2002). Individual plants

were cultured as ‘spot inocula’ on BCD agar medium supplemented with 1 mM CaCl₂ and 5 mM ammonium tartrate (BCDAT medium), or as lawns of protonemal filaments by subculture of homogenized tissue on BCDAT agar medium overlaid with cellophane discs (Focus Packaging & Design, UK) in growth chambers with 18/6 h day/night cycle at 22/18 °C.

For subculture and preparation of 1-day-old protonemal tissue, 1-week-old tissue scraped from plates was suspended in 8 mL of BCD medium and sheared by a T25 homogenizer (IKA, Germany) at 24,000 rpm for two 1-minute cycles and let 24 h to recover in a cultivation chamber with gentle shaking at 100 rpm. This treatment yielded a suspension of 3–5 cell protonema filaments, which readily settle for recovery. Settled protonemata could be handled without excessive losses by tweezers on Petri plates.

Counting of apical cells in *P. patens* branching culture

Cells cultivated on agar plates were counted manually by eye using a stereoscopic binocular light microscope (Olympus SZX16 research stereo microscope), and the field in sharp focus was evaluated on a computer monitor. Only objects in the focused area were included for counting. Specific fields were selected randomly across the plate, and usually areas with a lower density of cells were considered. Cells were counted on ten independent plate sections containing 25–204 cells for each time period using four independently grown cultures.

Cloning and analysis of *PpTERT* gene structure

Total RNA was isolated from *P. patens* cultures using the RNeasy Plant Mini Kit (Qiagen) followed by DNaseI treatment (TURBO DNA-free, Applied Biosystems) according to the manufacturers’ instructions. cDNA was prepared by reverse transcription of 1 µg of RNA using M-MuLV reverse transcriptase (NEB) and Random Nonamers (Sigma). The predicted *PpTERT* gene sequence (Sykorova and Fajkus 2009) was used for designing specific primers and cloning of the cDNA sequence (Table S1, Fig. 1 b). RT-PCR conditions for primer combinations (1Fw or 1–10Fw and 9Rev primers, 9Fw and 12Rev primers, Table S1) were optimized using gradient PCR and the *PpTERT* sequences were amplified with *DyNAzyme* II DNA Polymerase (Finnzymes) as follows: 2 min of initial denaturation and 35 cycles of 30 s at 94 °C, 30 s at 57 °C and 90 s at 72 °C. Sequences covering the overlapping cDNA regions (exons 1–9 and exons 9–12, GenBank KM886460–KM886468, KP001262, KP091459) were cloned, sequenced and manually aligned on the predicted *PpTERT* gene sequence (Sykorova and Fajkus 2009). The

prevailing splicing pattern of the *PpTERT* transcripts was verified by sequencing of the RT-PCR products spanning regions with frequent alternative splicing sites (see below, Table S1, Fig. 1c). The PpTERT protein sequence was examined for the presence of conserved motifs and manually aligned to the experimentally verified plant TERT sequences of *Arabidopsis thaliana*, *Oryza sativa*, *Doryanthes excelsa*, and *Scilla peruviana* (see (Sykorova and Fajkus 2009) for review), and to predicted sequences from the transcriptome of *Lygodium japonicum* (Aya et al. 2015) and the genome scaffolds of *Selaginella moellendorffii* (Banks et al. 2011), *Amborella trichopoda* (Albert et al. 2013), *Nelumbo nucifera* (Ming et al. 2013) and the prasinophyte alga *Micromonas* sp. RCC299 (Worden et al. 2009).

Analysis of the *PpTERT* gene transcripts

Quantification of the *PpTERT* transcript levels was done using FastStart SYBR Green Master (Roche) and primers derived from the exon 10 coding for the reverse transcription domain of the protein (Table S1); ubiquitin was chosen as a reference gene (Harries et al. 2005). One microliter of $2 \times$ diluted cDNA (see above) was added to the 20 μ l reaction mix, and the final concentration of each forward and reverse primer was 0.25 μ M. Reactions were done in triplicates; the PCR cycling consisted of 15 min of initial denaturation followed by 40 cycles of 30 s at 94 °C, 30 s at 56 °C and 30 s at 72 °C. At least two biological replicates in two technical replicates were analysed. Relative *TERT* transcription was calculated by the $\Delta\Delta$ Ct method (Pfaffl 2004). Additional RT-PCR experiments were performed to verify exon/intron structure of the *PpTERT* gene and the presence of mRNA variants during development.

Analysis of telomerase activity (TRAP—telomere repeat amplification protocol)

In vitro analysis of telomerase activity is based on the elongation of a substrate primer by the telomerase, and the extension product is then amplified by PCR. A telomerase extract from *P. patens* cultures was prepared as previously described (Fitzgerald et al. 1996; Sykorova et al. 2003a), and the maximum of telomerase activity was detected in fractions precipitated by 7.5–10.0 % PEG 8000. The quantitative version of the TRAP assay was performed according to (Herbert et al. 2006) using FastStart SYBR Green Master (Roche) and TS21 substrate primer and TelPr reverse primer (Table S1). Samples were analysed in triplicates in a 20- μ l reaction mix, and at least two biological replicates (independently grown cultures) were evaluated.

Relative telomerase activity was calculated by the Δ Ct method (Pfaffl 2004).

Analysis of telomere lengths

Analysis of telomere lengths by the Terminal Restriction Fragments (TRF) method is based on the digestion of genomic DNA by a frequently cutting restriction endonuclease without a recognition site in the G-rich telomeric repeats. After hybridization with a radioactively labeled telomeric probe, the signal corresponds to non-digested telomeric tracts (plus subtelomeric regions up to the first restriction site upstream of the telomeres). Analysis was performed as previously described (Ruckova et al. 2008; Jaske et al. 2013). Briefly, a *P. patens* culture was homogenized in liquid nitrogen, DNA was isolated according to (Dellaporta et al. 1983) and digested by either *Mse*I or *Taq*I restriction enzymes. Southern hybridization was performed with a telomeric probe synthesized as described in (Ijdo et al. 1991). Signals were visualized on a FLA7000 phosphorimager (FujiFilm). Evaluation of fragment lengths was done by using the Gene Ruler 1-kb DNA Ladder (Fermentas) as a standard; hybridization patterns were analysed by Multi Gauge software (FujiFilm). The unweighted mean telomere length was calculated as $\sum(\text{OD}_i \times L_i) / \sum(\text{OD}_i)$, where OD_i is the signal intensity above background within interval i and L_i is the molecular weight (kb) at the midpoint of interval i .

Analysis of induced DNA double strand breaks (DSBs) and of their repair in *P. patens*

Bleomedac inj. (Medac, Hamburg, Germany) was used for Bleomycin treatment as previously described (Hola et al. 2013). One day regenerated protonemal tissues (>50 % of apical cells) from wild type and mutant lines were treated with Bleomycin for 1 h prior to nuclear extraction and analysis. DSBs were detected by a comet assay using a fully neutral N/N protocol (Olive and Banath 2006; Rensing et al. 2008; Kozak et al. 2009). Comets were stained with SYBR Gold (Molecular Probes/Invitrogen), viewed in epifluorescence with a Nikon Eclipse 800 microscope and captured and evaluated by the LUCIA Comet cytogenetic software (LIM Inc., Czech Republic). The fraction of DNA in comet tails was used as a measure of DNA damage and for calculation of the percentage of DSBs remaining (Kozak et al. 2009). Data in this study were obtained in at least three independent experiments. Measurements of blindly labeled comet slides included four independent gel replicas of 25 evaluated comets with a total of at least 300 comets analyzed per experimental point.

Results and discussion

Structure of *PpTERT* gene

In order to track a possible involvement of telomerase expression in *P. patens* telomere dynamics, we analysed *P. patens TERT* gene structure and transcription. According to the *P. patens* genome annotation v1.6 (Rensing et al. 2008), the *PpTERT* gene sequence was predicted in silico with only three exons covering the C-part of the PpTERT protein thus possibly missing specific N-terminal telomerase motifs. Taking advantage of our knowledge about *TERT* gene structure and possible mRNA splicing (Rensing et al. 2005) we predicted 12 exons in the *PpTERT* gene (6971 bp long, inside contig ABEU01012720 (Sykorova and Fajkus 2009), Fig. 1b) similarly to other known plant *TERT* genes. To verify the predicted *PpTERT* gene and mRNA structure, we cloned cDNA sequences to cover the entire *PpTERT* (GenBank KM886460–KM886468, KP001262). Our gene structure prediction differed from the experimental results only in details, e.g. alignments of cloned *PpTERT* sequences revealed that exons 1 and 2 used the alternative splice donor site GC (Fig. 1c) instead of the consensus splice site GT reported in *Physcomitrella* transcriptome analysis (Rensing et al. 2005). This splicing pattern was found in all cloned cDNA sequences (Fig. 1c) and confirmed by sequencing of RT-PCR products spanning exon 1–4 (Fig. 1b, d, e). The exon lengths and cDNA sequence also correspond to the EST sequence (Genbank CN203080) covering exons 1–4 of the putative *TERT* of the bryophyte *Syntricha ruralis*. Moreover, we identified a surprisingly high number of alternative splicing events in *PpTERT*. These comprise different combinations of alternative donor and acceptor sites, especially in the 5' region of the *PpTERT* transcript, and retention of the intron 10 (Fig. 1c). Variation between the predicted and the cloned *PpTERT* cDNA sequences originated mostly from alternative splicing of exons 5–7 that code for a non-conserved protein linker between the nuclear localisation signal (NLS) and CP telomerase motifs. Majority of identified splicing events lead to out-of-frame mRNA variants (Fig. 1c). The high number of identified alternative transcripts necessitated a detailed analysis of major splicing patterns via sequencing of RT-PCR products that span exons 1–4, 1–6, 4–7, 7–9 and 9–12 (Table S1, Fig. 1b, d). For the 5' region of *PpTERT*, the results verified the presence of two major variants (Fig. 1b–d, primer combination 6–10Fw and 9–1Rev) found in the representative clone 21–3 (in-frame variant, Genbank KM886462) and in the representative clone 31–X1 (out-of-frame, premature stop codon in exon 7). Sequencing of RT-PCR products for the 3' region of *PpTERT* showed the presence of a major variant 56–35 (in-frame, Genbank KM886460) in addition to a low abundance variant 56–33 (out-of frame, premature stop codon in intron 10) (Fig. 1b–d, primer combination 10–2Fw and 11–5Rev). The

major mRNA splicing represented by in-frame variant clone 56–35 was also verified with the EST sequences from the GENBANK database (Unigene ID: 2850076).

Analysis of the PpTERT protein sequence (1301 AA, 148 kDa, pI 9.371) clearly showed the presence of all telomerase specific motifs (Fig. 1a) including the conserved NLS motif and highly conserved regions in the C-terminal extension similar to other plant TERTs (Sykorova et al. 2006a, b; Sykorova and Fajkus 2009). To compare telomerase structure from evolutionary distinct plant groups we analyzed a representative set comprising eudicots (*Arabidopsis*, sacred lotus), monocots (rice, *Doryanthes*, *Scilla*), basal angiosperm (*Amborella*), fern (*Lygodium*), lycophyte (*Selaginella*) and green alga (*Micromonas*). The experimentally verified sequences and the *Lygodium* isotig derived from transcriptome data were used for prediction or improvement of predicted TERT gene and protein structures (Fig. 1a). For example, analysis of the predicted *Amborella TERT* sequence revealed a misannotated gene structure and analysis of the corresponding genome scaffold clearly showed the presence of 12 exons similarly to the prediction from *Selaginella* scaffold 16, and the predicted *Nelumbo TERT*. Together with the presented *Physcomitrella TERT* data, these results suggest a 12 exon gene structure for an ancestral plant *TERT* (Fig. 1f) and also emphasize the necessity of experimental verification of predicted *TERT* gene structures.

RT-PCR analysis of *PpTERT* mRNA variants during development

The spectrum of *PpTERT* alternative splicing events is in agreement with the moss genome re-annotation that was reported after implementation of *Physcomitrella* transcriptome data (Zimmer et al. 2013) confirming intron retention as the most frequent form (~40 %) among gene loci with alternate transcripts (~21 % of all genes). However, its abundance in a single gene is quite unusual—for example, alternative *TERT* transcripts amount to only a few per cent in *Arabidopsis* (Zachova et al. 2013). The almost equal representation of in-frame and out-of-frame *PpTERT* variants during protonema development (Fig. 1e) may be of functional relevance, possibly related to the haploid protonema status. To our knowledge, equimolar representation of more *TERT* gene variants was only detected in the polyploid species *Nicotiana tabacum*, where three sequence variants of the *TERT* gene derived from the progenitor *N. tomentosiformis* and *N. sylvestris* genomes were identified (Sykorova et al. 2012). However, even in this case the level of the pseudogene *TERT* variant transcript was negligibly low (close to the detection limit). Potential translation of the out-of-frame *PpTERT* variant would lead to a protein comprising the N-terminal telomerase domain similar to the

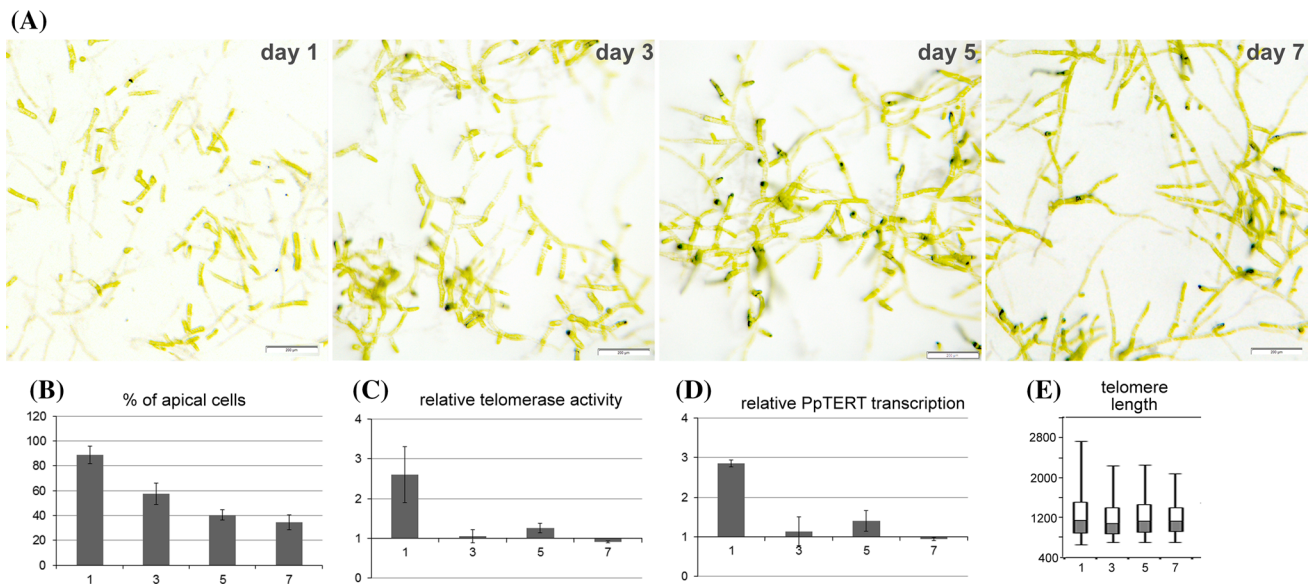


Fig. 2 Telomere dynamics in *P. patens* protonema. **a** Morphology of *P. patens* cells, **b** percentage of apical cells, **c** telomerase activity, **d** *PpTERT* gene transcription, and **e** telomere lengths in the course of 7-day culturing. A 7-day old culture was mechanically disrupted to destroy branched cells chains and cultivated under standard conditions. Samples were taken in 1, 3, 5 and 7 days after sub-culturing for respective analyses. Telomerase activity and *TERT* gene transcription

were related to the values obtained for a 7-day culture. The length of telomeres is presented using a box-and-whisker plot where the bottom part (gray) and the top (white) of the box are the lower and upper quartiles, respectively, separated by the median. The ends of the whiskers represent the minimum and maximum length corresponding to the hybridization signal range. Analyses were performed using three independently grown cultures

Arabidopsis TERT V(I8) variant. This variant interacts with POT1a, one of the paralogs of POT1 (Protection of Telomeres 1), a single-stranded-DNA-binding protein (Rosignol et al. 2007) and was suggested to provide additional telomerase function and regulation (reviewed in Majerska et al. 2011). Since *P. patens* also harbours a gene coding for POT1 protein (only a single-copy) and, moreover, its role for telomere integrity has already been demonstrated (Shakirov et al. 2010), this hypothesis is plausible.

Telomere dynamics during protonema growth

When sub-culturing the *P. patens* protonemata, highly branched chains of cells were mechanically disrupted and transferred to fresh medium; during the growth phase, the protonemata lengthened and divided forming branched chains. Since in higher plants telomerase is active in organs and tissues containing dividing meristem cells (seedlings, root tips, blossoms, floral buds), we monitored the percentage of apical cells in a growing *P. patens* culture and correlated this parameter to the telomerase activity, *PpTERT* transcript levels, and telomere length. One day after sub-culturing, the level of apical cells was highest and decreased relatively sharply during the subsequent 2 days, while a further drop was significantly slower (Fig. 2a, b). Telomerase activity and *PpTERT* gene transcripts increased moderately but reproducibly in the first day after the sub-culturing (Fig. 2c, d), when about 85 % of

the cells were located at the chain termini (Fig. 2b). In the following time intervals, telomerase activity and *PpTERT* transcripts were at the level comparable to standard 7-day-old culture which was used as the source culture. Importantly, the accrual of telomerase activity and transcription after sub-culturing was not correlated with a possible stress connected to the mechanical disruption of protonemata; telomerase activity and transcription in the 7-day-old culture collected from the plate and the same culture after mechanical treatment were quite comparable (data not shown). Telomere lengths were stable during the *P. patens* protonema culturing (Fig. 2e, Fig. S1) which accords with the results obtained in higher plants where telomere lengths are preserved in all tissues throughout development (Fajkus et al. 1998; Riha et al. 1998). Based on these results, telomerase activity and expression correlates with the proportion of apical cells in a protonema culture and telomere lengths remain stable during 7-day culturing in *P. patens*. We conclude that our results provide a direct experimental support of the general validity of the key principles of telomere dynamics during plant development which so far have only been predicted.

Telomere maintenance in *P. patens* mutants in selected DSB repair factors

In the *Arabidopsis thaliana* model plant, telomere homeostasis was shown to be disrupted in mutants with loss of

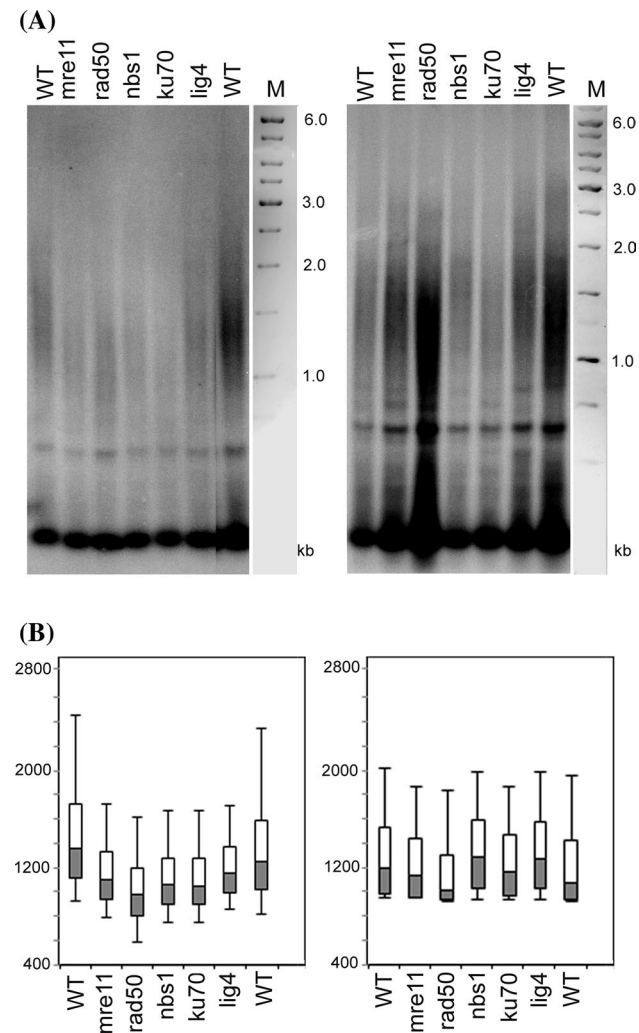


Fig. 3 Telomere length in *P. patens* mutants. The length of telomeric repeats was assayed by the TRF protocol in 7-day old cultures (two biological replicates are shown). **a** After hybridization of DNA digested by a restriction endonuclease against the telomeric probe, the radioactive signals in mutants lines reflecting the length of telomeres were either slightly shifted towards shorter lengths compared to wild type (WT) samples (*left*) or were maintained at the wild type level (*right*). Five independent analyses of telomere length were performed, and representative results are presented. **b** Hybridization signals were evaluated by MultiGauge software (Fujifilm) and are presented using a *box-and-whisker* plot as described in Fig. 2

function of genes coding for proteins involved in repair and recombination processes (see below). Although one of the crucial functions of telomeres is prevention of aberrant recombination events at the chromosome termini, proteins participating in recombination are essential for proper telomere structure and functions and are even involved in alternative mechanisms of telomere lengthening (Draskovic et al. 2009; Amiard et al. 2011). We took advantage of the extremely efficient system of homologous recombination in *P. patens* (Schaefer 2002) which enables relatively

simple and highly effective targeting of any non-essential gene, and analyse telomere length, telomerase activity and transcription of the *PpTERT* gene in mutant lines as follows: (i) In mutants in genes of the MRN complex (*mre11*, *rad50*, *nbs1*) which is involved in recognition of DSBs in DNA and subsequent phosphorylation signalling. Vertebrate cells with *MRE11* gene loss of function are even not viable, but in *A. thaliana* telomere lengthening was observed and mutants were hypersensitive to DNA damaging agents and suffered from developmental defects (Bundock and Hooykaas 2002). Similarly, *RAD50* function is essential for telomere maintenance in *A. thaliana*; in plants with a T-DNA insertion in the *AtRAD50* gene a significant telomere shortening and meiotic and DNA repair defects were observed (Gallego and White 2001). Finally, *A. thaliana nbs1* mutants are without morphological defects and telomere length is at the wild type level, but in *nbs1/tert* double-mutants telomere erosion was more progressive compared to *tert* mutants suggesting interplay of NBS1 and telomerase in telomere homeostasis processes (Najdekrova and Siroky 2012). (ii) In a *ku70* mutant; KU70 protein is a part of the KU70/KU80 complex which binds and stabilizes DSBs. In *Arabidopsis*, KU70 loss led to the formation of extra-long telomeres, elongation of single-strand telomere overhangs and significantly increased level of telomeric circles (Riha et al. 2002; Gallego et al. 2003; Akimcheva et al. 2008). (iii) In a *lig4* mutant with loss of function of the major DNA ligase participating in non-homologous end joining. In *Arabidopsis*, telomeres in *lig4* mutant are more heterogeneous but have the same average length as wild type telomeres (Heacock et al. 2007).

In the *P. patens* mutants tested, telomerase activity and *TERT* gene transcripts assayed by quantitative approaches do not significantly differ from the values obtained for wild type cultures (not shown). Interestingly, lengths of telomeres in mutants, including *ku70* mutant, are similar to the wild type telomeres, and no significant changes were observed (Fig. 3, Fig. S2). Basic telomere protective functions appear to be preserved as well, as suggested by unchanged morphology and growth parameters of mutant cultures (results not shown). Altogether, malfunction of the proteins examined involved in repair and recombination pathways does not influence telomere homeostasis substantially in *P. patens*, in contrast to the common higher plant model *Arabidopsis thaliana* (Table 1). The striking absence of a telomeric phenotype in *ku70* and other mutants in NHEJ factor genes in *P. patens* presumably corresponds to the general dominance and higher efficiency of homologous recombination over NHEJ in this system, contrasting with the opposite situation in flowering plants. These results further suggest that KU70 is not directly involved in protection of telomeres in *P. patens*, contrary to the situation described in *A. thaliana* (Kazda et al. 2012).

Table 1 Comparison of the telomere phenotype in mutants with loss of function of genes involved in the DNA DSB repair pathways in plant models *A. thaliana* and *P. patens*

Mutant	<i>Arabidopsis thaliana</i>	<i>Physcomitrella patens</i>
<i>mre11</i>	Elongated telomeres ^a	No significant changes in telomere lengths
<i>rad50</i>	Shortened telomeres ^b	No morphological or growth defects in protonema cultures
<i>nbs1</i>	WT morphology and telomere length, in <i>nbs/tert</i> more progressive telomere erosion than in <i>tert</i> mutants ^c	
<i>ku70</i>	Extra long telomeres ^d	
<i>lig4</i>	Length of telomeres heterogeneous ^e	

^a Bundock and Hooykaas (2002); ^b Gallego and White (2001); ^c Najdekrova and Siroky (2012); ^d Riha et al. (2002), Gallego et al. (2003) and Akimcheva et al. (2008); ^e Heacock et al. (2007)

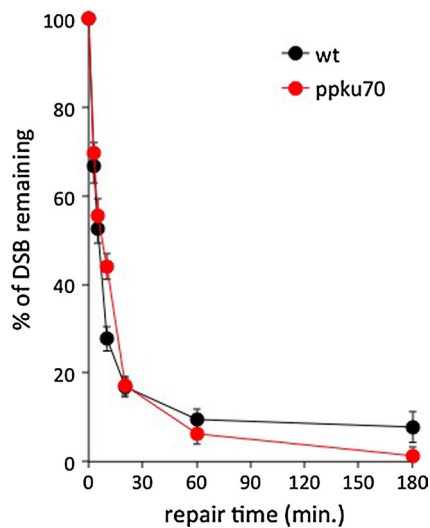


Fig. 4 DSBs repair kinetics determined by comet assay. One day regenerated protonemal tissue from wild type and *ku70* mutant lines was treated with 30 $\mu\text{g/ml}$ Bleomycin for 1 h prior to nuclear extraction and analysis. DSBs were determined by the N/N protocol: black—wild type, red—*ku70*. Repair kinetics is plotted as % of DSBs remaining after 0, 3, 5, 10, 20, 60 and 180 min period of repair. Maximum damage is normalised as 100 % at $t = 0$ for both lines. Error bars show standard error

Repair kinetics of DSBs in *ku70* mutants

In order to assess the interpretation of the surprising absence of a telomeric phenotype in *ku70* mutants, DNA repair kinetics were analysed in these mutants. The results of comet assays demonstrate (Fig. 4) that inactivation of the C-NHEJ pathway in *P. patens* by knocking out the *KU70* gene, whose product is responsible for DSB recognition, does not affect the overall ability to repair DSBs. Similarly mutations of *LIG4* (Hola et al. 2013), a factor involved in the final step of C-NHEJ, and of *MRE11*, *RAD50* and *NBS1*, components of the key repair complex MRN involved in both NHEJ and homologous recombination pathways (Kamisugi et al. 2012), do not affect overall DSB

repair in *P. patens* apical cells. In this respect, the moss *P. patens* parallels the situation in *Arabidopsis* where mutants of *KU80* and *LIG4* also efficiently repair DSBs (Kozak et al. 2009; Amiard et al. 2010; Charbonnel et al. 2010, 2011) but in contrast to *Physcomitrella*, the *Arabidopsis* mutants repair DSBs during the 1st phase even faster than wt Col0 (Kozak et al. 2009). Thus, *P. patens* wild type and mutants used in these studies exercise efficient and rapid DSB repair that in the case of deprotected telomeres can detect them as substrates for joining. However, the absence of a telomere phenotype in the corresponding *P. patens* mutants suggests that the loss of neither of these factors results in telomere deprotection.

Conclusion

We report here on the characterisation of *PpTERT* gene and its major splicing variants in growing protonemata. The overall *PpTERT* exon structure and the arrangement of telomerase-specific functional motifs in the amino acid sequence is conserved with respect to the previously characterised plant *TERTs*. A surprisingly rich spectrum and high abundance of alternate splicing products was observed and subsequent studies should address their functional importance. Further, we investigated telomere maintenance in growing *P. patens* protonemata and our results demonstrate telomere length stability and association of telomerase activity and expression with dividing apical cells. These findings provide experimental evidence for previously anticipated principles governing plant telomere biology and suggest their general validity among both lower and land plants. Next, we examined *P. patens* mutants in DSB repair factors for a possible telomere phenotype. Particularly interesting is the absence of a telomere phenotype in mutants depleted of *KU70*, the key factor in NHEJ, whose absence in *Arabidopsis* results in extremely elongated telomeres. Our results suggest that contrary to the situation in *A. thaliana*, *KU70* is not essential for protection of

telomeres in *P. patens*. Thus, our study identifies both conserved and distinct features between the telomere biology of lower and land plants which may initiate further studies directed to deeper understanding of their strategies to protect genome integrity.

Acknowledgments This work was supported by the Czech Science Foundation (13-06595S), project CEITEC (CZ.1.05/1.1.00/02.0068) of the European Regional Development Fund and project EVOGEN (CZ.1.07/2.3.00/20.0189) co-financed from European Social Fund and the State Budget of the Czech Republic.

References

- Akimcheva S, Zellinger B, Riha K (2008) Genome stability in Arabidopsis cells exhibiting alternative lengthening of telomeres. *Cytogenet Genome Res* 122:388–395. doi:[10.1159/000167827](https://doi.org/10.1159/000167827)
- Albert VA et al (2013) The Amborella genome and the evolution of flowering plants. *Science* 342:1467. doi:[10.1126/science.1241089](https://doi.org/10.1126/science.1241089)
- Amiard S, Charbonnel C, Allain E, Depeiges A, White CI, Gallego ME (2010) Distinct roles of the ATR kinase and the Mre11-Rad50-Nbs1 complex in the maintenance of chromosomal stability in Arabidopsis. *Plant Cell* 22:3020–3033. doi:[10.1105/tpc.110.078527](https://doi.org/10.1105/tpc.110.078527)
- Amiard S, White C, Gallego ME (2011) Recombination proteins and telomere stability in plants. *Curr Protein Pept Sci* 12:84–92
- Aya K, Kobayashi M, Tanaka J, Ohyanagi H, Suzuki T, Yano K, Takano T, Yano K, Matsuoka M (2015) De novo transcriptome assembly of a fern, *Lygodium japonicum*, and a web resource database, Ljtrans DB. *Plant Cell Physiol* 56:e5. doi:[10.1093/pcp/pcu184](https://doi.org/10.1093/pcp/pcu184)
- Banks JA, Nishiyama T, Hasebe M et al (2011) The Selaginella genome identifies genetic changes associated with the evolution of vascular plants. *Science* 332:960–963. doi:[10.1126/science.1203810](https://doi.org/10.1126/science.1203810)
- Benkova E, Ivanchenko MG, Friml J, Shishkova S, Dubrovsky JG (2009) A morphogenetic trigger: is there an emerging concept in plant developmental biology? *Trends Plant Sci* 14:189–193. doi:[10.1016/j.tplants.2009.01.006](https://doi.org/10.1016/j.tplants.2009.01.006)
- Bundock P, Hooykaas P (2002) Severe developmental defects, hypersensitivity to DNA-damaging agents, and lengthened telomeres in Arabidopsis MRE11 mutants. *Plant Cell* 14:2451–2462. doi:[10.1105/Tpc.005959](https://doi.org/10.1105/Tpc.005959)
- Charbonnel C, Gallego ME, White CI (2010) Xrcc1-dependent and Ku-dependent DNA double-strand break repair kinetics in Arabidopsis plants. *Plant J* 64:280–290. doi:[10.1111/j.1365-3113X.2010.04331.x](https://doi.org/10.1111/j.1365-3113X.2010.04331.x)
- Charbonnel C, Allain E, Gallego ME, White CI (2011) Kinetic analysis of DNA double-strand break repair pathways in Arabidopsis. *DNA Repair (Amst)* 10:611–619. doi:[10.1016/j.dnarep.2011.04.002](https://doi.org/10.1016/j.dnarep.2011.04.002)
- de Lange T (2009) How telomeres solve the end-protection problem. *Science* 326:948–952. doi:[10.1126/science.1170633](https://doi.org/10.1126/science.1170633)
- Dellaporta SL, Wood J, Hicks JB (1983) A Plant DNA miniprep. Version II. *Plant Mol Biol Rep* 1:19–21
- Draskovic I, Arnoult N, Steiner V, Bacchetti S, Lomonte P, Londono-Vallejo A (2009) Probing PML body function in ALT cells reveals spatiotemporal requirements for telomere recombination. *Proc Natl Acad Sci U S A* 106:15726–15731. doi:[10.1073/pnas.0907689106](https://doi.org/10.1073/pnas.0907689106)
- Fajkus J, Kovarik A, Kralovics R, Bezdek M (1995) Organization of telomeric and subtelomeric chromatin in the higher plant *Nicotiana tabacum*. *Mol Gen Genet* 247:633–638. doi:[10.1007/Bf00290355](https://doi.org/10.1007/Bf00290355)
- Fajkus J, Kovarik A, Kralovics R (1996) Telomerase activity in plant cells. *FEBS Lett* 391:307–309
- Fajkus J, Fulneckova J, Hulanova M, Berkova K, Riha K, Matyasek R (1998) Plant cells express telomerase activity upon transfer to callus culture, without extensively changing telomere lengths. *Mol Gen Genet* 260:470–474
- Fajkus J, Sykorova E, Leitch AR (2005) Telomeres in evolution and evolution of telomeres. *Chromosome Res* 13:469–479. doi:[10.1007/s10577-005-0997-2](https://doi.org/10.1007/s10577-005-0997-2)
- Fitzgerald MS, McKnight TD, Shippen DE (1996) Characterization and developmental patterns of telomerase expression in plants. *Proc Natl Acad Sci U S A* 93:14422–14427
- Friml J, Benfey P, Benkova E et al (2006) Apical-basal polarity: why plant cells don't stand on their heads. *Trends Plant Sci* 11:12–14. doi:[10.1016/j.tplants.2005.11.010](https://doi.org/10.1016/j.tplants.2005.11.010)
- Fulneckova J, Hasikova T, Fajkus J, Lukesova A, Elias M, Sykorova E (2012) Dynamic evolution of telomeric sequences in the green algal order Chlamydomonadales. *Genome Biol Evol* 4:248–264. doi:[10.1093/gbe/evs007](https://doi.org/10.1093/gbe/evs007)
- Fulneckova J, Sevcikova T, Fajkus J, Lukesova A, Lukes M, Vlcek C, Lang BF, King E, Elias M, Sykorova E (2013) A broad phylogenetic survey unveils the diversity and evolution of telomeres in eukaryotes. *Genome Biol Evol* 5:468–483. doi:[10.1093/Gbe/Evt019](https://doi.org/10.1093/Gbe/Evt019)
- Gallego ME, White CI (2001) RAD50 function is essential for telomere maintenance in Arabidopsis. *Proc Natl Acad Sci U S A* 98:1711–1716. doi:[10.1073/pnas.98.4.1711](https://doi.org/10.1073/pnas.98.4.1711)
- Gallego ME, Bleuyard JY, Daoudal-Cotterell S, Jallut N, White CI (2003) Ku80 plays a role in non-homologous recombination but is not required for T-DNA integration in Arabidopsis. *Plant J* 35:557–565
- Graham LE, Cook ME, Busse JS (2000) The origin of plants: body plan changes contributing to a major evolutionary radiation. *Proc Natl Acad Sci U S A* 97:4535–4540. doi:[10.1073/pnas.97.9.4535](https://doi.org/10.1073/pnas.97.9.4535)
- Greider CW, Blackburn EH (1985) Identification of a specific telomere terminal transferase activity in Tetrahymena extracts. *Cell* 43:405–413. doi:[10.1016/0092-8674\(85\)90170-9](https://doi.org/10.1016/0092-8674(85)90170-9)
- Greider CW, Blackburn EH (1987) The telomere terminal transferase of Tetrahymena is a ribonucleoprotein enzyme with 2 kinds of primer specificity. *Cell* 51:887–898. doi:[10.1016/0092-8674\(87\)90576-9](https://doi.org/10.1016/0092-8674(87)90576-9)
- Greider CW, Blackburn EH (1989) A telomeric sequence in the RNA of Tetrahymena telomerase required for telomere repeat synthesis. *Nature* 337:331–337. doi:[10.1038/337331a0](https://doi.org/10.1038/337331a0)
- Harries PA, Pan AH, Quatrano RS (2005) Actin-related protein2/3 complex component ARPC1 is required for proper cell morphogenesis and polarized cell growth in *Physcomitrella patens*. *Plant Cell* 17:2327–2339. doi:[10.1105/tpc.105.033266](https://doi.org/10.1105/tpc.105.033266)
- Heacock ML, Idol RA, Friesner JD, Britt AB, Shippen DE (2007) Telomere dynamics and fusion of critically shortened telomeres in plants lacking DNA ligase IV. *Nucleic Acids Res* 35:6490–6500. doi:[10.1093/nar/gkm472](https://doi.org/10.1093/nar/gkm472)
- Herbert BS, Hochreiter AE, Wright WE, Shay JW (2006) Nonradioactive detection of telomerase activity using the telomeric repeat amplification protocol. *Nat Protoc* 1:1583–1590. doi:[10.1038/nprot.2006.239](https://doi.org/10.1038/nprot.2006.239)
- Hola M, Kozak J, Vagnerova R, Angelis KJ (2013) Genotoxin induced mutagenesis in the model plant *Physcomitrella patens*. *Biomed Res Int* 2013:535049. doi:[10.1155/2013/535049](https://doi.org/10.1155/2013/535049)
- Ijdo JW, Wells RA, Baldini A, Reeders ST (1991) Improved telomere detection using a telomere repeat probe (TTAGGG)_n generated by PCR. *Nucleic Acids Res* 19:4780. doi:[10.1093/nar/19.17.4780](https://doi.org/10.1093/nar/19.17.4780)
- Jaske K, Mokros P, Mozgova I, Fojtova M, Fajkus J (2013) A telomerase-independent component of telomere loss in chromatin assembly factor 1 mutants of *Arabidopsis thaliana*. *Chromosoma* 122:285–293. doi:[10.1007/s00412-013-0400-6](https://doi.org/10.1007/s00412-013-0400-6)

- Kamisugi Y, Schlink K, Rensing SA, Schween G, von Stackelberg M, Cuming AC, Reski R, Cove DJ (2006) The mechanism of gene targeting in *Physcomitrella patens*: homologous recombination, concatenation and multiple integration. *Nucleic Acids Res* 34:6205–6214
- Kamisugi Y, Schaefer DG, Kozak J, Charlot F, Vrielynck N, Holá M, Angelis KJ, Cuming AC, Nogue F (2012) MRE11 and RAD50, but not NBS1, are essential for gene targeting in the moss *Physcomitrella patens*. *Nucleic Acids Res* 40:3496–3510. doi:10.1093/nar/gkr1272
- Kazda A, Zellinger B, Rossler M, Derboven E, Kusenda B, Riha K (2012) Chromosome end protection by blunt-ended telomeres. *Genes Dev* 26:1703–1713. doi:10.1101/gad.194944.112
- Knight CD, Cove DJ, Cuming AC, Quatrano RS (2002) Moss gene technology. In: Gilman PM, Bowler C (eds) *Molecular plant biology*, vol 2. Oxford University Press, Oxford, pp 285–299
- Kozak J, West CE, White C, da Costa-Nunes JA, Angelis KJ (2009) Rapid repair of DNA double strand breaks in *Arabidopsis thaliana* is dependent on proteins involved in chromosome structure maintenance. *DNA Repair (Amst)* 8:413–419. doi:10.1016/j.dnarep.2008.11.012
- Majerska J, Sykorova E, Fajkus J (2011) Non-telomeric activities of telomerase. *Mol BioSyst* 7:1013–1023. doi:10.1039/C0mb00268b
- McClintock B (1941) The stability of broken rinds of chromosomes in *Zea mays*. *Genetics* 26:234–282
- Ming R, VanBuren R, Liu Y et al (2013) Genome of the long-living sacred lotus (*Nelumbo nucifera* Gaertn.). *Genome Biol* 14:R41. doi:10.1186/Gb-2013-14-5-R41
- Najdekrova L, Siroky J (2012) NBS1 plays a synergistic role with telomerase in the maintenance of telomeres in *Arabidopsis thaliana*. *BMC Plant Biol* 12:167. doi:10.1186/1471-2229-12-167
- Olive PL, Banath JP (2006) The comet assay: a method to measure DNA damage in individual cells. *Nat Protoc* 1:23–29. doi:10.1038/nprot.2006.5
- Olovnikov AM (1971) Principle of marginotomy in template synthesis of polynucleotides. *Dokl Akad Nauk SSSR* 201:1496–1499
- Pfaffl MW (2004) Quantification strategies in real-time PCR. In: Bustin SA (ed) *A-Z of quantitative PCR*. International University Line, La Jolla, pp 87–112
- Pich U, Fuchs J, Schubert I (1996) How do Alliaceae stabilize their chromosome ends in the absence of TTTAGGG sequences? *Chromosome Res* 4:207–213. doi:10.1007/Bf02254961
- Prigge MJ, Bezanilla M (2010) Evolutionary crossroads in developmental biology: *Physcomitrella patens*. *Development* 137:3535–3543. doi:10.1242/Dev.049023
- Rensing SA, Fritzwosky D, Lang D, Reski R (2005) Protein encoding genes in an ancient plant: analysis of codon usage, retained genes and splice sites in a moss, *Physcomitrella patens*. *BMC Genom* 6:43. doi:10.1186/1471-2164-6-43
- Rensing SA, Lang D, Zimmer AD et al (2008) The *Physcomitrella* genome reveals evolutionary insights into the conquest of land by plants. *Science* 319:64–69. doi:10.1126/science.1150646
- Riha K, Fajkus J, Siroky J, Vyskot B (1998) Developmental control of telomere lengths and telomerase activity in plants. *Plant Cell* 10:1691–1698
- Riha K, Watson JM, Parkey J, Shippen DE (2002) Telomere length deregulation and enhanced sensitivity to genotoxic stress in *Arabidopsis* mutants deficient in Ku70. *EMBO J* 21:2819–2826. doi:10.1093/emboj/21.11.2819
- Rosignol P, Collier S, Bush M, Shaw P, Doonan JH (2007) Arabidopsis POT1A interacts with TERT-V(18), an N-terminal splicing variant of telomerase. *J Cell Sci* 120:3678–3687. doi:10.1242/jcs.004119
- Ruckova E, Friml J, Schrupfova PP, Fajkus J (2008) Role of alternative telomere lengthening unmasked in telomerase knock-out mutant plants. *Plant Mol Biol* 66:637–646. doi:10.1007/s11103-008-9295-7
- Schaefer DG (2002) A new moss genetics: targeted mutagenesis in *Physcomitrella patens*. *Annu Rev Plant Biol* 53:477–501. doi:10.1146/annurev.arplant.53.100301.135202
- Shakirov EV, Perroud PF, Nelson AD, Cannell ME, Quatrano RS, Shippen DE (2010) Protection of Telomeres 1 is required for telomere integrity in the moss *Physcomitrella patens*. *Plant Cell* 22:1838–1848. doi:10.1105/tpc.110.075846
- Smidkova M, Holá M, Angelis KJ (2010) Efficient biolistic transformation of the moss *Physcomitrella patens*. *Biol Plant* 54:777–780
- Suzuki K (2004) Characterization of telomere DNA among five species of pteridophytes and bryophytes. *J Bryol* 26:175–180. doi:10.1179/037366804x5279
- Sykorova E, Fajkus J (2009) Structure-function relationships in telomerase genes. *Biol Cell* 101:375–392. doi:10.1042/Bc20080205
- Sykorova E, Lim KY, Chase MW, Knapp S, Leitch IJ, Leitch AR, Fajkus J (2003a) The absence of Arabidopsis-type telomeres in *Cestrum* and closely related genera *Vestia* and *Sessea* (Solanales): first evidence from eudicots. *Plant J* 34:283–291
- Sykorova E, Lim KY, Kunicka Z, Chase MW, Bennett MD, Fajkus J, Leitch AR (2003b) Telomere variability in the monocotyledonous plant order Asparagales. *Proc Biol Sci* 270:1893–1904. doi:10.1098/rspb.2003.2446
- Sykorova E, Fajkus J, Meznikova M, Lim KY, Nepelchova K, Blattner FR, Chase MW, Leitch A (2006a) Minisatellite telomeres occur in the family Alliaceae but are lost in *Allium*. *Am J Bot* 93:814–823
- Sykorova E, Rowland A, Leitch AR, Fajkus J (2006b) *Asparagales* telomerases which synthesize the human type of telomeres. *Plant Mol Biol* 60:633–646. doi:10.1007/s11103-005-5091-9
- Sykorova E, Fulneckova J, Mokros P, Fajkus J, Fojtova M, Peska V (2012) Three TERT genes in *Nicotiana tabacum*. *Chromosome Res* 20:381–394. doi:10.1007/s10577-012-9282-3
- Viaene T, Landberg K, Thelander M, Medvecka E, Pederson E, Feraru E, Cooper ED, Karimi M, Delwiche CF, Ljung K, Geisler M, Sundberg E, Friml J (2014) Directional auxin transport mechanisms in early diverging land plants. *Curr Biol* 24:2786–2791. doi:10.1016/j.cub.2014.09.056
- Worden AZ, Lee JH, Mock T et al (2009) Green evolution and dynamic adaptations revealed by genomes of the marine picoeukaryotes *Micromonas*. *Science* 324:268–272. doi:10.1126/science.1167222
- Zachova D, Fojtova M, Dvorackova M, Mozgova I, Lermontova I, Peska V, Schubert I, Fajkus J, Sykorova E (2013) Structure-function relationships during transgenic telomerase expression in *Arabidopsis*. *Physiol Plant* 149:114–126. doi:10.1111/Ppl.12021
- Zimmer AD, Lang D, Buchta K, Rombauts S, Nishiyama T, Hasebe M, van de Peer Y, Rensing SA, Reski R (2013) Reannotation and extended community resources for the genome of the non-seed plant *Physcomitrella patens* provide insights into the evolution of plant gene structures and functions. *BMC Genom* 14:498. doi:10.1186/1471-2164-14-498

Holokinetic centromeres and efficient telomere healing enable rapid karyotype evolution

Maja Jankowska¹ · Jörg Fuchs¹ · Evelyn Klocke² · Miloslava Fojtová^{3,4} · Pavla Polanská^{3,4} · Jiří Fajkus^{3,4} · Veit Schubert¹ · Andreas Houben¹

Received: 20 April 2015 / Revised: 21 May 2015 / Accepted: 22 May 2015
© Springer-Verlag Berlin Heidelberg 2015

Abstract Species with holocentric chromosomes are often characterized by a rapid karyotype evolution. In contrast to species with monocentric chromosomes where acentric fragments are lost during cell division, breakage of holocentric chromosomes creates fragments with normal centromere activity. To decipher the mechanism that allows holocentric species an accelerated karyotype evolution via chromosome breakage, we analyzed the chromosome complements of irradiated *Luzula elegans* plants. The resulting chromosomal fragments and rearranged chromosomes revealed holocentromere-typical CENH3 and histone H2AThr120ph signals as well as the same mitotic mobility like unfragmented chromosomes. Newly synthesized telomeres at break points become detectable 3 weeks after irradiation. The presence of active telomerase suggests a telomerase-based mechanism of chromosome healing. A successful transmission of holocentric chromosome fragments across different

generations was found for most offspring of irradiated plants. Hence, a combination of holokinetic centromere activity and the fast formation of new telomeres at break points enables holocentric species a rapid karyotype evolution involving chromosome fissions and rearrangements.

Keywords Chromosome fusion and fission · De novo telomere synthesis · Holocentric chromosome · Holocentric genome evolution · *Luzula elegans*

Introduction

Fragmentation of monocentric chromosomes by ionizing irradiations (e.g., γ -, X-rays) and UV irradiation causes the formation of centric and acentric fragments. Acentric fragments due to the absence of kinetochores do not segregate and get consequently lost during mitosis which might lead to lethal mutations. In contrast, breakage of holocentric chromosomes generates mainly fragments possessing an active centromere, and thus, fragments can segregate normally in somatic cells (Hughes-Schrader and Ris 1941). Holocentric chromosomes lack a primary constriction and form holokinetic centromeres distributed along almost the entire length of the chromatids. In addition, in holocentric species, irradiation-induced chromosome rearrangements such as reciprocal translocations do not result in dicentric chromosomes, which often fail to segregate properly if both centromeres are active (McClintock 1939). Therefore, irradiation of holocentric species rarely results in anaphase bridge and micronuclei formation (Hughes-Schrader and Ris 1941; Nordenskiöld 1964; Pazy and Plitmann 1994). Consequently, chromosome fragment behavior was analyzed to demonstrate the presence of holokinetic centromeres in different species of green algae (Godward 1954), flowering plants (Håkansson 1954), nematodes (Albertson and

Electronic supplementary material The online version of this article (doi:10.1007/s00412-015-0524-y) contains supplementary material, which is available to authorized users.

✉ Andreas Houben
houben@ipk-gatersleben.de

- ¹ Leibniz Institute of Plant Genetics and Crop Plant Research (IPK), OT Gatersleben, Correnstrasse 3, D-06466 Stadt Seeland, Germany
- ² Julius Kühn-Institute, Institute for Breeding Research on Horticultural Crops, Erwin-Baur-Straße 27, D-06484 Quedlinburg, Germany
- ³ Mendel Centre for Plant Genomics and Proteomics, CEITEC, Masaryk University, Kamenice 5, CZ-625 00 Brno, Czech Republic
- ⁴ Laboratory of Functional Genomics and Proteomics, NCBR, Faculty of Science, Masaryk University, Kamenice 5, CZ-625 00 Brno, Czech Republic

Thomson 1982), and arthropods (Tempelaar 1979). The sporadic and polyphyletic occurrence of holocentricity in the tree of life suggests that holocentric centromere evolved from monocentric chromosomes at least 13–times independently in different clades (Melters et al. 2012).

Fragments of holocentric chromosomes are inherited stably throughout many generations and can give rise to a stable progeny (Nordenskiöld 1962, 1963, 1964; LaChance and Degrugillier 1969). In the genus *Luzula*, the haploid chromosome number varies in a broad range, and species with 3, 6–16, 18, 21, 23, 24, 26, 31, 33, 35, 36, and 42 chromosomes were reported (Nordenskiöld 1951; Kuta et al. 2004; Závěská Drábková 2013). A comparable situation was found for *Cyperus* plant species or holocentric butterflies of *Nymphalidae* with nearly continuous chromosome numbers from 5 to 134 (reviewed in Bureš et al. 2013). Moreover, within one holocentric species, the number of chromosomes can vary between different individuals as shown for plant species *Carex blepharicarpa* with $2n=26–32$ and 41 (Hoshino and Okamura 1994), *Luzula multiflora* with $2n=12, 18, 24, 28, 36,$ and 48 (Bolkhovskikh et al. 1969), or *Eleocharis kamschatica* with $2n=41–47$ (Yano and Hoshino 2006). It has been speculated that stably inherited chromosome fragments and the lack of dicentric translocation products are the reasons that number and size of chromosomes may vary considerably and may be tolerated in species with holocentric chromosomes.

Obviously, due to the fragmentation of holocentric chromosomes in different species of the genus *Luzula*, a negative correlation between chromosome number and chromosome size was found. When the chromosome number is doubled from 12 to 24, the length of chromosomes is about halved (Nordenskiöld 1951). Similarly, in *Juncus biglumis*, two cytotypes with $2n=60$ and $2n=120$ chromosomes were observed. Chromosomes of the $2n=60$ cytotype are about twice as big as the chromosomes of the cytotype with $2n=120$ while the relative DNA content differs by only 6 % between them (Schönschwetter et al. 2007). Interestingly, in *Luzula* hybrids derived from parents possessing small and large chromosomes, meiotic pairing occurs between one large and two half-sized chromosomes (Nordenskiöld 1961).

Malheiros-Garde and Garde (1950) and Nordenskiöld (1951) postulated the occurrence of so-called chromosome “fusion and fission” events during the evolution as an explanation for differently sized chromosomes in holocentric species. However, the term “chromosome fusion” should be used with caution because fusions *sensu stricto* imply the combination of two chromosomes without any loss of chromatin, which is usually prevented by telomeres (Schubert and Lysak 2011). Interstitial telomere repeats as indication of translocations with a break point inside with telomere repeat arrays were found in the spike rush *Eleocharis subarticulata* (Da

Silva et al. 2005). In contrast, other holocentric species, e.g., aphids (Monti et al. 2011), the plants *Luzula luzuloides* (Fuchs et al. 1995), and *Rhynchospora tenuis* (Vanzela et al. 2003), the and cabbage moths *Mamestra brassicae* (Mandrioli 2002), did not display interstitial telomeres. Likely, the so-called fusion events are based on translocations and subsequent loss of small translocation products including telomeres resulting in terminally truncated “fused” chromosomes. In addition to chromosome fragmentation and translocation, polyploidy and proliferation/removal of high-copy sequences are mechanisms involved in the genome evolution of holocentric species (Kuta et al. 2004; Bačič et al. 2007; Bozek et al. 2012; Zedek et al. 2010; Závěská Drábková 2013).

Beside the segregation failure due to centromere loss, broken ends of centric fragments of monocentric chromosomes may be mis-repaired, yielding dicentric and ring chromosomes causing breakage–fusion–bridge (BFB) cycles (; Muller 1938; McClintock 1941, 1942). Alternatively, chromosome fragments can be healed by adding telomeric sequences to the broken chromosome ends (McClintock 1941; Day et al. 1993). Telomeres are synthesized by a specialized reverse transcriptase, the telomerase, which can replenish already existing telomeres or add new telomeric sequences directly to non-telomeric DNA, for example, at the break points of chromosome fragments (reviewed in Melek and Shippen 1996). Telomeres are added gradually, and the start of the process might require passing through a certain number of cell cycles and/or a certain developmental stage (Tsujimoto 1993; Britt-Compton et al. 2009).

Alternatively, broken chromosome ends can be healed by a telomerase-independent mechanism termed telomere capture. In this case, broken chromosomes are stabilized by a transfer of telomeres from unbroken chromosomes to the broken ends likely via a conversion-like recombination process (Meltzer et al. 1993), which may also occur between broken and intact homologues (Slijepcevic and Bryant 1998; Lundblad 2002).

Here, we investigated the consequences of fragmentation of holokinetic chromosomes across three generations. Furthermore, we address the question whether or not, and if so, when telomere healing of chromosome fragments occurs. For this purpose, we selected the wood rush *Luzula elegans* Lowe (formerly *L. purpurea* Link), a plant species for which fragmentation caused by X-irradiation has been reported previously (Nordenskiöld 1962, 1963, 1964).

L. elegans (*Juncaceae*) is a self-fertilizing holocentric species with a diploid chromosome number of $2n=6$ (3.81 Gbp/1C) (Heckmann et al. 2013). The chromosomes of this species are characterized by a longitudinal CENH3-positive groove-like structure along each sister chromatid (throughout mitosis and meiosis), flanked by *Arabidopsis*-type telomeres (Heckmann et al. 2011, 2014; Wanner et al. 2015). As an adaption to the holokinetic centromere organization,

L. elegans performs an inverted sequence of meiotic sister chromatid segregation events (Nordenskiöld 1962; Heckmann et al. 2014).

Materials and methods

Plant material and X-ray irradiation

Seeds of *Luzula elegans* Lowe (2n=6) (herbarium vouchers of IPK Gatersleben: GAT 7852–7856) were germinated on wet filter paper at 21 °C. Three leaf stage plantlets (28 days old) were irradiated with various doses ranging from 10 to 30 Gy with an X-ray apparatus (Yxlon, International Hamburg). The dose rate amounted to 0.9 Gy/min. Subsequently, plantlets were harvested in 7-day intervals and fixed for 45 min in ice-cold 4 % (w/v) paraformaldehyde in 1× MTSB buffer (50 mM PIPES, 5 mM MgSO₄, and 5 mM EGTA, pH 7.2) for immunolabeling or in ethanol–acetic acid (3:1, v/v) fixative for fluorescence in situ hybridization (FISH). To induce flowering, the plants were transmitted to soil and subjected to vernalization for a minimum of 3 months (10 h light/14 h dark, 4 °C). Afterwards, the plants were grown under long-day conditions (13 h light/11 h dark, 20 °C/16 °C). Flower buds were collected and fixed as described above. The M1 offspring was a selfing product of irradiated plants.

Fluorescence in situ hybridization

Mitotic chromosome spreads, derived from acetocarmine-stained root and apical meristems, were prepared from fixed plantlets by squashing (Houben et al. 1999). Meiotic chromosomes were prepared from fixed flower buds (Heckmann et al. 2014). PCR generated FISH probes for the subtelomeric satellite repeat LeSAT7, and telomeres were labeled with ChromaTide Texas Red-12-dUTP or Alexa Fluor 488-5-dUTP (<http://www.invitrogen.com>) by nick translation. FISH was performed according to (Heckmann et al. 2013).

Indirect immunolabeling

Fixed flower buds were used to prepare spreads by squashing. Immunostaining was performed as described (Houben et al. 2007). The following dilutions of primary antibodies were used: 1:100 of rabbit anti-LnCENH3 (Nagaki et al. 2005) and 1:200 of rabbit anti-H2AThr120phos (Abcam, www.abcam.com). A FITC-conjugated anti-rabbit Alexa488 antibody (Molecular Probes, <http://www.invitrogen.com>) at 1:400 dilution was used as secondary antibody.

Microscopy

Fluorescence images were captured using an Olympus BX61 microscope equipped with an ORCA-ER CCD camera (Hamamatsu). Deconvolution of image stacks of 10 slices each and maximum intensity projections were done using the program AnalySIS (Soft Imaging System). All images were acquired in grey scale and afterwards pseudo-colored and merged with Adobe Photoshop CS5 (Adobe). To achieve an optical resolution of ~120 nm (super-resolution), we applied structured illumination microscopy (SIM) using a C-Apo 63×/1.2W Korr objective of an Elyra PS.1 microscope system and the software ZEN (Carl Zeiss GmbH). A SIM image stack was used to produce the 3D movie by the Imaris 8.0 (Bitplane) software.

Flow cytometric genome size measurement

The *Luzula* DNA content was estimated using young, fresh leaves according to (Fuchs et al. 2008) using *Pisum sativum* ‘Viktoria, Kifejtő Borsó’ (Genebank Gatersleben accession number PIS 630; 2C=9.09 pg) (Doležel et al. 1998), as an internal reference standard. Measurements were performed either on a FACStar^{PLUS} flow sorter (BD Biosciences) equipped with an argon ion laser INNOVA 90C (Coherent) adjusted to 514 nm or on a CyFlow space flow cytometer (Partec) equipped with a 532 nm solid-state laser. Each measurement was repeated at least two times on different days.

Analysis of telomerase activity according to the telomere repeat amplification protocol

Three leaf stage plantlets and flower buds of *L. elegans*, and 7-day seedlings of *Arabidopsis thaliana* were manually homogenized in extraction buffer (Fitzgerald et al. 1996; Sykorova et al. 2003). Crude extracts obtained after centrifugation were 5× and 10× diluted for analysis of telomerase activity as described (Fitzgerald et al. 1996; Fajkus et al. 1998). Briefly, 1 µl of 10 µM substrate primer TS21 (5′GACAATCCGT CGAGCAGAGTT3′) was mixed with 1 µl of diluted crude protein extract, and elongation of the primer by the telomerase proceeded for 45 min at 26 °C in 25 µl reaction buffer (Fitzgerald et al. 1996). Telomerase was heat inactivated (5 min, 94 °C); 1 µl of 10 µM reverse primer TelPr (5′CCGAATTCAACCCTAAACCCTAAACCCTAAACCC3′) and 2U of DyNAzymeII DNA polymerase (Finnzymes) were added, and extension products were amplified in PCR (35 cycles of 95 °C/30 s, 65 °C/30 s, 72 °C/30 s; final extension 72 °C/5 min). Aliquot samples of telomere repeat amplification protocol (TRAP) reactions were analyzed on 12.5 % polyacrylamide gel in 0.5×TBE buffer. Gels were stained by GelStar nucleic acid gel stain (LONZA) and signals were visualized using the LAS-3000 system (FujiFilm).

Results

X-ray radiation induces aberrations in holocentric chromosomes in a dosage-dependent manner

Three leaf stage plantlets of *L. elegans* were X-ray irradiated with 10, 20, 25, and 30 Gy to induce fragmentation of the holocentric chromosomes. In agreement with previous findings (Prakken 1959; Li et al. 2010), DNA double-strand breaks occurred more frequently with increasing radiation dosage. Both, the non-irradiated plant and the plant irradiated with 10 Gy did not show any chromosome fragmentation and possessed three equally sized chromosome pairs. FISH with the *Arabidopsis*-type telomere (TTTAGGG)_n repeat and the satellite repeat LeSAT7, which clusters at the ends of all *L. elegans* chromosomes (Fig. 1a) (Heckmann et al. 2011), confirmed the absence of major structural changes in these low- or non-irradiated samples. In contrast, irradiation doses of 20, 25, and 30 Gy induced numerous chromosome fragments detectable in metaphase cells 1 day after irradiation. Whereas 7 chromosomes/fragments was the most frequent number in plants irradiated with 20 Gy (66 %, *n*=61) and 25 Gy (70 %, *n*=50), an increase to 9 was found in the plant irradiated with 30 Gy (54 %, *n*=67) (Fig. 1b). Irradiated plants were cytogenetically heteromorphic exhibiting a variability in the newly formed chromosome/fragment sizes between cells and plants. In the plant irradiated with 25 Gy, we observed in addition to small fragments also an abnormally large chromosome (Fig. 1c). The absence of interstitial telomeres or LeSAT7 signals indicates that this chromosome might be the result of a translocation event combining two or more fragments.

Chromosome fragments containing a holokinetic centromere are stabilized by de novo formed telomeres

In order to test whether the fragments and the rearranged chromosomes possess normal centromere activity, the position of kinetochores was evaluated by immunostaining with CENH3- or histone H2AThr120ph-specific antibodies. Both antibodies label only functionally active centromeres (Allshire and Karpen 2008; Kawashima et al. 2010). Colocalization of the centromeres and the *Arabidopsis*-type telomeres revealed telomere signals at both ends of the longitudinal centromeres (Fig. 2a, Supporting Information Movie S1). Hence, the centromere spans over the entire chromosome, from telomere to telomere in non-irradiated plants. The CENH3-negative regions appearing distal to the telomere signals likely represent out-looped subtelomeric chromatin.

The chromosome fragments showed similar CENH3 and H2AThr120ph signals as unfragmented chromosomes (Fig. 2b, c). Extraordinary long chromosomes, presumably products of translocation events, revealed centromere proteins along the entire chromosome length (Fig. 2c). No interstitial signal gap was found by the centromere labeling. These observations and the absence of micronuclei indicate that fragmented and translocated chromosomes segregate normally in somatic cells due to the presence and activity of the holokinetic centromeres.

To study whether the ends of broken chromosomes are stabilized by de novo formed telomeres, in situ hybridization with the *Arabidopsis*-type telomere probe was performed in plants irradiated with 20 Gy 7, 14, and 21 days after irradiation. To distinguish between pre-existing and newly formed telomere sites, the subtelomere-specific probe LeSAT7 was

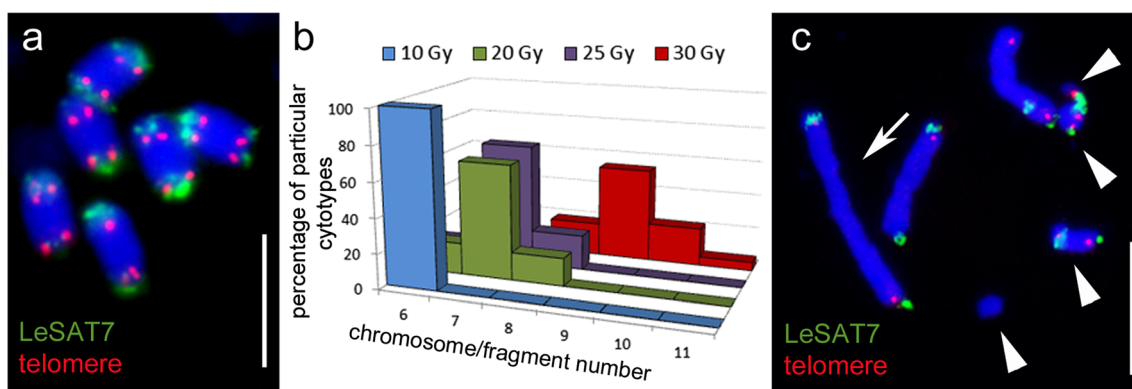


Fig. 1 X-ray irradiation induces chromosome fragmentation in *L. elegans*. **a** Non-irradiated mitotic metaphase with three equally sized chromosome pairs after FISH with the *Arabidopsis*-type telomere and the terminal satellite repeat LeSAT7. **b** Chromosome fragmentation rises with increasing radiation dosage. The plant irradiated with 10 Gy did not show any fragmentation and possessed six chromosomes. The most frequent number of chromosomes/fragments in the plant irradiated with 20 Gy was 7 (40 cells). In 11 cells 6 and in 10 cells 8 chromosomes could be counted. The most frequent chromosome number in the plant irradiated with 25 Gy was 7 (35 cells), followed by 8 (10 cells) and 6 (5 cells). In the plant

irradiated with 30 Gy, cells with 9 (36 cells), 10 (15 cells), 8 (13 cells), and 11 (3 cells) chromosomes/fragments were observed. **c** Mitotic metaphase of a plant irradiated with 25 Gy possessing seven chromosomes/fragments of different size after FISH with the *Arabidopsis*-type telomere probe and the terminal satellite repeat LeSAT7. Arrowheads indicate the chromosome fragments. The arrow points to an abnormally large chromosome, presumably the product of a translocation event. DNA was counterstained with DAPI (blue). Bars= 10 μ m

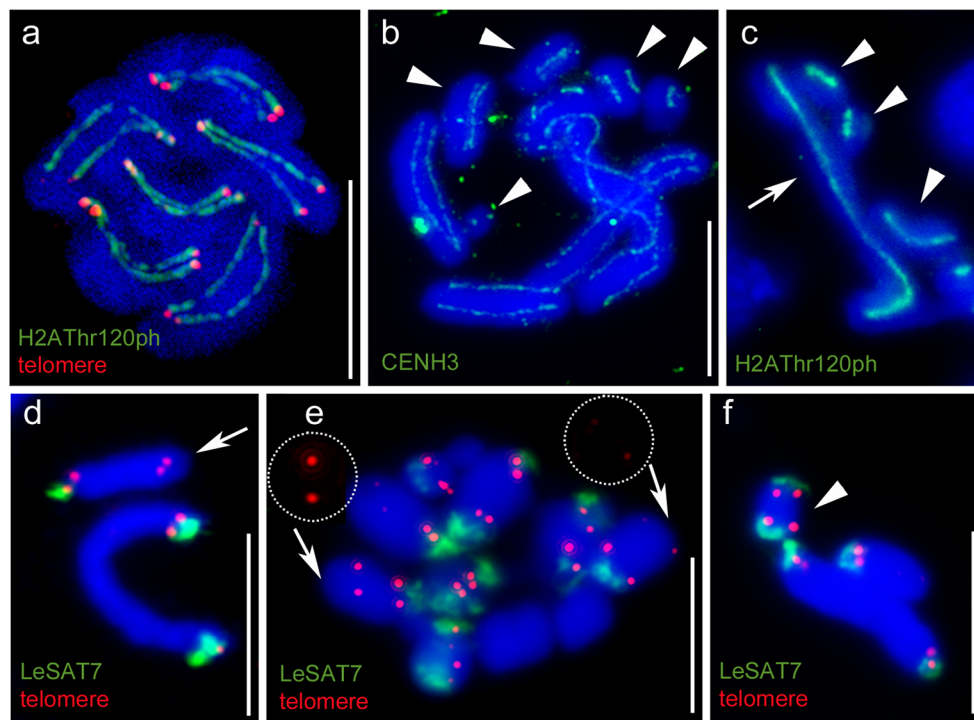


Fig. 2 Chromosome fragments of *L. elegans* possess holokinetic centromeres and de novo formed telomeres. **a** SIM of double labeled non-irradiated mitotic metaphase chromosomes with anti-H2AThr120ph immunostaining and FISH using the *Arabidopsis*-type telomere probe. The centromeres span the entire chromosome length from telomere to telomere (see also Supporting Information Movie S1). Immunolabeling of irradiated cells with anti-CENH3 (**b**) and anti-H2AThr120ph (**c**). Fragmented (**arrowheads**) and translocated (**arrow**) chromosomes possess active holocentromeres. **d** FISH with the terminal satellite

LeSAT7 and telomere repeats (**red**) enable to distinguish between pre-existing telomeres (carrying signals of both probes) and the newly synthesized telomeres (carrying only telomere signals, **arrow**). **e** The signal intensities of the newly synthesized telomeres differ between the fragmented chromosome ends (see further enlarged telomere signals, **arrowed**). **f** A chromosome fragment with pre-existing telomeres at both termini (**arrowhead**). Chromatin was counterstained with DAPI (**blue**). Bars=10 μ m

used in addition. Telomeric regions carrying both LeSAT7 and telomere repeats were assumed to be the pre-existing chromosome ends, while ends lacking LeSAT7 but exhibiting telomere signals were considered as those with newly synthesized telomeres (Fig. 2d). The first chromosome fragments exhibiting a newly formed telomere were found 21 days after irradiation. At this time point, newly formed telomeres were detectable at 51 % of 37 analyzed fragments. The hybridization signal intensity differed severely among the newly formed telomeres (Fig. 2e). Around 3 months after radiation, when the plants enter meiosis, the intensity of telomere signals was compared between chromosome fragments carrying a pre-existing and a newly formed telomere. In 70 % of 69 analyzed fragments, the hybridization intensity of newly formed telomeres was weaker than that of the pre-existing ones. In 17 % of the fragments, no obvious difference between “new” and “old” telomere sites was detectable, and 9 % of the newly formed telomeres showed an even more intense hybridization signal than the “pre-existing” ones. Only 4 % of chromosome fragments revealed no telomere signal at the newly formed chromosome ends. In addition, small chromosome fragments carrying telomeres and LeSAT7 repeats at both

ends could be observed (Fig. 2f), likely due to the fusion of two subteleromic regions.

To test whether the newly formed telomeres may be the product of active telomerase, we used a PCR-based TRAP assay which permits the detection of telomerase activity in vitro. Semi-quantitative analysis of TRAP products showed detectable levels of telomerase in extracts isolated from non-irradiated *L. elegans* seedlings and flower buds. Regular ladders of TRAP product showing the same periodicity as in the *A. thaliana* sample which was used as a positive control were reproducibly detected in both *L. elegans* tissues (Fig. 3). This observation suggests that de novo synthesized telomeres observed in somatic and generative cells are the likely result of telomerase-mediated healing process.

Successful transmission of holocentric fragments across several generations

L. elegans performs an inverted meiosis meaning that sister chromatids separate from each other during anaphase I and homologous non-sister chromatids separate during anaphase II (Heckmann et al. 2014). For several *Luzula* species, the

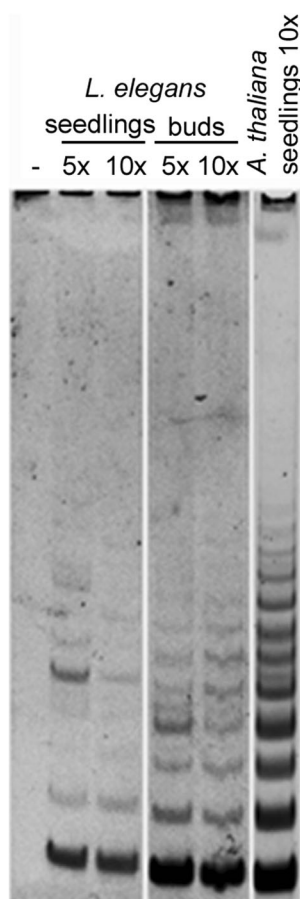


Fig. 3 Telomerase activity in seedlings and flower buds assayed by TRAP. Seedlings and flower buds of *L. elegans* show telomerase activity, as evidenced by the 7-bp incremental TRAP ladder. Total protein extracts from seedlings and flower buds were analyzed in 5× and 10× dilutions. An *A. thaliana* extract was used as a positive control. – negative control (no extract in the reaction)

stable transmission of holocentric chromosome fragments was described (Nordenskiöld 1962, 1963; Kusanagi 1973). Irradiated plants exhibited a bouquet formation in zygotene, like non-irradiated ones (Fig. 4a). However, at prometaphase I, multivalent configurations interconnected by terminal satellite repeats were detected, which have never been observed in non-irradiated plants (Fig. 4b). Additionally, we found the terminal satellite at an interstitial position as a product of a translocation event (Fig. 4c).

To further investigate whether meiosis is disturbed by the irradiation-induced aberrations, we determined the DNA content of the progeny of the plant irradiated with 20 Gy. Nineteen out of 20 analyzed M1 plants revealed a genome size comparable to non-irradiated plants ($3.81 \text{ Gbp/1C} \pm 1.5 \%$) indicating a balanced segregation of all chromosomes including fragments. All chromosome fragments in the self-progeny of the irradiated plant possess telomeric repeats at their newly formed chromosome ends (Fig. 4d). In one plant, a 7 % larger genome was detected (4.08 Gbp/1C). Analyses of this plant in prometaphase I showed three chromosome

fragments of different size (Fig. 4e) in addition to three bivalents. The corresponding tetrads revealed unequal numbers of telomere and LeSAT7 signals in daughter cells indicating a random segregation of these chromosome fragments. Furthermore, in 20 % of 100 examined tetrads of this M1 plant, micronuclei were observed (Fig. 4f) but not present in the other M1 plants. The DNA content of the M2 progeny of the M1 plant with 7 % bigger genome size ranged from 7.74 pg/2C (−0.76 %) to 8.87 pg/2C (+14 %) compared to 7.80 pg/2C of non-irradiated plants. In addition, the number and size of chromosomes and fragments in the M2 plants varied, but all chromosome and fragment ends contained telomere repeats. Plants possessing 3.35, 6.46, and 11.03 % bigger genomes harbored chromosome complements with $2n=6+2$ small fragments, $2n=6+2$ big+2 small fragments, and $2n=7+1$ small fragment, respectively (Fig. 4g, h, i) indicating a stable transmission of fragments independent of their size. Despite this severe variation in DNA content and karyotype constitution, no obvious phenotypic differences were observed.

The balanced segregation of the chromosome fragments to the progeny in 95 % of the cells indicates a correct process of inverted meiosis independent of irradiation induced fragmentations, translocations, and multivalent formation. The presence of telomere repeats at all broken ends in the progeny implies a significant role of telomere de novo formation for stable fragment transmission across generations.

Discussion

Species with holocentric chromosomes are characterized by a rapid karyotype evolution (Bureš et al. 2013). In contrast to organisms with monocentric chromosomes where acentric fragments are mostly lost during cell division, the breakage of holocentric chromosomes creates fragments with normal centromere activity. Therefore, no lagging anaphase chromosomes and micronuclei occur, and chromosome breakage and translocation events play an important role in the fast karyotype evolution of holocentric species (Heilborn 1924; Brown et al. 2004; Kuta et al. 2004; Da Silva et al. 2008; Hipp et al. 2009).

Using centromere-specific markers, we demonstrate that chromosome fragments independent of their size possess centromere activity along their sister chromatids. No abnormalities were found during mitotic divisions, similar as in γ -irradiated holocentric plant species *Rhynchospora pubera* (Vanzela and Colaço 2002) and the holocentric nematode *Caenorhabditis elegans*, where only very small fragments were rarely lost (Albertson and Thomson 1982). However, a holokinetic centromere is likely not sufficient to stabilize broken chromosomes as telomere-free chromosome ends are prone to “fuse”, and thus, form ring chromosomes when

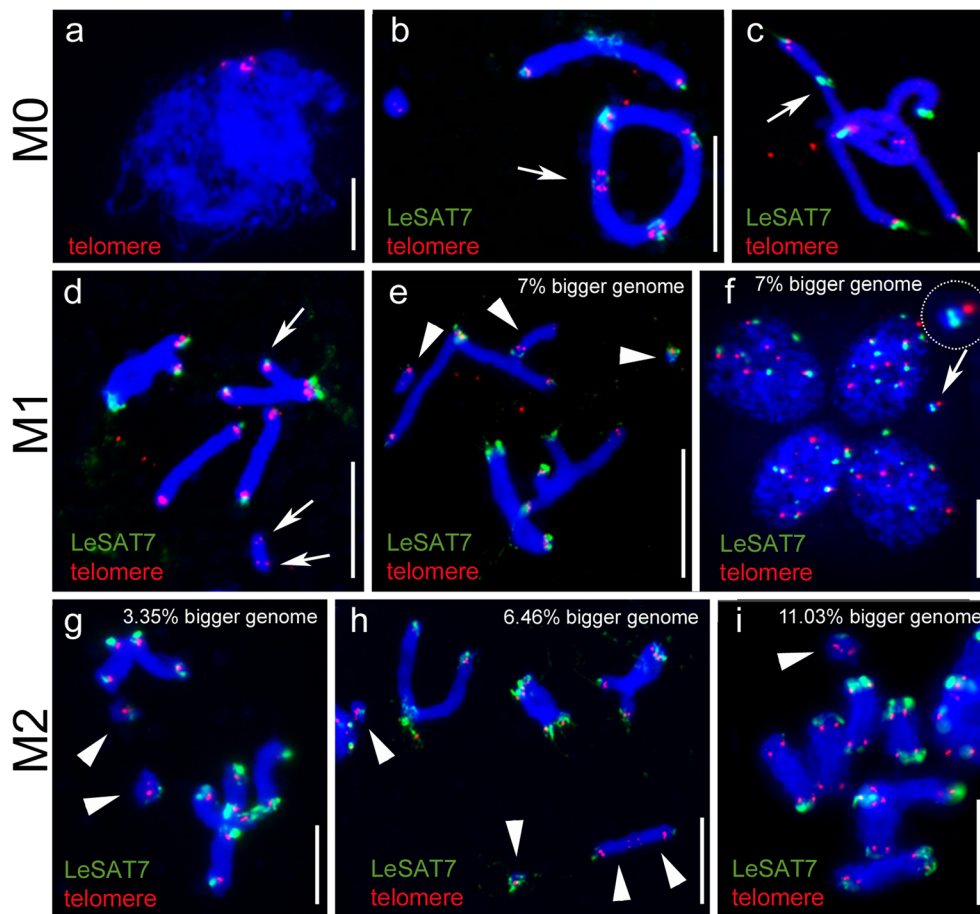


Fig. 4 Holocentric fragments in mutants (M0–M2) are stably transmitted to the next generation. **a** The formation of a bouquet-like configuration during zygotene of M0 mutants is not impaired by irradiation. **b** A multivalent configuration (*arrow*) is present at prometaphase I of irradiated M0 plants. **c** A translocation event caused by irradiation is indicated by the interstitial localization of the terminal satellite LeSAT7 (*arrow*). **d** Somatic metaphase of a mutant offspring (M1) with stably transmitted chromosome fragments ($2n=7$) and a similar genome size as non-irradiated plants. All chromosome fragments possess telomeric repeats at their newly formed chromosome ends (*arrows*). **e** Prometaphase I of a mutant offspring with a 7 % larger genome

possessing three bivalents and three fragments of different sizes (*arrowheads*). **f** Tetrads of the same mutant showing a micronucleus (further enlarged and *arrowed*). **g**, **h**, **i** M2 individuals of the progeny of the mutant with the 7 % larger genome revealed different combinations of the fragments (*arrowheads*) occurring in the mother plant. Number and size of fragments correlate with the estimated genome size: $2n=6+2$ small fragments (3.4 % enlarged genome), $2n=6+2$ big+2 small fragments (6.5 % enlarged genome), and $2n=7+1$ small fragment (11.0 % enlarged genome). FISH with the terminal satellite LeSAT7 and the telomere repeat. Chromatin was counterstained with DAPI (*blue*). Bars=10 μ m

fragments without terminal telomeric repeats are involved (McClintock 1941, 1942). We did not observe ring chromosomes, probably due to rapid telomere healing. Ring chromosome formation was also not present in irradiated *C. elegans* cell (Albertson and Thomson 1982). However, in the holocentric common spikerush, *Eleocharis palustris*, ring chromosomes were found after irradiation (Håkansson 1958).

In our study, cytologically detectable small telomere repeats at ~50 % of broken termini appeared already 21 days after irradiation. This indicates a telomerase-based mechanism of chromosome healing in *Luzula*, similar as described for monocentric human (Chabchoub et al. 2007) and *Tetrahymena* (Harrington and Harrington 1991; Yu and Blackburn 1991) chromosomes. Stabilization of break points by telomere de novo synthesis was also found in the

holocentric aphid *Myzus persicae* (Monti et al. 2011). In root meristems of maize, 50 % of the chromosome fragments caused by BFB cycles were stabilized after 3 weeks and up to 93 % after 10 weeks (Zheng et al. 1999). Similarly, in wheat, BFB cycles taking place after induced chromosome breakage were inhibited via adding telomeric sequences by telomerase to the break points (Tsujiimoto 1993; Tsujiimoto et al. 1997).

The lack of detectable amounts of newly formed telomeres and the differences in new telomeres signal intensities at some break points of *L. elegans* chromosomes might indicate a preferential binding of telomerase to specific repeats or other sequences at the fragment termini. Indeed, in *Saccharomyces cerevisiae*, the de novo telomere formation occurs preferentially at TG-rich sequences (Putnam et al. 2004). Additionally,

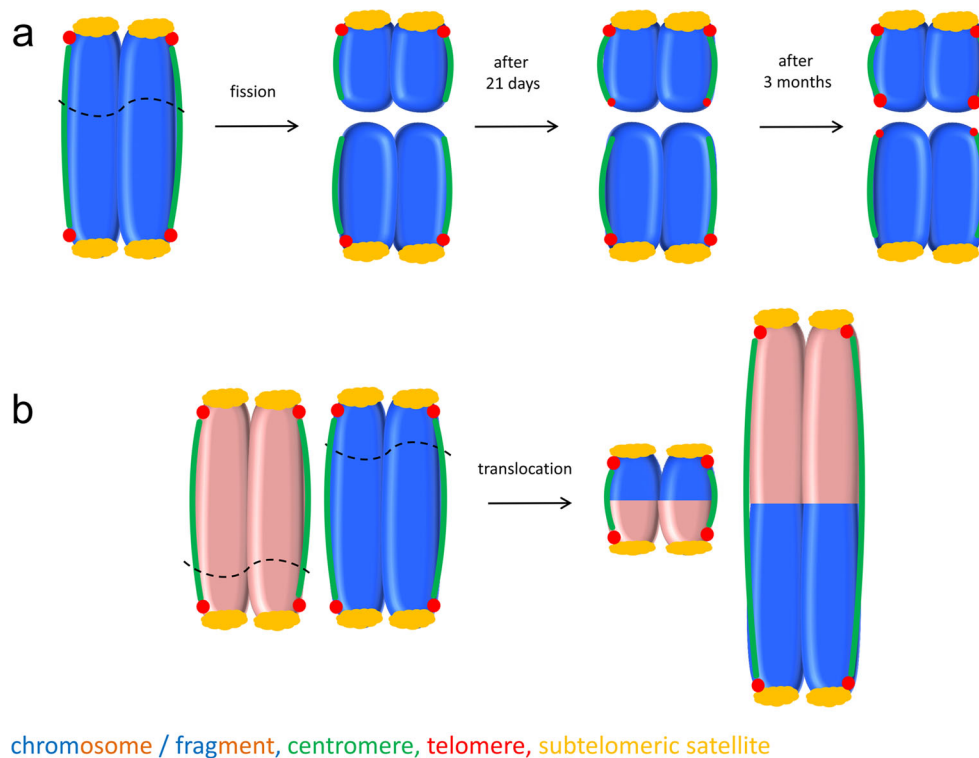


Fig. 5 Model illustrating possible karyotype alterations after fragmentation of holocentric chromosomes based on the interplay between holocentricity and telomere healing according to the behavior of *L. elegans* chromosomes. Irradiation of holocentric chromosomes induces chromosomal fragments of different size. Centromere activity is present along all chromosome fragments. Break points are indicated by black dotted lines. **a** Broken ends are negative for the terminal satellite

probe and become gradually healed by de novo telomere syntheses, detected by a telomere-specific probe. **b** Translocations between non-homologous chromosomes form fragments of different size which are stabilized by pre-existing telomeres and the holocentromeres. Note that the distal location of LeSAT7 compared with the telomeres is likely caused by a fold back of telomere repeats (Heckmann et al. 2014)

the telomerase might preferentially extend shorter telomeres than longer ones causing different telomere signal intensities. The preferential elongation of shorter telomeres has been demonstrated in yeast (Teixeira et al. 2004), mouse (Hemann et al. 2001), and human (Britt-Compton et al. 2009). The occurrence of new telomeres displaying a similar FISH signal intensity as the pre-existing ones, as well as the presence of chromosomal fragments carrying telomere and LeSAT7 repeats at both ends, a short time after radiation, suggest the additional action of a telomerase-independent process such as terminal translocation or recombination. Simultaneous mechanisms of broken chromosome stabilization, de novo telomere synthesis by telomerase and telomere capture, were also reported in other species, e.g., human (Chabchoub et al. 2007).

Irradiation-induced fragments, translocations, and multivalent configurations do not impair the course of inverted meiosis in *L. elegans*. Similarly, no abnormalities in meiosis were detected after chromosome fragmentation in the holocentric *Cuscuta babylonica* and *R. pubera* species (Pazy and Plitmann 1994; Vanzela and Colaço 2002). The occurrence of multivalent configurations caused by irradiation was observed also in the holocentric plant *E. subarticulata* probably

as the result of multiple translocations involving terminal heterochromatic region (Da Silva et al. 2005). The process of chromosome healing occurs gradually in *L. elegans*, and the cells have to pass several cell divisions to acquire a detectable number of telomeric repeats. All chromosome fragments present in the progeny of irradiated plants revealed telomeres at break points indicating their importance for fragment stabilization. In wheat, 2–4 weeks after chromosome fragmentation, stabilizing telomere repeats were observed only occasionally in root tip meristems, but during meiosis, all broken ends displayed cytologically detectable telomeres (Friebe et al. 2001).

The occasional occurrence of micronuclei in post-meiotic cells as well as the sporadic increase of the DNA amount in progeny plants might suggest missegregation of some chromosomal fragments during meiosis. Different factors may affect meiotic stability of fragments, e.g., fragment size, the presence of telomeres, and/or subtelomeric satellite repeats. A significant role of telomere repeats in chromosome end stabilization was demonstrated in the holocentric insect *Bombyx mori*. Here, fragments with telomeres at both ends were lost less often (25 %) during gametogenesis than fragments with telomeres present only at one end (56 %)

(Fujiwara et al. 2000). The importance of the terminal satellite repeats LeSAT7 and LeSAT11 during the inverted meiosis of *L. elegans* was previously demonstrated in (Heckmann et al. 2014). Additionally, other mechanisms, such as inappropriate attachment of spindle microtubules, kinetochore damage, and defects in the cell cycle control system might contribute to micronuclei formation (Luzhna et al. 2013).

In summary, we demonstrate that the combination of a holokinetic chromosome structure and the rapid formation of new telomeres at break points enable chromosome fragments to be successfully transmitted through mitotic and meiotic cell divisions. Thus, holocentric species may undergo a rapid karyotype evolution involving chromosome translocations and fissions (Fig. 5).

Acknowledgments We are grateful to Ingo Schubert and all members of the Chromosome Structure & Function group for their fruitful discussions and to Katrin Kumke for excellent technical assistance. This work was supported by the Deutsche Forschungsgemeinschaft (SPP 1384, HO 1779/17-1) and the IPK (Gatersleben). The work performed at the Masaryk University was supported by the Czech Science Foundation (13-06943S), project CEITEC (CZ.1.05/1.1.00/02.0068) of the European Regional Development Fund and project CZ.1.07/2.3.00./20.0189 co-financed from European Social Fund and the State Budget of the Czech Republic.

Conflicts of interest No conflicts of interest exists.

Research involving human participants and/or animals No research involving human participants or animals was performed.

References

- Albertson DG, Thomson JN (1982) The kinetochores of *Caenorhabditis elegans*. *Chromosoma* 86:409–428
- Allshire RC, Karpen GH (2008) Epigenetic regulation of centromeric chromatin: old dogs, new tricks? *Nat Rev Genet* 9:923–937
- Bačič T, Jogan N, Koče JD (2007) *Luzula* sect. *Luzula* in the south-eastern Alps-karyology and genome size. *Taxon* 56:129–136
- Bolkhovskikh Z, Grif V, Matvejeva T, Zakhareva O (1969) Chromosome number of flowering plants. *Nauka, Leningrad*: Academy of Sciences, U.S.S.R.
- Bozek M, Leitch AR, Leitch IJ, Závěská Drábková L, Kuta E (2012) Chromosome and genome size variation in *Luzula* (*Juncaceae*), a genus with holocentric chromosomes. *Bot J Linn Soc* 170:529–541
- Britt-Compton B, Capper R, Rowson J, Baird DM (2009) Short telomeres are preferentially elongated by telomerase in human cells. *FEBS Lett* 583:3076–3080
- Brown J, Keith S, Von Schoultz B, Suomalainen E (2004) Chromosome evolution in neotropical *Danainae* and *Ithomiinae* (Lepidoptera). *Hereditas* 141:216–236
- Bureš P, Zedek F, Marková M (2013) Holocentric chromosomes. In: Greilhuber J, Doležel J, Wendel JF (eds) *Plant genome diversity*. Vol 2. Springer, Vienna, pp 187–208
- Chabchoub E, Rodriguez L, Galan E, Mansilla E, Martinez-Fernandez ML, Martinez-Frias, ML, Fryns JP, Vermeesch JR (2007) Molecular characterisation of a mosaicism with a complex chromosome rearrangement: evidence for coincident chromosome healing by telomere capture and neo-telomere formation. *J Med Genet* 44:250–256
- Da Silva CRM, González-Elizondo MS, Vanzela ALL (2005) Reduction of chromosome number in *Eleocharis subarticulata* (*Cyperaceae*) by multiple translocations. *Bot J Linn Soc* 149:457–464
- Da Silva CRM, González-Elizondo MS, Vanzela ALL (2008) Chromosome reduction in *Eleocharis maculosa* (*Cyperaceae*). *Cytogenet Genome Res* 122:175–180
- Day JP, Marder BA, Morgan WF (1993) Telomeres and their possible role in chromosome stabilization. *Environ Mol Mutagen* 22:245–249
- Doležel J, Greilhuber J, Lucretti S, Meister A, Lysák M, Nardi L, Obermayer R (1998) Plant genome size estimation by flow cytometry: Inter-laboratory comparison. *Ann Bot Lond* 82:17–26
- Fajkus J, Fulnečková J, Hulánová M, Berková K, Říha K, Matyášek R (1998) Plant cells express telomerase activity upon transfer to callus culture, without extensively changing telomere lengths. *Mol Gen Genet* 260:470–474
- Fitzgerald MS, McKnight TD, Shippen DE (1996) Characterization and developmental patterns of telomerase expression in plants. *Proc Natl Acad Sci U S A* 93:14422–14427
- Friebe B, Kynast RG, Zhang P, Qi LL, Dhar M, Gill BS (2001) Chromosome healing by addition of telomeric repeats in wheat occurs during the first mitotic divisions of the sporophyte and is a gradual process. *Chromosome Res* 9:137–146
- Fuchs J, Brandes A, Schubert I (1995) Telomere sequence localization and karyotype evolution in higher plants. *Plant Syst Evol* 196:227–241
- Fuchs J, Jovtchev G, Schubert I (2008) The chromosomal distribution of histone methylation marks in gymnosperms differs from that of angiosperms. *Chromosome Res* 16:891–898
- Fujiwara H, Nakazato Y, Okazaki S, Ninaki O (2000) Stability and telomere structure of chromosomal fragments in two different mosaic strains of the silkworm, *Bombyx mori*. *Zool Sci* 17:743–750
- Godward MBE (1954) The diffuse centromere or polycentric chromosomes in *Spirogyra*. *Ann Bot Lond* 18:143–155
- Håkansson A (1954) Meiosis and pollen mitosis in X-rayed and untreated spikelets of *Eleocharis palustris*. *Hereditas* 40:325–345
- Håkansson A (1958) Holocentric chromosomes in *Eleocharis*. *Hereditas* 44:531–540
- Harrington LA, Harrington LA (1991) Telomerase primer specificity and chromosome healing. *Nature* 353:451–454
- Heckmann S, Schroeder-Reiter E, Kumke K, Ma L, Nagaki K, Murata M, Wanner G, Houben A (2011) Holocentric chromosomes of *Luzula elegans* are characterized by a longitudinal centromere groove, chromosome bending, and a terminal nucleolus organizer region. *Cytogenet Genome Res* 134:220–228
- Heckmann S et al (2013) The holocentric species *Luzula elegans* shows interplay between centromere and large-scale genome organization. *Plant J* 73:555–565
- Heckmann S, Jankowska M, Schubert V, Kumke K, Ma W, Houben A (2014) Alternative meiotic chromatid segregation in the holocentric plant *Luzula elegans*. *Nat Commun* 5:4979
- Heilborn O (1924) Chromosome numbers and dimensions, species-formation and phylogeny in the genus *Carex*. *Hereditas* 5:129–216
- Hemann MT, Strong MA, Hao L-Y, Greider CW (2001) The shortest telomere, not average telomere length, is critical for cell viability and chromosome stability. *Cell* 107:67–77
- Hipp AL, Rothrock PE, Roalson EH (2009) The evolution of chromosome arrangements in *Carex* (*Cyperaceae*). *Bot Rev* 75:96–109
- Hoshino T, Okamura K (1994) Cytological studies on meiotic configurations of intraspecific aneuploids of *Carex blepharicarpa* (*Cyperaceae*) in Japan. *J Plant Res* 107:1–8
- Houben A, Wako T, Furushima-Shimogawara R, Presting G, Künzel G, Schubert I, Fukui K (1999) The cell cycle dependent

- phosphorylation of histone H3 is correlated with the condensation of plant mitotic chromosomes. *Plant J* 18:675–679
- Houben A, Schroeder-Reiter E, Nagaki K, Nasuda S, Wanner G, Murata M, Endo T (2007) CENH3 interacts with the centromeric retrotransposon *cereba* and GC-rich satellites and locates to centromeric substructures in barley. *Chromosoma* 116:275–283
- Hughes-Schrader S, Ris H (1941) The diffuse spindle attachment of coccids, verified by the mitotic behavior of induced chromosome fragments. *J Exp Zool* 87:429–456
- Kawashima SA, Yamagishi Y, Honda T, Ishiguro K, Watanabe Y (2010) Phosphorylation of H2A by Bub1 prevents chromosomal instability through localizing shugoshin. *Science* 327:172–177
- Kusanagi A (1973) Preferential orientation of interchange multiples in *Luzula elegans*. *Jap J Genet* 48:175–183
- Kuta E, Bohanec B, Dubas E, Vižintin L, Przywara L (2004) Chromosome and nuclear DNA study on *Luzula-A* genus with holokinetic chromosomes. *Genome Natl Res Counc Can* 47:246–256
- LaChance LE, Degrugillier M (1969) Chromosomal fragments transmitted through three generations in *Oncopeltus (Hemiptera)*. *Science* 166:235–236
- Li R, Bruneau AH, Qu R (2010) Morphological mutants of St. Augustine grass induced by gamma ray irradiation. *Plant Breed* 129:412–416
- Lundblad V (2002) Telomere maintenance without telomerase. *Oncogene* 21:522–531
- Luzhna L, Kathiria P, Kovalchuk O (2013) Micronuclei in genotoxicity assessment: from genetics to epigenetics and beyond. *Front Genet* 4: 131
- Malheiros-Garde N, Garde A (1950) Fragmentation as a possible evolutionary process in the genus *Luzula* DC. *Genet Iber* 2: 257–262
- Mandrioli M (2002) Cytogenetic characterization of telomeres in the holocentric chromosomes of the lepidopteran *Mamestra brassicae*. *Chromosom Res* 10:279–286
- McClintock B (1939) The behavior in successive nuclear divisions of a chromosome broken at meiosis. *Proc Natl Acad Sci USA* 25:416, pp 405–416
- McClintock B (1941) The stability of broken ends of chromosomes in *Zea mays*. *Genetics* 26:282
- McClintock B (1942) The fusion of broken ends of chromosomes following nuclear fusion. *Proc Natl Acad Sci U S A* 28:458, pp 458–463
- Melek M, Shippen DE (1996) Chromosome healing: spontaneous and programmed de novo telomere formation by telomerase. *BioEssays* 18:301–308
- Melters DP, Paliulis LV, Korf IF, Chan SWL (2012) Holocentric chromosomes: convergent evolution, meiotic adaptations, and genomic analysis. *Chromosome Res* 20:579–593
- Meltzer PS, Guan XY, Trent JM (1993) Telomere capture stabilizes chromosome breakage. *Nat Genet* 4:252–255
- Monti V, Giusti M, Bizzaro D, Manicardi GC, Mandrioli M (2011) Presence of a functional (TTAGG)_n telomere-telomerase system in aphids. *Chromosome Res* 19:625–633
- Muller H (1938) The remaking of chromosomes. *Collect Net* 13: 181–195
- Nagaki K, Kashihara K, Murata M (2005) Visualization of diffuse centromeres with centromere-specific histone H3 in the holocentric plant *Luzula nivea*. *Plant Cell* 17:1886–1893
- Nordenskiöld H (1951) Cyto-taxonomical studies in the genus *Luzula*. *Hereditas* 37:325–355
- Nordenskiöld H (1961) Tetrad analysis and course of meiosis in three hybrids of *Luzula campestris*. *Hereditas* 47:203–238
- Nordenskiöld H (1962) Studies of meiosis in *Luzula purpurea*. *Hereditas* 48:503–519
- Nordenskiöld H (1963) A study of meiosis in progeny of x-irradiated *Luzula purpurea*. *Hereditas* 49:33–47
- Nordenskiöld H (1964) The effect of x-irradiation on diploid and polyploid *Luzula*. *Hereditas* 51:344–374
- Pazy B, Plitmann U (1994) Holocentric chromosome behavior in *Cuscuta (Cuscutaceae)*. *Plant Syst Evol* 191:105–109
- Prakken R (1959) Induced mutation. *Euphytica* 8:270–322
- Putnam CD, Pennaneach V, Kolodner RD (2004) Chromosome healing through terminal deletions generated by de novo telomere additions in *Saccharomyces cerevisiae*. *Proc Natl Acad Sci U S A* 101:13262–13267
- Schönswetter P, Suda J, Popp M, Weiss-Schneeweiss H, Brochmann C (2007) Circumpolar phylogeography of *Juncus biglumis (Juncaceae)* inferred from AFLP fingerprints, cpDNA sequences, nuclear DNA content and chromosome numbers. *Mol Phylogenet Evol* 42:92–103
- Schubert I, Lysak MA (2011) Interpretation of karyotype evolution should consider chromosome structural constraints. *Trends Genet* 27:207–216
- Slijepcevic P, Bryant PE (1998) Chromosome healing, telomere capture and mechanisms of radiation-induced chromosome breakage. *Int J Radiat Biol* 73:1–13
- Sykorova E, Lim KY, Chase MW, Knapp S, Leitch IJ, Leitch AR, Fajkus J (2003) The absence of *Arabidopsis*-type telomeres in *Cestrum* and closely related genera *Vestia* and *Sessea (Solanaceae)*: first evidence from eudicots. *Plant J* 34:283–291
- Teixeira MT, Arneric M, Sperisen P, Lingner J (2004) Telomere length homeostasis is achieved via a switch between telomerase-extendible and nonextendible states. *Cell* 117:323–335
- Tempelaar MJ (1979) Fate of fragments and properties of translocations of holokinetic chromosomes after X-irradiation of mature sperm of *Tetranychus urticae* Koch (*Acar*, *Tetranychidae*). *Mutat Res* 63: 301–316
- Tsujimoto H (1993) Molecular cytological evidence for gradual telomere synthesis at the broken chromosome ends in wheat. *J Plant Res* 106: 239–244
- Tsujimoto H, Yamada T, Sasakuma T (1997) Molecular structure of a wheat chromosome end healed after gametocidal gene-induced breakage. *Proc Natl Acad Sci U S A* 94:3140–3144
- Vanzela ALL, Colaço W (2002) Mitotic and meiotic behavior of γ irradiated holocentric chromosomes of *Rhynchospora pubera (Cyperaceae)*. *Acta Sci* 24:611–614
- Vanzela ALL, Cuadrado A, Guerra M (2003) Localization of 45S rDNA and telomeric sites on holocentric chromosomes of *Rhynchospora tenuis* Link (*Cyperaceae*). *Genet Mol Biol* 26:199–201
- Wanner G, Schröder-Reiter E, Ma W, Houben A, Schubert V (2015) The ultrastructure of mono and holocentric plant centromeres: An immunological investigation by electron and structured illumination microscopy. *Chromosoma*. doi:10.1007/s00412-015-0521-1
- Yano O, Hoshino T (2006) Cytological studies of aneuploidy in *Eleocharis kamschatkica (Cyperaceae)*. *Cytologia* 71:141–147
- Yu G-L, Blackburn EH (1991) Developmentally programmed healing of chromosomes by telomerase in *Tetrahymena*. *Cell* 67:823–832
- Záveská Drábková L (2013) A survey of karyological phenomena in the *Juncaceae* with emphasis on chromosome number variation and evolution. *Bot Rev* 79:401–446
- Zedek F, Šmerda J, Šmarda P, Bureš P (2010) Correlated evolution of LTR retrotransposons and genome size in the genus *Eleocharis*. *BMC Plant Biol* 10
- Zheng YZ, Roseman RR, Carlson WR (1999) Time course study of the chromosome-type breakage-fusion-bridge cycle in maize. *Genetics* 153:1435–1444

Characterisation of an unusual telomere motif (TTTTTTAGGG)_n in the plant *Cestrum elegans* (Solanaceae), a species with a large genome

Vratislav Peška^{1,2}, Petr Fajkus^{1,2}, Miloslava Fojtová^{1,2}, Martina Dvořáčková^{1,2}, Jan Hapala², Vojtěch Dvořáček¹, Pavla Polanská², Andrew R. Leitch³, Eva Sýkorová^{1,2} and Jirí Fajkus^{1,2,*}

¹Institute of Biophysics, Academy of Sciences of the Czech Republic, v.v.i., Královopolská 135, CZ-61265 Brno, Czech Republic,

²Faculty of Science, and CEITEC-Central European Institute of Technology, Masaryk University, Kamenice 5, CZ-62500 Brno, Czech Republic, and

³School of Biological and Chemical Sciences, Queen Mary University of London, London E1 4NS, UK

Received 26 January 2015; revised 20 March 2015; accepted 23 March 2015; published online 31 March 2015.

*For correspondence (e-mail fajkus@sci.muni.cz).

SUMMARY

The characterization of unusual telomere sequence sheds light on patterns of telomere evolution, maintenance and function. Plant species from the closely related genera *Cestrum*, *Vestia* and *Sessea* (family Solanaceae) lack known plant telomeric sequences. Here we characterize the telomere of *Cestrum elegans*, work that was a challenge because of its large genome size and few chromosomes (1C 9.76 pg; $n = 8$). We developed an approach that combines BAL31 digestion, which digests DNA from the ends and chromosome breaks, with next-generation sequencing (NGS), to generate data analysed in RepeatExplorer, designed for *de novo* repeats identification and quantification. We identify a unique repeat motif (TTTTTTAGGG)_n in *C. elegans*, occurring in ca. 30 400 copies per haploid genome, averaging ca. 1900 copies per telomere, and synthesized by telomerase. We demonstrate that the motif is synthesized by telomerase. The occurrence of an unusual eukaryote (TTTTTTAGGG)_n telomeric motif in *C. elegans* represents a switch in motif from the 'typical' angiosperm telomere (TTAGGG)_n. That switch may have happened with the divergence of *Cestrum*, *Sessea* and *Vestia*. The shift in motif when it arose would have had profound effects on telomere activity. Thus our finding provides a unique handle to study how telomerase and telomeres responded to genetic change, studies that will shed more light on telomere function.

Keywords: *Cestrum elegans*, NGS analysis, RepeatExplorer, telomerase, telomeric sequence, unusual telomere, GenBank KM573817–573822.

INTRODUCTION

The origin of linear chromosomes with the divergence of eukaryotes led to the evolution of mechanisms that reversed the incomplete replication of chromosome ends (telomeres) at each round of the cell cycle. The best known and probably the commonest occurring mechanism that overcomes the end-replication problem (Olovnikov, 1971; Watson, 1972) in eukaryotes involves telomerase, a nucleoprotein enzyme complex which compensates for replicative telomere shortening by using reverse transcription to elongate the DNA strand at the chromosome 3' terminus. Telomerase itself has two core subunits, the telomerase reverse transcriptase (TERT) protein subunit, which provides catalytic activity, and the telomerase RNA (TR) subunit, a small part of which serves as a template for

synthesis of short sequence motifs of telomeric DNA. Repeated telomerase reaction cycles results in both telomere elongation and the repetitive nature of telomeric DNA (Greider and Blackburn, 1985, 1987). Appropriate telomere elongation is known to be vital for genome stability and to counteract cell ageing.

In addition to the telomerase-dependent strategy, some other mechanisms function to solve the end-replication problem, collectively these are termed Alternative Lengthening of Telomeres (ALT). For example, telomeres can be formed by tandem arrays that elongate by recombination, DNA can be synthesized on telomeric loops (t-loops), and extrachromosomal telomeric circles can elongate by rolling-circle amplification and recombination with linear

telomeres. In addition, the formation of terminal hairpin loops can prime chromosome elongation, there can be transposition of mobile retroelements, and telomere DNA replication can be primed with covalently bound terminal proteins [all these mechanisms are reviewed in (Nosek *et al.*, 2006)]. ALT mechanisms are usually observed as a backup pathway, or part of multiple pathways, that emerge in response to the loss of telomerase-based mechanism of telomere synthesis, as e.g. in telomerase deficient yeast or plant mutants (McEachern and Hicks, 1993; Ruckova *et al.*, 2008), or in a fraction of telomerase-negative tumours (Bryan *et al.*, 1997). However, ALT mechanisms are also functional in species that do not use telomerase. The best known is exemplified by *Drosophila melanogaster*, which uses retrotransposition of mobile elements to reverse DNA losses associated with incomplete end replication (Pardue and DeBaryshe, 2003).

In flowering plants (angiosperms) there are two groups known where there has been significant evolutionary divergence in telomere biology. The first group is in plant order Asparagales, a group of petaloid monocots. During the radiation of Asparagales, one large clade of species is thought to have lost the typical angiosperm telomeric motif (TTTAGGG)_n synthesized by telomerase and which was first reported in *Arabidopsis thaliana* (Figure 1). Instead a new motif is found (TTAGGG)_n. That switch in motif was likely to have had profound consequences for telomerase activity and the function and activity of telomere binding proteins (Sykorova *et al.*, 2003c, 2006b; Fajkus *et al.*, 2005b). Then later, in this same clade, a second switch happened with the divergence of plant genus *Allium* (onion, family Alliaceae). Here the (TTAGGG)_n motif itself was lost, and another, as yet undiscovered, telomeric motif evolved (Figure 1), which is elongated by a mechanism that is probably independent of telomerase (Pich *et al.*, 1996; Sykorova *et al.*, 2006a).

The second plant group known with unusual telomere biology is in family Solanaceae. Most genera studied in this family (e.g. *Nicotiana* or *Solanum*) have typical Arabidopsis-type telomere repeats synthesized by telomerase (Fajkus *et al.*, 1995, 1996, 2002), encoded by gene with 13 exons (Sykorova *et al.*, 2012). But with the divergence of three closely related genera, *Cestrum*, *Vestia* and *Sessea*, the motif switched (Figure 1) to an unknown sequence and mechanism of telomere synthesis (Sykorova *et al.*, 2003b). In previous studies aimed at finding the telomeres of this group, we showed in *C. elegans*, that degenerate A/T-rich minisatellite sequences were dispersed around the genome along with short interstitial telomeric (TTTAGGG) sequences (ITS). We speculated that the occurrence and distribution of these sequences may be related to ancestral telomerase activity, or instabilities caused by telomere malfunction when the Arabidopsis-type telomere was lost (Sykorova *et al.*, 2003a). However, without a functional

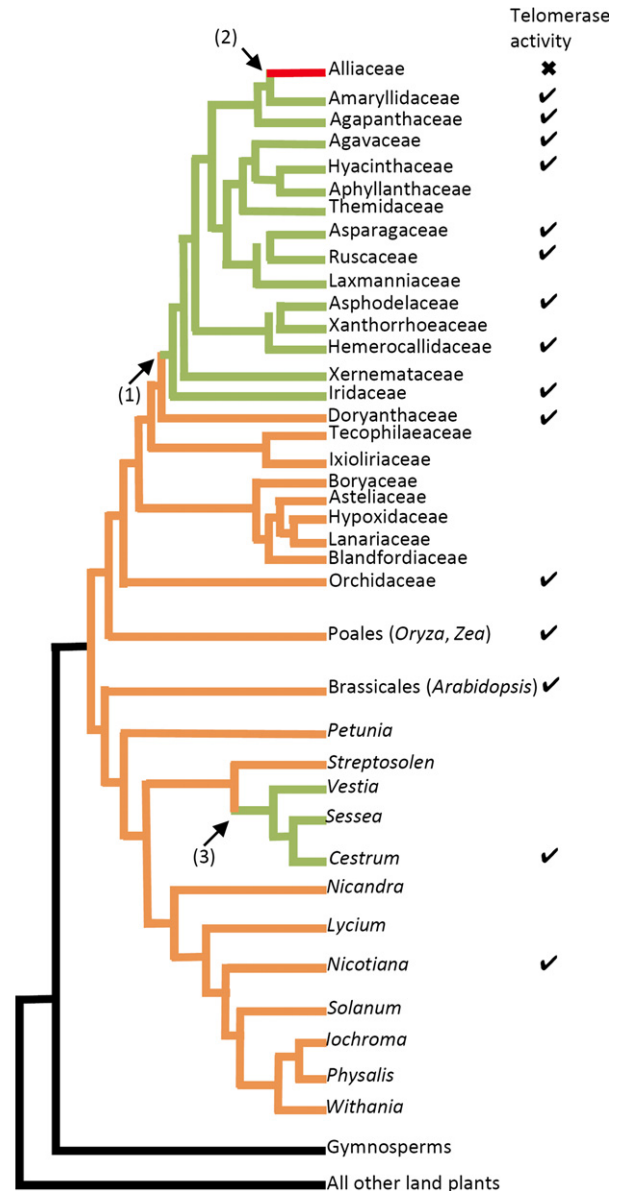


Figure 1. Two groups of flowering plants show significant divergence in telomere sequence.

The first group is in plant order Asparagales (1), where the typical Arabidopsis-type telomere motif (TTTAGGG)_n is replaced with the motif (TTAGGG)_n, more typical of vertebrates. Later in the evolution of the clade, with the divergence of genus *Allium* (2), the TTAGGG motif was replaced by another, unknown sequence synthesized by ALT mechanisms. The second plant group known with unusual telomere biology is in family Solanaceae (3) and occurred with the divergence of three closely related genera, *Cestrum*, *Vestia* and *Sessea*. Here the Arabidopsis-type telomere motif was again lost. Here we show that in *C. elegans* at least, it is replaced by the (TTTTTTAGGG)_n motif synthesized by telomerase. The relationships between families and genera are adapted from schematic phylogenetic trees in Sykorova *et al.* (2003a,b,c, 2006a,b).

telomeric DNA sequence and a corresponding mechanism of its synthesis, deeper understanding of this telomere biology was not possible. One problem in finding the telomere of these species was that the genome sizes are large

and chromosome numbers small (e.g. *C. elegans*; $1C = 9.76 \text{ pg} \approx 9.55 \text{ Gbp}$; $n = 8$). This meant that the telomere motifs themselves were likely to be only a tiny fraction of the total DNA. Furthermore, our approaches to find the telomere were confounded by a high occurrence of experimentally induced double strand breaks.

We developed an original assay to overcome the problem of the large genome size of the study material. From *C. elegans*, we obtained high molecular weight DNA (hwm DNA), which was split into two pools, one of which was treated with BAL31, an enzyme that digests DNA from double strand DNA (dsDNA) breaks, telomeres, single-strand DNA (ssDNA) nicks and local structures in DNA (e.g. cruciform folded DNA), which occur in native chromatin (Varga *et al.*, 1999; Szilagy *et al.*, 2003). We then obtained next-generation sequencing (NGS) data (Illumina HiSeq) of these two DNA pools. We reasoned that any repeat that was under-represented in the BAL31 digested genomic component would be a likely candidate DNA sequence because all telomeres should be digested by BAL31 while breaks and other BAL31-sensitive structures are likely to be more randomly distributed or less focussed at a particular repeat. To find under-represented repeats we used the bioinformatic pipeline RepeatExplorer (Novak *et al.*, 2013). Candidate sequences identified were then analysed using cytogenetic and molecular biology tools that are frequently used in telomere biology (Fajkus *et al.*, 2005a; Bennett and Leitch, 2012). Using this integrated approach, we characterize the unusual telomeric sequence of *C. elegans* and the mechanism of its synthesis.

RESULTS

Sequence clustering using RepeatExplorer

We analysed four million 100 bp paired end reads from *C. elegans*, two million reads from each of the untreated and BAL31-treated hwm DNA samples. The DNA C-value of *C. elegans* is estimated to be $1C = 9.76 \text{ pg}$ (Sykorova *et al.*, 2003b). Assuming that 1 pg of DNA is equivalent to 978 Mb, then the NGS data represent 4.2% of the genome. Despite the low genome coverage, we were able to assemble repetitive elements from *C. elegans* with RepeatExplorer using these data. RepeatExplorer groups the reads into clusters based on their sequence similarity, so that each cluster represents a distinctive repeat. The abundance of reads in a cluster reflects the proportion of repeats in the genome. Approximately 1.4 million reads from each sample (2 879 047 reads from both samples) were assigned into 126 912 clusters (called CL1–CL126912), representing 72% of the input dataset. The remaining reads (1 120 953 from both samples) remained as ‘singlets’, corresponding to low-copy and single-copy sequences.

BAL31 sensitivity–telomere sequence candidates

We focused our search for telomere candidates to clusters that contained eight or more reads. We examined clusters with a low number of reads because the telomeric DNA may represent only a small fraction of the total genome. All clusters were statically analysed with Chi-squared tests to determine whether the number of reads in untreated and BAL31-treated genomic hwm DNA samples were significantly different from a 1:1 ratio, the latter being expected if BAL31 had no effect on repeat copy number. The number of clusters (and their *P*-values) that differed significantly from a 1:1 ratio are shown in Figure 2. The sensitivity of the clusters to BAL31 and their size (number of reads in the cluster) is shown in Figure 3. We obtained 126 BAL31-sensitive clusters ($P \leq 0.01$).

RepeatExplorer not only groups reads to clusters, but within each cluster assembles one or more sequence contigs. The 126 clusters contained 19 267 contigs. Of these contigs, we removed 49 contigs that matched in BLAST to rRNA, cpDNA and mtDNA. We analysed the contigs to determine which were significantly influenced by BAL31-treatment. We found 206 BAL31-sensitive contigs ($P \leq 0.01$). From these we interrogated the contig sequences searching for potential repeats that might be telomeric. Five contigs revealed a tandem repeat arrangement in dot-plot analyses (Table S1 and Figure S1). One of them (CL401Contig2, see BAL31-sensitive cluster CL401 in Figure 3) carried a minisatellite repeat of unit sequence TTTT TAGGG. This sequence corresponds to the consensus $T_n A G_m$ motif (Figure S2) typical for most known telomeric minisatellites, as well as our previously characterized irregular interstitial A/T-tract sequences in

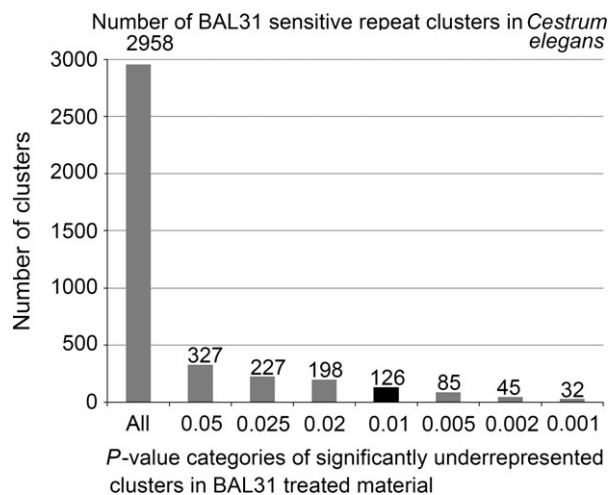


Figure 2. Number of BAL31 sensitive repeat clusters in *C. elegans* showing the total number of clusters at different significance thresholds that have reduced numbers of reads in BAL31-treated samples compared with control ($\leq P$ -values given, chi-squared tests).

We analysed in detail the 126 significant clusters that were significant different at $P \leq 0.01$ (black column).

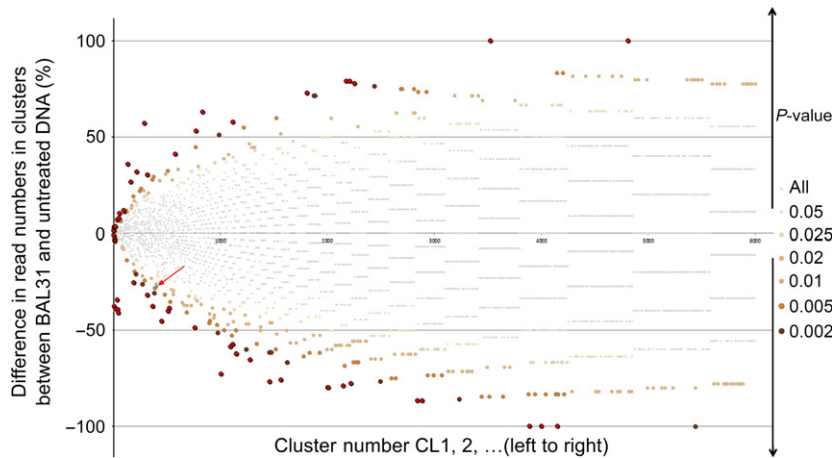


Figure 3. Distribution of BAL31 sensitive/resistant clusters in Illumina HiSeq 2000 data from *C. elegans*.

The percentage difference in number of reads in clusters between BAL31 and untreated DNA is shown. If the cluster is composed of the same number of reads from BAL31 and untreated DNA the value is 0, it is a BAL31 neutral cluster. If the cluster is solely composed of reads from untreated DNA, then the value is -100, a BAL31-sensitive cluster. If the cluster is solely composed of reads from BAL31 treated DNA, the value is 100, a BAL31 resistant cluster. BAL31 sensitive clusters are under zero on the Y axis, BAL31 resistant clusters are above 0 on the Y axis. The clusters are numbered in decreasing order of size from cluster 1 (left with most reads) to the cluster with the fewest numbers of reads (right). The statistical significance of the differences in read numbers ($P = 0.05\text{--}0.001$) is illustrated by the colour of dots. Grey clusters are not statistically distinct from BAL31 neutral clusters. The most significant clusters are on the edge of the distribution. The red arrow shows the cluster containing (TTTTTTAGGG)_n reads.

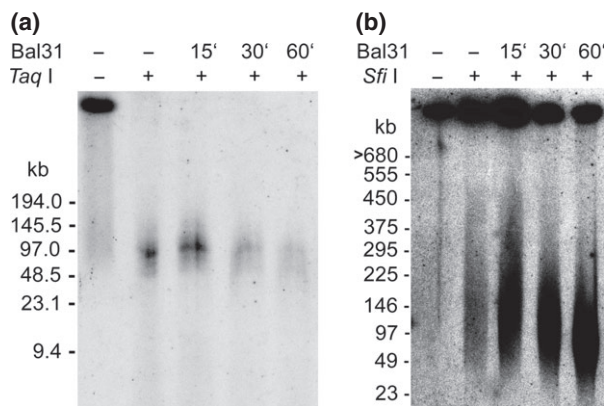


Figure 4. Analysis of terminal restriction fragments from *C. elegans*.

High molecular weight DNA from *C. elegans* was treated with BAL31 and either endonuclease *Taq*I (a) or *Sfi*I (b). *Taq*I generates shorter telomeric fragments (48–97 kb) than *Sfi*I (48–500 kb). The loss of total telomeric signal with increasing BAL31 digestion is apparent after *Taq*I digestion (15, 30, 60 min) and the size of *Taq*I fragments without BAL31 treatment are an estimate of the range in telomeres sizes. With *Sfi*I digestion the progressive shortening of terminal fragments with BAL31 digestion is clearly visible.

C. elegans (Sykorova *et al.*, 2003a). We also searched for contigs carrying these A/T-rich tract sequences, but none showed BAL31 sensitivity. No other contigs found included satellite repeats that may indicate a telomerase-based, end-replication system.

Analysis of terminal restriction fragment (TRF) lengths and BAL31-sensitivity with (TTTTTTAGGG)_n probe

To further test BAL31 sensitivity of the candidate telomeric sequence, we conducted Southern hybridization using the

(TTTTTTAGGG)_n probe to hmw DNA isolated from *C. elegans* and digested for varying amount of time with BAL31 and further digested with *Sfi*I or *Taq*I restriction enzymes. In the experiment using *Sfi*I, the probe hybridized to a large range of restriction fragments (48–500 kb). With increasing BAL31 treatment, fragment sizes were revealed with decreasing molecular weights (30–150 kb) (Figure 4b), providing evidence for the terminal position of (TTTTTTAGGG)_n sequences. However, the sizes of the fragments do not reflect the length of the telomeres because the fragments also potentially carry high proportions of subtelomeric DNA (in theory *Sfi*I restriction sites are expected to occur every 65 kb). Therefore, the experiment was repeated using *Taq*I, which cuts more frequently than *Sfi*I. This resulted in three hybridization bands between 48 and 97 kb. These bands blurred, decreased in intensity and shifted towards shorter lengths with increasing BAL31 digestion times (Figure 4a). Thus, this experiment also demonstrates the terminal position of hybridizing *Taq*I restriction fragments. However, the length of the telomeric (TTTTTTAGGG)_n tandem arrays is likely to be shorter than the TRFs, because of sequences between the proximal border of the telomere and the closest subtelomeric *Taq*I cleavage site.

An independent assessment of telomere lengths was derived from NGS data. Given that there were 63 telomeric reads in the genomic dataset of 2 million reads, then these sequences constitute a genome proportion of 0.0000315 (1C genome = 9.54528 Gb), arranged over 16 telomeres ($n = 8$). Thus telomere sequences constitute around 300 kb of DNA (per 1C genome), giving an average telomere length of about 19 kb, approximately 1900 copies per telomere.

The difference between the telomere length estimates based on TRF analysis and NGS data is probably caused by long telomere-associated region that lack the restriction sites of the enzymes used. Indeed, even long Bal31 digestion times, resulting in the near complete erosion of sequences hybridizing with the (TTTTTTAGGG)_n, terminal fragments still had a mean length of *ca.* 50 kb. Potentially these telomere-associated regions may be composed of degenerated telomere repeats, potentially including the A/T-rich tracts which we described earlier in *Cestrum* chromosomes (Sykorova *et al.*, 2003a).

C. elegans telomeric-FISH (fluorescence *in situ* hybridization)

Using the (TTTTTTAGGG)_n probe in FISH experiments to *C. elegans* root tip cell spreads, signals were located exclusively at both ends of all 16 chromosomes in cells at metaphase (see Figure 5a–c). No interstitial sites of probe hybridization were observed [interstitial telomeric sequence (ITS)], and there was no cross-hybridization to the A/T-rich tract sequences previously identified (Sykorova *et al.*, 2003a).

C. elegans TERT gene cloning

We used tblastn to the Illumina HiSeq 2000 data to identify *TERT* gene-like fragments using the *N. tabacum TERT* gene as a query (Figure 6). Although we did not obtain the entire gene sequence, we found 510 reads that covered all exons of *N. tabacum TERT* (*NtTERT*). Comparison of sequence coverage showed the exons 9–12 are covered better than the other parts of the gene. Interestingly, we observed few hits to introns.

Using PCR with gene specific primers, we obtained four overlapping genomic clones for *C. elegans TERT* (*CeTERT*) forming a 7299 nt long consensus sequence that contains

almost the entire gene (Table S2). Such *CeTERT* consensus sequence shows 58% query cover to genomic sequence of *NtTERT* (11 831 nt), (bl2seq tool). Based on similarity of *CeTERT* to *NtTERT*, we predict that *CeTERT* has 13 exons and 12 introns, including the 4/5a exon, as previously shown for *NtTERT* (Sykorova *et al.*, 2012) (Figure 6a). *CeTERT* contains the telomerase specific motifs (T2, CP, QFP and T), reverse transcriptase motifs (1, 2, A–E) and the nuclear localisation-like signal (NLS) reported for plant TERTs (Sykorova *et al.*, 2006b; Zachova *et al.*, 2013) (Figure 6a).

C. elegans TERT cDNA cloning

Sequence specific primers were used to capture transcripts corresponding to putative exons of the *CeTERT* gene using the 5' and 3' rapid amplification cDNA ends (RACE) protocol. We obtained two clones (Table S2) for 5' RACE and 3' RACE products respectively, that overlap each other in the exon 4–8 region (GenBank: KM573822, KM573821). Their sequences confirm that *CeTERT* gene is composed of 13 exons and 12 introns. The *CeTERT* coding regions (CDS; 3318 nt) shows 98% query cover to *NtTERT* CDS (3687 nt) and 76% of nucleotides in the covered regions are identical (bl2seq tool). Thus, comparisons between *NtTERT* and *CeTERT*, in either CDS or genomic DNA sequence show a low conservation of intron sequences, while exon structures and sequences are highly homologous.

C. elegans telomerase synthesizes TTTTTAGGG repeats *in vitro*

To confirm that *CeTERT* is active, we performed *in vitro* TRAP (Telomere Repeat Amplification Protocol) assays using protein extracts from shoot apex and adjacent young leaves. The products were then sequenced to confirm the identity of the telomere units added by *CeTERT*. Products

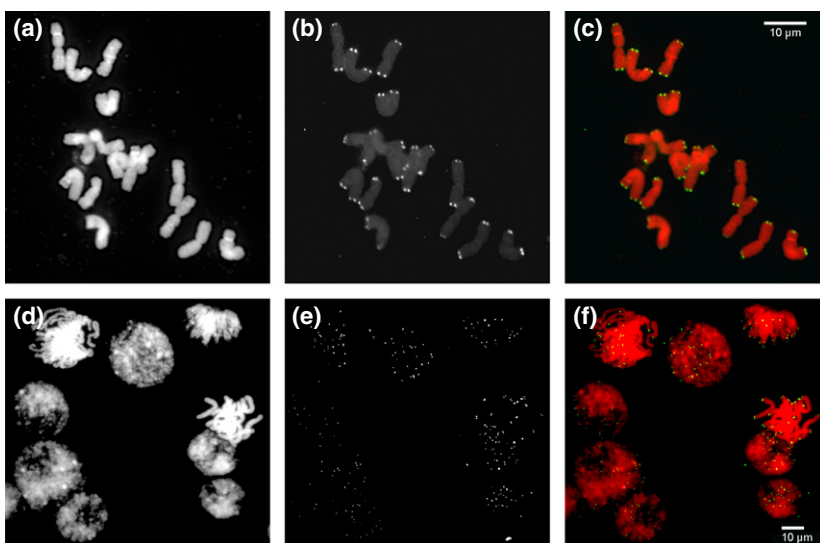


Figure 5. Fluorescent *in situ* hybridization of (TTTTTTAGGG)_n probe to *C. elegans* chromosomes.

(a, d) Chromosomes stained for DNA with DAPI. (b, e) (TTTTTTAGGG)_n probe labelled directly by AF488 showing sites of probe hybridization (grey). (c, f) Merged images and coloured (red for DAPI; green for FISH signal). Note the terminal location of the signal on the metaphase and prophase chromosomes.

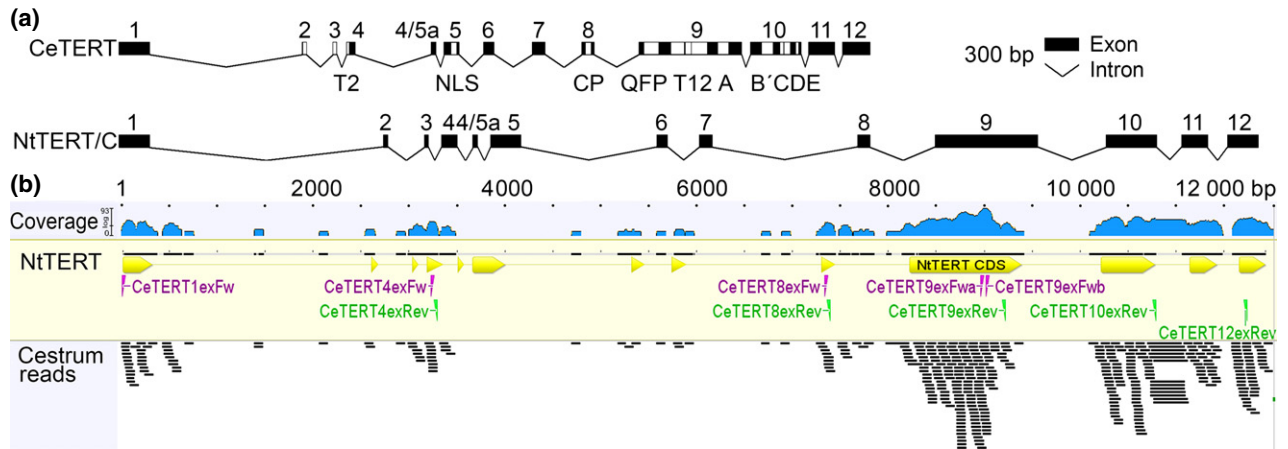


Figure 6. Comparative analysis of *CeTERT* and *NtTERT* genes.

(a) Models of exon-intron structure *CeTERT* and *NtTERT*. Model structure for *CeTERT* is based on comparison between cDNA and genomic DNA clones (for GenBank accessions see Table S2). The model of *NtTERT/Cb* is taken from (Sykороva *et al.*, 2012). Both TERT genes share 13 exons and the telomerase specific motifs: T2, CP, QFP and T, the reverse transcriptase motifs 1 and 2, A-E and nuclear localisation-like signal-NLS (grey blocks).

(b) Mapping of Illumina HiSeq 2000 reads from *C. elegans* with similarity to *NtTERT* used as a query in tblastn. Illumina reads (short black bars at the bottom of the picture) from tblastn were mapped to assembled queries of *NtTERT* (large black bar labelled *NtTERT*_Assembly). Yellow arrows indicate exons, violet and green text in the figure indicates forward and reverse gene primers designed for RACE and genomic PCR against *C. elegans* samples.

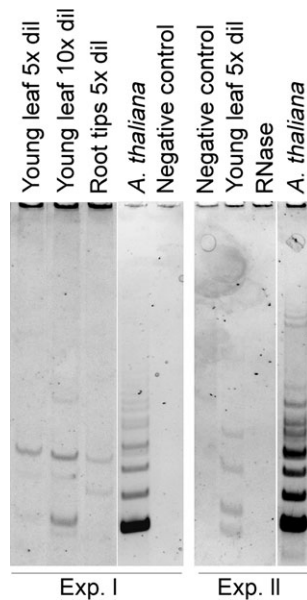


Figure 7. Telomerase activity detection in *C. elegans*.

The products of the TRAP assay using young leaf extracts diluted with reaction buffer five or 10 times. *A. thaliana* telomerase extracts were used as a positive control, the negative control contained the complete reaction mix but lacking the telomerase extract. Pre-treatment of the *C. elegans* telomerase extract with RNase A caused the TRAP assay to fail. Two independent experiments (exp I, exp II) are shown.

of telomerase extension amplified by PCR were detected as faint bands on native polyacrylamide gel (Figure 7). Comparison were made with the regular ladder of bands generated by *A. thaliana* telomerase, where the periodicity of TRAP ladder follows the (TTTAGGG)_n pattern of its 7 bp repeat length. For *C. elegans* there was a larger distance

between individual bands, as expected for a 10-bp telomeric monomer unit. Correspondingly, sequencing of the cloned TRAP products revealed the occurrence of TTTTTTAGGG sequences (Table S4). It is not clear whether the observed low processivity of *C. elegans* telomerase in TRAP assay (Figure 7) reflects specific conditions of the *in vitro* assay (e.g. high T-A content and, consequently, a low melting temperature of the TelCe3 reverse primer), or a general feature of this enzyme. Nevertheless, the sequence of the telomeric repeat unit exactly corresponds with the NGS results, as well as to FISH and TRF data.

DISCUSSION

A general strategy to find an unknown telomere sequence

We present here a general strategy to find telomere sequences in eukaryotes, with particular utility to species with large genomes. Such species have previously been intractable to motif identification, probably because their telomeres represent a tiny fraction of the genome and because of high numbers of double strand breaks induced by DNA isolation. The approach we developed involves digesting hmw DNA with BAL31, an enzyme which digests DNA from telomeres, DNA nicks and breaks and specific local structures in native chromatin (Varga *et al.*, 1999; Szilagyi *et al.*, 2003). We obtained several million Illumina HiSeq 2000 reads of genomic DNA sequence from untreated and BAL31-treated hmw DNA. These data were analysed with RepeatExplorer – a pipeline that reconstructs repetitive DNA from relatively low volume of genomic reads (typically amounting to <10% of the genome). This enabled us to identify all those repeats that are under-represented in the BAL31-treated DNA and were therefore

likely to include candidate telomere sequences. In this way, we identified and then verified using established approaches in telomere biology, an unusual telomere motif in *C. elegans*. That motif is (TTTTTAGGG)_n. This result paves the way for further studies on telomere maintenance, function and evolution in *Cestrum*, *Sessea* and *Vestia* (related genera in family Solanaceae; Figure 1), all of which lack the telomere motif that is typical of *A. thaliana* (TTTAGGG)_n (Sykorova *et al.*, 2003b). Our approach may also be used to find the telomere of plant genus *Allium*, the other angiosperm group where the telomere motif remains unknown and where the genome size is large (diploids range from 1C = 7.6–35.4 pg, (Bennett and Leitch, 2012)) and the number of chromosomes few (typically $n = 8$).

One possible caveat to the general utility of the method may be found in species with high copy numbers of ITSs, as in, for example, *Arabidopsis thaliana* (Uchida *et al.*, 2002). Here ITSs may be problematic if the high copy numbers mask the effects of BAL31 activity at the telomere. However ITSs are typically degenerate in nature, and that could enable resolution of ITS from telomere sequences in RepeatExplorer clusters. This is because RepeatExplorer groups similar sequences into the same cluster, but then variants are distributed into different contigs. Indeed, we observed in the *C. elegans* repeat cluster that contained the (TTTTTTAGGG)_n telomere motif that some contigs were influenced by BAL31, whilst others were not.

(TTTTTTAGGG)_n telomere motif in *C. elegans*

Previous data from our laboratory had shown that *C. elegans* did not have the telomere repeats that were typical of plants and several other well studied eukaryotes (i.e. *Arabidopsis* TTTAGGG)_n, human TTAGGG)_n, *Bombyx* TTAGG)_n, *Chlamydomonas* TTTTAGGG)_n, *Oxytricha* TTTTGGGG)_n and *Tetrahymena* TTGGGG)_n) (Sykorova *et al.*, 2003a,b). Following identification of (TTTTTTAGGG)_n motifs from the Illumina HiSeq datasets, we demonstrated using FISH and Southern hybridization approaches that the motif is telomeric. Then using TRAP assays and cloning strategies we demonstrated that the motif is likely to be maintained by telomerase. As far as we are aware this is a new variant of the consensus T_nAG_m motif (Figure S2) typical for telomerase-generated telomeric minisatellite sequences. Previously, Fulneckova *et al.* (2013) found the same minisatellite motif (TTTTTTAGGG)_n in publically available whole genome sequence data of the fungus *Mortierella alpina*, but there was no evidence that the motif is telomeric as far as we know (Watson, 1972; Fulneckova *et al.*, 2013). We estimate that there are approximately 1900 copies of the (TTTTTTAGGG)_n sequences at each telomere in *C. elegans* genome. This telomere size is comparable with those described previously in other Solanaceae species (Ganal *et al.*, 1991; Kovarik *et al.*, 1996; Fajkus *et al.*, 2002).

In our previous searches for telomeres in *Cestrum*, we had identified interstitial A/T tracts of a minisatellite with the consensus [TTTT(T)AGCAG]_n. These minisatellites are similar to the telomeric repeats, but exhibit relatively high variability in AGCAG region (Sykorova *et al.*, 2003a). These sequences did not show BAL31 sensitivity and are not likely to be involved in telomere function.

Telomerase in *Cestrum*

Given that the telomere motif is new for eukaryotes, it was possible that they are amplified using telomerase- or ALT-based systems. Consequently, we searched for active telomerase in our Illumina dataset. Using tblastn, we identified reads with similarity to several exons of NtTERT from *N. tabacum* (Figure 6b). However the coverage was low and these sequences could have been derived from dysfunctional telomerase remnants. Consequently, we designed specific primers from the partial TERT-like genomic sequences (Figure 6b and Tables S2 and S3) and used these to amplify CeTERT from genomic DNA and cDNA. We showed that CeTERT shares high similarity with NtTERT, including the presence of exon 4/5a, which is not usually observed in plants and may be restricted to Solanaceae (Figure 6a) (Sykorova *et al.*, 2012). TRAP assays further confirmed the (TTTTTTAGGG)_n motif was maintained by telomerase (Figure 7).

Evolution of telomeres in higher plants

There are three switch-points known in the divergence of telomere motifs in land plants. Two of these occur in order Asparagales (Figure 1). The first involved a telomere motif change from that found in *A. thaliana* (TTTAGGG)_n to a motif more usually found in vertebrates (TTAGGG)_n. Both repeats are synthesized at the telomere by telomerase (Sykorova *et al.*, 2003c, 2006b; Fajkus *et al.*, 2005b). Then at another switch point, the (TTAGGG)_n motif itself was lost, and a new as yet undiscovered telomere evolved in association with a loss of telomerase function (Figure 1). The third known switch point in telomere motif occurred in Solanaceae and we show is not associated with loss of telomerase function. The motif changed from the Arabidopsis-type telomere motif to the (TTTTTTAGGG)_n motif in *C. elegans*. It is likely, although untested at present, that the same, new (TTTTTTAGGG)_n telomeric motif is also found in all species of *Cestrum*, *Sessea* and *Vestia*, all of which are known to lack the Arabidopsis-type telomere (Sykorova *et al.*, 2003b).

There are several possible mutations that can explain the divergence of the telomere motif in the evolution of *C. elegans*. These are: (i) There was a mutation in the template site in the TR subunit. Typically the template site carries about one and half telomere motifs, so the template may have diverged to a *circa* 15 nucleotide template from a *circa* 10 nucleotide template. (ii) The template may have

changed through a shift, or removal of a pausing signal in telomere synthesis, which is thought responsible for the precise synthesis of telomere repeats. In human TR, the template region has a single-residue that pauses nucleotide addition at an exact position, maintaining the 5' boundary of the template region. This 5' boundary is defined by a region known as the helix paired region 1 (P1), which constrains and restricts the functions of the template for DNA synthesis (Brown *et al.*, 2014). (iii) Telomerase itself may have diverged, perhaps altering the annealing preferences between substrate and the TR template site, as we argued for the divergence of telomeres in Asparagales (Sykorova *et al.*, 2006b). These hypotheses can be tested when both telomerase subunits from *Cestrum* and related genera are characterized in more details.

Whatever mechanism caused the motif shift at the telomere, there would have been strong selection pressures for mutational change cascading to all proteins that bind telomere-specific sequences at the telomere. Thus our finding here provides a unique opportunity to study how telomerase and telomeres functions and evolves in higher plants, since divergence of the motif will have had profound effects on how telomeres are maintained and are folded.

EXPERIMENTAL PROCEDURES

Plant material

The plant *Cestrum elegans* (Brongn.) Schltldl was studied in this work (herbarium voucher specimen: Lim 002 (Natural History Museum, London, <http://data.nhm.ac.uk/>). The genome size of *C. elegans* ($n = 8$) is $1C = 9.76$ pg (Sykorova *et al.*, 2003b).

DNA isolation

Agarose plugs (Agarose Low Melt 3; Applichem, <https://www.applichem.com/start.html>) with high molecular weight (hmw) DNA samples were prepared from young plant leaves as described previously (Sykorova *et al.*, 2006a). Deproteinized plugs were washed twice in TE (10 mM Tris-HCl pH 8.0; 1 mM EDTA pH 8.0) for 30 min, then twice in TE with 1 mM phenylmethylsulphonyl fluoride (PMSF) for 30 min, and finally in $0.1 \times$ TE for subsequent enzyme treatment, or stored in 50 mM EDTA (pH 8.0).

BAL 31 digestion

Samples in agarose plugs were equilibrated for 30 min in BAL31 nuclease buffer (New England Biolabs, NEB, <https://www.neb.com/>) with addition of bovine serum albumin (BSA) to a final concentration $1 \mu\text{g ml}^{-1}$ and then digested with 3 units of BAL31 nuclease in a total volume 300 μl at 30°C. Reactions were stopped after varying incubation times by washing in 50 mM EGTA (pH 8.0) and incubating the sample at 50°C for 40 min.

DNA extraction from agarose

Agarose plugs with genomic DNA (gDNA) and BAL31-treated genomic DNA (BAL31-DNA) were washed in TE for 15 min. The washing buffer was replaced with $1 \times$ β -Agarase I buffer (NEB) to a final volume of 300 μl (including the plug). The plugs were

melted for 15 min by heating to 70°C with a gentle mixing. The samples were then incubated at 42°C for a further 15 min prior to the application of two units of β -Agarase I (NEB) and incubation for 2 h at 42°C with gentle agitation (using a thermomixer). The samples were then centrifuged (10 min, 14 000 *g*, room temperature). The supernatant was precipitated with ammonium acetate and ethanol. Precipitated DNA was dissolved in $1 \times$ TE and sent for Illumina HiSeq 2000 sequencing (for more details see the next paragraph).

Illumina HiSeq 2000 sequencing

Samples of genomic DNA and BAL31 treated DNA were processed into two barcoded libraries and sequenced by EMBL Genomics Core Facilities (<http://www.genecore.embl.de/>). The average length of inserts in libraries was 300 bp. Paired end sequencing was performed on Illumina HiSeq 2000 in a single lane that yielded 350 millions of reads 100 bp long.

NGS data analysis

The bioinformatic analyses, quality filtering as well as all other pre-processing were conducted on a local installation of Galaxy (<http://galaxyproject.org/>) (Giardine *et al.*, 2005; Blankenberg *et al.*, 2010; Goecks *et al.*, 2010). Repeats were identified using RepeatExplorer implemented in Galaxy using two million paired end reads per sample. The sequencing reads were clustered on the basis of similarity (Novak *et al.*, 2010, 2013; Macas *et al.*, 2011). All parameters for clustering were default parameters (minimum overlap length for clustering: 55, [%] Cluster size threshold for detailed analysis: 0.0001, RepeatMasker database: Viridiplantae, Search conserved domain database: yes, Minimal overlap for assembly: 40). We used custom made scripts to extract from the RepeatExplorer output file the numbers of reads in each repeat cluster and its contigs with the sample identification affixed to each read (either gDNA or BAL31-DNA).

BAL31 sensitivity for every cluster was calculated from any decrease from expectation in numbers of BAL31-DNA reads compared with gDNA reads in each cluster. The numbers were tested for significant differences using chi-squared tests. In the same way, we also tested for significant losses of repeats in BAL31-DNA contigs (sequence assemblies within each cluster) (Figure S3). Visualization of cluster sensitivity to BAL31 was carried out using MICROSOFT EXCEL 2010. Differences in numbers of reads in each cluster were expressed as a graph showing the percentage difference in copy number between BAL31-DNA and gDNA reads. Sequences that matched in BLAST to rRNA, cpDNA and mtDNA were removed from further analysis (see Results).

For identification of tandem repeats and the estimations of repeat unit lengths, we used dot plots (Sonnhammer and Durbin, 1995). The repeat unit consensus sequence of CL401 was reconstructed from the most frequent k-mers from reads in this cluster. K-mer frequencies were calculated using a set of modified scripts from Jiri Macas (Macas *et al.*, 2010).

Cestrum elegans TERT (*CeTERT*) BLAST

We used BLAST algorithm tblastn (<http://www.ncbi.nlm.nih.gov/books/NBK1763/#CommandLineAppsManual.Installation>) to identify TERT gene or its remnants in nucleotide database created from HiSeq Illumina reads. As a query we used *Nicotiana tabacum* TERT variants (*NtTERT*, GenBank: HM057433, HM057434 and HM057436) (Sykorova *et al.*, 2012). The identified reads were mapped to query in Geneious (Biomatters Ltd., <http://www.biomatters.com/#/>). We aligned *CeTERT* assembly of genomic clones and *NtTERT*

consensus sequences using nucleotide sequences in web tool *blast2seq* (option *blastn*, default), (http://blast.ncbi.nlm.nih.gov/Blast.cgi?PAGE_TYPE=BlastSearch&BLAST_SPEC=blast2seq&LINK_LOC=align2seq) to get information about sequence homology of entire genes and also CDSs. *CeTERT* assembly was used as a query sequence and *NtTERT* assembly as a subject.

***CeTERT* gene PCR**

Genomic DNA from *C. elegans* leaves was isolated using GenE-lute™ Plant Genomic DNA Miniprep Kit (Sigma-Aldrich, <http://www.sigmaaldrich.com/czech-republic.html>). We used *TERT*-like reads identified by *tblastn* from *C. elegans* (see above) to design primers for gene specific PCR. Primers were designed manually and analysed in OLIGOANALYZER 3.1 (IDT, <https://eu.idtdna.com/calc/analyzer>). We finally optimised PCR using *Ex Taq* DNA polymerase (TaKaRa, <http://www.clontech.com/takara>) and various primer combinations (Table S2) covering the putative *TERT* gene sequence in *C. elegans*. PCR products were cloned with TOPO^R-TA Cloning^R Kit for Sequencing using One Shot^R TOP10 Competent Cells and vector pCR™4-TOPO^R (Life Technologies/Invitrogen, <http://www.lifetechnologies.com/cz/en/home/brands/invitrogen.html>). Clones were sequenced and four representative clones were submitted to GenBank (Table S2).

***CeTERT* cDNA RACE**

Total RNA was isolated from the mixed sample of callus and roots from *C. elegans* using the RNeasy Plant Mini Kit (Qiagen, <https://www.qiagen.com/cz/>) followed by DNase I treatment (TURBO DNA-free, Life Technologies/Ambion, <http://www.lifetechnologies.com/cz/en/home/brands/ambion.html>) according to the manufacturers' instructions. The *C. elegans* cDNA templates for 5' and 3' RACE were prepared using 1 µg of total RNA. Amplification was conducted according to manual using 5'-RACE or 3'-RACE CDS primers and SMARTScribe Reverse Transcriptase (SMARTer RACE cDNA amplification Kit; Clontech, <https://www.clontech.com/>). Gene specific primers *CeTERT8exRev* and *CeTERT4exFw* (Table S3) were designed for predicted exon loci and used to amplify the *CeTERT* cDNA sequence from 5' resp. 3' RACE products using the Advantage 2 Polymerase Mix and the Universal Primer Mix (UPM; Clontech). The cloned PCR products were sequenced and submitted to (GenBank: KM573821, KM573822).

Slides preparation and fluorescence *in situ* hybridization (FISH)

Cestrum elegans root tips were fixed in freshly made mixture of ethanol:acetic acid (3:1) overnight, and processed according to (Mandakova and Lysak, 2008). We used an enzyme mix to soften the root tips [0.3% (w/v) in water each of: cellulase (Onozuka RS, Serva), pectolyase Y-23 (Duchefa) and cytohelicase (Sigma-Aldrich)]. Chromosomes and nuclei were then spread using the squashing method in 60% acetic acid. Slides were treated with RNase A (100 µg ml⁻¹, 1 h at 37°C), pepsin (10 µg ml⁻¹ in 10 mM HCl, 10 min at 37°C), and fixed in 4% (w/v) formaldehyde in 2 × SSC (saline-sodium citrate buffer, 0.3 M sodium chloride and 30 mM trisodium citrate, pH 7.0) solution. After each step, washing steps 3 × 5 min in 2 × SSC were introduced. Slides were finally dried in an ethanol series (70%–80%–96%).

Probes for FISH were prepared by oligonucleotides *CeTelC* and *CeTelG* (Table S3) in non-template PCR (Ijdo *et al.*, 1991) and subsequently labelled by AF488-dUTP (Life Technologies) with a nick-translation reaction (Mandakova and Lysak, 2008). For *in situ* hybridization, 200 ng of the probe was used in the hybridization

mixture containing 50% deionised formamide/2 × SSC/10% dextran sulphate, with a volume of 30 µl added per slide. Slides were denatured together with probes at 80°C and hybridized overnight in a moist chamber at 37°C. Post hybridization washing steps included 3 × 5 min in 35% formamide/2 × SSC at 42°C, 2 × 5 min in 2 × SSC at 42°C, 2 × 5 min in 2 × SSC at room temperature. Chromosomes were counterstained with 4',6-diamidino-2-phenylindole (DAPI; 1 µg ml⁻¹) in Vectashield (Vector Laboratories, <http://www.vectorlabs.co.uk/>) and analysed on Zeiss Axioimager Z1 microscope, with a cooled charged coupled device (CCD) camera and appropriate filter set (ZEISS, http://www.zeiss.com/corporate/en_de/home.html). Images were processed in ADOBE® PHOTOSHOP® CS6.

Analysis of terminal restriction fragments lengths and BAL31-sensitivity

hmw DNA from *C. elegans* plants was prepared in agarose plugs as described above and previously (Sykorova *et al.*, 2006b). The terminal position of probed sequences was tested by sensitivity to BAL31 nuclease digestion. Samples in agarose plugs (ca. 2 µg of DNA) were equilibrated for 15 min in 200 µl of BAL31 nuclease buffer (NEB) and then digested in a new portion of the buffer with 3 units of BAL31 nuclease (NEB) in Thermomixer (Eppendorf AG, Hamburg, Germany, <http://www.eppendorf.com/int/?l=1&action=start>) at 30°C for various periods of time. Reactions were stopped by buffer exchange with 50 mM EGTA pH 8.0, and BAL31 nuclease was irreversibly inactivated by incubation at 55°C for 40 min. The plugs were then washed in 0.1 × TE buffer (3 × 15 min) and equilibrated in the appropriate restriction buffer (*SfiI* or *TaqI*, NEB) for subsequent restriction enzyme digestion to measure telomere lengths by Terminal restriction fragment (TRF) analysis (Fajkus *et al.*, 1998). DNA samples in the agarose plugs were analysed by pulsed-field gel electrophoresis (PFGE) using the CHEF Mapper system under the following conditions: 1% Pulsed-Field Certified™ Agarose (Bio-Rad, <http://www.bio-rad.com/>) in 0.5 × TBE buffer, 6 V cm⁻¹, pulse time ramped from 0.5 sec to 45 sec for 20 h at 14°C (*SfiI* digestion, NEB) or from 0.25 sec to 36 sec for 14 h at 14°C (*TaqI* digestion, NEB). PFGE gels were alkali blotted onto Hybon XL membranes (GE Healthcare Life Sciences, <http://www.gelifesciences.com/>) and hybridized with radioisotope-labelled probes for (TTTTTTAGGG)_n telomeres produced by oligonucleotides *CeTelC* and *CeTelG* (Table S3) in non-template PCR (Ijdo *et al.*, 1991; Neplechova *et al.*, 2005). Hybridization signals were visualized using the FLA-7000 phosphorimaging system (FujiFilm, <http://www.fujifilm.com/>).

Telomere repeat amplification protocol (TRAP)

TRAP assay for plant telomerase activity was performed as described previously (Fitzgerald *et al.*, 1996; Sykorova *et al.*, 2003c). Shoot apex samples including very young leaves of *C. elegans* were manually homogenized in extraction buffer, crude extracts obtained after centrifugation were 5× and 10× diluted for analysis of telomerase activity. A volume of 0.5 µl of 10 µM substrate oligonucleotide (TS21 5'-GACAATCCGTCGAGCAGAGTT-3' (Fajkus *et al.*, 1998) or 47F 5'-CGCGGTAGTGATGTGGTTGTGTT-3' (Fojtova *et al.*, 2002), Table S3) was mixed with 1 µl of diluted crude protein extract. Primer extension by telomerase proceeded for 45 min at 26°C in the 25 µl of the reaction buffer (Fitzgerald *et al.*, 1996). Telomerase was heat-inactivated (5 min, 94°C) and telomerase extension products were amplified using substrate oligonucleotide as forward primer and with the reverse primer *TelCe3* (5'-CGTACACCCTAAAAGACCCTAGAAAACC-3'; Table S3)

reflecting the predicted sequence of the *C. elegans* telomeric repeat. PCR with 2 U of DyNAzyme II DNA polymerase (Thermo Scientific/Finnzymes, <https://www.lifetechnologies.com/cz/en/home/brands/thermo-scientific.html>) was performed as follows: 35 cycles of 95°C per 30 sec, 58°C per 30 sec, 72°C per 30 sec; final extension 72°C per 5 min. The TRAP reaction products were resolved on 12.5% polyacrylamide gel in 0.5 × TBE buffer and stained by GelStar™ Nucleic Acid Gel Stain 10 000× (LONZA, <http://www.lonza.com/>) and signals were visualized using LAS-3000 system (FujiFilm). The protein extract from the *Arabidopsis thaliana* seedlings was used as a control sample for rough estimation of the length of the *C. elegans* telomeric unit. Finally the *C. elegans* TRAP products were cloned using TOPO® TA Cloning® Kit (Life Technologies/Invitrogen) and sequenced.

ACKNOWLEDGEMENTS

We wish to acknowledge the help provided by Šarlota Štemberová in FISH probe labelling, Jiří Macas for providing us an image of RepeatExplorer and scripts for k-mer analysis logo and Vladimír Beneš for advising us with proper NGS libraries selection. This work was supported by the Czech Science Foundation [13-10948P to V.P.]; the Czech Academy of Sciences [M200041206 to J.F.]; project CEITEC (CZ.1.05/1.1.00/02.0068) of the European Regional Development Fund and projects CZ.1.07/2.3.00./20.0189 and CZ.1.07/2.3.00/30.0019 co-financed from European Social Fund and the State Budget of the Czech Republic. Access to computing and storage facilities owned by parties and projects contributing to the National Grid Infrastructure MetaCentrum, provided under the programme 'Projects of Large Infrastructure for Research, Development, and Innovations' (LM2010005), is greatly appreciated.

SUPPORTING INFORMATION

Additional Supporting Information may be found in the online version of this article.

Figure S1. Dot-plot of five BAL31 sensitive clusters containing tandem repeats from *C. elegans*.

Figure S2. Reconstructed fragments with telomeric repeat motif from *C. elegans*.

Figure S3. Example calculation of (a) expected number of BAL31 and untreated gDNA reads in cluster CL401; (b) – Chi-squared test to determine whether observed values of numbers BAL31 and gDNA reads in CL401 differ from expected value; (c) calculation of percentage decrease in BAL31 reads (see Figure 3).

Table S1. BAL31 sensitive contigs containing tandem repeats (analysed as candidate telomeric sequences) from *C. elegans*.

Table S2. Summary of primer combinations for *CeTERT* RACE and PCR with genomic DNA.

Table S3. List of primers and their sequences used in PCR, RACE, TRAP and probe preparation for FISH and TRF analysis.

Table S4. List of sequences obtained by cloning TRAP products.

REFERENCES

- Bennett, M.D. and Leitch, I.J. (2012) *Plant DNA C-values database (release 6.0, Dec. 2012)*.
- Blankenberg, D., Von Kuster, G., Coraor, N., Ananda, G., Lazarus, R., Mangano, M., Nekrutenko, A. and Taylor, J. (2010) Galaxy: a web-based genome analysis tool for experimentalists. *Curr. Protoc. Mol. Biol.* Chapter 19, Unit 19 10 11–21.
- Brown, A.F., Podlevsky, J.D., Qi, X., Chen, Y., Xie, M. and Chen, J.J. (2014) A self-regulating template in human telomerase. *Proc. Natl Acad. Sci. USA*, **111**, 11311–11316.
- Bryan, T.M., Englezou, A., DallaPozza, L., Dunham, M.A. and Reddel, R.R. (1997) Evidence for an alternative mechanism for maintaining telomere

length in human tumors and tumor-derived cell lines. *Nat. Med.* **3**, 1271–1274.

- Fajkus, J., Kovarik, A., Kralovics, R. and Bezdek, M. (1995) Organization of telomeric and subtelomeric chromatin in the higher-plant *Nicotiana tabacum*. *Mol. Gen. Genet.* **247**, 633–638.
- Fajkus, J., Kovarik, A. and Kralovics, R. (1996) Telomerase activity in plant cells. *FEBS Lett.* **391**, 307–309.
- Fajkus, J., Fulneckova, J., Hulanova, M., Berkova, K., Riha, K. and Matyasek, R. (1998) Plant cells express telomerase activity upon transfer to callus culture, without extensively changing telomere lengths. *Mol. Gen. Genet.* **260**, 470–474.
- Fajkus, J., Novotna, M. and Ptacek, J. (2002) Analysis of chromosome termini in potato varieties. *Rostlinna Vyroba*, **48**, 477–479.
- Fajkus, J., Sykorova, E. and Leitch, A.R. (2005a) Techniques in plant telomere biology. *Biotechniques*, **38**, 233–243.
- Fajkus, J., Sykorova, E. and Leitch, A.R. (2005b) Telomeres in evolution and evolution of telomeres. *Chromosome Res.* **13**, 469–479.
- Fitzgerald, M.S., McKnight, T.D. and Shippen, D.E. (1996) Characterization and developmental patterns of telomerase expression in plants. *Proc. Natl Acad. Sci. USA*, **93**, 14422–14427.
- Fojtova, M., Fulneckova, J., Fajkus, J. and Kovarik, A. (2002) Recovery of tobacco cells from cadmium stress is accompanied by DNA repair and increased telomerase activity. *J. Exp. Bot.* **53**, 2151–2158.
- Fulneckova, J., Svecikova, T., Fajkus, J., Lukesova, A., Lukes, M., Vlcek, C., Lang, B.F., Kim, E., Elias, M. and Sykorova, E. (2013) A broad phylogenetic survey unveils the diversity and evolution of telomeres in eukaryotes. *Genome Biol. Evol.* **5**, 468–483.
- Ganal, M.W., Lapitan, N.L.V. and Tanksley, S.D. (1991) Macrostructure of the tomato telomeres. *Plant Cell*, **3**, 87–94.
- Giardine, B., Riemer, C., Hardison, R.C. et al. (2005) Galaxy: a platform for interactive large-scale genome analysis. *Genome Res.* **15**, 1451–1455.
- Goecks, J., Nekrutenko, A., Taylor, J. and Galaxy, T. (2010) Galaxy: a comprehensive approach for supporting accessible, reproducible, and transparent computational research in the life sciences. *Genome Biol.* **11**, R86.
- Greider, C.W. and Blackburn, E.H. (1985) Identification of a specific telomere terminal transferase activity in *Tetrahymena* extracts. *Cell*, **43**, 405–413.
- Greider, C.W. and Blackburn, E.H. (1987) The telomere terminal transferase of tetrahymena is a ribonucleoprotein enzyme with 2 kinds of primer specificity. *Cell*, **51**, 887–898.
- Ijdo, J.W., Wells, R.A., Baldini, A. and Reeders, S.T. (1991) Improved telomere detection using a telomere repeat probe (TTAGGG)_n generated by PCR. *Nucleic Acids Res.* **19**, 4780.
- Kovarik, A., Fajkus, J., Koukalova, B. and Bezdek, M. (1996) Species-specific evolution of telomeric and rDNA repeats in the tobacco composite genome. *Theor. Appl. Genet.* **92**, 1108–1111.
- Macas, J., Neumann, P., Novak, P. and Jiang, J. (2010) Global sequence characterization of rice centromeric satellite based on oligomer frequency analysis in large-scale sequencing data. *Bioinformatics*, **26**, 2101–2108.
- Macas, J., Kejnovsky, E., Neumann, P., Novak, P., Koblikova, A. and Vyskot, B. (2011) Next generation sequencing-based analysis of repetitive DNA in the model dioecious [corrected] plant *Silene latifolia*. *PLoS One*, **6**, e27335.
- Mandakova, T. and Lysak, M.A. (2008) Chromosomal phylogeny and karyotype evolution in x = 7 crucifer species (Brassicaceae). *Plant Cell*, **20**, 2559–2570.
- McEachern, M.J. and Hicks, J.B. (1993) Unusually large telomeric repeats in the yeast *Candida albicans*. *Mol. Cell. Biol.* **13**, 551–560.
- Neplechova, K., Sykorova, E. and Fajkus, J. (2005) Comparison of different kinds of probes used for analysis of variant telomeric sequences. *Biophys. Chem.* **117**, 225–231.
- Nosek, J., Kosa, P. and Tomaska, L. (2006) On the origin of telomeres: a glimpse at the pre-telomerase world. *BioEssays*, **28**, 182–190.
- Novak, P., Neumann, P. and Macas, J. (2010) Graph-based clustering and characterization of repetitive sequences in next-generation sequencing data. *BMC Bioinformatics*, **11**, 378.
- Novak, P., Neumann, P., Pech, J., Steinhaisl, J. and Macas, J. (2013) RepeatExplorer: a Galaxy-based web server for genome-wide characterization of eukaryotic repetitive elements from next-generation sequence reads. *Bioinformatics*, **29**, 792–793.
- Olovnikov, A.M. (1971) Principle of marginotomy in template synthesis of polynucleotides. *Dokl. Akad. Nauk SSSR*, **201**, 1496–1499.

- Pardue, M.L. and DeBaryshe, P.G. (2003) Retrotransposons provide an evolutionarily robust non-telomerase mechanism to maintain telomeres. *Annu. Rev. Genet.* **37**, 485–511.
- Pich, U., Fuchs, J. and Schubert, I. (1996) How do Alliaceae stabilize their chromosome ends in the absence of TTTAGGG sequences? *Chromosome Res.* **4**, 207–213.
- Ruckova, E., Friml, J., Schrupfova, P.P. and Fajkus, J. (2008) Role of alternative telomere lengthening unmasked in telomerase knock-out mutant plants. *Plant Mol. Biol.* **66**, 637–646.
- Sonnhammer, E.L. and Durbin, R. (1995) A dot-matrix program with dynamic threshold control suited for genomic DNA and protein sequence analysis. *Gene*, **167**, GC1–GC10.
- Sykorova, E., Lim, K.Y., Fajkus, J. and Leitch, A.R. (2003a) The signature of the *Cestrum* genome suggests an evolutionary response to the loss of (TTTAGGG)_n telomeres. *Chromosoma*, **112**, 164–172.
- Sykorova, E., Lim, K.Y., Chase, M.W., Knapp, S., Leitch, I.J., Leitch, A.R. and Fajkus, J. (2003b) The absence of Arabidopsis-type telomeres in *Cestrum* and closely related genera *Vestia* and *Sessea* (Solanaceae): first evidence from eudicots. *Plant J.* **34**, 283–291.
- Sykorova, E., Lim, K.Y., Kunicka, Z., Chase, M.W., Bennett, M.D., Fajkus, J. and Leitch, A.R. (2003c) Telomere variability in the monocotyledonous plant order Asparagales. *Proc. R. Soc. B Biol. Sci.* **270**, 1893–1904.
- Sykorova, E., Fajkus, J., Meznikova, M., Lim, K.Y., Neplechova, K., Blattner, F.R., Chase, M.W. and Leitch, A.R. (2006a) Minisatellite telomeres occur in the family Alliaceae but are lost in *Allium*. *Am. J. Bot.* **93**, 814–823.
- Sykorova, E., Leitch, A.R. and Fajkus, J. (2006b) Asparagales telomerases which synthesize the human type of telomeres. *Plant Mol. Biol.* **60**, 633–646.
- Sykorova, E., Fulneckova, J., Mokros, P., Fajkus, J., Fojtova, M. and Peska, V. (2012) Three TERT genes in *Nicotiana tabacum*. *Chromosome Res.* **20**, 381–394.
- Szilagyi, I., Varga, T., Szekvolgyi, L. et al. (2003) Non-random features of loop-size chromatin fragmentation. *J. Cell. Biochem.* **89**, 1193–1205.
- Uchida, W., Matsunaga, S., Sugiyama, R. and Kawano, S. (2002) Interstitial telomere-like repeats in the *Arabidopsis thaliana* genome. *Genes Genet. Syst.* **77**, 63–67.
- Varga, T., Szilagyi, I. and Szabo, G. Jr (1999) Single-strand breaks in agarose-embedded chromatin of nonapoptotic cells. *Biochem. Biophys. Res. Commun.* **264**, 388–394.
- Watson, J.D. (1972) Origin of concatemeric T7 DNA. *Nat. New Biol.* **239**, 197–201.
- Zachova, D., Fojtova, M., Dvorackova, M., Mozgova, I., Lermontova, I., Peska, V., Schubert, I., Fajkus, J. and Sykorova, E. (2013) Structure-function relationships during transgenic telomerase expression in Arabidopsis. *Physiol. Plant.* **149**, 114–126.

Centromere and telomere sequence alterations reflect the rapid genome evolution within the carnivorous plant genus *Genlisea*

Trung D. Tran^{1,†}, Hieu X. Cao^{1,†}, Gabriele Jovtchev^{1,‡}, Pavel Neumann², Petr Novák², Miloslava Fojtová³, Giang T.H. Vu¹, Jiří Macas², Jiří Fajkus^{3,4}, Ingo Schubert^{1,3} and Joerg Fuchs^{1,*}

¹Leibniz Institute of Plant Genetics and Crop Plant Research (IPK), OT Gatersleben, Corrensstrasse 3, D-06466, Stadt Seeland, Germany,

²Biology Centre of the Academy of Sciences of the Czech Republic, Institute of Plant Molecular Biology, Branišovská 31/1160, 37005, České Budějovice, Czech Republic,

³Central European Institute of Technology (CEITEC) and Faculty of Science, Masaryk University, Kamenice 5, 62500 Brno, Czech Republic, and

⁴Institute of Biophysics, Academy of Sciences of the Czech Republic v.v.i., Královopolská 135, 61265 Brno, Czech Republic

Received 3 March 2015; revised 7 October 2015; accepted 15 October 2015.

*For correspondence (e-mail fuchs@ipk-gatersleben.de).

†These authors contributed equally to this work.

‡Present address: Department of Ecosystem Research, Environmental Risk Assessment and Conservation Biology, Institute of Biodiversity and Ecosystem Research, Bulgarian Academy of Sciences, 2 Gagarin Street, Sofia, 1113, Bulgaria.

SUMMARY

Linear chromosomes of eukaryotic organisms invariably possess centromeres and telomeres to ensure proper chromosome segregation during nuclear divisions and to protect the chromosome ends from deterioration and fusion, respectively. While centromeric sequences may differ between species, with arrays of tandemly repeated sequences and retrotransposons being the most abundant sequence types in plant centromeres, telomeric sequences are usually highly conserved among plants and other organisms. The genome size of the carnivorous genus *Genlisea* (Lentibulariaceae) is highly variable. Here we study evolutionary sequence plasticity of these chromosomal domains at an intrageneric level. We show that *Genlisea nigrocaulis* (1C = 86 Mbp; 2n = 40) and *G. hispidula* (1C = 1550 Mbp; 2n = 40) differ as to their DNA composition at centromeres and telomeres. *G. nigrocaulis* and its close relative *G. pygmaea* revealed mainly 161 bp tandem repeats, while *G. hispidula* and its close relative *G. subglabra* displayed a combination of four retroelements at centromeric positions. *G. nigrocaulis* and *G. pygmaea* chromosome ends are characterized by the Arabidopsis-type telomeric repeats (TTTAGGG); *G. hispidula* and *G. subglabra* instead revealed two intermingled sequence variants (TTCAGG and TTTCAGG). These differences in centromeric and, surprisingly, also in telomeric DNA sequences, uncovered between groups with on average a > 9-fold genome size difference, emphasize the fast genome evolution within this genus. Such intrageneric evolutionary alteration of telomeric repeats with cytosine in the guanine-rich strand, not yet known for plants, might impact the epigenetic telomere chromatin modification.

Keywords: Lentibulariaceae, *Genlisea nigrocaulis*, *G. hispidula*, centromeric tandem repeat, centromeric retrotransposons, plant telomeric repeat variants, telomerase, genome evolution.

INTRODUCTION

The nuclear genome of eukaryotic organisms is packed into chromosomes. Although the number and size of chromosomes may vary even between closely related species, linear eukaryotic chromosomes invariably possess as essential constituents a centromere and two telomeres. The centromere is required for sister chromatid cohesion

until it becomes involved in chromosome segregation during nuclear divisions. Telomeres protect chromosome ends from degradation and fusion and prevent chromosome shortening during DNA replications.

Although centromere and telomere functions are highly conserved, their DNA sequences show different degrees of

conservation across eukaryotic organisms. In vascular plants, the heptanucleotide repeat (TTTAGGG) which was first discovered in *Arabidopsis thaliana* (Richards and Ausubel, 1988) is the most common telomere sequence (Fuchs *et al.*, 1995). Nevertheless, this plant-type telomere repeat is replaced completely or partially by other repeats such as (TTAGGG) or (TTGGGG) or by unknown sequences within families of the monocotyledonous order Asparagales (Adams *et al.*, 2001; Weiss and Scherthan, 2002; Sykorova *et al.*, 2003c, 2006). Telomere repeat alteration was also detected within species of the dicotyledonous family Solanaceae (Sykorova *et al.*, 2003a; Peska *et al.*, 2015).

Variation of centromere-associated sequences is even more widespread. From numerous centromere DNA sequences reported for plants and animals, centromere-specific tandem repeats are the most common. A typical characteristic of these centromeric repeats is their rapid divergence (Henikoff *et al.*, 2001; Ma *et al.*, 2007). A comparative analysis of centromeric repeats in hundreds of plant and animal species revealed that the overall similarity of these elements is very low (Melters *et al.*, 2013). Variation in sequence and length of repeated monomers of centromeric repeats has been detected e.g. in *A. thaliana* (centromeric repeat family pAL1) (Martinez-Zapater *et al.*, 1986), *Oryza sativa* (CentO, formerly RCS2 family) (Dong *et al.*, 1998; Cheng *et al.*, 2002) and barley (AGGGAG) (Hudakova *et al.*, 2001). Other important components of centromeric DNA are transposable elements. Centromeres of a number of angiosperm species are colonized by centromeric retrotransposons (CR) belonging to the CRM (centromeric retrotransposon of maize) clade of chromoviruses, a lineage of *Ty3/gypsy* retrotransposons possessing an integrase chromodomain (Gorinsek *et al.*, 2004; Neumann *et al.*, 2011). Centromeric tandem repeats and CRs, either alone or together, contribute to the structure of centromeres which may span from hundreds of kbp to several Mbp in different species, and vary regarding their extension even among chromosomes of a complement (Hosouchi *et al.*, 2002; Jiang *et al.*, 2003; Plohl *et al.*, 2014). However only the core part of such extended and complex structures is defined as functional centromere which binds kinetochore proteins and contains the centromeric histone variant cenH3 (for review see Houben and Schubert, 2003; Jiang *et al.*, 2003; Fukagawa and Earnshaw, 2014). Further (peri)centromere-specific histone marks are histone H2A phosphorylated at threonine 133 in maize (Dong and Han, 2012) or at threonine 120/121 (see Materials and Methods and Demidov *et al.* (2014)) and histone H3 phosphorylated at serines 10 or 28 (Houben *et al.*, 1999) in all tested plants.

The carnivorous genus *Genlisea* comprises at least 29 species distributed in South and Central America and in Africa (Fleischmann, 2012) (Figure 1). This genus gained

increasing scientific interest since *G. aurea* (63.6 Mbp/1C) and *G. margaretae* (63.4 Mbp/1C) were shown to possess the smallest nuclear genome sizes recorded for angiosperms (Greilhuber *et al.*, 2006). Later analyses including our own measurements could not confirm the ultra-small genome size for *G. margaretae* (Fleischmann, 2012; Veleba *et al.*, 2014). However, with *G. tuberosa* (approximately 63 Mbp/1C) another species with an ultra-small genome was reported (Fleischmann *et al.*, 2014). Other *Genlisea* species, such as *G. hispidula* (1417–1510 Mbp/1C) and *G. subglabra* (1471 Mbp/1C), were reported having an up to 24-fold larger genome (Greilhuber *et al.*, 2006; Veleba *et al.*, 2014). In spite of a very similar morphology, *Genlisea* species display with a 25-fold difference one of the largest genome size ranges reported within a genus.

The genomes of *G. nigrocaulis* and *G. hispidula* (86 Mbp and 1550 Mbp, respectively) were sequenced for a comprehensive comparative analysis and revealed divergent genome size evolution within this genus (Vu *et al.*, 2015). These two species have the same chromosome number ($2n = 40$), but, in correlation with their difference in genome size, they possess different proportions of repetitive DNA. Screening repetitive DNA profiles, we identified a 161-bp tandem repeat (GnCent satellite) for *G. nigrocaulis*, and four families of potentially centromeric retrotransposons (GhCR) for *G. hispidula* (Vu *et al.*, 2015).

Here we confirm the centromeric localization of the respective repeats by fluorescence *in situ* hybridization (FISH) in combination with immunofluorescence of centromere-specific histone marks in both species and their close relatives. Furthermore, studying the telomere composition of both species, we detected an alteration in telomere repeats within the genus. The Arabidopsis-type telomere repeat present in *G. nigrocaulis* were replaced by two variant sequences (TTCAGG) and (TTTCAGG) in *G. hispidula* and its close relative *G. subglabra*. The observed alterations regarding centromere and telomere sequences are in accordance with the presumed rapid evolution of genome size and organization as postulated previously by us (Vu *et al.*, 2015) and others (Ibarra-Laclette *et al.*, 2013).

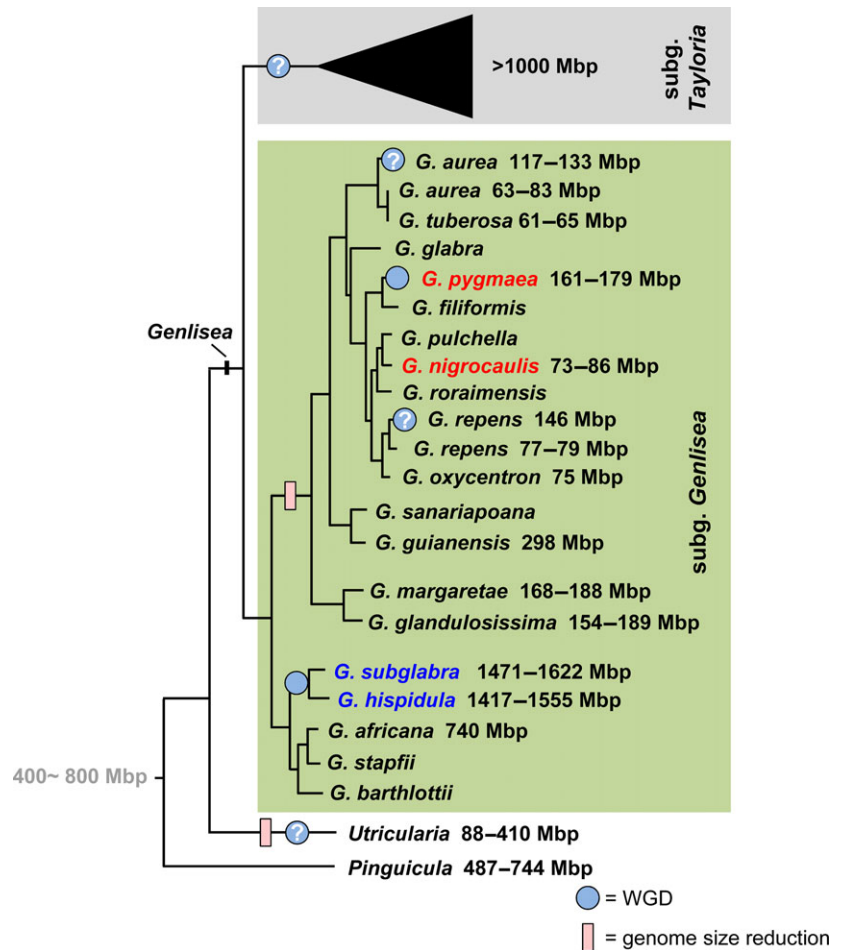
RESULTS

A 161-bp tandem repeat and four CR elements were identified as putative centromeric sequences in *Genlisea nigrocaulis* and *G. hispidula*, respectively

Graph-based clustering analysis of unassembled randomly selected whole genome sequence reads revealed a different composition of repetitive DNA for the genomes of *G. nigrocaulis* and *G. hispidula* (Vu *et al.*, 2015). The *G. nigrocaulis* genome comprised only 15.9% repetitive DNA; 0.07% belong to the chromovirus clade of *Ty3/gypsy* long terminal repeat (LTR) retrotransposons, and 2.3% are

Figure 1. Simplified phylogenetic tree of the genus *Genlisea* modified according to Fleischmann *et al.* (2014) indicating switch points of genome diminution or confirmed (or presumed) whole genome duplication.

All numbers indicate genome sizes (Mbp) from Greilhuber *et al.* (2006), Fleischmann *et al.* (2014), Veleba *et al.* (2014), Tran *et al.* (2015), Vu *et al.* (2015) and own measurements.



tandem repeats. Among the few tandem repeats, a 161 bp tandem repeat (GnCent) is the most abundant one (Vu *et al.*, 2015). Used as FISH probe on *G. nigrocaulis* interphase nuclei, GnCent showed strong clustered signals colocalized with intensely 4',6-diamidino-2-phenylindole (DAPI)-stained chromocenters (Figure 2a). In metaphase plates, GnCent yielded a distinct signal on every *G. nigrocaulis* chromosome (Figure 2b).

In *G. hispidula*, 64.1% of the genome were characterized as repetitive sequences, most of them as *Ty3/gypsy* LTR retrotransposons (24.64%) (Vu *et al.*, 2015). Among the only 1.96% of tandem repeats, several motifs were identified but none of them showed a hybridization signal on more than two chromosome pairs of *G. hispidula*. However, four families of *Ty3/gypsy* elements classified as members of the CRM clade (Gorinsek *et al.*, 2004) were found highly enriched in centromeric regions of *G. hispidula*. Further phylogenetic classification based on the reverse transcriptase domain of these retroelements showed that these elements, namely GhCR1, 2, 3 and 4, were clustered into a distinct branch of group A (Figure 3a), which was previously

shown to include genuine CRs (Neumann *et al.*, 2011). Importantly, integrase C-termini of all four GhCR elements possessed a CR motif domain which is assumed to be responsible for targeting of centromeric retrotransposons to the centromeric region (Neumann *et al.*, 2011). This suggested that the four GhCR elements are constituents of the centromeres in *G. hispidula*. FISH analysis revealed clustered signals on each chromosome, mainly in a side-by-side arrangement, and some weaker dispersed signals of the individual or combined GhCR elements (Figure 3b,c).

The presence of GnCent and GhCR elements in other *Genlisea* species was tested by PCR and FISH analysis. The GnCent satellite was also amplifiable from genomic DNA (gDNA) of the tetraploid *G. pygmaea* ($2n = 4x = 80$, 179 Mbp/1C, Vu *et al.*, 2015), a close relative of *G. nigrocaulis*, but not from *G. aurea* and *G. margaretae*, all belonging to the lineage with small genomes (Figure 1). Except *G. nigrocaulis*, only chromosomes of *G. pygmaea* revealed FISH signals for GnCent (Figure 2f,g). Sequence comparison of GnCent repeats, cloned from PCR products amplified from gDNA of *G. nigrocaulis* and *G. pygmaea*,

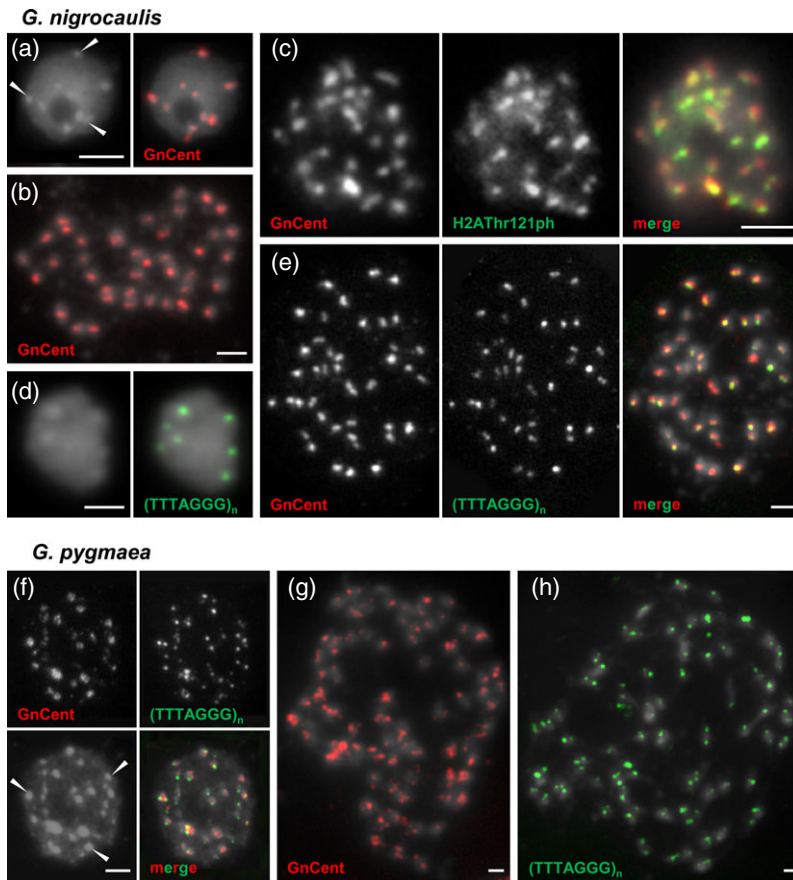


Figure 2. Cytogenetic characterization of centromeres and telomeres of *Genlisea nigrocaulis* and *G. pygmaea*.

(a, b) FISH with GnCent resulted in signal clusters co-localizing with intensely DAPI-stained chromocenters (white arrowheads) in interphase nuclei (a) and in a single hybridization signal per metaphase chromosome in *G. nigrocaulis* (b).

(c) Adjacent localization of GnCent FISH signals and H2AThr121ph immunostaining signals on metaphase chromosomes confirms the location of GnCent repeats in the (peri)centromere region of *G. nigrocaulis*.

(d, e) The Arabidopsis-type telomere repeat clusters in distinct foci in interphase nuclei (d) and localizes adjacent to the GnCent signals on metaphase chromosomes (e) of *G. nigrocaulis*.

(f) Also in *G. pygmaea* the GnCent signals co-localize with chromocenters and are closely associated with the Arabidopsis-type telomere repeat in interphase nuclei.

(g, h) These two repeats reveal strong FISH signals on each of the 80 metaphase chromosomes of *G. pygmaea*. Bars represent 2 μm .

revealed an interspecific similarity of 85.2%. The variation between both species is mostly caused by a 3-bp insertion/deletion (Figure 4, blue box). Outside *G. hispidula*, the GhCR family was detectable by PCR and FISH only in *G. subglabra* (Figure 3).

Pericentromere-specific histone markers localize adjacent to the putative centromere sequences of *Genlisea nigrocaulis* and *G. hispidula*

To confirm the presumed centromere specificity of the GnCent satellite in *G. nigrocaulis* and of the four GhCR elements in *G. hispidula*, we combined FISH of these repeats

with immunostaining experiments using antibodies against phosphorylated threonine 121 of histone H2A (H2AThr121ph) and phosphorylated serine 10 of histone H3 (H3Ser10ph). Both modifications were previously shown to be highly conserved among plants and useful cytological markers to detect the (peri)centromeric region (Houben *et al.*, 1999; Demidov *et al.*, 2014). In *G. nigrocaulis*, we found adjacent signals for GnCent and H2AThr121ph on metaphase chromosomes (Figure 2c). Similarly, FISH signals of the four GhCR elements were immediately adjacent to immunosignals for H2AThr121ph on prophase nuclei and metaphase chromosomes

Figure 3. Cytogenetic characterization of centromeres and telomeres of *Genlisea hispidula* and *G. subglabra*.

(a) The neighbour-joining tree of the CRM clade, inferred from a comparison of reverse transcriptase domain sequences, reveals a distinct subgroup of GhCR family (blue shading) in group A (pink shading) comprising many elements with centromeric localization confirmed by FISH (red) or by *in silico* analysis (green) (modified from Neumann *et al.* (2011)).

(b) Combination of GhCR2 and GhCR4 shows signals clustered on each metaphase chromosome of *G. hispidula*.

(c) Partial metaphase of *G. hispidula* labeled by GhCR1 and GhCR3. Some chromosomes show enrichment of GhCR1 only (red arrows) or additional signals of either of the two sequences (white arrowheads).

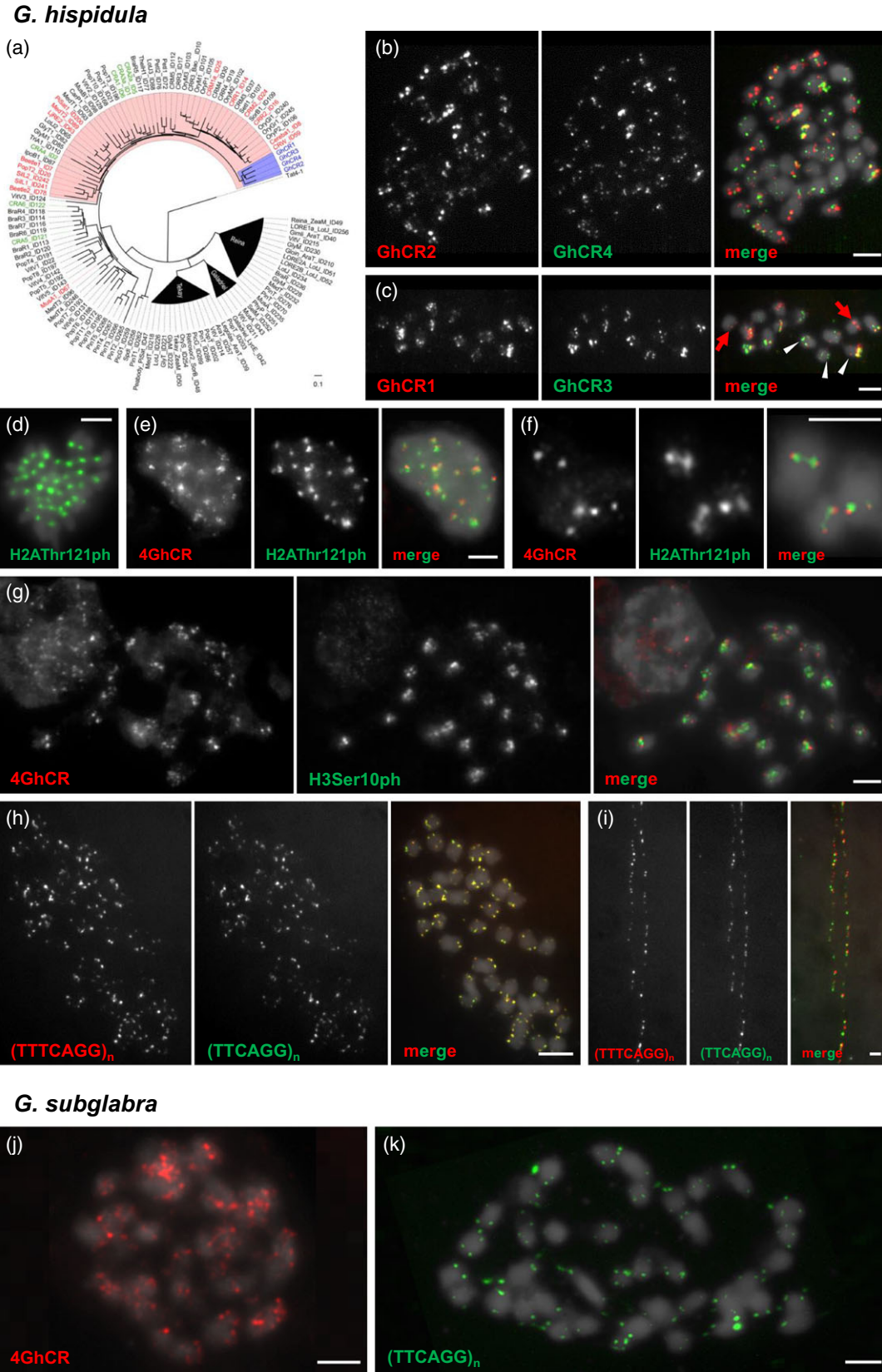
(d–f) Anti-H2AThr121ph signals suggest monocentric chromosomes for *G. hispidula* (d) and localize together with adjacent FISH signals for the four GhCR elements (4GhCR) on prophase nuclei (e) and metaphase chromosomes (f).

(g) FISH signals of 4GhCR join those of H3Ser10ph, another (peri)centromeric-specific marker, in a partial metaphase of *G. hispidula*.

(h) Double-FISH detected the two non-canonical telomere sequence variants (TTCAGG, TTTCAGG) on *G. hispidula* chromosome ends.

(i) These variants are intermingled on extended chromatin fibers.

(j, k) Chromosomal distribution of 4GhCR signals (j) and the telomeric sequence variant TTCAGG in *G. subglabra* (k). Bars represent 3 μm .



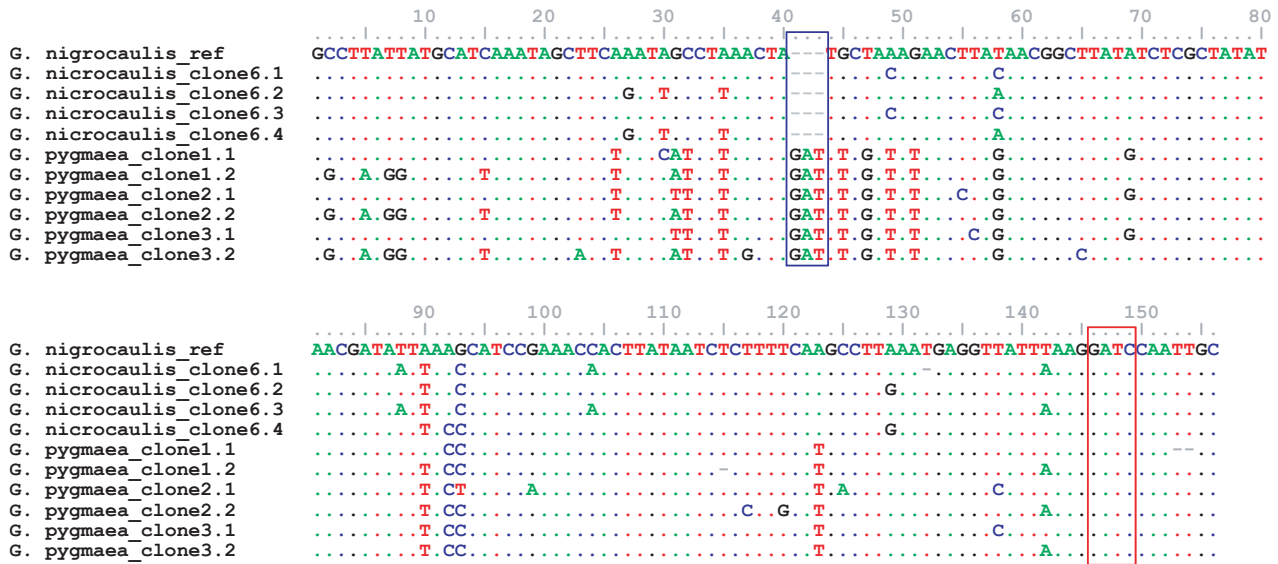


Figure 4. Sequence alignment of GnCent motifs shows significant variation between those cloned from gDNA of *Genlisea nigrocaulis* and *G. pygmaea*. The actual fragments amplified by a specific primer pair (Gn7c161, Table 1) were 153 bp and 156 bp for *G. nigrocaulis* and *G. pygmaea* clones, respectively. The blue and red boxes indicate the 3-bp insert/deletion region and the *MboI* recognition site, respectively.

(Figure 3d–f) and for H3Ser10ph on metaphase chromosomes (Figure 3g) in *G. hispidula*.

***Genlisea nigrocaulis* and *G. pygmaea* share the Arabidopsis-type telomere repeat**

FISH using the Arabidopsis-type telomere sequence (TTTAGGG) as probe revealed strong signal clusters on interphase nuclei and on metaphase chromosomes of *G. nigrocaulis* (Figure 2d,e) and *G. pygmaea* (Figure 2f,h). On metaphase chromosomes of *G. nigrocaulis* the signals were found closely adjacent to the centromere-specific GnCent signals (Figure 2e).

Due to limitations in the availability of sufficient amount of leaf material of *G. nigrocaulis*, we used *G. pygmaea* to confirm the terminal position of the Arabidopsis-type telomere repeat by terminal restriction fragment (TRF) analysis. To detect TRFs and a possible association between telomere and the GnCent satellite sequence in *G. pygmaea*, digestion with the 6-bp cutter *XbaI* and the 8-bp cutter *SfiI* (none of these have a recognition site in the GnCent satellite) was performed in BAL31-digested high-molecular-weight DNA. Using the Arabidopsis-type telomere sequence (TAAACCC)₄ as a probe, similar TRF patterns were found with both restriction enzymes (Figure 5a). Progressive TRF shortening with increasing BAL31 digestion times is visible in the pulse-field gel electrophoresis (PFGE) patterns (left panel) as well as in the blot from conventional electrophoresis (right panel); the latter detecting truncated TRFs diffusing out of the agarose plugs after BAL31 digestion. Re-probing of the membranes with GnCent revealed similar (but slightly stronger) hybridiza-

tion patterns as for the telomeric probe (Figure 5c), thus supporting the close association of GnCent repeats and telomeric sequences on chromosomes. Since the restriction enzymes chosen for TRF analysis in *G. pygmaea* produce long fragments (comprising presumably tens of kbp of subtelomeric DNA), an additional restriction enzyme, the 4-bp cutter *MboI*, with a recognition site within the GnCent repeat (Figure 4, red box), was used to determine telomere lengths more precisely. TRFs ranging between 10 and 18 kbp were detected, reflecting the telomere lengths in this species (Figure 5b).

To demonstrate the presence of the Arabidopsis-type telomere sequence in *G. pygmaea* by a further independent approach, the TRAP (telomere repeat amplification protocol) assay was performed using telomerase extracts from either shoots with flower buds or young leaves, and from *A. thaliana* seedlings as a positive control (Figure 6a). Regular ladders of telomerase products were obtained in both extracts of *G. pygmaea*, showing the same periodicity of the ladder bands as the control products of *A. thaliana* telomerase (Figure 6a). The TRAP products were cloned and sequenced. The obtained sequences revealed regular (TTTAGGG)_n repeats with four errors per 120 sequenced nucleotides (approximately 3% error rate).

***Genlisea hispidula* replaced the Arabidopsis-type telomeres by two sequence variants**

Surprisingly, the Arabidopsis-type telomere sequence was not detectable by FISH, and among the genomic reads of *G. hispidula* only as short interstitial fragments. Instead, two variant repeat motifs of either 6-bp TTCAGG or 7-bp

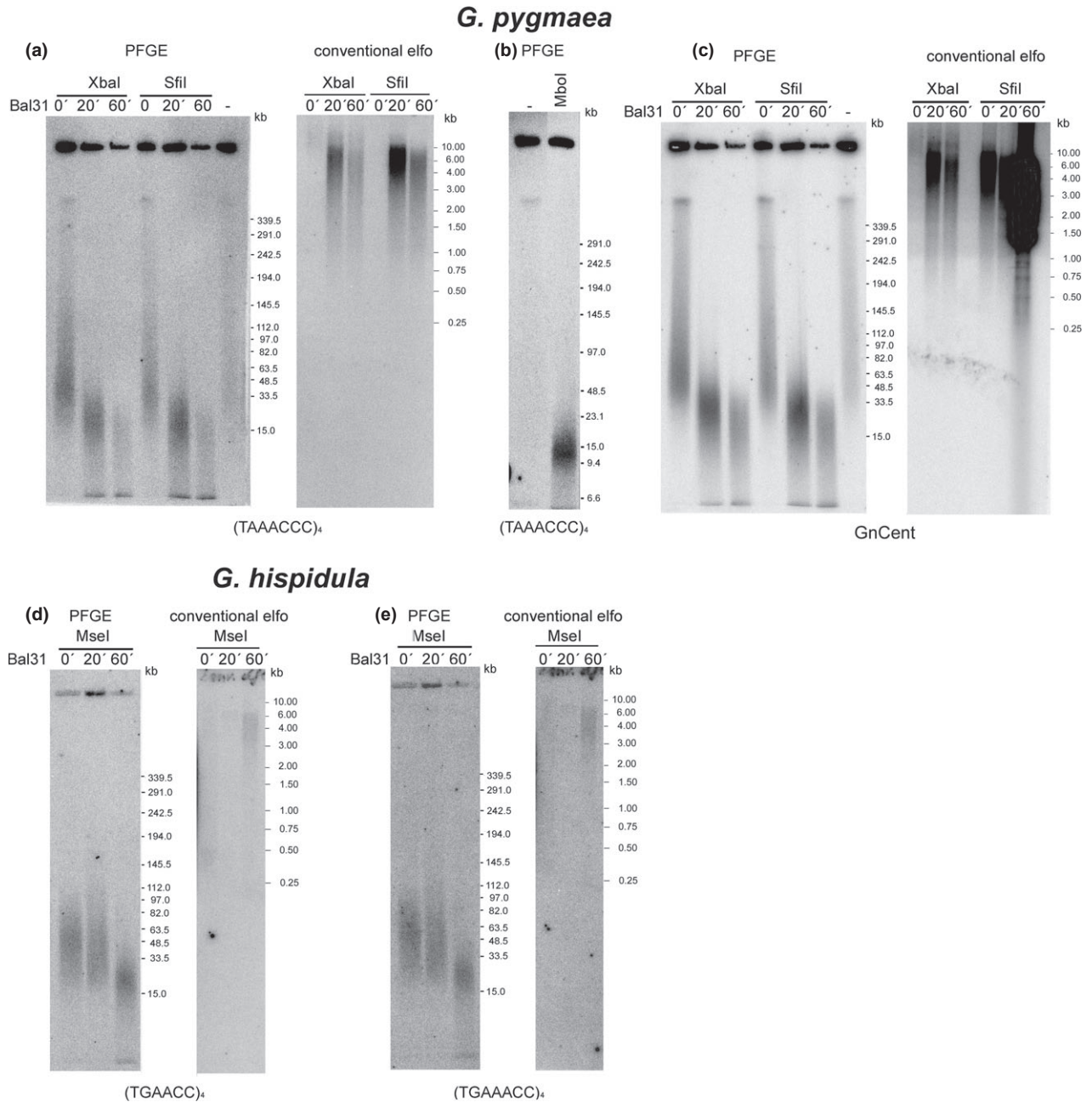


Figure 5. Telomere sequence analysis in *Genlisea pygmaea* and *G. hispidula*.

(a–c) BAL31 and TRF analysis in *G. pygmaea*. High-molecular-weight DNA in agarose plugs was digested with restriction enzymes *XbaI* or *SfiI* without (–) or after prior BAL31 digestion for times indicated above individual lanes. PFGE denotes Southern hybridization of PFGE-separated DNA retained in agarose plugs after digestion, conventional electrophoresis denotes Southern hybridization of DNA diffused out of the plugs after digestion, separated by conventional electrophoresis. Hybridization patterns obtained using the Arabidopsis-type telomere probe (a, b) and the putative centromeric repeat Gn7c161 (c) are shown (probed sequences are mentioned below each panel). Similar hybridization patterns of PFGE parts of panels (a) and (c) demonstrate association of both probed sequences in large TRF fragments, while TRF signal obtained using *MboI* (after cleavage of the 161-bp satellite) provides more precise assessment of genuine telomere lengths (between 10 and 18 kbp, b). Positions of LowRange PFG marker (NEB) and GeneRuler 1 kbp DNA ladder (Fermentas) are indicated on the right.

(d, e) BAL31 and TRF analysis in *G. hispidula*. High-molecular-weight DNA in agarose plugs was digested with *MseI* restriction enzyme without (–) or after prior BAL31 digestion for times indicated above individual lanes. PFGE denotes Southern hybridization of PFGE-separated DNA retained in agarose plugs after digestion; conventional electrophoresis denotes Southern hybridization of DNA diffused out of the plugs after digestion, separated by conventional electrophoresis. Hybridization patterns obtained using the short (d) and the long (e) variants of telomeric repeat units are shown (probed sequences are mentioned below each panel). Positions of MidRange PFG marker (NEB) and GeneRuler 1 kbp DNA ladder (Fermentas) are indicated on the right.

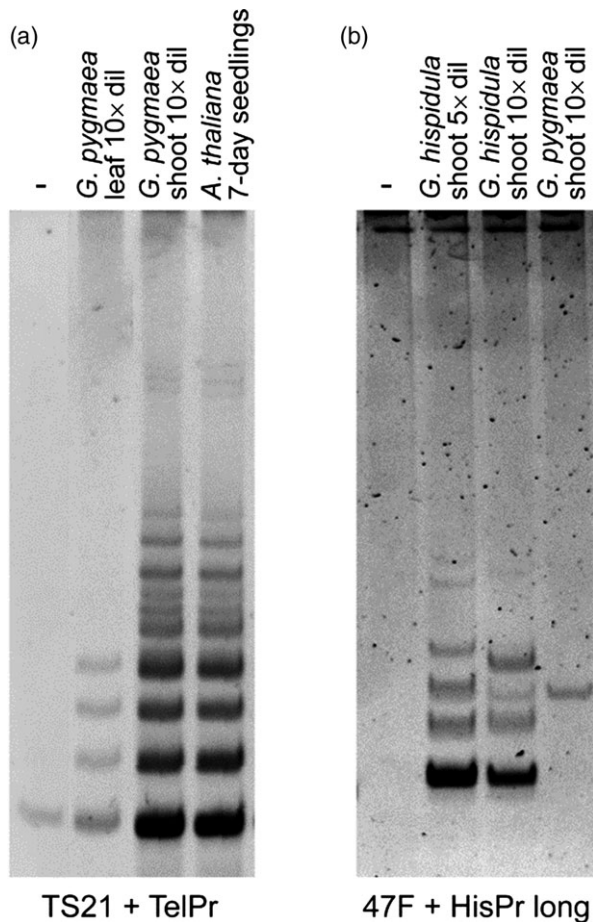


Figure 6. Telomerase activity detection in *Genlisea pygmaea* (a) and *G. hispidula* (b) using TRAP assay.

Substrate and reverse primers used in TRAP are given below each panel (see Table 1). *G. pygmaea* shows regular ladders of telomerase products, similar to *A. thaliana* extract used as positive control (a). While *G. hispidula* extracts produce irregular ladders of telomerase products, *G. pygmaea* extract shows only a single band of a non-specific product with *G. hispidula* primers (b).

TTTCAGG could be identified as putative telomere sequences. FISH using these motifs as probes indicated their terminal location on metaphase chromosomes of *G. hispidula* and of its close relative *G. subglabra* (Figure 3h,k). Fiber FISH experiments demonstrated that both sequences are intermingled (Figure 3i). Probes of both motifs, (TGAAACC)₄ and (TGAACC)₄, revealed similar patterns of TRFs ranging from 20 to 97 kbp at individual chromosome ends. Their sensitivity to BAL31 digestion proved the terminal chromosome position of the hybridizing fragments (Figure 5d,e). During the longest BAL31 exposure, the truncated TRFs diffuse from agarose plugs and can be detected in the DNA fraction obtained from the reaction solution (Figure 5d,e, right panels). No signal could be observed when re-probing the membranes with the Arabidopsis-type telomere sequence (TAAACCC)₄.

The identity of telomeric sequences was further tested using the TRAP assay with *G. hispidula* telomerase extracts and subsequent sequencing of the resulting products. Several combinations of substrate and reverse primers have been tested, but positive results were only obtained when the primer combinations 47F as substrate and either HisPr long or HisPr short as reverse primer (see Table 1) were used. Finally, the primer for the longer repeat variant, HisPr long, yielding well reproducible results, was chosen for the TRAP assay (Figure 6b). No product was obtained in the reaction without protein extract, and in the extract from *G. pygmaea* only a single, most likely unspecific band was detected (Figure 6b). *G. hispidula* displayed irregular ladders, presumably due to alternation of long and short variants of the synthesized telomere repeat (Figure 6b). Sequencing of the products demonstrated co-occurrence of both variants in all clones that contained more than one sequenced repeat unit. While it is not clear whether the observed low processivity of *G. hispidula* telomerase is due to *in vitro* conditions, or is an intrinsic feature of this telomerase, the observed alternation of both telomeric sequence variants confirmed next-generation sequencing results (see Table S2), as well as the co-localization of both sequences observed in FISH and TRF analyses.

DISCUSSION

Two small *Genlisea* genomes revealed predominantly tandem repeats, and two large genomes clusters of retroelements at their centromeres

Centromere-specific repeats were not found on *Tradescantia* chromosomes (Houben *et al.*, 1996). *De novo* centromere formation in barley may occur at positions that do not contain the centromeric repeats typical for this species (Nasuda *et al.*, 2005). Non-repetitive DNA sequences were characterized as centromere-specific for five chromosomes of potato (Gong *et al.*, 2012). Sequence and abundance of centromeric repeats can vary, even between centromeres of the same species (Berr *et al.*, 2006; Neumann *et al.*, 2012). Nevertheless, centromeric repeats and/or CR elements are the major constituents of plant centromeres, although their contribution can vary between chromosomes of a complement (Plohl *et al.*, 2014). In *G. nigrocaulis*, and in its tetraploid relative *G. pygmaea*, the 161 bp GnCent satellite apparently coincides with the centromere position. Taking into account the rapid divergence of centromeric satellite repeats (Henikoff *et al.*, 2001), the presence of the 161 bp tandem repeat in both species suggests their close relationship with a common ancestor. In *G. hispidula* FISH revealed GhCR elements in positional coincidence with immunosignals for the (peri)centromere marks H2AThr121ph and H3Ser10ph. The presence of these GhCRs on each chromosome of the close relative

Table 1 Sequences of primers used to generate FISH probes (a) or in analyses of telomerase activity in tissues of *Genlisea hispidula* and *G. pygmaea* (b)

(a) Primers for FISH probes		
Name	Sequence (5'→3')	Product
Gn7c161	F: GCCTATTATGCATCAAATAGCTTC; R: GCAATTGGATCCTTTAATAACCTC	161 bp tandem repeat (GnCent)
Gh_CR01	F: GCTTTGACAGAACCCTTAATC; R: AGCTTCCTTGGTCTCCACTT	Centromeric retrotransposon element (GhCR1, 4.8 kbp)
Gh_CR02	F: TGTCCTCAAGTAAAGATAAAGAAAAA; R: TCCACCTCAAATGAGTTCATAA	Centromeric retrotransposon element (GhCR2, 4.8 kbp)
Gh_CR03	F: TCTAGATAGCAAGATGATCCTTGAG; R: TTAGGCTCCTCGAATGTGAT	Centromeric retrotransposon element (GhCR3, 4.8 kbp)
Gh_CR04	F: ATGTCCAAGGATAAGGTGATTG; R: CTTGAGTGGTCTTGCTTGAT	Centromeric retrotransposon element (GhCR4, 5.2 kbp)
Atha_TEL	F: TTTAGGGTTTAGGGTTTAGGGTTTAGGG; R: CCCTAAACCCTAAACCCTAAACCCTAAA	Arabidopsis-type telomere
Gh_TEL6	F: TTCAGGTTTCAGGTTTCAGGTTTCAGG; R: CCTGAACCTGAACCTGAACCTGAA	6 bp telomeric variant of <i>G. hispidula</i>
Gh_TEL7	F: TTTAGGTTTCAGGTTTCAGGTTTCAGG; R: CCTGAACCTGAACCTGAACCTGAAA	7 bp telomeric variant of <i>G. hispidula</i>
(b) Primers for analyses of telomerase activity		
Name	Sequence (5'→3')	Species
TS21	S: GACAATCCGTCGAGCAGAGTT	<i>G. pygmaea</i>
TelPr	R: CCGAATCAACCCTAAACCCTAAACCCTAAACC	<i>G. pygmaea</i>
47F	S: CGCGGTAGTGATGTGGTTGTGTT	<i>G. hispidula</i>
HisPr long	R: CCGAATCAACCCTGAAACCTGAAACCTGAAACC	<i>G. hispidula</i>
HisPr short	R: CCGAATTCTGAACCTGAACCTGAACCTGAACC	<i>G. hispidula</i>

F: forward primer; R: reverse primer; S: substrate primer.

G. subglabra suggests that the last common ancestor of both species already recruited these elements as centromeric sequence.

While retrotransposons became accumulated at centromere positions in the *G. hispidula* clade, they were likely eliminated in the course of genome shrinking within the *G. nigrocaulis* clade during evolution from an ancestor with an intermediate genome size of 400–800 Mbp (Vu *et al.*, 2015). Additional weak and dispersed FISH signals of GhCRs along several metaphase chromosomes of *G. hispidula* might indicate remnants of the ancestral state or cross-hybridization with related elements (Figure 3c).

Two large *Genlisea* genomes display novel tandem repeats at their chromosome ends

In contrast to centromeric DNA, telomeric sequences are usually composed of highly conserved simple sequence repeats and vary little between different eukaryotic kingdoms. For instance, the vertebrate telomere sequence (TTAGGG)_n differs only by one T from the motif (TTTAGGG)_n of *Arabidopsis* (Richards and Ausubel, 1988) which is typical for most of the investigated plant species (Fuchs *et al.*, 1995). First evidence that not all plant species

protect their chromosome ends by the Arabidopsis-type telomere came from FISH with a (TTTAGGG)_n probe on chromosomes of several species of the genus *Allium* (Fuchs *et al.*, 1995). Pich *et al.* (1996) and Pich and Schubert (1998) confirmed the absence of (TTTAGGG)_n and suggested that highly repetitive satellite and/or rDNA sequences substituted the original telomeric sequence at the very ends of the *Allium* chromosomes. They also suggested a conversion-like mechanism for compensation of replication-mediated end-shortening. Later, Adams *et al.* (2000) reported the lack of Arabidopsis-type telomeres in *Aloe*, another genus of the order Asparagales to which *Allium* belongs. A large-scale screen using different minisatellite sequences identified the vertebrate-type telomere as the predominant satellite repeat, occasionally associated with (TTTAGGG) repeats, at the chromosome termini of Asparagales species which descend from an evolutionary switch-point leading to an extensive replacement of the Arabidopsis motif (Sykorova *et al.*, 2006). A second switch-point (inside the Alliaceae family) towards the evolution of the genus *Allium* is responsible for the loss of any of the known telomere minisatellites, and apparently also of an active telomerase gene in this genus (Fajkus

et al., 2005). Also three genera of the Solanaceae family, *Vestia*, *Sessea* and *Cestrum*, lack Arabidopsis- and vertebrate-type telomeres (Sykorova *et al.*, 2003a,b). Recently, an A/T rich (TTTTTTAGGG) minisatellite was characterized as telomeric sequence for *Cestrum elegans* (Peska *et al.*, 2015). However, it still needs to be confirmed whether this non-canonical telomeric repeat is also shared by the two sister genera *Vestia* and *Sessea*.

In the genus *Genlisea* we found in *G. nigrocaulis*, and in the closely related *G. pygmaea*, Arabidopsis-type telomere repeats. In the much larger genome of *G. hispidula*, and in that of its close relative *G. subglabra*, this sequence motif is replaced at the chromosome ends by two hitherto unknown telomeric sequence variants. In Asparagales, the change from the Arabidopsis-type (TTTAGGG) to the vertebrate-type (TTAGGG) telomere can be explained by point mutations in the telomerase catalytic protein subunit (TERT) which affect the telomere-telomerase interaction and result in a variant usage of template region in the telomerase RNA subunit (TR) and consequently in T-slippage (Sykorova *et al.*, 2006). In *Genlisea* however, the variant motifs observed in *G. hispidula* cannot be derived from the presumed ancestral Arabidopsis-type telomere sequence by less than two mutations. In particular, the presence of cytosine in the G-rich strand of both sequence variants is remarkable. This change is most likely associated with a corresponding mutation directly in the template region of the *G. hispidula* TR subunit. Variants having a C within the G-rich strand are rare (http://telomerase.asu.edu/sequences_telomere.html), and were to our knowledge hitherto not described for plants. An evolutionary switch of telomeric sequences within a genus has also not been reported so far (Figure 7). This switch occurs in parallel with an apparently high mutation rate (Ibarra-Laclette *et al.*, 2013) and a fast genome size evolution within the genus *Genlisea* (Vu *et al.*, 2015). Telomeric sequences of the neighbor clade (*G. africana*, *G. stapfii* and *G. barthlottii*) could not be investigated due to the lack of available plant material. Therefore, it remains an open question whether the new telomere repeat variants evolved immediately before separation of *G. hispidula* and *G. subglabra* or already earlier, at the basis of that branch of the subgenus *Genlisea* that displays large genomes (Figure 1).

Conclusions

The presented data strongly argue that centromeres and telomeres are evolutionarily flexible in a hitherto unknown scale, with different sequences being recruited to perform the same function. Whereas in a group of species of the genus *Genlisea* with very small genomes (86–179 Mbp) a tandem repeat occupies the centromeric position, in species of a group with almost 20-fold larger genomes four retroelements were found in the centromeres instead. Thus, even within the same genus, either tandem repeats

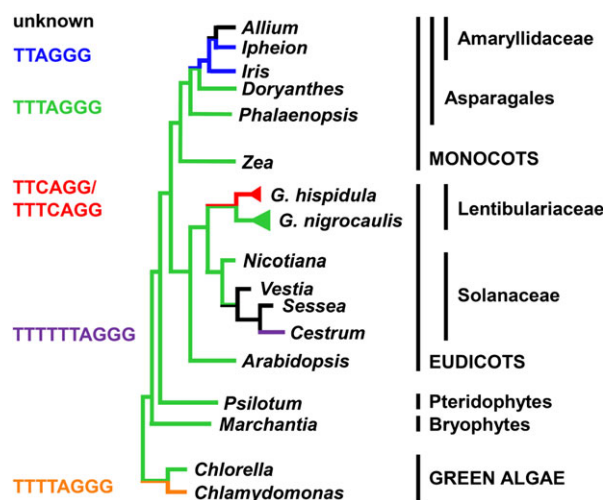


Figure 7. Phylogenetic tree of green plants indicating telomeric sequence deviations from TTTAGGG, the most widespread telomeric repeat among plants [modified according to Sykorova *et al.* (2006) and Peska *et al.* (2015)].

or retroelements can serve as centromeric sequences. Surprisingly, both groups differ also in the sequence of their telomeric repeats. The canonical plant telomeric repeat TTTAGGG, present at the chromosome termini of the small genomes, is replaced by two intermingled sequence variants (TTCAGG and TTTTCAGG) in species with the large genomes. Hence, also between closely related species intragenetic switches of telomeric repeats may occur. The presence of cytosine within the guanine-rich strand of the two described sequence variants has potential implications for the modification of telomeric chromatin.

EXPERIMENTAL PROCEDURES

Plant material

Plants of species used in this study (*G. nigrocaulis*, *G. hispidula*, *G. pygmaea*, *G. subglabra*) were obtained from Best Carnivorous Plants Store (<http://www.bestcarnivorousplants.net>; Ostrava, Czech Republic): *G. nigrocaulis*, *G. hispidula*, *G. pygmaea*; Carnivores and more (<http://www.carnivoresandmore.de>; Merzig, Germany): *G. nigrocaulis*, *G. subglabra* and Die Welt der Fleischfressenden Pflanzen (<http://www.falle.de>; Gartenbau Thomas Carow, Nüdlingen, Germany): *G. nigrocaulis*. All species were cultivated in a greenhouse. Herbarium vouchers of *G. nigrocaulis*, *G. pygmaea* and *G. hispidula* were deposited at the IPK Gatersleben (Table S1).

Preparation of genomic DNA, nuclei and chromosomes

Genomic DNA of *Genlisea* species was isolated using the DNeasy® Plant Mini kit (Qiagen, <https://www.qiagen.com/>). Concentration and quality of the DNA were estimated using a Nano-Drop spectrophotometer (Thermo Scientific, <http://www.thermoscientific.com/>) and by 1% (w/v) agarose-gel electrophoresis.

Interphase nuclei from leaves were isolated after formaldehyde fixation, flow sorted and dropped onto slides as described by (Lysak *et al.*, 2006). Slides were stored at -20°C until use.

For chromosome preparations either flower buds or very young leaf tips were used. Squashing was performed as described in Lysak *et al.* (2006) with minor modifications. In brief, plant material was treated in 20 mM 8-hydroxyquinoline for 2 h at room temperature followed by 4 h at 4°C to accumulate dividing cells. After washing briefly in distilled water, the material was fixed in ethanol: glacial acetic acid (3:1) for at least 24 h at room temperature. Fixed tissues were used immediately or stored at 4°C for several days. After three washes in citrate buffer (10 mM sodium citrate, pH 4.5) for 5 min each, the plant tissue was softened in 2% pectinase and 2% cellulose, (w/v) in citrate buffer, at 37°C, for 10 min (young leaves) or 15 min (flower buds). The digestion was stopped by adding ice-cold citrate buffer. Squashing on microscopic slides was performed in a drop of 75% glacial acetic acid. After freezing in liquid nitrogen, slides were rinsed in 2 × SSC, dehydrated in an ethanol series (70, 90 and 96%) and air dried. The quality of spreading was evaluated after DAPI staining. Slides harboring more than 10 well-spread metaphases were stored at 4°C until use for FISH. For immunofluorescence experiments, chromosomes were prepared according to Houben *et al.* (2003). For preparation of extended chromatin fibers, suspensions of nuclei were prepared according to Lysak *et al.* (2006), dropped on one end of a microscopic slide and dragged along the slide as described (Li *et al.*, 2005).

Fluorescence *in situ* hybridization (FISH) and immunostaining

To generate FISH probes, the GnCent repeat and four GhCR elements identified by graph-based clustering analysis (Novak *et al.*, 2010; Vu *et al.*, 2015) were PCR amplified with sequence-specific primers (Table 1) using either a GoTag Kit (Promega) or a Phusion High Fidelity DNA Polymerase Kit (Thermo Scientific). PCR products were analyzed by 1% (w/v) agarose-gel electrophoresis, cloned by pGEM-T Easy Vector Systems (Promega, <http://www.promega.com/>) and confirmed by Sanger sequencing. Telomere probes were amplified using tetramers of the telomeric sequences in the absence of DNA template as described by Ijdo *et al.* (1991). Probes were labeled by nick-translation (Lysak *et al.*, 2006) using either TexasRed-dUTP, Alexa 488-dUTP (Life Technologies, <http://www.thermofisher.com/>) or Cy3-dUTP (Amersham, <http://www.gelifesciences.com/>). FISH was performed according to Lysak *et al.* (2006).

For immunostaining, slides were incubated in blocking buffer (5% horse serum, 3% BSA in 1 × PBS) immediately after preparation for 1 h at 37°C, shortly washed in 1 × PBS and incubated with primary antibodies for 16 h at 4°C in a humid chamber. As primary antibodies rabbit anti-H2AThr121ph (MyBioSource, <http://www.mybiosource.com/>, cat-No. MBS004447, dilution 1:1000, considering the removal of the initial N-terminal methionine it corresponds to H2AThr120ph) and rabbit anti-H3Ser10ph (Merck Millipore, <http://www.merckmillipore.com/>, cat-No. 06-570, dilution 1:50) were used. Subsequently, slides were washed in 1 × PBS three times for 10 min each and then incubated with Alexa 488-conjugated anti-rabbit antibody (Life Technologies, dilution 1:200) in a humid chamber at 37°C for 1 h. After final washes in 1 × PBS (three times, 10 min each), slides were counter-stained with DAPI (1 µg ml⁻¹) in VectaShield.

Microscopy and image processing

FISH and immunostaining preparations were analyzed using a Zeiss Axioplan 2 epifluorescence microscope equipped with a cooled CCD camera (Diagnostic Instruments, Inc., <http://www.spotimaging.com/>). Fluorescence images for each fluorochrome

were captured separately using appropriate filter combinations and a 100× objective. The images were processed (brightness and contrast adjustment only), pseudo-colored and merged using ADOBE PHOTOSHOP software (Adobe Systems, <http://www.adobe.com/>).

Analysis of telomere lengths and BAL31-sensitivity

High-molecular-weight DNA from *Genlisea* plants was prepared in agarose plugs as described (Sykorova *et al.*, 2006). Briefly, plant tissues were homogenized in liquid nitrogen, resuspended in homogenization buffer [10 mM 2(*N*-morpholino) ethanesulphonic acid (MES), pH 5.6; 10 mM NaCl; 5 mM EDTA], mixed with an equal volume of 2% (w/v) low melting point agarose in 400 mM mannitol, 20 mM MES, pH 5.6 and transferred to a mould. Samples in agarose blocks were treated by proteinase K (0.1 mg ml⁻¹) in TES buffer [0.5 M EDTA, pH 8.0; 10 mM Tris-HCl, pH 8.0; 1.0% (w/v) lauroylsarcosine] at 37°C for 24 h. Deproteinised plugs were washed twice in TE buffer (10 mM Tris-HCl, pH 8.0; 1 mM EDTA, pH 8.0) for 30 min, twice in TE with 1 mM phenylmethylsulfonyl fluoride for 30 min and 3 × 30 min in 0.1 × TE. The terminal position of probed sequences was tested by BAL31 nuclease sensitivity. DNA samples in agarose plugs (approximately 2 µg) were equilibrated for 15 min in 200 µl of BAL31 nuclease buffer (NEB, cat-No. M0213S) and then digested in a new portion of buffer with 3 units of BAL31 nuclease for 20 or 60 min in a thermomixer (Eppendorf, <http://www.eppendorf.com/>) at 30°C. The reactions were stopped by buffer exchange with 50 mM EGTA pH 8.0, and BAL31 was irreversibly inactivated by incubation at 58°C for 30 min. Then the plugs were washed in 0.1 × TE buffer (three times for 15 min) and equilibrated in appropriate restriction buffer for subsequent restriction enzyme digestion to measure telomere lengths by TRF analysis (Fajkus *et al.*, 1998). After digestion, the low-molecular-mass fraction of digested DNA was precipitated with ethanol and dissolved in TE for analysis by conventional agarose-gel electrophoresis and Southern hybridization. High-molecular-mass fractions were retained in the agarose plugs, and analyzed by PFGE using the BioRad Chef Mapper instrument under the following conditions: 1% (w/v) FastLane agarose gel in 0.5 × TBE buffer, 6 V/cm, pulse time ramped from 0.5 to 26 sec at 14°C for 20 h. Conventional and PFGE gels were alkali blotted and hybridized with radioisotope-labeled probes (Fojtova *et al.*, 2010). Hybridization signals were visualized with a FLA-7000 phosphorimaging system (Fuji Film, <http://www.fujifilm.com/>).

Telomere repeat amplification protocol

Leaves and shoots of *Genlisea* species were manually homogenized in extraction buffer according to Fitzgerald *et al.* (1996). Crude extracts obtained after centrifugation were 5× and 10× diluted for analysis of telomerase activity. Primers usually applied in Telomere repeat amplification protocol (TRAP) assays for plants (Fajkus *et al.*, 1998) were used for analysis of *G. pygmaea*. Additional primers and primer combinations corresponding to putative telomere repeats in *G. hispidula* were tested (Table 1). One µl of 10 µM substrate primer (TS21 for *G. pygmaea* and 47F (Fojtova *et al.*, 2002) for *G. hispidula*) was mixed with 1 µl of diluted crude protein extract and elongation of the primer by the telomerase proceeded for 45 min at 26°C in 25 µl reaction buffer as described (Fojtova *et al.*, 2010). After heat inactivation of telomerase (5 min, 94°C), 1 µl of 10 µM reverse primer (TelPr for *G. pygmaea*; HisPr short or HisPr long for *G. hispidula*) and 2U of DyNAzymell DNA polymerase (Finnzymes, <http://www.thermofisher.com/>) were added and extension products were amplified (35 cycles of 95°C/30 sec, 65°C/30 sec, 72°C/30 sec; final extension 72°C/5 min). Aliquot samples of TRAP reactions were analyzed on 12.5% (w/v)

polyacrylamide gel in 0.5 × TBE buffer. Gels were stained by GelStar Nucleic Acid Gel Stain (LONZA) and signals were visualized using the LAS-3000 system (FujiFilm).

Products of TRAP were cloned using a TOPO-TA cloning kit (Invitrogen, <https://www.thermofisher.com/>) and sequenced to characterize sequences added by telomerase.

CONFLICT OF INTEREST

The authors declare that they have no conflict of interests.

ACKNOWLEDGEMENTS

We thank Martina Kühne and Achim Bruder for excellent technical assistance. This work was supported by a grant of the Deutsche Forschungsgemeinschaft to IS and JF (SCHU 951/16-1), by the European Social Fund (CZ.1.07/2.3.00/20.0189) to IS, JFa and MF, by grants GBP501/12/G090 and RVO: 60077344 to JM, by the Czech Academy of Sciences (M200041206) to JFa, by Czech Science Foundation (13-06943S) to MF, and by PhD scholarship of Vietnam Ministry of Education and Training to TDT.

SUPPORTING INFORMATION

Additional Supporting Information may be found in the online version of this article.

Table S1. List of herbarium vouchers of *Genlisea* species deposited at the IPK Gatersleben.

Table S2. Analysis of reads with telomeric motifs GGTTCa and GGTTCa in *Genlisea hispida*.

REFERENCES

- Adams, S.P., Leitch, I.J., Bennett, M.D. and Leitch, A.R. (2000) Aloe L.—a second plant family without (TTTAGGG)_n telomeres. *Chromosoma*, **109**, 201–205.
- Adams, S.P., Hartman, T.P., Lim, K.Y., Chase, M.W., Bennett, M.D., Leitch, I.J. and Leitch, A.R. (2001) Loss and recovery of Arabidopsis-type telomere repeat sequences 5'-(TTTAGGG)_n-3' in the evolution of a major radiation of flowering plants. *Proc. Biol. Sci.* **268**, 1541–1546.
- Berr, A., Pecinka, A., Meister, A., Kreth, G., Fuchs, J., Blattner, F.R., Lysak, M.A. and Schubert, I. (2006) Chromosome arrangement and nuclear architecture but not centromeric sequences are conserved between *Arabidopsis thaliana* and *Arabidopsis lyrata*. *Plant J.* **48**, 771–783.
- Cheng, Z., Dong, F., Langdon, T., Ouyang, S., Buell, C.R., Gu, M., Blattner, F.R. and Jiang, J. (2002) Functional rice centromeres are marked by a satellite repeat and a centromere-specific retrotransposon. *Plant Cell*, **14**, 1691–1704.
- Demidov, D., Schubert, V., Kumke, K. et al. (2014) Anti-phosphorylated histone H2A^{Thr120}: a universal microscopic marker for centromeric chromatin of mono- and holocentric plant species. *Cytogenet. Genome Res.* **143**, 150–156.
- Dong, Q. and Han, F. (2012) Phosphorylation of histone H2A is associated with centromere function and maintenance in meiosis. *Plant J.* **71**, 800–809.
- Dong, F., Miller, J.T., Jackson, S.A., Wang, G.-L., Ronald, P.C. and Jiang, J. (1998) Rice (*Oryza sativa*) centromeric regions consist of complex DNA. *Proc. Natl Acad. Sci. USA*, **95**, 8135–8140.
- Fajkus, J., Fulneckova, J., Hulanova, M., Berkova, K., Riha, K. and Matyasek, R. (1998) Plant cells express telomerase activity upon transfer to callus culture, without extensively changing telomere lengths. *Mol. Gen. Genet.* **260**, 470–474.
- Fajkus, J., Sýkorová, E. and Leitch, A.R. (2005) Telomeres in evolution and evolution of telomeres. *Chromosome Res.* **13**, 469–479.
- Fitzgerald, M.S., McKnight, T.D. and Shippen, D.E. (1996) Characterization and developmental patterns of telomerase expression in plants. *Proc. Natl Acad. Sci. USA*, **93**, 14422–14427.
- Fleischmann, A. (2012) *Monograph of the Genus Genlisea: Redfern Natural History Productions.*
- Fleischmann, A., Michael, T.P., Rivadavia, F., Sousa, A., Wang, W., Tensch, E.M., Greilhuber, J., Muller, K.F. and Heubl, G. (2014) Evolution of genome size and chromosome number in the carnivorous plant genus *Genlisea* (Lentibulariaceae), with a new estimate of the minimum genome size in angiosperms. *Ann. Bot.* **114**, 1651–1663.
- Fojtova, M., Fulneckova, J., Fajkus, J. and Kovarik, A. (2002) Recovery of tobacco cells from cadmium stress is accompanied by DNA repair and increased telomerase activity. *J. Exp. Bot.* **53**, 2151–2158.
- Fojtova, M., Wong, J.T.Y., Dvorackova, M., Yan, K.T.H., Sykora, E. and Fajkus, J. (2010) Telomere maintenance in liquid crystalline chromosomes of dinoflagellates. *Chromosoma*, **119**, 485–493.
- Fuchs, J., Brandes, A. and Schubert, I. (1995) Telomere sequence localization and karyotype evolution in higher plants. *Plant Syst. Evol.* **196**, 227–241.
- Fukagawa, T. and Earnshaw, W.C. (2014) The centromere: chromatin foundation for the kinetochore machinery. *Dev. Cell* **30**, 496–508.
- Gong, Z.Y., Wu, Y.F., Koblikova, A. et al. (2012) Repeatless and Repeat-Based Centromeres in Potato: implications for centromere evolution. *Plant Cell*, **24**, 3559–3574.
- Gorinsek, B., Gubensek, F. and Kordis, D. (2004) Evolutionary genomics of chromoviruses in eukaryotes. *Mol. Biol. Evol.* **21**, 781–798.
- Greilhuber, J., Borsch, T., Worberg, A., Porembski, S. and Barthlott, W. (2006) Smallest angiosperm genomes found in Lentibulariaceae, with chromosome of bacterial size. *Plant Biol.* **8**, 770–777.
- Henikoff, S., Ahmad, K. and Malik, H.S. (2001) The centromere paradox: stable inheritance with rapidly evolving DNA. *Science*, **293**, 1098–1102.
- Hosouchi, T., Kumekawa, N., Tsuruoka, H. and Kotani, H. (2002) Physical map-based sizes of the centromeric regions of *Arabidopsis thaliana* chromosomes 1, 2, and 3. *DNA Res.* **9**, 117–121.
- Houben, A. and Schubert, I. (2003) DNA and proteins of plant centromeres. *Curr. Opin. Plant Biol.* **6**, 554–560.
- Houben, A., Brandes, A., Pich, U., Manteuffel, R. and Schubert, I. (1996) Molecular-cytogenetic characterization of a higher plant centromere/kinetochore complex. *Theor. Appl. Genet.* **93**, 477–484.
- Houben, A., Wako, T., Furushima-Shimogawara, R., Presting, G., Kunzel, G., Schubert, I. and Fukui, K. (1999) The cell cycle dependent phosphorylation of histone H3 is correlated with the condensation of plant mitotic chromosomes. *Plant J.* **18**, 675–679.
- Houben, A., Demidov, D., Gernand, D., Meister, A., Leach, C.R. and Schubert, I. (2003) Methylation of histone H3 in euchromatin of plant chromosomes depends on basic nuclear DNA content. *Plant J.* **33**, 967–973.
- Hudakova, S., Michalek, W., Presting, G.G., ten Hoopen, R., dos Santos, K., Jasencakova, Z. and Schubert, I. (2001) Sequence organization of barley centromeres. *Nucleic Acids Res.* **29**, 5029–5035.
- Ibarra-Laclette, E., Lyons, E., Hernandez-Guzman, G. et al. (2013) Architecture and evolution of a minute plant genome. *Nature*, **498**, 94–98.
- Ijdo, J.W., Wells, R.A., Baldini, A. and Reeders, S.T. (1991) Improved telomere detection using a telomere repeat probe (TTAGGG)_n generated by PCR. *Nucleic Acids Res.* **19**, 4780.
- Jiang, J., Birchler, J.A., Parrott, W.A. and Dawe, R.K. (2003) A molecular view of plant centromeres. *Trends Plant Sci.* **8**, 570–575.
- Li, L., Yang, J., Tong, Q., Zhao, L. and Song, Y. (2005) A novel approach to prepare extended DNA fibers in plants. *Cytometry A*, **63A**, 114–117.
- Lysak, M.A., Franz, P. and Schubert, I. (2006) Cytogenetic analyses of *Arabidopsis*. *Methods Mol. Biol.* **323**, 173–186.
- Ma, J., Wing, R.A., Bennetzen, J.L. and Jackson, S.A. (2007) Plant centromere organization: a dynamic structure with conserved functions. *Trends Genet.* **23**, 134–139.
- Martinez-Zapater, J., Estelle, M. and Somerville, C. (1986) A highly repeated DNA sequence in *Arabidopsis thaliana*. *Mol. Gen. Genet.* **204**, 417–423.
- Melters, D., Bradnam, K., Young, H. et al. (2013) Comparative analysis of tandem repeats from hundreds of species reveals unique insights into centromere evolution. *Genome Biol.* **14**, R10.

- Nasuda, S., Hudakova, S., Schubert, I., Houben, A. and Endo, T.R. (2005) Stable barley chromosomes without centromeric repeats. *Proc. Natl Acad. Sci. USA*, **102**, 9842–9847.
- Neumann, P., Navratilova, A., Koblizkova, A., Kejnovsky, E., Hribova, E., Hobza, R., Widmer, A., Dolezel, J. and Macas, J. (2011) Plant centromeric retrotransposons: a structural and cytogenetic perspective. *Mobile DNA*, **2**, 4.
- Neumann, P., Navratilova, A., Schroeder-Reiter, E., Koblizkova, A., Steinbauerova, V., Chocholova, E., Novak, P., Wanner, G. and Macas, J. (2012) Stretching the rules: monocentric chromosomes with multiple centromere domains. *PLoS Genet*, **8**, e1002777.
- Novak, P., Neumann, P. and Macas, J. (2010) Graph-based clustering and characterization of repetitive sequences in next-generation sequencing data. *BMC Bioinformatics*, **11**, 378.
- Peska, V., Fajkus, P., Fojtova, M., Dvorackova, M., Hapala, J., Dvoracek, V., Polanska, P., Leitch, A.R., Sykorova, E. and Fajkus, J. (2015) Characterisation of an unusual telomere motif (TTTTTAgGG)n in the plant *Cestrum elegans* (Solanaceae), a species with a large genome. *Plant J.* **82**, 644–654.
- Pich, U. and Schubert, I. (1998) Terminal heterochromatin and alternative telomeric sequences in *Allium cepa*. *Chromosome Res.* **6**, 315–321.
- Pich, U., Fuchs, J. and Schubert, I. (1996) How do Alliaceae stabilize their chromosome ends in the absence of TTTAGGG sequences? *Chromosome Res.* **4**, 207–213.
- Plohl, M., Mestrovic, N. and Mravinac, B. (2014) Centromere identity from the DNA point of view. *Chromosoma*, **123**, 313–325.
- Richards, E.J. and Ausubel, F.M. (1988) Isolation of a higher eukaryotic telomere from *Arabidopsis thaliana*. *Cell*, **53**, 127–136.
- Sykorova, E., Lim, K.Y., Chase, M.W., Knapp, S., Leitch, I.J., Leitch, A.R. and Fajkus, J. (2003a) The absence of Arabidopsis-type telomeres in *Cestrum* and closely related genera *Vestia* and *Sessea* (Solanaceae): first evidence from eudicots. *Plant J.* **34**, 283–291.
- Sykorova, E., Lim, K.Y., Fajkus, J. and Leitch, A.R. (2003b) The signature of the *Cestrum* genome suggests an evolutionary response to the loss of (TTTAGGG)_n telomeres. *Chromosoma*, **112**, 164–172.
- Sykorova, E., Lim, K.Y., Kunicka, Z., Chase, M.W., Bennett, M.D., Fajkus, J. and Leitch, A.R. (2003c) Telomere variability in the monocotyledonous plant order Asparagales. *Proc. Biol. Sci.* **270**, 1893–1904.
- Sykorova, E., Fajkus, J., Meznikova, M., Lim, K.Y., Neplechova, K., Blattner, F.R., Chase, M.W. and Leitch, A.R. (2006) Minisatellite telomeres occur in the family Alliaceae but are lost in *Allium*. *Am. J. Bot.* **93**, 814–823.
- Tran, T.D., Cao, H.X., Jovtchev, G., Novák, P., Vu, G.T.H., Macas, J., Schubert, I. and Fuchs, J. (2015) Chromatin organization and cytological features of carnivorous *Genlisea* species with large genome size differences. *Front. Plant Sci.*, **6**, 613.
- Veleba, A., Bures, P., Adamec, L., Smarda, P., Lipnerova, I. and Horova, L. (2014) Genome size and genomic GC content evolution in the miniature genome-sized family Lentibulariaceae. *New Phytol.* **203**, 22–28.
- Vu, G.T., Schmutzer, T., Bull, F. *et al.* (2015) Comparative genome analysis revealed divergent genome size evolution in a carnivorous plant genus. *Plant Genome*, **8**, 3.
- Weiss, H. and Scherthan, H. (2002) Aloe spp.–plants with vertebrate-like telomeric sequences. *Chromosome Res.* **10**, 155–164.

1 **Tissue-specific expression of telomerase reverse transcriptase gene variants in**
2 ***Nicotiana tabacum***

3

4 Jana Jurečková¹, Eva Sýkorová², David Honys³, Jiří Fajkus^{1,2}, Miloslava Fojtová^{1*}

5

6 ¹ Mendel Centre for Plant Genomics and Proteomics, Central European Institute of Technology
7 (CEITEC) and Faculty of Science, Masaryk University, Kamenice 5, 625 00 Brno, Czech
8 Republic

9 ² Institute of Biophysics, Academy of Sciences of the Czech Republic v.v.i., Královopolská 135,
10 612 65 Brno, Czech Republic

11 ³ Institute of Experimental Botany, Academy of Sciences of the Czech Republic v.v.i., Rozvojová
12 263, 165 02 Prague, Czech Republic

13

14

15 * Correspondence:

16 Miloslava Fojtová

17 Central European Institute of Technology (CEITEC) and Faculty of Science

18 Masaryk University

19 Kamenice 5

20 625 00 Brno

21 Czech Republic

22 fojtova@sci.muni.cz

23

24

25 number of words: 5 269

26 number of figures: 6

27

28

29

30

31

32

1 **Abstract**

2
3 Telomerase is a ribonucleoprotein complex providing for the maintenance of telomeres,
4 structures delimiting ends of linear eukaryotic chromosomes. In the *Nicotiana tabacum* (tobacco)
5 allotetraploid plant, three sequence variants of the gene coding for the telomerase reverse
6 transcriptase protein subunit (*TERT*) were described; two of them derived from the maternal *N.*
7 *sylvestris* genome (*TERT_Cs*, *TERT_D*) and one originated from the *N. tomentosiformis* paternal
8 genome (*TERT_Ct*). To correlate the level of *TERT* variants transcripts and telomerase activity,
9 we analyzed transcription of *TERTs* in telomerase-positive and telomerase-negative tobacco
10 tissues. High and approximately comparable levels of *TERT_Ct* and *TERT_Cs* transcripts were
11 detected in seedlings, roots, flower buds and leaves while the transcript of the *TERT_D* variant
12 was markedly under-represented. Similarly, in *N. sylvestris* tissues, *TERT_Cs* transcript
13 significantly predominated over *TERT_D*. Transcripts of *TERT_C* variants and *TERT_D* variant
14 in tobacco and its progenitors seedlings were maintained at similar levels, evidencing that stable
15 *TERT* transcription is a parameter important for cell stability. A specific pattern of *TERT*
16 transcripts was detected in samples of tobacco pollen with the *TERT_Cs* variant clearly
17 dominating. Telomerase activity corresponded to *TERT_Ct* and *TERT_Cs* transcript levels in
18 tobacco seedlings, roots, flower buds and leaves; in pollen samples, telomerase activity appeared
19 to correlate with the rate of *TERT_Ct* transcription. We conclude that the existence of multiple
20 *TERT* gene variants in tobacco represents another level at which telomerase functions may be
21 modulated. Our results support the significance of *Nicotiana* species as interesting and profitable
22 models for plant telomere biology studies.

23
24
25

26 Key words: telomerase, transcription, gene sequence variant, *Nicotiana tabacum*, *Nicotiana*
27 *sylvestris*, *Nicotiana tomentosiformis*

28
29
30
31
32
33
34
35
36
37
38
39
40
41
42
43

1 Introduction

2
3 Telomeres, nucleoprotein structures delimiting ends of linear eukaryotic chromosomes, represent
4 functional elements essential for the maintenance of genome integrity. The basic function of
5 telomeres is to distinguish natural chromosome ends from un-repaired double stranded DNA
6 breaks and to protect the coding parts of the genome from the loss due to the non-effective
7 replication of the distal-most region of the lagging DNA strand. Incomplete DNA replication
8 leads to the progressive telomere shortening which may be or may not to be compensated by
9 specific pathways. In plant tissues containing dividing meristem cells like seedlings, root tips,
10 floral buds, blossoms, and in cultured cells, an active telomerase, a ribonucleoprotein enzyme
11 complex able to elongate telomeres, was detected (Fajkus et al., 1996; Fitzgerald et al., 1996).
12 Telomerase activity present throughout plant ontogenesis in meristems maintains stable telomere
13 lengths in cells that these meristems produce by serial division and differentiation, thus telomeres
14 do not shorten during developmental progression, in contrast to e.g., humans (Fajkus et al.,
15 1998). Even in the absence of telomerase activity, as occurs in the case of *Arabidopsis thaliana*
16 telomerase knock-out mutants, alternative telomere lengthening is activated, which partially
17 compensates for the lack of telomerase (Ruckova et al., 2008). Telomerase consists of two
18 subunits, a catalytic protein subunit TERT (TELomerase Reverse Transcriptase) and an RNA
19 subunit TER (TELomerase RNA). TER serves as a template for the synthesis of telomere repeat
20 sequences by TERT reverse transcriptase activity. It was shown that the determining factor for
21 telomerase activity was expression of its TERT subunit. Transcription of the *TERT* gene directly
22 correlates with the telomerase activity in plant tissues (Fitzgerald et al., 1996; Ogrocka et al.,
23 2012), while *TER* is transcribed in both telomerase-positive and telomerase-negative tissues
24 (Cifuentes-Rojas et al. 2011).

25 *Nicotiana tabacum* (tobacco) is a standard plant model used in telomere and telomerase
26 biology. Detection of active telomerase in tobacco BY-2 cell culture (Fajkus et al., 1996),
27 evidence of the maintenance of telomere length and dynamic regulation of telomerase activity
28 (Fajkus et al., 1998), description of chromatin structure of telomeric and subtelomeric repeats
29 (Fajkus et al., 1995a; Fajkus et al., 1995b), cell cycle-dependent regulation of telomerase activity
30 by plant hormones (Tamura et al., 1999; Yang et al., 2002), and characterization of epigenetic
31 properties of telomeric chromatin (Majerova et al., 2014) represent key studies in the field.

32 *N. tabacum* is an allotetraploid plant and its genome originated ~ 200 000 years ago from
33 diploid progenitors, *Nicotiana sylvestris* and *Nicotiana tomentosiformis* (Murad et al., 2002; Lim
34 et al., 2004). Many sequences in the tobacco genome – mainly those of repetitive nature (Renny-
35 Byfield et al., 2011) – passed through distinct evolution; the well-known example of this process
36 is so called concerted evolution of rDNA arrays (reviewed in Kovarik et al. (2008)).

37 Nevertheless, in the case of the gene coding for the telomerase protein subunit, allopolyploid
38 ancestry of tobacco has been maintained as three sequence variants of *TERT* were recently
39 identified in the tobacco genome; two of them derived from *N. sylvestris* (*TERT_Cs*, *TERT_D*)
40 and one variant sharing a high level of homology with the *TERT_Ct* sequence present in *N.*
41 *tomentosiformis* (Sykorova et al., 2012). Original abbreviations are Cs for Coding putative
42 functional *TERT* variant of the S-genome origin, Ct for Coding putative functional *TERT* variant
43 of the T-genome origin, and D for putative pseDogene *TERT* variant. All *TERT* gene variants
44 are transcriptionally active, although *TERT_D* shows a lower level of sequence similarity with
45 *TERT_C* variants, and due to insertions and deletions within exons and truncation at the 5' end it
46 was originally supposed to be a pseudogene. *Nicotiana TERT* genes demonstrate several specific

1 features, as presence of novel short exon 4/5a between canonical exons 4 and 5, and specific
2 repeats in the intron 9 in genomes of tobacco and both progenitors. Moreover, in tobacco and *N.*
3 *sylvestris*, transcript variants with different repeat motives in the exon 5 were described
4 (Sykorova et al., 2012).

5 Tobacco with three sequence variants of the *TERT* gene represents unique model system
6 because a single copy of the *TERT* gene is present in most eukaryotes studied, including the
7 common model plant *A. thaliana*. We designed this study (i) to analyze transcription of *TERT*
8 variants in *N. tabacum* tissues, and (ii) to correlate *TERT*'s transcription and telomerase activity.
9 Our results showed that in most tobacco tissues, telomerase activity was correlated to the level of
10 *TERT_C* transcripts and the amount of *TERT_D* transcript was about the detection limit. Specific
11 pattern of *TERT* transcripts was observed in pollen samples with very high level of *TERT_C*s,
12 while *TERT_Ct* transcript was at the level detected in seedlings. Moreover, our data supported
13 presence of two *TERT_C*s gene copies in the genome of *N. sylvestris*. The existence of more
14 genes coding for the protein subunit of telomerase in the genome of allotetraploid tobacco, which
15 is very interesting from the evolutionary point of view, opens up further levels at which activity
16 of telomerase may be regulated.

17 18 **Material and methods**

19 20 **Plant growth**

21
22 *Nicotiana tabacum*, *Nicotiana sylvestris* and *Nicotiana tomentosiformis* seeds were surface
23 sterilized with 90% bleach SAVO (Biochemie group a.s., active substance: NaClO), and
24 germinated on plates with Murashige-Skoog (MS) medium (Duchefa Biochemicals)
25 supplemented with 1% sucrose and 0.8% plant agar (Duchefa Biochemicals). After 12 days of
26 cultivation under short day conditions (light 150 mmolm⁻²s⁻¹ for 8 h at 21°C; dark for 16 h at
27 19°C), seedlings were either collected for analysis or potted into soil and plants were grown
28 under long day conditions (light for 16 h, dark for 8 h). For functional analysis, tobacco seeds
29 were germinated for 12 days in the presence of plant hormones: synthetic auxin NAA (1-
30 naphthalenacetic acid, Duchefa Biochemicals), synthetic auxin 2,4-D (2,4-dichlorophenoxyacetic
31 acid, Duchefa Biochemicals), synthetic cytokinin BAP (6-benzylaminopurine, Duchefa
32 Biochemicals); concentrations of hormones in the cultivation medium were 50 nM, 100 nM, 5
33 μM.

34 35 **Isolation of immature and mature pollen of *N. tabacum* and *in vitro* pollen tubes cultivation**

36
37 Wild-type *N. tabacum* (cv. Samsun) seeds were sown in a greenhouse at 22–25 °C and
38 under short-day conditions. Adult plants with fully developed roots were transplanted to an
39 outdoor greenhouse to compost soil. There the plants were grown under natural day–night
40 photoperiods in spring and summer.

41 Immature pollen grains at three stages of development were collected from August to
42 September. The appropriate developmental stages were determined by the length of the flower
43 buds including calyx, as published previously by (Tupy et al., 1983). Flower bud lengths were as
44 follows: early bicellular pollen (stage 3), 25–27 mm and late bicellular pollen (stage 5), 46–49
45 mm. After flower collection, freshly isolated anthers were immediately processed by gentle
46 crushing in a chilled mortar with 5% (w/v) sucrose in diethylpyrocarbonate (DEPC, Sigma-

1 Aldrich)-treated sterile water. The mixture containing released pollen was filtered through a
2 nylon mesh of approximately 100 µm to remove anther debris. Suspended pollen grains were
3 then sedimented by centrifugation (2000 g, 5 min, 4 °C), excess supernatant was decanted and
4 pollen was stored at -80 °C. For assessment of the correct pollen developmental stage, standard
5 4',6-diamidino-2 phenylindole (DAPI) staining in DAPI staining solution (0.1 M sodium
6 phosphate, pH 7; 1 mM EDTA; 0.1% (v/v) Triton X-100; 0.8 mg/ml DAPI) was used (Park et al.,
7 1998). Stained pollen grains were visualized with a NIKON TE2000 fluorescence microscope
8 and images were captured with NIS element software (NIKON).

9 Mature pollen was isolated aseptically as described previously (Petrů et al., 1964).
10 Flowers were collected 1 day before anthesis. Stamens were removed from the flowers into a
11 Petri dish to dehisce in a fume-hood overnight at room temperature. Dry pollen grains were then
12 filtered through a nylon mesh (Miracloth, pore size 50 µm), weighed and stored at -20°C. Over
13 80% of the collected pollen grains could successfully germinate and give rise to a pollen tube,
14 irrespective of the collection date. DAPI-stained images of pollen developmental stages and
15 mature pollen were presented in Bokvaj et al., 2015.

16 For *in vitro* pollen tube germination, approximately 10 mg of pollen was re-suspended in
17 10 ml of pollen germination medium (SMM: 0.3 M sucrose, 1.6 mM H₃BO₃, 3 mM Ca(NO₃)₂
18 .4H₂O, 0.8 mM MgSO₄.7H₂O, 1 mM KNO₃) and aliquoted into conical flasks. The 30 min and 4
19 h pollen tubes were cultivated with SMM medium supplemented with casein (1 mg/ml). Cultures
20 were incubated in a water-bath shaker at 140 rpm for 2 h and then slowed to 90 rpm for the
21 remaining cultivation time at 26°C in the dark. Aliquots of the samples were stained with aniline
22 blue and DAPI, and analyzed under a light microscope (Park et al., 1998). Pollen tubes were
23 vacuum-filtered, flash frozen in liquid nitrogen and stored at -80°C prior to RNA extraction.
24

25 **Proportion of *TERT* gene variants in genomes of *Nicotiana* species**

26
27 Total genomic DNA was isolated from 2 g of leaves of *Nicotiana* species according to
28 (Dellaporta et al., 1983). PCR using specific primer combinations for *TERT* gene sequence
29 variants (Table S1) and MyTaq polymerase (Bioline) was run under conditions as follows: 1 min
30 at 95 °C, 35 cycles of 20 s at 95 °C, 20 s at 62 °C, 20 s at 72 °C, and the final extension step (3
31 min at 72 °C). The concentration of primers in the reaction mix was 0.25 µM.

32 Quantitative analysis was carried out using 20 ng of genomic DNA as a template, KAPA
33 SYBR FAST qPCR master mix (Kapa Biosystems) and a Rotorgene 6000 cycler (Qiagen) in 20-
34 µl reactions. qPCR conditions were optimized *via* determination of reaction efficiencies using
35 diluted PCR products as templates for calibration curve constructions for amplification of each
36 *TERT* variant. Optimized qPCR conditions were as follows: 5 min at 95 °C, 40 cycles of 5 s at 95
37 °C, 20 s at 62 °C, 15 s at 72 °C (at the end of this step, fluorescence was measured); and the final
38 extension (3 min at 72 °C). Genomic DNA for quantification of *TERT* variants was isolated from
39 3 independently grown individual plants of each species and analyzed in 3 technical replicates.
40 The actin gene was used as a reference to precisely determine the amount of template DNA in
41 each reaction (sequences of primers are given in Table S1, annealing temperature of primers was
42 56 °C). Data were evaluated by the Rotorgene 6000 software (Qiagen).
43

44 **Transcription of *TERT* gene variants**

45
46 Total RNA from seedlings, leaves, flower buds and roots was isolated using the RNeasy Plant
47 Mini Kit (Qiagen), and RNA from immature and mature pollen and pollen tubes using

1 TriReagent (Molecular Research Center). RNA was purified by DNaseI treatment (TURBO
2 DNA-free, Life Technologies). The quality and quantity of RNA was checked by electrophoresis
3 on a 1% (w/v) agarose gel and by measurement of absorbance (NanoPhotometer, IMPLLEN).
4 cDNA was prepared by reverse transcription of 2 µg of RNA using M-MuLV reverse
5 transcriptase (NEB) and Random Nonamers (Sigma). Quantification of transcript levels of the
6 *TERT* variants in respective tissues was carried out by KAPA SYBR FAST qPCR master mix
7 (Kapa Biosystems), a Rotorgene 6000 (Qiagen) and using actin and *EFL* genes as suitable
8 references for quantitative analyses in tobacco (Schmidt and Delaney, 2010); sequences of
9 primers are given in the Table S1. It was determined by the BLAST search and confirmed by
10 calibration curves construction that these reference genes are applicable also for analysis of *N.*
11 *sylvestris* and *N. tomentosiformis* samples. One µl of 2× diluted cDNA was added to the 20-µl
12 reaction mix. Reactions were carried out in triplicate under conditions described in the above
13 paragraph. Analyses were performed for 2 - 8 biological replicates in three technical replicates.
14 Relative transcription in the respective tissues was calculated as the fold increase/decrease
15 relative to 12-day seedlings ($\Delta\Delta C_t$ method (Pfaffl, 2004)). The proportion of respective *TERT*
16 sequence variants in transcriptomes was calculated according to their C_t (the PCR cycle in which
17 a reasonable increase in fluorescence was detected; ΔC_t method (Pfaffl, 2004)). For evaluation of
18 the data and statistical analysis the program qbase+ (Biogazelle) (Hellemans et al., 2007) was
19 used.

21 **Telomerase activity**

23 Telomerase activity in tissues of *Nicotiana* species was analyzed by the TRAP (Telomere Repeat
24 Amplification Protocol) *in vitro* method. Telomerase extracts were prepared according to the
25 published protocol (Fitzgerald et al., 1996; Sykorova et al., 2003). Telomerase activity was
26 quantified (Herbert et al., 2006) using FastStart SYBR Green Master (Roche), TS21 and TELPR
27 primers (Table S1; concentration of each primer in the reaction mix was 0.25 µM) and 1 µl of
28 telomerase extract (protein concentration 200 ng/µl). The substrate primer, TS21, was extended
29 by telomerase (45 min at 26 °C) and after telomerase inactivation (15 min at 95 °C), extension
30 products were amplified in 30 cycles consisting of 15 s at 95 °C, 1 min at 60 °C (at the end of this
31 step, fluorescence was measured). Two to five biological replicates (independently cultivated
32 seedlings/plants) were analyzed in 3 technical replicates. C_t values were determined using the
33 Rotorgene 6000 (Qiagen) machine software and relative telomerase activity was calculated by the
34 ΔC_t method (Pfaffl, 2004).

36 **Results**

38 **Increased copy number of *TERT_C* variants in genomes of *N. tabacum* and *N. sylvestris***

40 To specifically amplify *TERT* gene sequence variants, we designed variant-specific reverse
41 primers from the 9th exon in respect to sequence polymorphisms as described by (Sykorova et
42 al., 2012). Using the combination of common forward primer 9ex Fw and specific reverse
43 primers (Table S1), the presence of *TERT* variants was confirmed in three *Nicotiana* species as
44 follows: *TERT_Ct* in *N. tabacum* and *N. tomentosiformis*, *TERT_Cs* and *TERT_D* in *N. tabacum*
45 and *N. sylvestris* (Figure 1A).

1 Quantitative PCR conditions were carefully optimized for all *TERT* sequence variants
2 with calibration curves constructed using diluted PCR products as templates. Reaction
3 efficiencies were determined for the amplification of *TERT*_Ct, *TERT*_Cs and *TERT*_D as 0.97,
4 0.97 and 0.99, respectively (Figure S1). Applying the optimized protocol and genomic DNAs as
5 templates, the presence and proportion of *TERT* variants were determined in genomes of common
6 tobacco and its progenitors (Figure 1B). As expected, only the *TERT*_Ct variant was amplified
7 from *N. tomentosiformis*. Interestingly, in *N. sylvestris*, the amount of the *TERT*_Cs variant was
8 three fold higher compared to the *TERT*_D variant, which is in agreement with the intensities of
9 variant-specific hybridization signals as demonstrated in the previous study (Sykorova et al.,
10 2012) and here supplemented by the densitometry analysis (Figure S2). A similar level of the
11 *TERT*_D variant was present in the *N. tabacum* genome (23% of total *TERT*) and the content of
12 *TERT*_Ct was slightly lower compared to *TERT*_Cs (33% and 44%, respectively). Previously we
13 have hypothesized the presence of two copies of *TERT*_Cs in the *N. sylvestris* genome (Sykorova
14 et al., 2012), however due to known similarities between *TERT*_Ct and *TERT*_Cs variants, tiny
15 differences among individual *TERT*_C sequences were not sufficient for verification at the
16 sequence level. In qPCR analysis using the C-variant universal reverse primer for amplification
17 of both *TERT*_C variants (primer 9ex Rev_C, Table S1), the signals normalized to actin were
18 comparable for *N. tabacum* and *N. sylvestris* samples (data not shown), supporting the presence
19 of more than one copy of the *TERT*_Cs variant in the *N. sylvestris* genome.
20

21 **Distinct prevalence of C variants in *N. tabacum* and *N. sylvestris* *TERT* transcripts**

22

23 To compare telomerase expression at the protein and RNA levels, we quantified telomerase
24 activity (Figure 2A) and the transcription of specific *TERT* gene variants (Figure 3) in *N.*
25 *tabacum* tissues with high telomerase activity (seedlings, roots, flower buds) and in mature leaves
26 with significantly reduced telomerase activity. A correlation between telomerase activity and
27 *TERT* transcription was observed for the *TERT*_Ct and the *TERT*_Cs transcripts (Figure 2A,
28 Figure 3A, B) whereas the *TERT*_D variant showed a different transcription pattern (Figure 3C).
29 *TERT*_Ct and *TERT*_Cs representation in the tobacco *TERT* transcriptome were as follows
30 (Figure 3D): seedlings 47% and 35%, roots 57% and 32%, flower buds 61% and 39%, and leaves
31 47% and 53%, respectively. The *TERT*_D transcript (Figure 3C, D) was detected only in
32 seedlings, representing here about 18% of all *TERT* transcripts, and in roots (11% of all *TERT*
33 transcripts). In flower buds and leaves, signal of the *TERT*_D transcript was below the detection
34 limit. As the *TERT*_D variant cannot produce a functional TERT protein, we recalculated the
35 ratio of dominant *TERT*_C variants transcripts in respective tissues (Figure 3E) to better estimate
36 a correlation between these functional *TERT* variants and telomerase activity. When *TERT*_D
37 transcription was ignored, portions of *TERT*_Ct and *TERT*_Cs in seedlings were 57% and 43%,
38 and in flower buds 64% and 36%, respectively. A detailed comparison of transcription profiles of
39 *TERT* gene variants in tobacco tissues clearly shows that both *TERT*_C variants were highly
40 transcribed with a mild prevalence of *TERT*_Ct in telomerase-positive tissues (Figure 3E).

41 In *N. sylvestris* tissues, the pattern of telomerase activity was similar to *N. tabacum*
42 (Figure 2B) and transcripts of the *TERT*_Cs variant clearly predominated (Figure 4). Although
43 the *TERT*_D variant transcript was detected in all tissues analyzed, its amount was only up to
44 about 10%. The highest *TERT*_D transcript level was detected in *N. sylvestris* seedlings (12% of
45 *TERT* transcripts) while the lowest *TERT*_D transcript level was in flower buds (2%) (Figure 4).

46 A direct comparison of *TERT*_C and *TERT*_D transcript levels in seedlings of all three
47 *Nicotiana* species was performed using primer combinations for amplification of both *TERT*_C

1 variants with the universal reverse primer 9ex Rev_C (Table S1) and amplification of the
2 *TERT_D* variant, respectively. Comparison of qPCR signals normalized to the actin reference
3 gene clearly showed that levels of *TERT_C* transcripts, which are presumably crucial for
4 telomerase activity in telomerase positive tissues, were comparable in *N. tabacum*, *N. sylvestris*
5 and *N. tomentosiformis* seedlings (Figure 5A). Regarding the *TERT_D* transcript in *N. tabacum*
6 and *N. sylvestris* seedlings, slightly higher level was found in *N. sylvestris*, but this increase was
7 not statistically significant (Figure 5B). These data demonstrate that transcripts of *TERT_C*
8 variants and the *TERT_D* variant in *N. tabacum* and in its progenitors are maintained at similar
9 levels.

10 It was reported that telomerase activity increased in tobacco cell culture BY-2 treated with
11 the plant hormone auxin (Tamura et al., 1999). We tested if plant hormones influenced
12 transcription of *TERT* gene variants and telomerase activity in tobacco seedlings. Synthetic
13 auxins NAA and 2,4-D and synthetic cytokinin BAP, at concentrations of 50 and 100 nM, did not
14 change transcription of *TERT* variants during tobacco seeds germination (data not shown). A
15 higher concentration of 2,4-D (5 μ M) resulted in only a slight increase in the relative level of
16 *TERT_Ct* transcript compared with untreated seedlings (Figure S3A, top panel) without
17 significant change in the proportion of *TERT* variants in the *TERT* transcriptome (Figure S3A,
18 bottom panel). A similar pattern was observed in seedlings treated by 5 μ M NAA (Figure S3B).
19 Slightly increased *TERT_D* level was detected in seedlings influenced by 5 μ M BAP (Figure
20 S3C). Telomerase activity was not significantly changed in seedlings germinated in the presence
21 of any of the plant hormones investigated (data not shown). Treatment of tobacco seedlings with
22 plant hormones is thus not directly reflected in the modulation of either transcription of *TERT*
23 variants or telomerase activity. Obviously, telomerase activity, as an important cellular parameter
24 involved in the maintenance of the genome stability, is under more complex and more robust
25 control in tobacco plants compared to cell culture.

26 27 **Specific pattern of *TERT* transcripts in tobacco pollen**

28
29 In general, plant telomerase is active in meristems and dedifferentiated tissues (Fitzgerald et al.,
30 1996). Pollen grains represent a differentiated plant tissue producing sperm cells; yet, active
31 telomerase was detected in *Silene latifolia* pollen (Riha et al., 1998). Mature pollen is a
32 metabolically quiescent structure designed for the pollination and for the delivery of its precious
33 cargo, male gametes (sperm cells), to the female reproductive tissues. Therefore although the
34 metabolism of dry pollen is negligible, its preceding developmental and following functional
35 (progamic) phases are metabolically extremely active. Pollen development is characterized by the
36 massive storage of metabolic reserves enabling the explosive and highly competitive growth of
37 pollen tubes through the pistil (Pacini et al., 2006; Honys et al., 2009). To get better insight to
38 telomerase dynamics during male gametophyte development and progamic phase, we
39 investigated telomerase activity and *TERT* variant transcripts in tobacco immature pollen
40 (developmental stages 3, 5), mature pollen grains and pollen tubes cultivated *in vitro* for 30 min
41 and 4 h. Active telomerase was detected in all analyzed samples including mature pollen (Figure
42 2C). Telomerase activity gradually decreased during pollen maturation but even in mature pollen,
43 the activity was comparable to 12 day-old seedlings. No changes in relative telomerase activity
44 were observed during *in vitro* cultivation of pollen tubes, but the data might be influenced by the
45 fact that in quantitative telomerase activity assays, samples are diluted to the same protein
46 concentration, which varies during pollen tubes cultivation (Rihova et al., 1996). Nevertheless,
47 we can reliably conclude that active telomerase is present in tobacco pollen samples.

1 Relative levels of *TERT*_Ct transcript were similar or slightly lower in all pollen samples,
2 except the early bicellular pollen, when compared to seedlings (Figure 6A). The amount of
3 *TERT*_Ct transcript was significantly increased in the early bicellular pollen (stage 3), about
4 eight-fold higher than in later developmental stages. Actually, profile of *TERT*_Ct transcripts in
5 pollen samples (Figure 6A) copied profile of telomerase activity (Figure 2C). Astonishingly high
6 levels of *TERT*_Cs transcript were detected in all pollen samples (Figure 6B) with a similar
7 profile as *TERT*_Ct but at a significantly higher level. *TERT*_Cs reached eight-fold accrual in
8 mature pollen and pollen tubes compared with seedlings, about 15-fold accrual in late bicellular
9 immature pollen (stage 5), and more than 35-fold higher level of *TERT*_Cs transcript was
10 detected in early bicellular immature pollen (stage 3). The *TERT*_D variant transcript was not
11 detected. In the pollen *TERT* transcriptome, the *TERT*_Cs clearly dominates, representing about
12 80% of total *TERT* transcript in immature pollen stage 3 and about 90% in other pollen samples
13 (Figure 6C), unlike the other tobacco tissues investigated (Figure 3). The transcription profile of
14 *TERT*_Cs and its dominance confirmed previously published microarray data (Hafidh et al.,
15 2012a; Hafidh et al., 2012b; Bokvaj et al., 2015). On an Agilent Tobacco 44K Genome Array,
16 only probes for *TERT*_Cs were present and from the tissues analyzed, the respective transcript
17 accumulation also peaked in early bicellular pollen (Figure 6D). In the study of Bokvaj et al.
18 (2015), uninucleate microspores (developmental stage 1) were analyzed too and the level of
19 *TERT*_Cs transcript was even in one order of magnitude higher compared to the early bicellular
20 pollen at stage 3 (data not shown).

21

22 Discussion

23

24 In both plant and mammalian kingdoms, telomerase is strictly regulated during development.
25 This regulation represents a complex process and is realized by the close interplay of multifarious
26 pathways e.g., binding of activators/repressors affecting activity of the telomerase protein subunit
27 promoter, chromatin structure and nucleosomal density in *TERT* regulatory regions, alternative
28 splicing of the *TERT* primary transcript, telomere transcripts TERRA, and/or posttranslational
29 modifications. The basic telomerase function – elongation of telomeric repeats at chromosome
30 ends – is further influenced by factors determining the structure of telomeres and their
31 accessibility for the telomerase enzyme. In the allotetraploid plant *Nicotiana tabacum*, the
32 complexity of telomerase regulation was extended to another level due to the presence of three
33 sequence variants of the gene coding for the telomerase reverse transcriptase protein subunit
34 (Sykorova et al., 2012). In this pilot study, presence of more than one copy of the *TERT*_Cs in the
35 *N. sylvestris* genome was hypothesized due to markedly different intensities of the *TERT*_Cs- and
36 *TERT*_D-specific hybridization bands (Figure S2). Using quantitative PCR we demonstrated that
37 the *TERT*_C gene-specific signal in *N. tabacum* genome comprising *TERT*_Ct and *TERT*_Cs
38 variants was comparable to *TERT*_Cs level in the *N. sylvestris* genome. It confirms our
39 presumption of two copies of the *TERT*_Cs variant in the *N. sylvestris* genome that might arise
40 from gene duplication. Searching of published *N. sylvestris* draft genome assembly (Sierro et al.,
41 2013) identified one *TERT*_C variant in two subsequent contigs (Figure S4). Absence of a gene
42 duplicate in the draft genome could be caused by technical difficulties due to putative high
43 sequence similarity between copies, which is 99.7% for *TERT*_Cs and 99.3% for *TERT*_D
44 between *N. tabacum* and ancestral *N. sylvestris* *TERT*s. Moreover, a close proximity of *TERT*
45 gene copies in *N. sylvestris* is suggested also from FISH experiment where only one *TERT* locus
46 was revealed (Sykorova et al., 2012).

1 Generally, *TERT* gene transcript level correlates directly with telomerase activity
2 (Fitzgerald et al., 1996; Ogrocka et al., 2012). In most tobacco tissues (seedlings, flower buds,
3 roots and leaves), telomerase activity (Figure 2A) correlated with levels of *TERT_Ct* and
4 *TERT_Cs* variant transcripts (Figure 3A, B), while the *TERT_D* transcript was under-represented
5 and in some tissues its abundance was even below the detection limit (Figure 3C). Since in the *N.*
6 *sylvestris* progenitor, only the *TERT_Cs* variant was present, and thus clearly responsible for
7 telomerase activity, and the same was true for *N. tomentosiformis* and *TERT_Ct*, it seems highly
8 probable that transcripts of both *TERT_C* variants contribute to synthesis of active TERT protein
9 in tobacco.

10 A specific *TERT* transcription pattern was detected in tobacco pollen. In contrast to other
11 tobacco tissues in which *TERT_Ct* and *TERT_Cs* transcripts were roughly comparable (Figure
12 3D, E), in all pollen samples, *TERT_Cs* transcript unequivocally dominated (Figure 6C). The
13 level of *TERT_Cs* transcript was extremely high in samples representing pollen mitosis I in
14 uninucleate microspheres and early bicellular pollen, stages 1 and 3, respectively (not shown and
15 Figure 6B, D). Highly asymmetrical pollen mitosis I is one of the most decisive events in male
16 gametophyte development since it leads to the establishment of two cell lineages, vegetative and
17 generative, representing the still proliferating male germline (reviewed in Berger and Twell,
18 2011). Comparison of the transcriptional pattern of *TERT_C* variants in pollen samples with
19 those in seedlings revealed interesting information. In the early bicellular pollen, in which about
20 eight-fold higher telomerase activity was detected compared with seedlings and other pollen
21 samples (Figure 2C), increased levels of *TERT_C* variants transcripts were also detected. The
22 increment of *TERT_Ct* transcript corresponded exactly to the increment of telomerase activity
23 (eight-fold higher level of *TERT_Ct* transcript compared with seedlings, Figure 6A), while an
24 increase in *TERT_Cs* transcripts was clearly marked, more than 35-fold compared with seedlings
25 (Figure 6B). In other pollen samples, telomerase activity and *TERT_Ct* transcription were at
26 levels similar to those measured in seedlings (Figures 2C, 6A), and *TERT_Cs* transcription was
27 significantly increased (Figure 6B), although the accrual was not as dramatic as in the case of
28 early bicellular pollen. Based on these data, we suggest that in tobacco pollen, the pattern of
29 *TERT_Ct* transcription correlates with telomerase activity, while *TERT_Cs* transcript level, which
30 is high in all pollen samples, is not directly reflected in the activity of telomerase. The cell-
31 lineage-specific or preferential expression of each *TERT_C* variant in vegetative and generative
32 cells cannot be ruled out and definitely deserves further investigation. The differences in
33 chromatin status in the vegetative nucleus and in the male germline were documented (reviewed
34 in She and Baroux, 2015) and therefore differential telomerase activity in these cell types is
35 likely. The reason for so high level of *TERT_Cs* transcript and the potential function of the
36 protein remain unclear.

37 A completely different transcription pattern was observed for the *TERT_D* variant, which
38 was inherited from the *N. sylvestris* maternal genome. Its transcription was very low in tobacco
39 tissues; actually, only in seedlings and flower buds it was above the detection limit in our
40 experimental set up (Figure 3C). In *N. sylvestris*, the *TERT_D* transcript was detected in all
41 samples analyzed, but it was significantly under-represented and encompassed less than 10% of
42 the *TERT* transcriptome (Figure 4). Our analyses focusing on tissue specific expression of *TERT*
43 variants did not reveal any link to a specific biological process; nevertheless the *TERT_D* gene
44 variant is transcribed and some hypothetical function (e.g., at RNA interference level for
45 regulation of the other variants) is possible.

46 Despite more than 200 000 years of ongoing evolution of the tobacco genome, some gene
47 homologues or other DNA sequences originating from parental genomes are maintained

1 (Fulnecek et al., 2009; Clarkson et al., 2010). Because *TERT* variants represent examples of such
2 long term stability of inherited sequences, we tried to specify the extent of this conserved state.
3 For this purpose, transcription of *TERT_C* variants (without distinguishing between Cs and Ct)
4 was compared in seedlings of tobacco and both its progenitors. Quantitative data showed that
5 transcription of *TERT_C* was comparable in *N. tomentosiformis*, *N. sylvestris* and *N. tabacum*
6 (Figure 5A) setting *TERT* equilibrium in *Nicotiana* transcriptomes. This means that the level of
7 *TERT_C* transcripts (sum of *TERT_Ct* and *TERT_Cs*) in tobacco must be maintained at the same
8 level as in both progenitors. A correlation between telomerase activity and *TERT_C* transcription
9 supports the hypothesis presented above that transcripts of both *TERT_C* gene variants are
10 templates for synthesis of active telomerase enzyme in tobacco seedlings and probably also in
11 other telomerase-positive tissues such as roots and flower buds. Moreover, similar transcription
12 profile of the *TERT_D* variant was observed in *N. tabacum* and *N. sylvestris* seedlings (Figure
13 5B) thus suggesting the importance of stable *TERT* transcription for execution of telomeric and
14 possibly non-telomeric functions of telomerase that are crucial for cell stability and survival.

15 One of highly disputed telomerase biology questions were mechanisms of activation or
16 deactivation of telomerase in different model systems. In tobacco cultured cells, telomerase
17 activation in S phase potentiated by the treatment with auxins was reported (Yang et al., 2002)
18 indicating hormonal cross-talk involved in cell cycle-dependent regulation of telomerase activity.
19 Moreover, in *A. thaliana*, a protein activating telomerase expression acts as a part of the auxin
20 signaling pathway (Ren et al., 2004). Tobacco, with three *TERT* gene variants that can be
21 regulated independently, appeared to be a promising experimental system to clarify the
22 relationship between plant hormones and regulation of telomerase expression and activity.
23 Nevertheless, in our experiments, plant hormones – two synthetic auxins and one synthetic
24 cytokinin – did not significantly change telomerase activity or the proportion of *TERT* variants
25 (Figure S3). The absence of response to auxin treatment in tobacco seedlings, in contrast to BY-2
26 cell culture, can be explained by the higher complexity of seedlings. Above all, directional, cell-
27 to-cell auxin transport occurs in seedlings, facilitated by plasma membrane-localized transport
28 proteins, namely due to the polar subcellular localization of PIN proteins (see e.g., Adamowski
29 and Friml, 2015 for a recent review), and this level of auxin regulation is absent in cell cultures.
30 Therefore, differential sets of responses to auxin treatment, including an impact on telomerase
31 activity, may be triggered in tobacco cultured cells (BY-2) and in differentiated tissues
32 (seedlings). In this context, analysis of the *TERT* variants transcription in synchronized tobacco
33 cell culture treated with plant hormones may provide relevant data.

34 Based on the these data we conclude that (i) additional analyses support presence of two
35 copies of *TERT_Cs* variant in the *N. sylvestris* genome; (ii) equilibrated *TERT* transcription in
36 tobacco and its progenitors manifests importance of this parameter for proper settings of cellular
37 functions; (iii) significantly unbalanced levels of *TERT_Ct* and *TERT_D* transcripts in *N.*
38 *tabacum* and *N. sylvestris* tissues indicate their differential regulation; (iv) specific *TERT*
39 transcription pattern in pollen samples evidences different regulation of *TERT* variant
40 transcription in these tissues and conjures up the question on the purpose of the *TERT_Cs*
41 transcript high level; (v) telomerase activity correlated with the both *TERT_C* variants transcript
42 levels in all tobacco tissue except pollen samples where *TERT_Ct* and telomerase activity are
43 matched; (vi) using the specific quantitative assay for the transcription of *TERT* variants in
44 tobacco tissues we are able to determine their changes due to e.g., suboptimal living conditions or
45 treatments, setting a methodology background for further telomere research. Finally, we can
46 speculate that three sequence variants of the *TERT* gene in the *Nicotiana tabacum* genome
47 represent attribute contributing to evolutionary prosperity of this tetraploid plant.

1
2
3
4
5
6
7
8
9
10
11
12
13
14
15
16
17
18
19
20
21
22
23
24
25
26
27
28
29
30
31
32
33
34
35
36
37
38
39
40
41
42
43
44
45

Conflict of interest statement

The authors declare that the research was conducted in the absence of any commercial or financial relationships that could be construed as potential conflict of interest.

Funding

The work was supported by the Grant Agency of the Czech Republic (13-06943S) and by the project “CEITEC - Central European Institute of Technology” (CZ.1.05/1.1.00/02.0068) from the European Regional Development Fund.

References

Adamowski, M., and Friml, J. (2015). PIN-dependent auxin transport: Action, regulation, and evolution. *Plant Cell* 27, 20-32. doi: 10.1105/tpc.114.134874.

Berger, F., and Twell, D. (2011). Germline specification and function in plants. *Annu. Rev. Plant Biol.* 62, 461-484. doi: 10.1146/annurev-arplant-042110-103824.

Bokvaj, P., Hafidh, S., and Honys, D. (2015). Transcriptome profiling of male gametophyte development in *Nicotiana tabacum*. *Genomics Data* 3, 106-111.

Cifuentes-Rojas, C., Kannan, K., Tseng, L., and Shippen, D.E. (2011). Two RNA subunits and POT1a are components of Arabidopsis telomerase. *Proc. Natl. Acad. Sci., U.S.A.* 108, 73-78. doi: 10.1073/pnas.1013021107 [pii]10.1073/pnas.1013021107.

Clarkson, J.J., Kelly, L.J., Leitch, A.R., Knapp, S., and Chase, M.W. (2010). Nuclear glutamine synthetase evolution in *Nicotiana*: Phylogenetics and the origins of allotetraploid and homoploid (diploid) hybrids. *Mol. Phylogenet. Evol.* 55, 99-112. doi: 10.1016/j.ympev.2009.10.003.

Dellaporta, S., Wood, J., and Hicks, J. (1983). A plant DNA miniprep: Version II. *Plant Mol. Biol. Rep.* 1, 19-21.

Fajkus, J., Fulneckova, J., Hulanova, M., Berkova, K., Riha, K., and Matyasek, R. (1998). Plant cells express telomerase activity upon transfer to callus culture, without extensively changing telomere lengths. *Mol. Gen. Genet.* 260, 470-474.

Fajkus, J., Kovarik, A., and Kralovics, R. (1996). Telomerase activity in plant cells. *FEBS Lett.* 391, 307-309.

Fajkus, J., Kovarik, A., Kralovics, R., and Bezdek, M. (1995a). Organization of telomeric and subtelomeric chromatin in the higher plant *Nicotiana tabacum*. *Mol. Gen. Genet.* 247, 633-638. doi: Doi 10.1007/Bf00290355.

Fajkus, J., Kralovics, R., Kovarik, A., and Fajkusova, L. (1995b). The telomeric sequence is directly attached to the HRS60 subtelomeric tandem repeat in tobacco chromosomes. *FEBS Lett.* 364, 33-35. doi: Doi 10.1016/0014-5793(95)00347-C.

Fitzgerald, M.S., Mcknight, T.D., and Shippen, D.E. (1996). Characterization and developmental patterns of telomerase expression in plants. *Proc. Natl. Acad. Sci., U.S.A.* 93, 14422-14427.

Fulnecek, J., Matyasek, R., and Kovarik, A. (2009). Faithful inheritance of cytosine methylation patterns in repeated sequences of the allotetraploid tobacco correlates with the expression

1 of DNA methyltransferase gene families from both parental genomes. *Mol. Genet.*
2 *Genomics* 281, 407-420. doi: 10.1007/s00438-008-0420-8.

3 Hafidh, S., Breznenova, K., and Honys, D. (2012a). De novo post-pollen mitosis II tobacco
4 pollen tube transcriptome. *Plant Signal. Behav.* 7, 918-921. doi:10.4161/psb.2074520745.

5 Hafidh, S., Breznenova, K., Ruzicka, P., Fecikova, J., Capkova, V., and Honys, D. (2012b).
6 Comprehensive analysis of tobacco pollen transcriptome unveils common pathways in
7 polar cell expansion and underlying heterochronic shift during spermatogenesis. *BMC*
8 *Plant Biol.* 12. doi: Artn 2410.1186/1471-2229-12-24.

9 Hellemans, J., Mortier, G., De Paepe, A., Speleman, F., Vandesompele, J. (2007) qBase relative
10 quantification network and software for amangement and automated analysis of real-time
11 quantitative PCR data. *Genome Biol.* 8.

12 Herbert, B.S., Hochreiter, A.E., Wright, W.E., and Shay, J.W. (2006). Nonradioactive detection
13 of telomerase activity using the telomeric repeat amplification protocol. *Nat. Protoc.* 1,
14 1583-1590. doi: nprot.2006.239 [pii]10.1038/nprot.2006.239.

15 Honys, D., Renak, D., Fecikova, J., Jedelsky, P.L., Nebesarova, J., Dobrev, P., and Capkova, V.
16 (2009). Cytoskeleton-associated large RNP complexes in tobacco male gametophyte
17 (EPPs) are associated with ribosomes and are involved in protein synthesis, processing,
18 and localization. *J. Proteome Res.* 8, 2015-2031. doi: 10.1021/pr8009897.

19 Kovarik, A., Dadejova, M., Lim, Y.K., Chase, M.W., Clarkson, J.J., Knapp, S., and Leitch, A.R.
20 (2008). Evolution of rDNA in Nicotiana allopolyploids: A potential link between rDNA
21 homogenization and epigenetics. *Ann. Bot.* 101, 815-823. doi: Doi 10.1093/Aob/Mcn019.

22 Lim, K.Y., Matyasek, R., Kovarik, A., and Leitch, A.R. (2004). Genome evolution in
23 allotetraploid Nicotiana. *Biol. J. Linn. Soc. Lond.* 82, 599-606. doi: DOI 10.1111/j.1095-
24 8312.2004.00344.x.

25 Majerova, E., Mandakova, T., Vu, G.T.H., Fajkus, J., Lysak, M.A., and Fojtova, M. (2014).
26 Chromatin features of plant telomeric sequences at terminal vs. internal positions. *Front.*
27 *Plant Sci.* 5. doi: DOI 10.3389/fpls.2014.00593.

28 Murad, L., Lim, K.Y., Christopodulou, V., Matyasek, R., Lichtenstein, C.P., Kovarik, A., and
29 Leitch, A.R. (2002). The origin of tobacco's T genome is traced to a particular lineage
30 within Nicotiana tomentosiformis (Solanaceae). *Am. J. Bot.* 89, 921-928. doi: Doi
31 10.3732/Ajb.89.6.921.

32 Ogrocka, A., Sykorova, E., Fajkus, J., and Fojtova, M. (2012). Developmental silencing of the
33 AtTERT gene is associated with increased H3K27me3 loading and maintenance of its
34 euchromatic environment. *J. Exp. Bot.* 63, 4233-4241. doi: Doi 10.1093/Jxb/Ers107.

35 Pacini, E., Guarnieri, M., and Nepi, M. (2006). Pollen carbohydrates and water content during
36 development, presentation, and dispersal: a short review. *Protoplasma* 228, 73-77. doi:
37 10.1007/s00709-006-0169-z.

38 Park, S.K., Howden, R., and Twell, D. (1998). The Arabidopsis thaliana gametophytic mutation
39 gemini pollen1 disrupts microspore polarity, division asymmetry and pollen cell fate.
40 *Development* 125, 3789-3799.

41 Petru, E., Hrabětová, E., and Tupý, J. (1964). The technique of obtaining germinating pollen
42 without microbilla contamination. *Biol. Plant.* 6, 68-69.

43 Pfaffl, M.W. (2004). "Quantification strategies in real-time PCR," in *A-Z of quantitative PCR*, ed.
44 S.A. Bustin. (La Jolla, CA, USA: International University Line), 87-112.

45 Ren, S.X., Johnston, J.S., Shippen, D.E., and Mcknight, T.D. (2004). TELOMERASE
46 ACTIVATOR1 induces telomerase activity and potentiates responses to auxin in
47 Arabidopsis. *Plant Cell* 16, 2910-2922. doi: DOI 10.1105/tpc.104.025072.

- 1 Renny-Byfield, S., Chester, M., Kovarik, A., Le Comber, S.C., Grandbastien, M.A., Deloger, M.,
2 Nichols, R.A., Macas, J., Novak, P., Chase, M.W., and Leitch, A.R. (2011). Next
3 generation sequencing reveals genome downsizing in allotetraploid *Nicotiana tabacum*,
4 predominantly through the elimination of paternally derived repetitive DNAs. *Mol. Biol.*
5 *Evol.* 28, 2843-2854. doi: DOI 10.1093/molbev/msr112.
- 6 Riha, K., Fajkus, J., Siroky, J., and Vyskot, B. (1998). Developmental control of telomere lengths
7 and telomerase activity in plants. *Plant Cell* 10, 1691-1698.
- 8 Rihova, L., Capkova, V., and Tupy, J. (1996). Changes in glycoprotein patterns associated with
9 male gametophyte development and with induction of pollen embryogenesis in *Nicotiana*
10 *tabacum* L. *J. Plant Physiol.* 147, 573-581.
- 11 Ruckova, E., Friml, J., Schrupfova, P.P., and Fajkus, J. (2008). Role of alternative telomere
12 lengthening unmasked in telomerase knock-out mutant plants. *Plant Mol. Biol.* 66, 637-
13 646. doi: 10.1007/s11103-008-9295-7.
- 14 She, W., and Baroux, C. (2015). Chromatin dynamics in pollen mother cells underpin a common
15 scenario at the somatic-to-reproductive fate transition of both the male and female
16 lineages in *Arabidopsis*. *Front. Plant Sci.* 6, 294. doi: 10.3389/fpls.2015.00294.
- 17 Schmidt, G.W., and Delaney, S.K. (2010). Stable internal reference genes for normalization of
18 real-time RT-PCR in tobacco (*Nicotiana tabacum*) during development and abiotic stress.
19 *Mol. Genet. Genomics* 283, 233-241. doi: DOI 10.1007/s00438-010-0511-1.
- 20 Sierro, N., Battey, J.N.D., Ouadi, S., Bovet, L., Goepfert, S., Bakaher, N., Peitsch, M.C., and
21 Ivanov, N.V. (2013). Reference genomes and transcriptomes of *Nicotiana sylvestris* and
22 *Nicotiana tomentosiformis*. *Genome Biol.* 14. doi: 10.1186/Gb-2013-14-6-R60.
- 23 Sykorova, E., Fulneckova, J., Mokros, P., Fajkus, J., Fojtova, M., and Peska, V. (2012). Three
24 TERT genes in *Nicotiana tabacum*. *Chromosome Res.* 20, 381-394. doi: DOI
25 10.1007/s10577-012-9282-3.
- 26 Sykorova, E., Lim, K.Y., Chase, M.W., Knapp, S., Leitch, I.J., Leitch, A.R., and Fajkus, J.
27 (2003). The absence of *Arabidopsis*-type telomeres in *Cestrum* and closely related genera
28 *Vestia* and *Sessea* (Solanaceae): first evidence from eudicots. *Plant J.* 34, 283-291. doi:
29 1731 [pii].
- 30 Tamura, K., Liu, H.T., and Takahashi, H. (1999). Auxin induction of cell cycle regulated activity
31 of tobacco telomerase. *J. Biol. Chem.* 274, 20997-21002. doi: DOI
32 10.1074/jbc.274.30.20997.
- 33 Tupy, J., Suss, J., Hrabetova, E., and Rihova, L. (1983). Developmental changes in gene
34 expression during pollen differentiation and maturation in *Nicotiana tabacum* L. *Biol.*
35 *Plant.* 25, 231-237. doi: Doi 10.1007/Bf02902110.
- 36 Yang, S.W., Jin, E., Chung, I.K., and Kim, W.T. (2002). Cell cycle-dependent regulation of
37 telomerase activity by auxin, abscisic acid and protein phosphorylation in tobacco BY-2
38 suspension culture cells. *Plant J.* 29, 617-626. doi: DOI 10.1046/j.0960-
39 7412.2001.01244.x.

40

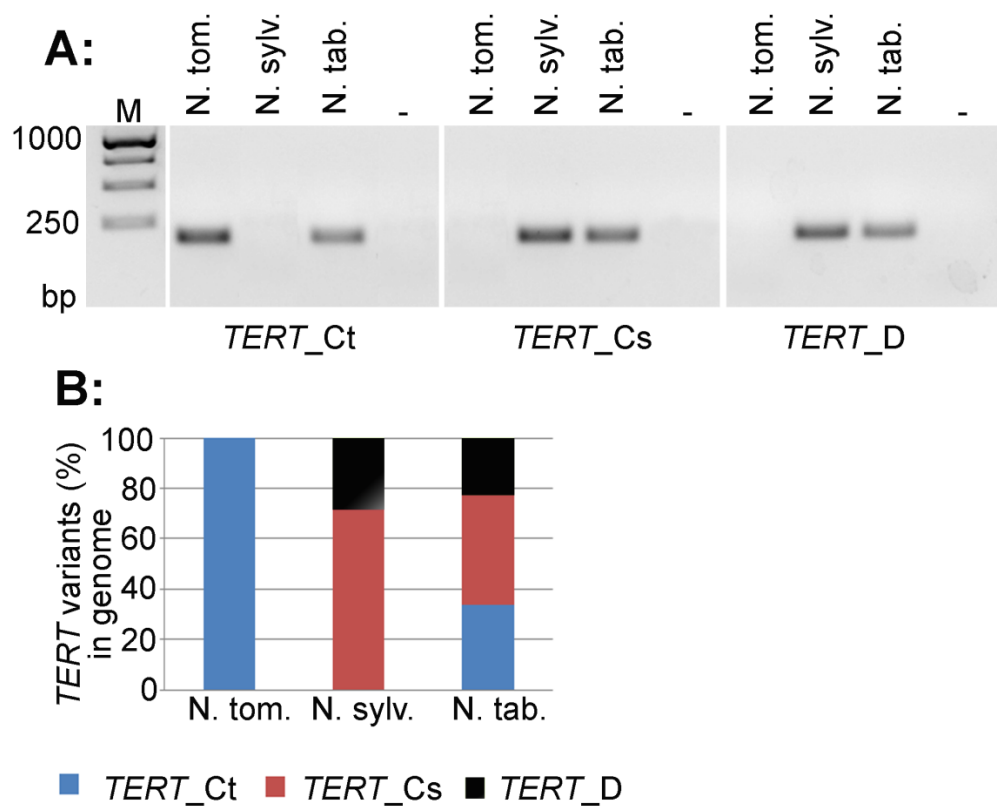


Figure 1: *TERT* gene variants in genomes of *N. tabacum*, *N. sylvestris* and *N. tomentosiformis*.

A: PCR amplification confirmed the presence of the *TERT_Ct* variant in genomes of *N. tabacum* and *N. tomentosiformis*, bands of *TERT-Cs* and *TERT_D* products were detected in *N. tabacum* and *N. sylvestris*. N. tom., *N. tomentosiformis*; N. sylv., *N. sylvestris*; N. tab., *N. tabacum*; -, no template reaction; M, DNA ladder (GeneRuler 1 kb DNA Ladder, Life Technologies).

B: The representation of *TERT* gene variants (in %) in genomes of tobacco and its progenitors was determined by qPCR. Abbreviations for *Nicotiana* species are as in A; *TERT* gene variants are indicated by colors (*TERT_Ct* in blue; *TERT-Cs* in red; *TERT_D* in black).

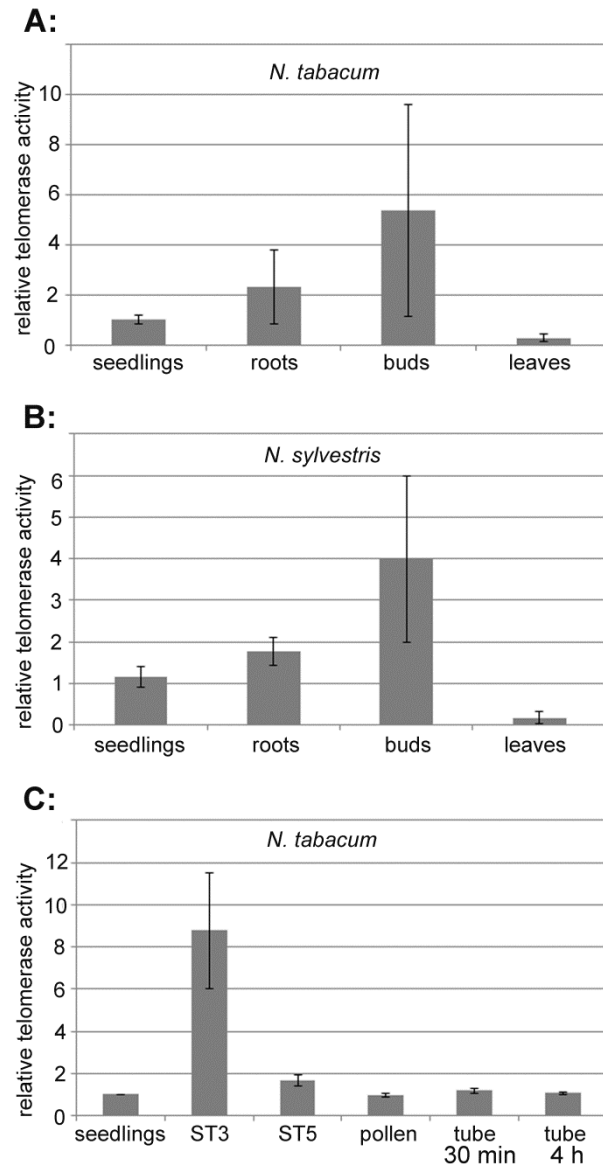


Figure 2: Relative telomerase activity in tissues of *Nicotiana* species.

A: Relative telomerase activity in *N. tabacum* tissues. Three samples of 12-day seedlings, three samples of roots, four samples of flower buds and five samples of mature leaves were analyzed in three technical replicates by quantitative TRAP. Results were related to telomerase-positive seedlings (telomerase activity in seedlings was arbitrarily chosen as 1). Relatively high heterogeneity of telomerase activity in flower buds reflects subjective evaluation of the flower buds developmental stage during sample collection.

B: Relative telomerase activity in *N. sylvestris* tissues. Three samples of respective tissues were analyzed in three technical replicates. Results were related to seedlings.

C: Relative telomerase activity in *N. tabacum* pollen. Two samples of respective tissues were analyzed in three technical replicates. Results were related to seedlings.

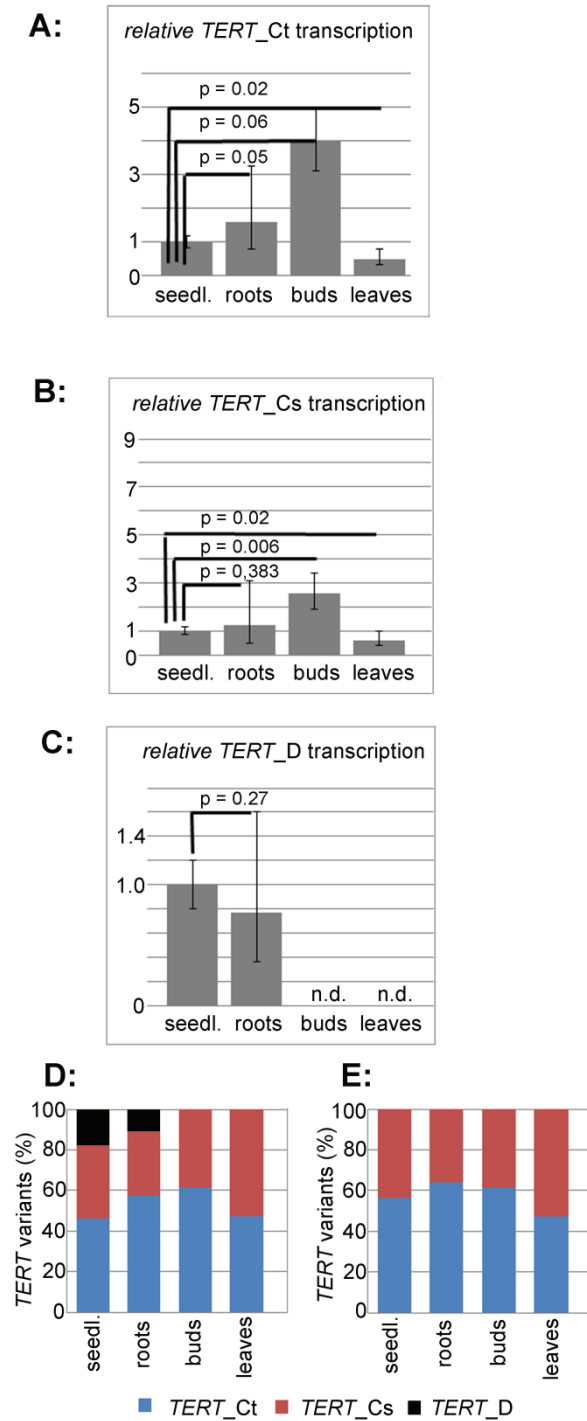


Figure 3: Transcripts of *TERT* variants in *N. tabacum* tissues. Transcript levels of *TERT_Ct* (A) *TERT-Cs* (B) and *TERT_D* (C) variants were determined in eight samples of 12-day seedlings, flower buds and mature leaves, and six samples of roots in three technical replicates. Data were related to seedlings. Level of *TERT_D* transcript was below the detection limit in flower buds and leaves (n.d., not detected). Statistical analysis was done using qbase+ software and “p” levels for respective tissues were determined.

D: The representation of individual *TERT* variants (in %) in total *TERT* transcripts of respective tissues was calculated using Ct values obtained for amplification of respective *TERT* variants by the Δ Ct method. *TERT* gene variants are indicated by colors (*TERT*_Ct in blue; *TERT*_Cs in red; *TERT*_D in black).

E: The representation of *TERT*_C variants (in %) in total *TERT* transcripts of respective tissues; *TERT*_D transcript was not considered in this calculation. *TERT*_Ct is in blue; *TERT*_Cs is in red.

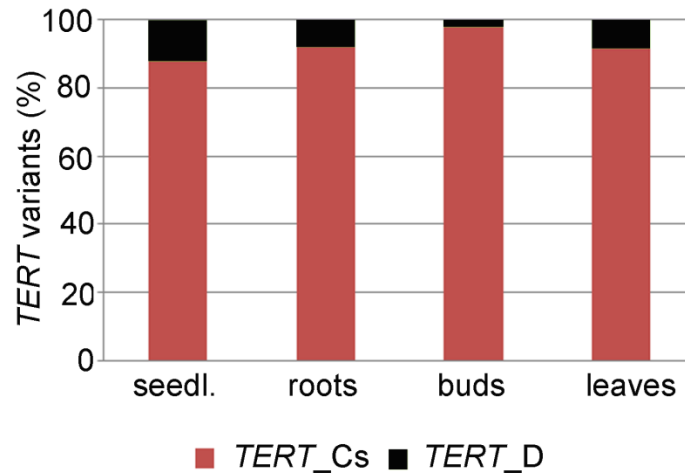


Figure 4: Transcripts of *TERT* variants in *N. sylvestris* tissues.

The representation of *TERT* variants (in %) in transcriptomes of respective tissues was calculated using Ct values obtained for *TERT*_Cs and *TERT*_D amplifications by the Δ Ct method. *TERT*_Cs is in red; *TERT*_D is in black.

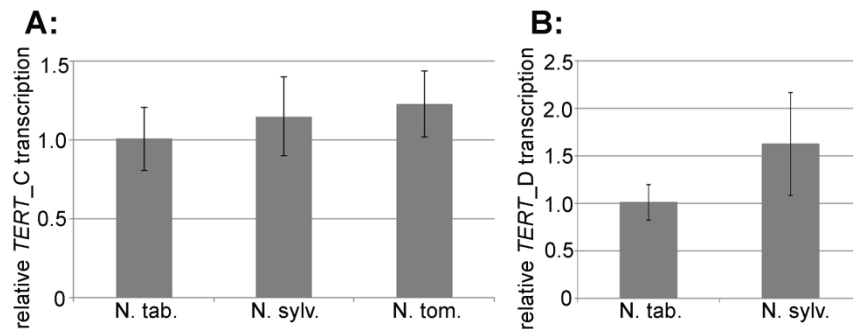


Figure 5: Comparison of transcript levels of *TERT* variants in *Nicotiana* species.

A: Relative levels of *TERT*_C variant transcripts in *N. tabacum* (N. tab.), *N. sylvestris* (N. sylv.) and *N. tomentosiformis* (N. tom.) seedlings, four samples of each species were analyzed in three technical replicates. Data were related to tobacco seedlings.

B: Relative levels of *TERT*_D transcript in *N. tabacum* and *N. sylvestris* seedlings, four samples of both species were analyzed in three technical replicates. Data were related to tobacco seedlings.

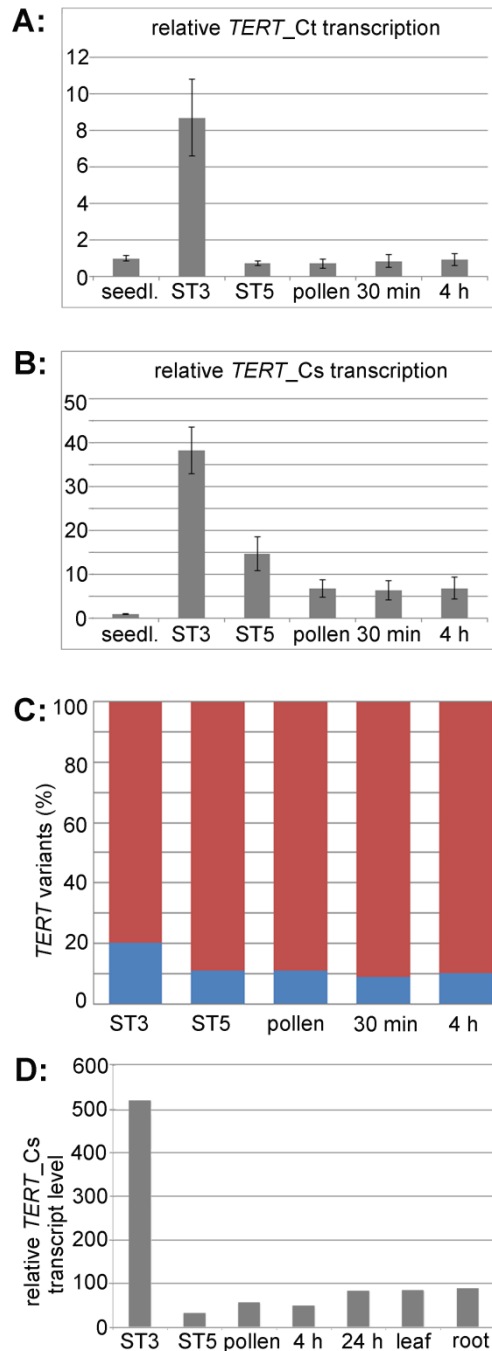


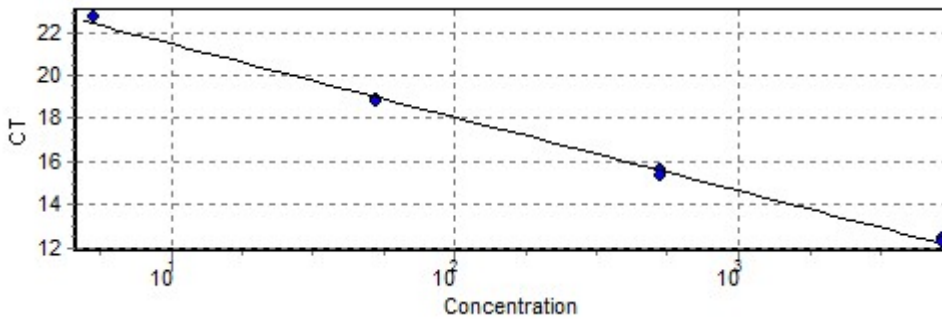
Figure 6: Transcripts of *TERT* variants in tobacco pollen.

Transcription of *TERT_Ct* (A) and *TERT-Cs* (B) was determined in two samples of immature pollen, mature pollen and pollen tubes in three technical replicates. Data were related to seedlings. Statistical analysis of data was not done, results of analyses of two biological replicates were not sufficient for reliable comparisons. ST3, immature pollen stage 3; ST5, immature pollen stage 5; pollen, mature pollen grains; 30 min, pollen tube cultivated *in vitro* for 30 min; 4 h, pollen tube cultivated *in vitro* for 4h.

C: The representation of *TERT* variants in total *TERT* transcripts of tobacco pollen samples was calculated using Ct values obtained for *TERT_Ct* and *TERT_Cs* amplifications by the Δ Ct method. *TERT_Ct* is in blue; *TERT_Cs* is in red.

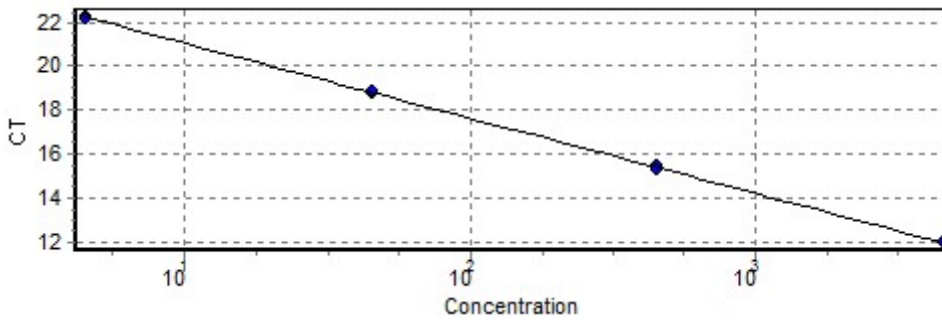
D: Expression profile of *TERT_Cs* transcript during tobacco pollen development and in two sporophytic tissues according to published microarray data (for details see text).

TERT_Ct calibration curve



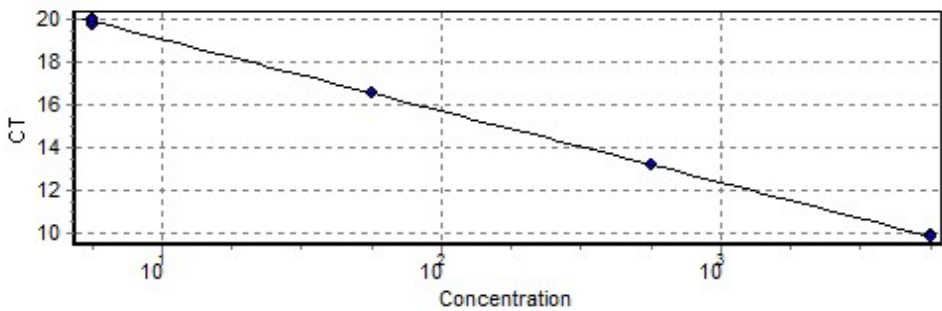
Reaction efficiency = 0.97
M = -3.3941
R value = 0.99842
R2 value = 0.99785

TERT-Cs calibration curve



Reaction efficiency = 0.97
M = -3.4067
R value = 0.99992
R2 value = 0.99983

TERT_D calibration curve

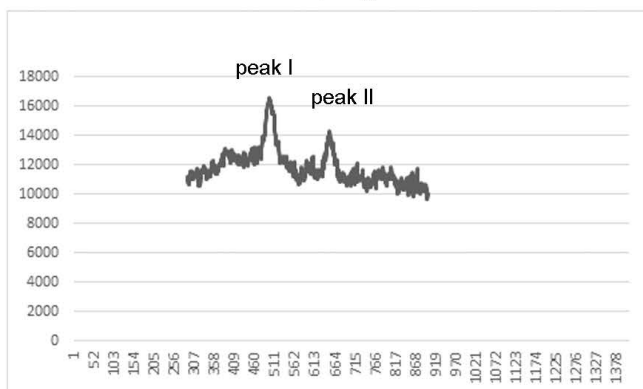


Reaction efficiency = 0.99
M = -3.3375
R value = 0.99985
R2 value = 0.99971

Figure S1: Calibration curves for qPCR analyses of *TERT_Ct*, *TERT-Cs* and *TERT_D* variants. Parameters were calculated by the Rotorgene6000 (Qiagen) software from calibration curves which were constructed using gradually diluted genomic DNA isolated from tobacco leaves.

A:

EcoRI + MspI digestion

**B:**

EcoRI digestion

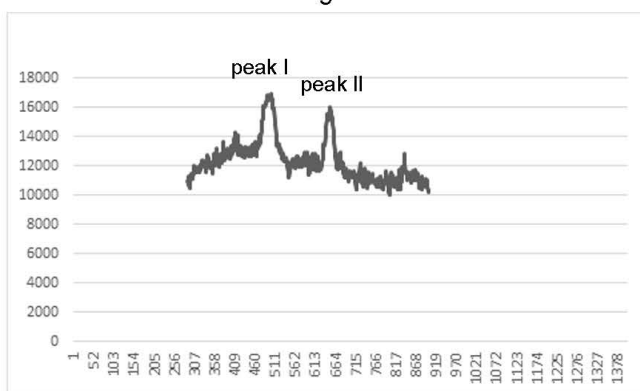


Figure S2: Densitometric evaluation of the *TERT*_Cs- and *TERT*_D-specific hybridization bands intensities.

As described in Sykorova et al., 2012, restriction digestion of genomic DNA (gDNA) and Southern hybridization using radioactively labeled probe specific for the *NtTERT* allowed identification of all three variants in the *N. tabacum* genome as separate bands. The same probe and experimental design was used for analysis of *N. sylvestris* gDNA digested by restriction endonucleases. Two bands were revealed, representing the *TERT*_Cs and *TERT*_D variant. Evaluation of the intensity of hybridization signals of the *N. tabacum* and *N. sylvestris* bands showed the tobacco bands as approximately equal, but the band corresponding to the *N. sylvestris* *TERT*_Cs variant much stronger compared to the *TERT*_D variant band. This opened the question about the copy number of *TERT* variants in the *N. sylvestris* genome (Sykorova et al., 2012).

Here we presented results of quantitative evaluation of *TERT*-specific signals from Southern hybridization of *N. sylvestris* gDNA digested by EcoRI + MspI (A) and EcoRI (B) using densitometry (not shown in Sykorova et al., 2012). It is evident that the peak I corresponding to the *TERT*_Cs-specific band is more developed in both digested samples compared to the peak II representing the *TERT*_D-specific band. Comparison of the hybridization signal intensities in both bands showed ratio 8:2 (*TERT*_Cs : *TERT*_D) in EcoRI + MspI digested DNA; and 7:3 in EcoRI digested DNA (the sum of the signals intensities was arbitrarily chosen as 10).

Relative intensities of bands in variant-specific hybridization bands in *N. tabacum* DNA digested by EcoRI + MspI were as follows: *TERT*_Cs - 3.5; *TERT*_Ct - 3.5; *TERT*_D - 3, which is in good agreement with the data obtained by qPCR analysis (Figure 1B).

Density of the hybridization signal along respective lane was evaluated using the Multi Gauche program (FujiFilm).

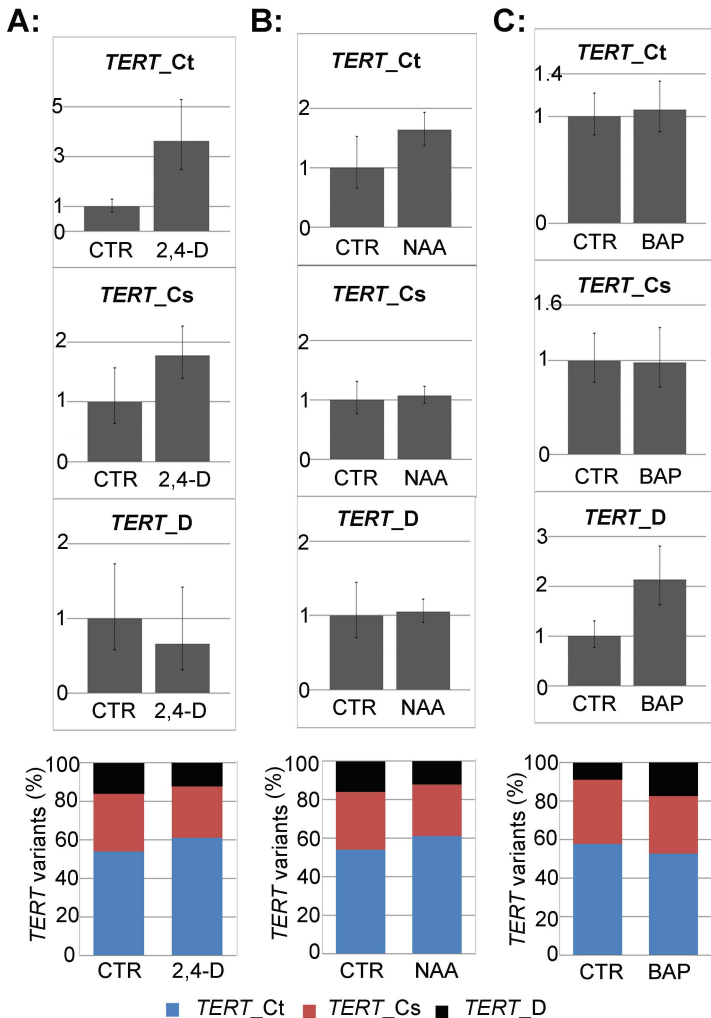


Figure S3: Transcripts of *TERT* variants in tobacco seedlings treated with plant hormones. Transcripts of *TERT* variants in seedlings cultivated in the presence of 5 μ M 2,4-D (A), 5 μ M NAA (B) and 5 μ M BAP (C) were determined in three independently cultivated samples in three technical replicates. Data were related to control untreated seedlings (CTR). In bottom panels, representations of individual *TERT* variants in total *TERT* transcripts, calculated using Ct values obtained for amplification of respective *TERT* variants by the Δ Ct method, are presented. *TERT_Ct* is in blue; *TERT_Cs* is in red; *TERT_D* is in black.

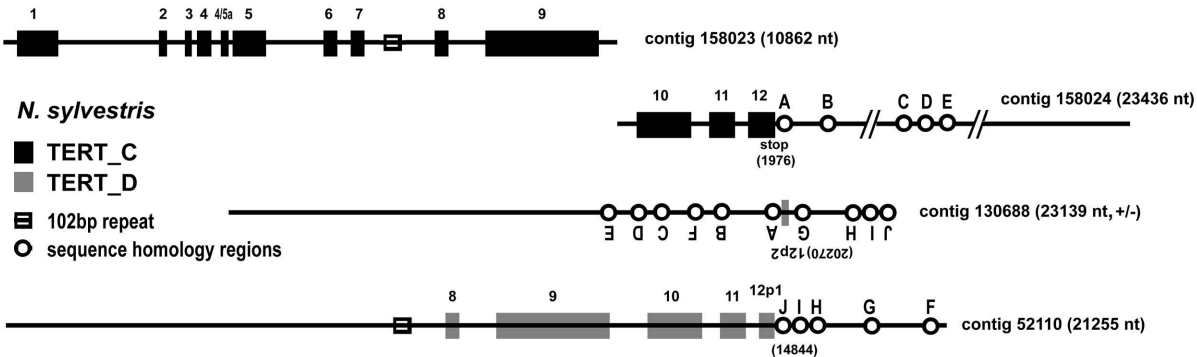


Figure S4: *In silico* analysis of *TERT* variants present in draft genome assembly of *N. sylvestris* identified four contigs with sequence homology to *TERT_C* and *TERT_D* variants. The non-overlapping contigs 158023 and 158024 contain *TERT_C* variant. The *N. sylvestris* *TERT_D* sequence corresponding to *TERT_D* variants reported in Sykorova et al. (2012) matches to the contig 52110 including partial exon 12 (12p1) and sequence similarity enabled mapping of putative regions upstream of exon 9 (up to 102bp repeat found in intron 7). Missing part of the exon 12 (12p2) could be found in the contig 13688. Sequence homology regions (circles) reflect rearrangements of these gene parts and their origin. Scheme is not in scale.

PRIMER	SEQUENCE (5' → 3')	METHOD
9ex Fw	GTGCTGGATGATCTCAATTTGGAG	forward primer for amplification of all <i>TERT</i> gene variants
9ex Rev_Ct	GAAGACAAGACCTGGCATTAGCAG	reverse primer for amplification of Ct variant of the <i>TERT</i> gene
9ex Rev_Cs	GGAAGATAAGACCTAGCATTGGCG	reverse primer for amplification of Cs variant of the <i>TERT</i> gene
9ex Rev_C	CAAGAATGCCATGCAATGAGCC	reverse primer for amplification of C variants of the <i>TERT</i> gene
9ex Rev_D	GAAGACAAGACCTGGCATTGACG	reverse primer for amplification of D variant of the <i>TERT</i> gene
actin Fw	CTGGATTTGCTGGTGATGAT	forward primer for amplification of actin reference gene
actin Rev	CYCTCTTGGATTGAGCTT	reverse primer for amplification of actin reference gene
EF1 Fw	TGAGATGCACCACGAAGCTC	forward primer for amplification of <i>EF1</i> reference gene
EF1 Rev	CCAACATTGTCACCAGGAAGTG	reverse primer for amplification of <i>EF1</i> reference gene
TS21	GACAATCCGTCGAGCAGAGTT	qTRAP
TELPR	CCGAATTCAACCCTAAACCCTAAACCCTAAACCC	qTRAP

Table S1: Sequences of primers used for specific amplification of *TERT* gene variants and quantification of telomerase activity. Actin primers are designed to amplify act54 and act103 members of the actin multigene family.